Synthesis and Reactivity of Sulfamoyl Fluoride Imines: Applications to Strained Ring Synthesis



Benedict A. Williams

Oriel College

University of Oxford

Michaelmas Term, 2024

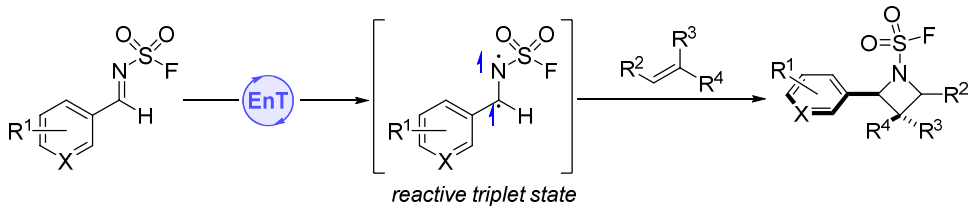
A thesis submitted in partial fulfilment of the requirements for the for the degree of Doctor of Philosophy in Organic Chemistry

Abstract

The work in this thesis describes the discovery, development and study of an intermolecular aza Paternò–Büchi reaction of an acyclic imine.

Chapter 1 is a literature review covering the properties, applications and synthetic strategies towards azetidines. The physical principles of photochemistry and energy transfer catalysis is also highlighted.

Chapter 2 describes the development of an intermolecular aza Paternò–Büchi reaction of acyclic sulfamoyl fluoride imines. This discovery is contextualised with a review of the photochemistry of imines, including the strategies towards the intermolecular aza Paternò–Büchi reaction. The scope of the transformation with respect to both components is explored and a brief mechanistic study is described to give support to our mechanistic hypothesis that the reaction proceeds *via* a triplet imine.



Chapter 3 documents a density functional theory computational study of the developed intermolecular aza Paternò–Büchi reaction of acyclic sulfamoyl fluoride imines. In particular, contextualising the reactivity of sulfamoyl fluoride aldimines against other sulfonyl aldimines in order to rationalise the unique reactivity of this imine.

Chapter 4 discusses the conclusion of these projects and provides potential future work.

Chapter 5 provides the experimental data and procedures used.

Declaration

I declare that the work in this thesis had not been previously submitted for a degree at the university of Oxford or any other higher education institution.

The experimental work in Chapter 2 was carried out in collaboration with Dr. Nicholas A. Parker a former post-doctoral researcher in the Willis group. The experiments and procedures performed by Dr. Nicholas A. Parker are clearly labelled NAP within Chapter 2 and the experimental section.

The computational work in Chapter 3 was carried out in collaboration with Dr. Michael J. Tilby, a former DPhil student in the Willis group. NBO calculations and analysis was performed by Dr. Michael J. Tilby.

The work in both Chapters 2 and 3 has been prepared and submitted for publication.

Benedict Williams

October 2024

Acknowledgements

Firstly, I have to thank Prof. Michael C. Willis, or M in email correspondences. The supervision and training I have received from starting as a Part II student until my DPhil has been world-class, I cannot think of anyone better to have guided me through this journey. Not only that but your constant belief in me and encouragement will never be forgotten. Thank you.

Next thank you is to my other academic supervisors and mentors I have had throughout my DPhil. To Prof. Fernanda Duarte, my time in the group was an invaluable learning experience being able to learn from such great people was a joy. In particular, I want to thank Alistair Sterling for his generosity and wisdom, without which I would have been lost. To Nils Frank for being an such an aspirational figure, it was truly a pleasure lending you MCW chemicals. I would also like to thank my industrial collaborators Mycah R. Uehling, Caleb Hethcox and Dipannita Kalyani for our great discussions over the years, your ideas and insight never ceased to inspire me. I would also like to thank the X-ray crystallography team and in particular Kirsten for taking me under your wing and the hours of patient help you have given me. A thank you of course goes to the funding bodies paying for me: the SBM doctoral training program. A special thanks goes to Lara in particular.

As part of my DPhil, I have worked directly work with some great people on my projects. To Nick Parker, thank you for putting your time and effort into synthesising some challenging molecules. To Tony ‘lazy bastard’ Lo I will never forget your patience and mentorship. To Michael Tilby (Tilby), goes the biggest thanks for helping push me out of my comfort zone to be the best computational chemist I can be and whilst being a great

person to talk to. Special thanks go to the absolute legends who have helped proofread this thesis: Jonny Andrews, Michael Tilby, May Merino, Charlie Bell, Mingkai Wei and Joshua Baxter.

Not only have I been able to learn from some great people but, I have had the chance to mentor some excellent students. Charlie Perry, your infectious joy and enthusiasm was a pleasure to be around! To Josh Mitchell, I hope one day you will learn why bad things always happen to good people like yourself. Being even such a small part of your chemistry journey has been such a joy and I know you will continue on to great things in the Aggarwal group. And finally, to Em, your headstrong determination and bravery will always be an inspiration.

To all the people that I have had the joy of working with in F1 over the years you really have made working in the Willis group feel like home including: Antoine, Janette, Kangtao, Damien, Jagadeesh, Russell, Wyman, Chris, Maddison and George. To the boys: Dan and Jonny, it has been pleasure going on so many unforgettable luncheons, pub, horsebox and ATS trips together. It has been an honour getting to know you two and I would never have made it as far as I have without you guys. I want to also thank Suzie, in spite of your unacceptable mess, you have been an amazing fumehood neighbour and have truly made F1 a joy to be in, keep on being you and look after F1 for me when I am gone. Baxter, I will never tire of being regaled with the same anecdotes of your rugby days, Tyson Fury related sheep-stealing incidents, the SAS, Canadian war crimes during WW1… Thank you also for services to DJing and the dogged enthusiasm and good humour you bring to life and chemistry. To Matt, I am sure I will see again at the next conference and get some more excellent dining recommendations which, hopefully I can get to enjoy your company at. Ivan, it has been fantastic to get to know you over all these

years and your one-liners will never fail to crack me up. Cian, it has been a pleasure to know get to know you right at the end and it has been great to see your journey in the Willis group so far and best of luck going forward in an excellent group.

To F1's visitors: Nerea, Lucia and Nikki, you have all made a such a big impact in such a short amount of time you were here whether it be chemistry-wise and also being a big part of the group bringing the good vibes from all over the world when F1 needed it most.

Next stop F2, you guys are the best and a big shout out goes to all of you: Xinlan, Ndi, Mingyan, Zexin, Maia, Presiyan, Dom, Niklas B, Ria, Gabby, Sajal, Erik and Luca. May and Katherine, thank you for being the beating hearts of the Willis group social scene. Whether it be in organising cheese and wine night or the perennial Friday lunch club, these social gatherings and your company at these events will be (and are already) sorely missed. Mingkai your work ethic has always inspired me but what is even more inspiring to me is your boundless enthusiasm and infectious kindness, you have made the Willis group a pleasure for not only me but for everyone to be a part of! Di, a man like no one I have ever met! I can honestly say there is never a dull moment with you with your sense of humour providing me endless laughs and your sharp mind always keep me on my toes. Cherry good luck with carrying on this work going forward and I hope you enjoy being the next Willis group crystallographer. Here is an apt time to thank Charlie not only for being the glue holding the Willis group together, your excellent advice or for being a friend to rely on. But, most importantly for helping organise dinner at the Magdalen Arms, which typified the way your sense of duty drives you to always go above and beyond in everything you do.

To all my friends outside of the MCW group goes a massive thanks and in particular SBM crew for being such a great group of people to be around: Jess, Junfu, Tim, Josh, Tom, Steve and Diana. Last and certainly not least Calum Patel, for all the things we have been through together from our time in the Duarte group together and beyond. You've been a true friend to me; always supporting me; cheering me on when I succeeded and picked me up when I was down.

Lastly and most importantly, I want to thank my family for supporting me through thick and thin, good times and bad. The most important acknowledgement goes ultimately to Aoife. I have no clue how you have put up with me all these years, stood by my side and kept on loving me. I can't wait to see what is next in store for us.

Table of Contents

1 Introduction 1
1.1 Importance of Azetidines 1
1.2 Synthesis of Azetidines 2
1.2.1 Cyclisation of Linear Precursors 3
1.2.2 Thermal [2+2]-Cycloaddition 9
1.2.3 Ring Opening of aza-BCBs 13
1.2.4 Ring Expansions and Contractions 18
1.2.5 Reduction of β-Lactams 23
1.3 Principles of Photochemistry 24
1.3.1 Energy Transfer Catalysis 26
2 Sulfamoyl Fluoride Aldimines as Sensitisable Partners in the aza Paternò–Büchi reaction 29
2.1 Introduction 29
2.1.1 Photochemistry of Imines 29
2.1.2 Photoisomerisation 30
2.1.3 Photofragmentation and Photoelimination 32
2.1.4 Aza Paternò–Büchi Reaction using Triplet Imines 41
2.1.5 Aza Paternò–Büchi Reaction *via* a Singlet Exciplex 48
2.1.6 Aza Paternò–Büchi Reaction *via* an Excited State Alkene 51
2.2 Origin and Outline of Project 52
2.3 Synthesis of Sulfamoyl Fluoride Aldimines 57
2.4 Optimisation of aza Paternò–Büchi Reaction 62
2.4.1 Preliminary Optimisation System 62
2.4.2 Optimisation with 1,1-Disubstituted Olefin 63
2.5 Scope of aza Paternò–Büchi reaction 71
2.5.1 Imine Scope 71
2.5.2 Alkene Scope 76
2.6 Derivatisation and Scale-Up 84
2.7 Indane Formation through a Dearomative Mechanism 91
2.8 Mechanistic Investigation 92
2.8.1 Stern-Volmer Quenching 94

2.8.2 Cyclic Voltammetry 97
2.8.3 Time Course Experiment 98
2.9 Summary and Outlook 99
3 Computational Investigation of the aza Paternò–Büchi Reaction of Sulfamoyl Fluoride Imines 101
3.1 Introduction 102
3.2 Photochemistry of imines 102
3.2.1 Triplet Energy 102
3.2.2 Minimum Energy Crossing Point 104
3.2.3 Photoisomerisation 106
3.3 Fragmentation of Imines 107
3.4 Addition of Imines into Alkenes 109
3.4.1 Potential Energy Surfaces 109
3.4.2 Born-Oppenheimer Molecular Dynamics of Addition 117
3.4.3 Comparison of Imine Addition Barriers 120
3.4.4 Alternative Transition State 121
3.4.5 Regioselectivity of Addition 123
3.5 Intersystem Crossing 125
3.6 Alternative alkene 126
3.6.1 Addition of Imine 127
3.6.2 Intersystem Crossing 128
3.7 Calculated Reduction Potentials 130
3.7.1 Imine 130
3.7.2 Photochemistry and Electrochemical Studies on Thioxanthone Photocatalysts 132
3.8 NBO Analysis 133
3.9 Summary and Outlook 135
4 Conclusions and Future Work 137
5 Experimental Procedures 139
5.1 General Information 139
5.2 Experimental Data for Chapter 2 141
5.2.1 General Procedures 141
5.2.2 Substrate Synthesis 143

5.2.2.1 Alkene Substrates 143
5.2.2.2 Aldehyde Substrates 156
5.2.2.3 Imine Substrates 165
5.2.3 Azetidine Substrate Scope 183
5.2.4 Product Derivatisation 262
5.2.5 Indane Preparation 271
5.2.6 Photocatalyst Preparation 272
5.2.7 Stern-Volmer Data 275
5.2.8 Cyclic Voltammetry 277
5.3 Computational Data and Procedures for Chapter 3 278
5.3.1 Computational Methods 278
5.3.2 Tables of Energies 280
References 284
Spectra 292

Abbreviations and Acronyms

1,2-DCE	1,2-dichloroethane
2-MeO-TX	2-methoxy-9H-thioxanthen-9-one
3-F-TX	3-fluoro-9H-thioxanthen-9-one
5CzBN	2,3,4,5,6-Penta(9H-carbazol-9-yl)benzonitrile
Å	Angstrom
Ac	Acetyl
Alk	alkyl
app.	Apparent
aq.	Aqueous
Ar	Aryl
atm	atmosphere
BCB	Bicyclo[1.1.0]butane
BET	Back electron transfer
Bn	Benzyl
Boc	tert-Butyloxycarbonyl
BOMD	Born-Oppenheimer molecular dynamics
bp	Boiling point
br	Broad
BS-DFT	Broken Symmetry Density Functional Theory
BSIE	Basis set incompleteness error
BSSE	Basis set superposition error
Bu	Butyl
Bz	Benzoyl

CASSCF	complete active space self-consistent field
cat	Catalyst
Cbz	carboxybenzyl
CCDC	Cambridge crystallographic data centre
Cy	Cyclohexyl
Cyp	Cyclopentyl
CYP450	Cytochrome p450
d	Doublet
DABCO	1,4-diazabicyclo[2.2.2]octane
DCM	Dichloromethane
DFT	Density functional theory
DIPEA	N, N'-Diisopropylethylamine
DMA	N, N-Dimethylacetamide
DMAP	4-dimethylaminopyridine
DMF	N, N-Dimethylformamide
DMSO	Dimethyl sulfoxide
dr	diastereomeric ratio
dtbbpy	4,4'-di-tert-butyl-2,2'-dipyridyl
E	electrophile
EDG	electron-donating group
ee	enantiomeric excess
EI	Electron ionisation
Epin	1,1,2,2-tetraethylethylene glycol
equiv.	Equivalent(s)

ESI	Electrospray Ionisation
Et	Ethyl
eV	electron Volts
EWG	Electron-withdrawing group
fac	facial
FDA	Food and Drug Administration
g	Gram(s)
G	gibbs free energy
GGA	generalised gradient approximation
h	Hour(s)
H	enthalpy
HAD	hydrogen atom donor
HAT	hydrogen atom transfer
Het	Heteroaryl
HOMO	highest occupied molecular orbital
HPLC	High Performance Liquid Chromatography
HRMS	High Resolution Mass Spectrometry
Hz	Hertz
i	iso
IC	internal conversion
IR	Infrared Spectrometry
ISC	intersystem crossing
ITX	2-isopropyl-9H-thioxanthen-9-one
J	Coupling constant (Hz)

kcal	kilocalorie
LRMS	Low resolution mass spectrometry
LSOMO	lowest singly occupied molecular orbital
LSUMO	lowest singly unnoccupied molecular orbital
LUMO	lowest unoccupied molecular orbital
m	meta or Multiplet
M	Molar
m/z	Mass to charge ratio
M06-2X	Minnesota 06 54% Hartree-Fock exchange
m-CPBA	meta-chloroperoxybenzoic acid
Me	Methyl
MIDA	N-methyliminidiacetic acid
mol	Mole
mp	Melting point
MS	Molecular sieves
Ms	methanesulfonyl
n	normal
N	normality
NBD	Norbornadiene
NMP	N-methyl pyrrolidone
NMR	Nuclear magnetic resonance
nr	No reaction
Nu	nucleophile
o	ortho

p	para
PDEA	N-phenyldiethanolamine
PES	potential energy surface
PET	Photoinduced electron transfer
Petrol	Petroleum ether (40 – 60 °C)
Ph	Phenyl
Phth	phthalimide
pin	Pinacol
Piv	pivaloyl
PMP	para-methoxyphenyl
ppm	Parts per million
ppy	2-phenyl pyridine
Pr	Propyl
Pyr	Pyridine
q	quartet
R	Generic group / substituent
rbf	Round bottom flask
RDS	Rate determining step
Red	reduction
rt	Room temperature
s	Singlet
S	entropy
sat.	Saturated
SCE	saturated calomel electrode

SEM	Trimethylsilylethoxymethyl
SET	Single electron transfer
SIE	self-interaction error
SMD	solvent model based on density
S_N1	Nucleophilic unimolecular substitution
S_N2	Nucleophilic bimolecular substitution
S_NAr	Nucleophilic aromatic substitution
SuFEx	Sulfur(VI) Fluoride exchange
t	Triplet or tertiary
TBA	Tetrabutylammonium
TBDMS	tert-Butyldimethylsilyl
TDDFT	Time dependent density functional theory
Temp	Temperature
Tf	Triflate
TFA	trifluoroacetate
THF	Tetrahydrofuran
TLC	Thin Layer Chromatography
TMS	Trimethylsilyl
TMS	trimethylsilyl
Tol	Tolyl
Ts	toluenesulfonyl (tosyl)
TS	transition state
TX	9H-thioxanthen-9-one
UV	Ultra-Violet

Vis	Visible
vs.	versus
X	(Pseudo)halide (unless stated otherwise)
Z	carboxybenzyl
ZPE	zero-point energy

Chapter 1 - Introduction

1.1 Importance of Azetidines

Saturated *N*-heterocycles are ubiquitous in nature in the form of alkaloid natural products, including a multitude of biologically active molecules used in agrochemistry and medicinal chemistry (**Figure 1-1A and B**).[1, 2] In medicinal chemistry, >80% of all drugs approved by the FDA in the last ten years incorporate at least one *N*-heterocycle.[3] In contrast, azetidines, the 4-membered homologues of piperidines, occupy only a small fraction of chemical space, ranking only 26th on the list of heterocycles used in FDA approved drugs from 2013 – 2023.[3] The underutilisation of azetidines as a scaffold in drug design is a direct consequence of the limitations in established methods for their synthesis rather than a result of their structural features or properties.[4, 5]

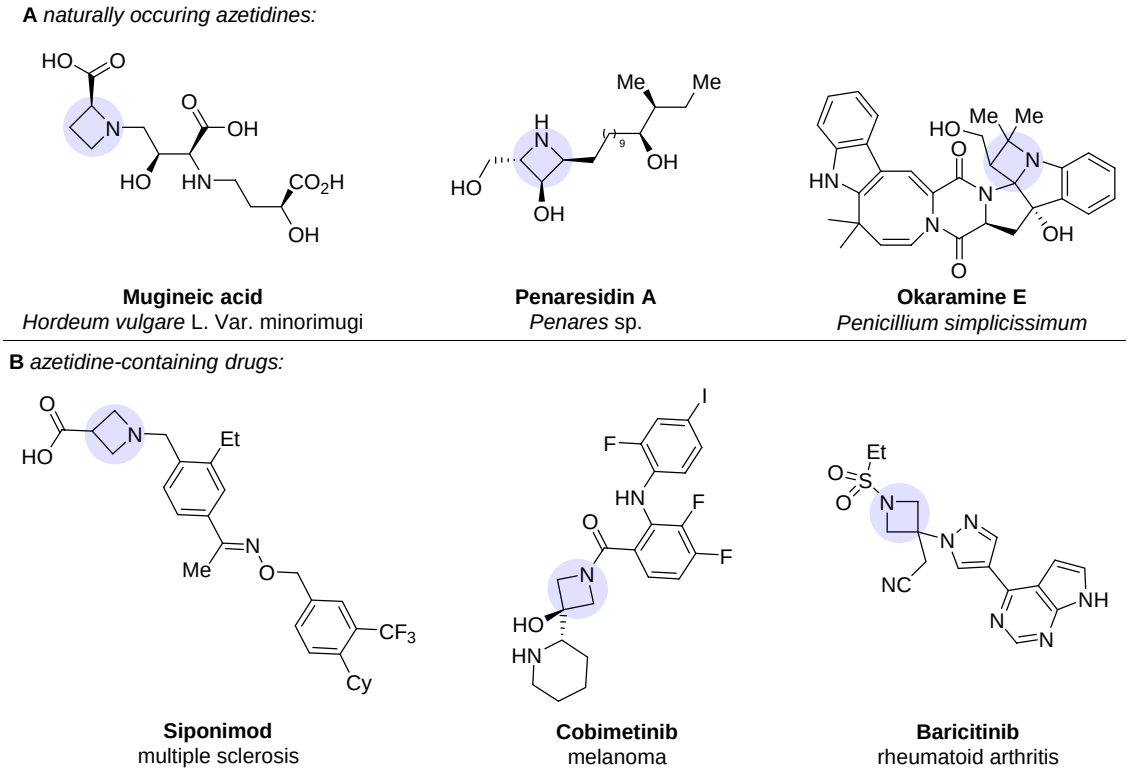
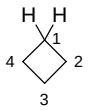


Figure 1-1A Examples of azetidine-containing natural products. **B** Examples of azetidine-containing drugs.

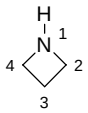
Structurally, azetidines are similar to the carbocyclic cyclobutane sharing similar median bond lengths, angles and puckering angles (**Figure 1-2A and B**). Their small size, coupled with their rigidity and high Fsp^3 character represents an atom-efficient three-dimensional scaffold with defined vectors to present pendant functionality.[6] As a result, incorporation of azetidines into bioactive molecules has been shown to impart myriad desirable properties, including improved stability to oxidative metabolism stemming from the increased strength of the α-C-H bonds by CYP450 enzymes as a result of poorer dative stabilisation of the resulting radical.[7] Replacement of unsaturated ring systems with azetidines leads to increased aqueous solubility due to the loss of aromatic groups, which have been shown to limit aqueous solubility.[8, 9] Finally, replacement of 1,4-substituted piperidines by symmetrically similar 1,3-substituted azetidines has been shown to reduce lipophilicity and improve lipophilic ligand efficiency whilst maintaining potency.[10]

A cyclobutane



Distances / Å	Angles / °
C_1—C_2: 1.51	C-C-C: 88.9
C_2—C_4: 2.16	C-C-C-C dihedral: 15.5

B azetidine



Distances / Å	Angles / °
C_2—C_3: 1.54	C-C-C: 87.1
N_1—C_2: 1.47	N-C-C: 89.1
C_2—C_4: 2.15	C-N-C: 90.3
N_1—C_3: 2.10	N-C-C-C dihedral: 15.3

Figure 1-2A Selected geometric parameters of cyclobutane. **B** Selected geometric parameters of azetidine.

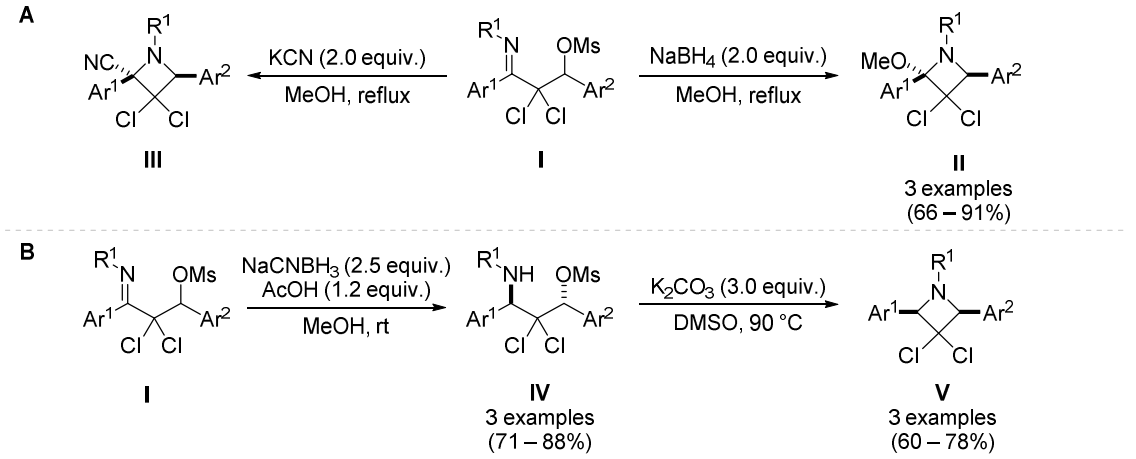
Beyond application to the biological sciences, dendrameric poly(propylenimine), which can be synthesised from ring opening polymerisation of azetidines, has found applications in metal binding, water purification and CO_2 adsorption.[11-13]

1.2 Synthesis of Azetidines

As alluded to in the previous section, the widespread application of azetidines has been constrained by shortcomings in established methods for their synthesis. As opposed to the larger unstrained congener of azetidine, piperidine, methods of synthesising must also factor in the large strain energy associated with azetidine (25.2 kcal mol^{-1} relative to piperidine).[14] There are several strategies for the synthesis of azetidines including: cyclisation of a linear precursor, thermal- or photochemical cycloaddition, ring opening of azabicyclo[1.1.0]butanes and the reduction of *β*-lactams. In this section, representative examples of these methods will be summarised.

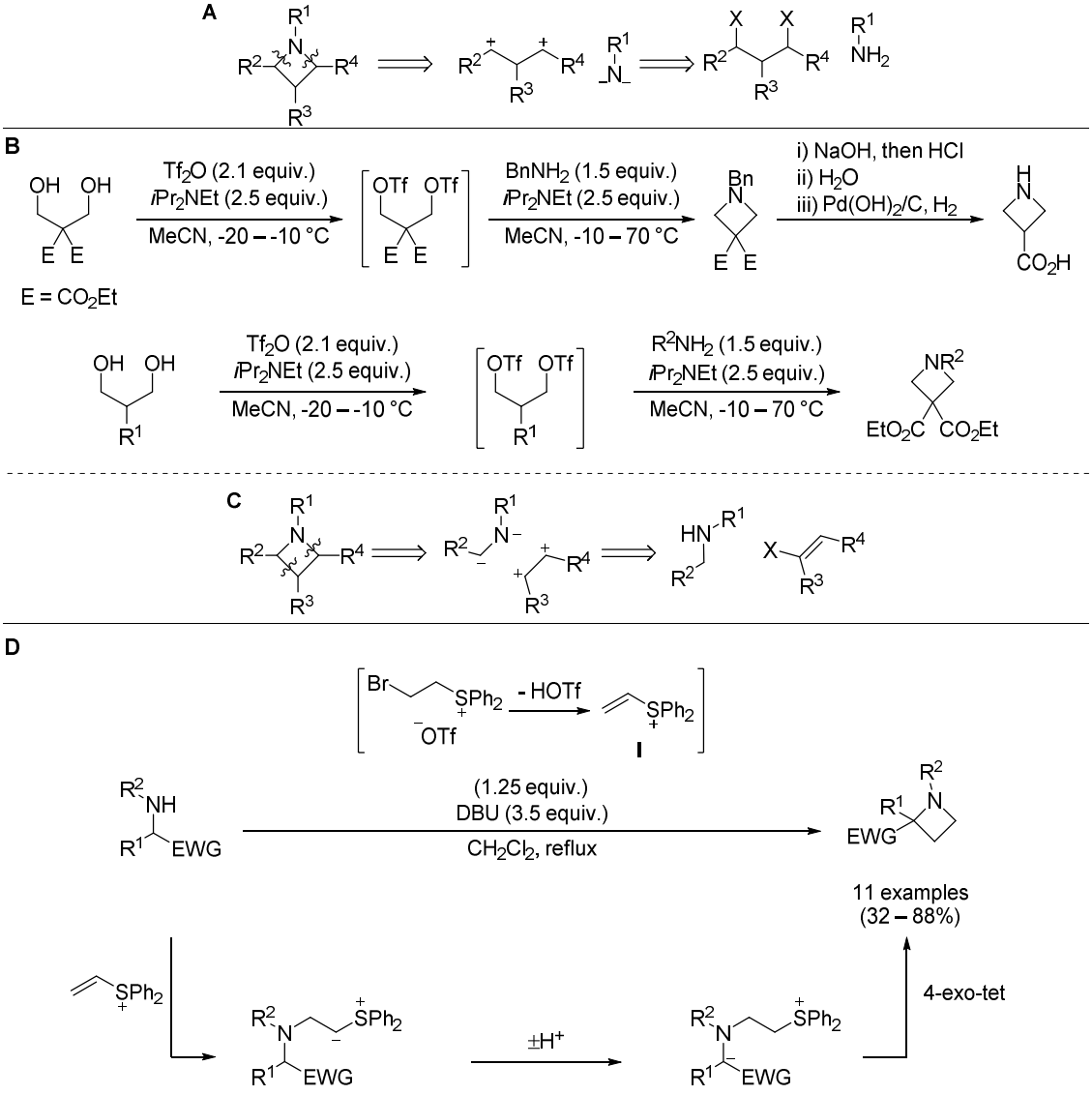
1.2.1 Cyclisation of Linear Precursors

The most common method to synthesise azetidines is the cyclisation of a linear precursor by nucleophilic displacement of a leaving group, most commonly by an amine nucleophile. Due to the high energy conformational alignment required to achieve productive orbital overlap these reactions tend to suffer from competitive elimination of HX.[15] One archetypal example is by De Kimpe where they show that *β*-(mesyloxy) imines **I** upon treatment with methoxide or potassium cyanide can generate *in-situ* the requisite nucleophile to effect the required cyclisation to form azetidine **II** and **III**, respectively (**Scheme 1-1A**). 3-(Mesyloxy) amines **IV** could also be formed by reduction of **I** with $NaCNBH_3$, isolated and subjected to basic nucleophilic substitution conditions to form azetidines **V** (**Scheme 1-1B**). However, in some cases formation of an imidoyl alkyne *via* an elimination pathway was a problematic side reaction which led to purification issues.[16]



Scheme 1-1A Redox neutral cyclisation of dichloro *β*-(mesyloxy) imines. **B** Reductive cyclisation of dichloro *β*-(mesyloxy) imines.

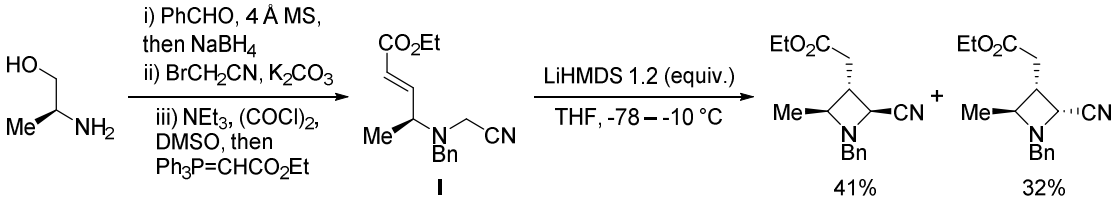
A step efficient method to generate azetidines is to employ a bis electrophile and a doubly nucleophilic *N*-nucleophile. One retrosynthetic strategy is two make C-N disconnections which leads back to a primary amine and a 1,3-bis Csp^3 electrophile (**Scheme 1-2A**). Scientists at Merck's Process Research facility demonstrated that 1,3-bis-triflates generated from the corresponding diol were suitable electrophiles for selective azetidine ring-forming over elimination. In separate reports, they were able to develop a practical route to 3-azetidine carboxylic acid and a general approach to 3-substitued azetidines (**Scheme 1-2B**).[17, 18] An alternative disconnection is to cut the C-C and C-N bonds across the ring to give a C, N-bis nucleophile and C, C bis electrophile (**Scheme 1-2C**). Vinyl sulfonium salts have been shown to behave as excellent bis carbon electrophiles in this transformation. The Aggarwal group demonstrated that *in-situ* generation of vinyl sulfonium **I** could be employed in conjunction with protected amino acids to deliver azetidines (**Scheme 1-2D**).[19] The Ritter group later demonstrated it was possible to perform the same transformation using a bench-stable vinyl sulfonium salt derived from thianthrene instead of generating the electrophile *in-situ*.[20]



Scheme 1-2A Retrosynthetic disconnection of azetidine to bis-nucleophile and bis-electrophile. **B** Merck's 1,3- double triflate electrophile. **C** Alternative disconnection to give bis-nucleophile and bis-electrophile. **D** Aggarwal's vinyl sulfonium electrophile to synthesize azetidines.

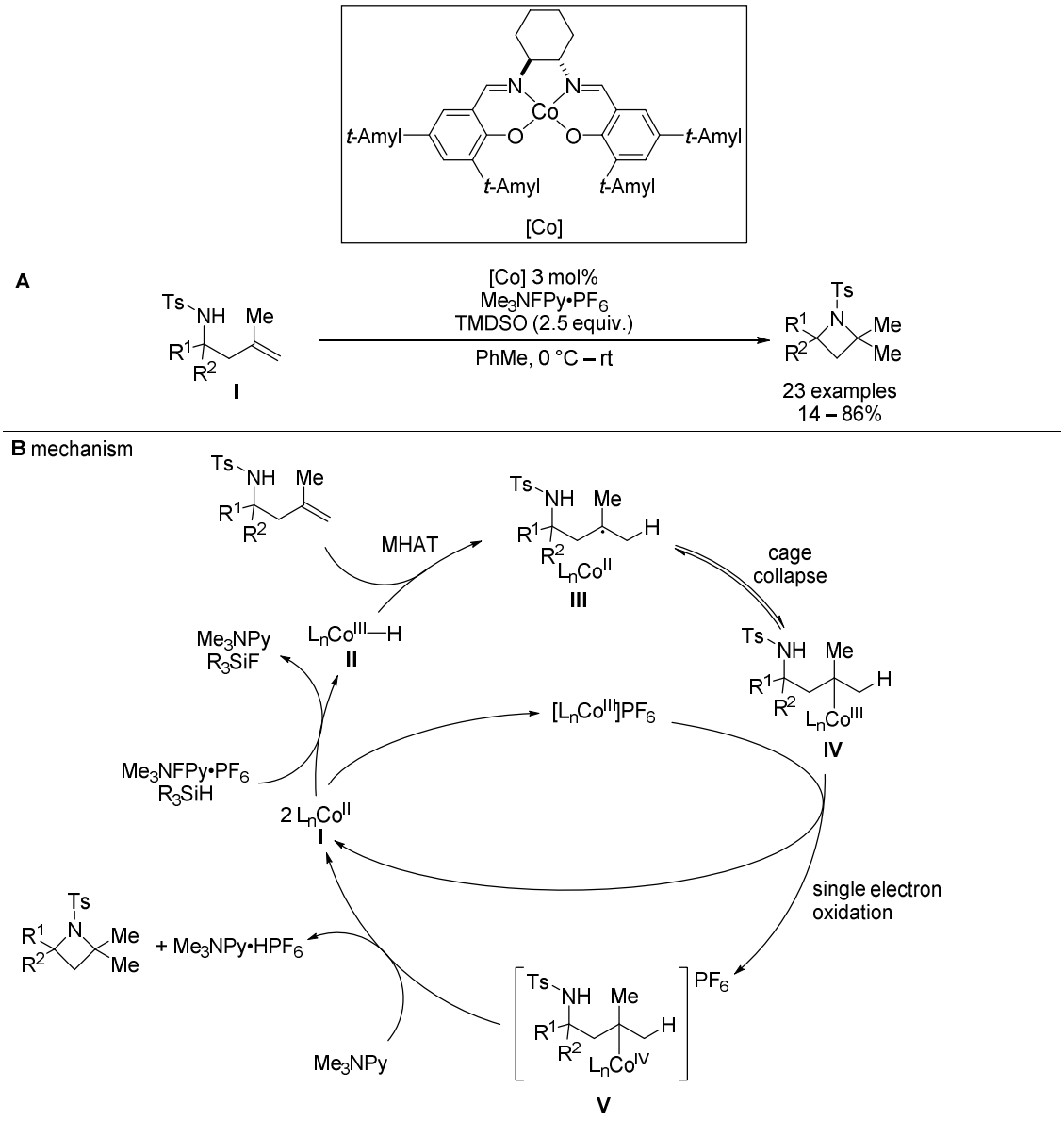
Alternatively, it is possible to synthesize an azetidine by cyclisation of a linear precursor with a tethered carbon nucleophile. Couty used an intramolecular 4-exo-trig conjugate addition of enantiopure α-lithiated nitriles **I** to generate a range of azetidines which upon deprotection gave conformationally constrained glutamic acid derivatives (**Scheme 1-3**). The diastereoselectivity observed was determined to be as a result of thermodynamic

control as subjecting either diastereomer of the product to the reaction conditions delivered the same diastereomeric ratio as the parent reaction.[21, 22]



Scheme 1-3 Intramolecular conjugate addition to form azetidines.

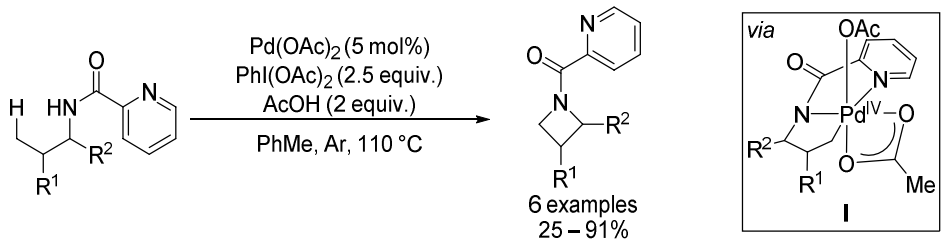
Recently, advances in transition metal catalysis have enabled its application to azetidine synthesis. Shigehisa demonstrated that it is possible to use Co-catalysed metal hydride atom transfer/radical-polar crossover to synthesise azetidines from homoallylic sulfonamides **I** (**Scheme 1-4**). The mechanism of this reaction starts with the generation of a Co(III)-H species **II** from Co(II) **I** by an oxidant and silyl hydride—in this case, *N*-fluoro-2,4,6-collidinium hexafluorophosphate and 1,1,3,3-tetramethyldisiloxane. This reacts with the alkene to generate a tertiary carbon-centred radical and a Co(II) radical pair **III**. This radical pair can then undergo collapse to form a Co(III) organometallic species **IV**, which undergoes oxidation to Co(IV) to form a cationic alkyl cobalt complex **V**, representing a radical-polar crossover. This complex can ultimately be displaced by the pendant nucleophile to deliver the azetidine and regenerate the Co(II) **I** catalyst (**Scheme 1-4B**).



Scheme 1-4A Cobalt-hydride catalysed cyclisation of homoallylic sulfonamides to give azetidine. **B** Mechanism of cobalt-hydride catalysed cyclisation.

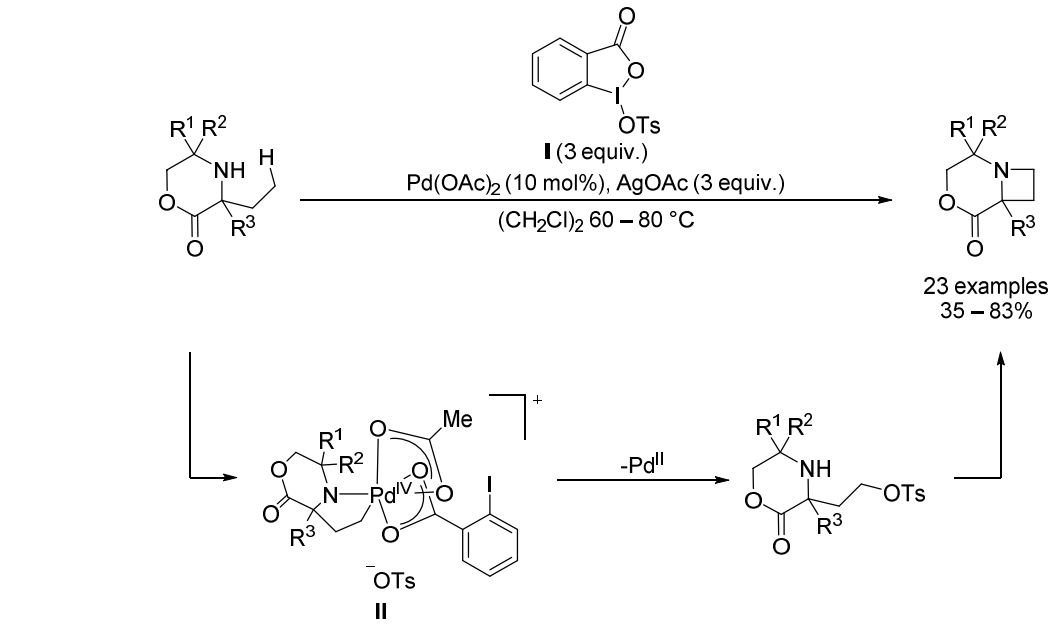
It has also been demonstrated that it is possible to leverage Pd-catalysed *γ*- C-H-amination of alkyl amines to deliver azetidines The first application of *γ*- C-H-amination to an azetidine was reported by the Chen lab using picolinamide protected amines which could undergo C-H activation at the *γ*-position and selectively form azetidines under Pd(II/IV) catalysis (**Scheme 1-5**).[23] Mechanistically, this proceeds by first chelation of Pd(II) to the substrate, followed by C-H activation at Pd(II). Oxidation of this Pd(II) complex to

Pd(IV) intermediate **I** then promotes direct Csp^3-N reductive elimination, delivering the azetidine product.



Scheme 1-5 Chen's Pd-catalysed cyclisation of picolinamides to give azetidines.

Later, Gaunt demonstrated that through careful, mechanistically informed catalyst design and the selection of an appropriate hypervalent iodine oxidant **I**, it is possible to employ simple amines as substrates for C-H activation, without the need for a directing group, to synthesise a range of azetidines in excellent yields across a broad range of substrates (**Scheme 1-6**). Mechanistically, following coordination, C-H activation, and oxidation, a Pd(IV) complex **II** forms. To generate the azetidine, an oxidant bearing a tosylate was crucial. Instead of an inner-sphere Pd(IV)-mediated Csp^3-N reductive elimination, the authors proposed that the tosylate anion is responsible for mediating an outer-sphere reductive elimination, generating a γ-tosylate, which subsequently cyclises *via* an intramolecular S_N2 process.[24]



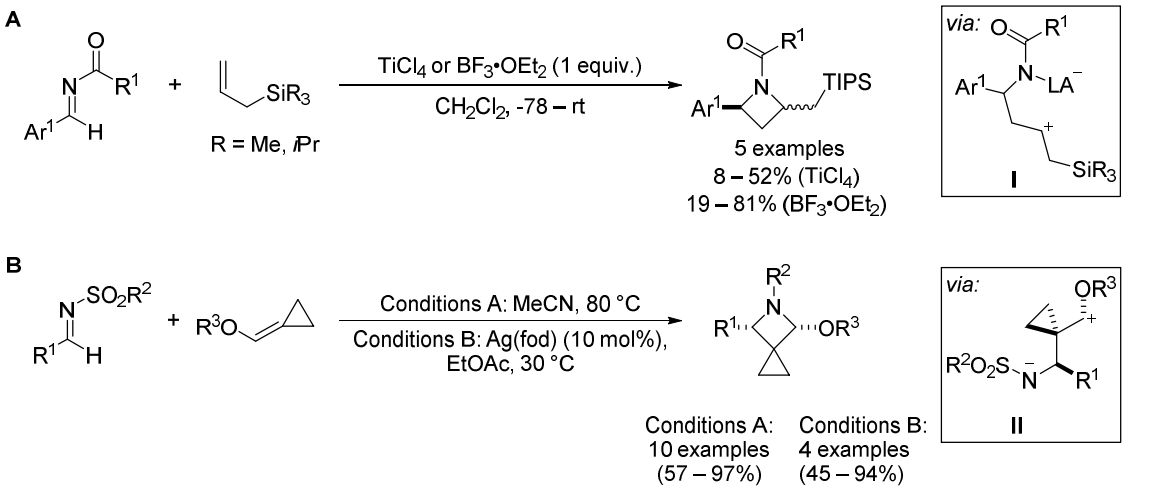
Scheme 1-6 Gaunt's Pd-catalysed C-H activation, cyclisation of amines to form azetidines.

1.2.2 Thermal [2+2]-Cycloaddition

The [2+2]-cycloaddition between an imine and a C-C double bond represents a direct and atom-economical route to an azetidine. Typically, this class of reaction is often mediated by light to enable access to electronically excited states of either component to overcome limitations imposed by orbital symmetry rules in the ground state.[25] Photochemical, transformations will be discussed in detail in a later section. Thermally mediated [2+2]-cycloadditions between alkenes and imines have been reported to occur despite the constraints of orbital symmetry rules. This is made possible by stepwise mechanisms, which allow the formation of ionic intermediates, bypassing the typical symmetry restrictions. Some historical examples rely on unusual reaction conditions such as elevated pressures, which promote the polar [2+2] cycloaddition as a result of their large negative activation volumes, or extremely protracted reaction times (50 days).[26, 27]

Lewis acids have also been shown to be capable of promoting cycloadditions, Uyehara showed that it is possible to generate azetidines derived from aromatic imines and allyl

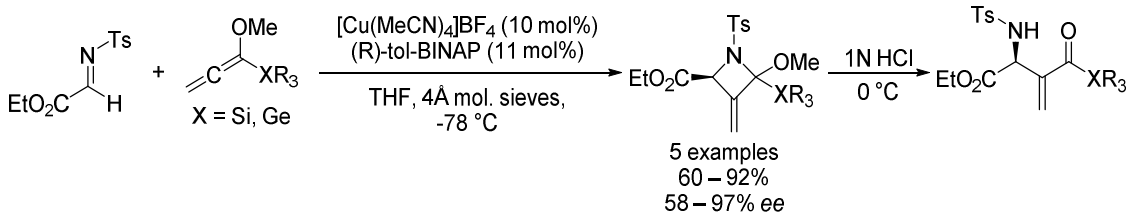
silanes mediated by either $TiCl_4$ or $BF_3{\cdot}OEt_2$ as Lewis acids (**Scheme 1-7A**).[28] In this case, symmetry orbital rules are circumvented by the generation of an zwitterionic intermediate **I** following the addition of allyl silane into the imine, as a result of stabilisation of the carbocation by the *β*-silicon. Subsequently, Nakamura demonstrated that (alkoxymethylene)cyclopropanes could react with imines to deliver azetidines thermally upon heating to 80 °C, or at 30 °C upon addition of a silver Lewis acid catalyst (**Scheme 1-7B**). The authors propose that the stabilisation of the adjacent carbocation by the cyclopropane ring in the zwitterionic intermediate **II** is critical for reactivity as non-cyclopropyl alkenes do not perform this transformation.[28]



Scheme 1-7A Lewis acid mediated formal [2+2]-cyclisation between imine and allyl silane. **B** formal [2+2]-cycloaddition between sulfonyl aldimines and alkoxymethylene cyclopropanes.

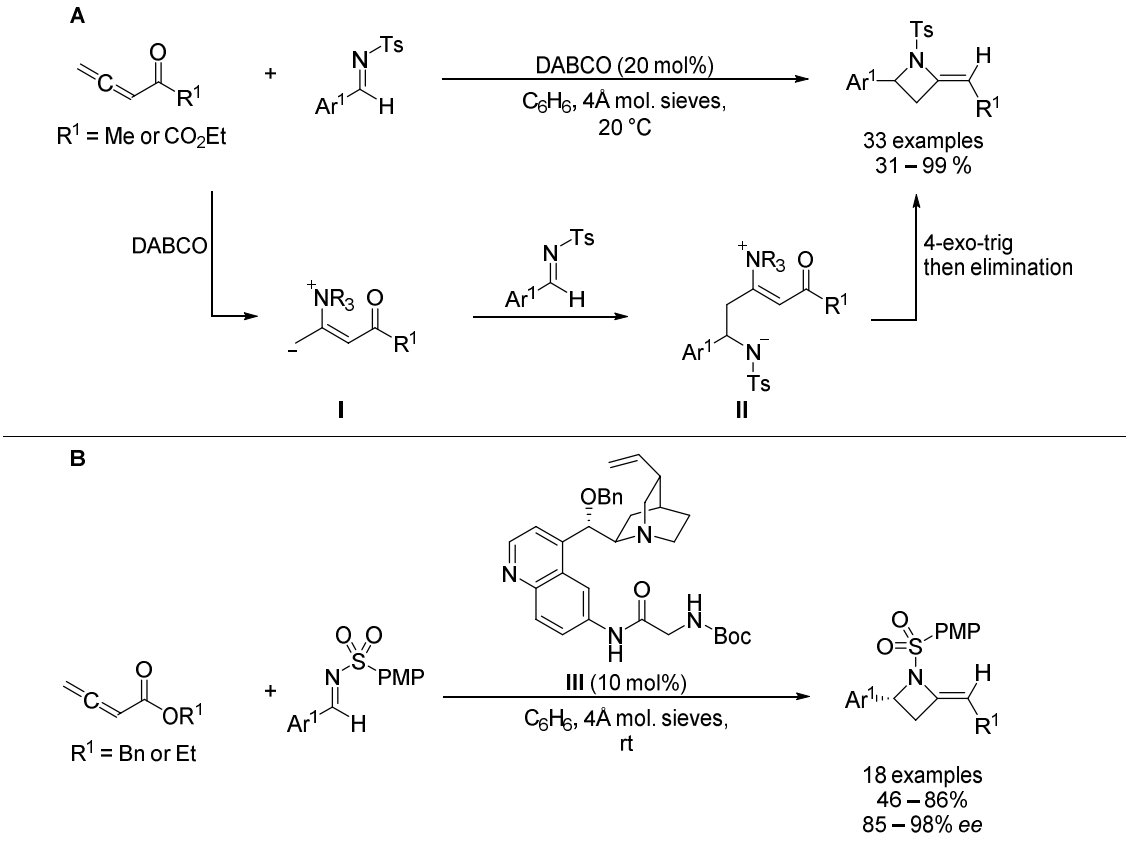
Alternatively, allenes can be employed as an alkene equivalent in the reaction, and the orthogonal π system enables orbital overlap for cycloaddition.[29] Direct thermal cycloaddition of electron-rich allenes and electron-deficient imines can deliver exocyclic alkenyl azetidines, but this was unselective and low yielding with the main product being an acyclic alkyne.[30] However, employing a Lewis acid catalyst enables the reaction between electron-rich allenes with electron-deficient imines to proceed in high yields and

with high stereoselectivity. Moreover, Akiyama showed that if a chiral ligand is employed, highly enantioenriched methylene azetidines can be formed (**Scheme 1-8**). Treating these allenes with 1N HCl gives the corresponding acyl silanes.[31]



Scheme 1-8 Lewis-acid mediated enantioselective [2+2]-cycloaddition between nucleophilic allenes and an electrophilic imine.

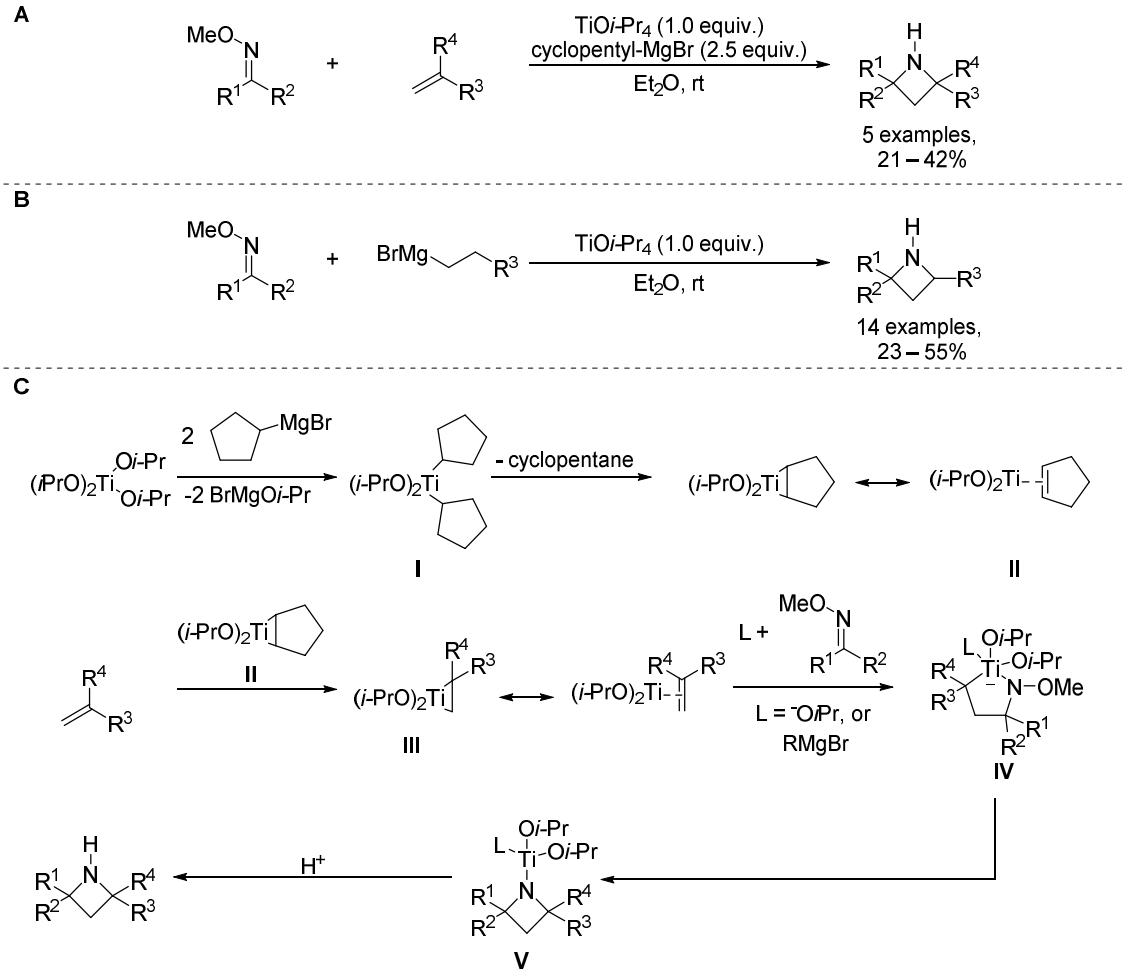
Alternatively, if an electron-deficient allene is employed, it is possible to use a tertiary alkyl amine as a nucleophilic catalyst to react with imines and form azetidines in a mechanistically similar manner to the Morita-Baylis-Hillman reaction (**Scheme 1-9A**). Here zwitterionic intermediate **I** generated by addition of DABCO into the allene can be intercepted by the imine to form intermediate **II**, which subsequently cyclises to deliver the azetidine product. The choice of base employed is crucial in determining the regioselectivity; DABCO selectively gave the methylene azetidine whereas DMAP gives dihydropyridines derived from addition of the allene to two equivalents of imine.[32] Masson and Zhu showed that employing a Cinchona alkaloid **III** as chiral tertiary amine catalyst can be rendered enantioselective to generate a range of methylene azetidines in high *ee*'s (**Scheme 1-9B**).[33]



Scheme 1-9A DABCO catalysed formal [2+2] cycloaddition between electron deficient allenes and imines. **B** A catalytic enantioselective formal [2+2]-cycloaddition employing a cinchona alkaloid catalyst.

Kürti demonstrated that when ketoximines are employed as electrophiles in a Kulinkovich reaction an azetidine can be directly obtained, using both terminal alkenes and cyclopropyl magnesium bromide as a reductant, representing a formal [2+2] cycloaddition (**Scheme 1-10A**). The Grignard reagent can be used as both the coupling partner and reductant, and the authors demonstrated a broad scope of this reaction in (**Scheme 1-10B**). The mechanism for the formal [2+2] cycloaddition begins with a double ligand exchange of alkoxide with cyclopentylmagnesium bromide to form organotitanium complex **I**, which subsequently undergoes β-hydride elimination to deliver the cyclopentene-Ti(II) intermediate **II** (**Scheme 1-10C**). Exchange of the cyclopentene with the terminal alkene generates the active titanocyclopropane **III**, which adds into the oxime to form a five-membered titanocycle **IV**. This intermediate collapses

with the loss of methoxide to give titanium amide **V**, which, upon aqueous work-up, yields the azetidine.[34]

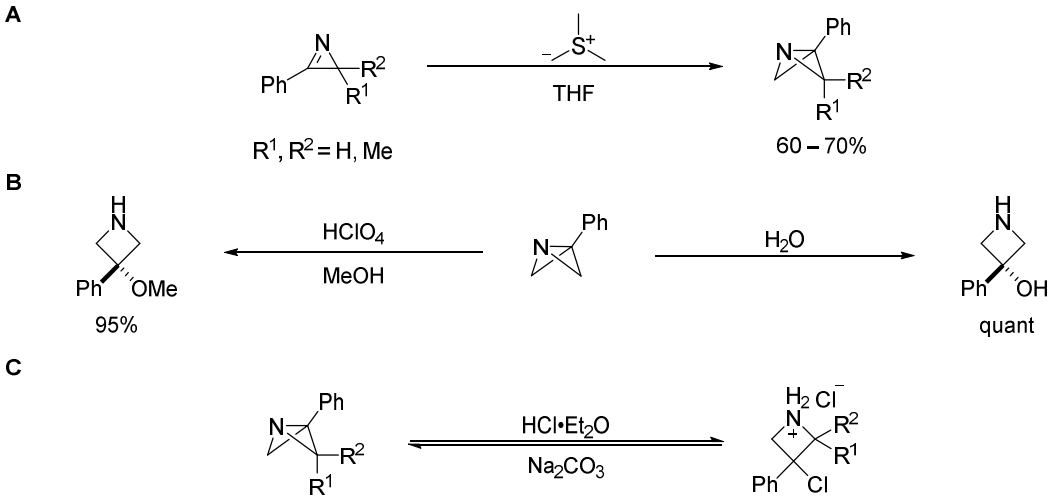


Scheme 1-10A Kulinkovich reaction between ketoximes and alkene with cyclopentyl magnesium bromide as reductant. **B** Kulinkovich reaction between ketoximines and Grignard reagent. **C** Mechanism of Kulinkovich-type reaction between alkene and ketoximine.

1.2.3 Ring Opening of aza-BCBs

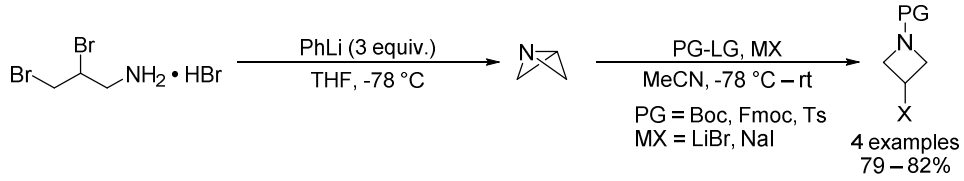
The 1-azabicyclobutane group was first reported in 1967 by Hortmann which was synthesised from 2-phenylazirine and dimethylsulfonium methylide (**Scheme 1-11A**).[35] In follow up publications the authors detail the ring-opening reactivity of the bridgehead bond which delivered azetidines either through the proton-initiated addition of water or methanol (**Scheme 1-11B**). Alternatively, treatment of azabicyclobutane with dry HCl

afforded 3-chlorophenylazetidine hydrochlorides. Attempts to liberate the free amines led to reformation of the parent azabicyclobutane (**Scheme 1-11C**).[36]



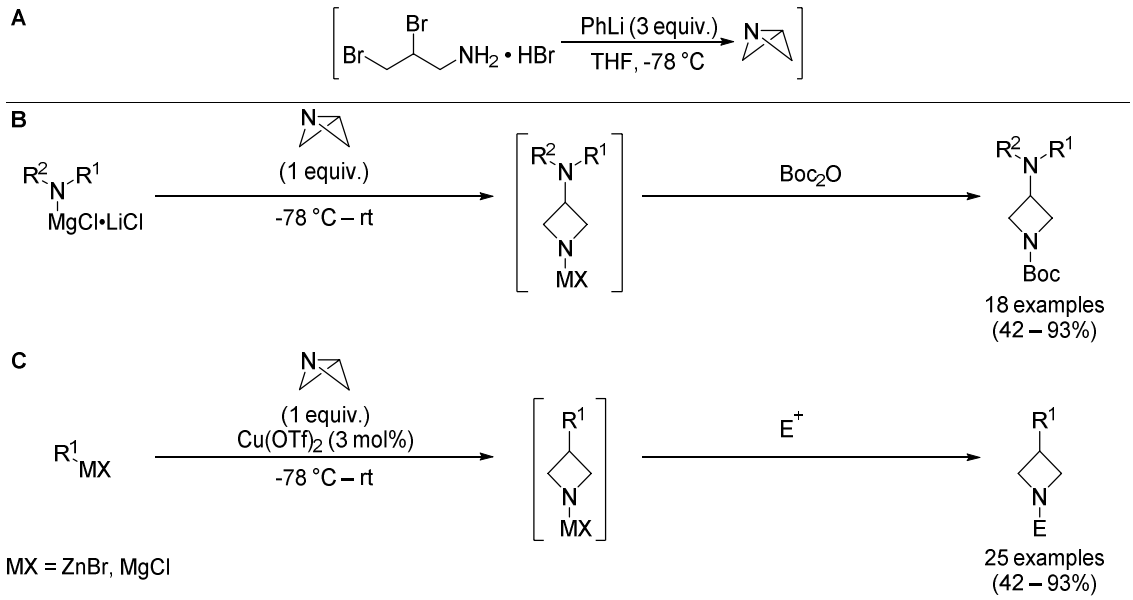
Scheme 1-11A Synthesis of substituted aza-bicyclobutane. **B** Ring opening of aza-BCB by MeOH and water. **C** Ring opening of aza-BCB by dry HCl and ring closing of 3-chloro azetidinium hydrochloride upon treatment with base.

Since this initial report, there have been numerous examples of the synthesis of 3-substituted azetidines from the reaction of 1-azabicyclobutanes and an appropriate electrophile such as BzCl or TsCl.[37] Typically, these proceed first by nucleophilic attack of the nitrogen atom which displaces nucleofuge X. This forms a more electrophilic cationic species which is intercepted by X to open the cationic intermediate to give azetidine product.[38] A recent example of this is Lopchuk's procedure which leverages this reaction for the gram-scale preparation of protected 3-haloazetidines (**Scheme 1-12**).[39]



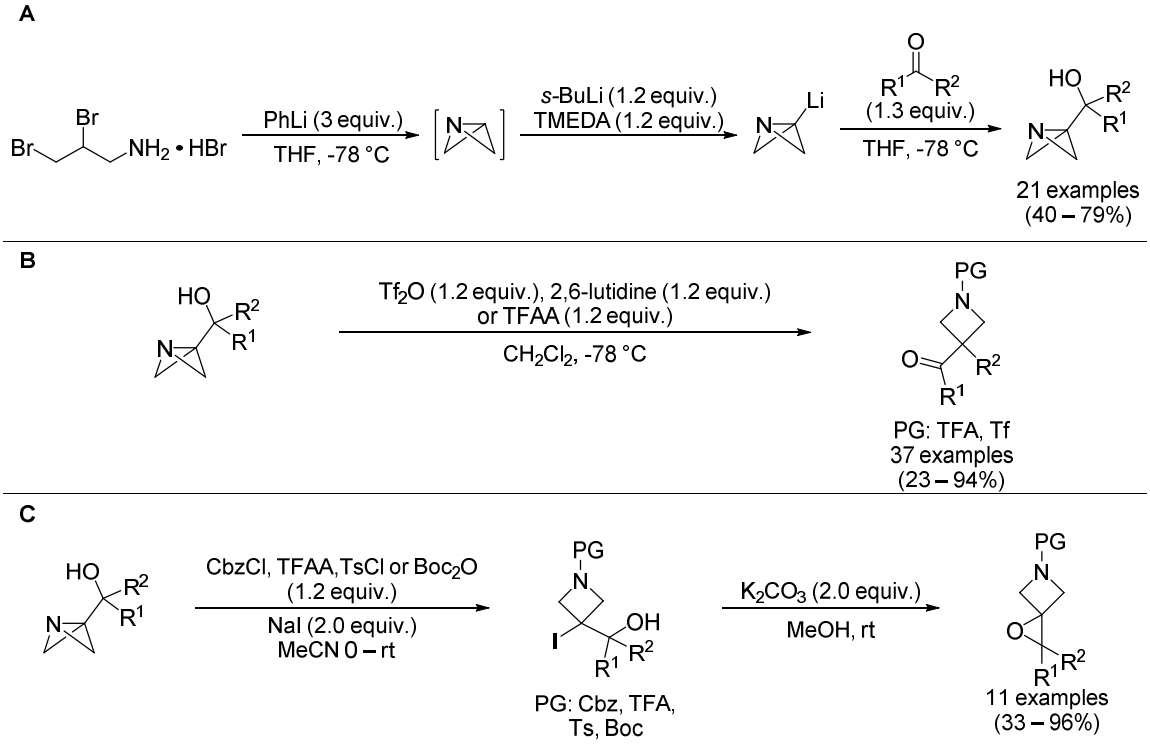
Scheme 1-12 Gram-scale synthesis of protected 3-halo azetidines.

Nucleophilic addition across 1-azabicyclobutanes can also be achieved without the use of an electrophilic activator. A recent example includes Baran's influential strain-release amination report where they were able synthesise a broad range of 3-amino azetidines by addition of turbo-Hauser amides across 1-azabicyclobutane (**Scheme 1-13B**).[40] The scope of nucleophiles was expanded to include carbon nucleophiles when Gianatassio demonstrated it was possible to add organo- magnesium and zinc reagents, in the presence of 3 mol% copper (II) triflate, to the 3-position to 1-azabicyclobutanes delivering 3-substituted azetidines (**Scheme 1-13C**).[41]



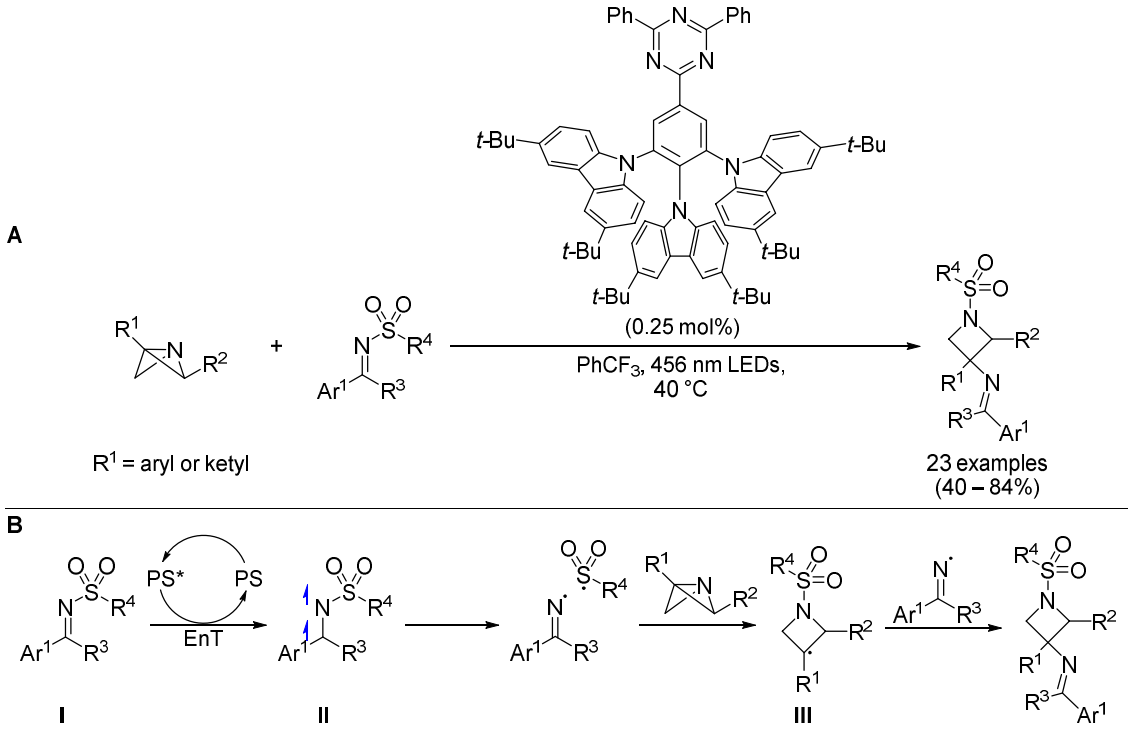
Scheme 1-13A Synthesis of aza-bicyclobutane. **B** Baran's strain-release amination of aza-BCB. **C** Giantassio's addition of organometallics to aza-BCB.

Recently, the Aggarwal group have developed the use of lithiated 1-azabicyclobutanes as versatile synthetic intermediates, allowing rapid access to densely functionalised 1-azabicyclobutanes which can further be elaborated to azetidine products.[42-44] One example is the reaction of -azabicyclobutyl lithiums with aldehydes and ketones which forms 1-azabicyclobutyl carbinols that can undergo divergent reactivity (**Scheme 1-14A**). For example, reaction with a strong electrophile such as Tf_2O can mediate a semi-pinacol rearrangement to deliver keto 1,3,3-substituted azetidines (**Scheme 1-14B**). Treatment with a less electron withdrawing activating group, such as benzyl chloroformate, and the addition of sodium iodide leads instead to an iodohydrin intermediate, which subsequently undergoes ring closure to form spiroepoxy azetidines upon treatment with base (**Scheme 1-14C**).[45]



Scheme 1-14A One-pot synthesis 1-azabicyclobutyl carbinols. **B** Semi-pinacol rearrangement of 1-azabicyclobutyl carbinols to give keto-azetidine. **C** Spiroepoxyazetidine synthesis *via* formation of iodohydrin intermediate.

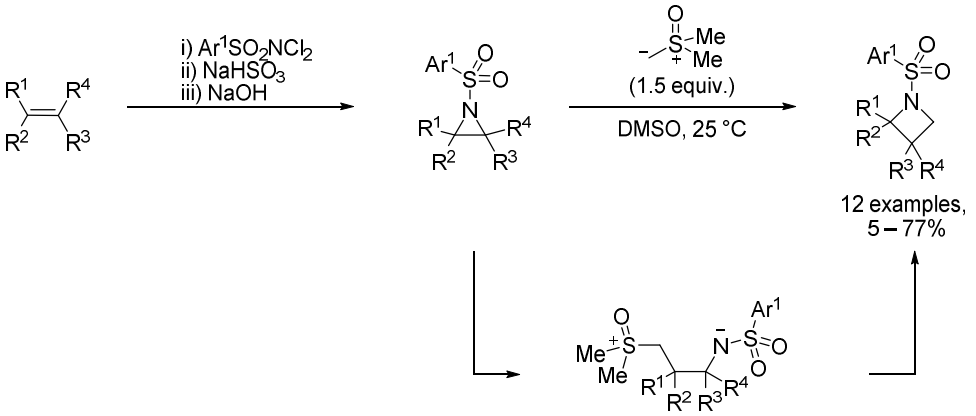
As opposed to the plethora of radical strain release methods that exist for bicyclobutane, there is currently only one report for radical strain release for their aza- analogue.[46] Dell'Amico and co-workers developed a method to synthesise 3-amino sulfonyl azetidines from 3-phenyl and 3-keto aza-bicyclobutanes using energy transfer catalysis and *N*-sulfonyl imines (**Scheme 1-15A**). Sensitisation of the *N*-sulfonyl imine **I** to the triplet state **II** by the photocatalyst precedes fragmentation of N-S bond simultaneously generating a sulfonyl radical and an iminyl radical. The sulfonyl radical adds at nitrogen of the aza-BCB to give a carbon-centred radical **III** which is intercepted by the iminyl radical to give the product (**Scheme 1-15B**). Precisely tuning the triplet energy sensitization rate, through modulation of the singlet-triplet energy gap of the photocatalyst, was critical to the success of the reaction as this suppressed the competitive dimerization of the iminyl radical. The authors were able to generalise the method to a three component coupling to accommodate other functionalities at the 3-position of the azetidines ring by intercepting the transient carbon-centred radical with different somophiles.[47]



Scheme 1-15A Energy-transfer catalysed sulfonyl radical addition into aza-BCB. **B** Proposed mechanism of the transformation.

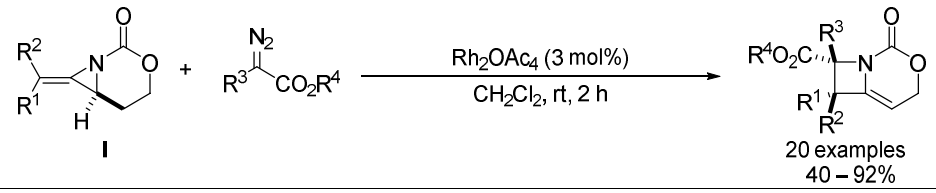
1.2.4 Ring Expansions and Contractions

An attractive strategy for the synthesis of azetidines is the one-carbon insertion into aziridines, which are much more synthetically tractable because they can be readily accessed through the insertion of carbenes or nitrenes into imines and alkenes, respectively.[48] One early report showed that *N*-sulfonyl aziridines could be opened by dimethylsulfoxonium methylide followed by 4-exo-tet ring closure with extrusion of DMSO to give the desired azetidine (**Scheme 1-16**). Mechanistically, as this transformation proceeds *via* two sequential S_N2 reactions this reaction is stereospecific, so cis-aziridines yield trans-azetidines and vice versa.[49]



Scheme 1-16 One-carbon ring expansion of aziridines to azetidines by sulfoxonium ylide.

Schomaker showed that ylides of methyleneaziridines (**I**), generated from donor-acceptor diazoacetates under dirhordium catalysis, can undergo ring expansion to deliver endocyclic, bicyclic methylene azetidines in high yields and stereoselectivities (**Scheme 1-17**). When enantioenriched material is used the reaction shows excellent chirality transfer from the aziridine stereocentre.[50] In a later study, DFT modelling showed that the reaction may proceed either by radical or ionic intermediates.[51]

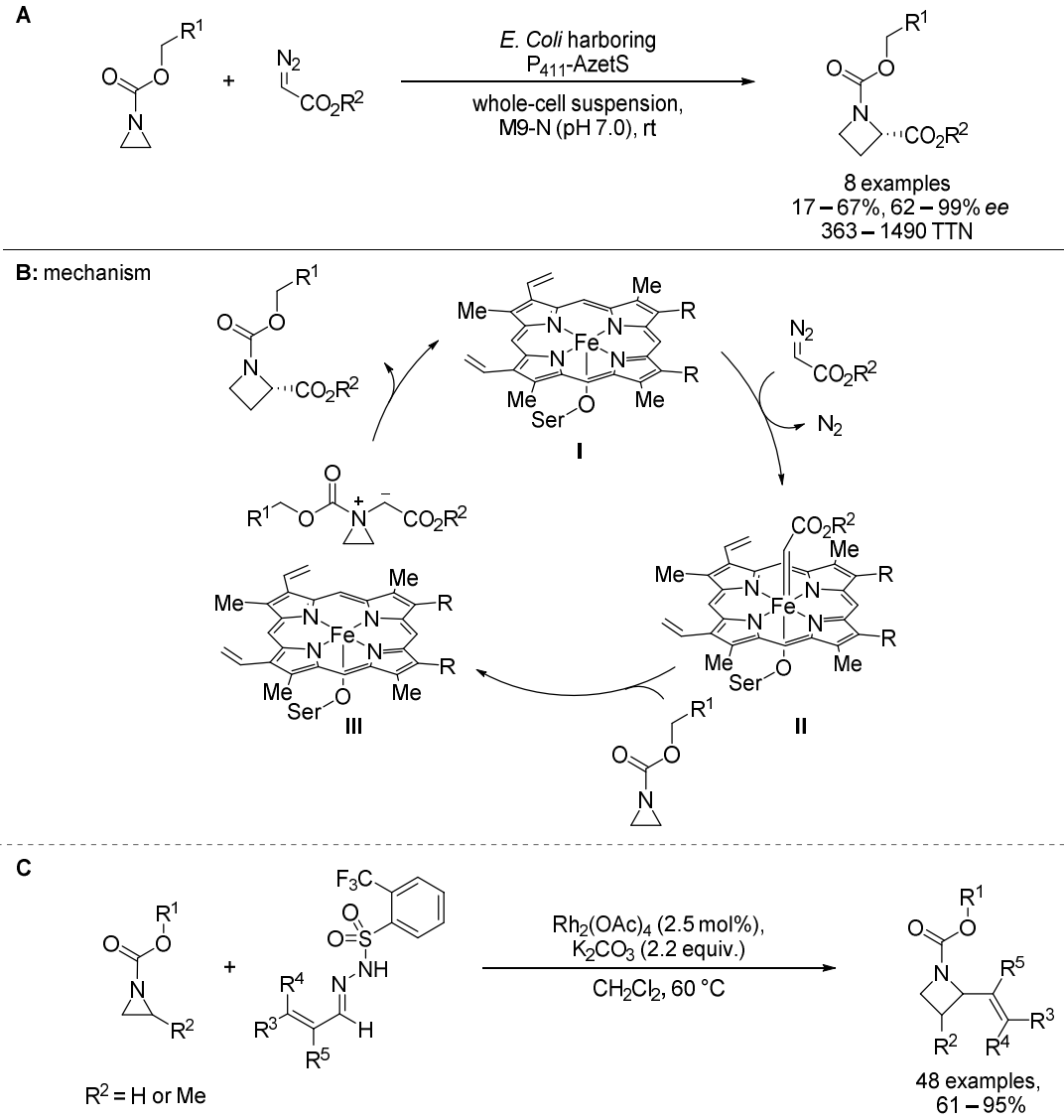


Scheme 1-17 Rhodium catalysed ring expansion of methyleneaziridines.

With regards to monocyclic azetidines, the Arnold group demonstrated that one of their carbene transfer haemoprotein enzymes, derived from cytochrome P450BM3, could be evolved to perform a one-carbon ring expansion of carbamate-protected aziridines. This transformation was achieved using a whole-cell suspension of *E. coli* bacteria, which harboured their evolved P411-AzetS enzyme (**Scheme 1-18A**). They were able to demonstrate a modest scope modifying the benzylic alcohol of the carbamate and the

ester group of the diazo compound, whilst generally maintaining excellent enantioselectivities, high TTNs and good yields. Mechanistically this reaction proceeds by initial formation of the iron carbene **II** from the diazo ester and the iron heme complex **I** in the active site which is then intercepted by the nucleophilic aziridine to generate an aziridine ylide **III**. This ylide then selectively undergoes a [1,2]-Stevens rearrangement mediated by the active site of the enzyme, which prevents competitive cheletropic extrusion of ethylene, to generate the azetidine (**Scheme 1-18B**).[52, 53]

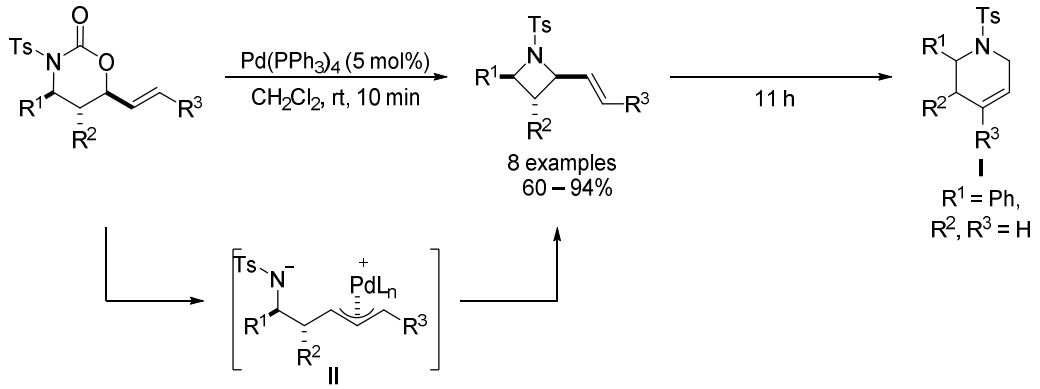
Using the same [1,2]-Stevens rearrangement of an aziridine ylide strategy the Bi group showed that it is possible to use a wide range of vinyl-N-triftosylhydrazones as a carbene precursor and $Rh_2(OAc)_4$ as a catalyst to ring-expand aziridines to form vinyl-substituted azetidines with broad scope with respect to the nitrene (**Scheme 1-18C**).[54]



Scheme 1-18A Iron carbene transfer haemoprotein enzyme mediated ring expansion of aziridine to azetidine. **B** Mechanism of protein mediated aziridine ring expansion. **C** Rhodium catalysed ring expansion of aziridines with allyl carbenes.

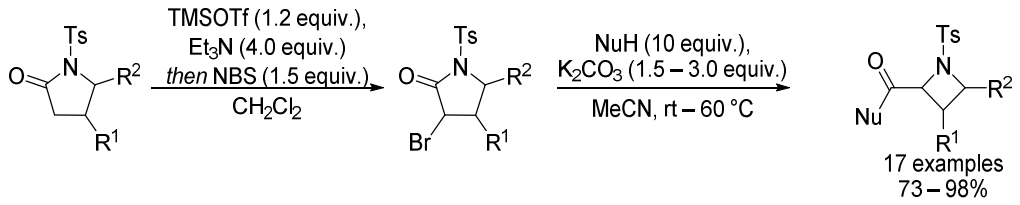
The ring contraction of larger, more synthetically accessible N-heterocycles into azetidines offers a viable strategy for azetidine synthesis, owing to the lower strain energy of larger rings. Building upon the investigations of Pd-catalysed reactions of allyl carbamates by Tamaru,[55-57] Tunge showed that it possible to perform a Tsuji-Trost decarboxylative diastereoselective ring contraction of 6-vinyl oxazinanones to form azetidines as the kinetic product (**Scheme 1-19**). Leaving the reaction longer resulted in

tetrahydropyridine **I** as the thermodynamic product. Subjecting both diastereomers of the starting material to the reaction led to the same diastereomeric ratio showing that epimerisation through a π-σ-π mechanism is faster than cyclisation. Based on the reaction of a substrate which cannot epimerise through a π-σ-π mechanism, the authors proposed that the reaction proceeds *via* an ionised π-allyl complex **II** and backside of the amide nucleophile resulting in a stereoretentive process.



Scheme 1-19 Decarboxylative Tsuji-Trost ring contraction of 6-vinyl oxazinanones to kinetic azetidine product.

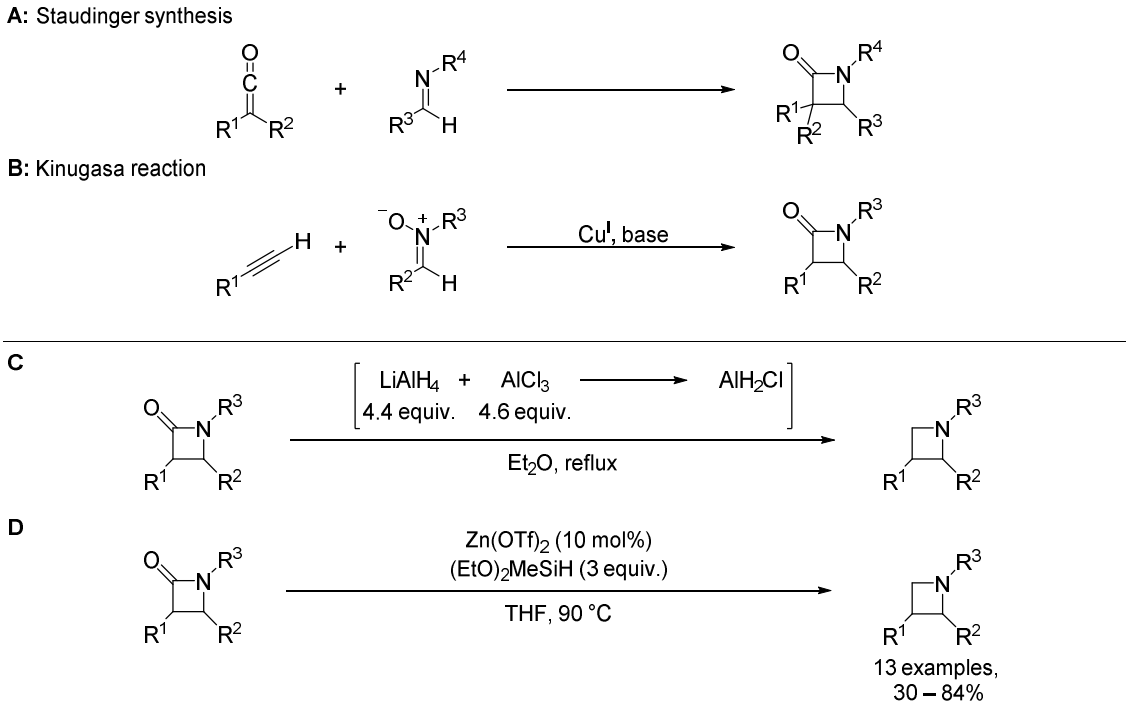
In 2014, Pale and Blanc reported that α-bromo *N*-sulfonyl pyrrolidinones, which can be prepared in three steps from 2-pyrrolidinones, undergo nucleophilic addition followed by ring contraction to deliver α-carbonyl sulfonyl azetidines when combined with alcohols, anilines, and phenols.[58] Simply treating the substrate with ten equivalents of nucleophile and potassium carbonate results in nucleophilic attack and ring opening of the amide to give a linear intermediate which then undergoes a 4-exo-tet cyclisation to yield the azetidine.[58]



Scheme 1-20 Ring contraction of *α*-bromo-2-pyrrolidinones to form α-amino carbonyl azetidines.

1.2.5 Reduction of *β*-Lactams

β-lactams provide an excellent starting point for the synthesis of azetidines as they can quickly be synthesised through the Staudinger reaction between imines and ketenes, or bythe Kinugasa reaction between nitrones and copper acetylides (**Scheme 1-21A and B**).[59, 60] The choice reductant for reducing *β*-lactams to azetidines is a mixture of $LiAlH_4$ and $AlCl_3$; mechanistically this generates mono- and di- chloroalanes ($AlClH_2$ and $AlCl_2H$) *in-situ* which affect the selective reduction without forming *γ*-amino alcohols.[61, 62] However, these reaction conditions are not tolerant of a range of electrophiles including esters, nitriles and azides (**Scheme 1-21C**). In order to ameliorate this issue Alcaide and Almendros developed more selective conditions using hydrosilanes coupled with $Zn(OTf)_2$ to selectively reduce *β*-lactams to azetidines in the presence of esters and nitriles without erosion of stereochemistry of the azetidine (**Scheme 1-21D**).[61]



Scheme 1-21A Staudinger synthesis of *β*-lactams between ketenes and imines. **B** Kinugasa reaction between nitrones and alkynes mediated by copper. **C** Chloroalane reduction of *β*-lactams. **D** Lewis acid enabled silane reduction of *β*-lactams.

1.3 Principles of Photochemistry

The first step in a photochemical process is photoexcitation where a substrate is promoted to a higher energy electronic state. This process is governed by two laws: the Grotthuss-Draper law, and the Stark-Einstein law. The first law of photochemistry, the Grotthuss-Draper law, states that in order for a photochemical reaction to take place, a molecule must first absorb light. The second law of photochemistry, the Stark-Einstein law, states that for each photon of light absorbed by a chemical system only one molecule is activated for a photochemical transformation. The efficiency at which a photochemical process occurs is given by the quantum yield (φ).

Upon absorption of light by a ground-state molecule (S_0), an electron is promoted to a higher-energy molecular orbital, maintaining the same spin, as dictated by spin selection

rules, since a change in spin state is forbidden by the law of conservation of angular momentum. The excited electron may be promoted from the HOMO or from a lower-energy orbital to the LUMO, leading to a range of excited singlet states (S_1, S_2, S_3, etc.). However, rapid internal conversion from $S_n>1$ to the S_1 state means that this is often the only relevant singlet excited state; this is known as Kasha's rule.[63]

From S_1, a molecule may undergo several processes, including radiative decay to the ground state, known as fluorescence. Photoexcited molecules may also undergo non-radiative decay processes, including internal conversion when the spin of the system is conserved, or intersystem crossing to generate a triplet excited state, T_1, where spin is not conserved. Radiative decay of T_1 back to the ground state (S_0), known as phosphorescence, is spin-forbidden and generally quite slow, resulting in T_1 being a long-lived excited state.[64] However, spin selection rules can be relaxed if spin-orbit coupling is induced, either by a change in electronic configuration (also known as El-Sayed's rule) or by the presence of a heavy atom, referred to as the heavy atom effect.[65, 66] Photochemical processes are detailed below in a Jablonski diagram (**Figure 1-3**).

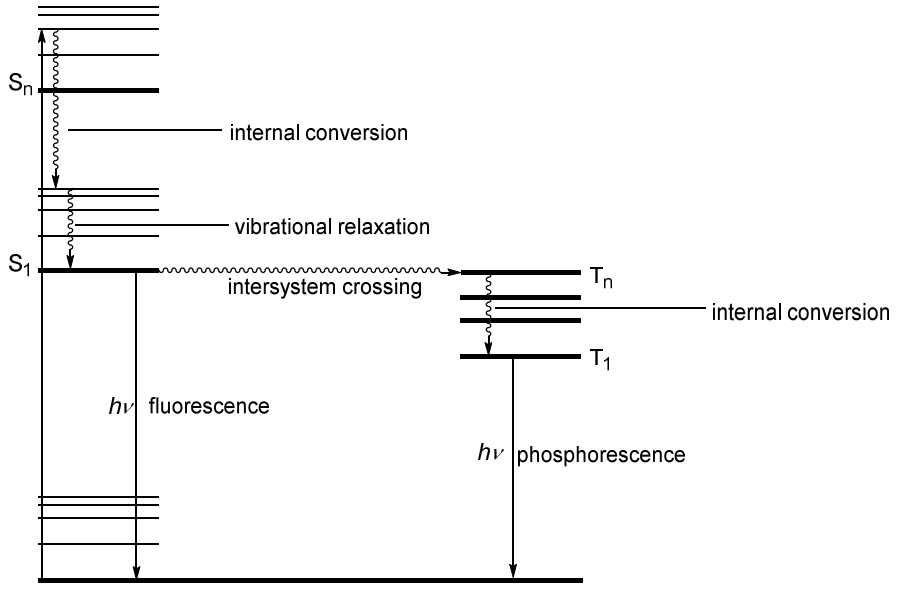


Figure 1-3 Annotated Jablonski diagram, displaying some example photochemical processes.

Non-radiative decay, specifically from T_1 or S_1 to S_0, may either occur intramolecularly or intermolecularly, transferring its energy to another molecule. This collisional process is termed quenching when the focus is on the initially excited species or sensitisation if the newly excited species is the molecule of interest. Intermolecular quenching of T_1 (triplet-triplet energy transfer) has seen widespread uptake in the synthetic organic chemistry in the form of energy transfer catalysis.[67, 68]

1.3.1 Energy Transfer Catalysis

Excited triplet states can enable access to transformations that would otherwise be extremely challenging in the ground state. Their unique reactivity stems from their biradical-like electronic structure and long lifetimes in solution, which result from the spin-forbidden nature of relaxation back to the ground state, enabling efficient intermolecular reactivity. Accessing the T_1 state by photonic excitation followed by intersystem crossing is inefficient for many organic molecules, as they often exhibit weak absorption, low rates of intersystem crossing, and radiative decay, leading to low triplet

quantum yield and inefficient reactions. This, coupled with the fact that most molecules absorb light in the UV region, and the numerous concerns associated with the use of UV light sources, makes such an approach impractical.[67]

Energy transfer catalysis (more specifically triplet-triplet energy transfer catalysis) is intrinsically more efficient as the light-harvesting molecule used is specifically designed to use visible light and to possess a high triplet quantum yield. This is either achieved through spin-orbit coupling resulting from the heavy atom effect in polypyridyl transition metal complexes or a change in electronic configuration in carbonyl compounds. This energy can then be transferred intermolecularly to the desired substrate to access the T_1 state without the absorption-relaxation-ISC manifold (**Figure 1-4**).[67]

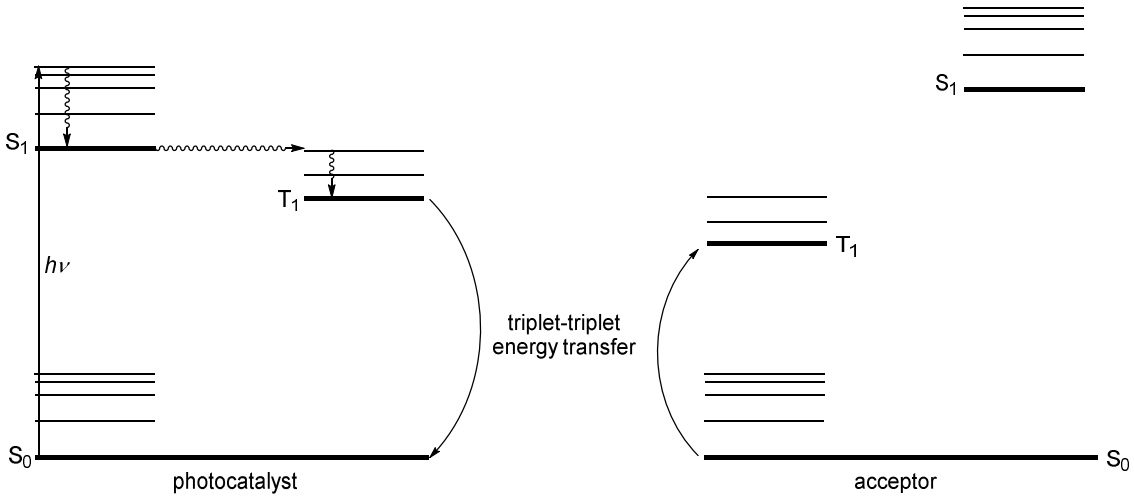


Figure 1-4 Jablonski diagram showing triplet-triplet energy transfer between a photocatalyst an acceptor molecule.

The mechanism operative for triplet energy transfer is most likely a Dexter mechanism, which involves the simultaneous exchange of electrons from the HSOMO of the excited state donor to the LUMO of the acceptor and the from the HOMO of the acceptor to the LSOMO of the donor (**Figure 1-5**). As a result, this electron exchange mechanism

depends on the orbital overlap between the excited state donor and acceptor and is very sensitive to distance, with the efficiency decreasing exponentially as distance increases. Thus, the formation of an in-solvent encounter complex is required, and these reactions are diffusion-limited.[67, 68]

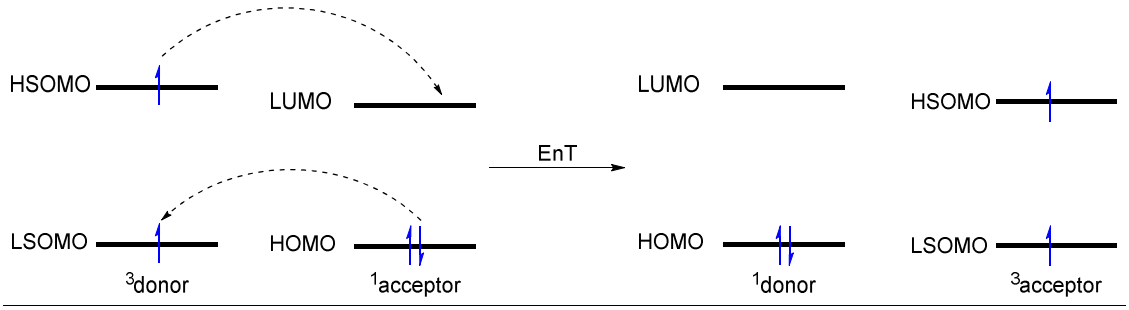


Figure 1-5 Energy level diagram detailing the mechanism of Dexter energy transfer.

Some applications of energy transfer catalysis to synthesis will be discussed in the next chapter in the context of the aza Paternò–Büchi reaction.

Chapter 2 - Sulfamoyl Fluoride Aldimines as Sensitisable Partners in the aza Paternò–Büchi Reaction

2.1 Introduction

Although azetidines are an important, biologically active class of molecules,they are vastly underrepresented in marketed pharmaceuticals as a direct result of their challenging synthesis. Of the myriad methods reviewed, a [2+2]-cycloaddition approach presents a direct and efficient disconnection comprised of two components of similar size and complexity. Polar [2+2]-cycloaddition reactions between imines and alkenes are generally challenging, often requiring high pressure or specific, bespoke pairs of substrates. However, the photo-mediated [2+2] cycloaddition, the aza Paternò–Büchi reaction, presents an opportunity for a transformation that is much broader in scope. The aza Paternò–Büchi reaction is comparatively underdeveloped compared to its oxo-counterpart, due to the poor reactivity of excited-state imines.[69, 70] Here, a brief overview of the photochemistry of imines, detailing some of the processes that preclude imines from undergoing the aza Paternò–Büchi reaction is presented. A brief review of [2+2] photocyclisations to synthesise azetidines is also detailed, with a focus on the strategies employed to circumvent the poor photoreactivity of imines.

2.1.1 Photochemistry of Imines

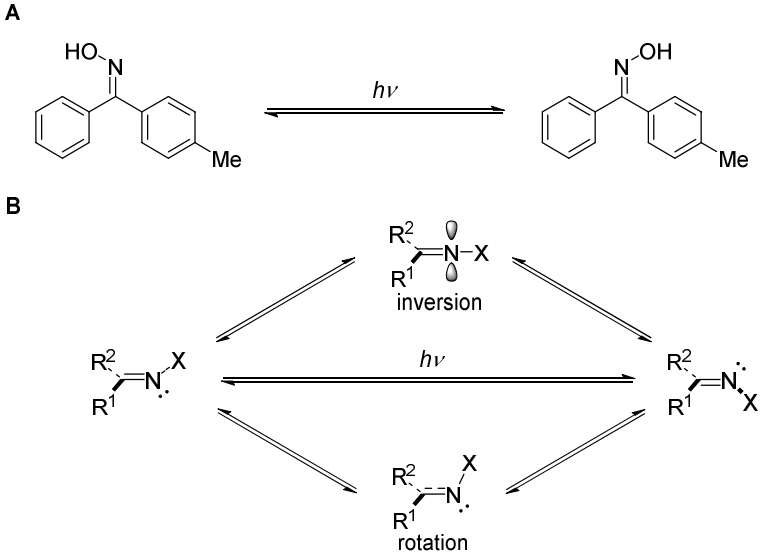
Spectroscopically, imines not in conjugation exhibit two absorption bands in UV/Vis spectra a shorter, more intense band at 170 – 180 nm, with a molar absorptivity of ~10^4 M^{-1} cm^{-1} assigned to a π–π^* transition; a weaker band at 230 – 260 nm, with a much smaller molar absorptivity of ~2×10^2 M^{-1} cm^{-1} designated to the forbidden n–π^* transition.[71, 72] Conjugation of the azomethine group shifts the absorption to longer

wavelengths, hence the weak bands due to n–π^* transitions are now submerged by strong absorption associated with π–π^* transitions.[72]

2.1.2 Photoisomerisation

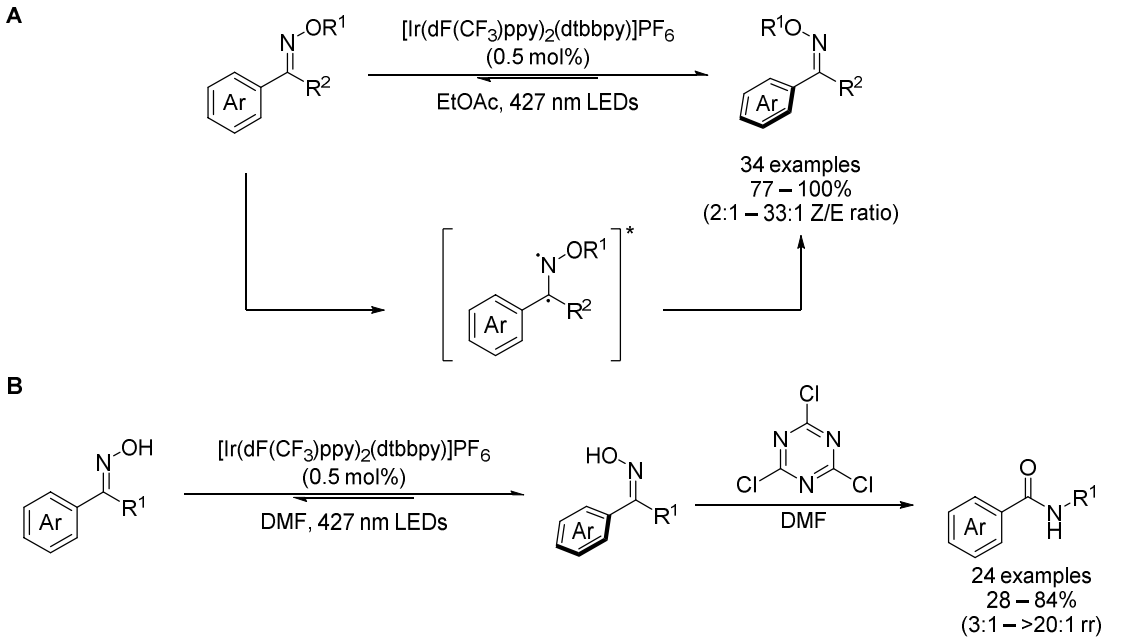
Photoisomerisation is an important process in nature being the operative mechanism in the conversion of a light signal in photoreceptors in the retina to an electrical pulse responsible for vision.[73] In the eye 11-cis-retinal condensed with a terminal amine forms an iminium ion which upon absorption of a photon isomerises.

Geometric isomerisation of oximes using UV light has been known as far back as the 19th century, this equilibration occurring analogously to olefin photoisomerization (**Scheme 2-1A**).[74, 75] Studying photoisomerization for other imines, including 1,2-diaryl imines, is significantly more challenging as they undergo rapid thermal isomerisation at ambient temperatures.[76] In contrast, oximes are configurationally stable, which makes them a more suitable candidate for studies of photochemical isomerisation.[77, 78] Quenching studies have shown that photo-equilibration of oximes can either occur from the singlet state through direct irradiation or the triplet state by sensitisation. There are currently two prevailing mechanisms for *E/Z* photoisomerization: a torsion mechanism involving rotation about the carbon-nitrogen double bond or an inversion mechanism, which involves increasing the C=N-X bond angle from ~120° to 180° and a rehybridization of the N-lone pair from sp^2 to sp (**Scheme 2-1B**).[79]



Scheme 2-1A Photo-isomerisation of ketoximine reported by Hantzsch. **B** Proposed mechanisms of imine isomerisation: inversion and rotation.

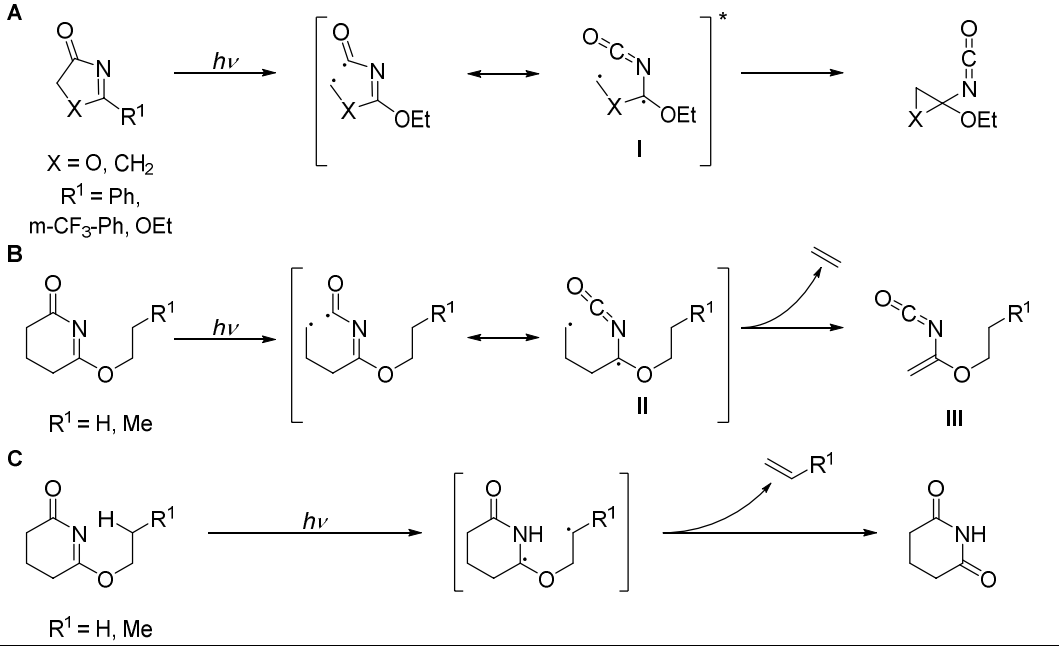
From a synthetic standpoint, Rovis developed an energy transfer catalysed isomerisation of *E*-oximes to the less accessible *Z*-oximes using an Ir photosensitiser and visible light to enable the isomerisation of *E*-oximes to the less accessible *Z*-oximes (**Scheme 2-2A**). In this case the contrathermodynamic process is possible as a result of the *Z*-oxime product having a reduced rate of energy transfer compared to the *E*-isomer, resulting diminished conjugation of the C=N bond and aryl ring due to steric hindrance. The authors utilised the previously inaccessible Z-oximes to give Beckmann rearrangement products in which the alkyl group migrates instead of the aryl group to deliver benzamides as opposed to anilides (**Scheme 2-2B**).[80]



Scheme 2-2A Energy transfer catalysed isomerisation of *E* oximes to *Z*. **B** One pot photoisomerisation Beckmann rearrangement procedure to deliver benzamides.

2.1.3 Photofragmentation and Photoelimination

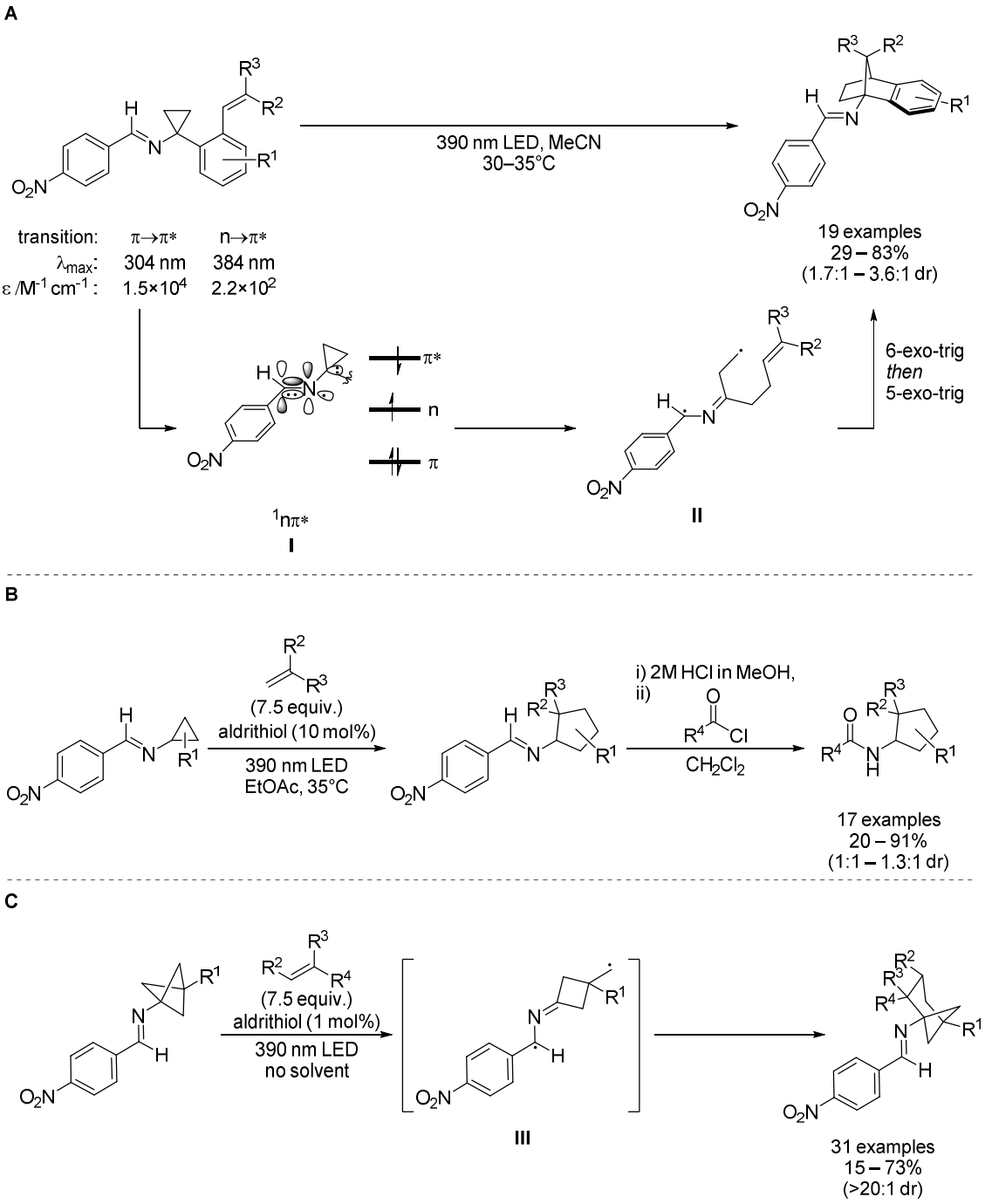
Imines have been shown to fragment by both type I and II Norrish mechanisms. With regards to type I fragmentations Koch reported a series of keto imino ethers that undergo *β*-scission of a C-C bond and rearrangement to the corresponding isocyanate with complete exclusion of both photodimerisation and photo-addition with olefins when there is an alkoxy group at the 2-position (**Scheme 2-3A**).[81, 82] The reactions were proposed to proceed *via* the nπ* singlet state which fragments to form a 1,3-biradical **I**, before collapsing to form the cyclopropane. When the analogous 6-membered cyclic imine was photoexcited, instead of recombining from the resulting 1,4-biradical **II** to give the corresponding cyclobutanes, extrusion of ethene gave vinyl isocyanate **III,** which was detected spectroscopically (**Scheme 2-3B**).[82] This compound also undergoes a competing Norrish type II rearrangement through abstraction of a γ-hydrogen atom to extrude ethylene delivering glutarimide (**Scheme 2-3C**).[82]



Scheme 2-3A Norrish type I rearrangement of imine. **B** Norrish type I rearrangement with extrusion of ethylene. **C** Norrish type II rearrangement to give glutarimide

Synthetic applications of the homolysis of the N-C bond of photo-excited imines has been evaluated by Stephenson using cyclopropyl *p*-nitrobenzimines.[83] Upon direct excitation using longer wavelength light (390 nm), the imine is selectively excited to the lower lying ^{1}n,π* electronic state **I**, which is capable of undergoing strain induced β-scission as a result of the overlap of the nitrogen lone pair SUMO with the σ_{cc} of the cyclopropane. However, excitation to the higher energy $^1\pi,\pi$* state, which results from an absorption with a much larger molar absorptivity, is precluded from undergoing this fragmentation due to the orthogonality of the π* and σ_{cc} orbitals.[83] By tethering a 2-styrene substituent to the cyclopropane, the authors were able to synthesise a range of (het)aryl-fused norbornyl imines by sequential radical cyclisation sequence forming two C—C bonds from intermediate biradical **II** (**Scheme 2-4A**).[83] In a subsequent publication the authors showed that the 1,5-biradical cyclopropylimine intermediates could be intercepted intermolecularly with an exogenous alkene to ultimately deliver aminocyclopentanes

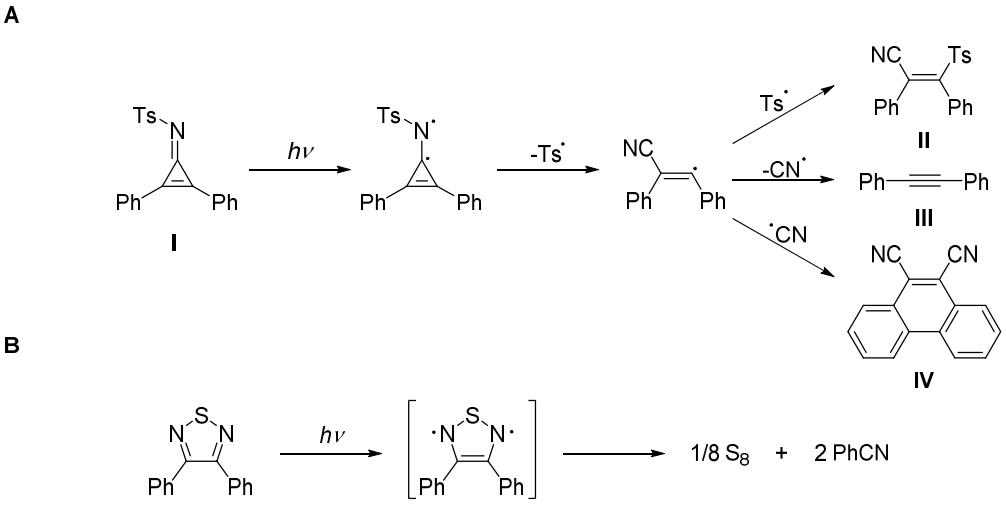
(**Scheme 2-4B**).[84] When imines derived from bicyclo[1.1.1]pentan-1-amines are subjected 390 nm irradiation, the resulting 1,6-biradical **III** could be intercepted by an alkene to convert the bicyclopentylimines to bicycloheptylimines (**Scheme 2-4C**).[85]



Scheme 2-4A Stephenson's strain-release fragmentation double cyclisation to give norbornyl imines. **B** Strain-release intermolecular [3+2] cycloaddition between cyclopropyl imines and olefins. **C** Photochemical ring-expansion of BCP-imines to bicycloheptylimines.

Photoexcited imines have also been shown to extrude heteroatom centred radicals including oxygen and sulfur. With regards to sulfur; irradiation of N-(*p*-toluenesulfonyl)diphenylcyclopropenlmine **I** with UV light in benzene generated a

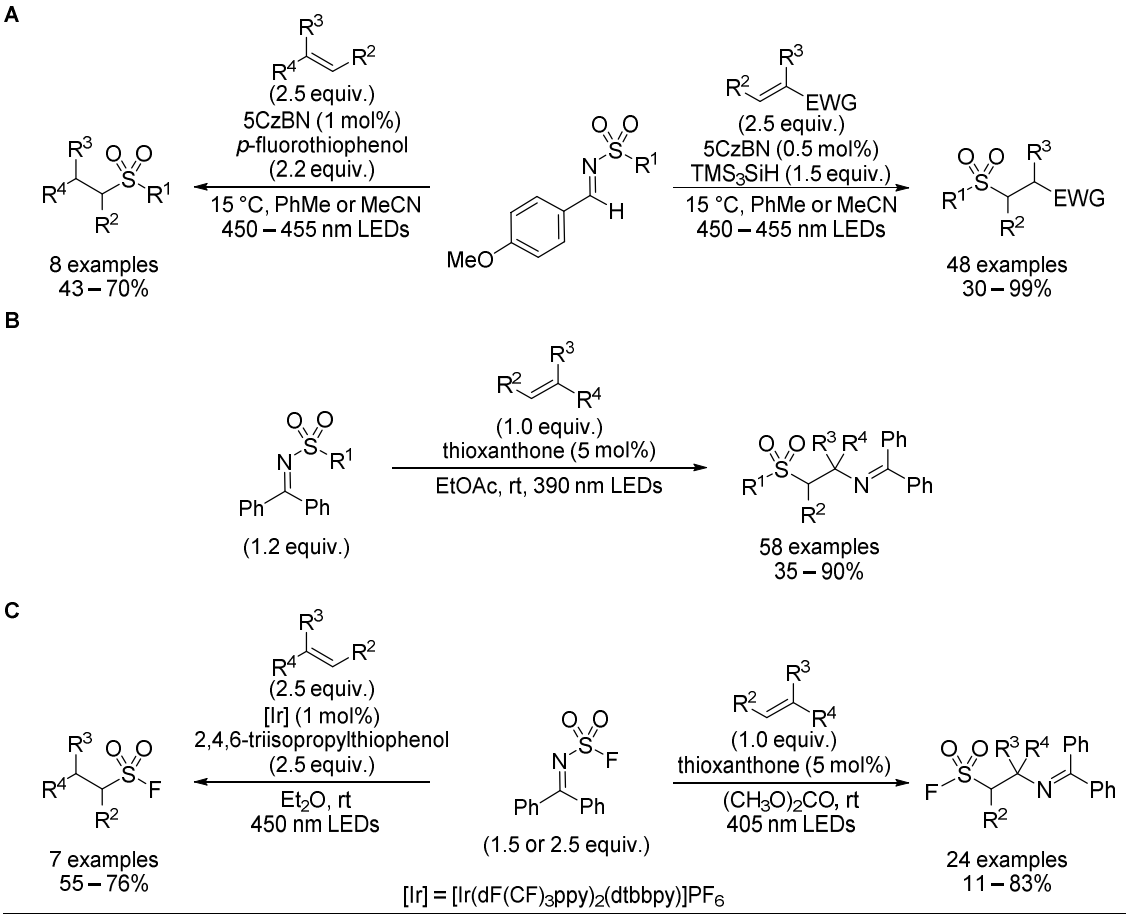
mixture 1-cyano-2-ptoluenesulfonyl-cis-stilbene **II**, diphenylacetylene **III**, 9-cyano-10-9,10-dicyanophenanthrene **IV**, and *p*-toluenesulfonylphenanthrene (**Scheme 2-5A**). This photodegradation is attributed to scission of the α-C—C bond, followed by sequential extrusion of a sulfonyl radical and cyano radical.[86] Hetero-aromatic 1,2,5-thiadiazoles also undergo photolysis *via* the singlet state undergoing a double extrusion producing elemental sulfur and benzonitrile (**Scheme 2-5B**).[87]



Scheme 2-5A Fragmentation of N-(*p*-toluenesulfonyl)diphenylcyclopropenlmine to give sulfonyl radicals. **B** Fragmentation of thiadiazole to give elemental sulfur.

Recently, the radical scission of S-centred radicals from excited state imines has been utilised to significant effect to make functionalised sulfonyl containing products. In 2022, the Willis group disclosed that N-sulfonyl imines, derived from *p*-anisaldehyde and the corresponding sulfonamide behave as excellent sulfonyl radical precursors under triplet energy transfer conditions. The authors demonstrated the synthetic utility of the platform by performing hydrosulfonylation reactions of both electron-rich and electron-poor olefins by tuning the philicity of the H-atom source (**Scheme 2-6A**).[88] If instead benzophenone derived imines are employed, Du showed that it is possible to generate β-amino sulfones with alkenes. This is due to the increased stability of the iminyl radical,

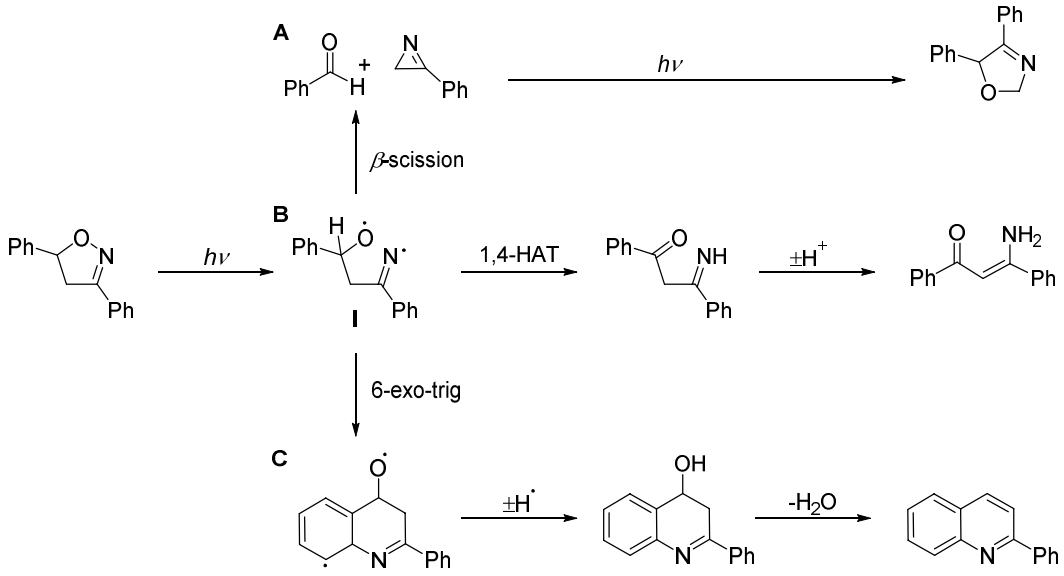
which facilitates the selective radical-radical combination with the carbon-centred radical resulting from the addition of the sulfonyl radical to the olefin *via* the persistent radical effect (**Scheme 2-6B**).[89, 90] Glorius also developed a related procedure using sulfamoyl fluoride ketimines to generate *β*-amino sulfonyl fluorides which the authors demonstrated behave as versatile substrates for further elaboration (**Scheme 2-6C**). When an HAT-donor (2,4,6- triisopropylthiophenol) is employed in the photochemical step, a hydrosulfonylation reaction was also realised.[91]



Scheme 2-6A Energy transfer catalysed hydrosulfonylation of alkenes using sulfonyl aldimines as a radical precursor. **B** Amino-sulfonylation of olefins using sulfonyl ketimines. **C** Energy transfer catalysed synthesis of aliphatic sulfonyl fluorides from sulfamoyl fluoride ketimines.

With respect to extrusion of O-centred radicals, an early example involves irradiating 3,5-diphenyl-2-isoxazoline with UV light giving rise to a mixture of 4,5-diphenyl-3-

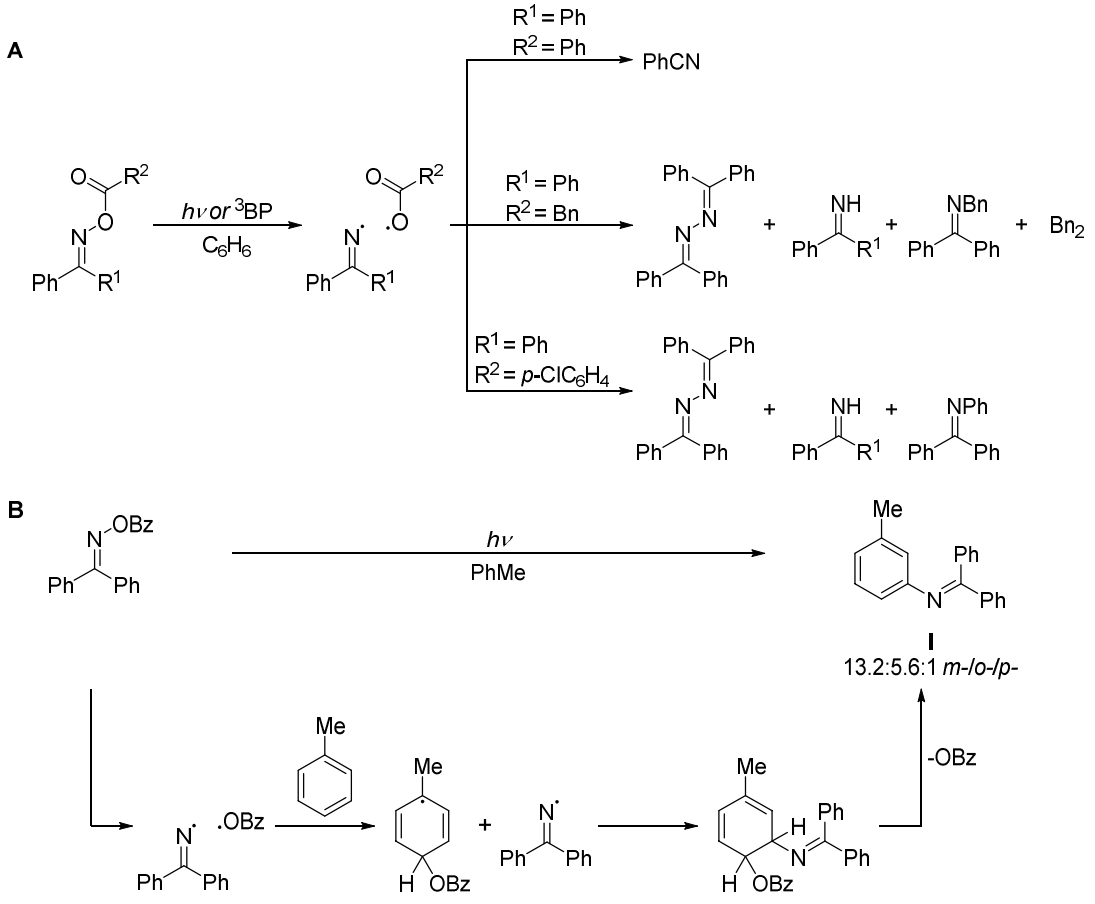
oxazoline, *β*-aminochalcone, and 2-phenylquinoline (**Scheme 2-7**). These compounds are a result of scission of the N—O to form a common 1,5-biradical parent intermediate **I**; scission of the C—C bond *α*- to the alkoxy radical, forming an azirine and benzaldehyde, which subsequently undergo a photomediated recombination to give 4,5-diphenyl-3-oxazoline (**Scheme 2-7A**); *β*-aminochalcone stems from a 1,5-HAT process (**Scheme 2-7B**) and 2-phenyl quinoline results from initial intramolecular cyclisation of the iminyl radical into a neighbouring phenyl group and *β*-aminochalcone stems from a 1,5-HAT (**Scheme 2-7C**).[92, 93]



Scheme 2-7 Photo-fragmentation of 4,5-diphenyl-3-oxazoline.

The photolysis of aromatic ketoxime carboxylates has been known since at least the 1960s.[94] This fragmentation, induced either by direct excitation with UV light or triplet energy sensitisation, in benzene, results in the homolytic fission of the N-O bond to give a carboxyl radical and an iminyl radical. Depending on the structure of the oxime ester, a different distribution of degradation products is observed (**Scheme 2-8A**).[95, 96] Phenylmethelenimino radicals from the photolysis of aldoximine esters do not dimerise,

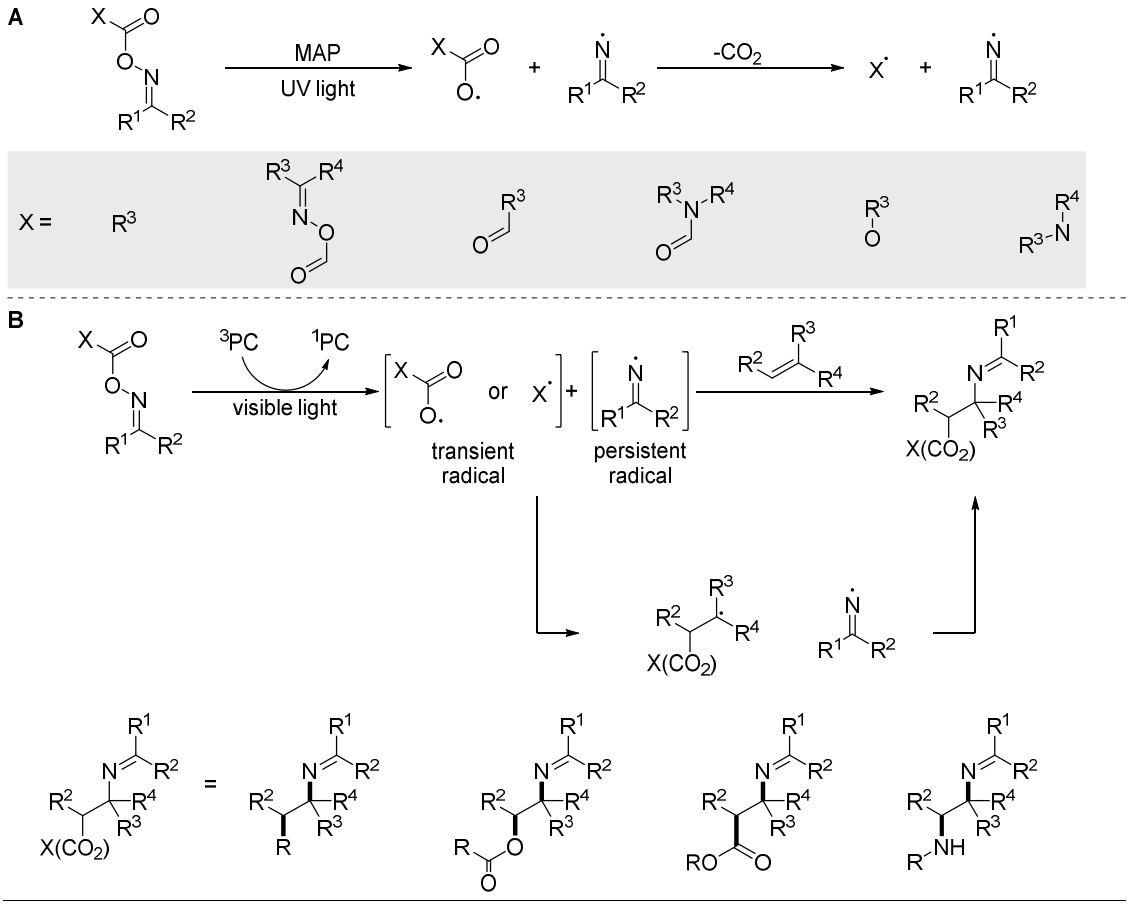
but instead are oxidised to the nitrile as a result of HAT by either a carboxyl or aryl radical.[97] Benzyl carboxylate ketoximines (R^2 = Bn) instead give significant recombination with the iminyl radical and dimerisation.[95] Aromatic carboxylate ketoximes (R^2 = *p*-ClC_6H_4) yield azine as a result of iminyl radical dimerization and aromatic substitution reactions of benzene, a process proposed to be facilitated by the addition of a carboxyl radical, as evidenced by the observed preference for the *meta*-isomer of **I** when toluene is used as the solvent (**Scheme 2-8B**).[95]



Scheme 2-8A Product distribution of the fragmentation of ketoximine carboxylates. **B** Mechanism proposed by Tokumaru for the formation of anilide imines.

Since, these initial reports, reaction has been generalised to other oxime functionalitities including, dioxime oxalates, oxime glyoxylates, oxalate amides, carbonates, and

carbamates, and applied to a range of different reactions including radical cyclisations.[98-104] Much of this work has been pioneered by Walton, who studied this photofragmentation (triggered using UV light and 4-methoxyacetophenone as a photosensitiser) in detail using EPR spectroscopy to detect open-shell intermediates *in-situ* (**Scheme 2-9A**).[99-102, 104] As the photo-fragmentation of ketoximine carbonyls occurs through the triplet state it is amenable to sensitisation using a photocatalyst and visible light, resulting in widespread application as a platform for alkene difunctionalisation. The Glorius group, amongst others, have demonstrated that using appropriately tuned ketoximines it is possible to affect a wide range of different difunctionalisation reactions including carbo-, carbonyl-, oxy- and amino-imination with a wide range of different olefins (**Scheme 2-9B**).[105-109]



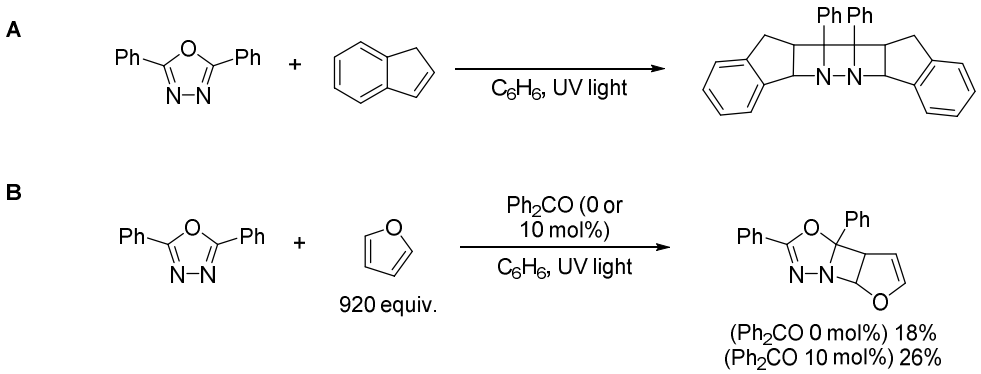
Scheme 2-9A Overview of carboxylate imines studied by EPR spectroscopy. MAP = 4-methoxyacetophenone. **B** Overview of synthetic methods for energy transfer catalysed alkene difunctionalisation by ketoximine carboxylates.

2.1.4 Aza Paternò–Büchi Reaction Using Triplet Imines

In order to circumvent deleterious processes of excited state imines and achieve intermolecular reactivity when employing a triplet imine, methods have focused on tethering the C-N double bond in either a 5- or 6- membered ring to prevent rotation about the double bond, thus adding an entropic penalty to fragmentation. However, this solution makes these methods synthetically less appealing as the formed azetidine is bicyclic, with ring cleavage leaving part of the imine tethering group still attached to the azetidine.

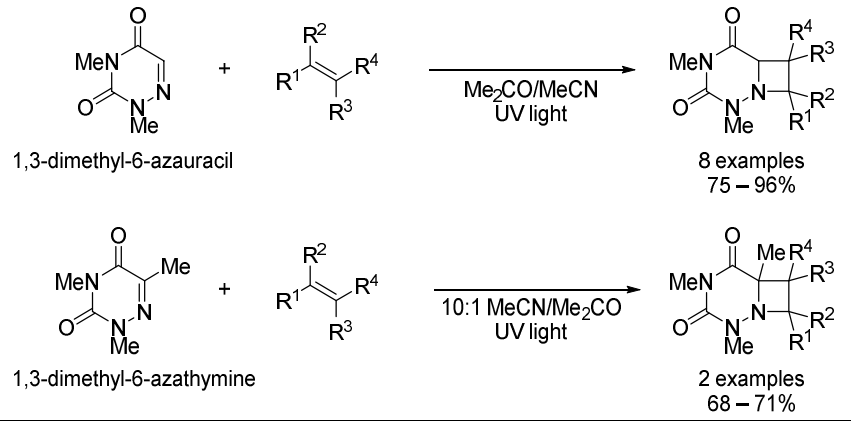
The first reported aza Paternò–Büchi reaction was disclosed by Tsuge in 1968. Here it was disclosed that under direct UV irradiation 2,5-diphenyl-1,3,4-oxadiazole forms a 2:1

diazetidine adduct with indene along with extrusion of an oxygen atom (**Scheme 2-10A**).[110] Later, the scope of this reaction was expanded to also include furan as a coupling partner, giving the mono cycloadduct in 26% when using benzophenone as a triplet sensitiser, and in 18% yield without the sensitiser, which is consistent with the reaction proceeding *via* the triplet state of the oxadiazole (**Scheme 2-10B**).[111]



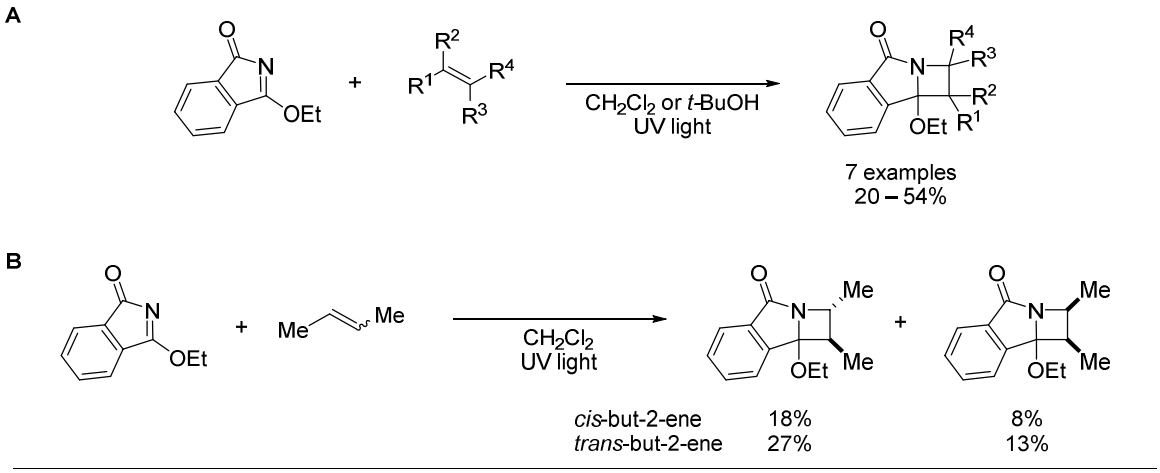
Scheme 2-10A First reported aza Paternò–Büchi. **B** Reaction of substituted oxadiazole with furan.

Later, Swenton and coworkers disclosed in 1972 that 1,3-dimethyl-6-azauracil was capable of undergoing [2+2]-photocycloaddition with ethyl vinyl ether in greater than 90% yield, using acetone as a cosolvent and triplet energy sensitizer.[112] In a follow up report, the authors showed that both 1,3-dimethyl-6-azauracil and 1,3-dimethyl-6-azathymine underwent [2+2]-photocycloaddition reactions regioselectively with a range of electron -rich and -neutral alkenes with various substitution patterns (**Scheme 2-11**).[113]



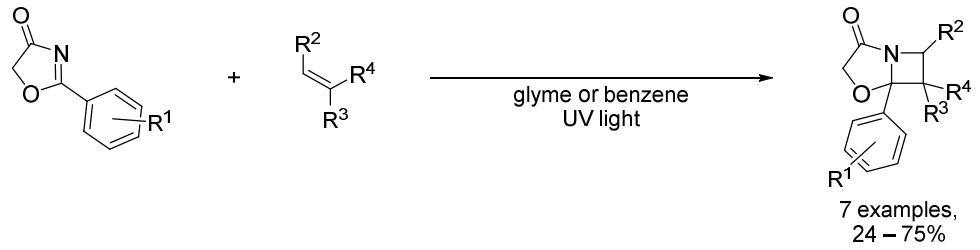
Scheme 2-11 Aza Paternò–Büchi reaction of aza-uracil and aza-thymine with alkenes.

Almost concurrently with Swenton's report, Koch reported that 3-ethoxyisoindolone is also a competent substrate in the aza Paternò–Büchi reaction, showing reactivity with 1,1-dimethoxyethylene in *t*-BuOH and methylenecyclohexane, the latter requiring a solvent change to CH_2Cl_2 (**Scheme 2-12A**).[114] In Koch's follow up report the scope of this transformation was expanded with respect to the olefin, and the quantum yield of the transformation was measured at a range of olefin concentrations to determine that the excited state of the imine is quenched by the olefin. The lack of stereospecificity observed when the imine was subjected to *cis*- and *trans*- isomers of but-2-ene led the authors to conclude that the reaction occurs *via* the triplet state of the imine, as this is consistent with formation of a long-lived 1,4-triplet biradical able to undergo rotation (**Scheme 2-12B**).[115]



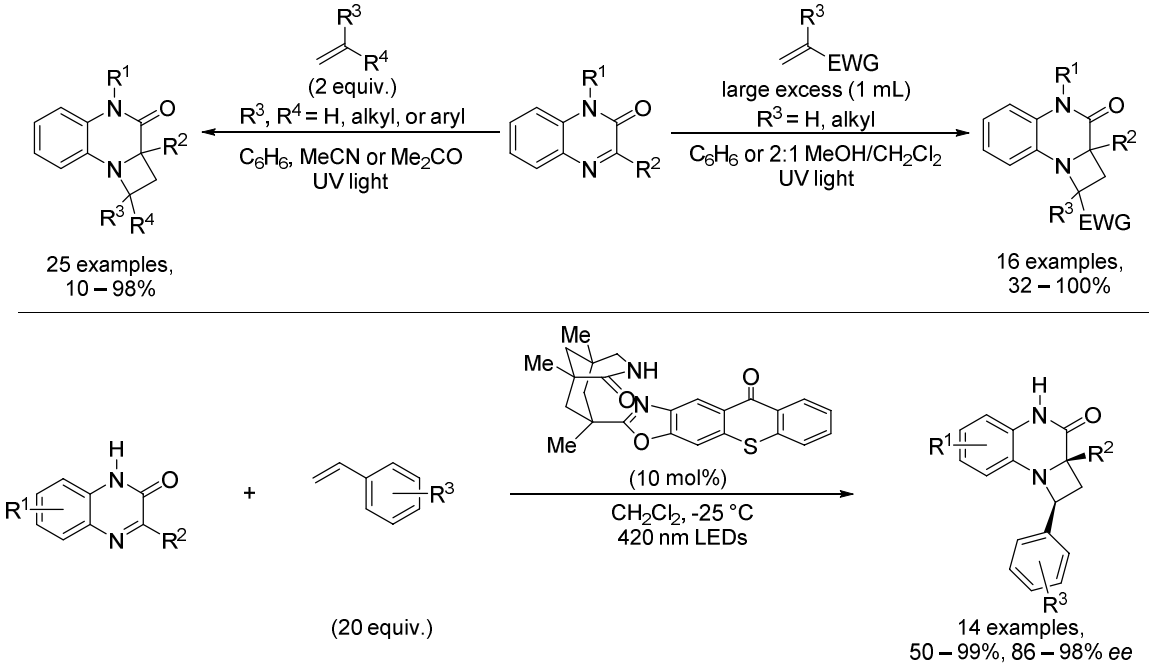
Scheme 2-12A Aza Paternò–Büchi reaction of 3-ethoxyisoindolone. **B** Mechanistic probe into the spin state of the 1,4-biradical intermediate.

Removing the benzo-fused ring from the chromophore of 3-ethoxyisoindolone significantly affects its photoreactivity (as discussed in **section 2.1.3**). The non-benzo-fused compounds do not undergo intermolecular [2+2] photocycloaddition; instead, partly due to the weakened C–C bond α to the carbonyl, they undergo a rearrangement *via* an initial Norrish type I cleavage to form an isocyanate (**Scheme 2-3**). This was also attributed to a change in electronic configuration from $\pi\pi^*$ in the case of the isoindolone substrate, to $n\pi^*$.[81] However, changing the functional group from an imine to an imidoate and substituting the ethoxy group for an aromatic group changes the reactive excited state back to $\pi\pi^*$, enabling the [2+2]-photocycloaddition with furan and 1,1-dimethoxyethylene to occur for a range of aromatic groups on the cyclic imidoate (**Scheme 2-13**).[81]



Scheme 2-13 Aza Paternò–Büchi reaction of 3- aryl cyclic imidoates.

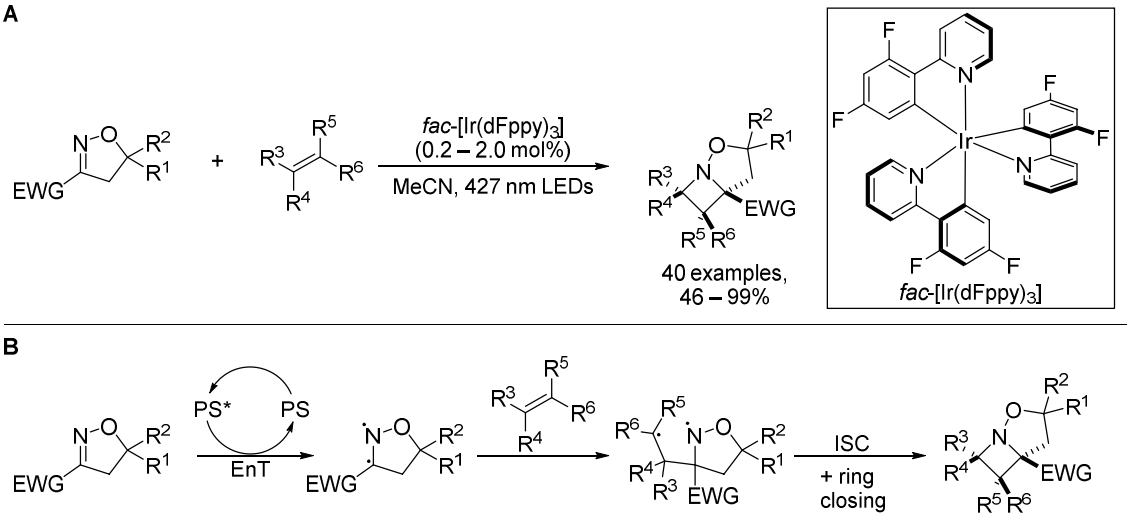
Nishio reported that quinoxalin-2(1*H*)-ones are capable of undergoing an inter-molecular aza Paternò–Büchi reaction with electron-deficient olefins, demonstrating broad scope with respect to both components and later expanding the scope to styrenes (**Scheme 2-14A**). [116, 117] Bach expanded on this latter work by employing a chiral thioxanthone derivative, rendering the transformation enantioselective. This approach resulted in a broad scope with respect to both components, with excellent yields and *ee*s observed in all cases. Enantioinduction is achieved by the photocatalyst hydrogen-bonding with the quinoxalinone to first facilitate energy transfer and the subsequent C-C bond formation with the styrene, allowing attack of the alkene only on one face. The intermediate 1,4-biradical then undergoes intersystem crossing diastereoselectively to form the azetidine product (**Scheme 2-14B**).[118]



Scheme 2-14A Nishio's original report of the aza Paternò–Büchi of quinoxzalines with styrenes and electron-deficient olefins. **B** Bach's catalytic, enantioselective version of the transformation.

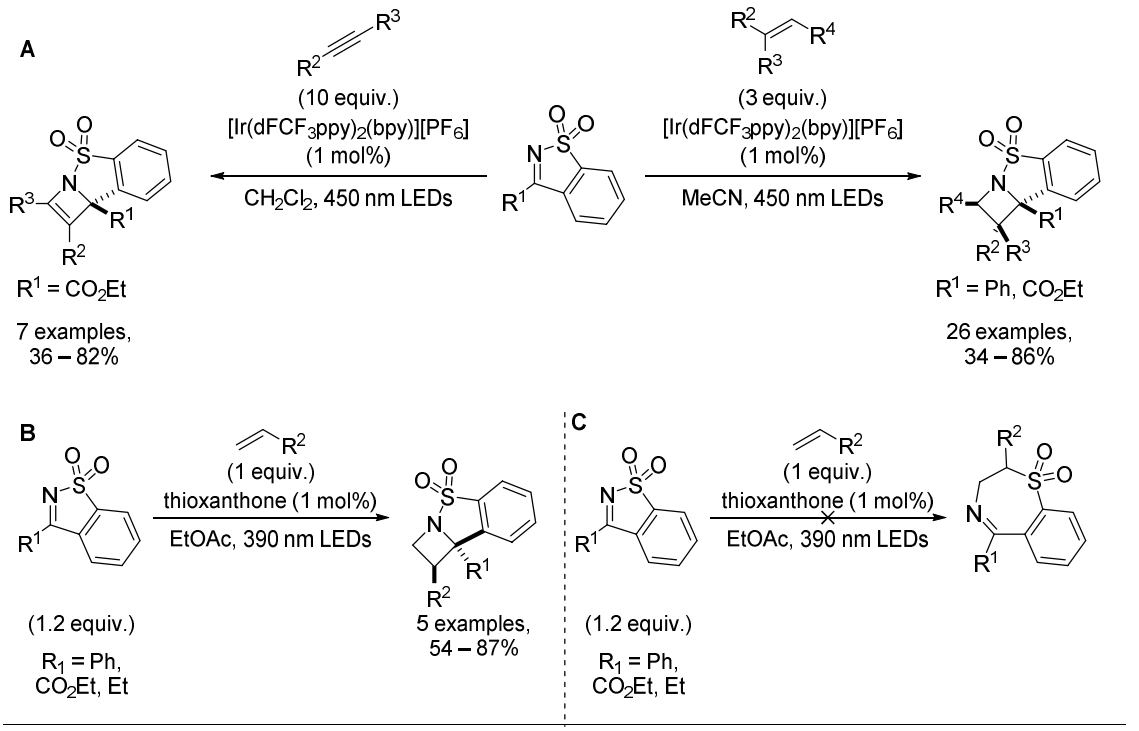
Contemporaneous examples of the intermolecular aza Paternò–Büchi reaction often employ an energy sensitiser as opposed to direct excitation of the imine. This is in part due to the advent of photoredox catalysis whereby the use of photoexcited polypyridyl transition metal complexes, which are capable of behaving simultaneously as strong oxidants and reductants, has enabled the mild generation of open-shelled intermediates using mild visible light.[119] The same features that make these catalysts appealing for photoredox catalysis: high triplet quantum yields as a result of the heavy atom effect, and long-lived triplet lifetimes and high triplet energies also makes these compounds effective triplet energy sensitisers.[68] One example, reported by Schindler in 2020, involves the use of isoxazolines as a cyclic imine equivalent, unactivated alkenes, and the Ir complex *fac*-[Ir(dFppy)$_3$] as a photosensitiser, along with blue light. The authors report a broad scope with over 40 examples total, including a broad range of alkene components ranging from mono- to tetra- substituted alkenes examples, *B*-, *O*- and *Si*-substituents and electron-

deficient alkenes (**Scheme 2-15A**). The scope of the oxime is more limited, with an electron-withdrawing substituent at the 2- position of the isooxazoline necessary and the heterocycle must be a 5-membered ring.[120]



Scheme 2-15A Schindler's aza Paternò–Büchi reaction between isoxazolines and alkenes. **B** Proposed mechanism of the reaction.

More recently, Brown showed cyclic sulfonyl imines, 3-substituted benzo[d]isothiazole 1,1-dioxides, used along with the Ir photosensitiser $[Ir(dFCF_3ppy)bpy][PF_6]$ are also capable of undergoing [2+2]-photocycloadditions with either an excess of alkene to form azetidines or with alkynes to from 2-azetines, depending on the substituent on the benzoisothiazole (**Scheme 2-16A**). An aromatic substituent (R^1) enabled the reactivity with alkenes only, whereas an ester group enabled reactivity with both alkenes and alkynes.[121] This reaction was also inadvertently disclosed by Du during the study of hydrosulfonylimination reaction of alkenes where they mischaracterise the [2+2]-photocycloaddition (**Scheme 2-16B**) of 3-substituted benzoisothiadiazole dioxides as a 2 carbon ring expansion evidenced by the compounds having spectral data that matches Brown's (**Scheme 2-16C**).[89]



Scheme 2-16A Brown's energy transfer catalysed aza Paternò–Büchi reaction of benzo[d]isothiazole 1,1-dioxides with alkenes and alkynes. **B** Du's energy transfer catalysed reported ring expansion benzo[d]isothiazole 1,1-dioxides. **C** Actual aza Paternò–Büchi reaction of benzo[d]isothiazole 1,1-dioxides under energy transfer catalysed conditions.

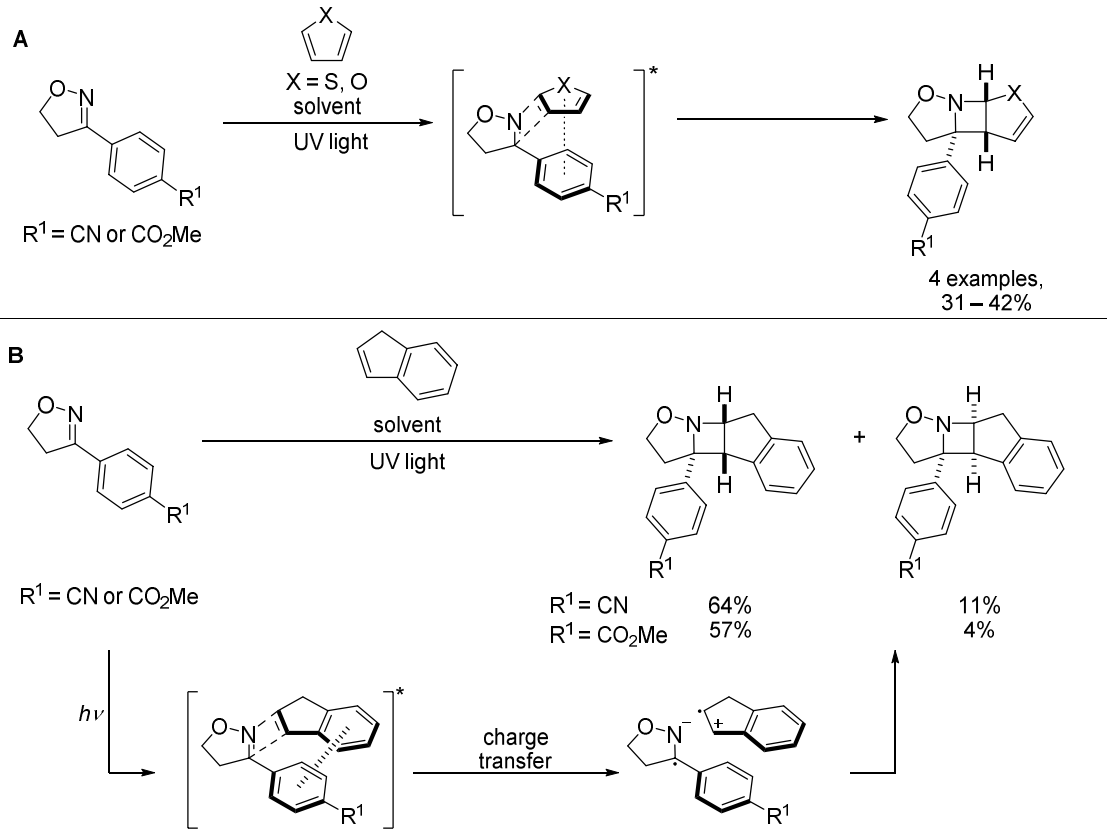
2.1.5 Aza Paternò–Büchi Reaction *via* a Singlet Exciplex

Rather than achieving reactivity *via* the triplet state of the imine generated either by direct excitation or triplet energy transfer, another feasible strategy is to achieve reactivity through the singlet state.

In 1981, Mukai disclosed that 3-(4-cyanophenyl)-2-isoxazoline is capable of forming a 1:1 photoproduct upon irradiation with benzene as a single regio- and stereoisomer. In this report the authors confirm that reactivity occurs from the singlet state of the imine and not benzene. They propose that either the formation of an exciplex or a charge transfer interaction is necessary for photocycloadduct formation (**Scheme 2-17A**).[122]

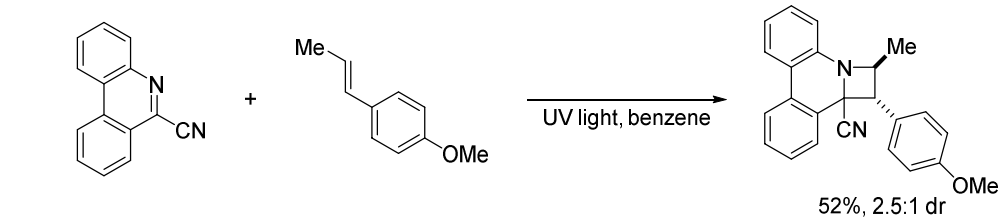
In a follow-up publication the authors report the reaction also proceeds in a regio- and stereospecific manner with furan and thiophene. However, the authors also reported that the reaction doesn't work with non-aromatic double bonds, including 2,3-dihydrofuan, ethylvinylether, 1,1-dimethoxyethene, enamines or cycloalkenes.[123] This may be further evidence that the C-C double bond used must be capable of forming an exciplex with a sandwich type conformation with isooxazolines (**Scheme 2-17A**). The authors confirmed that an electron-withdrawing group on the arene is critical to the success of the [2+2]-photocycloaddition.

With indene however, the reaction instead gives a mixture of diastereomers (**Scheme 2-17B**). This observation was rationalized by the possibility that, in addition to the previously described singlet exciplex mechanism, a second mechanism may also be occurring simultaneously. In this alternative mechanism, charge transfer may occur, generating a radical ion pair that then recombines in a stepwise manner, producing a mixture of diastereomers.[124]



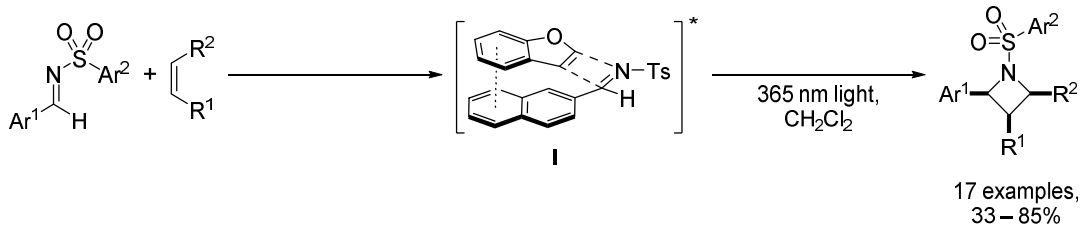
Scheme 2-17A Aza Paternò–Büchi reaction of aryl isoxazolines *via* the formation of a singlet exciplex. **B** Stereodivergent aza Paternò–Büchi reaction of aryl isoxazolines as a result of charge transfer from the singlet exciplex.

In the early 1980s Ohta communicated in a pair of reports, photocycloadditions of 6-substituted phenanthridines and electron-rich olefins, including a [2+2]-photocycloaddtion between 6-cyano phenanthridine and *trans*-anethole, using UV light (**Scheme 2-18**).[125, 126] This product however is not stable under the reaction conditions and was shown to decompose to the corresponding azocine. The reaction was shown to proceed *via* the singlet state ($^1\pi\pi^*$) of the phenathridine as the addition of a triplet quencher (1,3-pentadiene), did not quench the formation of the photoadduct. The addition of *trans*-anethole did quench the fluorescence of phenathridine and weak emission from an exciplex was detected at 503 nm, which was shown to be responsible for the formation of the azetidine.[125]



Scheme 2-18 Aza Paternò–Büchi reaction reaction of phenthridine *via* formation of singlet exciplex.

In 2016, Maruoka demonstrated that either naphthyl *N*-sulfonyl imines or naphthylsulfonyl aromatic imines can be employed with an alkene containing an aromatic group to stereospecifically form azetidines in good to excellent yields (**Scheme 2-19**). The stereospecificity was attributed to the formation of a singlet exciplex **I**, facilitated by π-stacking interactions between the imine and the alkene, enabling a concerted addition. However, this mechanistic requirement restricts the scope to imines with a naphthyl group and alkenes with an aromatic group.[127]

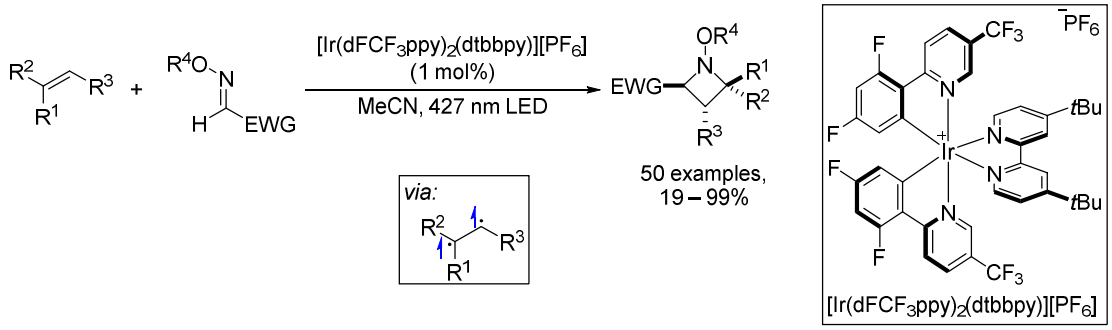


Scheme 2-19 Maruoka's UV light, direct excitation aza Paternò–Büchi with naphthyl sulfonyl aldimines.

2.1.6 Aza Paternò–Büchi Reaction *via* an Excited State Alkene

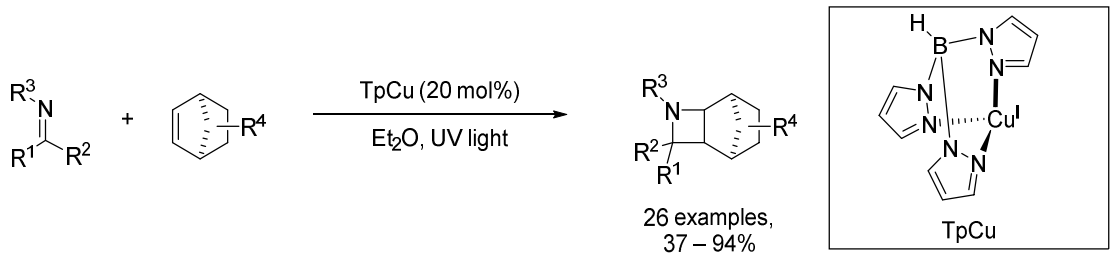
An alternative strategy to circumvent the challenges associated with excited state imines is to induce a formal aza Paternò-Büchi reaction by using activated alkenes that are excited in preference to the imine. A notable recent example from the Schindler and Kulik laboratories utilizes acyclic oximes as imine-equivalents, in combination with activated alkenes including styrenes, cyclic alkenes and dienes (**Scheme 2-20**). A computational

investigation revealed this was enabled by careful matching of the frontier molecular orbital energies of the two reaction components to deliver an efficient process.[128]



Scheme 2-20 [2+2]-photocycloaddition between triplet alkenes and acyclic oximes to produce monocyclic azetidines.

In 2022, Schmidt reported a similar approach whereby the use of copper catalysis activates alkenes for addition into aliphatic imines (**Scheme 2-21**). In this approach the copper complex, TpCu, first binds to the olefin to form a complex, which absorbs a photon of ultraviolet light (<300 nm) and subsequently undergoes MLCT to formally reduce the alkene, which chemoselectively reacts with an imine to form an azetidine.[129] However, the scope of the reaction with respect to the olefin component is quite limited as alkene must be cyclic with most examples also being norbornene derivatives.

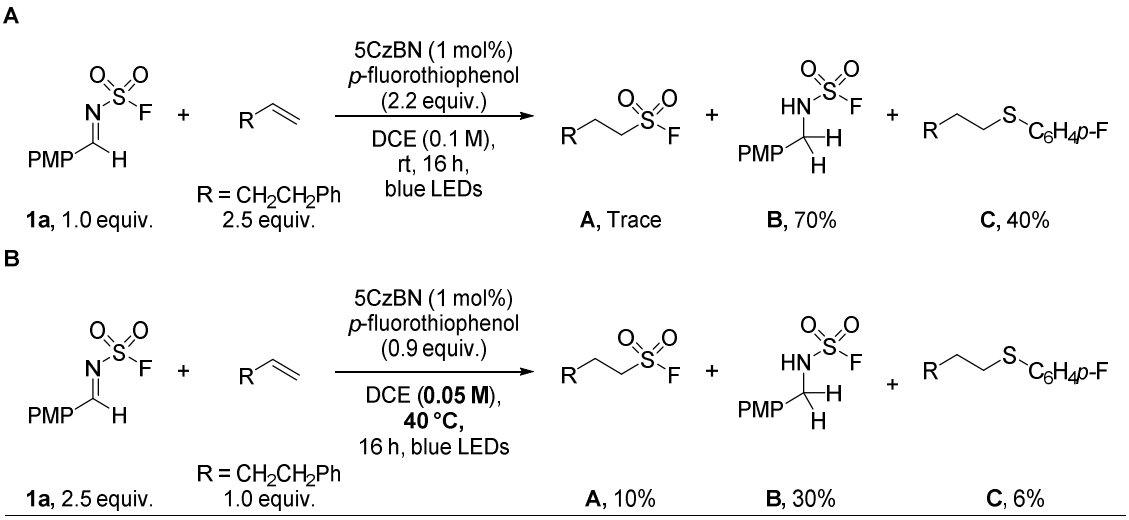


Scheme 2-21 Schmidt's copper catalysed [2+2]-photocycloaddition.

2.2 Origin and Outline of Project

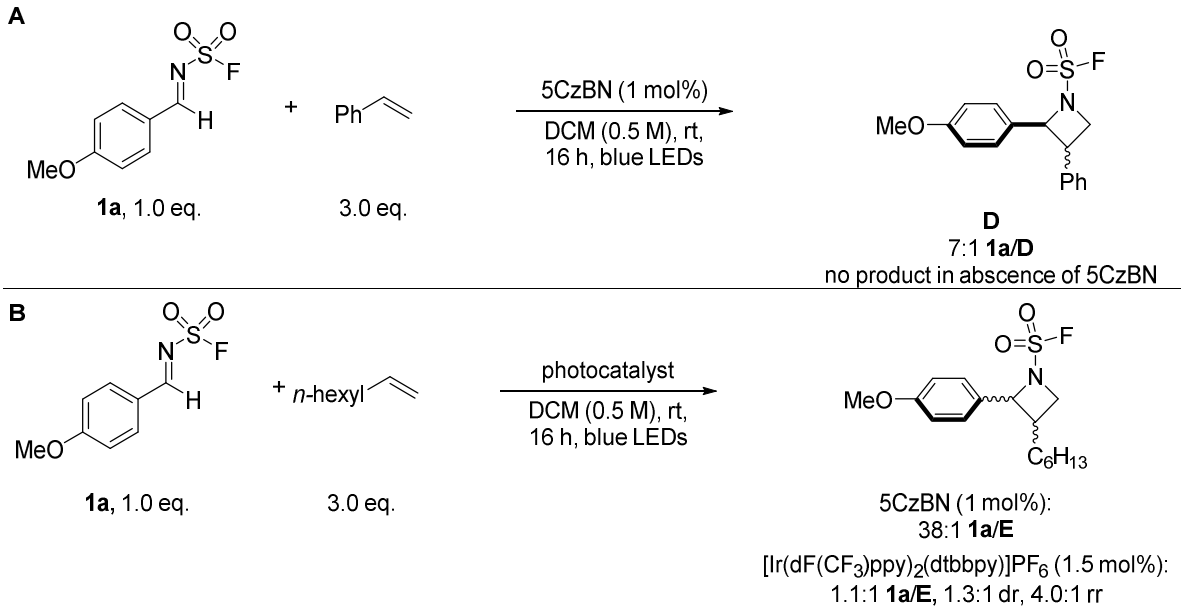
As outlined in the previous section, *N*-sulfonyl aldimines when promoted to the triplet state by energy transfer catalysis, can behave as competent sulfonyl radical precursors.[88] Our initial aim was to apply and adapt the chemistry in order to the generate other sulfonyl radicals. Already this chemistry was shown to work with sulfamoyl and sulfonyl radicals, and we wanted to show this reaction could be extended to the elusive SO_2F radical, from the bench-handleable solid, (*p*-methoxybenzylidene)sulfamoyl fluoride (**1a**). Up to this point the only methods to generate the SO_2F radical involved flash vacuum pyrolysis of fluorosulfonyl nitrene or using highly reactive $ClSO_2F$ gas.[130-132]

However, when we applied conditions previously reported with N-sulfonyl aldimines and electron deficient aldimines to the imine (**1a**) we only observed trace hydrosulfonylated product (**A**), and principally observed reduction of the sulfamoyl fluoride imine to the sulfamoyl fluoride amine (**B**) and sulfide (**C**) as a side-product (**Scheme 2-22A**).[88] After a short optimisation campaign, the yield of the product (**A**) increased to 10% (**Scheme 2-22B**). Given the poor fragmentation of imine observed under these conditions, we hypothesized that we may instead be able to intercept the triplet aldimine directly with an alkene to form an azetidine.



Scheme 2-22A Initial conditions for hydrosulfonylation of unactivated alkenes with 1a. **B** Optimised conditions for hydrosulfonylation.

Our initial hit for this project came from a set modified conditions from the fragmentation work using 5CzBN as an energy sensitiser and using styrene as a coupling partner. The appearance of 2 new peaks in the ^{19}F NMR spectrum at around ~ +30 ppm was strongly indicative of shielded $NSO_2\mathbf{F}$ environments, which are characteristic of azetidines.[133] In this case we observed a 7:1 starting material/product **(D)** ratio, and no reaction in absence of 5CzBN, hence excluding the possibility of a thermal pathway (**Scheme 2-23A)**. Next, we wanted to test if the reaction was also applicable to unactivated alkenes. We found that by swapping the photocatalyst to $[Ir(dF(CF_3)ppy)_2dtbbpy][PF_6]$ and employing octene, we also observed reactivity, which resulted in a 1.1:1 starting material/product (**E**) ratio (**Scheme 2-23B**).

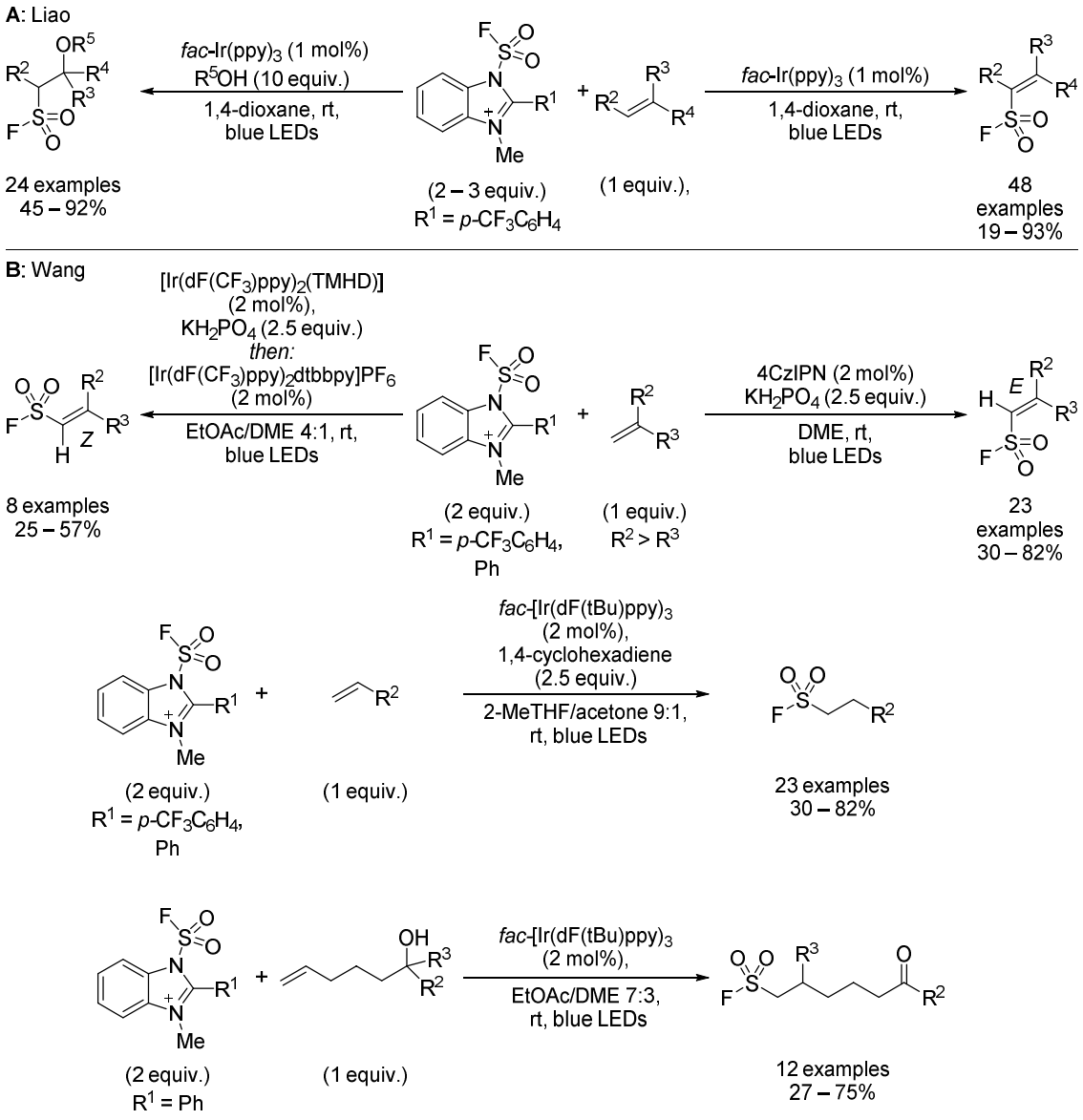


Scheme 2-23A Initial conditions for aza Paternò–Büchi with activated alkene. **B** Initial results for an unactivated alkene.

From these results, we postulated that we could develop an intermolecular aza Paternò–Büchi reaction that would not only be feasible but also capable of broad application. As this reaction became the main focus of the project, we aimed to design a process that: (a) was general with respect to both the alkene and imine components; (b) used substrates that were rapidly accessible in a single step from feedstock aldehydes; and (c) had a cleavable group on nitrogen. Regarding (a), our result with a simple unsubstituted alkene suggested that the scope with respect to the alkene could be broad. Concerning the imine, we reasoned, based on previous [2+2] photocycloadditions of triplet styrenes that it would be possible to modify the arene ring on our imine and still have a successful aza Paternò–Büchi reaction.[134] Sulfamoyl fluoride aldimines can be conveniently prepared by condensing aldehydes with fluorosulfonyl isocyanate, producing only CO_2 as a by-product, hence fulfilling criterion (b) and also giving the possibility of telescoping imine synthesis into the aza Paternò–Büchi reaction. Regarding (c), reports of the cleavage of the tertiary sulfamoyl fluoride moiety are scarce and are limited to activated examples,

so it was imperative to develop a protocol to achieve this, as it would enable the -SO_2F to behave as a traceless activating group.[135, 136]

Meanwhile a number of reports surfaced on the development of solid sources of SO_2F radicals. These included, benzimidazolium derived sulfamoyl fluoride salts simultaneously disclosed by the Liao and Wang groups, and Glorius' sulfamonyl fluoride ketimine (as discussed previously in section **2.1.3**).[91, 137, 138] The imidazolium salt was shown to operate *via* a photoredox manifold reacting with alkenes to give either alkenyl or alkyl sulfonyl fluorides when either a nucleophile or a H-atom source was also present (**Scheme 2-24A and B**). With the advent of these methods our investigation into sulfamoyl aldimines fluorides as SO_2F radical precursors was paused indefinitely.



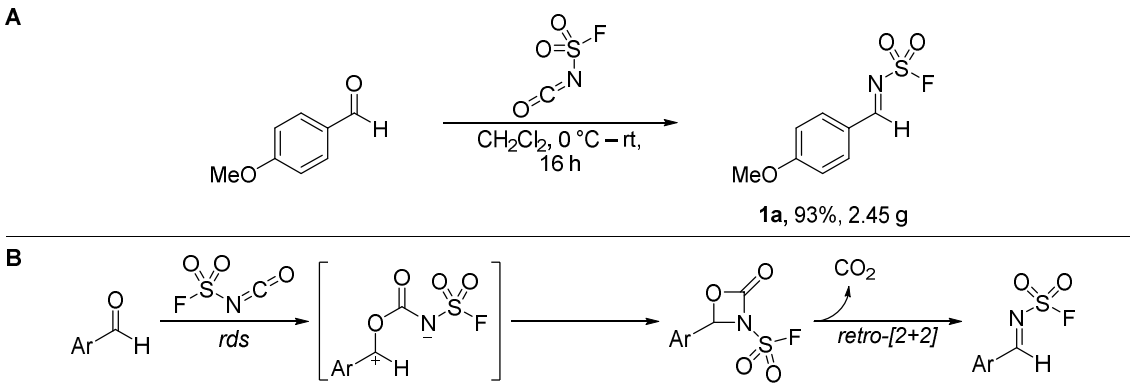
Scheme 2-24A Liao's report of fluorosulfamoyl benzimidazolium salt as a SO_2F radical precursor, with two transformations disclosed. **B** Wang's simultaneously published report, with four transformations disclosed.

The current chapter seeks to explore the photochemistry of sulfamoyl fluoride imines in order to deliver an aza Paternò–Büchi reaction that enables an effective modular disconnection of azetidines.

2.3 Synthesis of Sulfamoyl Fluoride Aldimines

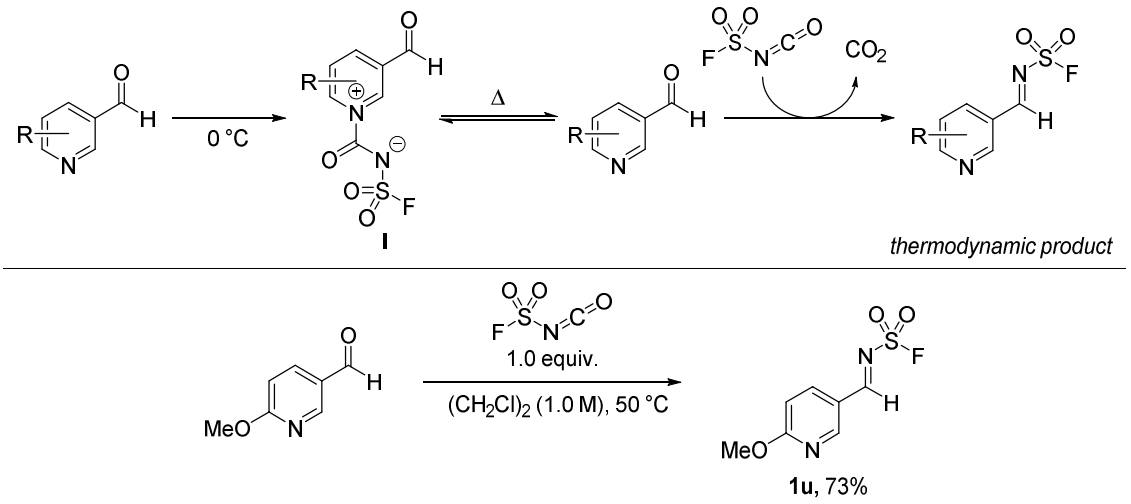
Sulfamoyl fluoride imines were first reported by Graf in 1963 and have been synthesised a handful of times in the 1960s and 1970s; however, their reactivity was never significantly explored and only hydrolysis and addition of phosphorus nucleophiles were reported and this imine has been largely ignored since.[139-141] Sulfamoyl fluoride imines are synthesised *via* condensation of sulfamoyl fluoride isocyanate with carbonyl compounds with extrusion of CO_2, the scope with regard to aromatic aldehydes has only been examined for benzaldehyde and *p*-tolylaldehyde.[141]

The first substrate we prepared was aldimine (**1a**), which was synthesised by a modified procedure from Jensen, and isolated in 93% yield (**Scheme 2-25A**).[141] Fluorosulfonyl isocyanate (FSI) was prepared by a halogen exchange reaction between SbF_3 and chlorosulfonyl isocyanate.[142] This method worked well for electron-rich and electron-neutral aldehydes, however, lower conversion was observed when an electron-poor aldehyde (for example 4-chlorobenzaldehyde) was employed. For these substrates it was found that elevated temperatures of 50 °C to 80 °C were required for full conversion of aldehydes. This is consistent with the mechanism of a disconcerted [2+2]-cycloaddition between the isocyanate and the aldehyde followed a retro cyclisation to extrude CO_2, whereby the rate limiting step is the addition of isocyanate to aldehyde (**Scheme 2-25B**).[143]



Scheme 2-25A The synthesis of **1a**. **B** Proposed mechanism for the condensation reaction between FSI and an aldehyde to form a sulfamoyl fluoride imine.

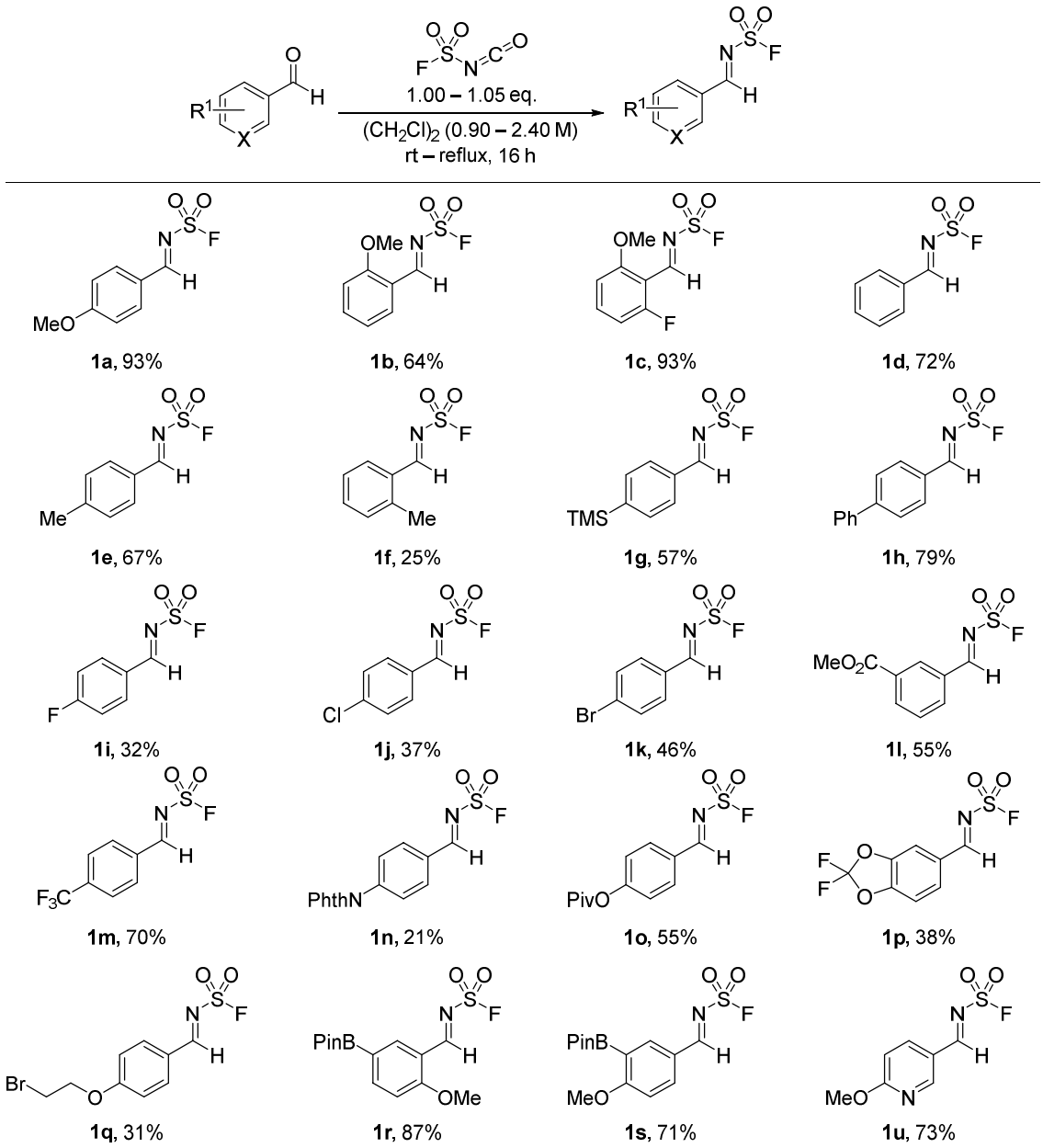
For the synthesis of heteroaromatic sulfamoyl fluoride imines there is the additional complication that at low temperature the Lewis basic nitrogen atom of the heterocycle forms a zwitterionic adduct **I** with FSI which, crashes out of the reaction mixture, as is the case with 6-methoxy-3-pyridinecarboxaldehyde.[144] However, the formation of this adduct is reversible at high temperature and upon further heating the zwitterionic adduct can decompose back to FSI and nucleophile, consistent with the reaction mixture becoming homogenous upon further heating. The liberated FSI can then undergo attack by the aldehydic oxygen to deliver the imine, as the final retro-[2+2] step is irreversible (**Scheme 2-26A**).[144] With this method it was possible to isolate **1u** in 73% yield (**Scheme 2-26B**).



Scheme 2-26A Proposed mechanism for the synthesis of heteroaromatic sulfamoyl fluoride imines. **B** Synthesis of **1u**.

One limitation of this route was that imines bearing amides could not be synthesised, as the amide would also react under these conditions to give amidines, producing a complicated mixture of products.

The imines synthesised, isolated and characterised in our study are given in **Scheme 2-27**, and details of the specific conditions to synthesise each imine substrate is given in **Chapter 5**. The reaction to synthesise the imines was relatively broad in scope, capable of tolerating electrophiles such as primary alkyl bromides **1q**, esters **1l** and **1o** and phthalimide **1n**. The pattern of substitution on the aromatic ring did not have a deleterious effect on whether the reaction was successful as ortho substituted imines **1b**, **1f** and **1r**, and di-ortho substituted imine **1c** were well tolerated, as well as para substituted imines (**1e**, **1i**, **1j** and **1m**), and meta substituted imines (**1l**, **1p**, **1r** and **1s**). In addition, electron-rich aldehydes, such as **1a** and electron deficient aldehydes **1m**, worked equally well in the transformation.



Scheme 2-27 Scope of imines synthesised and isolated in this study. (See **Chapter 5** for details of synthetic procedures.)

Almost all the imines synthesised were highly moisture sensitive and decomposed immediately upon exposure to either silica gel or alumina and therefore could not be purified by column chromatography. Instead, the compounds had to be either recrystalised or washed with the appropriate solvent to remove any remaining aldehyde or FSO_2NH_2. Many heteroaromatic imines synthesised were exceptionally moisture

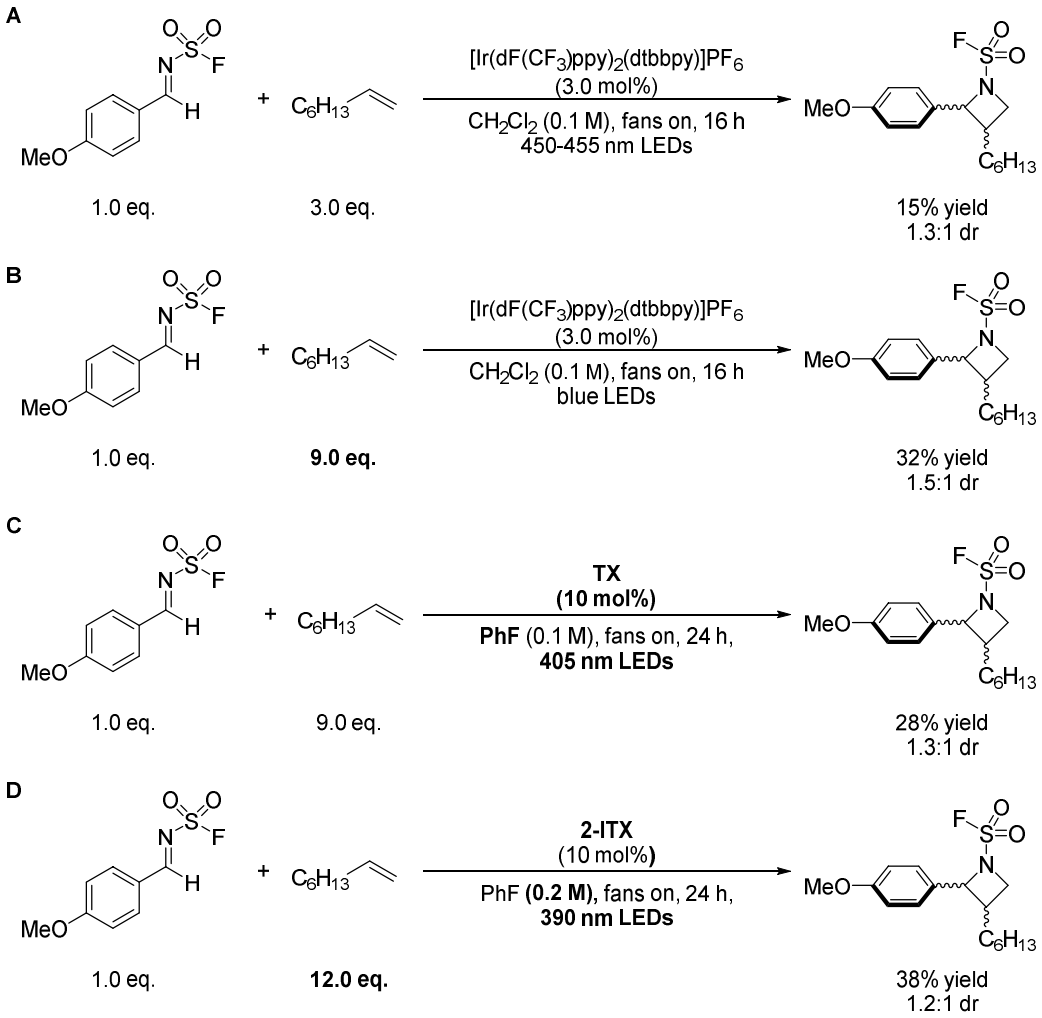
sensitive including **1v** and **1w**. These imines would hydrolyse upon standing in air in a matter of minutes. To mitigate this, these imines were generated *in-situ* and telescoped through to the photochemical step directly.

2.4 Optimisation of aza Paternò–Büchi Reaction

2.4.1 Preliminary Optimisation System

Initially, we attempted to optimise the aza Paternò–Büchi reaction between 1-octene and aldimine (**1a**), monitoring the diastereomeric ratio (dr) and yield using ^{1}H and ^{19}F NMR spectroscopy. After conducting the optimisation campaign and performing a preliminary scope of the transformation, we found that 1-octene was not a representative alkene for evaluating reaction performance. For completeness, and to provide a through line to the final conditions, the key findings are briefly summarised here.

First, we observed that the dr remained relatively constant throughout the optimisation, and none of the variables examined had a significant effect. Using an iridium photocatalyst and 450 – 455 nm blue light we found that increasing alkene loading from 3 to 9 equivalents increased the yield from 15% to 32 % (**Scheme 2-28A and B**). The reaction performed well in a variety of solvents, with fluorobenzene emerging as the best, at a 0.2 M concentration of the limiting aldimine and it was found that it was possible to use a cheaper, commercially available organophotocatalyst, thioxanthone (TX), along with 405 nm to get a similar yield of 28% (**Scheme 2-28C**). Swapping the organic photocatalyst to 2-isopropyl-thioxanthone (ITX) coupled with shorter 390 nm light, and increasing the alkene loading to 12 equivalents provided a 38% yield of the major regioisomer of (**E**) with a 1.3:1 dr (**Scheme 2-28D**). When the alkene was made the limiting reagent, the yield dropped precipitously.



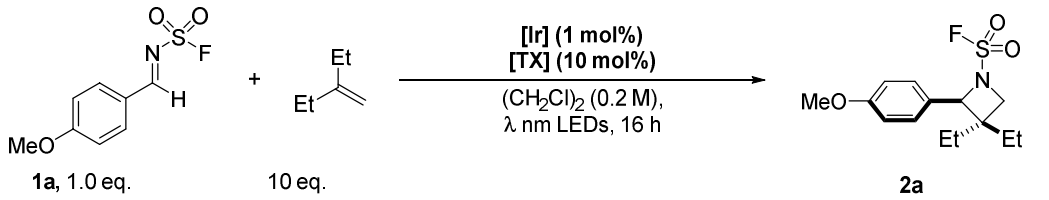
Scheme 2-28A Initial conditions for aza Paternò–Büchi reaction. **B** Increased alkene loading. **C** Organophotocatalytic conditions**. D** Final optimised conditions.

2.4.2 Optimisation with 1,1-Disubstituted Olefin

From the preliminary scope it was noted that 1,1-disubstituted alkenes performed particularly well in the transformation so we decided to use 3-methylene pentane to perform further optimisation studies. We started with a set of slightly modified conditions based on those developed for 1-octene, with two main changes. First, the solvent was changed to 1,2-dichloroethane as in some in cases a precipitate would form after the reaction and we found that when using 1,2-dichloroethane the reaction was homogenous throughout. Secondly, we lowered the alkene loading to ten equivalents.

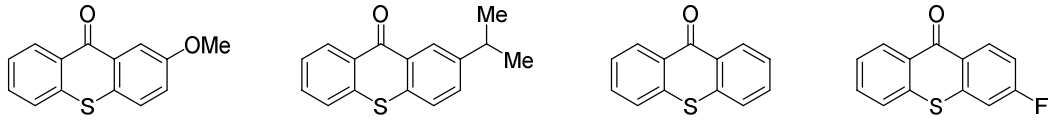
The first parameter we examined was the photocatalyst (**Table 2-1**). Generally, we found that photocatalysts with a triplet energy above ~60 kcal mol^{-1} delivered the product in >90% yield, with ITX, TX, 3-F-TX and $[Ir(dF(CF)_3ppy)_2(dtbbpy)][PF_6]$ (entries 3 – 5 and 7) all performing well. 3-F-TX performed the best with 97% spectroscopic yield and 94% isolated yield (entry 5); however, this photocatalyst is not yet commercially available, so we decided to use ITX moving forward, given the small difference in yield with ITX. The high performance of the Ir photocatalyst with blue LEDs represents a good alternative photocatalytic system and is useful if only access to blue LEDs (>400nm) is possible.

Using photocatalysts with lower triplet energies resulted in diminished yields, as in the case of 2-OMe-TX, where we observed a yield of 33% consistent with a reduced rate of energy transfer. The energy transfer process is likely endergonic and slow as a result of competitive back energy transfer.[68] In the case of *fac*-$Ir(ppy)_3$ there is no consumption of starting material and no product formed, which is consistent with energy transfer not being competitive with unproductive SET from the photocatalyst and subsequent BET from the imine. In the absence of a photocatalyst the reaction gives some product, showing that it is possible to access an excited state of the imine by absorption of a photon and reacting via either the singlet or triplet state, this is relatively inefficient as the excitation wavelength is very far from the maximum of the absorption spectrum of the imine (λ_{max} = 324 nm). Both of these two observations are consistent with a photoredox mechanism being unlikely under these conditions.



1a, 1.0 eq. 10 eq. **2a**

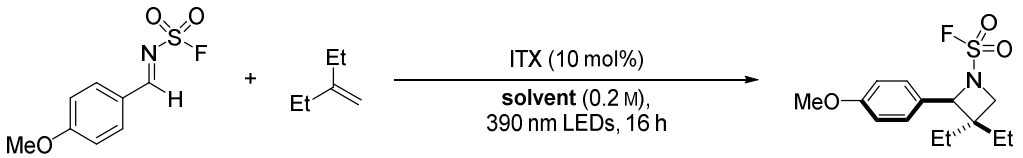
entry	photocatalyst	E_T / kcalmol^{-1}	λ / nm	SM remaining[a] / %	yield of 2a[a] / %
1	none	-	390	61	15
2	2-MeO-TX	57.8	390	38	33
3	ITX	63.5	390	0	94
4	TX	65.4	390	0	93
5	3-F-TX	67.4	390	0	97(94)
6	*fac*-Ir(ppy)$_3$	54.5	450-455	100	0
7	[Ir(dF(CF$_3$)ppy)$_2$(dtbbpy)][PF$_6$]	60.1	450-455	0	95



2-MeO-TX ITX TX 3-F-TX

Table 2-1 Photocatalyst evaluation; [a]Yields determined using ^{19}F NMR spectroscopy with 1,4-difluorobenzene as an internal standard. Structures of thioxanthone and thioxanthone derived photocatalysts below table.

The next parameter we examined was the reaction solvent (**Table 2-2**). Generally, polar solvents worked well for this transformation (entries 1 – 4 and 6). Solvents containing weak hydridic C-H bonds such as DMF and THF led to significantly diminished yields, potentially as result of HAT from the electrophilic *N*-centred unpaired electron (entries 5 and 7). Apolar solvents were not investigated as the imine was not soluble in these.

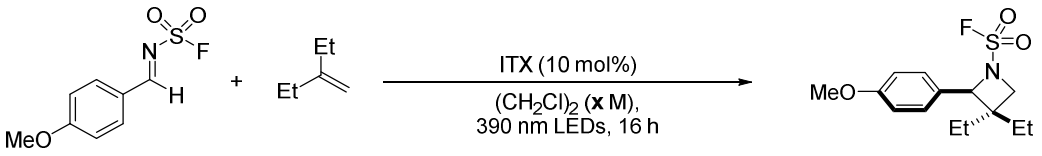


1a, 1.0 eq. 10 eq. **2a**

entry	solvent	SM remaining[a] / %	yield of 2a[a] / %
1	$(CH_2Cl)_2$	0	94
2	CH_2Cl_2	0	92
3	MeCN	0	82
4	EtOAc	0	85
5	DMF	0	39
6	PhF	0	94
7	THF	0	50

Table 2-2 Screening of solvents. [a]Yields determined using ^{19}F NMR spectroscopy using 1,4-difluorobenzene as an internal standard

The next parameter investigated was concentration (**Table 2-3**). Here we found that either increasing or decreasing the concentration (entries 1 and 3) of the reaction from 0.2 M led to a small decrease in the yield of the transformation, thus the 0.2 M concentration was maintained (entry 2).

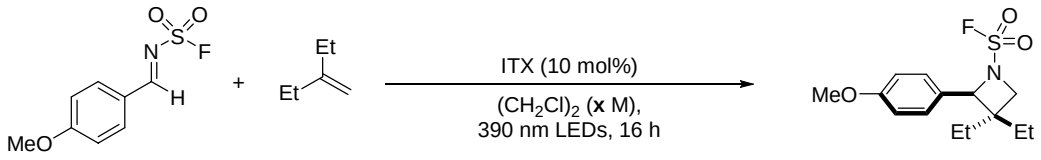


1a, 1.0 eq. 10 eq. **2a**

entry	concentration / M	SM remaining[a] / %	yield of 2a[a] / %
1	0.1	0	92
2	0.2	0	94
3	0.4	0	91

Table 2-3 Screen of concentration. [a]Yields determined using ^{19}F NMR spectroscopy using 1,4-difluorobenzene as an internal standard

The next parameter we investigated was alkene loading (**Table 2-4**), whereby we found that upon lowering the alkene loading to 5 or 3 equivalents we observed a small progressive increase in the yield to 98% and 100%, respectively (entries 1 – 3). Further reducing the alkene loading to 1 equivalent led to a decrease in the yield to 70% (entry 4); a stark contrast to what we had observed for exocyclic alkenes. This result was not general to other classes of alkene, and even very closely related exocyclic 1,1-disubstituted alkenes including methylenetetrahydro-2H-thiopyran 1,1-dioxide required high loadings (**21**) (**Table 2-5**).



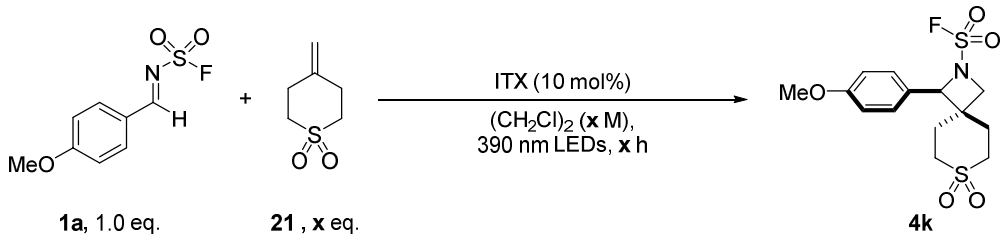
1a, 1.0 eq. 10 eq. **2a**

entry	alkene loading / eq.	SM remaining[a] / %	yield of 2a[a] / %
1	10	0	94
2	5.0	0	98
3	3.0	0	100
4	1.0	0	70

Table 2-4 Evaluation of alkene loading. [a]Yields determined using ^{19}F NMR spectroscopy using 1,4-difluorobenzene as an internal standard

The first set of conditions are based on those from the optimisation campaign for another exocyclic cyclobutene, 3-methylenecyclobutane-1-carbonitrile, which is omitted here for brevity. The key finding was that in this system, an alkene loading of 7.5 equivalents was required for the optimum yield. However, when these conditions were applied to alkene **21,** we observed only 50% of the azetidine product and 24% of the starting material remaining (entry 1). When increasing the loading to 10 equivalents the yield improved to 61% with only 2% starting material remaining (entry 2). In order to lower the loading of

alkene, we hypothesised that if we could keep the concentration of alkene the same but increase the total reaction concentration we could achieve the same effect; however we observed similar results as before, with a significant amount of starting material remaining (25%) (entry 3). Concentrating the reaction and lowering the alkene loading further to 4 equivalents reduced the yield of the reaction from 44% to 36% but improved the overall mass balance (entry 4). The reaction time was increased to 3 days to allow the reaction to go to completion and we achieved a comparable 57% yield (entry 5). Halving the photocatalyst loading to 5 mol% decreased the yield slightly to 54% (entry 6).

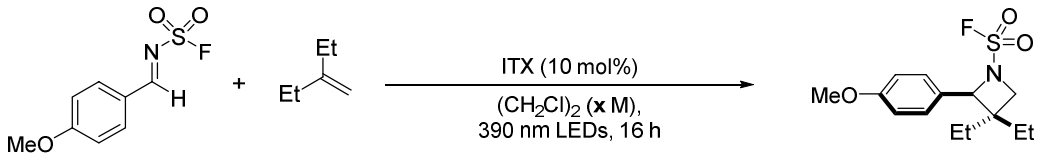


entry	alkene loading / eq.	concentration / M	time / h	SM remaining[a] / %	yield of 4k[a] / %
1	7.5	0.2	16	24	50
2	10	0.2	16	2	61
3	5.0	0.4	16	25	44
4	4.0	0.5	16	50	36
5	4.0	0.5	72	0	57
6[b]	4.0	0.5	72	0	54

Table 2-5 Evaluation of alkene loading, concentration and time of a cyclic alkene. [a]Yields determined using ^{19}F NMR spectroscopy using 1,4-difluorobenzene as an internal standard. [b]5 mol% of ITX employed

In cases where the alkene starting material is precious it is possible to run the reaction longer and achieve a similar result to using increased alkene loading, alternatively we later demonstrate that at different loadings, any unreacted alkene can be recovered. Moving forward we decided to use 10 equivalents of alkene as this represented the most general set of conditions and allowed for shorter reaction times.

To conclude the optimisation studies, we performed some control reactions and firstly showed that the yield drops to 15% (entry 2) when the photocatalyst is removed as discussed earlier (**Table 2-6**). Running this reaction in the dark resulted in no consumption of the starting material and no product (entry 3), and finally we showed that no product was formed under thermal conditions rather than photochemical conditions (entry 4).

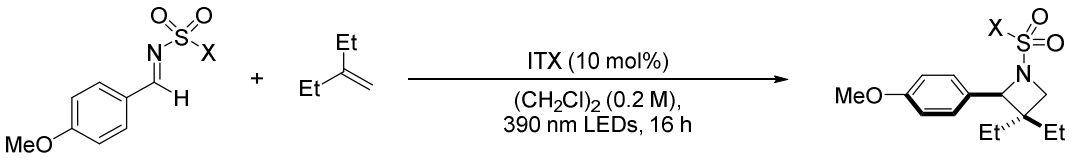


1a, 1.0 eq. 10 eq. **2a**

entry	variations from conditions above	SM remaining[a] / %	yield of 2a[a] / %
1	none	0	94
2	no ITX	61	15
3	no light	100	0
4	no light, no ITX and 80 °C	68	0

Table 2-6 Control experiments. [a]Yields determined using 19F NMR spectroscopy using 1,4-difluorobenzene as an internal standard.

With a set of optimised conditions for the aza Paternò–Büchi reaction we wanted to re-examine other sulfonyl aldimines and see if this reactivity was limited to the -SO_2F group (**Table 2-7**). As expected, the tosyl aldimine (entry 1) did not yield any product and fully decomposed under photochemical conditions producing a complex reaction profile. However, the triflyl aldimine (**1x)** did give 56% yield of the corresponding azetidine (**2x**). These results suggest that in order for a substrate to be successful in the aza Paternò–Büchi reaction, the nitrogen atom of the aldimine must bear an extremely electron-withdrawing group in order to be sufficiently electrophilic.



entry	X	SM remaining[a] / %	yield[a] / %
1	4-MePh	0	0
2	CF_3	0	56
3	F	0	94

Table 2-7 Scope of alternative imines. [a]Yields determined using $^1H/^{19}F$ NMR spectroscopy using 1,4-difluorobenzene as an internal standard.

Before embarking on a full-scale scoping study, a preliminary scope was conducted using ITX as catalyst with a small range of electronically diverse imines (**Table 2-8**). Both ITX and 3-F-TX performed well with the electron-rich para-methoxy substituted imine (**1a**), yielding 91% and 94%, respectively. However, for the electron-neutral phenyl imine (**1d**), ITX gave a 15% lower yield of azetidine **2d** compared to 3-F-TX. The difference in performance between the two catalysts was even more pronounced with the electron-deficient *p*-CF_3 imine (**1m**), where a more than 40% decrease in yield of **2m** was observed. Both photocatalysts have similar triplet energies (E_T(3-F-TX) = 67.4 kcal mol^{-1} vs E_T(ITX) = 63.6 kcal mol^{-1}).[145] However, given that more electron-deficient imines performed worse, we hypothesised that for ITX, single electron reduction was competitive with energy transfer in these substrates. In contrast, for 3-F-TX, the electronegative fluorine destabilises the resulting radical cation formed upon reduction of the imine, reducing the magnitude of the reduction potential. Therefore, to have a method that was more general with respect to the imine we swapped to the 3-F-TX photocatalyst.

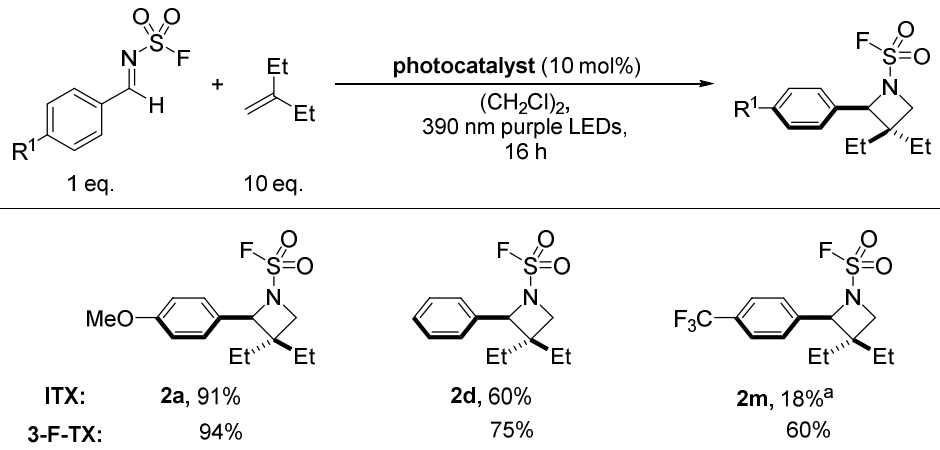


Table 2-8 Preliminary scope comparing photocatalyst 3-F-TX and ITX. Reaction conditions: imine (0.20 mmol, 1.0 eq.), alkene (2.0 mmol, 10 eq.), $(CH_2Cl)_2$ (0.20 M) and photocatalyst (0.020 mmol, 0.10 eq.), 390 nm irradiation, 16 h. Isolated yields. [a]Yields determined using ^{19}F NMR spectroscopy relative to 1,4-difluorobenzene as an internal standard.

2.5 Scope of aza Paternò–Büchi Reaction

2.5.1 Imine Scope

With optimized conditions for the aza Paternò-Büchi reaction in hand, we first proceeded to assess the generality with respect to the imine component. Pleasingly, we were able to observe good yields of azetidine regardless of the electronics of the aryl imine with a variety of substitution patterns, often proceeding in excellent yields. Sterically encumbered substrates could also be incorporated, with a number of bulky substituents successfully placed on the azetidine ring in spite of the proximity to a quaternary carbon (**2b**, **2c**, **2f**, **2r**, **2v**, **2w**). Example **2f** is of note as like the parent aldehyde, [2+2]-photocycloaddition is competitive with the Norrish-Yang cyclisation and the benzocyclobutylamine was not observed.[146, 147] The mild nature of the conditions is highlighted by the tolerance of a range of sensitive functionalities including a selection of esters (**2l**, **2o**), primary alkyl bromides (**2q**), and boronic esters (**2r**-**2t**), which would likely not survive traditional basic conditions for forming azetidines *via* S_N2 processes [17]. Alongside imines derived from arenes, a range of heteroaromatic imines can also be

successfully employed, including pyridines (**2t**, **2u**) which provide access to 4-membered derivatives of nicotine, as well as pyrimidines and pyrimidones (**2v**, **2w**).

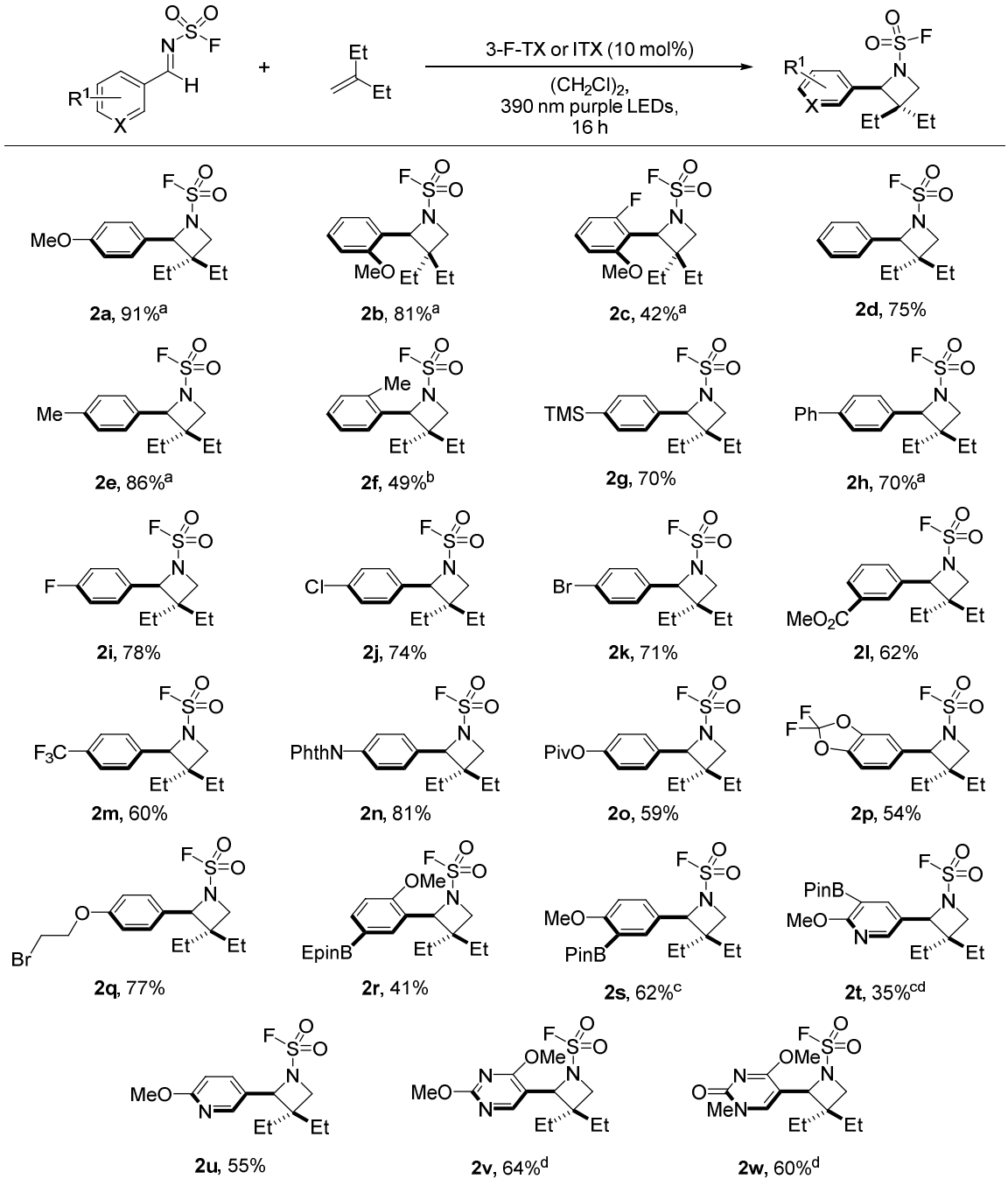


Table 2-9 Scope of the imine. Reaction conditions: imine (0.20 mmol, 1.0 equiv.), alkene (2.0 mmol, 10 equiv.), $(CH_2Cl)_2$ (0.20 M) and 3-F-TX (0.020 mmol, 0.10 equiv.), 390 nm irradiation, 16 h. Isolated yields. [a]ITX used as photocatalyst. [b]3 equiv. alkene used. [c]Isolated as the corresponding phenol.

To confirm that we were indeed forming azetidines, single crystals suitable for an X-ray diffraction (XRD) were obtained for compound **2h** (CCDC 2375437) which supported the assignment by NMR spectroscopy and mass spectrometry.

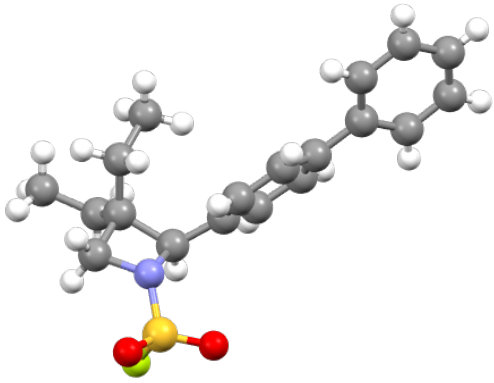


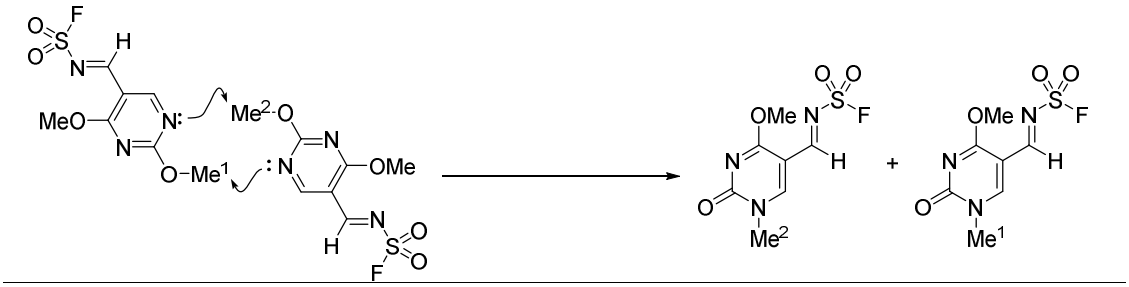
Figure 2-1 X-ray crystal structure of **2h**.

As a result of their hydrolytic sensitivity, heteroaromatic imines leading to azetidines **2t**, **2v**, and **2w** were not isolated, and were instead synthesised in situ using a telescoped procedure. Boronic ester **2s** and **2t** were further elaborated to the corresponding phenol for ease of purification. Products **2v** and **2w** are both derived from the same starting material, 2,4-dimethoxypyrimidine carbaldehyde (**36**); however, by modifying the conditions used to synthesise the imine, we were able to selectively form either the pyrimidine (**2v**) or pyrimidone (**2w**) substituted azetidine.

When 2,4-dimethoxypyrimidine carbaldehyde was first implemented using the standard telescoped procedure, we were surprised to find that two azetidine products were formed in the reaction. From the ^{1}H NMR spectrum of the reaction, we proposed that one product resulted from a [2+2] photocycloaddition of the pyrimidine imine with the alkene, while the other arose from a [2+2] photocycloaddition with a rearranged imine, which now

contained two vastly different CH_3 environments and a significantly shielded aromatic proton. This is consistent with our attempt to synthesise 2,4-dimethoxypyrimidine sulfamoyl imine, where the product hydrolysed upon standing, and another aldehyde product was observed.

We hypothesised that one of the methyl groups from the methoxy group migrated from oxygen onto one of the nitrogen atoms to form a pyrimidone, and that this transposition occurred thermally during the imine formation *via* the Hilbert–Johnson reaction, rather than photochemically (**Scheme 2-29**).[148] To access the pyrimidone-substituted azetidine in high yield, we needed to accelerate the Hilbert–Johnson reaction. Therefore, the imine synthesis was performed at a higher temperature and concentration to favour the intermolecular rearrangement.



Scheme 2-29 Mechanism for the Hilbert-Johnson reaction of 2,4-dimethoxypyrimidine imine.

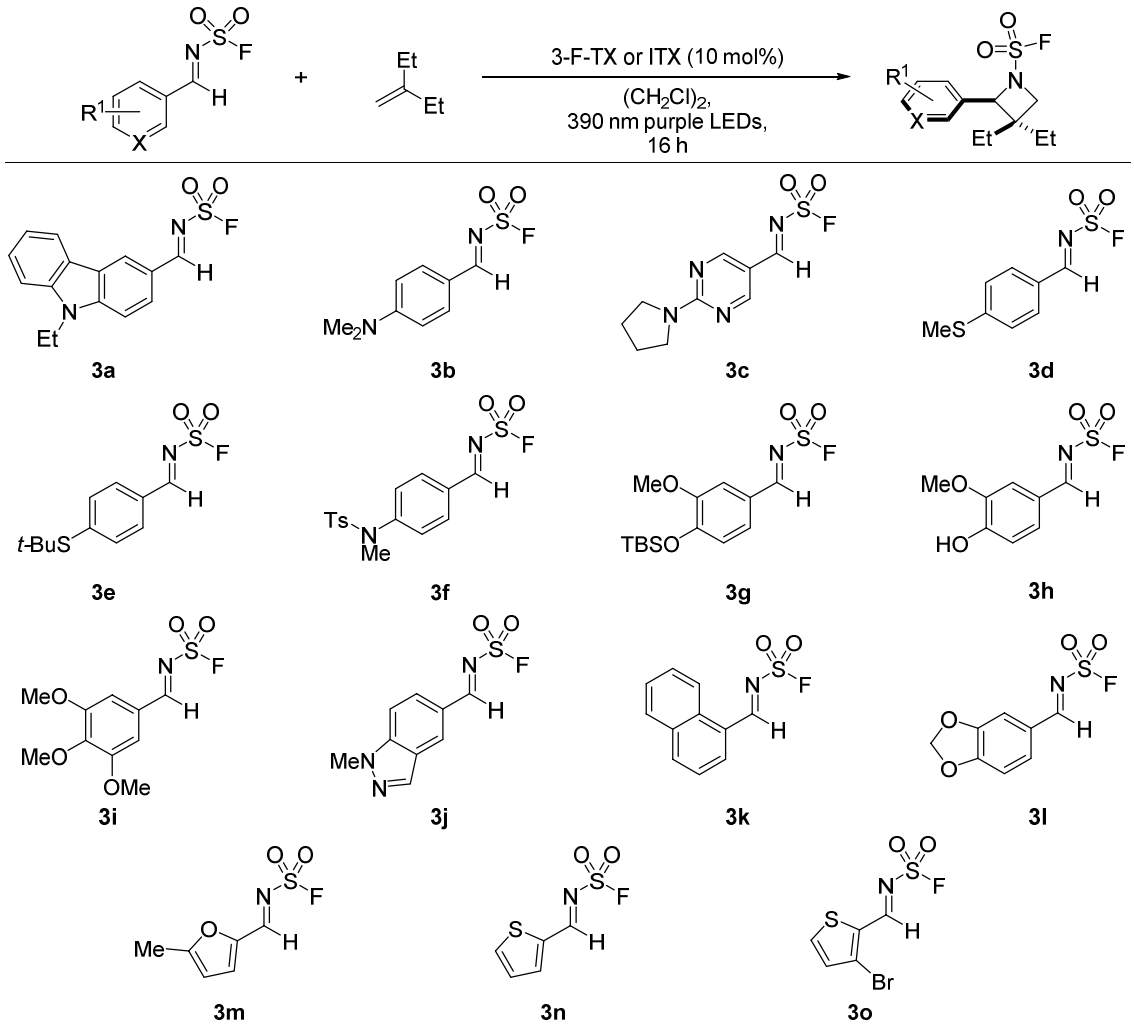
Pleasingly, this proved effective, as we were able to obtain the pyrimidone azetidine **2w** exclusively in 60% yield. Reducing the temperature of the imine synthesis to 55 °C and diluting the reaction to 0.2 M suppressed the Hilbert–Johnson reaction, yielding the pyrimidine imine and providing azetidine **2v** in 64% yield.

The figure below summarises the imines that were unsuccessful in the transformation giving either little or no azetidine product (**Scheme 2-30**). When 4-*N* aldimines **3a–c** were subjected to our conditions full recovery of starting material was observed. One possible

explanation could be that the lifetime of the triplet excited state is not long enough to permit intermolecular reactivity, as these types of donor-acceptor imines can undergo rapid intersystem crossing through intramolecular charge transfer.[149]

When sulfide imines **3d** and **3e** were employed the reaction yield was poor (<20%) and there was still significant starting material remaining. In both cases the reaction profiles were complicated as there were imidic ^{1}H signals in the ^{1}H NMR spectrum, likely a result of the imine rearranging under photochemical conditions, most likely through cleavage of the C-S bond. For the *t*-Bu sulfide, both imines were competent in the aza Paternò–Büchi reaction, as two azetidine products were observed in the NMR spectra. In contrast, only one product was observed when the Me sulfide imine was used. Scission of the weak N—S bond in substrate **3f** was observed, as it was possible to isolate the N-H imine following the reaction.

When particularly electron-rich aldimines, **3g**, **3h** and **3i** were employed the reactions typically proceeded with low conversion and in the case of **3i** only the indane product was observed (see **section 2.7**). Bicyclic indazole **3j**, 1-naphthyl **3k** and 1,3-benzodioxole **3l** imines resulted in complete degradation of starting material with no product formed. 5-membered rings were also not well tolerated resulting in complete degradation, shown in the cases of methylfuran **3m** and thiophene imines **3n** and <20% for 3-bromothiophene **3o**.



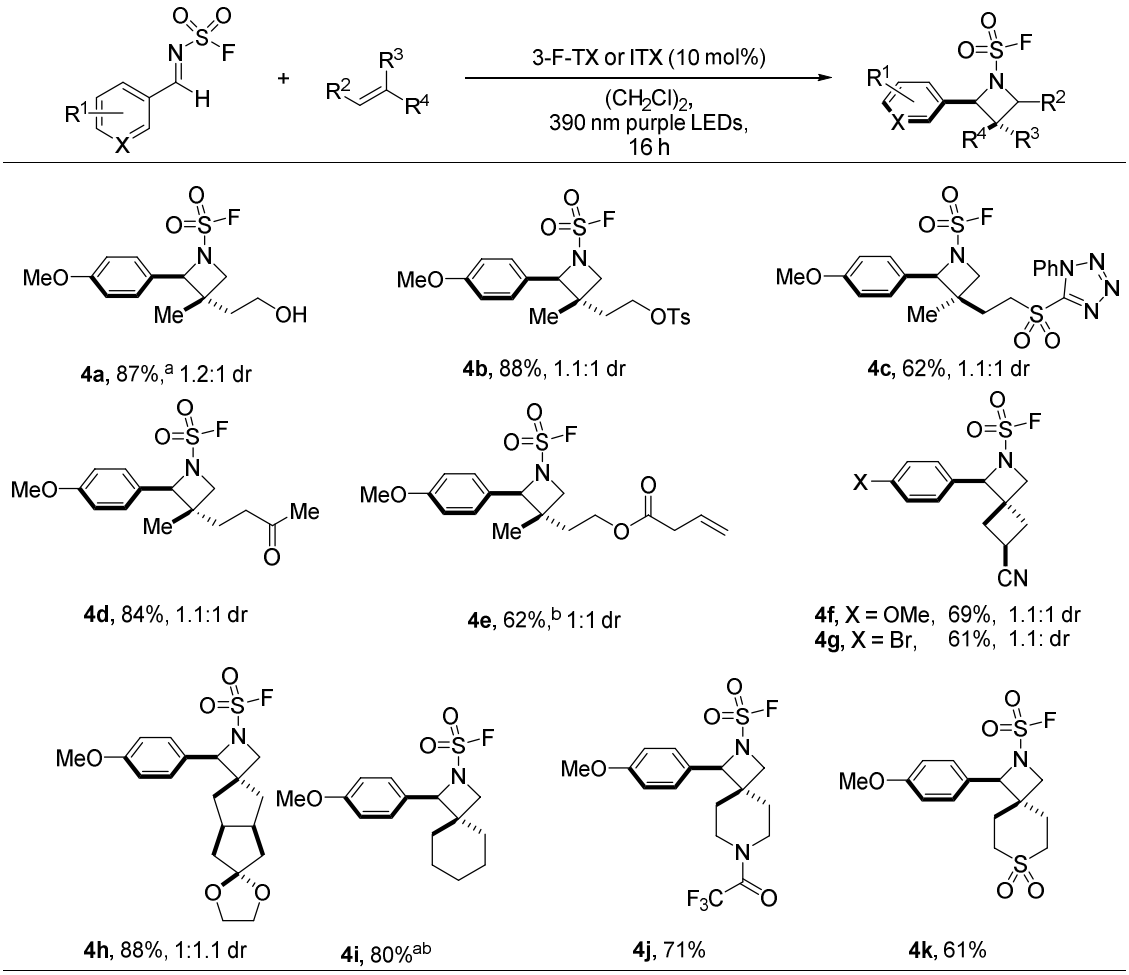
Scheme 2-30 Unsuccessful imine substrates.

2.5.2 Alkene Scope

We then investigated the scope of the transformation with respect to the alkene component was performed in collaboration with my colleague Dr. Nicholas A. Parker, the compounds synthesised by Dr. Nicholas A. Parker are clearly indicated. First, we looked at a number of acyclic 1,1-dialkyl substituted olefins varying the functional group appended to the alkene, to investigate the functional group tolerance of the photochemical conditions (**Scheme 2-31**). Pleasingly, the reaction proceeded in excellent yields whilst tolerating a range of sensitive nucleophilic groups such as alcohol **4a** and electrophilic reactive handles including tosylate **4b**, methyl-ketone **4d** and sulfonyl tetrazole **4c**, the

latter of which may be labile under photoredox conditions.[150, 151] For the sulfonyl tetrazole example we demonstrated that it is possible to lower the loading of alkene to 3 equivalents and recover 64% of the alkene used. Also, for the substrate **4e** that feature two different alkenes, the reaction occurs exclusively at the 1,1-disubstituted olefin over the terminal alkene.

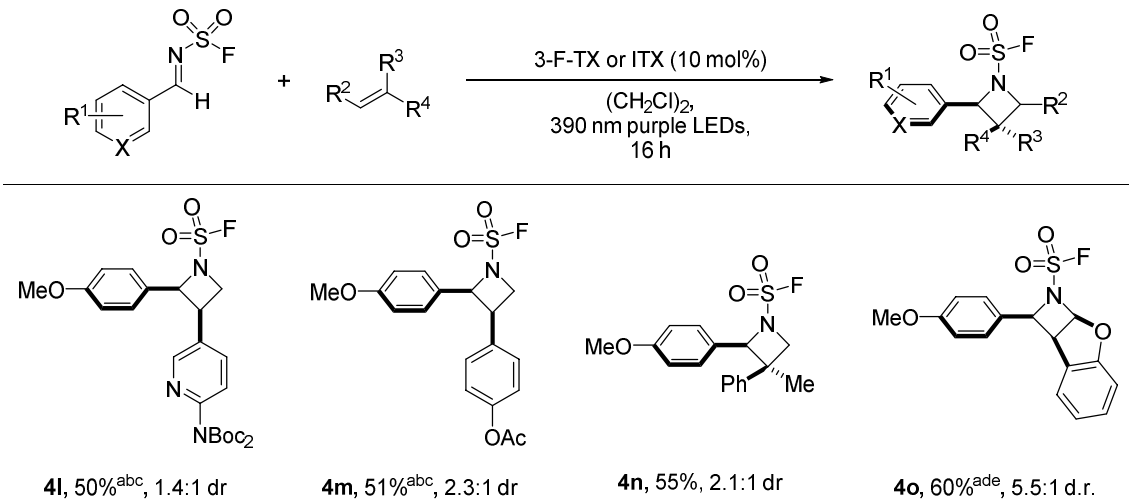
When exocyclic 1,1-disubstituted alkenes were employed, we could generate a range of spirocyclic azetidines **4f–k**, which are attractive, 3D scaffolds that often require laborious multistep sequences to prepare.[152-154] Here we demonstrate it was possible to vary the size of the spirocyclic ring and introduce heteroatoms whilst maintaining very good to excellent yields across all substrates. For **4k** we showed that it was possible to isolate and recover 85% (8.5 equivalents of the alkene relative to the imine) of the olefin. Across the 1,1-disubstituted alkene scope we observed poor diastereoselectivity, in part due to the alkyl substituents on the alkene being similar in size. Hence making it difficult to discriminate between the diastereomers. In the case of the exocyclic alkenes, this is also due to the stereocentre being far away from the reactive centre of the molecule.



Scheme 2-31 Scope of 1,1-dialkyl alkenes. Reaction conditions: imine (0.20 mmol, 1.0 equiv.), alkene (2.0 mmol, 10 equiv.) and 3-F-TX (10 mol%) in $(CH_2Cl)_2$ (0.20 M), 390 nm irradiation, 16 h, isolated yields of both diastereomers. Diastereomeric ratios were determined by ^{19}F NMR spectroscopic analysis of the crude reaction mixture. [a]10 mol% ITX used as photocatalyst. [b]Reaction performed by Dr. Nicholas A Parker.

Next, we looked at a series of conjugated alkenes (**Scheme 2-32**). Under our developed conditions it was possible to employ styrenes (**4l** and **4m**) as a coupling partner, however, typically only in moderate yields, and full conversion was only achieved when using extended reaction times of 3 days. The complications that arise are likely a result of styrenes possessing a lower triplet energy than the aldimines employed resulting in styrene performing as a more efficient quencher.[155, 156] The competitive quenching not only slows down the desired transformation but the triplet styrene is also reactive under these conditions, resulting in the formation of large amounts of cyclobutane homodimer

and the opposite regioisomer as a minor product, further complicating purification of the product. α-Methyl styrene performed better (**4n**), as no homodimerisation of the alkene was observed and an extended reaction time was not required to achieve full conversion. Benzofuran could also be employed as a coupling partner to deliver a dearomative [2+2]-photocyclisation product **4o** in good yield, however in this case only the major diastereomer could be obtained as the minor diastereomer decomposed during purification on silica gel. The diastereoselecitivity observed for these alkenes is modest at <2.3:1 dr with the exception of the bicyclic benzofuran substrate **4o** imparting higher diastereoselectivitiy due to the bicyclic structure displaying a preference for all-*syn* bowl shaped diastereomer.



Scheme 2-32 Scope of aromatic conjugated alkenes. Reaction conditions: imine (0.20 mmol, 1.0 equiv.), alkene (2.0 mmol, 10 equiv.) and 3-F-TX (10 mol%) in $(CH_2Cl)_2$ (0.20 M), 390 nm irradiation, 16 h, isolated yields of both diastereomers. Diastereomeric ratios were determined by ^{19}F NMR spectroscopic analysis of the crude reaction mixture. [a]10 mol% ITX used as photocatalyst [b]Yield determined by ^{19}F NMR relative to 1,4-dFPh. [c]Reaction times 3 days. [d]Isolated yield of a single diastereomer. [e]Reaction performed by NAP.

To confirm the relative configuration of **4o**, single crystals suitable for an X-ray diffraction (XRD) were obtained (CCDC 2375438) which confirmed our assignment (**Figure 2-2**).

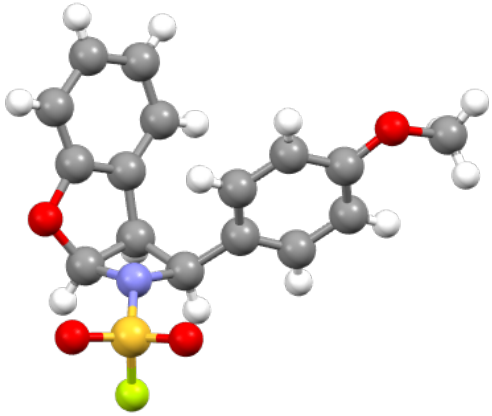


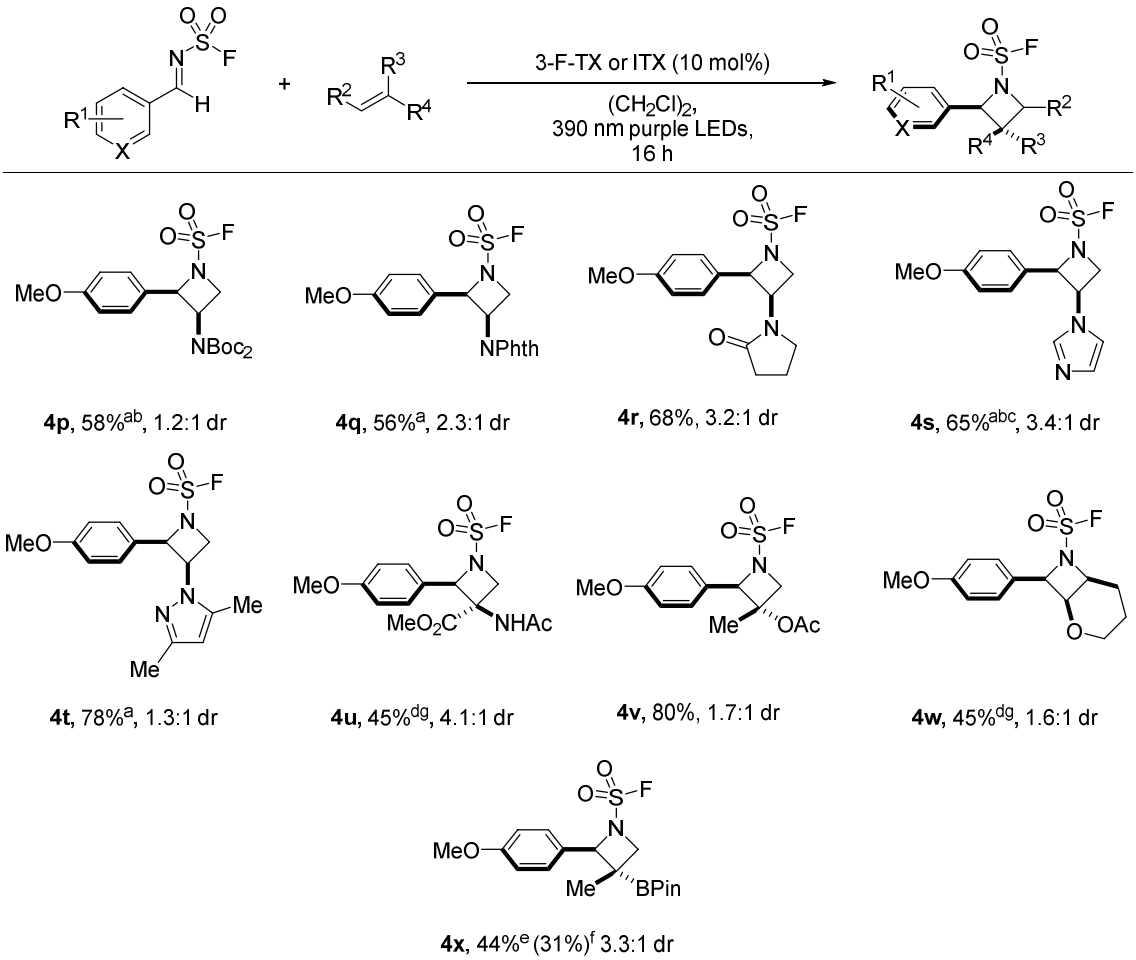
Figure 2-2 X-ray structure of **4o**.

A diverse range of different heteroatom substituted olefins could be successfully employed in the transformation (**Scheme 2-33**).

Doubly protected enamides performed well to deliver nitrogen-substituted azetidines **4p** and **4q** in good to moderate yields. Using our initial conditions for **4p** led to a complicated reaction profile and a lower yield of 30%; analysis of the crude reaction mixture by ^{1}H NMR spectroscopy was indicative of significant polymerisation of the 1,4-biradical. In order to attenuate this side reaction, we employed 10 mol% of 2,2'-dithiodipyridine as an inhibitor to prevent intermolecular reactivity and promote the desired azetidine formation.[84]

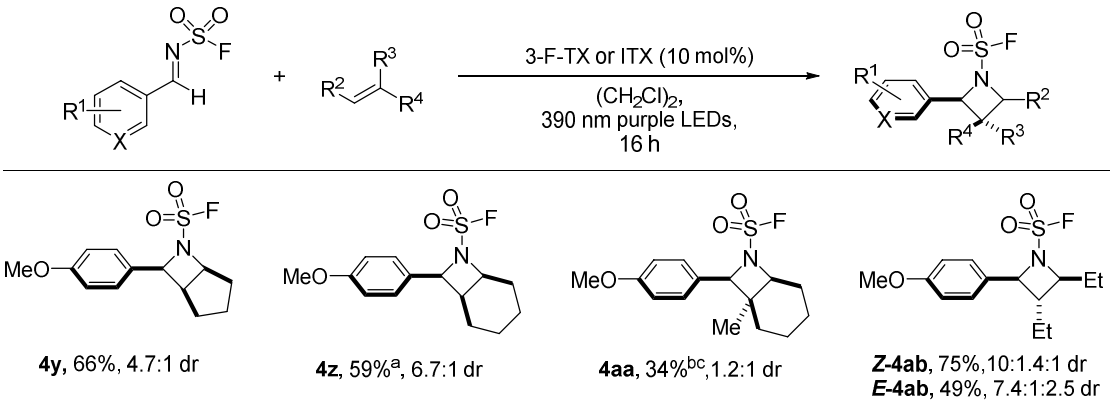
Next, we demonstrated we could employ a range of vinyl heterocycles including: 2-pyrrolidinone (**4r**), imidazole (**4s**), this example also benefitting from addition of 2,2'-

dithiodipyridine), and pyrazole (**4t**), the latter representing an azetidine derivative of Baricitinib. The dehydroalanine derived product **4u** displayed a relativley good dr, potentially as a result of intramolecular hydrogen bonding stabilising the productive conformation of the 1,4-biradical intermediate. Oxygen containing alkenes could also be employed in the transformation to deliver tertiary ester **4v** and fused cyclic ether **4w** in 80% and 45% yields, respectively.



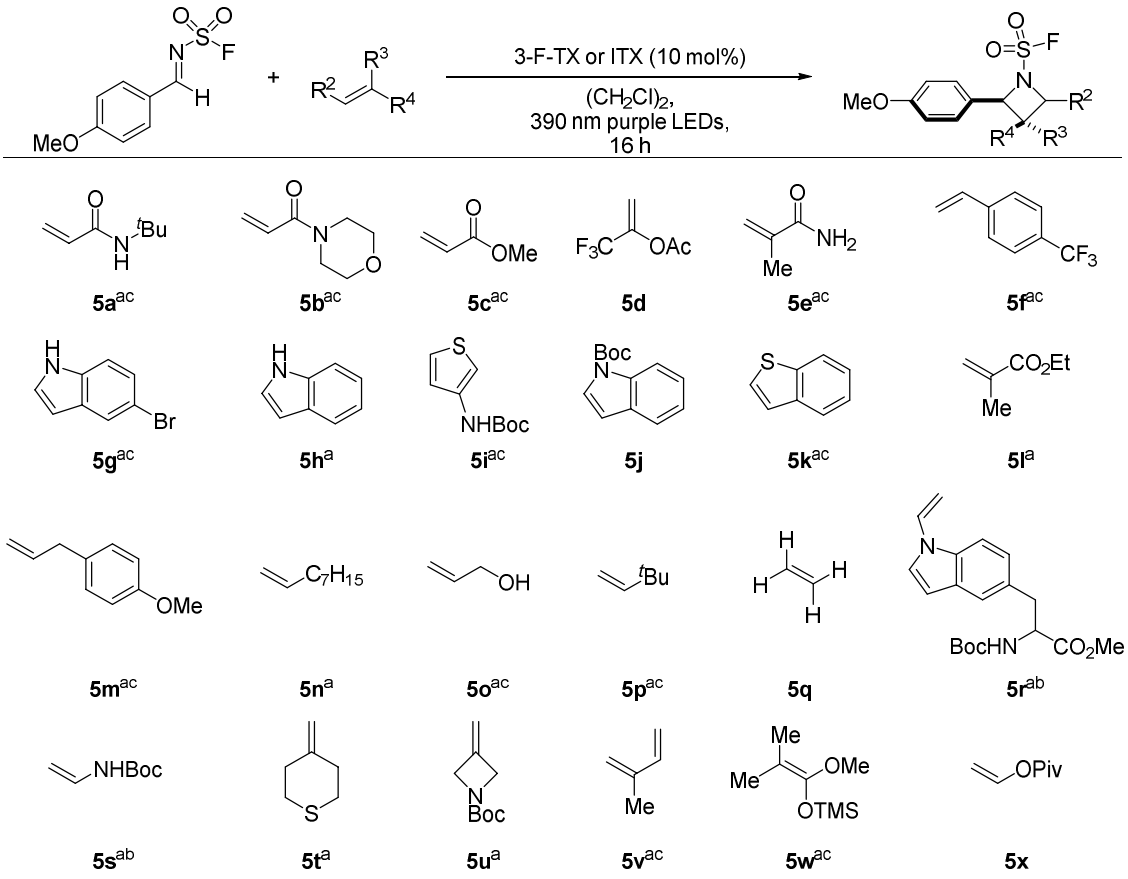
Scheme 2-33 Scope of heteroatom substituted alkenes. Reaction conditions: imine (0.20 mmol, 1.0 equiv.), alkene (2.0 mmol, 10 equiv.) and 3-F-TX (10 mol%) in $(CH_2Cl)_2$ (0.20 M), 390 nm irradiation, 16 h, isolated yields of both diastereomers. Diastereomeric ratios were determined by ^{19}F NMR spectroscopic analysis of the crude reaction mixture. [a]3 equiv. of alkene used. [b]Aldrithiol-2 (5 mol%) added. [c][Ir(dFCF$_3$ppy)$_2$dtbbpy][PF$_6$] (1 mol%) and 427 nm LEDs [d]10 mol% ITX used as photocatalyst. [e]Yield determined by ^{19}F NMR spectroscopy relative to 1,4-dFPh. [f]Yield of alcohol after oxidative workup. [g]Reaction performed by NAP.

The final class of alkenes investigated were 1,2-disubstituted and tri substituted alkyl alkenes (**Scheme 2-35**). Employing 1,2-disubstituted cyclic alkenes delivered fused bicyclic azetidines **4y** and **4z** in good yields with good dr's yet trisubstituted olefins were not as successful, delivering only a moderate yield and dr of azetidine **4aa**. Acyclic 1,2-disubstituted olefins could also be utilised to synthesise trisubstituted azetidines and pleasingly in this case it was possible to isolate the major diastereomer from the mixture of three diastereomers (***E*- and *Z*- 4ab**). When both *E*- and *Z*- stereoisomers of hex-3-ene were used the reaction produces the same major diastereomer, demonstrating that during the reaction the stereochemical information of the starting material is lost. This is evidence of the reaction proceeding through the triplet state consistent with the formation of an intermediate 1,4-biradical that is capable of free rotation. However, it is worth noting that the *E*- and *Z*-isomers gave different yields and non-identical diastereomeric distribution. The discrepancy in yield can be rationalised by the *Z*- alkene being more reactive due to strain-release upon addition. The difference in distribution of diastereomers may be that even though there is scrambling of stereochemical information in the intermediate 1,4-biradical the lifetime of this reactive intermediate is not long enough to enable full equilibration of between all accessible conformers.



Scheme 2-34 Scope of 1,2- and tri- substituted alkenes. Reaction conditions: imine (0.20 mmol, 1.0 equiv.), alkene (2.0 mmol, 10 equiv.) and 3-F-TX (10 mol%) in $(CH_2Cl)_2$ (0.20 M), 390 nm irradiation, 16 h, isolated yields of both diastereomers. Diastereomeric ratios were determined by ^{19}F NMR spectroscopic analysis of the crude reaction mixture. [a]Isolated yield of a single diastereomer. [b]10 mol% ITX used as photocatalyst. [c]Reaction performed by NAP.

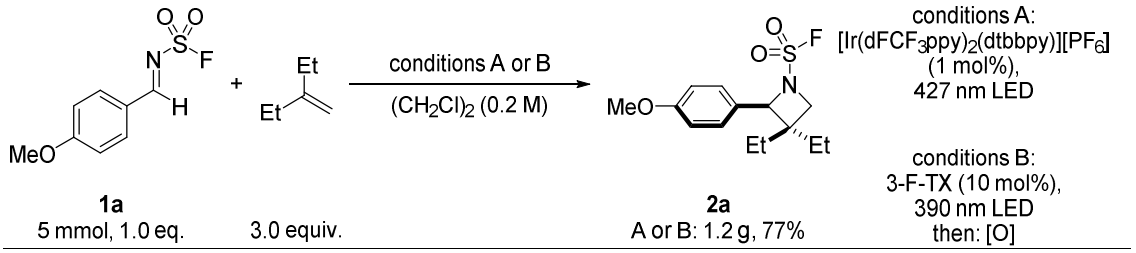
During our study we encountered a number of alkene examples that did not perform well in the azetidine formation (**Scheme 2-35**). Olefins bearing electron-withdrawing groups (**5a–f**) and heterocycles (**5g–k**) did not engage with the triplet imine and deliver product. Ethyl methacrylate (**5l**) gave a moderate yield of the major diastereomer, however, the minor diastereomer was inseparable from both diastereomers of the minor regioisomer. Mono-alkyl alkenes (**5m–p**) were also too unreactive and not electronically biased enough to deliver satisfactory yields of azetidine. Running the reaction under an atmosphere of ethylene (**5q**) did not deliver the product. *N*-vinyl tryptophan derivative (**5r**) and *N*-Boc vinyl enamide (**5s**) performed poorly likely due to competitive oligomerisation even with the addition of an inhibitors. 1,1-disubstituted olefins bearing weak C-H groups (**5t and 5u**) also did not give the product, likely a result of competitive HAT. Alkenes **5v**, **5w** and **5x** also all performed poorly



Scheme 2-35 Poor yielding substrates. Reaction conditions: imine (0.20 mmol, 1.0 equiv.), alkene (2.0 mmol, 10 equiv.) and 3-F-TX (10 mol%) in $(CH_2Cl)_2$ (0.20 M), 390 nm irradiation, 16 h [a]10 mol% ITX used as photocatalyst. [b]3 equiv. of alkene used. [c]Reaction performed by NAP.

2.6 Derivatisation and Scale-Up

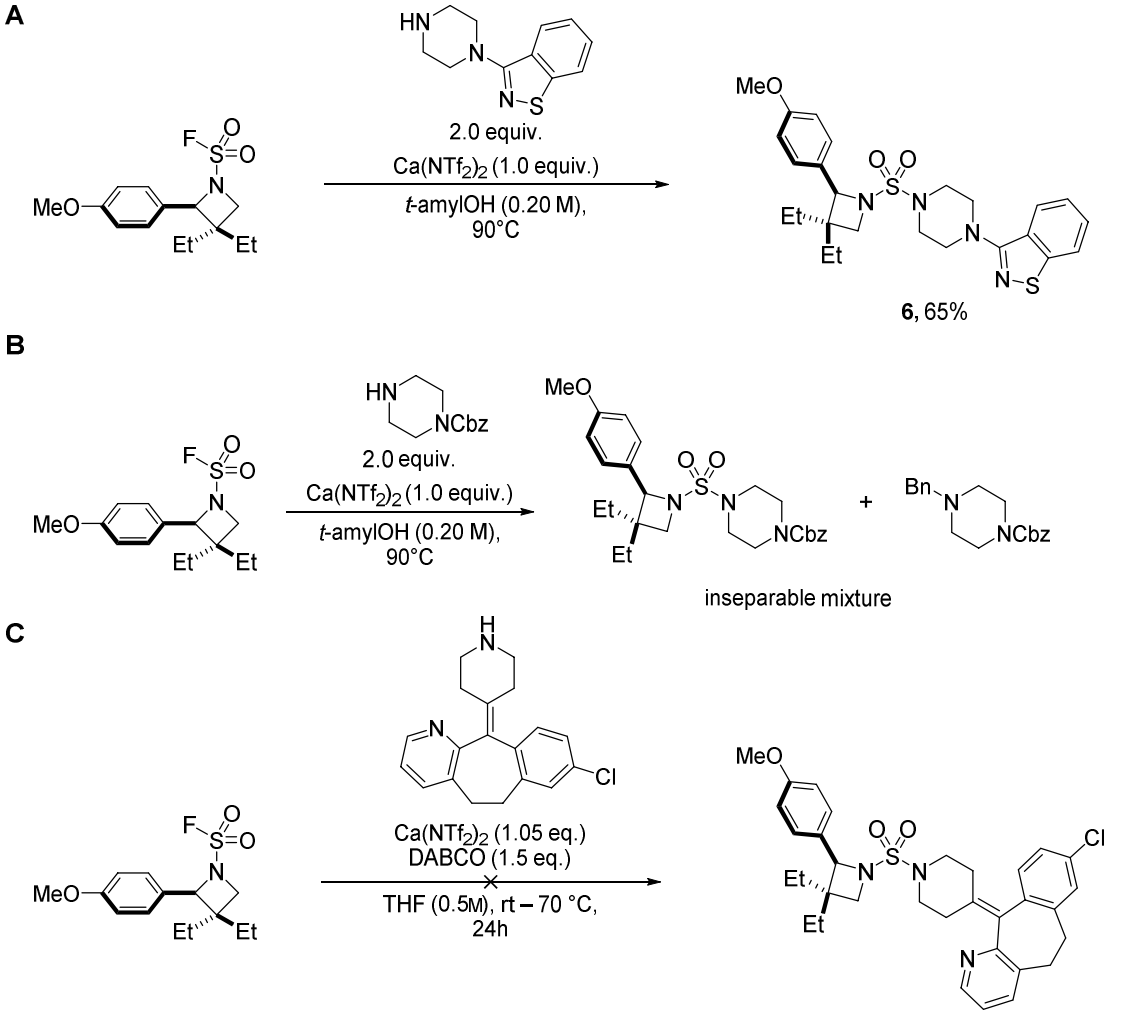
To generate enough product to conduct our derivatisation campaign we scaled the reaction up to 5 mmol scale (**Scheme 2-36**). To do this we reduced the loading of alkene to 3 equivalents. During the scale up, we found that the photocatalyst co-eluted with the product, therefore we treated the crude reaction mixture with *m*-CPBA to oxidise the thioxanthone photocatalyst to the corresponding sulfone, which allowed us to isolate the product in 77% yield. It was also demonstrated that this oxidative work-up procedure can be avoided if an Ir photocatalyst coupled with blue light was employed, without compromising the yield of the reaction.



Scheme 2-36 Reaction scale-up to 5 mmol.

In our derivatisation study we firstly demonstrated that it was possible to use the sulfamoyl fluoride as an electrophilic hub and displace the fluoride with an amine to generate sulfamide **6** using the $Ca(NTf_2)_2$ activation conditions developed by Ball (**Scheme 2-37A**).[157] When we first employed Cbz-piperazine as the amine nucleophile we obtained benzylated Cbz-piperazine which co-eluted with the sulfamide product, demonstrating that the Cbz group is not tolerated under these conditions (**Scheme 2-37B**).

It is worth noting that the 2nd generation conditions developed by Ball specifically for less reactive sulfamoyl fluorides, in our case did not work, even upon heating the reaction to 70 °C (**Scheme 2-37C**).[158] Our hypothesis is that these conditions have been shown to operate *via* an S_N2-like mechanism and as our sulfamoyl-fluoride is particularly hindered the increased steric hindrance shuts down the reaction.[159] The 1st generation conditions may favour a more disconcerted S_N1-like mechanism where hydrogen-bonding from the solvent may allow fluoride to leave slightly before addition of the nucleophile, leading to a less congested transition-state.



Scheme 2-37A $Ca(NTf_2)_2$ mediated SuFEx reaction of sulfamoyl fluoride. **B** Failed attempt at SuFEx reaction.

We also explored the use of using organometallic reagents to displace fluoride to generate sulfonamides. Grignard reagents, specifically containing an iodide counterion, have been shown to be capable of displacing fluoride to generate sulfonamides.[135] When we attempted these reactions with our substrate, we observed no reaction with methyl magnesium iodide at temperatures up to 60 °C. Upon heating the reaction to 90 °C we instead observed a complex mixture of products and starting material remaining, the major component of the reaction being the secondary amine as a result of attack of the

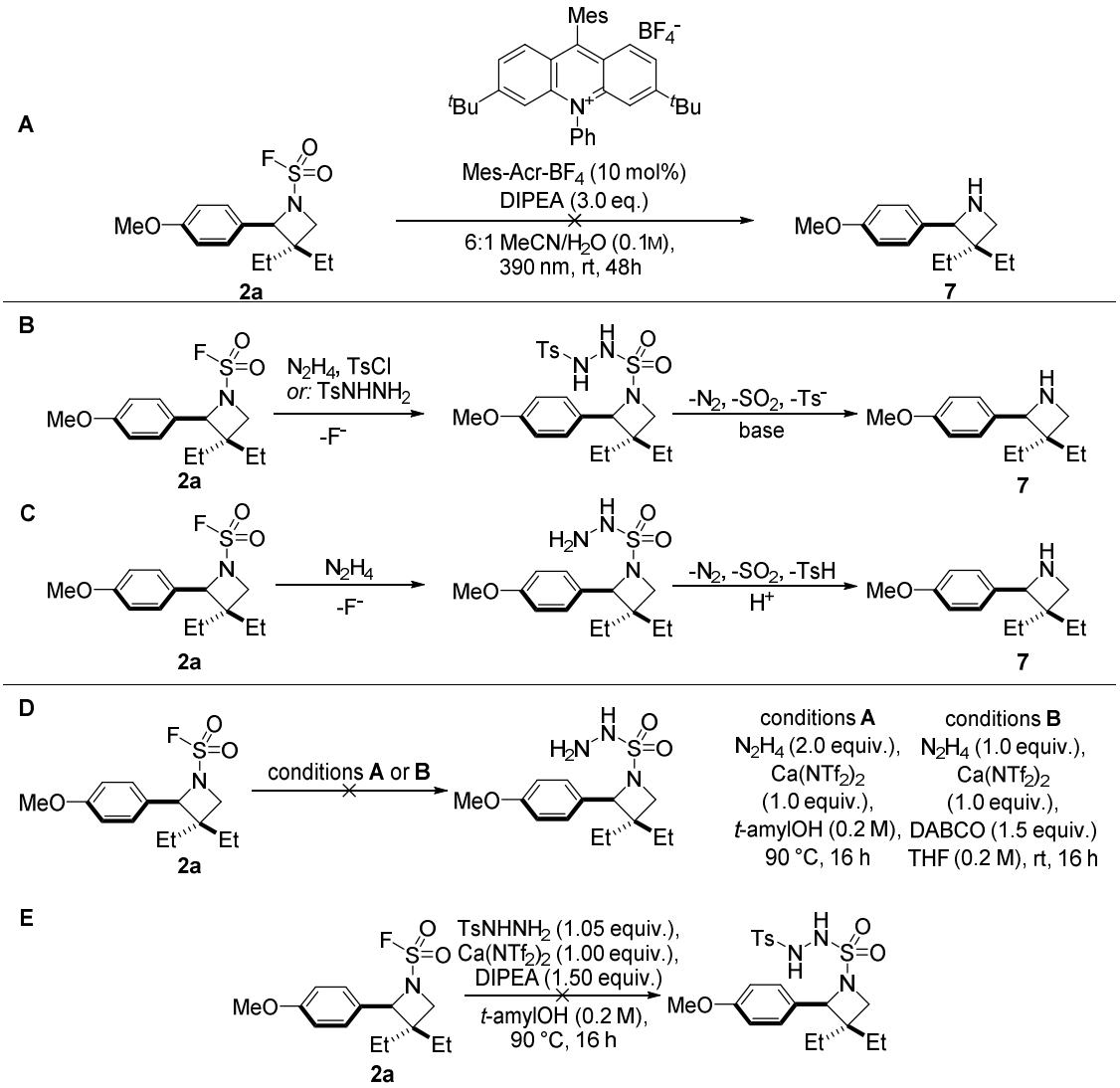
Grignard at fluorine to generate the unstable amino-sulfinate which decomposes to the amine.

In order to fulfil one of the goals of this study, we needed to be able cleave the -SO_2F activating group in order to access the free amine. In the case of the molecules synthesised in this study, which were all tertiary sulfamoyl fluorides, -SO_2F cleavage is not a known transformation and in fact this group had been shown to be impervious to a range of nucleophiles including amines, phosphines, organolithium and Grignard reagents, as well as oxidising agents hydride reducing agents, radicals and strong acids and bases.[160] This is in stark contrast to secondary sulfamoyl fluorides which undergo facile elimination to azasulfene under basic conditions by virtue of the acidic nature of the *N*-sulfamoyl proton.[135, 160] Aniline derived tertiary sulfamoyl fluorides are more susceptible to basic hydrolysis and can be hydrolysed by LiOH at room temperature.[136]

We hypothesised that the N-S reactivity of sulfamoyl fluorides would be most similar to *p*-toluenesulfonamides. We were attracted to Nicewicz's photochemical cleavage of sulfonamides using acridinium catalyst and DIPEA due to the broad scope and functional group tolerance displayed; however, when applied to our system we observed no reactivity and full recovery of starting material (**Scheme 2-38A**).[161]

Next, we wanted to see if we could deprotect the sulfamoyl fluoride in a unique manner that takes advantage of the electrophilicity of the sulfamoyl fluoride. Displacement of fluoride by hydrazine will give a sulfamoyl hydrazine. This can either be tosylated to give an *N*-sulfonyl, *N'*-sulfamoyl hydrazine which upon treatment of base would eliminate SO_2, N_2 and tosylate analogously to 1,2-ditosylhydrazine (**Scheme 2-38B**).[162] Alternatively, the acid-sensitive sulfamoyl hydrazine can be treated directly with acid to

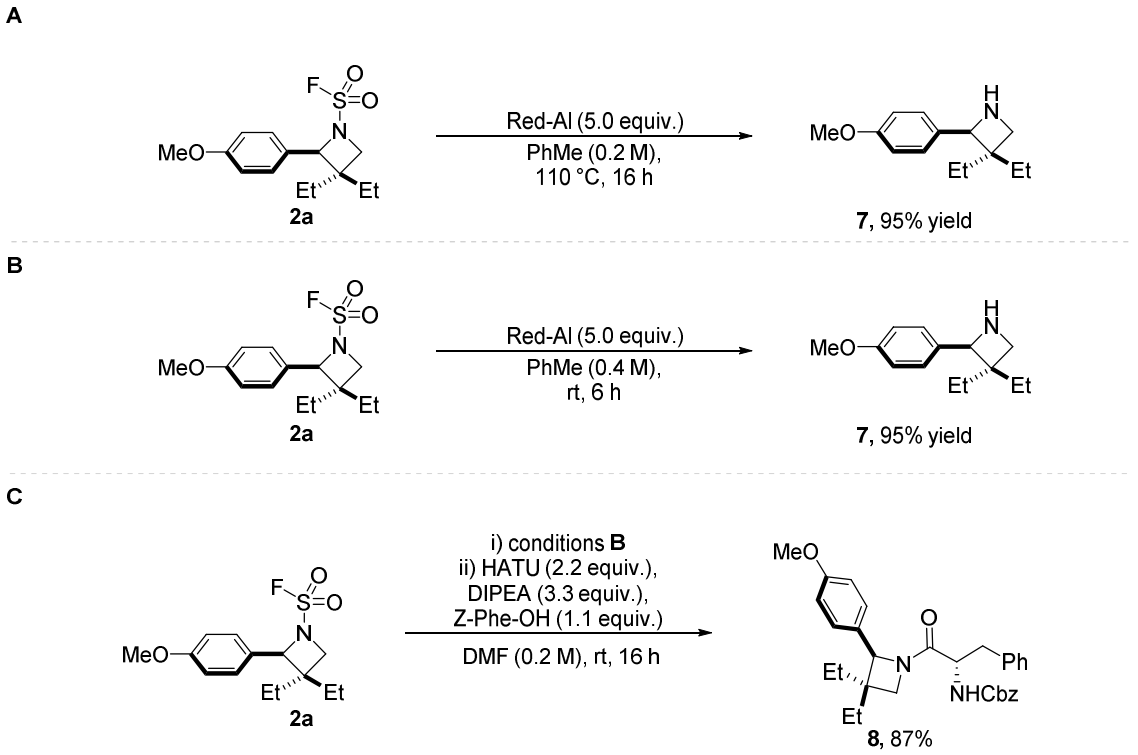
give the amine (**Scheme 2-38C**).[163] The sulfamoyl fluoride was treated with hydrazine or tosyl hydrazine under a variety of different conditions to promote nucleophilic substitution of fluoride. Under milder conditions the S-F bond either remained intact, or upon treatment with more forcing conditions the azetidine ring decomposed (**Scheme 2-38D, E**).



Scheme 2-38A Attempted photoreductive cleavage of sulfamoyl fluoride group. **B** Base-mediated reductive cleavage of sulfamoyl fluoride. **C** Acid-mediated deprotection of sulfamoyl fluorides. **D** Attempted displacement of fluoride with hydrazine of sulfamoyl fluoride. **E** Attempted displacement of fluoride with tosyl hydrazine of sulfamoyl fluoride.

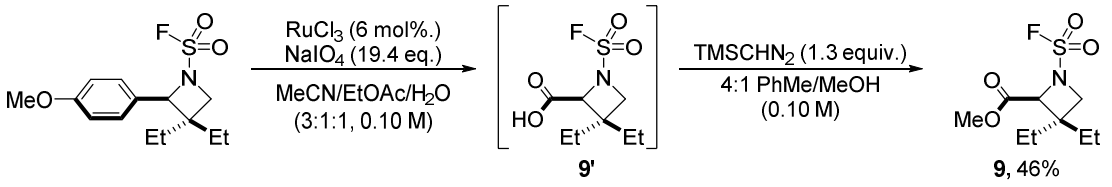
A detailed literature survey showed that Red-Al was known to be a privileged reductant for the cleavage of sulfonamides demonstrating superior reactivity to $LiAlH_4$.[164] Encouragingly, Miyamoto had shown Red-Al ® could reduce triflyl- protected secondary amines, which are more electronically similar to sulfamoyl fluoride protected azetidines than to tosyl protected amines.[165] We applied a modified set of conditions employed by Nagib for sulfonamides to our system and we were delighted to find that we obtained the pure N-H azetidine **7** in 95% yield without the need for any further purification (**Scheme 2-39A**). However, given that Miyamoto's report for triflyl protected amines shows reactivity at temperatures as low −40 °C we thought it would be possible to produce a much milder set of conditions.

We first tried performing the reaction at 0 °C for three hours, however, this was not sufficient to achieve full conversion of the starting material resulting in a 13:1 product/starting material ratio. Given practicality concerns of keeping reaction at 0 °C for longer than 3 hours we decided to perform the reaction at room temperature, and in this case we improved the conversion achieving an 18:1 product/starting material ratio. In order to push the reaction to completion the reaction time and concentration were doubled to 6 h and 0.4 M respectively, and pleasingly this resulted in obtaining the pure unprotected azetidine **7** in 95% yield (**Scheme 2-39B**). Next, we showed that the azetidine could be directly into an amide bond coupling reaction with a protected phenyl alanine, to give amide **8** in 87% overall yield across two steps (**Scheme 2-39C**).



Scheme 2-39A Literature conditions for reductive RedAl ® cleavage of sulfonamides. **B** Optimised conditions for reduction of sulfamoyl fluoride. **C** Telescoped conditions for formation of amide.

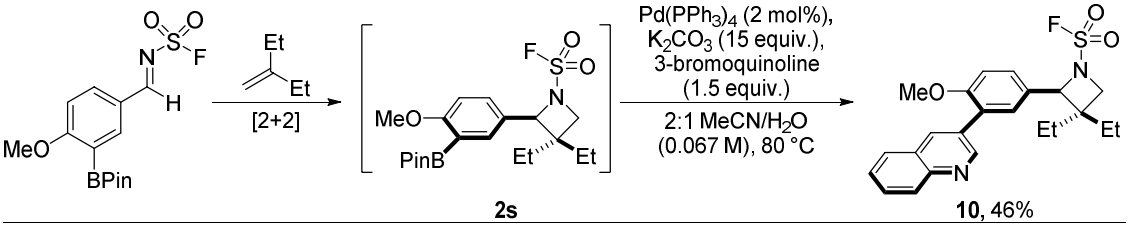
Taking advantage of the oxidative stability of sulfamoyl fluorides, we demonstrated it was possible to cleave the PMP group using RuO_4 to furnish directly α-amino-acid **9'**, which we protected *in-situ* using TMS-diazomethane to isolate methyl ester **9** (**Scheme 2-40**). This represents a route to synthesise conformationally restricted unnatural α-amino-acids, which were a class of targets our collaborators at Merck were interested in.



Scheme 2-40 RuO_4 oxidative cleavage of PMP group and methylation of carboxylic acid.

We also attempted to cleave the Me-O bond of the methoxy group of the molecule as this would allow us to demonstrate that it was possible to cleave one simple molecule at four distinct points. Reactions using both BBr_3 at room temperature, and heating NaSEt in DMF resulted in complete decomposition of the molecule and no intact -NSO_2F environments were visible in the ^{19}F NMR spectra.

The simplicity of the aza-Paternò–Büchi conditions allowed us to telescope further transformations after the photochemical step. Boronic esters were able to be oxidised following the reaction to generate the corresponding phenol, which is a functional group that is not tolerated in the photochemical conditions. Apart from simple oxidations, we could also perform Suzuki-Miyaura cross coupling with the crude boronic ester to generate heterobiaryl **10** in 46% yield from the imine (**Scheme 2-41**).

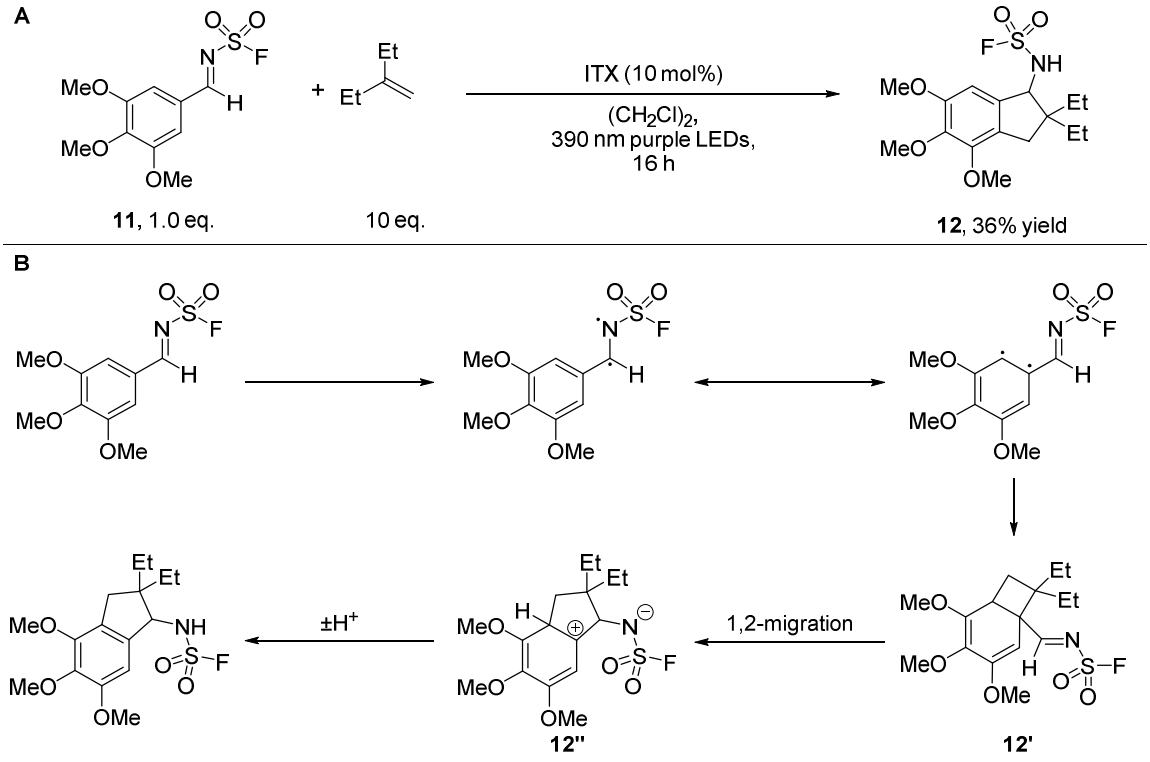


Scheme 2-41 Telescoped Suzuki coupling of boronic ester.

2.7 Indane Formation through a Dearomative Mechanism

When imine **11** was subjected to the photochemical conditions, we did not observe the formation of any azetidine product and instead observed the formation of indane product **12** (**Scheme 2-42A**). Along with other spectroscopic data, we were able to unequivocally verify the structure of **12** by single crystal X-ray diffraction. One plausible mechanism is that addition of the imine occurs at the ortho- position of the arene ring, followed by intersystem crossing and radical recombination to form reactive cyclobutane **12'**. This

then undergoes a ring expansion to form zwitterion **12''** which after proton transfer forms product **12** (**Scheme 2-42B**). The change in mechanism may likely be a result of increased electron-spin density of the ortho- position of the arene ring as a result of mesomeric donation of the two *meta* methoxy groups.

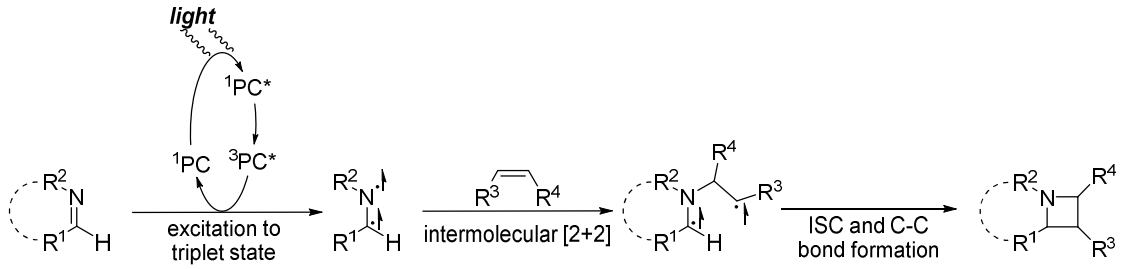


Scheme 2-42A Indane formation conditions. **B** Proposed mechanism of dearomative indane formation.

2.8 Mechanistic Investigation

Following the conclusion of our synthetic investigations we sought to elucidate the mechanism of the transformation. The proposed mechanism, is analogous to other energy transfer catalysed (aza-)Paternò–Büchi reactions.[120, 121, 166-168] The first step is efficient sensitisation of our substrate to the T_1 triplet state by the excited photocatalyst, and then the nitrogen of the triplet imine then adds into the alkene to deliver a long-lived triplet 1,4-biradical which can undergo free rotation scrambling the initial stereochemistry of

the substrates. The triplet biradical then undergoes intersystem crossing to the singlet state which subsequently enables radical recombination and C-C bond formation.

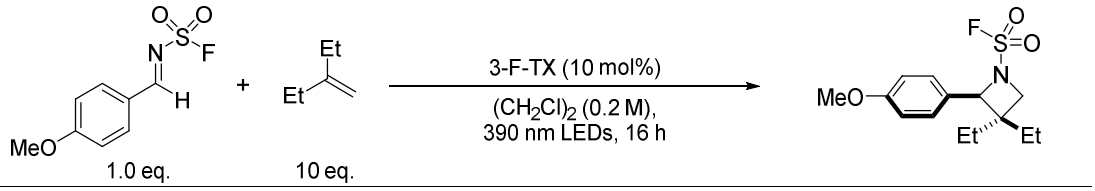


Scheme 2-43 Proposed mechanism for aza-Paternò–Büchi reactions of sulfamoyl fluoride imines.

Earlier in this chapter we noted several observations consistent with this mechanism, which will be briefly summarised. First, a triplet energy transfer process, rather than a photoredox process, is likely operative, as the success of the transformation is not dictated by the magnitude of the reduction potential of the catalyst. For example, *fac*-Ir(ppy)$_3$ does not lead to a successful transformation, but a photocatalyst with a high triplet energy does. The oxidation potentials of even electron-rich imines, such as N-(tertiary alkyl)-(2,4,6-trimethoxyphenyl) aldimines and N-tosyl, 4-methoxyphenyl aldimine have an oxidation potential of +1.42 V and N-tosyl 1.98 V vs SCE respectively,[88, 169] are well beyond the range of the photocatalysts tested in this study and will therefore not be discussed further.

The hypothesis that an energy transfer process is operative is supported by the reaction proceeding—albeit poorly—even in the absence of a photocatalyst. This suggests that an excited state of the imine is the reactive species, rather than a singly reduced species. The proposal that this excited state is a triplet is further substantiated by the reaction of the imine with both the *E*- and *Z*- isomers of hex-3-ene, delivering the same major diastereomer. This is consistent with the formation of a long-lived triplet biradical.

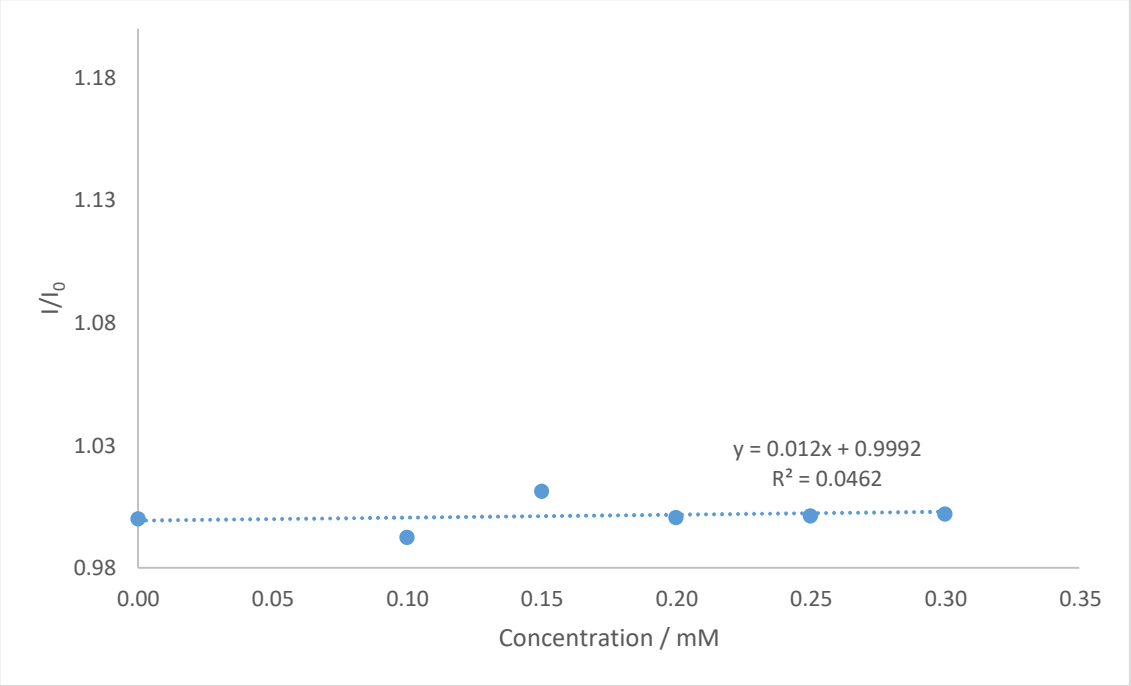
In this section we will describe further mechanistic experiments conducted in order to support the proposed mechanism. The model system we will be using is the same used for the optimisation and control study shown in (**Scheme 2-44**).



Scheme 2-44 Model system for control experiments.

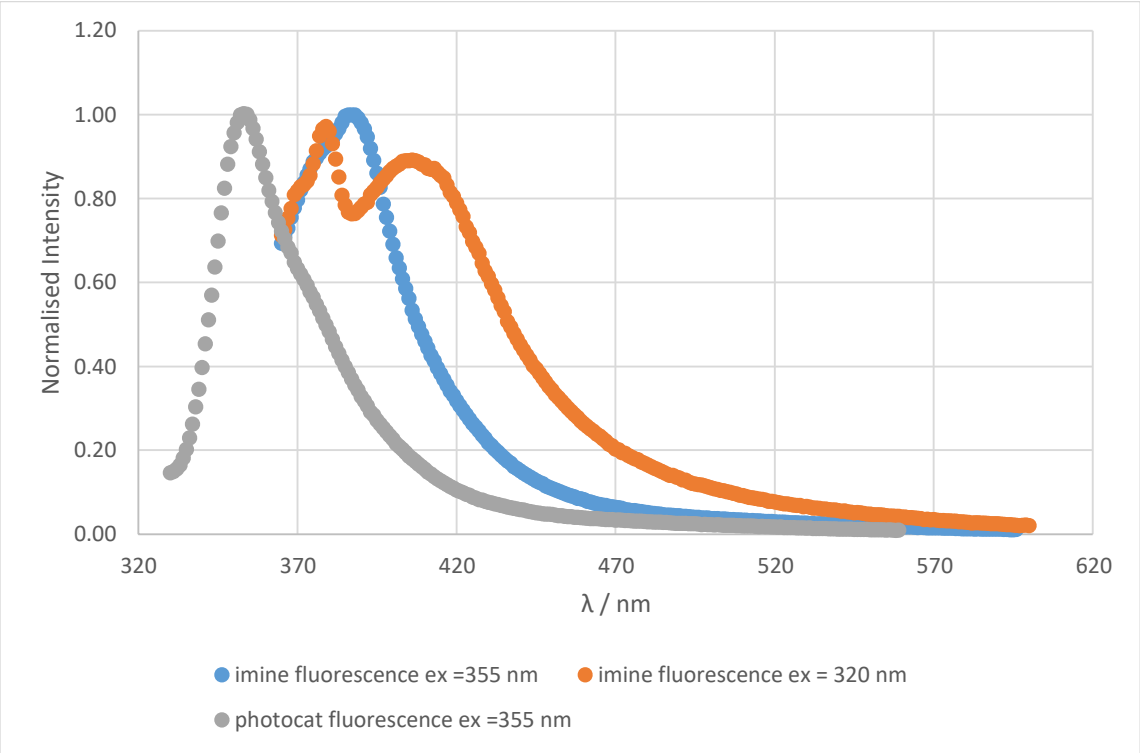
2.8.1 Stern-Volmer Quenching

In order to support our conclusion that our reaction proceeds through the excited state of the imine and not the alkene, we measured the emission spectra of the photocatalyst, 3-F-TX, in the presence of varying concentration of the other components in the reaction. This enables one to assess which species is responsible for quenching the excited state of the photocatalyst and can be represented by constructing a Stern-Volmer plot.



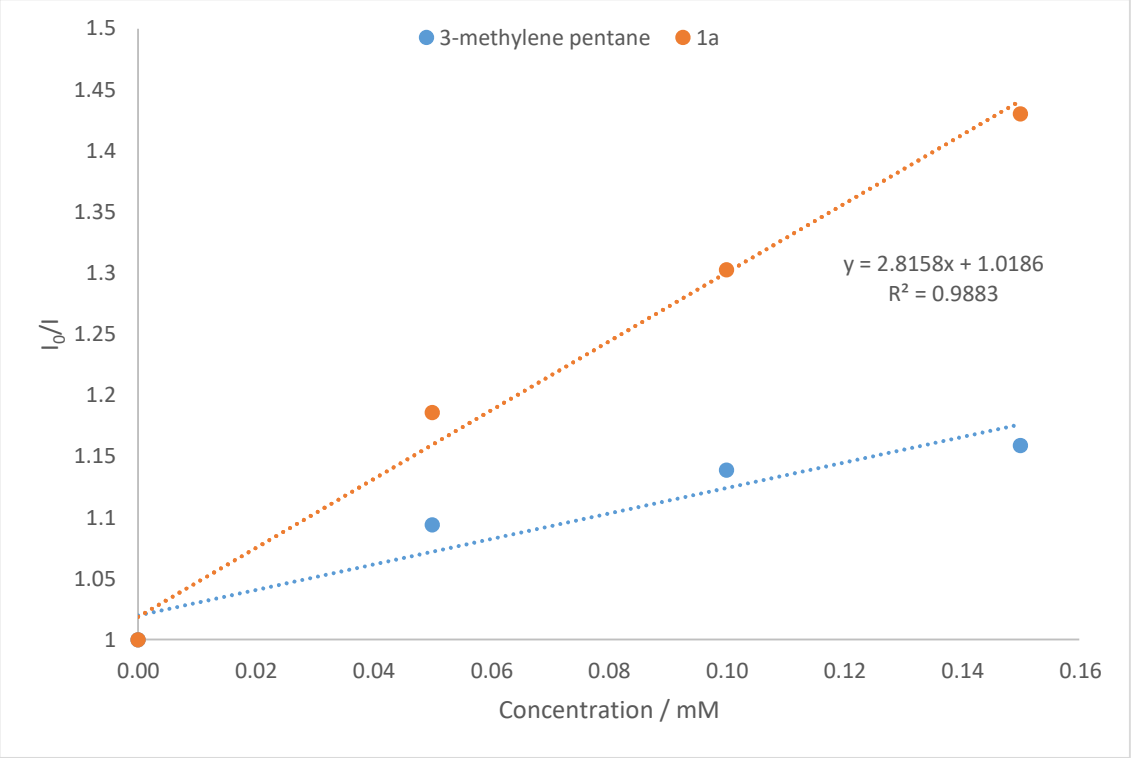
Graph 2-1 Stern-Volmer quenching of 3-F-TX with 3-methylene pentane.

With 3-F-TX as the photocatalyst we were only able to construct a Stern-Volmer plot with the alkene 3-methylene pentane (**Graph 2-1**). This is because when we use an excitation wavelength of 355 nm to excite the photocatalyst, at this wavelength it is short enough to overlap with absorption spectrum of the imine and it fluoresces in a similar part of the EM spectrum as 3-F-TX (**Graph 2-2**). Therefore, it was not possible to measure quenched fluorescence of the photocatalyst 3-F-TX as this was eclipsed by the fluorescence of the imine. However, we were able to show that the fluorescence was not quenched by the alkene, showing that the excited state of 3-F-TX and the alkene have minimal interaction. This provides further evidence that the excited state of the alkene was not responsible for the success of the transformation and indirect evidence that the imine is the species being excited.



Graph 2-2 Normalised fluoresence spectra of **1a** and 3-F-TX.

In order to obtain direct evidence that the imine was the species being excited we needed to use a photocatalyst with an absorption spectrum that does not overlap with the imine. Here we selected $[Ir(dF(CF)_3ppy)_2dtbbpy]PF_6$, which was also shown to be a competent photocatalyst for this transformation (see **Table 2-1**), as it has a λ_{max} of 380 nm. In this case we were able to show that indeed the imine is the most efficient quencher in the system and that the direct interaction of the imine and photocatalyst is important in the reaction (**Graph 2-3**). However, it is worth noting that this data does not distinguish the mechanism of quenching.



Graph 2-3 Stern Volmer quenching plot of $[Ir(dF(CF)_3ppy)_2dtbbpy]PF_6$ with **1a** and 3-methylene pentane.

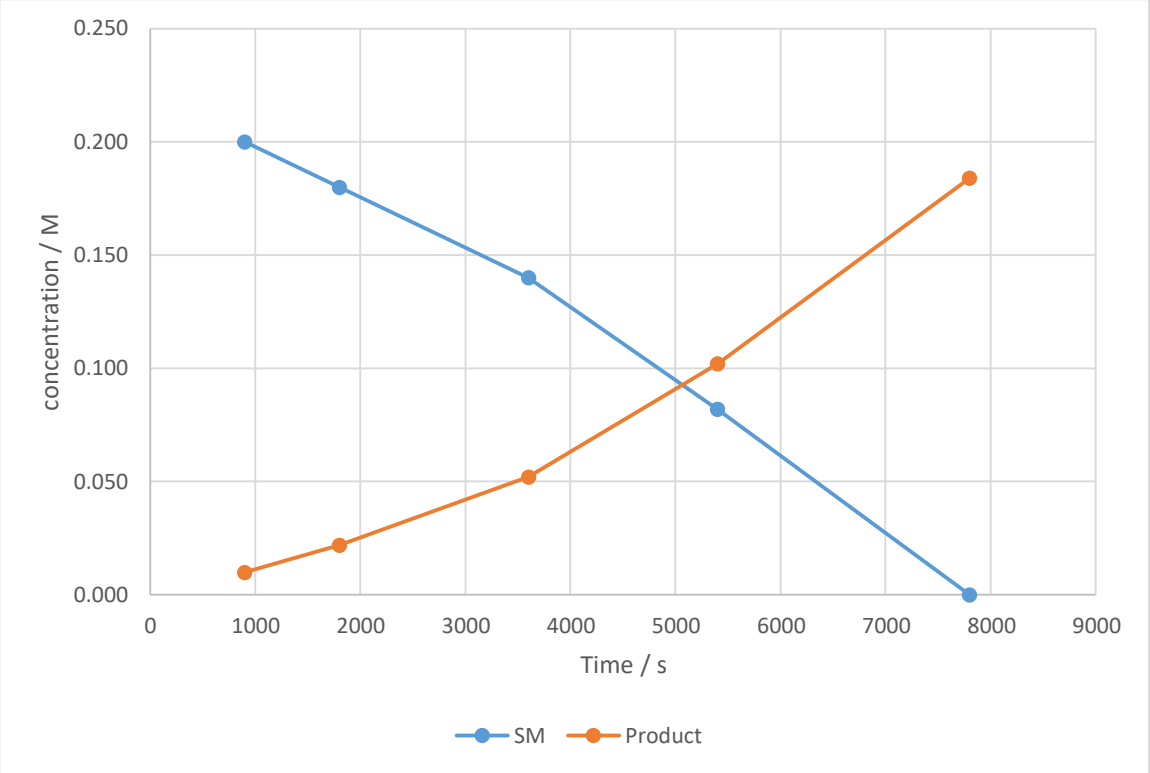
2.8.2 Cyclic Voltammetry

Next, we wanted to study the feasibility of electron transfer occurring in our system. To do this we measured the reduction potential of our model imine in acetonitrile using cyclic voltammetry. We found that the imine had a reduction potential of –1.1 V (vs SCE) and was irreversible suggesting that further chemical or electron transfer processes occurred after the initial redox event. The ground state or excited state oxidation potentials have not been measured for 3-F-TX, however, in the course of this study (see section **3.7.2**) they have been calculated at -0.99 V with respect to SCE and $[Ir(dF(CF)_3ppy)_2tbbpy]PF_6$ ($E_{red}(PC^+/PC^*)$ = -0.89), both photocatalysts shown to mediate the aza Paternò–Büchi in excellent yields (97% and 93% yields respectively).[119, 170] With single electron reduction of the model substrate being endergonic for both photocatalysts, it is unlikely that a photoredox process is taking place. This data coupled with the reduced performance of

electron deficient substrates with ITX in the aza-Paternò–Büchi reaction, which would have even more accessible reduction potentials, is further suggestive of an energy transfer mechanism taking place.

2.8.3 Time Course Experiment

In order to acquire kinetic data, a time course experiment was conducted in which we monitored the concentrations of the product and starting material over time (**Graph 2-4**). For our model system with a large excess of alkene, it was found that the reaction was finished after just over 2 hours and that the rate of reaction increased over time. The increasing rate of reaction is intriguing and hints at further complexity than in our initially proposed mechanism. Possible explanations are that: (1) the reaction is autocatalytic and the product catalyses the reaction (unlikely), or (2) that the imine quenches its excited state bimolecularly, reducing the rate of the reaction most at the beginning when the imine concentration is greatest.



Graph 2-4 Time-course experiment.

2.9 Summary and Outlook

One of the guiding design principles of prior work focused on aza Paternò–Büchi reactions was that acyclic imines must be avoided, as their erratic photochemistry is not conducive to successful intermolecular reactions.[128] Instead, the imine must be tethered in a cyclic framework to achieve reactivity, or alternatively, the alkene component must be excited. However, the constraining ring leaves a vestigial appendage that is difficult to cleave, limiting the accessible chemical space for the transformation. Despite being a desirable synthetic route to azetidines, the engineered imine equivalents required for success have relegated this method to little more than a curiosity in organic synthesis.

In the present investigation it was found that by modulating the activating group on nitrogen of simple acyclic aldimines this principle is no longer the case, and we have tamed this elusive biradical intermediate and realised an intermolecular aza Paternò–

Büchi reaction. We have shown that this reaction is synthetically useful with broad scope with respect to both components to give a wide array useful azetidine products. We go on to show that it is possible to further derivatise these substrates and in particular show that substituents attached to both the C and N of the C=N bond can be cleaved to leave no vestige of the initial imine if desired. Here all the requirements are now in place to make the aza Paternò–Büchi reaction a workhorse reaction for the synthesis of azetidines. However, the reaction developed is not without limitations including: electron deficient alkenes not being compatible, poor diastereoselectivities and high loadings of alkene required.

Given the unusual kinetics displayed by this transformation, a full detailed mechanistic investigation is warranted to determine the intricacies of the reaction including the mechanism by which the rate of the reaction accelerates. Further mechanistic understanding may lead to rational design of a more productive reaction or even broader scope. Insight into the rate acceleration phenomenon for example may be of particular importance on scale where this run-away may lead to unwanted exotherms and reduced yields.

With the unprecedented reactivity of these acyclic triplet imines in the aza Paternò–Büchi reaction established, this may lead to development of further transformations. Here we have already disclosed that changing substituents of the imine can lead to an indane can being formed instead of an azetidine. By modulating the alkene component, it may be possible to realise even more exciting transformations.

Chapter 3 - Computational Investigation of the aza Paternò–Büchi Reaction of Sulfamoyl Fluoride Imines

3.1 Introduction

In order to rationalise the privileged reactivity displayed by sulfamoyl fluoride aldimines in the aza Paternò–Büchi reaction we next studied this reaction computationally using density functional theory (DFT). As this reaction does not produce any isolable intermediates, a computational approach is particularly valuable as it is possible to study these species *in-silico*. In our study we will model, each of the steps in our proposed mechanism for a range of different sulfonyl aldimines in order to ascertain what are the defining characteristics of an imine that is successful in this transformation.

In this study we used the ORCA suite of programs (version 5.0.3), using the meta-GGA functional M06-2X functional on Ahlrich's def2-TZVP triple-zeta basis set and Grimme D3 atom-pairwise dispersion correction.[171-176] In order to take in the effects of solvent an implicit solvation was introduced by employing the SMD explicit solvent model using default parameters for 1,2-dichloroethane.[177] M06-2X was chosen due to its high performance across a range of benchmarking studies for main group chemistry, as well being employed in a number of studies of triplet energy transfer reactions.[108, 178-182]

In order to reduce the computational cost and limit the total number of possible conformers, we truncated the experimental model system, removing the methoxy group of the arene and truncating the Et groups on the alkene to Me. The different substituents on sulfur we chose to study are: F, Cl, CN, CF_3, Me, Ph and Bn. In the course of this investigation not only was the main reaction pathway studied, but a number of side

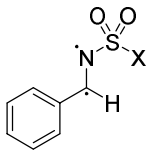
reactions were also considered in order to ascertain why these processes did not predominate.

3.2 Photochemistry of Imines

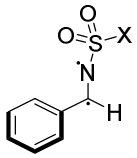
3.2.1 Triplet Energy

The first step in the proposed mechanism is triplet energy transfer (likely a Dexter mechanism) from the photocatalyst in the T_1 state to the imine substrate. By calculating the energy of the lowest lying triplet states of the imines we can ascertain the feasibility of this process. However, this is only an approximation as this model does not take into account hot-band effects (whereby energy transfer to molecules in the ground state occurs through vertical excitation along a vibrational normal mode, leading to a reduction in energetic separation between the S_0 and T_1 hypersurfaces).[183] This is a non-adiabatic method. Despite this, the adiabatic triplet energy transfer model has demonstrated success in predicting the feasibility of energy transfer.[145, 184]

For each imine, two triplet states were located during this study (**Table 3-1**). For triplet sulfamoyl imine, ^{3}A, we found a planar geometry around the C—N bond, ^{3}A1 and a twisted geometry around the C—N bond, ^{3}A2. The twisted state was found to be lower for all imines investigated bar the CN sulfonyl imine. Triplet energies were calculated using the planar conformer in order to minimise structural reorganisation during triplet-triplet energy transfer as described in a previous report.[88, 185]



planar



twisted

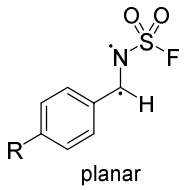
X	Cl	CF_3	CN	F	Me	Bn	Ph
E_T / kcalmol^{-1}	61.5	63.8	65.9	67.3	69.3	69.3	69.6
E_T(twisted) / kcalmol^{-1}	61.4	63.1	66.9	66.5	60.9	62.7	61.8
ΔE_T / kcalmol^{-1}	0.1	0.7	-1.0	0.8	8.4	6.6	7.8

Table 3-1 Triplet energies for planar and twisted conformations of sulfonyl imines.

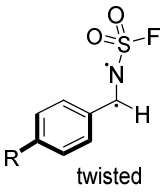
E_T for the array of imines investigated was found to be in the range 61.5 – 69.6 kcal mol^{-1} whereas as for the twisted geometries the E_T(twisted) was found to have a smaller range of 61.4 – 66.9 kcal mol^{-1}. Generally, the difference between the two E_T values (ΔE_T) is smaller for sulfonyl aldimines bearing electronegative groups: Cl, CF_3, CN and F (0.1, 0.7, 1.0 and 0.8 kcal mol^{-1} respectively), than the more electropositive substituents: Me, Bn and Ph (8.4, 6.6 and 7.8 kcal mol^{-1} respectively). Energy transfer for the main photocatalyst used in our study, 3-F-TX (E_T = 67.4 kcal mol^{-1}), is exergonic and thus energy transfer is anticipated to be a rapid and efficient process. However, for [Ir(dFCF_3ppy)$_2$dtbbpy][PF_6] (E_T = 60.1 kcal mol^{-1}) the process is endergonic and despite this the reaction still proceeds well. In this case energy transfer likely a thermally activated process, proceeding through thermally excited rotational and vibrational levels. Back EnT from the substrate to the photocatalyst can also become a significant and decrease the efficiency of energy transfer.[68]

Next, we looked at the effect of adding substituents to the arene ring on the triplet energy of the imine (**Table 3-2**). Both an electron-withdrawing CN group and an electron-donating OMe group result in a lower E_T compared to the electron-neutral imine (R = H). This can be rationalised by the fact that the CN group decreases the LUMO energy more

than it affects the HOMO, while the OMe group increases the HOMO energy more than it affects the LUMO. Like the parent electron-neutral imine, the twisted geometry of the CN substituted imine is lower in energy than the planar geometry, in contrast for the methoxy substitution the relative energies of these two geometries is inverted and the planar conformer is significantly lower in energy. This may be due to conjugation of the *N*-lone pair into the π-system that occurs in the twisted geometry being destabilised by the electron donating methoxy group.



planar



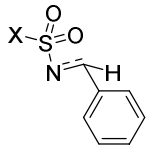
twisted

R	OMe	H	CN
E_T / kcalmol^{-1}	61.5	67.3	64.9
E_T(twisted) / kcalmol^{-1}	67.6	66.5	63.2

Table 3-2 Triplet energies for planar and twisted conformations of range sulfamoyl fluoride imines.

3.2.2 Minimum Energy Crossing Point

Following on, we looked at the minimum energy crossing point (MECP), between the singlet and triplet states for each of the imines in the series (**Table 3-3**). The MECP is represented by the structure where two different potential energy surfaces, in this case the singlet and triplet potential energy surfaces cross each other. In ORCA this is achieved by minimising the energy of the first potential energy surface while minimising the difference between the two surfaces. The MECP in this case was interpreted as a proxy for triplet state lifetimes of the imines without having to resort to the use of more complex, multireference methods combined with time-dependant density functional theory (TDDFT). The results are summarised below.



X	Ph	Me	Bn	Cl	CF_3	F	CN
MECP / $kcalmol^{-1}$	5.9	7.3	8.8	9.9	11.5	11.9	13.2

Table 3-3 MECPs for sulfonyl aldimines relative to twisted triplet imine.

The imidic *C*- and *N*- atoms of the triplet aldimines possess geometry consistent with atoms bearing sp^2 hybridisation, with trigonal planar geometry around the imidic *C* and bond angles close to 120°, as well as a bent geometry around *N* with a bond angle of 114.9° (**Figure 3-1A**). In the MECP geometry these atoms have bond angles consistent with sp^3 hybridisation, with trigonal pyramidal geometry around the imidic *C*, hence bond angles close to 109.5° and a bent geometry around *N* with a bond angle of 107.4°. Inspection of spin densities and charges show that electronically the singlet state species that is converged to is a closed shell species, attempts to find an open shell species using broken symmetry DFT were unsuccessful (**Figure 3-1B**). Generally, more electronegative groups on the sulfonyl group such as CF_3, F and CN increase the energy of the MECP, while more electropositive Ph, Me and Bn have lower energy MECPs.

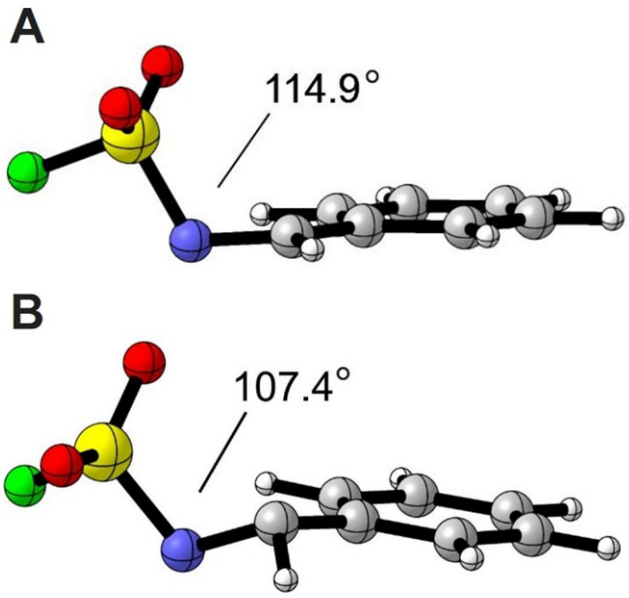
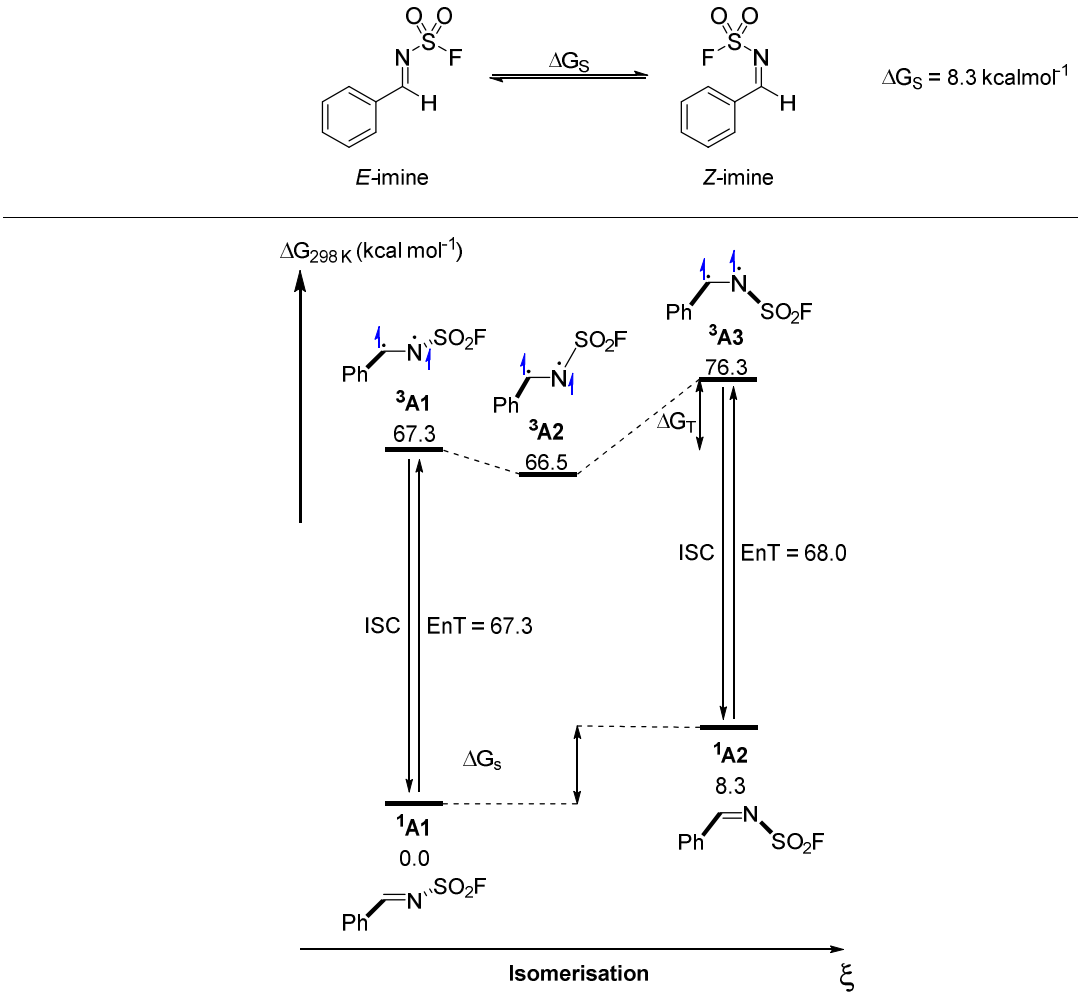


Figure 3-1A Structure of twisted triplet sulfamoyl fluoride aldimine. **B** Structure of MECP for sulfamoyl fluoride aldimine.

3.2.3 Photoisomerisation

During our experimental investigation the *Z*-aldimine was never observed, in order to establish why this was the case photochemical isomerisation was studied computationally (**Scheme 3-1**). The position of equilibrium between *E*- and *Z*-isomers for both ground state and excited state aldimines were found to lie strongly towards the *E*- aldimine (ΔG_s = 8.3 kcal mol^{-1} and ΔG_T = 9.0 kcal mol^{-1} respectively. The triplet energies for both of the aldimine geometries are very similar (67.3 vs 68.0 kcal mol^{-1}), given this, we may assume that the difference in the rates of energy transfer is negligible. Therefore, if we assume that rates of intersystem crossing are similar for both geometries of the triplet imine, the distribution of geometries is only determined by the difference in Gibbs free energy of the two species in the ground state (ΔG_s). This gives a value of the equilibrium constant for the reaction below to be K = 8.14×10^{-7}, or one in every 1.2 million molecules, consistent with the observation that the *Z*-imine is not detected under our conditions.



Scheme 3-1 Photoisomerisation of sulfamoyl fluoride aldimine.

3.3 Fragmentation of Imines

Fragmentation is commonly observed in photoexcited imines, making it essential to understand the extent of this process when rationalising the success of the developed aza Paternò–Büchi reaction. In particular, we examined fragmentation along the N–S bond, which yields an imidoyl radical and a sulfonyl radical. Focusing on the -SO_2F imine, the transition state originates from the twisted triplet imine, as confirmed by the backward intrinsic reaction coordinate (IRC) calculation. This transition state also exhibits a twisted geometry around the C–N bond, with a dihedral angle of -87.7° (**Figure 3-2**). At this stage, the S–N bond elongates to 2.01 Å, while the C–N bond contracts to 1.30 Å, nearly

matching the C–N bond length in the sulfamoyl fluoride imine ground state (1.28 Å). This results in a late transition state, where the C=N double bond has almost reformed before fragmentation.

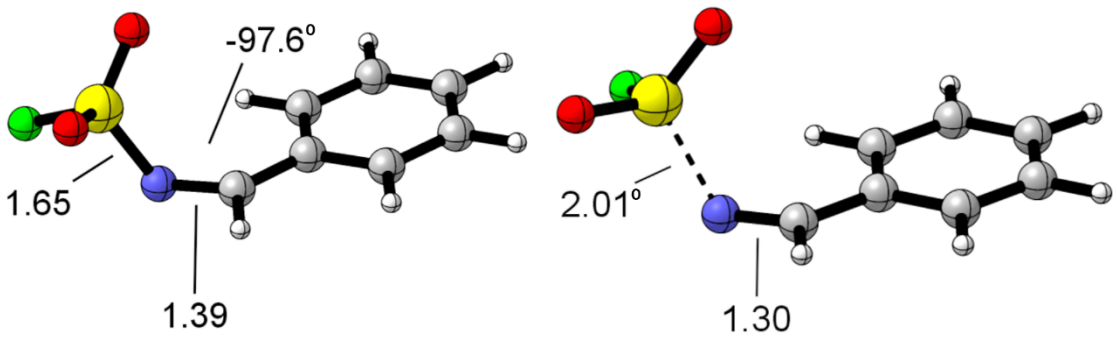
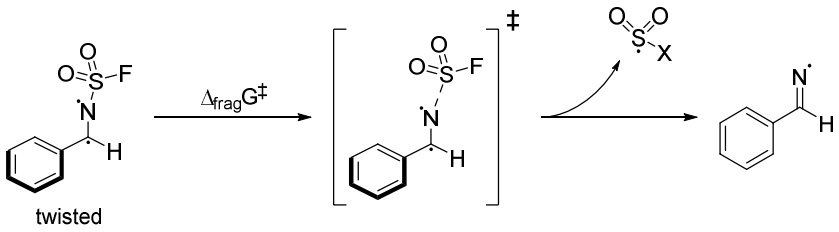


Figure 3-2 Annotated structures of twisted triplet sulfamoyl fluoride (left) and fragmentation transition state (right).

The transition states for fragmentation were then located for the rest of the imines selected for this study and the results are summarised below. For all the imines the barriers are relatively low less than 10 kcal mol^{-1}, with $MeSO_2$- bearing the largest barrier to fragmentation at 9.5 kcal mol^{-1} and $ClSO_2$- bearing the lowest barrier at only 2.4 kcal mol^{-1}. The data presented may explain partly why some imines, such as $PhSO_2$- imine, are unsuccessful in the aza Paternò–Büchi reaction as their fragmentation barriers are too low to compete with an intermolecular process. Experimentally, products arising from fragmentation from *N*-tosyl or *N*-SO_2F imines under photochemical aza Paternò–Büchi reaction conditions were rarely observed.



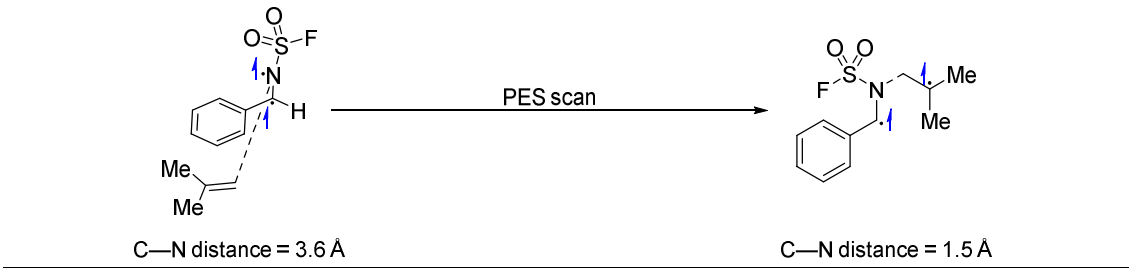
X	Cl	CN	Ph	CF_3	Bn	F	Me
$\Delta_{frag}G^{\ddagger}$ / kcalmol^{-1}	2.4	5.8	6.8	7.3	8.3	8.6	9.5

Table 3-4 Fragmentation barriers of sulfonyl imines.

3.4 Addition of Imines into Alkenes

3.4.1 Potential Energy Surfaces

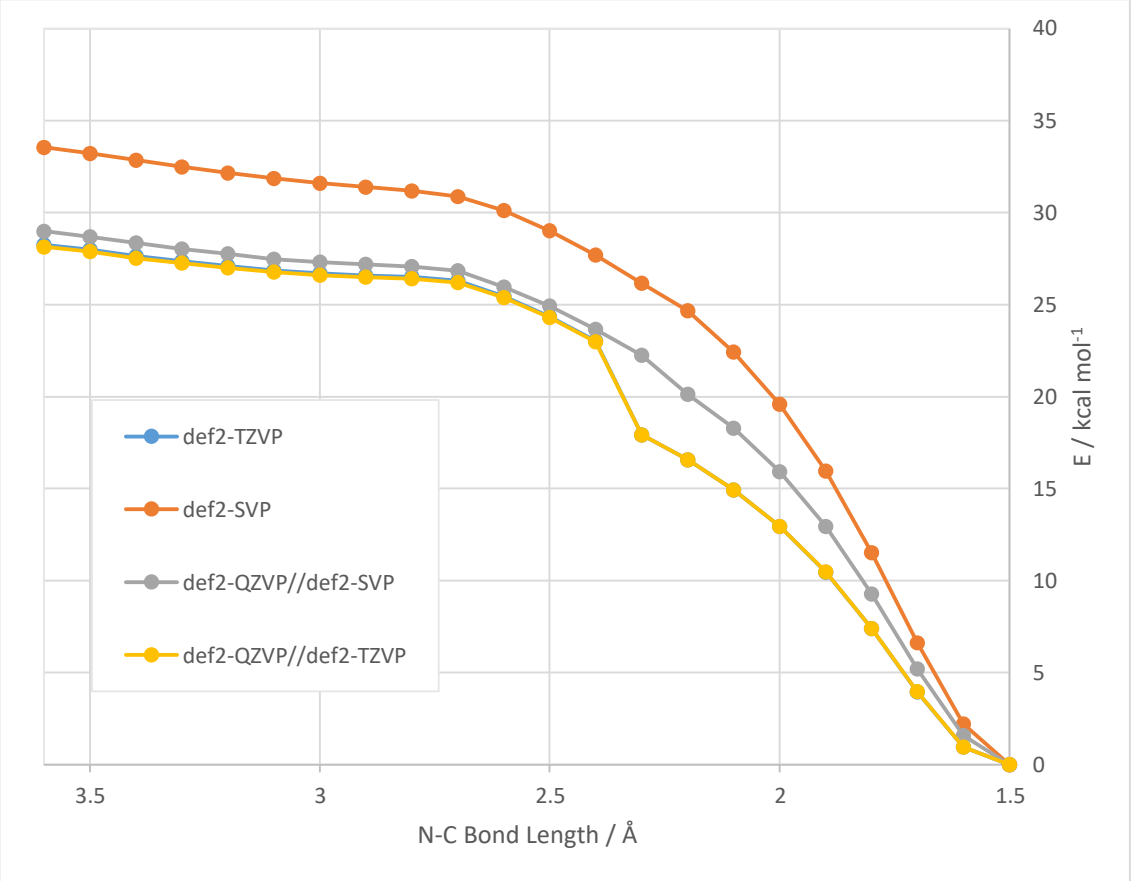
We examined the potential energy surface for the addition of ^{3}A into isobutene scanning from a C—N distance of 1.5 to 3.6 Å (**Scheme 3-2**). To ensure that our results were not specific to the level of theory used we examined a number of different variables including: the effect of basis set, solvent model, % of Hartree-Fock exchange and a range of alternative functionals. In particular, this approach helped to ensure that self-interaction error (SIE), arising from some density functionals incorrectly including an electron's interaction with its own density, and basis set superposition error (BSSE), resulting from basis functions being borrowed between interacting fragments, were minimised. Solutions were checked for the possibility of charge-transfer type mechanisms occurring and ensure the validity of the triplet solutions.[186, 187] We found that in almost all cases there was no maximum in the surface, which is indicative of a barrierless process.



Scheme 3-2 Diagramatic representation of PES scan. C-N distance indicated by dashed line.

Considering the size of the basis set, all basis sets with M06-2X produced potential energy surfaces that are entirely downhill over the range examined (**Graph 3-1**). The smaller def2-SVP basis set results in the steepest potential energy surface, which is likely the result of basis set incompleteness error (BSIE). As the two fragments are moved further apart each component cannot adversely increase the size of its basis set and stabilise the adduct, therefore the energy increases. When running these geometries with the larger def2-QZVP basis set the relative energies decrease by about ~4 kcal mol^{-1} (median ΔE = 4.1 kcal mol^{-1}) corroborating that there is BSIE with def2-SVP basis set.

Increasing the size of the basis set to the triple zeta def2-TZVP leads to a less steep potential energy surface which has a discontinuity at 2.3 Å, this is as a result of a sudden flattening of the imine resulting in a lower energy conformation. Taking these geometries and evaluating them with a larger quadruple zeta basis set, def2-QZVP, the energies converge (largest ΔE = 0.14 kcal mol^{-1}) indicating that the def2-TZVP basis set is sufficiently large to model the system.

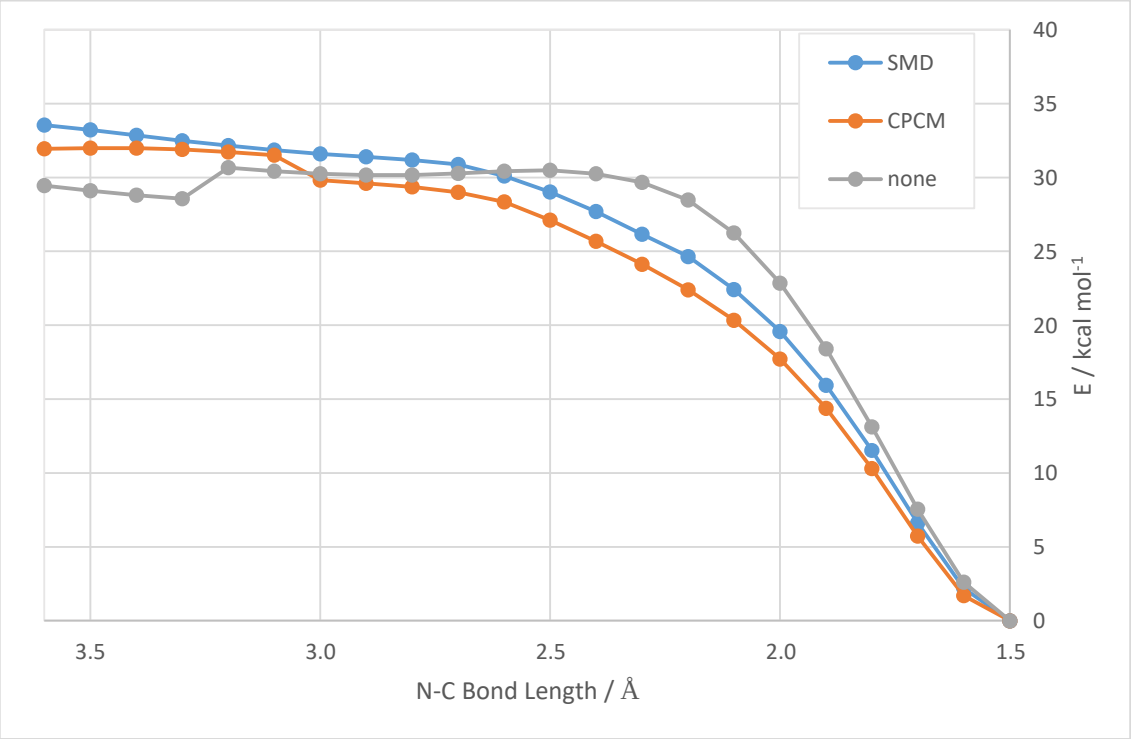


Graph 3-1 Potential energy surface scan varying the size of the basis set.

Next the effect of the solvent model was investigated. In the solution state both CPCM and SMD solvent models do not give a point corresponding to a transition state in the potential energy surface, and have continuously downhill PES's (**Graph 3-2**). At medium distances, the CPCM solvent model gives a lower energy surface than SMD but the overall shapes of the curves are very similar, showing that the choice of solvent model has little effect on the conclusions drawn.

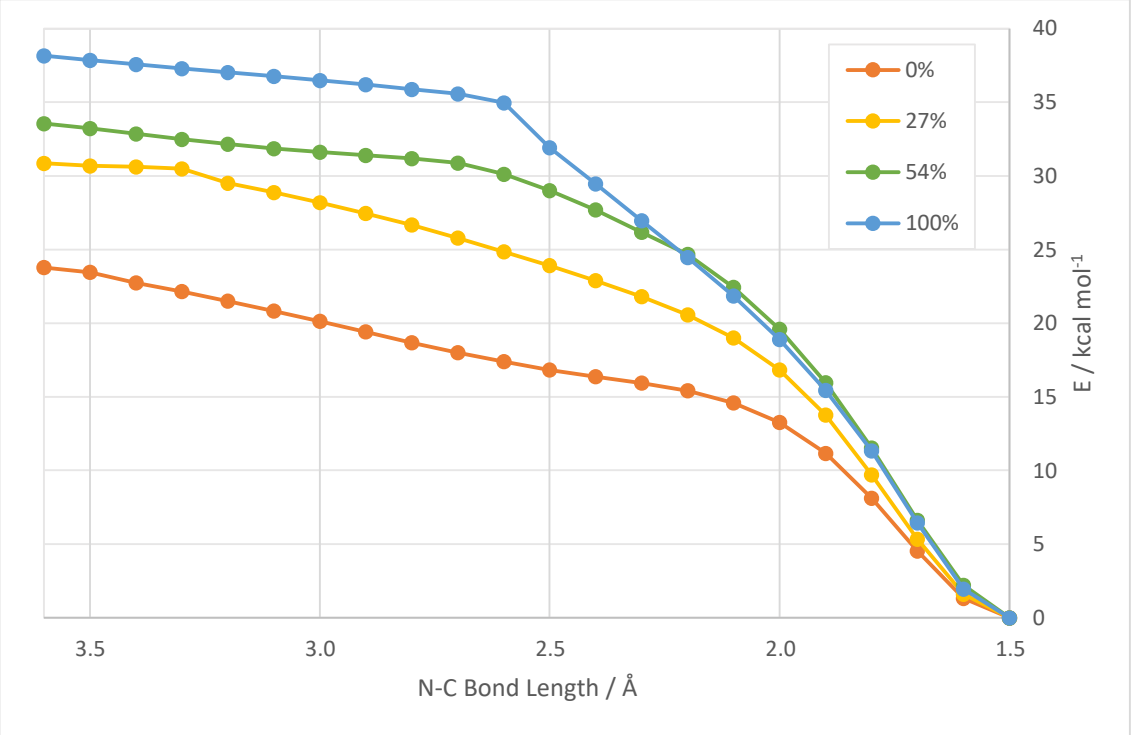
However, in the gas phase a smooth potential energy surface results yielding a shallow maximum at 2.5 Å. Taking this geometry, it is possible to find a transition state with $\Delta^{\ddagger}G$ = 5.4 kcal mol^{-1} and $\Delta^{\ddagger}G$ = 9.1 kcal mol^{-1} with a larger basis set (def2-TZVP). Even though in the gas phase there is a transition state present it is still very low (below 10 kcal mol^{-1}). Given the different conclusions resulting from the absence of a solvent model, it

was determined that it was important to model the solvent in order to obtain a valid conclusion for our system.



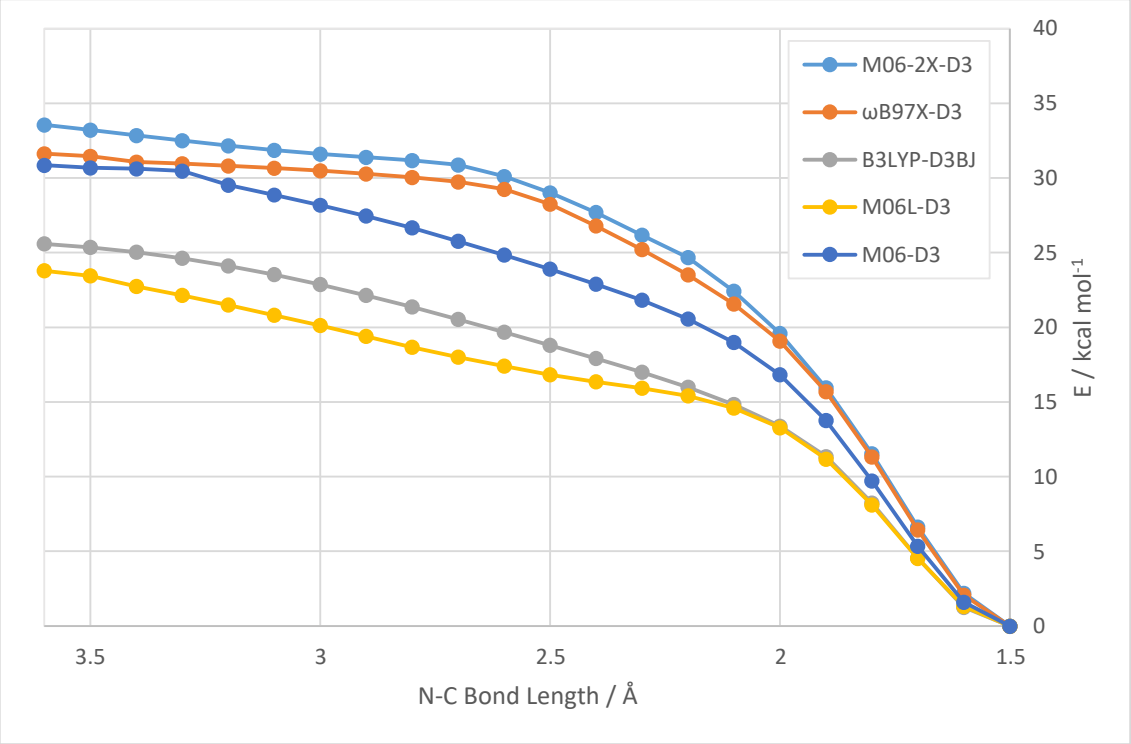
Graph 3-2 Potential energy surface scan varying the solvent model.

Increasing the amount of exact exchange included in the density functional used leads to an increase in the energy of the system particularly at larger C—N distances (**Graph 3-3**). This observation can be interpreted as increasing the amount of exact exchange in the density functional allows a better description of dynamic correlation in the system, hence leading to a reduction in self-interaction error and a reduction in the spurious lowering of potential energy. Increasing exchange from 54% to 100% shows no significant change in the potential energy surface from 1.5 Å to 2.3 Å and beyond 2.6 Å, implying that 54% exchange is sufficient to account for the dynamic correlation in this system. The difference in the gradient of the potential energy surface of M06-HF-D2 at distances between 2.3 Å and 2.6 Å may be a result of the D2 dispersion correction underestimating dispersion forces at this intermediate distance.



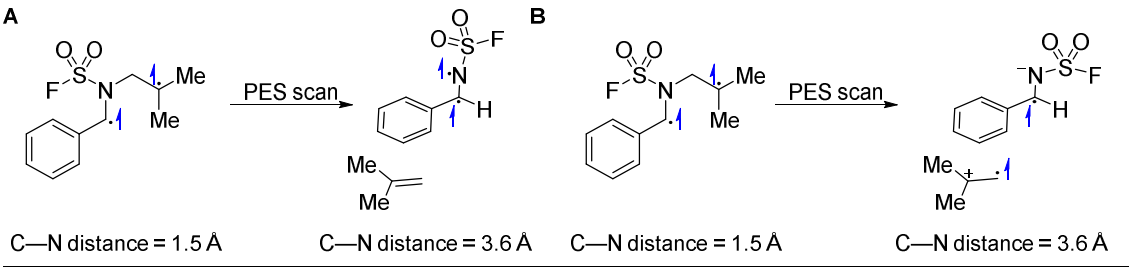
Graph 3-3 Potential energy surface scan varying % of Hartree-Fock exchange in functional. 0% is M06L-D3/def2-SVP, 27% is M06-D3/def2-SVP, 54% is M06-2X-D3/def2-SVP and 100% M06-HF-D2/def2-SVP (this functional uses the D2 dispersion correction as the D3 M06-HF-D3.

Across the range of functionals tested they all produce potential energy surfaces of similar shape without any maxima in the range investigated (**Graph 3-4**). Range-separated functional ωB97X-D3 and hybrid meta-GGA functional M06-2X, often two of the highest performing hybrid functionals in benchmarking studies, produced very similar PES's. Hybrid functionals M06 and in particular B3LYP produced much shallower surfaces possibly due these functionals underestimating long range interactions between the imine and alkene. M06L, a meta-GGA functional not including any Hartree-Fock exchange, performs very similarly to B3LYP at distances <2.1Å however at longer distances it produces the lowest energy potential energy surface.



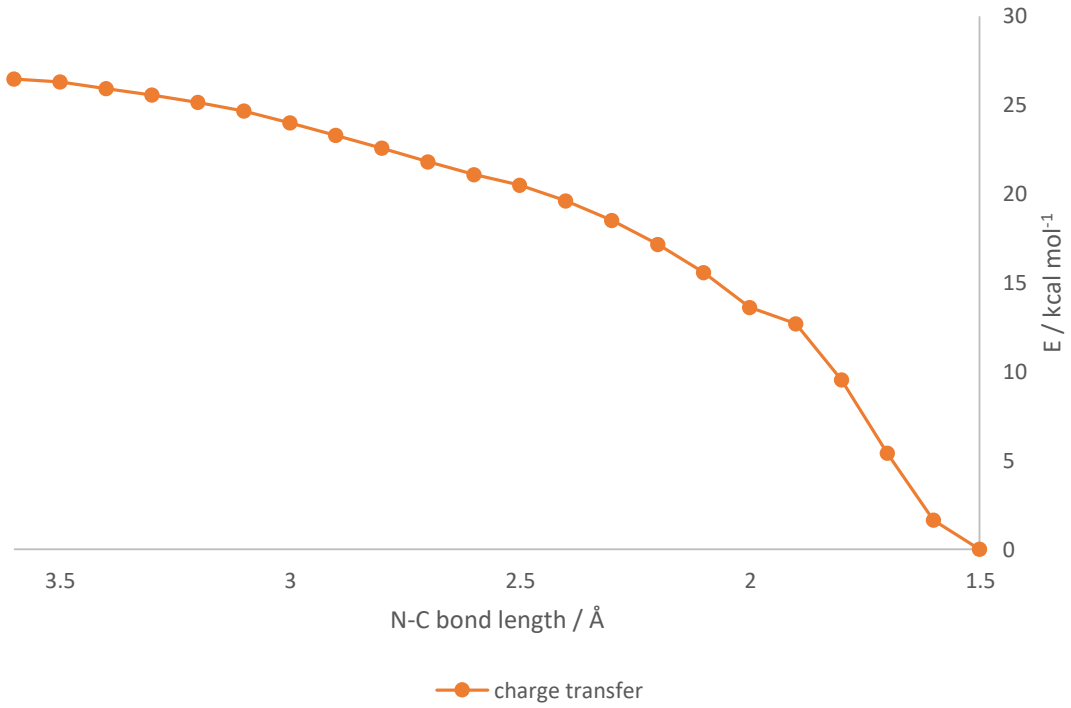
Graph 3-4 Potential energy surface scans varying the functionals.

When performing a geometry scan with SMD(DCE)-M06-2X-D3/def2-TZVP and scanning from the 1,4-biradical and increasing the C-N distance from 1.5 Å, instead of dissociating to a triplet imine and isobutene (**Scheme 3-3A**), the charge partitions unevenly forming a radical cation alkene and a radical anion imine (**Scheme 3-3B**).



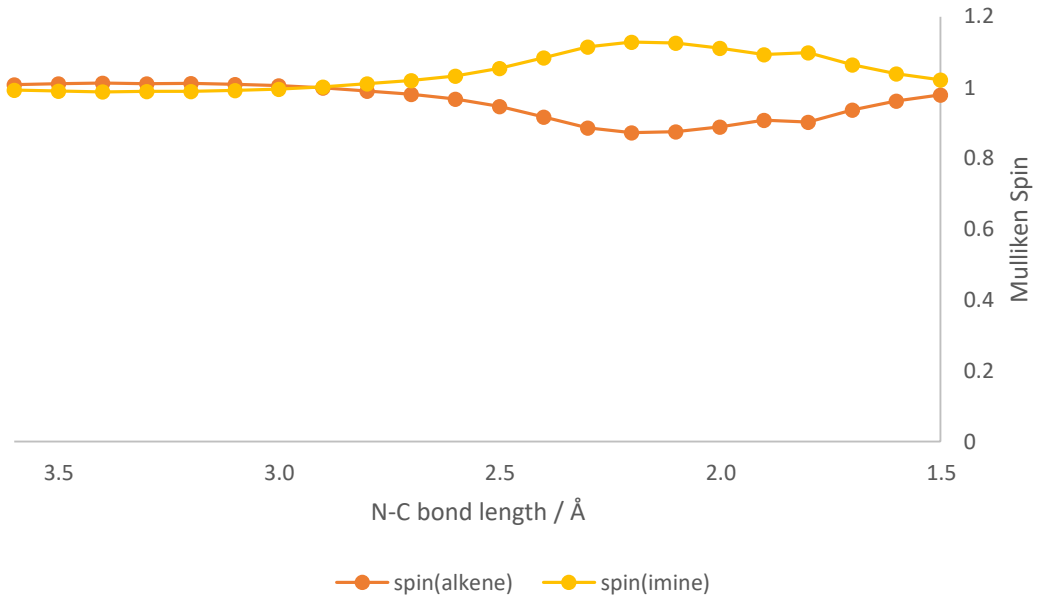
Scheme 3-3A Intended behaviour of the PES scan. **B** Behaviour observed of PES scan with SMD(DCE)-M06-2X-D3/def2-TZVP.

Moving along the PES in the other direction, the addition of the imine radical anion into the isobutene radical cation, like the addition of the triplet imine into the neutral alkene, also gives a downhill process (**Graph 3-5**).

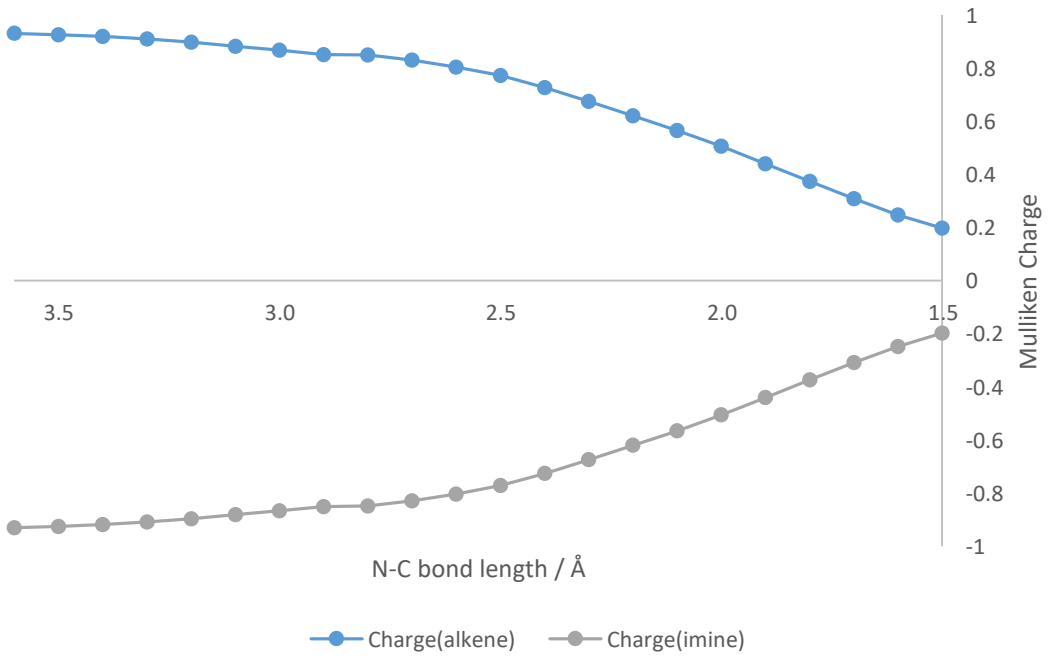


Graph 3-5 Potential energy surface (SMD(DCE)-M06-2X-D3/def2-TZVP) resulting in alkene radical cation and imine radical anion.

The electronic nature of the PES can be visualised by plotting the sum of the Mulliken spin and charge densities of the imine and alkene against the C-N distance. From these graphs it is clear that instead of portioning onto only the imine to form a triplet biradical, the spin partitions evenly to form two radical species (**Graph 3-6**). By plotting the Mulliken charges against distance, it is also clear that while at a distance of 1.5 Å in the 1,4-biradical there is only a small degree of charge separation, at large distances the charge fully separates forming a cationic alkene and anionic imine (**Graph 3-7**).

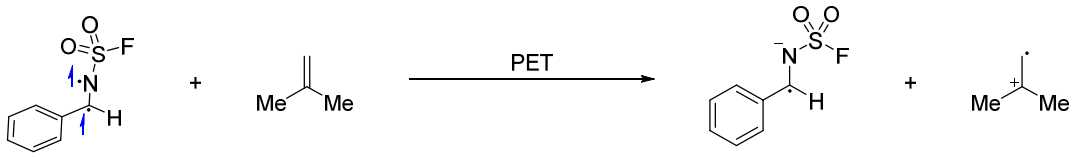


Graph 3-6 Plot of the sum of Mulliken spin for the imine and alkene component for the potential energy surface resulting in charge transfer.



Graph 3-7 Plot of the sum of Mulliken charge for the imine and alkene component for the potential energy surface resulting in charge transfer.

Given that photoinduced electron transfer between the imine and isobutene is endergonic ($\Delta_{PET}G$ = 8.1 kcal mol^{-1}), a charge transfer mechanism can be excluded (**Scheme 3-4**).



Scheme 3-4 Photoinduced electron transfer between triplet imine and isobutene.

Overall, the potential energy surfaces generated after assessing all variables resulted in downhill potential energy surfaces, indicating that this process is likely either barrierless or has an extremely small barrier. In all bar one case we see no maximum in the potential energy surface, except in the gas phase. Here we also demonstrate that results obtained from our selected level of theory (SMD(DCE)-M06-2X-D3/def2-TZVP) and the conclusions drawn about the addition of the alkene into the imine are general and the same conclusions may be drawn from choosing other functionals, basis set or solvent model.

3.4.2 Born-Oppenheimer Molecular Dynamics of the Addition Step

To further investigate the addition of the triplet sulfamoyl fluoride to the alkene and to show that there was no barrier to addition we performed molecular dynamics simulations using ORCA.

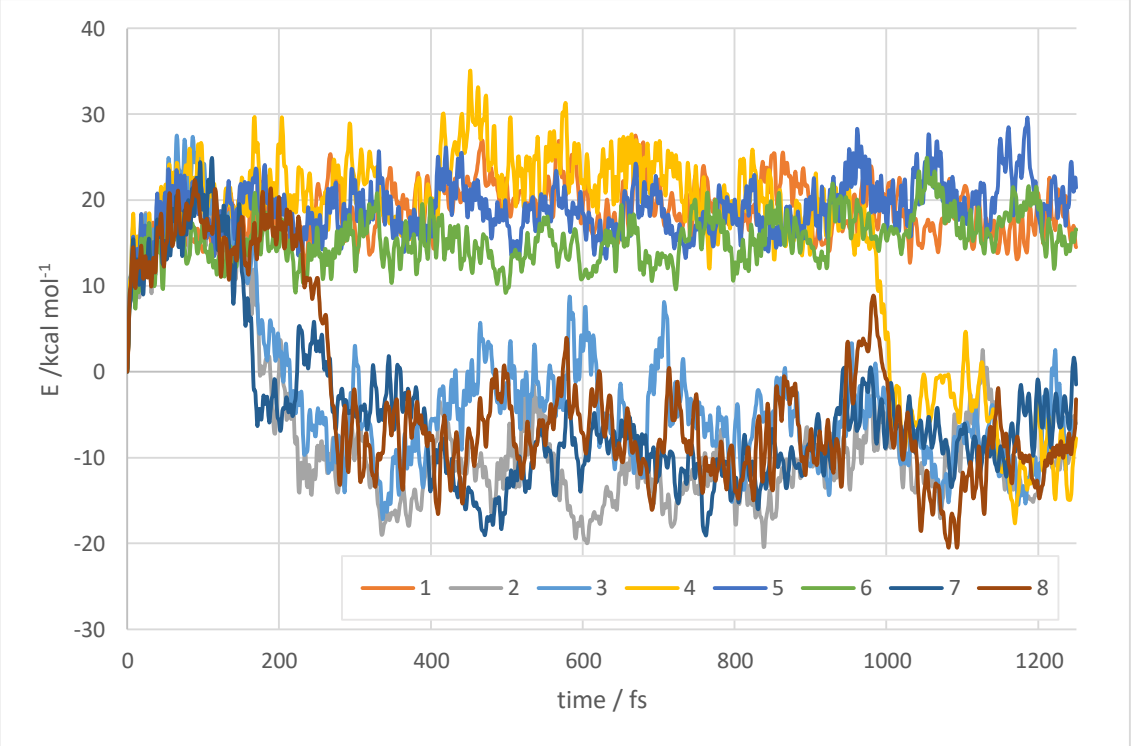
By solving Newton's equations of motion acting on all the atoms of the system and using DFT to calculate the forces we can see how the system evolves over time. As an analytical solution is not possible, numerical solution methods are applied, and in the case of ORCA the velocity Verlet integration algorithm is employed, by taking discreet time steps. For our study we chose a step size of 0.5 fs and a maximum simulation time of 1.25 ps; these

parameters are commonly used in MD simulations of organic molecules.[188] To minimise energy drift, and therefore temperature drift in the system resulting from bond stretching and numerical errors due to the finite time step, a thermostat was employed to conserve the initial temperature of the canonical ensemble. In our case we chose the Nosé-Hoover thermostat and the temperature was set at 298 K.[189, 190] Each MD run was randomised using a stated seed.

The starting geometry for the simulation was chosen from a position along the M06-2X-D3/def2-SVP potential energy surface (3.2 Å C—N bond distance). This distance was chosen as it is greater than twice the equilibrium bond length of the C—N bond and is much greater than the C—N bond distance in the solventless transition state with M06-2X-D3/def2-SVP level of theory (2.51 Å).

In our study, we performed eight simulation runs, and the imine added to the alkene in five out of these eight runs. When addition occurred, it took place within the first 400 fs of the simulation in runs 2, 3, 7, and 8. However, in run 4, additions only occurred after 1000 fs. When the imine and the alkene did not combine (runs 1,5 and 6), the distance between the two species may initially decrease however the distance between the species then increases beyond their initial separated distance, this is a consequence of the changed random initial velocities. When the D3 dispersion correction was excluded, it was found that the imine added into the alkene in 2 of the 4 runs and when addition did occur it occurred in the first 300 fs of the simulation. Similar to when D3 dispersion was included, when the imine and the alkene did not combine the distance between the two species may initially decrease however the distance between the species then increases beyond their initial separated distance.

Addition of the imine and olefin coincides with a sharp decrease of the potential energy of the system, indicating the formation of a bond (**Graph 3-8**). Once the two species combined, the adduct remained intact for the duration of the simulation, implying that addition of the imine into the alkene is irreversible, indicating there is no recrossing effect.

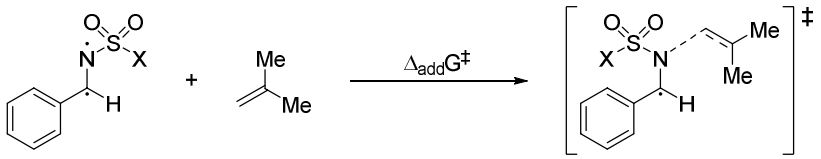


Graph 3-8 Potential energy surfaces for MD runs.

Addition of the alkene into the imine on the femtosecond timescale over multiple runs is strong evidence that there is no barrier to addition up to a distance of 3.2 Å and that this addition is incredibly fast. Hence the only barrier for the addition is likely the diffusion of the two species and the formation of an encounter complex. In this study, only one conformation of the imine and alkene was investigated; however, in future, MD simulations from a distribution of conformations could be examined to provide a more realistic picture.

3.4.3 Comparison of Imine Addition Barriers

After carefully considering the effect of the level of theory used to calculate the potential energy surface for the addition of imine-derived triplets into the alkene, we next explored if triplet derived from other imines had activation energies associated with addition (**Table 3-5**). Transitions states were located for Me, Ph and Bn substituted sulfonyl aldimines all displaying relatively large barriers to addition compared to fragmentation ($\Delta G^{‡}$ = 14.0, 12.1 and 10.7 kcal mol^{-1} respectively). However, when attempting to find the activation barriers for the addition of imines featuring strong electron-withdrawing groups (-SO_2CN, -SO_2Cl -SO_2F, -SO_2CF_3) we were unable to locate transition states, and instead found a series of relentlessly downhill potential energy surfaces, implying that there is either no transition state or an extremely low-lying transition state for these processes.



X	Me	Ph	Bn	Cl	CN	CF_3	F
$\Delta_{add}G^{‡}$ / kcalmol^{-1}	14.0	12.1	10.7	-	-	-	-

- barrierless

Table 3-5 Calculated Gibbs energy barrier of addition into isobutene in kcal mol^{-1}.

Taking the transition state for Me sulfonyl aldimine as an example, it is worth noting that this is an early transition state displaying very little breaking of the C=C bond, with the bond only increasing in length by 0.03 Å or by 2% (**Figure 3-3**). Given that theses imines display higher barriers to addition than to fragmentation ($\Delta\Delta G^{‡}$ = 4.5, 5.3 and 2.4 kcal mol^{-1} respectively), intermolecular [2+2] photocyclization could not be competitive with

fragmentation and therefore these substrates would perform poorly in the aza Paternò–Büchi reaction. Combined with the fact that the standard state used in this investigation is 1 M, which is greater than the concentration used in our reaction of 0.2 M, this further disfavours the bimolecular addition process over unimolecular fragmentation.

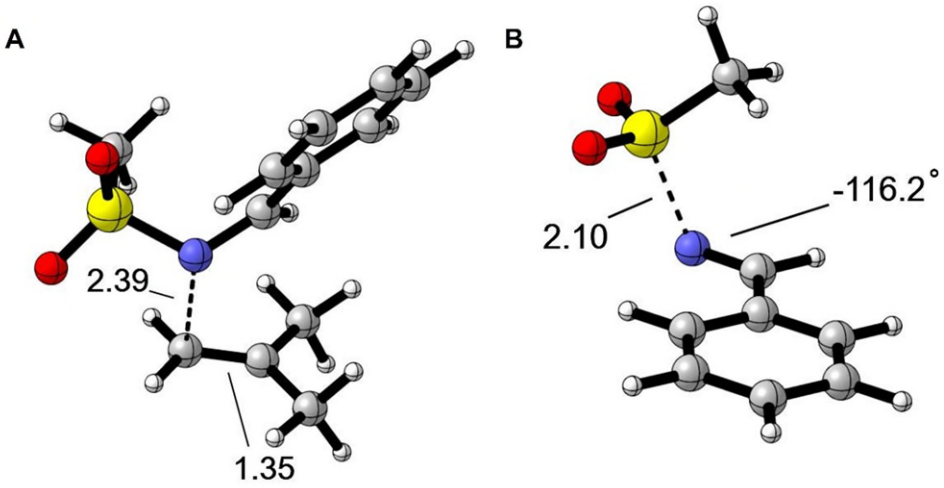


Figure 3-3A Transition state for addition of Ms-imine into isobutene. **B** Transition for fragmentation of Ms-aldimine. Distances in Angstroms (Å)

3.4.4 Alternative Transition States

For completeness, addition of the imine into the alkene with other orientations was considered (**Figure 3-4**). For the -SO_2F aldimine a transition state was located with the gem-dimethyl portion of the alkene is eclipsing the sulfonyl group (θ(S-N-C(alkene)-C(alkene)) = -62.1°) with a barrier of 3.2 kcal mol^{-1} (**Figure 3-5**). By inspecting the Mulliken atomic charges and spin densities we noted that this transition state is consistent with the formation of an exciplex with significant charge transfer. Spin density is almost equally distributed between the imine and isobutene (1.09 and 0.91 respectively) accompanied by a charge transfer of +0.8 and -0.8 for the alkene and imine respectively. Although these transition states would produce feasible processes, as discussed, PET is endergonic, which would preclude the initial electron transfer. Moreover, from the

investigation of the level on theory on the PES's for addition discussed previously, some of the trajectories gave the gauche conformation through the triplet biradical without any barrier, suggesting that this mechanism would be dominant.

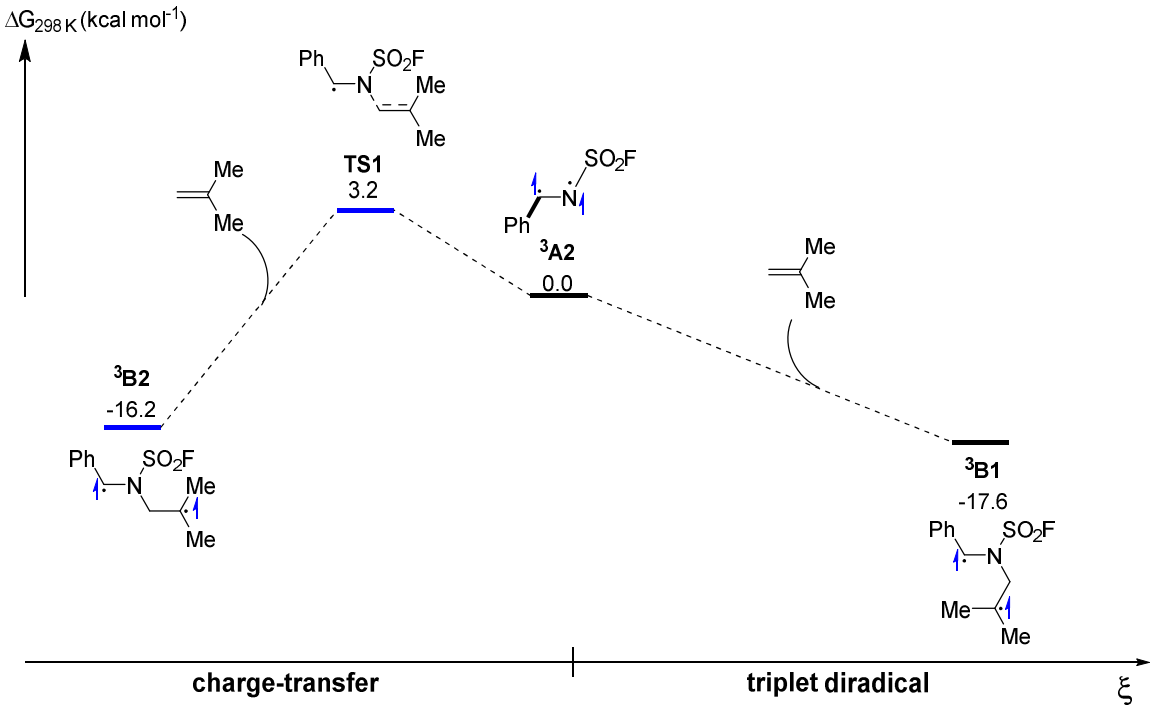


Figure 3-4 Comparison of reactivity profiles for charge transfer addition mechanism vs. triplet imine addition.

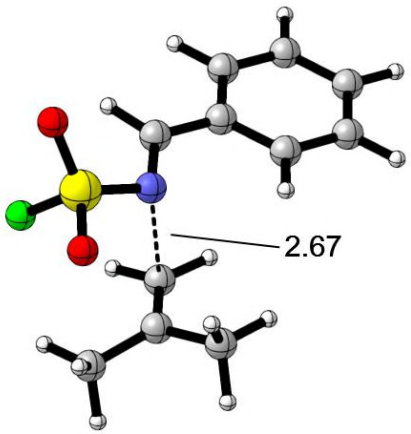
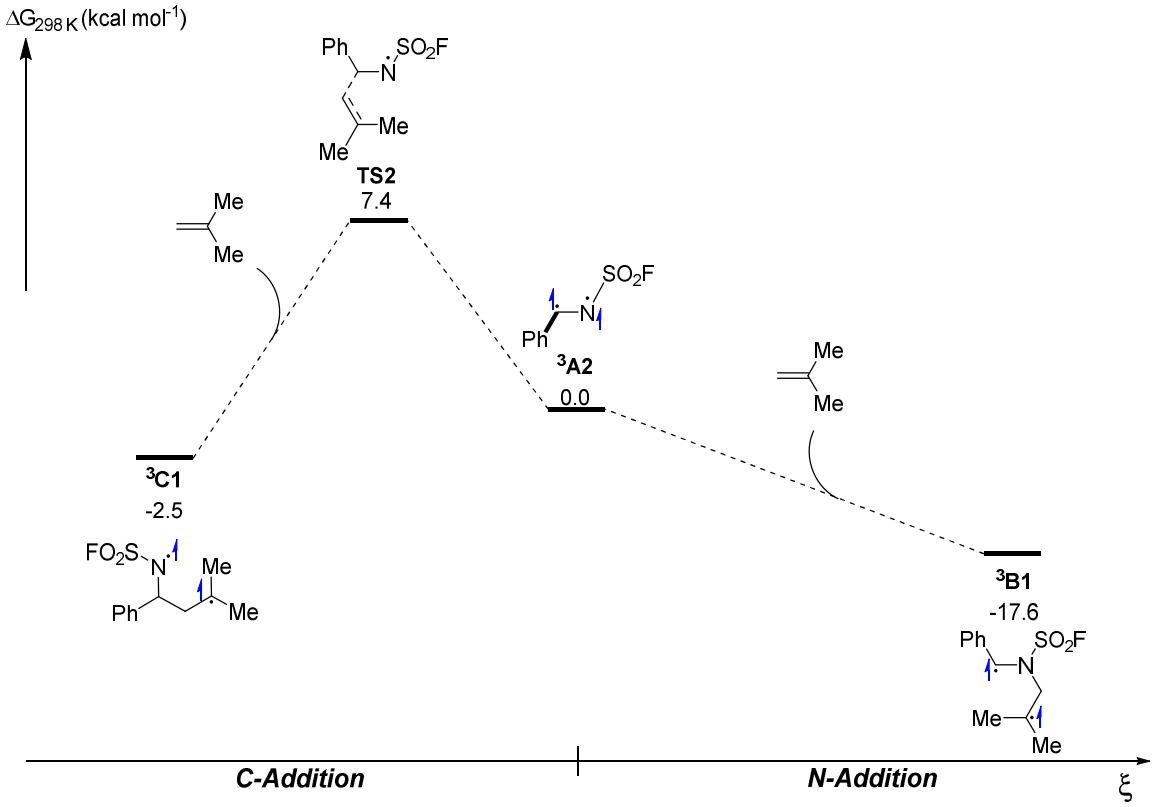


Figure 3-5 Structure of transition state (TS1) for addition into isobutene for the gauche conformation. Labelled distance in angstroms (Å).

3.4.5 Regioselectivity of Addition

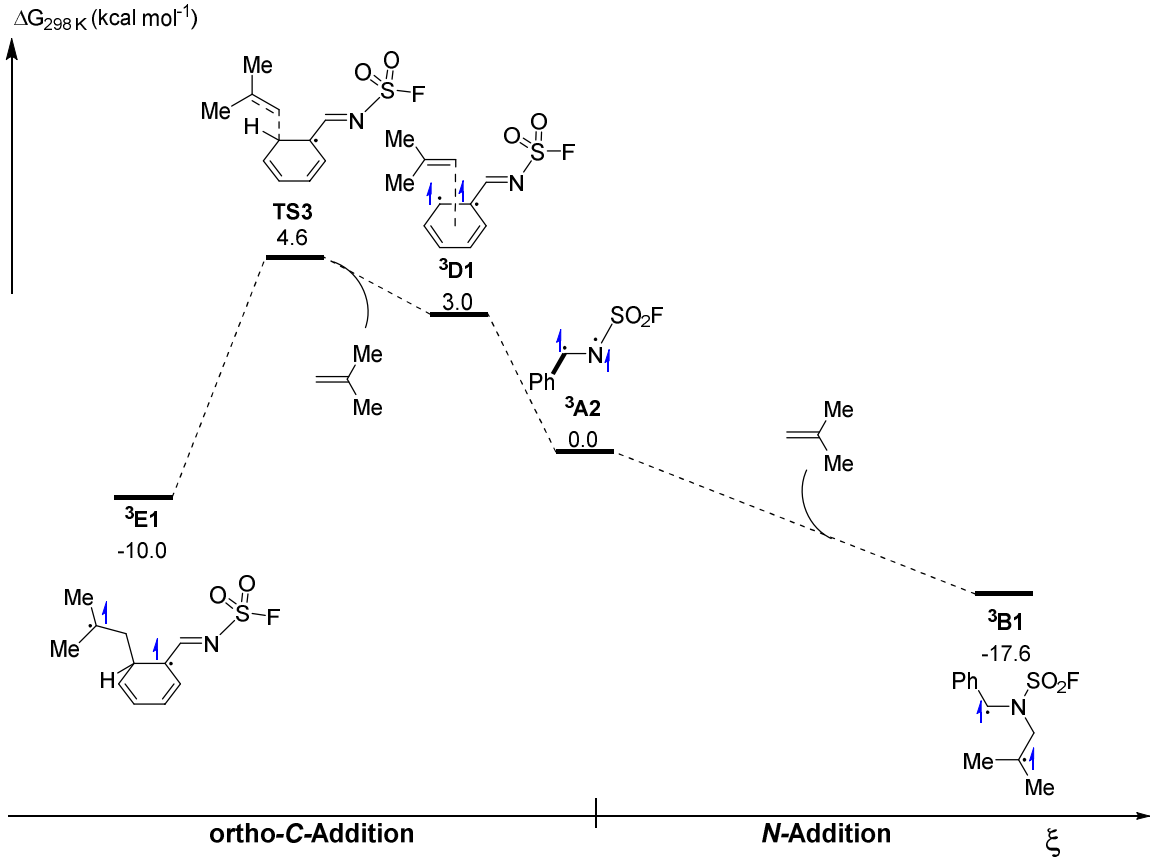
Given the excellent regioselectivity observed experimentally for the product resulting from initial *N*- addition, the barrier to *C*- addition was investigated (**Scheme 3-5**). It was found that unlike addition at *N*-, there is a barrier for *C*-addition of 7.4 kcal mol^{-1}, which would preclude the formation the resulting regioisomer as it would not be kinetically competitive with addition at *N*. This computational data strongly supports the experimental observation, showing that the nucleophilic alkene reacts more rapidly at the electrophilic *N* than at the nucleophilic *C*, and that any process with a barrier greater than 7.4 kcal mol^{-1} would likewise be unable to compete, including fragmentation.



Scheme 3-5 Addition of reaction profile for *N*-addition vs. *C*-addition.

In order to determine other possible reactive positions on the imine the spin densities were inspected and it was found there was significant spin density on the *ortho*- positions

(0.22 and 0.24) of the arene ring. It was hypothesised that addition into this position may be feasible. An encounter complex, ^{3}D1, was located and following this endergonic encounter complex the transition state is a further 1.6 kcal mol^{-1} higher in energy for a total barrier of 4.6 kcal mol^{-1} to *o*- addition (**Scheme 3-6**). For our model system this precludes this regioisomer from forming relative to addition at *N*, however given that 3,4,5-trimethoxybenzaldehyde derived imine gives exclusively an indane product this pathway may be more relevant for other imines. It is worth noting that the transition state for *ortho*-addition (TS3) is actually lower in energy than transition state for addition at the imidic-*C* (TS2) ($\Delta\Delta G^{\ddagger}$ = 2.8 kcal mol^{-1}), despite the imidic-*C* possessing Mulliken spin density (0.67) higher than both *o*- carbons combined. This observation suggests that radical philicity may be a more important factor in determining reaction rates than spin density alone.

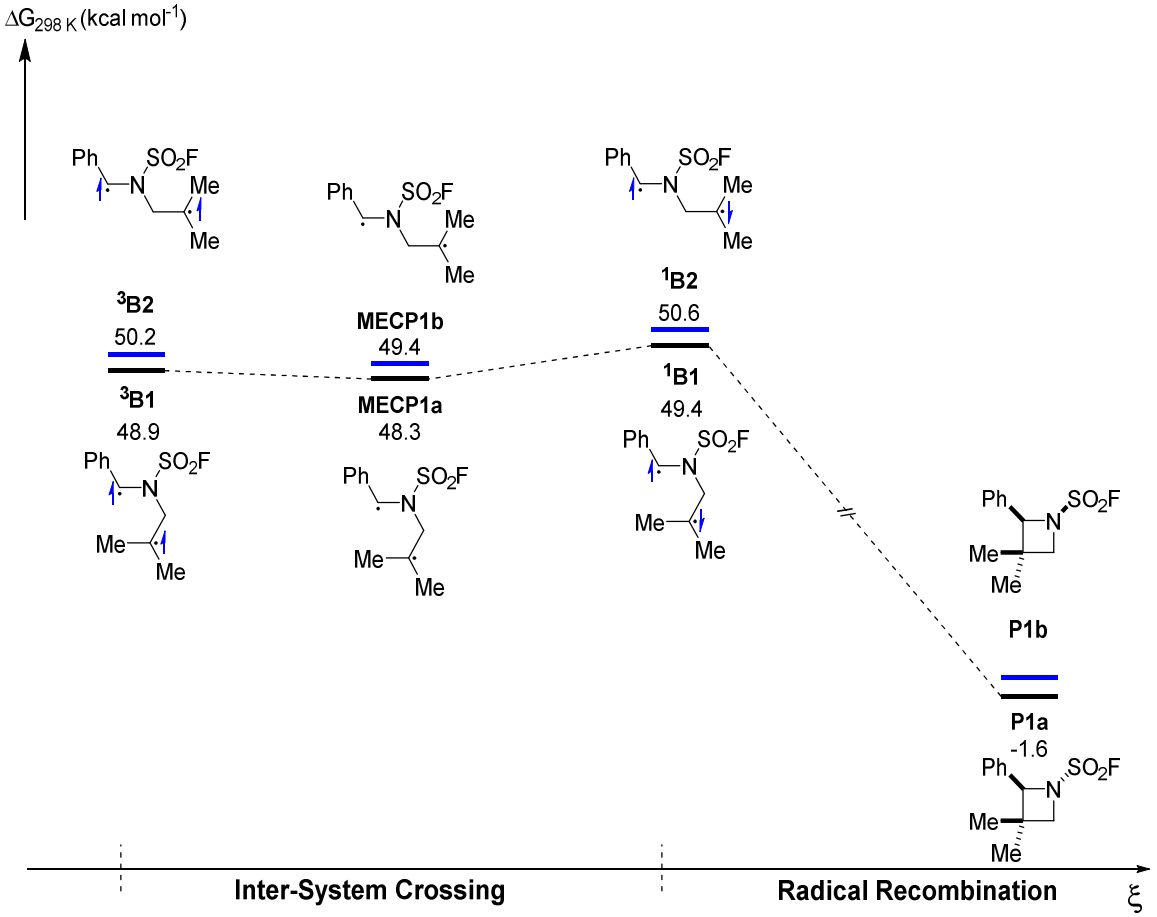


Scheme 3-6 Addition of reaction profile for *N*-addition vs. *ortho C*-addition.

3.5 Intersystem Crossing

Following addition of the triplet imine into isobutene two conformers for the triplet diradical intermediate were located; a lower energy conformer with the isopropyl radical anti-periplanar to the -SO_2F group and a higher energy gauche conformation (**Scheme 3-7**). Next, for the resulting biradical from addition into isobutene, the minimum energy crossing point (MECP) was located and was very close in energy to the initial triplet state, implying that intersystem crossing is very rapid. Following inter-system crossing, an open-shelled singlet biradical is formed of which two conformations were found with the same order of energy as the MECP and triplet states. The singlet biradical subsequently undergoes a radical-radical recombination step, which is expected to barrierless and is highly exergonic resulting in the product being formed irreversibly. Although DFT

methods may result in static correlation effects, the broken system solution and MECP provide an initial approximation to indicate a straightforward route to the product. Within the BS-DFT formulation the spin densities of the relevant atoms were checked to ensure a diradical species was formed and not a zwitterionic species.



Scheme 3-7 Reaction profile following the fate of the 1,4-biradical.

3.6 Alternative Alkene

To rationalise why exocyclic 1,1-dialkyl alkenes required an increased loading relative to their non-exocyclic counterparts, we decided to investigate the reaction profile computationally and determine which step in the mechanism may explain this difference. Our model alkene for this study was methylene cyclobutene, as this class of alkene was shown to work experimentally and is computationally inexpensive.

3.6.1 Addition of Imine

Two conformations of the triplet biradical are formed from the addition of the imine into methylene cyclobutene: a higher-energy extended conformation and a lower-energy contracted conformation (**Figure 3-6**).

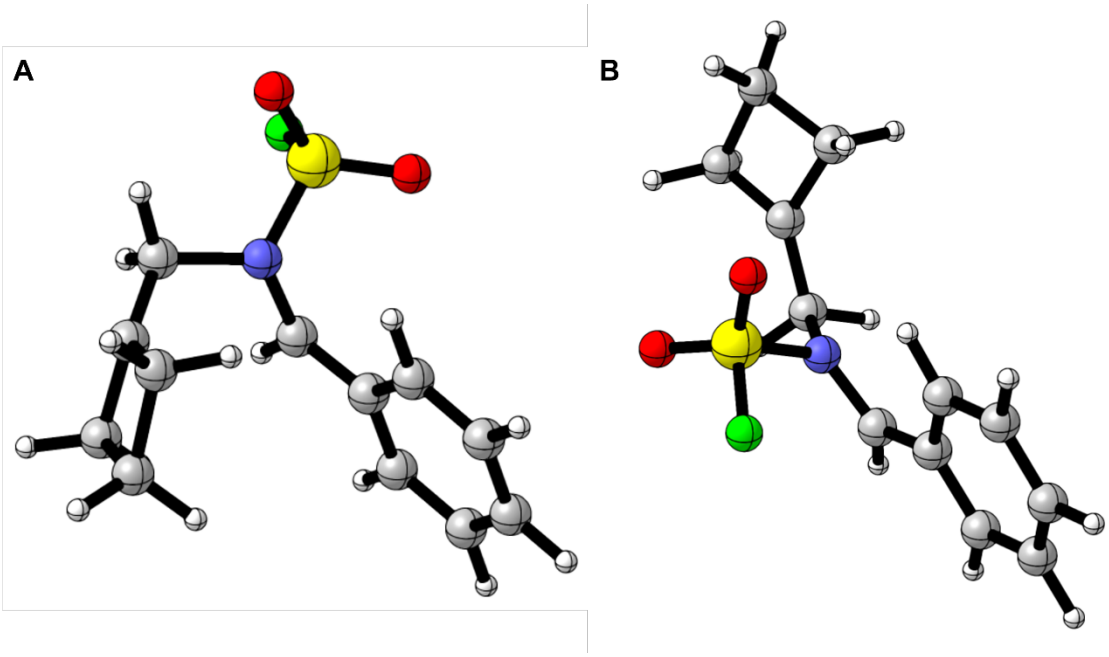
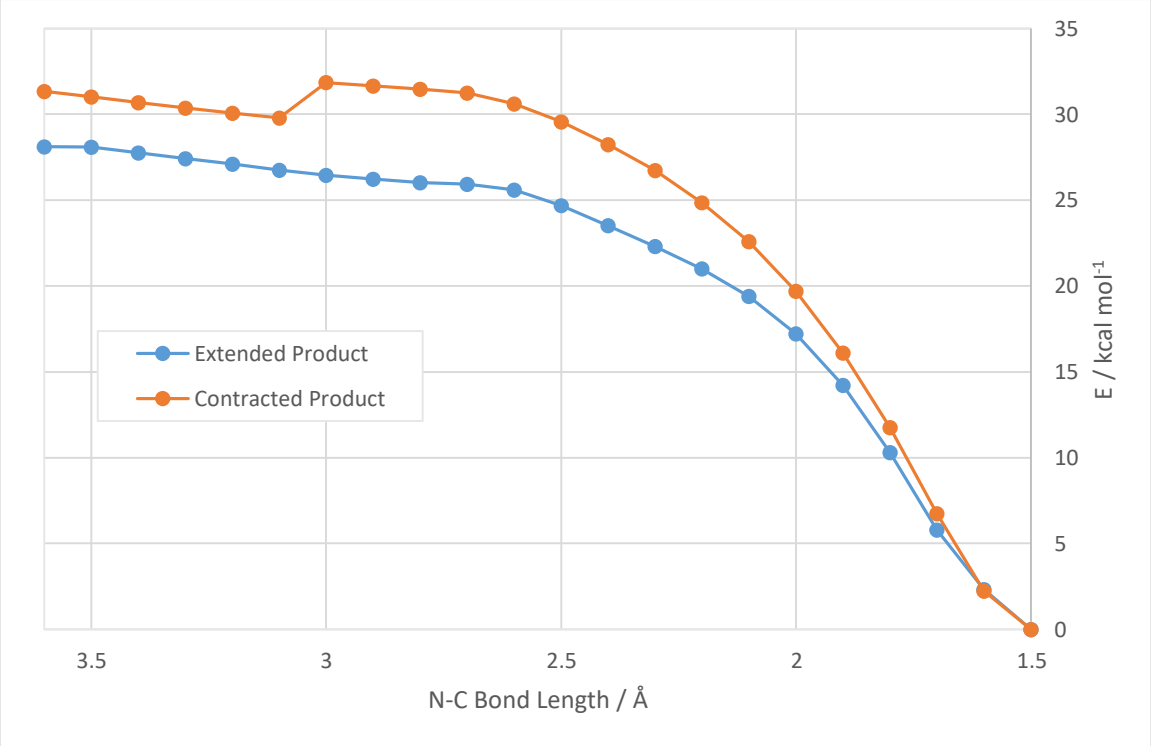


Figure 3-6 A Lower energy conformation triplet biradical ^{3}E1 resulting from addition of imine into methylene cyclobutene. **B** Higher energy extended conformation ^{3}E2.

PES scans were calculated using SMD(DCE)-M06-2X-D3/def2-SVP, resulting in both conformations from the addition of the triplet imine into the alkene (**Graph 3-9**). For the surface leading to the extended product, the energy surface was entirely downhill with no maxima from 3.6 Å onward. For the surface leading to the contracted conformation, the addition of the imine into cyclobutene resulted in a downhill surface from 3.0 Å. Beyond this distance, there is a decrease in energy due to a change in the orientation of the alkene as the imine begins to add to the more substituted carbon, resulting in an artificial maximum. Indeed, it was difficult to obtain a potential energy surface where the imine did not add to the more substituted carbon when starting from the separated imine and

alkene. The 'extended' PES appears lower in energy compared to the 'contracted' surface because the extended product is higher in energy, effectively transposing the entire surface downward. During the scans, we sometimes observed surfaces where full charge transfer occurred. However, this possibility could be ruled out due to the endergonicity of PET for this system($\Delta_{PET}G$ = 8.6 kcal mol^{-1}).



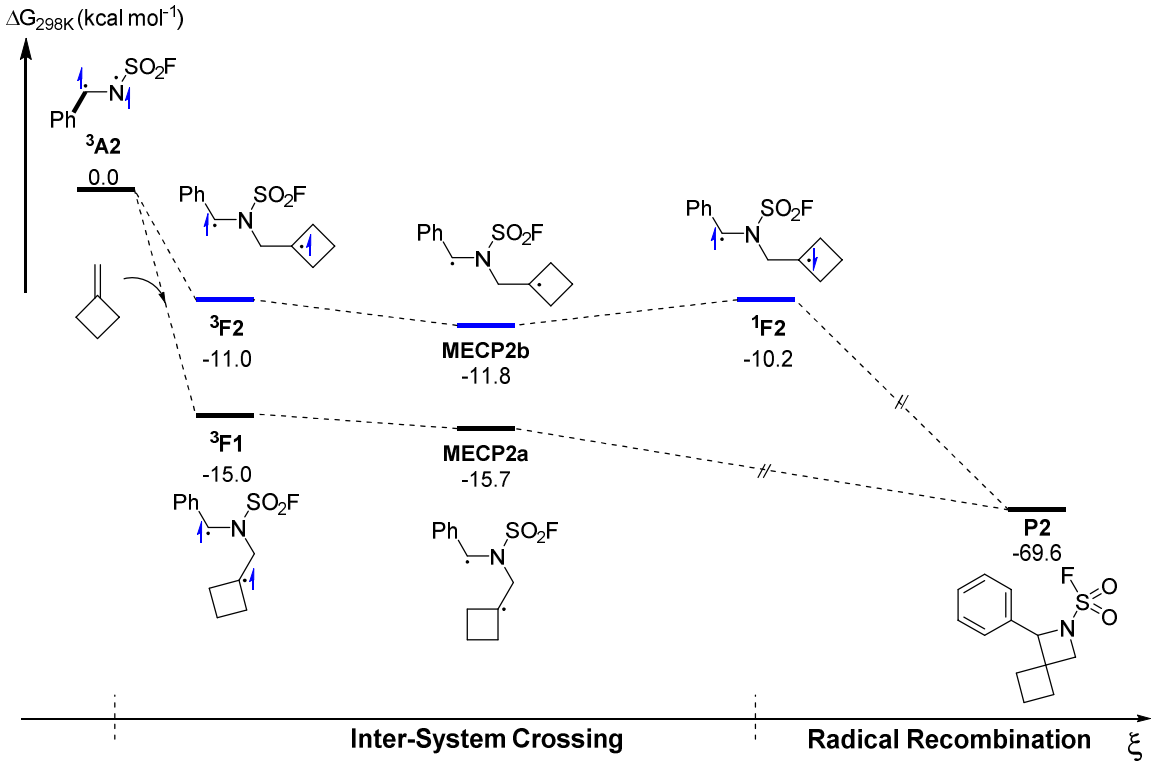
Graph 3-9 PES surface for the addition of methylene cyclobutane.

Therefore, we ruled that addition of the imine into methylene cyclobutene like isobutene is also barrierless, therefore another step in the mechanism is likely responsible for the difference in reactivity observed.

3.6.2 Intersystem Crossing

Following on from the formation of the triplet biradical, intersystem crossing was investigated to see if intersystem crossing was substantially different for the exocyclic alkene to the previous system (**Scheme 3-8**). To give a first approximation of the rate of

intersystem crossing the MECP for both conformations was investigated. However, in this case we obtained similar results to the previous system with an MECP very close in energy to the initial triplet species and likely very rapid. We were able to locate the corresponding open-shell singlet biradical after MECP for the extended conformer however, it was not possible to locate a stable open-shelled singlet biradical species for the contracted species which was unstable relative to the closed shell product.



Scheme 3-8 Reaction profile following the fate of the 1,4-biradical.

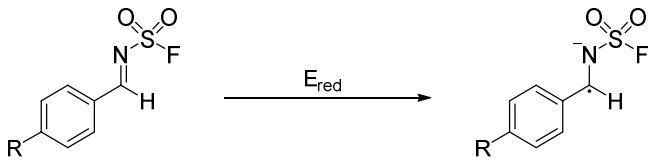
The relative energy of the MECP to the triplet state do not necessarily reflect the rate of inter-system crossing as this not an adiabatic process and the dynamics of the system need to be taken into account. In order to fully understand the rate of the intersystem crossing step, one would need to turn to time CASSCF, however this is outside the scope of this study.

Ultimately, it is not possible to conclusively state why the seemingly small structural difference of an exocyclic alkene *vs* acyclic alkene results in a large difference in reactivity. It is unlikely to be as a result of the addition step as these are very similar for both alkenes and are well described by DFT and is more likely a result of difference in intersystem crossing which even though this has an MECP that is close in energy to the parent triplet, is not well described by DFT.

3.7 Calculated Reduction Potentials

3.7.1 Imines

To further rule out the possibility of a photoredox catalysed reaction manifold operating in our system we looked at the reduction potential for a series of aldimines varying the electronics of the arene ring (**Table 3-6**). This data along with calculated excited triplet state oxidation potentials allows the determination of the feasibility of the generation of a radical anion.



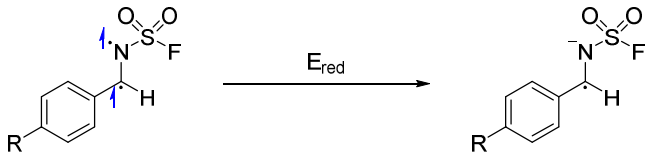
R	σ_p	E_{red}(calculated) /V	E_{red}(experimental) /V
H	+0.00	-1.13	-
OMe	-0.27	-1.28	-1.12
CN	+0.66	-0.77	-

Table 3-6 Computed reduction potentials of sulfamoyl fluoride imines vs. SCE in DCE. Experimental value is in MeCN.

The calculated reduction potential for the OMe substituted imine (E_{red} = -1.28 V) was benchmarked against the experimental reduction potential in MeCN (E_{red} = -1.12 V) and the two results show good agreement. In general, the calculated reduction potentials of

sulfamoyl fluoride imines are very low, and are much lower than the experimental values for tosyl aldimines (for *N*-(4-methoxybenzylidene)-4-methylbenzenesulfonamide E_{red} = -1.44 V. [88]. From the limited dataset above adding a more electron-withdrawing group onto the imine and increasing the Hammett parameter significantly reduces the reduction potential of the aldimine. This puts the aldimine reduction potential in range of the more reducing ITX photocatalyst (*vide infra*) resulting in lower yield as a result reduction being competitive with sensitisation.

Next, we wanted to look at how the oxidising power of the same aldimines as above in the triplet state (**Table 3-7**). Adding electron withdrawing groups stabilises the resulting radical anion, making the aldimine more oxidising and *vice versa* for -OMe. We hypothesized that in some cases reductive quenching of the triplet aldimine with a ground state aldimine may possibly become competitive with [2+2]-photocyclisation. For these calculations the planar geometry of the imines was implemented as this allowed for the lowest structural reorganisation and therefore fastest rate of electron-transfer.



R	E_{red}
OMe	+1.38
H	+1.74
CN	+2.04

Table 3-7 Computed reduction potentials of triplet sulfamoyl fluoride aldimines.

More electron-withdrawing substituents on the arene led to more positive reduction potentials, reflecting the increased stability of the resulting radical anion.

3.7.2 Photochemistry and Electrochemical Studies on Thioxanthone Photocatalysts

In order to gain further understanding of the photocatalysts employed in this study, the photochemical and electrochemical properties were investigated. First the triplet energies were computed using SMD(DCE)/M06-2X-D3/def2-TZVP (calculated values are E_T(ITX) = 64.2 kcal mol^{-1} and E_T(3-FTX) = 68.3 kcal mol^{-1}) which are consistent with the experimental values (E_T(ITX) = 63.6 kcal mol^{-1} and E_T(3-FTX) = 67.4 kcal mol^{-1}), previously determined by phosphorescence emission spectroscopy (**Figure 3-7**).[145] Comparing the triplet energies (E_T) calculated in this study and triplet energy calculated for sulfamoyl fluoride aldimine A (E_T = 67.3 kcal mol^{-1}), energy transfer is predicted to be slightly endergonic for ITX and slightly exergonic for 3-FTX which may account for the improved performance of 3-FTX over ITX in our system for the simple phenyl aldimine.

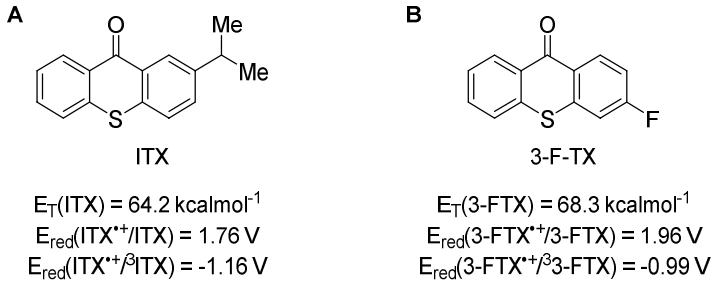


Figure 3-7 Photochemical and electrochemical properties of **A** ITX and **B** 3-FTX.

The less negative reduction potential of 3-FTX compared to ITX should also be taken into account particularly with respect to the improved performance of 3-FTX for aldimines bearing an electron-withdrawing groups on the aromatic group, which we would expect to reduce the triplet energy of the aldimine. In the case of ITX, single electron reduction and back electron transfer of electron-deficient aldimines becomes

competitive with energy transfer, which reduces the efficiency of energy transfer resulting in a diminished yield of the aza-Paternò Büchi reaction.

3.8 NBO Analysis

With the complete reaction profile for the -SO_2F substituted imine computed and the reactivity of sulfamoyl fluoride imines better understood, we next wanted to rationalise and understand why this imine displayed such excellent reactivity as compared to other sulfonyl aldimines. To this effect we carried out natural bond orbital (NBO) analysis as this allows us to transform the wavefunction into a localised form more in line with a chemist's Lewis structure picture.

Looking at the SUMOs on the SO_2F imine we see that the lower energy singly occupied orbital is *N*-based, $n_{N\text{-}NBO}$, and the HSUMO is *C*-based (**Figure 3-8A**). As we observe regioselective reaction at *N*, the reactivity of the imine can then be rationalised as the electrophilic component accepting an electron into the *N* based LSUMO from the alkene (**Figure 3-8B**). This also rationalises why this transformation performs well with electron-rich and nucleophilic alkenes and poorly with electron-poor, electrophilic alkenes.

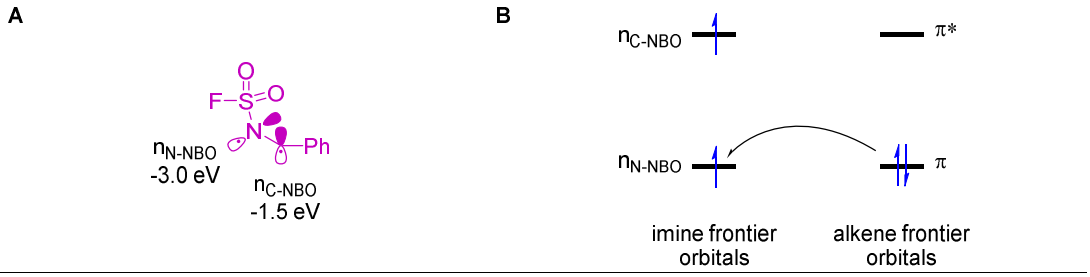
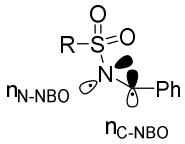


Figure 3-8A Annotated orbital diagram. **B** Energy level diagram for addition of imine into alkene.

Looking across the range of imines employed in this study, how negative the $n_{N\text{-}NBO}$ is and thus the electrophilicity of the imine correlates to the success of the imine in the aza

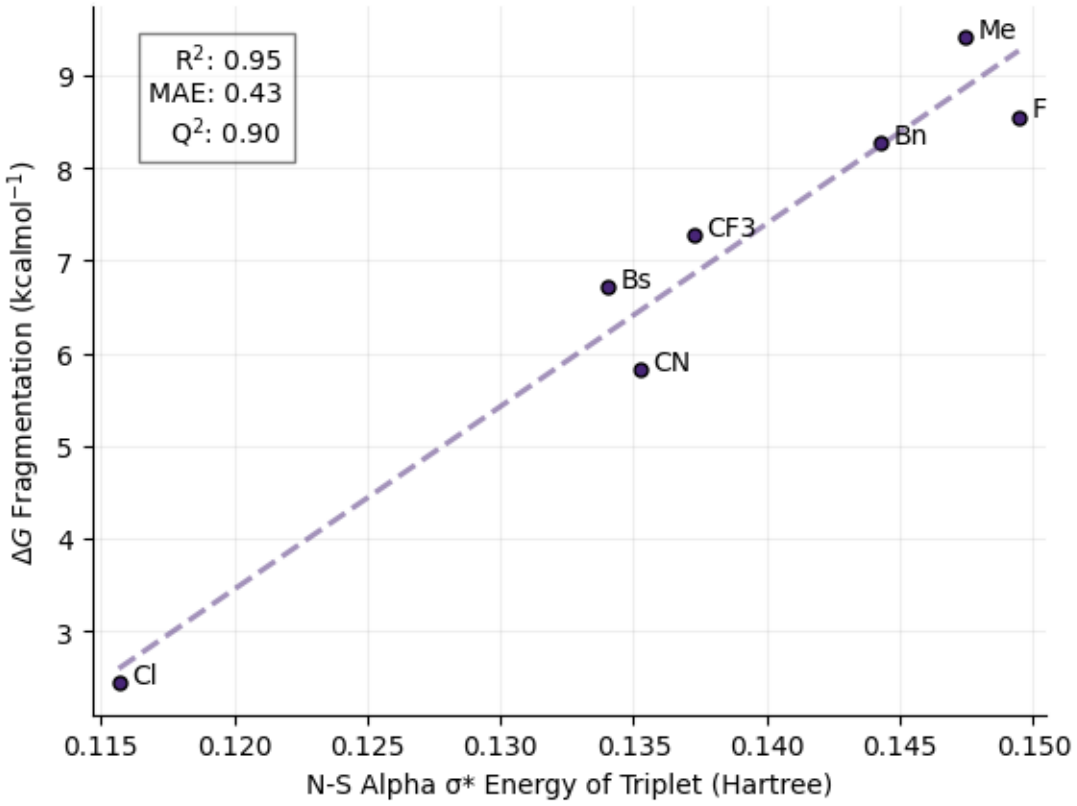
Paternò–Büchi reaction (**Table 3-8**). The successful -SO_2F and -SO_2CF_3 imines have very low $n_{N\text{-}NBO}$'s of -3.02 and -3.00 eV respectively while the $n_{N\text{-}NBO}$ of -SO_2Ph has a much higher value of-2.30 eV.



R	CN	F	CF_3	Cl	Bn	Me	Ph
$n_{N\text{-}NBO}$/eV	-3.11	-3.02	-3.00	-2.88	-2.39	-2.38	-2.30

Table 3-8 N LSUMOs for the range of imines.

Regarding the fragmentation of triplet sulfonyl aldimines, the most predictive property was the N-S σ* orbital energy in the triplet imine, which showed a strong correlation with the fragmentation barrier, as demonstrated by the graph below (R^2 = 0.95, **Graph 3-10**). A lower N-S σ* orbital energy naturally indicates a weaker N-S bond, and in this case, the thermodynamic parameter correlates well with the kinetics of fragmentation.



Graph 3-10 Best correlating feature with the sulfonyl aldimine fragmentation process.

3.9 Summary and Outlook

To conclude, this computational study has provided valuable insights into the mechanism of the developed aza Paternò–Büchi reaction, as well as rationalising why the sulfamoyl fluoride aldimine is privileged in this transformation. The triplet sulfamoyl fluoride aldimine has a relatively high barrier to β-scission as compared to other sulfonyl aldimines, allowing it to be resistant to photochemical fragmentation. Additionally, it has been shown that there is no barrier to addition of the sulfamoyl fluoride imine into an unactivated alkenes, as a result its high electrophilicity at nitrogen. Finally, when considering photocatalysts, a photocatalyst with a high triplet energy alone is not sufficient for designing an efficient energy transfer catalysed reaction, and the competing single electron transfer pathways must also be considered.

With these key features of a successful aza Paternò–Büchi reaction in mind, it may be possible to design other acyclic aldimines capable of undergoing this reaction. Rather than computing an entire reaction profile, one could focus on just a few key parameters. This approach would enable the screening of a large number of virtual compounds at a significantly reduced computational cost. Parameters that may predict successful substrates include a low $n_{N\text{-}NBO}$, indicative of an electrophilic imine, along with a high N-S σ* orbital, which suggests resistance to fragmentation. To further refine the model, predicted imines could be evaluated experimentally, with the results fed back into the model.

Chapter 4 Conclusions and Future Work

At the beginning of this thesis, the importance of azetidines, along with the established methods for their synthesis and the challenges associated with these methods (often stemming from their inherent strain), was described. The application of modern methods to these challenges has enabled expedient access to azetidines that would otherwise be cumbersome to synthesise or entirely inaccessible. Despite its origins in the 1960s and the attractive disconnection it offers, the aza Paternò–Büchi reaction has not been considered a viable synthetic route due to the extensive engineering required to enable an imine to undergo this reaction without succumbing to numerous side reactions. To address this, we sought to rectify these limitations and develop an aza Paternò–Büchi reaction that utilises simple acyclic aldimines.

We described how a simple modification to the sulfonyl group of sulfonyl aldimines allowed us to perturb the electronic character of the triplet state, reducing the extent of fragmentation typically observed for this class of aldimines. This enabled the aza Paternò–Büchi reaction with alkenes. We found that, under a visible-light energy transfer manifold, aryl sulfamoyl fluoride aldimines are capable of undergoing this reaction in excellent yields. The reaction demonstrated a broad scope with respect to both the imine and alkene components, enabling the synthesis of a diverse array of azetidines with underrepresented substitution patterns. The utility of the resulting azetidine sulfamoyl fluoride products was also demonstrated through key derivatisation reactions. Most importantly, we showed that the -SO_2F group could be removed, rendering it a traceless activating group. Due to the simplicity of this disconnection and the breadth of the transformation, this methodology is likely to find applications in both academic and industrial settings.

Following the development of this new methodology, we conducted a computational study to rationalise and explain why the imines selected in this study behave so differently from structurally similar substrates. Using DFT calculations, we proposed a plausible reaction mechanism akin to the Paternò–Büchi reaction. Within this framework, we identified the key characteristics of imines required for successful [2+2] photocycloaddition. With the mechanistic insights gained from this computational study, the potential for extending this transformation or discovering other classes of acyclic imines may now be realised.

Future work could focus on elaborating this aza Paternò–Büchi reaction to facilitate the stereoselective synthesis of azetidines. This could be achieved by integrating computational and experimental studies to design chiral aza-sulfur groups on nitrogen that act as chiral auxiliaries, thereby enabling the aza Paternò–Büchi reaction. This, in turn, would allow the synthesis of enantioenriched azetidines. Alternatively, to address the poor diastereoselectivity observed, tuning non-covalent interactions such as hydrogen bonding between the substrates may enable the selective formation of a single diastereomer.

Chapter 5 Experimental Procedures

5.1 General Information

All reactions were performed under an atmosphere of N_2 with constant magnetic stirring, unless otherwise stated, using clean, oven dried glassware. All inert gases were sourced from the University of Oxford's internal supplies and dried through a $CaCl_2$ drying columns. Reactions were monitored by thin-layer chromatography (TLC) which was performed on Merck Millipore Kieselgel 60 PF254 pre-coated aluminium backed TLC sheets and visualized by UV lamp (λ = 254 nm and 365 nm) and/ or staining using $KMnO_4$, phosphomolybdic acid or anisaldehyde stain. All chemicals used were obtained from commercial sources, unless otherwise stated, including Sigma Aldrich, Fluorochem, Alfa Aesar and Strem. $Pd(PPh_3)_4$ was triturated with MeOH before use and stored under N_2 at -20 ^oC. Dry solvents were obtained from the University of Oxford internal solvent drying system (Innovative Technology Inc. PS-400-7), wherein they are purified through dried alumina columns. Solvents used in the [2+2] photocyclisation were kept under an atmosphere of N_2 and stored over 3Å molecular sieves. Solvents used for purification, or not needed dry, were HPLC grade purchased from either Alfa Aesar or Sigma Aldrich. When referring to the solvent 'Petrol' and 'pet. ether', what is meant is the fractions of petroleum ether which boil within the range 40 – 60 ^oC. Flash column chromatography was performed by loading the compound as an oil or concentrated solution onto a column, using Geduran® Si 60, 40–63-micron silica gel, and then run with the indicated eluent system.

^1H NMR, ^{13}C NMR and ^{19}F NMR spectra were recorded on a Brüker AVIII spectrometers (400-700 MHz). Acquisitions were carried out at rt unless otherwise stated. Chemical shifts (δ/ ppm) are reported in parts per million (ppm) and referenced relative to the

residual solvent peak; ^{1}H NMR: $CHCl_3$ (7.26 ppm), ^{13}C NMR: $CHCl_3$ (77.2 ppm). Coupling constants (*J*) are given in Hertz (Hz) and rounded to the nearest 0.5 Hz. ^{1}H NMR is recorded to two decimal places and ^{13}C NMR is recorded to 1 decimal place. Proton multiplicity is assigned using the following abbreviations: singlet (s), doublet (d), triplet (t), quartet (q), pentet (p), multiplet (m), broad (br). Assignments were made using the help of a variety of 2D NMR experiments (COSY, HSQC, HMBC and NOESY).

High resolution mass spectra were obtained *via* the University of Oxford in-house service, utilising using either a Thermo Exactive High-Resolution Orbitrap FTMS spectrometer or Waters BioAccord TOF spectrometer under electrospray ionisation conditions (ESI). Values quoted are a ratio of mass to charge in Daltons to four decimal places on the high resolution. For high resolution mass spectra, the mass found was compared to the mass calculated from the monoisotopic molecular formula, and all results were found to be within a 5 ppm error of the calculated values.

Melting point values were found using a Reich Melting Point Apparatus and are reported uncorrected. Infrared spectra were determined using neat samples with a Brüker Tensor 27 FT-IR spectrometer with an internal range of 600-4000 cm^{-1} and all absorptions are given in wavenumbers (cm^{-1}).

All UV-vis absorption spectra were recorded at 298 K, with temperature control by a PTP-1 Peltier unit from Perkin Elmer, with baseline correction.

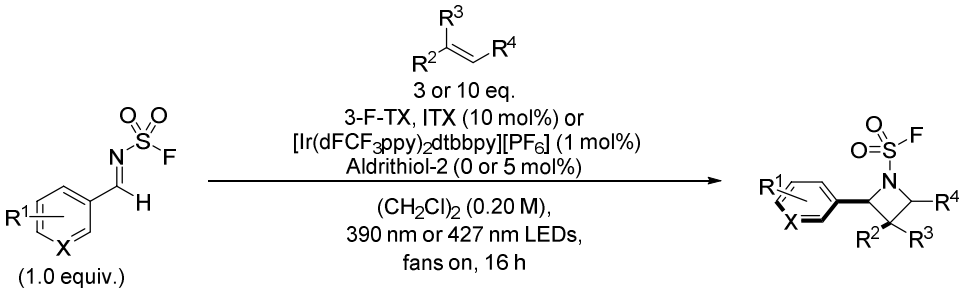
The HPLC data was obtained from an Agilent Technologies 1200 series HPLC Hypersol ODS, ϱ μm column (100 π 4.0 MM) using an extended 20 min method H_2O (0.1 % v/v H_3PO_4): Acetonitrile 10-95% (17 min) to 100% (18.5 min) to 10% (20 min).

For the relative stereochemistry nomenclature of final ring diastereoisomers, the terms *R** and *S** have been used denote the configuration of a stereocenter, relative to that of a co-existing stereocenter, within a racemic compound. This is not to be confused with absolute stereochemical terms *R* and *S*, used to depict absolute configuration within an enantiopure compound. Accordingly, a compound of number ***A***, with a name prefixed x*R**,z*S** ((x*R**,z*S**)-***A***), will be the diastereoisomer of compound ***A***, prefixed with x*R**,z*R** ((x*R**,z*R**)-***A***), where x and z are integers representing the stereocenter position.

5.2 Experimental Data for Chapter 2

5.2.1 General Procedures

Energy-transfer mediated intermolecular aza-Paternò-Büchi reaction (GP1)



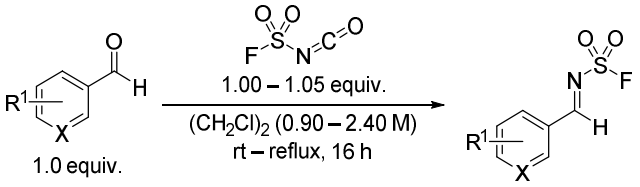
Fluorosulfamoyl imine (0.20 mmol, 1.0 equiv.), 3-F-TX (4.6 mg, 0.020 mmol, 10 mol%), ITX (5.1 mg, 0.020 mmol, 10 mol%) or [Ir(dFCF$_3$ppy)$_2$(dtbbpy)][PF$_6$] (2.2 mg, 0.002 mmol, 0.01 equiv.), Aldrithiol-2 (0 or 2.2 mg, 0.00 or 0.01 mmol, 0 or 5 mol%) and (if solid) alkene (0.60 –2.0 mmol, 3.0 – 10 equiv.) were added to an oven-dried tapered microwave vial equipped with a stirrer bar and a septum. The vial was evacuated and backfilled with N_2 3 times, followed by addition of anhydrous $(CH_2Cl)_2$ (1.0 – 3.0 ml, 0.067 – 0.20 M) and (if liquid) alkene (0.60 –2.0 mmol, 3.0 – 10 equiv.). The reaction was then stirred under irradiation with 390 nm LED (3-F-TX and ITX) or 427 nm LED

$[Ir(dFCF_3ppy)_2(dtbbpy)][PF_6]$ at ambient temperature for 16 h, with the fans on. The reaction mixture was diluted with CH_2Cl_2, and the solvent removed under reduced pressure, followed by purification by flash column chromatography.

Note: For particular azetidines obtained using General Procedure 1, flash column chromatography afforded the product as an inseparable mixture of the photocatalyst or photocatalyst-derived impurity. These by-products can be removed *via* straightforward process detailed below:

Workup 1: Following chromatography, the impure azetidine was redissolved in CH_2Cl_2 (1 ml) *m*-CPBA (1 equiv.) was added. Reaction mixture was stirred at rt for 16 h. Following completion, the reaction mixture was quenched with aq. sat. $NaHSO_3$ and layers partitioned. The aqueous layer was extracted with CH_2Cl_2 three times, combined organic layers were washed sequentially with aq. sat. $NaHCO_3$, brine, dried over anhydrous $MgSO_4$ subsequently filtered and concentrated under reduced pressure. The residue was then purified by flash column chromatography

Synthesis of sulfamoyl fluoride imines (GP2)

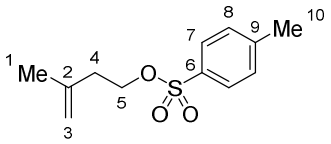


Fluorosulfonyl isocyanate (FSI) (1.00-1.80 equiv.) was added dropwise to a stirred solution of aldehyde (1.00 equiv.) in dry $(CH_2Cl)_2$ (0.9 – 2.4 M) under N_2 at 0 °C or rt. (Caution: CO_2 evolution). The reaction was warmed to (rt – reflux) and stirred for a further 16 h. The solvent was removed under reduced pressure to give the crude product, which was either recrystalised or triturated to give the desired product.

5.2.2 Substrate Synthesis

5.2.2.1 Alkene Substrates

3-Methylbut-3-en-1-yl 4-methylbenzenesulfonate (13)



3-Methyl-3-buten-1-ol (1.52 ml, 15.0 mmol, 1.00 equiv.) was added dropwise to a solution of DMAP (2.75 g, 22.5 mmol, 1.50 equiv.) and TsCl (3.58 g, 18.8 mmol, 1.25 equiv.) in CH_2Cl_2 (75 ml, 0.20 M) under N_2, at 0 °C. The reaction was warmed slowly to rt and stirred for a further 16 h. The reaction was cooled to 0 °C, quenched with water and stirred for a further 10 minutes. The phases were then partitioned and the aqueous layer was washed with CH_2Cl_2. The combined organic layers were washed with brine, dried over anhydrous $MgSO_4$ and concentrated under reduced pressure. Purification by flash column chromatography (4 – 5% EtOAc in pet. ether) afforded 3-methylbut-3-en-1-yl 4-methylbenzenesulfonate (**13**) as a colourless oil (3.28 g, 91%).

R_f (14% EtOAc in pet ether) = 0.54.

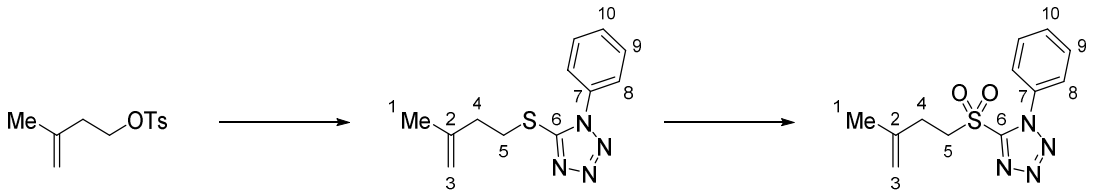
^{1}H NMR (400 MHz, $CDCl_3$) δ 7.82 – 7.73 (m, 2H, C(7)*H*), 7.38 – 7.30 (m, 2H, C(8)*H*), 4.78 (dq, *J* = 2.3, 1.1 Hz, 1H, C(3)H_a), 4.67 (dq, *J* = 2.2, 1.2 Hz, 1H, C(3)H_b), 4.12 (t, *J* = 6.9 Hz, 2H, C(5)H_2), 2.44 (s, 3H, C(10)H_3), 2.34 (t, *J* = 6.6 Hz, 2H, C(4)H_2), 1.65 (t, *J* = 1.1 Hz, 3H, C(1)H_3).

^{13}C NMR (101 MHz, $CDCl_3$) δ 144.8, 140.2, 133.3, 129.9, 128.0, 113.2, 68.6, 36.9, 22.4, 21.7.

HRMS (ESI) *m/z* $C_{12}H_{16}O_3SNa$ requires 263.0712 ($[M+Na]^+$), found 263.0724.

Data consistent with literature.[191]

5-((3-methylbut-3-en-1-yl)thio)-1-phenyl-1H-tetrazole (14) and 5-((3-Methylbut-3-en-1-yl)sulfonyl)-1-phenyl-1H-tetrazole (15)



5-((3-methylbut-3-en-1-yl)thio)-1-phenyl-1H-tetrazole (14): Prepared according to a modified procedure.[192] 3-Methylbut-3-en-1-yl 4-methylbenzenesulfonate (**13**) (1.49 g, 6.20 mmol, 1.0 equiv.) was added to a solution of 1-phenyl-1H-tetrazole-5-thiol (1.22 g, 6.82 mmol, 1.1 equiv.) and K_2CO_3 (4.28 g, 31.0 mmol, 5.0 equiv.) in MeCN (30 ml, 0.21 M) under N_2. The reaction was heated at 50 °C for 16 h. The reaction was cooled to rt and partitioned between water and EtOAc. The aqueous layer was extracted with EtOAc thrice, the combined organic layers were washed with aq. sat. $NaHCO_3$, dried over anhydrous $MgSO_4$, filtered and concentrated under reduced pressure. Purification by flash column chromatography (4 – 5% EtOAc in pet. ether) afforded 5-((3-methylbut-3-en-1-yl)thio)-1-phenyl-1H-tetrazole (**14**) as a colourless oil (1.13 g, 74%).

R_f (10% Et_2O in pentane) = 0.31.

^{1}H NMR (400 MHz, $CDCl_3$) δ 7.60 – 7.46 (m, 5H, Ar*H*), 4.81 (s, 1H, C(3)H_a), 4.75 (s, 1H, C(3)H_b), 3.50 (t, *J* = 7.4 Hz, 2H, C(5)H_2), 2.51 (t, *J* = 7.4 Hz, 2H, C(4)H_2), 1.75 (s, 3H, C(1)H_3).

^{13}C NMR (101 MHz, $CDCl_3$) δ 154.4, 142.5, 133.7, 130.1, 129.8, 123.9, 112.5, 36.9, 31.5, 22.1.

HRMS (ESI) *m/z* $C_{12}H_{15}N_4S$ requires 247.1012 ($[M+H]^+$), found 247.1009.

IR (thin film, ν_{max} /cm^{-1}) 3075, 1650, 1597, 1500, 1412, 1388, 1413, 1388, 1243, 1090, 1015, 896, 761, 694.

Data consistent with literature.[193]

5-((3-Methylbut-3-en-1-yl)sulfonyl)-1-phenyl-1H-tetrazole (15): Prepared according to a modified procedure.[194] A solution of oxidant made from $Mo_7O_{24}(NH_4)_6 \cdot 4H_2O$ (742 mg, 0.60 mmol, 0.16 equiv.) in H_2O_2 (30% in H_2O, 4 ml) was added to a solution of sulfide (**14**) (900 mg, 3.65 mmol, 1.0 equiv.) at 0 °C in EtOH (40 ml 0.091 M). The reaction was slowly warmed to rt and stirred for 3 days. The reaction was diluted with EtOAc and the organic phase was sequentially washed with water, brine, dried over $MgSO_4$, filtered and concentrated under reduced pressure. Purification by flash column chromatography (4 – 10% EtOAc in pet. ether) afforded 5-((3-methylbut-3-en-1-yl)sulfonyl)-1-phenyl-1H-tetrazole (**15**) as a colourless oil (563 mg, 55%).

R_f (10% EtOAc in pet ether) = 0.30.

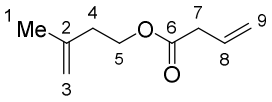
^{1}H NMR (400 MHz, $CDCl_3$) δ 7.71 – 7.66 (m, 2H, C(8)*H*), 7.66 – 7.57 (m, 3H, C(9)*H*, C(10)*H*), 4.87 (s, 1H, C(3)H_a), 4.81 (s, 1H, C(3)H_b), 3.91 – 3.82 (m, 2H, C(5)H_2), 2.69 – 2.60 (m, 2H, C(4)H_2), 1.80 (s, 3H, C(1)H_3).

^{13}C NMR (101 MHz, $CDCl_3$) δ 153.5, 140.5, 133.1, 131.6, 129.9, 125.2, 113.1, 54.7, 29.9, 22.3.

HRMS (ESI) *m/z* $C_{12}H_{15}N_4O_2S$ requires 279.0910 ($[M+H]^+$), found 279.0908.

IR (thin film, ν_{max} /cm^{-1}) 3080, 1652, 1596, 1498, 1157, 903, 764, 689, 624.

3-Methylbut-3-en-1-yl but-3-enoate (16)



A solution of crotonyl chloride (1.85 ml, 19.5 mmol, 1.1 equiv.) in CH_2Cl_2 (2.0 ml, 2.0 M) was added to a solution of 3-methyl-3-buten-1-ol (1.32 ml, 13.0 mmol, 1.0 equiv.) and NEt_3 (3.60 ml, 26.0 mmol, 2.0 equiv.) in CH_2Cl_2 under N_2 at 0 °C. The reaction was slowly warmed to rt and then stirred for a further 1 h and the reaction mixture was poured into cold water and the phases were partitioned. The aqueous phase was extracted with CH_2Cl_2 three times, dried over anhydrous $MgSO_4$, filtered and the solvent was removed under reduced pressure. Purification by flash column chromatography (0 – 40% CH_2Cl_2 in pet ether) afforded 3-methylbut-3-en-1-yl but-3-enoate (**16**) as a yellow oil (1.84 g, 92%).

R_f (5% CH_2Cl_2 in pentane) = 0.33.

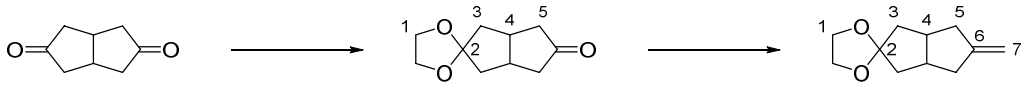
^{1}H NMR (400 MHz, $CDCl_3$) δ 5.97 – 5.84 (m, 1H, C(8)*H*), 5.19 – 5.14 (m, 1H, C(9)H_a), 5.14 – 5.11 (m, 1H, C(9)H_b), 4.79 (s, 1H, C(3)H_a), 4.72 (s, 1H, C(3)H_b), 4.20 (td, *J* = 6.9, 0.8 Hz, 2H, C(5)H_2), 3.07 (dq, *J* = 7.0, 1.3 Hz, 2H, C(7)H_2), 2.33 (t, *J* = 6.9 Hz, 2H, C(4)H_2), 1.74 (s, 3H, C(1)H_3).

^{13}C NMR (101 MHz, $CDCl_3$) δ 171.6, 141.7, 130.4, 118.5, 112.4, 63.0, 39.2, 36.8, 22.6.

HRMS (ESI) *m/z* $C_9H_{15}O_2$ requires 155.1067 ($[M+H]^+$), found 155.1067.

IR (thin film, ν_{max} /cm^{-1}) 2972, 1741, 1650, 1378, 1329, 1253, 1173, 1035, 994, 921, 894.

Tetrahydro-1H-spiro[pentalene-2,2'-[1,3]dioxolan]-5(3H)-one (17) and 5-Methylenehexahydro-1H-spiro[pentalene-2,2'-[1,3]dioxolane] (18)



Tetrahydro-1H-spiro[pentalene-2,2'-[1,3]dioxolan]-5(3H)-one (17): Ethylene glycol (0.89 ml, 15.8 mmol, 0.90 equiv.) was added to a solution of tetrahydropentalene-2,5(1H,3H)-dione (2.42 g, 17.5 mmol, 1.0 equiv.) and TsOH (329 mg, 1.75 mmol, 0.10 equiv.) in benzene (50 ml, 0.35 M). The flask was fitted with a Dean-Stark apparatus and heated at reflux for 6 h. The reaction mixture was cooled to rt, diluted with toluene and washed sequentially with 1N NaOH and brine solutions. The combined organic layers were dried over anhydrous $MgSO_4$, filtered and concentrated under reduced pressure. Purification by flash column chromatography (0 – 30% EtOAc in pet ether) afforded tetrahydro-1H-spiro[pentalene-2,2'-[1,3]dioxolan]-5(3H)-one (**17**) as a pale-yellow oil (915 mg, 29%).

R_f (30% EtOAc in pet ether) = 0.17.

^{1}H NMR (400 MHz, $CDCl_3$) δ 3.83 (s, 4H, C(1)H_2), 2.85 – 2.70 (m, 2H, C(4)H_2), 2.49 – 2.35 (m, 2H, C(5)H_a), 2.21 – 2.05 (m, 4H, C(3)H_a, C(5)H_b), 1.69 – 1.63 (m, 2H, C(3)H_b).

^{13}C NMR (101 MHz, $CDCl_3$) δ 220.3, 118.4, 64.7, 64.3, 44.5, 42.6, 37.1.

HRMS (ESI) *m/z* $C_{10}H_{15}O_3$ requires 183.1016 ($[M+H]^+$), found 183.1019.

Data consistent with literature.[195]

5-Methylenehexahydro-1H-spiro[pentalene-2,2'-[1,3]dioxolane] (18): Prepared according to a modified procedure.[196] NaHMDS in THF (2.0 M, 2.64 ml, 5.27 mmol, 1.2 equiv.) was added dropwise to a stirred solution of $MePPh_3Br$ (2.35 g, 6.59 mmol, 1.5

equiv.) in THF (20 ml, 0.22 M) at 0 °C for 30 minutes. A solution of 5-methylenehexahydro-1H-spiro[pentalene-2,2'-[1,3]dioxolane] (**17**) (800 mg, 4.39 mmol, 1.0 equiv.) in 5 ml THF was added dropwise at 0 °C. The reaction was stirred for a further 30 minutes at 0 °C after which, the reaction was slowly warmed to rt and stirred for a further 3 h. The reaction was diluted with Et_2O and washed sequentially with water, brine, dried over anhydrous $MgSO_4$ and then concentrated under reduced pressure. Purification by flash column chromatography (6% Et_2O in pentane) afforded 5-methylenehexahydro-1H-spiro[pentalene-2,2'-[1,3]dioxolane] (**18**) as a colourless oil (683 mg, 86%).

R_f (10% Et_2O in pentane) = 0.40.

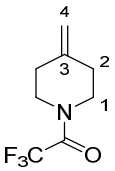
^{1}H NMR (400 MHz, $CDCl_3$) δ 4.81 (h, *J* = 1.8 Hz, 2H, C(7)H_2), 3.92 – 3.83 (m, 4H, C(1)H_2), 2.64 – 2.53 (m, 2H, C(4)H_2), 2.53 – 2.42 (m, 2H, C(5)H_a), 2.11 – 2.03 (m, 2H, C(5)H_b), 1.99 (ddt, *J* = 13.4, 6.5, 1.4 Hz, 2H, C(3)H_a), 1.56 (ddd, *J* = 13.5, 7.0, 1.5 Hz, 2H, C(3)H_b).

^{13}C NMR (101 MHz, $CDCl_3$) δ 152.4, 118.7, 106.3, 64.7, 64.0, 42.0, 40.0, 39.8.

HRMS (ESI) *m/z* $C_{11}H_{17}O_2$ requires 181.1223 ($[M+H]^+$), found 181.1232.

Data consistent with literature.[196]

2,2,2-Trifluoro-1-(4-methylenepiperidin-1-yl)ethan-1-one (19)



Prepared according to a modified procedure.[197] Trifluoroacetic acid (24 ml) was added to a stirred solution of *tert*-butyl 4-methylidenepiperidine-1-carboxylate (1.18 g, 6.0 mmol,

1.0 equiv.) in CH_2Cl_2 (24 ml). The reaction mixture was stirred at rt for 1 h and then concentrated thoroughly under reduced pressure. The flask was evacuated and backfilled with N_2 three times and the crude residue was dissolved in CH_2Cl_2 (10 ml, 0.60 M) and cooled to 0 °C. The reaction mixture was charged sequentially with NEt_3 (2.50 ml, 18 mmol, 3.0 equiv.) and TFAA (0.92 ml, 6.6 mmol, 1.1 equiv.). The flask was then warmed to rt and the mixture stirred for a further 16 h. The reaction was quenched with water and the aqueous layer was extracted 3 times with CH_2Cl_2. The combined organic layers were washed with brine, dried over anhydrous $MgSO_4$ and concentrated under reduced pressure. Purification by flash column chromatography (0 – 10% Et_2O in pentane) gave 2,2,2-trifluoro-1-(4-methylenepiperidin-1-yl)ethan-1-one (**19**) as a white solid (847 mg, 73%).

R_f (10% Et_2O in pentane) = 0.22.

^{1}H NMR (400 MHz, $CDCl_3$) δ 4.83 (s, 2H, C(4)H_2), 3.69 – 3.62 (m, 2H, C(1)H_a), 3.62 – 3.53 (m, 2H, C(1)H_b), 2.35 – 2.25 (m, 4H, C(2)H_2).

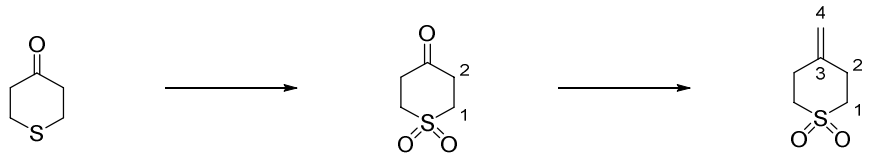
^{13}C NMR (101 MHz, $CDCl_3$) δ 155.6 (q, $^2J_{C\text{-}F}$ = 35.2 Hz), 142.9, 116.7 (q, $^1J_{C\text{-}F}$ = 288.0 Hz), 111.0, 47.1 (q, $^3J_{C\text{-}F}$ = 3.5 Hz), 45.2, 34.9, 33.9.

^{19}F NMR (377 MHz, $CDCl_3$) δ -68.88 (s).

HRMS (ESI) *m/z* $C_8H_{11}F_3NO$ requires 194.0787 ($[M+H]^+$), found 194.0787.

IR (thin film, ν_{max} /cm^{-1}) 3023, 2941, 1754, 1700, 1466, 1299, 1204, 1177, 1145, 988, 902.

Tetrahydro-4H-thiopyran-4-one 1,1-dioxide (20) and 4-Methylenetetrahydro-2H-thiopyran 1,1-dioxide (21)



Tetrahydro-4H-thiopyran-4-one 1,1-dioxide (20): Prepared according to a modified procedure.[198] A mixture of Oxone (31.7 g, 100 mmol, 2.9 equiv.) and $NaHCO_3$ (26.9 g, 32 mmol, 0.9 equiv.) was added portion wise within 30 min to a solution of tetrahydrothiopyran-4-one (3.95 g, 34 mmol, 1.0 equiv.) in MeCN (45 ml, 0.76 M) and aqueous Na_2·EDTA solution (30 mL, 4×10^{-4} M). at 0 °C. The reaction was warmed to rt and was stirred for 3 h. The reaction mixture was diluted with CH_2Cl_2, dried over anhydrous $MgSO_4$, and filtered through Celite. The filtrate was concentrated under reduced pressure to afford tetrahydro-4H-thiopyran-4-one 1,1-dioxide **(20**) as a white solid (4.16 g, 83% yield).

^{1}H NMR (400 MHz, $CDCl_3$) δ 3.37 – 3.27 (m, 4H, C(1)*H*$_2$), 2.96 – 2.87 (m, 4H, C(2)*H*$_2$).

^{13}C NMR (101 MHz, $CDCl_3$) δ 202.2, 49.7, 38.3.

LRMS (ESI) *m/z* 149.0 ($[M+H]^+$).

Data consistent with literature.[198]

4-Methylenetetrahydro-2H-thiopyran 1,1-dioxide (21): Methyltriphenylphosphonium bromide (5.89 g, 16.5 mmol, 1.1 equiv.) was added to a stirred solution of potassium *tert*-butoxide (2.22 g, 18.0 mmol, 1.2 equiv.) in THF (30 ml, 0.5 M) at 0°C under N_2. The reaction was stirred at 0 °C for 30 minutes. A solution of tetrahydro-4H-thiopyran-4-one 1,1-dioxide (**20**) (2.22 g, 15.0 mmol, 1.0 equiv.) in DMSO (15 ml) was added dropwise. The reaction warmed to rt and stirred for 16 h. The reaction mixture was quenched with aq. sat. NH_4Cl and the phases were partitioned. The aqueous phase was extracted three

times with EtOAc and the combined organic layers were washed with brine, dried over $MgSO_4$ and concentrated under reduced pressure. Purification by flash column chromatography (0 – 30% EtOAc in pet ether) afforded 4-methylenetetrahydro-2H-thiopyran 1,1-dioxide (**21**) as a white solid (730 mg, 33%).

R_f (40% EtOAc in pet ether) = 0.29.

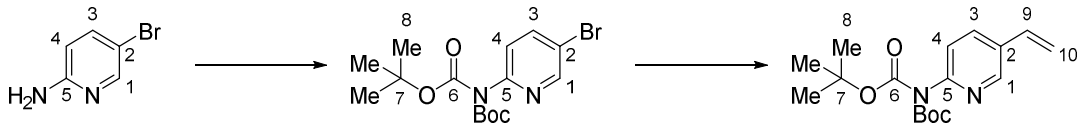
^{1}H NMR (400 MHz, $CDCl_3$) δ 4.94 (s, 2H, C(4)H_2), 3.09 – 2.99 (m, 4H, C(1)H_2), 2.76 – 2.67 (m, 4H, C(2)H_2).

^{13}C NMR (101 MHz, $CDCl_3$) δ 140.6, 114.9, 52.4, 32.1.

HRMS (ESI) *m/z* $C_6H_{10}O_2SNa$ requires 169.0294 ($[M+Na]^+$), found 169.0293.

Data consistent with literature.[199]

***Tert*-butyl (5-bromopyridin-2-yl)(*tert*-butoxycarbonyl)carbamate (22) and *Tert*-butyl (*tert*-butoxycarbonyl)(5-vinylpyridin-2-yl)carbamate (23)**



Tert-butyl (5-bromopyridin-2-yl)(tert-butoxycarbonyl)carbamate (22): Boc_2O (9.61 g, 44 mmol, 2.2 equiv.) was added portion wise to a stirred solution of 5-bromopyridin-2-amine (3.46 g, 20 mmol, 1.0 equiv.), DMAP (244 mg, 2.0 mmol, 0.10 equiv.) and NEt_3 (5.54 ml, 40 mmol, 2.0 equiv.) in CH_2Cl_2 (70 ml, 0.30 M). The reaction was stirred at rt for 16 h after which, the reaction mixture was partitioned over water and the aqueous layer was extracted 3 times with CH_2Cl_2. The combined organic extracts were washed with brine, dried over $MgSO_4$, filtered and the solvent was removed under reduced pressure. Purification by flash column chromatography (5 – 8% EtOAc in pentane)

afforded *tert*-butyl (5-bromopyridin-2-yl)(*tert*-butoxycarbonyl)carbamate (**22**) as a white solid (4.67 g, 63%).

R_f (5% EtOAc in pentane) = 0.23.

^{1}H NMR (400 MHz, $CDCl_3$) δ 8.51 (dd, *J* = 2.5, 0.7 Hz, 1H, C(1)*H*), 7.83 (dd, *J* = 8.5, 2.5 Hz, 1H, C(3)*H*), 7.17 (dd, *J* = 8.4, 0.7 Hz, 1H, C(4)*H*), 1.44 (s, 18H, C(8)H_3).

^{13}C NMR (101 MHz, $CDCl_3$) δ 151.1, 151.0, 149.8, 140.6, 123.0, 118.7, 83.6, 28.0.

HRMS (ESI) *m/z* $C_{15}H_{22}{}^{79}BrN_2O_4$ and $C_{15}H_{22}{}^{81}BrN_2O_4$ ($[M+H]^+$) requires 373.0757 and 375.0737, found 373.0765 and 375.0728.

Data consistent with literature.[200]

Tert-butyl (tert-butoxycarbonyl)(5-vinylpyridin-2-yl)carbamate (23): NEt_3 (1.04 ml, 7.5 mmol, 1.5 equiv.) was added to a suspension of potassium vinyltrifluoroborate (1.00 g, 7.5 mmol, 1.5 equiv.), *tert*-butyl (5-bromopyridin-2-yl)(*tert*-butoxycarbonyl)carbamate (**22**) (1.87 g, 5.0 mmol, 1.0 equiv.) and $PdCl_2dppf{\cdot}CH_2Cl_2$ (204 mg, 0.25 mmol, 5 mol%) in EtOH (75 ml, 0.10 M). The reaction mixture was then sparged with N_2 for 10 minutes and then heated at reflux for 1.5 h. Subsequently the reaction was cooled to rt, diluted with EtOAc and partitioned over water. The organic layer was dried over $MgSO_4$, filtered and concentrated under reduced pressure. Purification by flash column chromatography (5 – 8% EtOAc in pentane) afforded *tert*-butyl (*tert*-butoxycarbonyl)(5-vinylpyridin-2-yl)carbamate (**23**) as a white solid (1.34 g, 84%).

R_f (5% EtOAc in pentane) = 0.17.

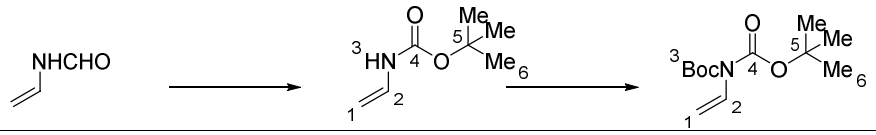
^{1}H NMR (400 MHz, $CDCl_3$) δ 8.46 (d, *J* = 2.4 Hz, 1H, C(1)*H*), 7.77 (dd, *J* = 8.3, 2.5 Hz, 1H, C(3)*H*), 7.19 (d, *J* = 8.3 Hz, 1H, C(4)*H*), 6.70 (dd, *J* = 17.7, 11.0 Hz, 1H, C(9)*H*), 5.81 (dd, *J* = 17.6, 0.6 Hz, 1H, C(10)*H*), 5.38 (dd, *J* = 11.0, 0.6 Hz, 1H, C(10)*H*), 1.44 (s, 18H).

^{13}C NMR (101 MHz, $CDCl_3$) δ 151.6, 151.4, 147.2, 134.7, 132.9, 131.9, 121.6, 116.6, 83.2, 28.0.

HRMS (ESI) *m/z* $C_{17}H_{25}N_2O_4$ requires 321.1809 ($[M+H]^+$), found 321.1810.

IR (thin film, ν_{max} /cm^{-1}) 2981, 2929, 1779, 1718, 1614, 1517, 1468, 1421, 1388, 1310, 1255, 1212, 1178, 1119, 1032, 848, 720, 652.

***Tert*-butyl vinylcarbamate (24) and Di-*tert*-butyl vinyliminodicarbonate (25)**



Tert-butyl vinylcarbamate (24): Boc_2O was added portionwise to a solution of N-vinyl formamide (0.71 ml, 10 mmol, 1.0 equiv.), NEt_3 (1.94 ml, 14 mmol, 1.4 equiv.) and DMAP (122 mg, 1.0 mmol, 0.10 equiv.) in THF (10 ml ,1.0 M) under N_2 at 0 °C. The reaction was then warmed to rt and stirred for 2 h. LiOH (0.84 g, 35 mmol, 3.5 equiv.) was then added and the reaction was then heated at 50 °C for 4 h, subsequently the reaction was cooled to rt and diluted with water and Et_2O. The phases were partitioned and the aqueous phase was washed with Et_2O. The combined organic phases were dried over anhydrous $MgSO_4$, filtered and concentrated under reduced pressure. Purification by flash column chromatography (10% EtOAc in pentane) afforded *tert*-butyl vinylcarbamate (**24**) as a white solid (1.02 g, 71%).

^{1}H NMR (400 MHz, $CDCl_3$) δ 6.73 – 6.58 (m, 1H, C(2)*H*), 6.30 (s, 1H, N(3)*H*), 4.40 (d, *J* = 15.7 Hz, 1H, C(1)H_a), 4.21 (d, *J* = 8.8 Hz, 1H, C(1)H_b), 1.46 (s, 9H, C(6)H_3).

Data consistent with literature.[201]

Di-tert-butyl vinyliminodicarbonate (25): Boc_2O (1.93 g, 8.82 mmol, 3.0 equiv.) and DMAP (35 mg, 0.29 mmol, 0.10 equiv.) were added sequentially to a stirred solution of *tert*-butyl vinylcarbamate (**24**) (421 mg, 2.94 mmol, 1.0 equiv.) in MeCN (7.0 ml, 0.40 M). The reaction mixture was stirred at rt for 2 h and subsequently concentrated under reduced pressure. Purification by flash column chromatography (0 – 5% Et_2O in pentane) afforded di-*tert*-butyl vinyliminodicarbonate (**25**) as a white solid (714 mg, 99%).

R_f (5% Et_2O in pentane) = 0.17.

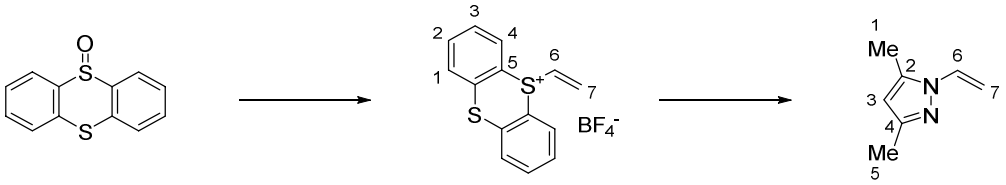
^{1}H NMR (400 MHz, $CDCl_3$) δ 6.68 – 6.57 (m, 1H, C(2)*H*), 4.82 (dd, *J* = 16.0, 0.9 Hz, 1H, C(1)H_a), 4.60 (dq, *J* = 9.1, 0.9 Hz, 1H, C(1)H_b), 1.51 (s, 18H, C(6)H_3).

^{13}C NMR (101 MHz, $CDCl_3$) δ 151.4, 130.3, 99.3, 83.3, 28.0.

HRMS (ESI) *m/z* $C_{12}H_{21}NO_4Na$ requires 266.1363 ([M+Na]$^+$), found 266.1374.

Data consistent with literature. [201]

Vinyl thianthrenium tetrafluoroborate (26) and 3,5-Dimethyl-1-vinyl-1H-pyrazole (27)



Vinyl Thianthrenium Tetrafluoroborate (26): TFAA (5.7 ml, 41 mmol, 3.0 equiv.) and TfOH (1.4 ml, 16 mmol, 4.2 equiv.) were added to a solution of thianthrene-S-oxide (3.14

g, 13.5 mmol, 1.0 equiv.) and trimethyl(vinyl)silane (4.0 ml, 27 mmol, 2.0 equiv.) in MeCN (65 ml, 0.20 M) at 0 °C. The mixture was then stirred at 0 °C for 30 minutes and then warmed to rt and stirred for a further 60 minutes. The reaction mixture was then concentrated under reduced pressure and the reaction mixture was dissolved in CH_2Cl_2 and transferred to a separatory funnel. The organic layer was washed with aq. sat. $NaHCO_3$ and the aqueous layer was washed twice with CH_2Cl_2. The combined organic layers were washed twice with 5% (w/w) $NaBF_4$ solution, dried over anhydrous $MgSO_4$, filtered and concentrated under reduced pressure. The crude product was dissolved in CH_2Cl_2 crashed out by addition of Et_2O, the precipitate was collected by filtration and washed thrice with Et_2O and dried under vacuum to afford vinyl thianthrenium Tetrafluoroborate (**26**) as an off-white solid (3.97 g, 88%).

^{1}H NMR (400 MHz, $CDCl_3$) δ 8.35 (dd, *J* = 7.9, 1.4 Hz, 2H, C(4)*H*), 7.84 (dd, *J* = 7.9, 1.4 Hz, 2H, C(1)*H*), 7.77 (td, *J* = 7.7, 1.3 Hz, 2H, C(2)*H* or C(3)*H*), 7.68 (td, *J* = 7.6, 1.4 Hz, 2H, C(2)*H* or C(3)*H*), 6.75 (dd, *J* = 16.0, 8.8 Hz, 1H, C(6)*H*), 6.30 (dd, *J* = 8.8, 2.9 Hz, 1H, C(7)H_a), 6.26 (dd, *J* = 16.0, 2.8 Hz, 1H, C(7)H_b).

^{13}C NMR (101 MHz, $CDCl_3$) δ 136.1, 134.9, 134.6, 134.5, 130.4, 130.3, 119.5, 118.6.

HRMS (ESI) *m/z* $C_7H_{11}N_2$ requires 243.0297 ($[M\text{-}BF_4]^+$), found 243.0294.

Data consistent with literature.[20]

3,5-Dimethyl-1-vinyl-1H-pyrazole (27): Prepared according to a modified procedure.[20] Under air, DBU (0.91 ml, 6.0 mmol, 2.0 equiv.) was added to a solution of 3,5-dimethyl-1*H*-pyrazole (288 mg, 3.0 mmol, 1.0 equiv.) and vinyl-thianthrenium tetrafluoroborate (**26**) (1.68 g, 5.1 mmol, 1.7 equiv.) in CH_2Cl_2 (30 ml, 0.10 M). The reaction was stirred

for 3 h at rt and then the solvent was removed under reduced pressure. Purification by flash column chromatography (0 – 10% Et_2O in pentane) afforded 3,5-dimethyl-1-vinyl-1H-pyrazole (**27**) as a colourless oil (320 mg, 87%).

R_f (10% Et_2O in pentane) = 0.24.

^{1}H NMR (400 MHz, $CDCl_3$) δ 6.86 (dd, *J* = 15.3, 8.9 Hz, 1H, C(6)*H*), 5.85 (s, 1H, C(3)*H*), 5.58 (d, *J* = 15.4 Hz, 1H, C(7)H_a), 4.74 (d, *J* = 8.9 Hz, 1H, C(7)H_b), 2.25 (s, 3H, C(1)H_3 or C(5)H_3), 2.24 (s, 3H, C(1)H_3 or C(5)H_3).

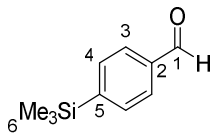
^{13}C NMR (101 MHz, $CDCl_3$) δ 150.0, 139.2, 129.3, 106.9, 99.4, 13.8, 11.0.

HRMS (ESI) *m/z* $C_7H_{11}N_2$ requires 123.0917 ($[M+H]^+$), found 123.0916.

Data consistent with literature.[202]

5.2.2.2 Aldehyde Substrates

4-(Trimethylsilyl)benzaldehyde (28)



Prepared according to a modified procedure.[203] Under N_2, *n*-butyllithium (2.35 M, 1.87 ml, 4.4 mmol, 1.1 equiv.) was added dropwise to a stirred solution of (4-bromophenyl)trimethylsilane (764 µl, 4.0 mmol, 1.0 equiv.) in THF (25 ml, 0.16 M) at -78 °C *via* syringe. The reaction mixture was stirred for 15 minutes at -78 °C. DMF was added dropwise at -78 °C following addition, the dry ice/acetone bath was removed and the reaction was warmed to rt and stirred for a further 16 h. Reaction was quenched with aq. sat. NH_4Cl and extracted twice with Et_2O. The combined organic extracts were dried over anhydrous $MgSO_4$, filtered and concentrated under reduced pressure. Purification

by flash column chromatography (0 – 3% Et_2O in pentane) afforded 4-(trimethylsilyl)benzaldehyde (**28**) as a colourless oil (558 mg, 78%).

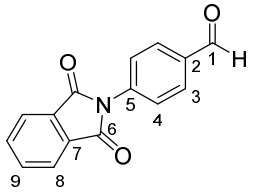
R_f (2% Et_2O in pentane) = 0.08.

^{1}H NMR (400 MHz, $CDCl_3$) δ 10.02 (s, 1H, C(1)*H*), 7.88 – 7.80 (m, 2H, C(3)*H*), 7.72 – 7.65 (m, 2H, C(4)*H*), 0.31 (s, 9H, C(6)H_3).

^{13}C NMR (101 MHz, $CDCl_3$) δ 192.7, 149.2, 136.5, 133.9, 128.7, -1.3.

HRMS (ESI) *m/z* $C_{10}H_{15}OSi$ requires 179.0887 ($[M+H]^+$), found 179.0892.

4-(1,3-Dioxoisoindolin-2-yl)benzaldehyde (29)



Prepared according to a modified procedure.[204] A pressure tube was charged with 4-bromobenzaldehyde (740 mg, 4.0 mmol, 1.0 equiv.) and potassium phthalimide (741 mg, 4.0 mmol, 1.0 equiv.). The vessel was then capped with a rubber septum and evacuated and backfilled with N_2 three times. Dry, degassed DMA (40 ml, 0.1 mmol) was added *via* syringe, the rubber septum was removed and CuI (762 mg, 4.0 mmol, 1.0 equiv.) was quickly added followed and the vial was sealed with a screw cap. The reaction was heated to 170 °C for 24h and then reaction was then cooled to rt and crude reaction mixture was diluted with EtOAc, transferred to a separating funnel and washed three times with 10% LiCl solution, followed by one wash with brine and then dried over anhydrous $MgSO_4$. The reaction mixture was filtered and concentrated under reduced pressure. Purification by flash column chromatography (0 – 5% EtOAc in CH_2Cl_2) afforded 4-(1,3-dioxoisoindolin-2-yl)benzaldehyde (**29**) as a yellow solid (517 mg, 51%).

R_f (2% EtOAc in CH_2Cl_2) = 0.41.

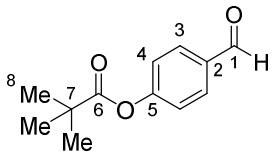
^{1}H NMR (400 MHz, $CDCl_3$) δ 10.06 (s, 1H, C(1)*H*), 8.06 – 7.98 (m, 2H, C(3)*H*), 7.98 (dd, *J* = 5.5, 3.1 Hz, 2H, C(8)*H*), 7.83 (dd, *J* = 5.5, 3.0 Hz, 2H, C(9)*H*), 7.73 – 7.69 (m, 2H, C(4)*H*).

^{13}C NMR (101 MHz, $CDCl_3$) δ 191.4, 166.8, 137.2, 135.2, 134.9, 131.6, 130.5, 126.6, 124.2.

HRMS (ESI) *m/z* $C_{15}H_9NO_3$ requires 252.0655 ($[M+H]^+$), found 252.0658.

Data consistent with literature.[204]

4-Formylphenyl pivalate (30)



Prepared according to a modified procedure.[205] Triethylamine (1.04 ml, 7.5 mmol, 1.5 equiv.) and pivaloyl chloride (923 µl, 7.5 mmol, 1.5 equiv.) were added sequentially *via* syringe to a stirred solution of 4-hydroxybenzaldehyde (611 mg, 5.00 mmol, 1.00 equiv.) in THF (5.0 ml, 1.0 M) at 0 °C. Subsequently the reaction was warmed gradually to rt and stirred for a further 16 h. The reaction mixture was quenched with aq. sat. NH_4Cl, diluted with Et_2O and the layers were partitioned. The aqueous layer was extracted three times and with Et_2O, the combined organic layers were washed with brine, dried over anhydrous $MgSO_4$ and concentrated under reduced pressure. Purification by flash column chromatography (0 – 10% EtOAc in pet. ether) afforded 4-formylphenyl pivalate (**30**) as a colourless oil (302 mg, 55%).

R_f (10% Et_2O in pentane) = 0.40.

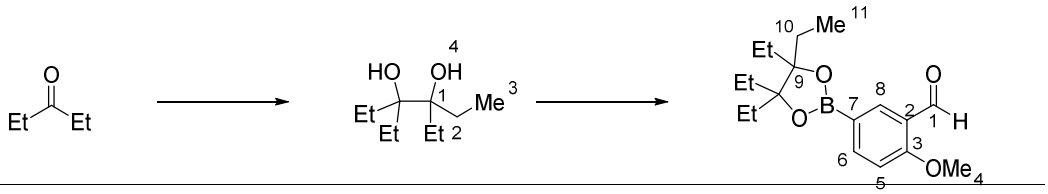
^{1}H NMR (400 MHz, $CDCl_3$) δ 9.96 (s, 1H, C(1)*H*), 7.93 – 7.85 (m, 2H, C(3)*H*), 7.26 – 7.18 (m, 2H, C(4)*H*), 1.35 (s, 9H, C(8)H_3).

^{13}C NMR (101 MHz, $CDCl_3$) δ 191.0, 176.4, 156.0, 133.9, 131.2, 122.4, 39.3, 27.1.

HRMS (ESI) *m/z* $C_{12}H_{15}O_3$ requires 207.1016 ($[M+H]^+$), found 207.1024.

Data consistent with literature.[205]

3,4-diethylhexane-3,4-diol (31) and 2-Methoxy-5-(4,4,5,5-tetraethyl-1,3,2-dioxaborolan-2-yl)benzaldehyde (32)



3,4-diethylhexane-3,4-diol (31): At -60 °C, $TiCl_4$ (3.3 ml, 30 mmol, 1.5 equiv.) was added slowly to a solution of pentan-3-one (2.13 ml, 20 mmol, 1.0 equiv.) in THF (50 ml, 0.4 M) under N_2. Subsequently the reaction was stirred at -60 °C for a further 30 minutes. Zn dust (3.92 g, 60 mmol, 3 equiv.) was added to the reaction mixture and the reaction was heated for a further 3 h at reflux. The reaction mixture was then cooled to 0 °C and quenched by slow addition of aq. sat. K_2CO_3 and stirred for a further 30 minutes. The reaction mixture was then filtered through Celite® and the filter cake was washed with EtOAc. The filtrate was extracted with EtOAc and the organic layer was washed with brine then dried over anhydrous $MgSO_4$, filtered and concentrated under reduced pressure. Purification by flash column chromatography (8 – 12% EtOAc in pentane) gave 3,4-diethylhexane-3,4-diol (**31**) as colourless oil which solidified upon standing (1.21 g, 70%).

R_f (8% EtOAc in petrol) = 0.19.

^{1}H NMR (400 MHz, $CDCl_3$) δ 2.00 (s, 2H, O(4)*H*),1.60 (qd, *J* = 7.4, 3.5 Hz, 8H, C(2)H_2), 0.93 (t, *J* = 7.5 Hz, 12H, C(3)H_3).

^{13}C NMR (101 MHz, $CDCl_3$) δ 79.0, 27.4, 9.1.

LRMS (ESI) *m/z* 197.2 ($[M+Na]^+$).

Data consistent with literature.[206]

2-Methoxy-5-(4,4,5,5-tetraethyl-1,3,2-dioxaborolan-2-yl)benzaldehyde (32): Prepared according to a modified procedure.[207] A round-bottom flask equipped with stirrer bar and reflux condenser was charged with 3-formyl-4-methoxyphenyl boronic acid (500 mg, 2.78 mmol, 1.00 equiv.), ethyl pinacol (**31**) (485 mg, 2.78 mmol, 1.00 equiv.) and 3 Å molecular sieves (1.25 g). The reaction vessel was evacuated and backfilled with N_2 and anhydrous CH_2Cl_2 (25 ml, 0.10 M) was added *via* syringe. The reaction mixture was heated at 40 °C for 16 h. The reaction mixture was filtered through celite and the filtrate was concentrated under reduced pressure. The crude mixture was purified by flash column chromatography (0 – 5% EtOAc in pentane), to give 2-methoxy-5-(4,4,5,5-tetraethyl-1,3,2-dioxaborolan-2-yl)benzaldehyde (**32**) as a white solid (817 mg, 92%).

R_f (5% EtOAc in pentane) = 0.48.

^{1}H NMR (400 MHz, $CDCl_3$) δ10.45 (s, 1H, C(1)*H*), 8.28 (d, *J* = 1.7 Hz, 1H, C(8)*H*), 7.99 (dd, *J* = 8.4, 1.8 Hz, 1H, C(6)*H*), 6.97 (d, *J* = 8.4 Hz, 1H, C(5)*H*), 3.94 (s, 3H, C(4)H_3), 1.84 – 1.64 (m, 8H, C(10)H_2), 0.95 (t, *J* = 7.5 Hz, 12H, C(11)H_3).

^{13}C NMR (101 MHz, $CDCl_3$) δ 190.1, 164.0, 142.7, 136.2, 124.5, 111.0, 89.1, 55.8, 26.6, 9.0.

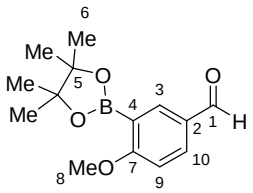
Note: The boron bearing quaternary carbon was not observed by ^{13}C NMR.

HRMS (ESI) *m/z* $C_{18}H_{28}BO_4$ requires 319.2075 ($[M+H]^+$), found 319.2089.

IR (thin film, ν_{max} /cm^{-1}) 2980, 1683, 1605, 1457, 1365, 1350, 1273, 1183, 1132, 1022, 906, 839, 669.

m.p. 50 – 52 °C.

4-Methoxy-3-(4,4,5,5-tetramethyl-1,3,2-dioxaborolan-2-yl)benzaldehyde (33)



Prepared according to a modified procedure.[208] A round-bottom flask equipped with stirrer bar and reflux condenser was charged with 3-bromo-4-methoxybenzaldehyde (1.29 mg, 6.00 mmol, 1.0 equiv.), B_2Pin_2 (2.03 g, 8.00 mmol, 1.30 equiv.), KOAc (1.18 g, 12.0 mmol, 2.00 equiv.) and [1,1′- $PdCl_2$dppf] 147mg, 0.18 mmol, 3.0 mol%). The reaction vessel was evacuated and backfilled three times with N_2 and then dioxane (20 ml, 0.30 M) was added *via* syringe. Reaction was heated at reflux for 16 h and then cooled to rt and filtered through a short pad of silica gel. The filtrate was concentrated under reduced pressure and purified by flash column chromatography (0 – 30% Et_2O in pentane) to give 4-methoxy-3-(4,4,5,5-tetramethyl-1,3,2-dioxaborolan-2-yl)benzaldehyde (**33**) as a white solid (1.38 g, 88%).

R_f (25% Et_2O in pentane) = 0.20.

^{1}H NMR (400 MHz, $CDCl_3$) δ 9.87 (s, 1H, C(1)*H*), 8.18 (d, *J* = 2.3 Hz, 1H, C(3)*H*), 7.93 (dd, *J* = 8.7, 2.3 Hz, 1H, C(10)*H*), 6.94 (d, *J* = 8.6 Hz, 1H, C(9)*H*), 3.89 (s, 3H, C(8)H_3), 1.34 (s, 12H, C(6)H_3).

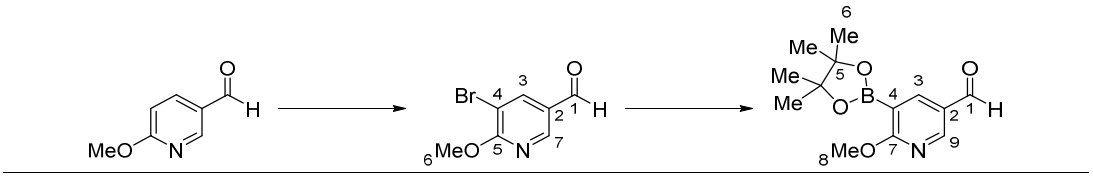
^{13}C NMR (101 MHz, $CDCl_3$) δ 191.1, 168.9, 140.0, 134.2, 129.4, 110.6, 84.0, 56.1, 24.9.

Note: The boron bearing quaternary carbon was not observed by ^{13}C NMR.

HRMS (ESI) *m/z* $C_{14}H_{20}BO_4$ requires 263.1449 ($[M+H]^+$), found 263.1457.

Data consistent with literature.[208]

5-Bromo-6-methoxynicotinaldehyde (34) and 6-Methoxy-5-(4,4,5,5-tetramethyl-1,3,2-dioxaborolan-2-yl)nicotinaldehyde (35)



5-Bromo-6-methoxynicotinaldehyde (34): Under an atmosphere of air, a solution of Br_2 in AcOH (3.1 M, 10 ml, 31 mmol, 1.4 equiv.) was added dropwise over a period of 30 mins *via* addition funnel to a stirred solution of NaOAc (3.5 g, 43 mmol, 1.9 equiv.) and 6-methoxynicotinaldehyde (3.0 g, 22 mmol, 1.0 equiv.) in AcOH (10 ml, 2.2 M). The mixture was then heated to 90 °C for 5 h, after which the reaction was cooled to rt, poured over ice water and neutralised to ~pH 7 with 1N aq. NaOH. The mixture was extracted with EtOAc three times and the combined organic layer was washed with brine and dried over anhydrous $MgSO_4$, filtered and concentrated under reduced pressure. Purification by flash column chromatography (0 – 50% CH_2Cl_2 in pentane) afforded 5-bromo-6-methoxynicotinaldehyde (**35**) as a white solid (1.77 g, 39%).

R_f (5% Et_2O in pentane) = 0.32.

^{1}H NMR (400 MHz, $CDCl_3$) δ 9.85 (s, 1H, C(1)*H*), 8.49 (d, *J* = 2.0 Hz, 1H, C(3)*H* or C(7)*H*), 8.22 (d, *J* = 2.1 Hz, 1H, C(3)*H* or C(7)*H*),), 4.04 (s, 3H, C(6)H_3).

^{13}C NMR (101 MHz, $CDCl_3$) δ 188.3, 163.6, 150.6, 140.3, 127.9, 108.6, 55.7.

HRMS (ESI) *m/z* $C_7H_7{}^{79}BrNO_2$ and $C_7H_7{}^{81}BrNO_2$ requires 215.9655 and 217.9634 respectively ($[M+H]^+$), found 215.9653 and 217.9633.

Data consistent with literature.[209]

6-Methoxy-5-(4,4,5,5-tetramethyl-1,3,2-dioxaborolan-2-yl)nicotinaldehyde (35): A 25 ml round-bottom flask equipped with reflux condenser and stirrer bar was sequentially charged with 5-bromo-6-methoxynicotinaldehyde (**34**) (648 mg, 3.0 mmol, 1.0 equiv.), B_2Pin_2 (990 mg, 4.0 mmol, 1.3 equiv.), KOAc (589 mg, 6.0 mmol, 2.0 equiv.) and $PdCl_2$dppf·CH_2Cl_2 (73.5 mg, 0.03 equiv., 0.09 mmol). The apparatus was placed under an atmosphere of N_2 and dioxane (10 ml, 0.3 M) was added *via* syringe. The reaction was heated to reflux for 16 h. The reaction was cooled to rt, filtered through a pad of Celite® and washed with copious EtOAc. Purification by flash column chromatography (0 – 30% EtOAc in pentane) afforded 6-methoxy-5-(4,4,5,5-tetramethyl-1,3,2-dioxaborolan-2-yl)nicotinaldehyde (**35**) as a white solid (544 mg, 69%).

R_f (20% EtOAc in pentane) = 0.15.

^{1}H NMR (400 MHz, $CDCl_3$) δ 9.96 (s, 1H, C(1)*H*), 8.70 (d, *J* = 2.5 Hz, 1H, C(3)*H* or C(9)*H*), 8.46 (d, *J* = 2.5 Hz, 1H, C(3)*H* or C(9)*H*)), 4.06 (s, 3H, C(8)H_3), 1.36 (s, 12H, C(6)H_3).

^{13}C NMR (101 MHz, $CDCl_3$) δ 189.7, 170.6, 154.4, 146.5, 126.2, 84.4, 54.9, 24.9.

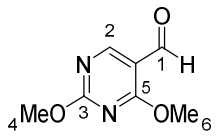
Note: The boron bearing quaternary carbon was not observed by ^{13}C NMR.

HRMS (ESI) *m/z* $C_{13}H_{19}BNO_4$ requires 264.1402 ($[M+H]^+$), found 264.1402.

IR (thin film, ν_{max} /cm^{-1}) 2981 ,1695, 1593, 1474, 1407, 1346, 1199, 1144, 1073, 854, 792, 676.

m.p. 104 – 108 °C.

2,4-Dimethoxypyrimidine-5-carbaldehyde (36)



Prepared according to a modified procedure.[203] Under N_2, n-butyllithium (2.12 M, 2.10 ml, 4.4 mmol, 1.1 equiv.) was added dropwise to a stirred solution of 5-bromo-2,4-dimethoxypyrimidine (876 mg, 4.0 mmol, 1.0 equiv.) in Et_2O (13 ml, 0.30 M) at -78 °C. The reaction mixture was stirred for 15 minutes at -78 °C. DMF (0.93 ml, 12.0 mmol, 3.0 equiv.) was added dropwise at -78 °C and stirred for 1h at that temperature. The dry ice/acetone bath was then removed and the reaction was warmed to rt and stirred for a further 1 h. The reaction was quenched with aq. sat. NH_4Cl and extracted thrice with Et_2O. The combined organic extracts were washed with brine, dried over anhydrous $MgSO_4$, filtered and concentrated under reduced pressure. Purification by flash column chromatography (0 – 3% Et_2O in pentane) afforded 2,4-dimethoxypyrimidine-5-carbaldehyde (**36**) as a white solid (373 mg, 55%).

R_f (20% Et_2O in pet ether) = 0.21.

^{1}H NMR (400 MHz, $CDCl_3$) δ 10.16 (s, 1H, C(1)*H*), 8.77 (s, 1H, C(2)*H*), 4.11 (s, 3H, C(4)H_3 or C(6)H_3), 4.07 (s, 3H, C(4)H_3 or C(6)H_3).

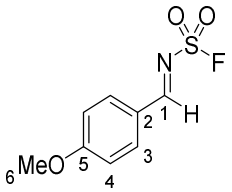
^{13}C NMR (101 MHz, $CDCl_3$) δ 186.6, 171.3, 167.7, 161.6, 112.4, 55.8, 54.7.

HRMS (ESI) *m/z* $C_7H_9N_2O_3$ requires 169.0608 ($[M+H]^+$), found 169.0613.

Data consistent with literature.[210]

5.2.2.3 Imine Substrates

(4-Methoxybenzylidene)sulfamoyl fluoride (1a)



Prepared according to **GP2**, FSI (1.00 ml, 12.72 mmol, 1.05 equiv.) was added dropwise to a stirred solution of anisaldehyde (1.50 ml, 12.12 mmol, 1.00 equiv.) in dry $(CH_2Cl)_2$ (5.0 ml, 2.4 M) under N_2 at 0 °C. The reaction was warmed to rt and stirred for a further 16 h. The solvent was removed under reduced pressure to give (4-methoxybenzylidene)sulfamoyl fluoride (**1a**), which was washed with hexane and isolated as an off-white solid (2.45 g, 93%).

^{1}H NMR (400 MHz, $CDCl_3$) δ 8.98 (s, 1H, C(1)*H*), 8.06 – 7.97 (m, 2H, C(3)*H*), 7.12 – 7.04 (m, 2H, C(4)*H*), 3.95 (s, 3H, C(6)H_3).

^{13}C NMR (101 MHz, $CDCl_3$) δ 176.0 (d, $^3J_{C\text{-}F}$ = 3.0 Hz), 167.2, 135.2, 124.0, 115.3, 56.0.

^{19}F NMR (377 MHz, $CDCl_3$) δ 44.48 (s).

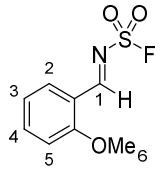
HRMS (ESI) *m/z* $C_8H_9FNO_3S$ requires 218.0282 ($[M+H]^+$), found 218.0293.

IR (thin film, ν_{max} /cm^{-1}) 1590, 1555, 1514, 1399, 1320, 1272, 1198, 1164, 1021, 837, 791.

m.p. 75–77 °C.

UV/Vis λ_{max}(fluorobenzene)/nm 324 (ε/dm^3 mol^{-1}cm^{-1} 9 420).

(2-Methoxybenzylidene)sulfamoyl fluoride (1b)



Prepared according to **GP2**, FSI (0.20 ml, 2.56 mmol, 1.05 equiv.) was added dropwise to a stirred solution of o-anisaldeyde (302 µl, 2.44 mmol, 1.00 equiv.) in dry $(CH_2Cl)_2$ (2.0 ml, 1.2 M) under N_2 at 0 °C. The reaction was warmed to rt and stirred for a further 16 h. The solvent was removed under reduced pressure to give (2-methoxybenzylidene)sulfamoyl fluoride (**1b**), which was washed with hexane and isolated as a light-yellow solid (340 mg, 64%).

^{1}H NMR (400 MHz, $CDCl_3$) δ 9.58 (s, 1H, C(1)*H*), 8.12 (dd, *J* = 7.9, 1.8 Hz, 1H, C(2)*H*), 7.71 (ddd, *J* = 8.9, 7.3, 1.8 Hz, 1H, C(4)*H*), 7.12 – 7.03 (m, 1H, C(3)*H*), 7.02 (d, *J* = 8.5 Hz, 1H, C(5)*H*), 3.96 (s, 3H, C(6)H_3).

^{13}C NMR (101 MHz, $CDCl_3$) δ 173.6 (d, $^3J_{C\text{-}F}$ = 3.8 Hz), 163.0, 139.5, 129.9, 121.5, 119.9, 112.0, 56.1.

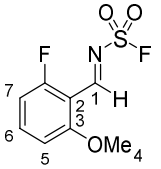
^{19}F NMR (377 MHz, $CDCl_3$) δ 43.82 (s).

HRMS (ESI) *m/z* $C_8H_9FNO_3S^+$ requires 218.0282 ([M+H]$^+$), found 218.0290.

IR (thin film, ν_{max} /cm^{-1}) 2924, 1606, 1590, 1564, 1488, 1405, 1264, 1201, 1165, 848, 798, 769, 636.

m.p. 50 – 52 °C.

(2-Fluoro-6-methoxybenzylidene)sulfamoyl fluoride (1c)



Prepared according to **GP2**, FSI (0.16 ml, 2.00 mmol, 1.05 equiv.) was added dropwise to a stirred solution of 2-fluoro-6-methoxybenzaldehyde (293 mg, 1.90 mmol, 1.00 equiv.) in dry $(CH_2Cl)_2$ (2.0 ml, 1.0 M) under N_2 at 0 °C. The reaction was warmed to rt and stirred for a further 16 h. The solvent was removed under reduced pressure to give (2-fluoro-6-methoxybenzylidene)sulfamoyl fluoride (**1c**), which was washed with hexane and isolated as an orange solid (416 mg, 93%).

^{1}H NMR (400 MHz, $CDCl_3$) δ 9.95 (d, *J* = 1.5 Hz, 1H, C(1)*H*), 8.12 (td, *J* = 8.5, 6.2 Hz, 1H, C(6)*H*), 7.34 – 7.30 (m, 1H, C(7)*H* or C(5)*H*), 7.30 – 7.27 (m, 1H, C(7)*H* or C(5)*H*), 4.45 (s, 3H, C(4)H_3).

^{13}C NMR (101 MHz, $CDCl_3$) δ 170.9 (d, $^{3}J_{C\text{-}F}$ = 4.1 Hz), 164.0 (d, $^{1}J_{C\text{-}F}$ = 269.0 Hz), 163.3 (d, $^{3}J_{C\text{-}F}$ = 4.8 Hz), 139.5 (d, $^{2}J_{C\text{-}F}$ = 12.3 Hz), 109.6 (d, $^{3}J_{C\text{-}F}$ = 10.3 Hz), 109.2 (d, $^{2}J_{C\text{-}F}$ = 21.0 Hz), 107.6 (d, $^{4}J_{C\text{-}F}$ = 3.6 Hz), 56.9.

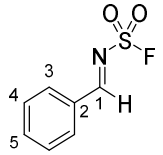
^{19}F NMR (377 MHz, $CDCl_3$) δ 43.16 (s), -102.13 – -102.33 (m).

HRMS (ESI) *m/z* $C_8H_8F_2NO_3S^+$ requires 236.0188 ($[M+H]^+$), found 236.0189.

IR (thin film, ν_{max} /cm^{-1}) 2925, 1620, 1566, 1481, 1407, 1378, 1291, 1256, 1202, 1091, 834, 790.

m.p. 84 – 87 °C.

Benzylidenesulfamoyl fluoride (1d)



Prepared according to **GP2**, FSI (0.16 ml, 2.00 mmol, 1.05 equiv.) was added dropwise to a stirred solution of benzaldehyde (202 µl, 1.90 mmol, 1.00 equiv.) in dry $(CH_2Cl)_2$ (2.0 mL, 1.0 M) under N_2 at 0 °C. The reaction was warmed to rt and stirred for a further 16 h. The solvent was removed under reduced pressure to give benzylidenesulfamoyl fluoride (**1d**), which was washed with hexane and isolated as a white solid (257mg, 72%).

^{1}H NMR (400 MHz, $CDCl_3$) δ 9.10 (s, 1H, C(1)*H*), 8.06 – 7.99 (m, 2H, C(3)*H*), 7.82 – 7.73 (m, 1H, C(5)*H*), 7.66 – 7.52 (m, 2H, C(4)*H*).

^{13}C NMR (101 MHz, $CDCl_3$) δ 177.7 (d, $^3J_{C\text{-}F}$ = 3.9 Hz), 137.2, 132.5, 131.3, 129.8.

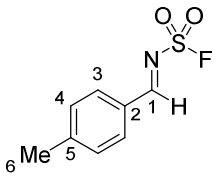
^{19}F NMR (377 MHz, $CDCl_3$) δ 43.65 (s).

IR (thin film, ν_{max} /cm^{-1}) 2924, 1598, 1572, 1455, 1409, 1377, 1206, 870, 846, 768, 687, 641.

m.p.: 45–46 °C.

Data consistent with literature.[211]

(4-Methylbenzylidene)sulfamoyl fluoride (1e)



Prepared according to **GP2**, FSI (0.15 ml, 1.92 mmol, 1.05 equiv.) was added dropwise to a stirred solution of 4-methylbenzaldehyde (220 mg, 1.83 mmol, 1.00 equiv.) in dry $(CH_2Cl)_2$ (2.0 mL, 0.9 M) under N_2 at 0 °C. The reaction was warmed to rt and stirred for a further 16 h. The solvent was removed under reduced pressure to give (4-methylbenzylidene)sulfamoyl fluoride (**1e**), which was recrystalised from Et_2O, as a white solid (245 mg, 67%).

^{1}H NMR (400 MHz, $CDCl_3$) δ 9.05 (s, 1H, C(1)*H*), 7.92 (d, *J* = 8.3 Hz, 2H, C(3)*H*), 7.39 (d, *J* = 7.9 Hz, 2H, C(4)*H*), 2.50 (s, 3H, C(6)H_3).

^{13}C NMR (101 MHz, $CDCl_3$) δ 177.3 (d, $^3J_{C\text{-}F}$ = 3.7 Hz), 149.3, 132.6, 130.6, 128.8, 22.4.

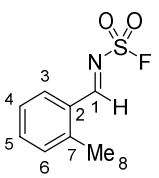
^{19}F NMR (377 MHz, $CDCl_3$) δ 43.89 (s).

IR (neat, ν_{max} /cm^{-1}) 3066, 1593, 1559, 1512, 1418, 1393, 1196, 1178, 874, 782, 762.

m.p. 77 – 79 °C.

Data consistent with literature.[141]

(2-Methylbenzylidene)sulfamoyl fluoride (1f)



Prepared according to **GP2**, FSI (0.20 ml, 2.56 mmol, 1.05 equiv.) was added dropwise to a stirred solution of 2-methylbenzaldehyde (228 μl, 1.90 mmol, 1.00 equiv.) in dry $(CH_2Cl)_2$ (2.0 mL, 1.2 M) under N_2 at 0 °C. The reaction was warmed to rt and stirred for a further 16 h. The ~80% solvent was removed under reduced pressure and the product was crashed out by adding heptane which was then washed with pentane to give (2-methylbenzylidene)sulfamoyl fluoride (**1f**) as a white solid (96.1 mg, 25%).

^{1}H NMR (400 MHz, $CDCl_3$) δ 9.39 (s, 1H, C(1)*H*), 8.10 (dd, *J* = 7.9, 1.5 Hz, 1H, C(3)*H*), 7.62 (td, *J* = 7.6, 1.5 Hz, 1H, C(5)*H*), 7.42 – 7.34 (m, 2H, C(4)*H*, C(6)H), 2.67 (s, 3H, C(8)H_3).

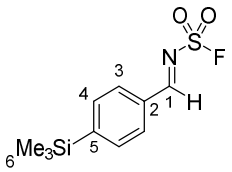
^{13}C NMR (101 MHz, $CDCl_3$) δ 176.2 (d, $^3J_{C\text{-}F}$ = 3.8 Hz), 144.2, 136.9, 132.2, 132.0, 129.4, 127.2, 20.0.

^{19}F NMR (377 MHz, $CDCl_3$) δ 43.81(s).

IR (thin film, ν_{max} /cm^{-1}) 1589, 1565, 1409, 1293, 1206, 851, 767.

m.p. 38 – 39 °C.

(4-(Trimethylsilyl)benzylidene)sulfamoyl fluoride (1g)



Prepared according to **GP2**, FSI (0.16 ml, 2.00 mmol, 1.05 equiv.) was added dropwise to a stirred solution of 4-trimethylsilylbenzaldehyde (**28**) (342 μl, 1.90 mmol, 1.00 equiv.) in dry $(CH_2Cl)_2$ (2.0 ml, 1.0 M) under N_2 at 0 °C. The reaction was warmed to rt and stirred for a further 16 h. The solvent was removed under reduced pressure to give (4-

(trimethylsilyl)benzylidene)sulfamoyl fluoride (**1g**), which was washed with pentane and isolated as a white solid (280 mg, 57%).

^{1}H NMR (400 MHz, $CDCl_3$) δ 9.09 (s, 1H, C(1)*H*), 8.00 – 7.93 (m, 2H, C(3)*H*), 7.78 – 7.69 (m, 2H, C(4)*H*), 0.33 (s, 9H, C(6)H_3).

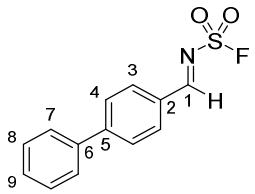
^{13}C NMR (101 MHz, $CDCl_3$) δ 177.9 (d, $^{3}J_{C\text{-}F}$ = 3.8 Hz), 153.4, 134.5, 131.3, 131.1, -1.4**.**

^{19}F NMR (377 MHz, $CDCl_3$) δ 43.74 (s).

IR (thin film, ν_{max} /cm^{-1}) 2957, 1595, 1545, 1412, 1252, 106, 1186, 1105, 845, 794, 761, 716, 624.

m.p. 59 – 60 °C.

([1,1'-Biphenyl]-4-ylmethylene)sulfamoyl fluoride (1h)



Prepared according to **GP2**, FSI (0.16 ml, 2.00 mmol, 1.05 equiv.) was added dropwise to a stirred solution of 4-phenylbenzaldehyde (346 mg, 1.90 mmol, 1.00 equiv.) in dry $(CH_2Cl)_2$ (2.0 ml, 1.0 M) under N_2 at 0 °C. The reaction was warmed to rt and stirred for a further 16 h. The solvent was removed under reduced pressure to give ([1,1'-biphenyl]-4-ylmethylene)sulfamoyl fluoride (**1h**), which was washed with hexane and isolated as a white solid (397mg, 79%).

^{1}H NMR (400 MHz, CDCl3) δ 9.13 (s, 1H, C(1)*H*), 8.13 – 8.06 (m, 2H, C(3)*H*), 7.85 – 7.78 (m, 2H, C(4)*H*), 7.72 – 7.62 (m, 2H, C(7)*H*), 7.56 – 7.42 (m, 3H, C(8)*H*, C(9)*H*).

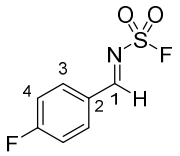
^{13}C NMR (101 MHz, CDCl3) δ 177.0 (d, $^{3}J_{C\text{-}F}$ = 3.7 Hz), 150.0, 139.0, 133.1, 130.0, 129.4, 129.3, 128.3, 127.6.

^{19}F NMR (377 MHz, CDCl3) δ 43.98 (s).

IR (thin film, ν_{max} /cm^{-1}) 2925, 1594, 1556, 1412, 1213, 883, 858, 766, 631.

m.p. 110–115 °C.

(4-Fluorobenzylidene)sulfamoyl fluoride (1i)



Prepared according to **GP2**, FSI (0.20 ml, 2.56 mmol, 1.05 equiv.) was added dropwise to a stirred solution of 4-fluorobenzaldehyde (275 µl, 2.44 mmol, 1.00 equiv.) in dry $(CH_2Cl)_2$ (2.0 mL, 1.2 M) under N_2 at 0 °C. The reaction was warmed to rt and stirred for a further 16 h. The solvent was removed under reduced pressure to give (4-fluorobenzylidene)sulfamoyl fluoride (**1i**), which was recrystalised successively from CPME and MTBE as a white solid (160 mg, 32%).

^{1}H NMR (400 MHz, CDCl$_3$) δ 9.07 (s, 1H, C(1)*H*), 8.14 – 8.03 (m, 2H, C(3)*H*), 7.34 – 7.24 (m, 2H, C(4)*H*).

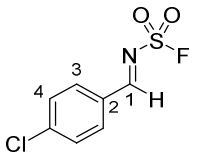
^{13}C NMR (101 MHz, CDCl$_3$) δ 176.0 (d, $^{3}J_{C\text{-}F}$ = 3.8 Hz), 168.3 (d, $^{1}J_{C\text{-}F}$ = 262.3 Hz), 135.2 (d, $^{3}J_{C\text{-}F}$ = 10.3 Hz), 127.8, 117.5 (d, $^{2}J_{C\text{-}F}$ = 22.5 Hz).

^{19}F(^{1}H) NMR (377 MHz, CDCl$_3$) δ 43.80, -96.70.

IR (thin film, ν_{max} /cm^{-1}) 2925, 1604, 1578, 1513, 1420, 1402, 1250, 1202, 1158, 881, 858, 805, 777.

m.p. 66 – 68 °C.

(4-Chlorobenzylidene)sulfamoyl fluoride (1j)



Prepared according to **GP2**, FSI (0.54 ml, 6.91 mmol, 1.80 equiv.) was added dropwise to a stirred solution of 4-chlorobenzaldehyde (540 mg, 3.84 mmol, 1.00 equiv.) in dry $(CH_2Cl)_2$ (2.0 mL, 1.9 M) under N_2 at 0 °C. The reaction was heated to 50 °C and stirred for a further 16 h. The solvent was removed under reduced pressure to give (4-chlorobenzylidene)sulfamoyl fluoride (**1j**), which was recrystalised from MTBE (313 mg, 37%).

^{1}H NMR (400 MHz, $CDCl_3$) δ 9.07 (s, 1H, C(1)*H*), 8.01 – 7.94 (m, 2H, C(3)*H*), 7.62 – 7.54 (m, 2H, C(4)*H*).

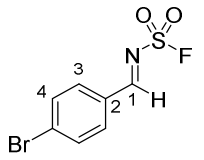
^{13}C NMR (101 MHz, $CDCl_3$) δ 176.2 (d, $^3J_{C\text{-}F}$ = 3.9 Hz), 144.1, 133.5, 130.3, 129.7.

^{19}F NMR (377 MHz, $CDCl_3$) δ 43.77 (s).

IR (neat, ν_{max} /cm^{-1}) 3092, 1590, 1559, 1489, 1412, 1200, 1089, 841, 831, 697.

m.p. 80 – 82 °C.

(4-Bromobenzylidene)sulfamoyl fluoride (1k)



Prepared according to **GP2**, FSI (0.16 ml, 2.00 mmol, 1.05 equiv.) was added dropwise to a stirred solution of 4-bromobenzaldehyde (352 mg, 1.90 mmol, 1.00 equiv.) in dry $(CH_2Cl)_2$ (2.0 mL, 1.0 M) under N_2 at rt. The reaction was heated to reflux and stirred for a further 16 h. The solvent was removed under reduced pressure to approximately ~50% original volume and triturated with heptane to give (4-bromobenzylidene)sulfamoyl fluoride (**1k**) as a white solid (232 mg, 46%).

^{1}H NMR (400 MHz, $CDCl_3$) δ 9.06 (s, 1H, C(1)*H*), 7.93 – 7.84 (m, 2H, C(3)*H*), 7.79 – 7.71 (m, 2H, C(4)*H*).

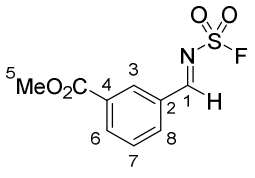
^{13}C NMR (101 MHz, $CDCl_3$) δ 176.4 (d, $^3J_{C\text{-}F}$ = 3.8 Hz), 133.4, 133.3, 133.1, 130.1.

^{19}F NMR (376 MHz, $CDCl_3$) δ 43.76 (s).

IR (neat, ν_{max} /cm^{-1}) 1586, 1556, 1485, 1220, 1069, 1011, 838, 674.

m.p. 98 – 100 °C.

Methyl 3-(((fluorosulfonyl)imino)methyl)benzoate (1l)



Prepared according to **GP2**, FSI (0.16 ml, 2.00 mmol, 1.05 equiv.) was added dropwise to a stirred solution of Methyl 3-formylbenzoate (312 mg, 1.90 mmol, 1.00 equiv.) in dry $(CH_2Cl)_2$ (2.0 mL, 1.0 M) under N_2 at 0 °C. The reaction was heated to reflux and stirred

for a further 16 h. The solvent was removed under reduced pressure to give the methyl 3-(((fluorosulfonyl)imino)methyl)benzoate (**1l**), which was washed with a 15:1 pentane/Et_2O mixture and isolated as a white solid (302 mg, 55%).

^{1}H NMR (400 MHz, $CDCl_3$) δ 9.16 (s, 1H, C(1)*H*), 8.66 (t, *J* = 1.8 Hz, 1H, C(3)*H*), 8.41 (dt, *J* = 7.8, 1.5 Hz, 1H, C(6)*H* or C(8)*H*), 8.24 (dt, *J* = 7.8, 1.5 Hz, 1H, C(6)*H* or C(8)*H*), 7.70 (t, *J* = 7.8 Hz, 1H, C(7)*H*), 3.98 (s, 3H, C(5)H_3).

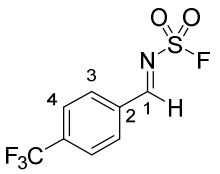
^{13}C NMR (101 MHz, $CDCl_3$) δ 176.7 (d, $^3J_{C\text{-}F}$ = 4.0 Hz), 165.4, 137.5, 135.5, 133.6, 132.0, 131.6, 130.0, 52.9.

^{19}F NMR (377 MHz, $CDCl_3$) δ 43.59 (s).

IR (thin film, ν_{max} /cm^{-1}) 2924, 1729, 1611, 1578, 1415, 1304, 1221, 1205, 1083, 852, 754, 646.

m.p. 97 – 100 °C.

(4-(Trifluoromethyl)benzylidene)sulfamoyl fluoride (1m)



Prepared according to **GP2**, FSI (0.16 ml, 2.00 mmol, 1.00 equiv.) was added dropwise to a stirred solution of 4-trifluoromethylbenzaldehyde (254 µl, 1.90 mmol, 1.00 equiv.) in dry $(CH_2Cl)_2$ (2.0 mL, 1.0 M) under N_2 at rt. The reaction was heated to reflux and stirred for a further 16 h. The solvent was removed under reduced pressure to

approximately ~20% original volume and triturated with heptane to give the (4-(trifluoromethyl)benzylidene)sulfamoyl fluoride (**1m**) as a white solid (337 mg, 70%).

^{1}H NMR (400 MHz, $CDCl_3$) δ 9.17 (s, 1H, C(1)*H*), 8.17 (dt, *J* = 7.9, 0.9 Hz, 2H, C(3)*H*), 7.86 (d, *J* = 8.2 Hz, 2H, C(4)*H*).

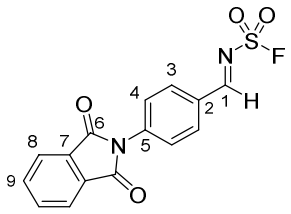
^{13}C NMR (101 MHz, $CDCl_3$) δ 176.2 (d, $^{3}J_{C\text{-}F}$ = 4.2 Hz), 137.7 (q, $^{2}J_{C\text{-}F}$ = 33.2 Hz), 134.1, 132.5, 128.7 (q, $^{1}J_{C\text{-}F}$ = 273.2 Hz), 126.7 (q, $^{3}J_{C\text{-}F}$ = 3.7 Hz).

^{19}F NMR (377 MHz, $CDCl_3$) δ 43.49 (s), -63.55 (s).

IR (neat, ν_{max} /cm^{-1}) 1609, 1574, 1516, 1422, 1379, 1327, 1212, 1175, 1131, 1112, 1067, 1019, 877, 835, 785, 662.

m.p. 72 – 75 °C.

(4-(1,3-Dioxoisoindolin-2-yl)benzylidene)sulfamoyl fluoride (1n)



Prepared according to **GP2**, FSI (0.16 ml, 2.00 mmol, 1.05 equiv.) was added dropwise to a stirred solution of 4-(1,3-dioxoisoindolin-2-yl)benzaldehyde (**29**) (477 mg, 1.9 mmol, 1.00 equiv.) in dry $(CH_2Cl)_2$ (2.0 mL, 1.0 M) under N_2 at 0 °C. The reaction was heated to reflux and stirred for a further 72 h. The reaction mixture was filtered to and the residue washed with copious CH_2Cl_2. The filtrate was then concentrated under reduced pressure and the compound was recrystalised from CH_2Cl_2 to give (4-(1,3-dioxoisoindolin-2-yl)benzylidene)sulfamoyl fluoride (**1n**) as a pale-yellow solid (133 mg, 21%).

^{1}H NMR (400 MHz, $CDCl_3$) δ 9.13 (s, 1H, C(1)*H*), 8.21 – 8.12 (m, 2H, C(3)*H*), 8.06 – 7.96 (m, 2H, C(8)*H*), 7.90 – 7.80 (m, 4H, C(4)*H*, C(9)*H*).

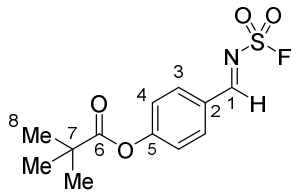
^{13}C NMR (101 MHz, $CDCl_3$) δ 176.4 (d, $^{3}J_{C\text{-}F}$ = 3.8 Hz), 166.5, 139.7, 135.2, 133.1, 131.5, 129.8, 126.6, 124.4.

^{19}F NMR (377 MHz, $CDCl_3$) δ 43.88 (s).

IR (neat, ν_{max} /cm^{-1}) 1719, 1700, 1590, 1560, 1413, 1219, 1089, 843, 719, 697.

m.p. 226 °C (decomp.).

4-(((Fluorosulfonyl)imino)methyl)phenyl pivalate (1o)



Prepared according to **GP2**, FSI (0.16 ml, 2.00 mmol, 1.05 equiv.) was added dropwise to a stirred solution of 4-formyl pivalate (**30**) (392 mg, 1.90 mmol, 1.00 equiv.) in dry $(CH_2Cl)_2$ (2.0 mL, 1.0 M) under N_2 at 0 °C. The reaction was heated to 35 °C and stirred for a further 16 h. The solvent was removed under reduced pressure to give 4-(((fluorosulfonyl)imino)methyl)phenyl pivalate (**1o**), which was washed with hexane and isolated as an orange solid (302 mg, 55%).

^{1}H NMR (400 MHz, $CDCl_3$) δ 9.07 (s, 1H, C(1)*H*), 8.10 – 8.02 (m, 2H, C(3)*H*), 7.36 – 7.28 (m, 2H, C(4)*H*), 1.38 (s, 9H, C(8)H_3).

^{13}C NMR (101 MHz, $CDCl_3$) δ 176.4 (d, $^{3}J_{C\text{-}F}$ = 3.8 Hz), 176.2, 158.2, 134.0, 128.5, 123.1, 39.5, 27.1.

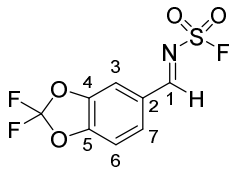
^{19}F NMR (377 MHz, $CDCl_3$) δ 43.86 (s).

HRMS (ESI) *m/z* $C_{12}H_{15}FNO_4S^+$ requires 288.0700 ($[M+H]^+$) found 288.0705.

IR (thin film, ν_{max} /cm^{-1}) 2926, 1748, 1600, 1572, 1478, 1410, 1235, 1121, 1165, 1112, 880, 844, 776, 630.

m.p. 96 – 98 °C.

((2,2-Difluorobenzo[d][1,3]dioxol-5-yl)methylene)sulfamoyl fluoride (1p)



Prepared according to **GP2**, FSI (0.16 ml, 2.00 mmol, 1.00 equiv.) was added dropwise to a stirred solution of 2,2-difluorobenzo[d][1,3]dioxole-5-carbaldehyde (354 mg, 1.90 mmol, 1.00 equiv.) in dry $(CH_2Cl)_2$ (2.0 mL, 1.0 M) under N_2 at 0 °C. The reaction was heated to reflux and stirred for a further 16 h. The solvent was removed under reduced pressure to give ((2,2-difluorobenzo[d][1,3]dioxol-5-yl)methylene)sulfamoyl fluoride (**1p**), which was washed with pentane and isolated as a white solid (195 mg, 38%).

^{1}H NMR (400 MHz, $CDCl_3$) δ 9.05 (s, 1H, C(1)*H*), 7.83 (s, 1H, C(3)*H*), 7.78 (d, *J* = 8.3 Hz, 1H, C(6)*H* or C(7)*H*), 7.29 (d, *J* = 8.2 Hz, 1H, C(6)*H* or C(7)*H*).

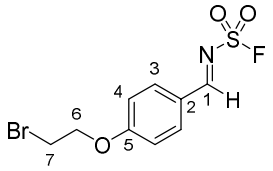
^{13}C NMR (101 MHz, $CDCl_3$) δ 175.8 (d, $^{3}J_{C\text{-}F}$ = 3.9 Hz), 150.1, 145.0, 132.5, 131.8 (t, $^{1}J_{C\text{-}F}$ = 260.0 Hz), 127.8, 110.6, 110.5.

^{19}F NMR (377 MHz, $CDCl_3$) δ 44.00 (s), -49.66 (s).

IR (thin film, ν_{max} /cm^{-1}) 2926, 1633, 1592, 1504, 1460, 1414, 1254, 1206, 1033, 902, 860, 788, 710.

m.p. 43 – 48 °C.

(4-(2-Bromoethoxy)benzylidene)sulfamoyl fluoride (1q)



Prepared according to **GP2**, FSI (0.15 ml, 1.92 mmol, 1.05 equiv.) was added dropwise to a stirred solution of 4-(2-bromoethoxy)benzaldehyde (435.3 mg, 1.90 mmol, 1.00 equiv.) in dry $(CH_2Cl)_2$ (2.0 mL, 1.0 M) under N_2 at 0 °C. The reaction was warmed to rt and stirred for a further 16 h. The solvent was removed under reduced pressure to give the (4-(2-bromoethoxy)benzylidene)sulfamoyl fluoride (**1q**), which was recrystalised from CH_2Cl_2/heptane and then washed with a 7:1 pentane/CH_2Cl_2 mixture to give the product as a yellow solid (182 mg, 31%).

^{1}H NMR (400 MHz, $CDCl_3$) δ 8.99 (s, 1H, C(1)*H*), 8.00 (d, *J* = 8.6 Hz, 2H, C(3)*H*), 7.07 (d, *J* = 8.5 Hz, 2H, C(4)*H*), 4.43 (t, *J* = 6.1 Hz, 2H, C(6)H_2), 3.69 (t, *J* = 6.1 Hz, 2H, C(7)H_2).

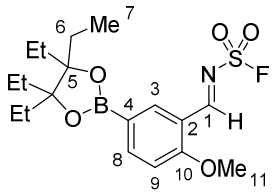
^{13}C NMR (101 MHz, $CDCl_3$) δ 175.9 (d, $^3J_{C\text{-}F}$ = 3.4 Hz), 165.4, 135.1, 124.6, 115.7, 68.3, 28.1.

^{19}F NMR (377 MHz, $CDCl_3$) δ 44.37 (s).

IR (thin film, ν_{max} /cm^{-1}) 2973, 2941, 1514, 1423, 1250, 1214, 1033, 732;

m.p. 88 – 90 °C.

(2-Methoxy-5-(4,4,5,5-tetraethyl-1,3,2-dioxaborolan-2-yl)benzylidene)sulfamoyl fluoride (1r)



Prepared according to **GP2**, FSI (0.16 ml, 2.00 mmol, 1.05 equiv.) was added dropwise to a stirred solution of 2-methoxy-5-(4,4,5,5-tetraethyl-1,3,2-dioxaborolan-2-yl)benzaldehyde (**32**) (605 mg, 1.90 mmol, 1.00 equiv.) in dry $(CH_2Cl)_2$ (2.0 mL, 1.0 M) under N_2 at 0 °C. The reaction was heated to 50 °C and stirred for a further 16 h. The solvent was removed under reduced pressure to approximately ~20% and crashed out by addition of heptane to give (2-methoxy-5-(4,4,5,5-tetraethyl-1,3,2-dioxaborolan-2-yl)benzylidene)sulfamoyl fluoride (**1r**), which was washed with pentane and isolated as a white solid (661 mg, 87%).

^{1}H NMR (400 MHz, $CDCl_3$) δ 9.58 (s, 1H, C(1)*H*), 8.56 (d, *J* = 1.7 Hz, 1H, C(3)*H*) 8.12 (dd, *J* = 8.4, 1.7 Hz, 1H, C(8)*H*), 7.00 (d, *J* = 8.5 Hz, 1H, C(9)*H*), 3.98 (s, 3H, C(11)H_3), 1.75 (ddt, *J* = 17.7, 14.4, 7.2 Hz, 8H, C(6)H_2), 0.97 (t, *J* = 7.5 Hz, 12H, C(7)H_3).

^{13}C NMR (101 MHz, $CDCl_3$) δ 173.6 (d, $^3J_{C\text{-}F}$ = 3.6 Hz), 164.9, 145.9, 137.2, 119.5, 111.2, 89.4, 56.2, 26.6, 9.0.

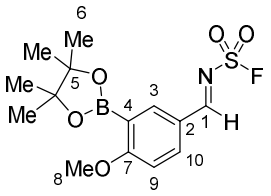
Note: The boron bearing quaternary carbon was not observed by ^{13}C NMR.

^{19}F NMR (377 MHz, $CDCl_3$) δ 43.93 (s).

IR (neat, ν_{max} /cm^{-1}) 2982, 1612, 1584, 1401, 1362, 1314, 1192, 1140, 1024, 910, 850, 823, 803, 784, 673.

m.p. 75 – 79 °C.

(4-Methoxy-3-(4,4,5,5-tetramethyl-1,3,2-dioxaborolan-2-yl)benzylidene)sulfamoyl fluoride (1s)



Prepared according to **GP2**, FSI (0.16 ml, 2.00 mmol, 1.00 equiv.) was added dropwise to a stirred solution of 4-methoxy-3-(4,4,5,5-tetramethyl-1,3,2-dioxaborolan-2-yl)benzaldehyde (**33**) (497 mg, 1.90 mmol, 1.00 equiv.) in dry $(CH_2Cl)_2$ (2.0 mL, 1.0 M) under N_2 at 0 °C. The reaction was heated to 50 °C and stirred for a further 16 h. The solvent was removed under reduced pressure to approximately ~20% original volume and the solid that crashed out was filtered off to give the (4-methoxy-3-(4,4,5,5-tetramethyl-1,3,2-dioxaborolan-2-yl)benzylidene)sulfamoyl fluoride (**1s**), which was washed with a 15:1 pentane/Et_2O mixture and isolated as a white solid (462 mg, 71%).

^{1}H NMR (400 MHz, $CDCl_3$) δ 8.98 (s, 1H, C(1)*H*), 8.33 (d, *J* = 2.3 Hz, 1H, C(3)*H*), 8.10 (dd, *J* = 8.8, 2.4 Hz, 1H,C(10)*H*), 7.02 (d, *J* = 8.8 Hz, 1H, C(9)*H*), 3.97 (s, 3H, C(8)H_3), 1.36 (s, 12H, C(6)H_3).

^{13}C NMR (101 MHz, $CDCl_3$) δ 176.2, 171.4, 143.0, 137.6, 123.5, 111.5, 84.3, 56.5, 24.9.

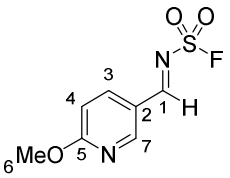
Note: The boron bearing quaternary carbon was not observed by ^{13}C NMR.

^{19}F NMR (377 MHz, $CDCl_3$) δ 44.54 (s).

IR (thin film, ν_{max} /cm^{-1}) 2984, 1588, 1560, 1492, 1412, 1274, 1198, 1146, 1068, 1021,968, 858.

m.p. 150 °C (decomp.).

((6-Methoxypyridin-3-yl)methylene)sulfamoyl fluoride (1u)



Prepared according to **GP2**, FSI (0.16 ml, 2.00 mmol, 1.00 equiv.) was added dropwise to a stirred solution of 5-formyl-2-methoxypyridine (274 mg, 2.00 mmol, 1.00 equiv.) in dry $(CH_2Cl)_2$ (2.0 mL, 1.0 M) under N_2 at rt. The reaction was heated to reflux and stirred for a further 16 h. The solvent was removed under reduced pressure to approximately ~50% original volume and triturated with heptane and washed with 9:1 Et_2O in pentane to give the ((6-methoxypyridin-3-yl)methylene)sulfamoyl fluoride (**1u**) as a white solid (320 mg, 73%).

^{1}H NMR (400 MHz, $CDCl_3$) δ 9.04 (s, 1H, C(1)*H*), 8.68 (d, *J* = 2.4 Hz, 1H, C(7)*H*), 8.26 (dd, *J* = 8.8, 2.4 Hz, 1H, C(3)*H*), 6.95 – 6.85 (m, 1H, C(4)*H*), 4.08 (s, 3H, C(6)H_3).

^{13}C NMR (101 MHz, $CDCl_3$) δ 174.5 (d, $^3J_{C\text{-}F}$ = 3.6 Hz), 169.6, 156.3, 138.8, 121.6, 113.4, 55.0.

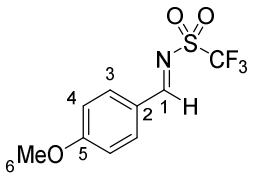
^{19}F NMR (377 MHz, $CDCl_3$) δ 44.19 (s).

HRMS (ESI) *m/z* $C_7H_8FN_2O_3S^+$ requires 219.0244 ($[M+H]^+$) found 219.0244.

IR (thin film, ν_{max} /cm^{-1}) 2926, 1779, 1607, 1553, 1504, 1404, 1203, 848, 773.

m.p. 108 – 113 °C.

1,1,1-trifluoro-*N*-(4-methoxybenzylidene)methanesulfonamide (1x)



Prepared according to a modified procedure.[212] Under air, a pressure tube was charged sequentially with trifluoromethanesulfonamide (358 mg, 2.40 mmol, 1.25 equiv.), 3Å molecular sieves (2.0 g), CH_2Cl_2 (7.5 ml, 0.3 M), *p*-anisaldehyde (0.24 ml, 1.90 mmol, 1.00 equiv.) and pyrrolidine (18 µl, 0.19 mmol, 10 mol%). The tube was sealed and heated to 60 °C for 16 h. After the elapsed time, the reaction was cooled to room temperature, filtered through a short pad of Celite® and concentrated under reduced pressure to give 1,1,1-trifluoro-N-(4-methoxybenzylidene)methanesulfonamide (**1x**), which was recrystalised from Et_2O, as a white solid (211 mg, 42%).

^{1}H NMR (400 MHz, $CDCl_3$) δ 9.03 (s, 1H, C(1)*H*), 8.03 (d, *J* = 8.5 Hz, 2H, C(3)*H*), 7.10 – 7.03 (m, 2H, C(4)*H*), 3.96 (s, 3H, C(6)H_3).

^{13}C NMR (101 MHz, $CDCl_3$) δ 178.4, 167.7, 135.8, 124.65, 119.3 (q, $^1J_{C-F}$ = 321.5 Hz), 115.5, 56.2.

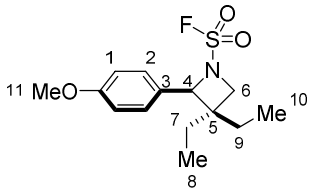
^{19}F NMR (377 MHz, $CDCl_3$) δ -76.97 (s).

IR (thin film, ν_{max} /cm^{-1}) 1602, 1585, 1546, 1512, 1430, 1356, 1266, 1205, 1168, 1119, 1020, 828, 758, 623.

Data consistent with literature.[213]

5.2.3 Azetidine Substrate Scope

(*R)-3,3-Diethyl-2-(4-methoxyphenyl)azetidine-1-sulfonyl fluoride (2a)**



Prepared according to **GP1** using (4-methoxybenzylidene)sulfamoyl fluoride (**1a**) (43.4 mg, 0.20 mmol, 1.0 equiv.), ITX (5.1 mg, 0.020 mmol, 0.10 equiv.) and 2-ethyl-1-butene (241 µl, 2.0 mmol, 10 equiv.) in $(CH_2Cl)_2$ (1.0 ml, 0.20 M). Purification by flash column chromatography (2% Et_2O in pentane) afforded (*R**)-3,3-diethyl-2-(4-methoxyphenyl)azetidine-1-sulfonyl fluoride (**2a**) as a yellow oil (55.4 mg, 91%).

Telescoped Procedure: Fluorosulfonyl isocyanate (FSI) (16 µl, 0.20 mmol, 1.0 equiv.) was added dropwise to a stirred solution of 4-anisaldehyde (0.20 mmol, 1.0 equiv.) in dry $(CH_2Cl)_2$ (0.50 ml, 0.4 M) under N_2 at 0 °C in a tapered microwave vial. (Caution: CO_2 evolution). The reaction mixture was then warmed to rt and stirred for 16 h. A solution of $[Ir(dFCF_3ppy)_2dtbbpy][PF_6]$ in $(CH_2Cl)_2$ (0.002 M, 1.0 ml, 1 mol%) was then added followed by the addition of 2-ethyl-1-butene (241 µl, 2.0 mmol, 10 eq). The reaction was then stirred under blue light irradiation (427 nm) at ambient temperature for 16 h. The reaction mixture was diluted with CH_2Cl_2, and the solvent removed under reduced pressure. Purification by flash column chromatography (0 – 2 Et_2O in pentane) afforded (*R**)-3,3-diethyl-2-(4-methoxyphenyl)azetidine-1-sulfonyl fluoride (**2a**) as a colourless oil (39.2 mg, 65%).

Scale-Up Method A: A Schlenk flask was charged with (4-methoxybenzylidene)sulfamoyl fluoride (**1a**) (1.09 g, 5.0 mmol, 1.0 equiv.) and $[Ir(dFCF_3ppy)_2(dtbbpy)][PF_6]$ (56.1 mg, 0.01 eq, 0.05 mmol). The flask was capped with a septum and evacuated and backfilled with N_2 thrice. $(CH_2Cl)_2$ (25 ml, 0.20 M) and 2-ethyl-1-butene (1.9 ml, 15 mmol, 3.0 equiv.) were added sequentially *via* syringe and the

reaction was stirred under irradiation with 427 nm light for 16 h. The reaction was concentrated under reduced pressure and purified by flash column chromatography (0 – 3% Et_2O in pentane) to give (*R**)-3,3-diethyl-2-(4-methoxyphenyl)azetidine-1-sulfonyl fluoride (**2a**) as a colourless oil (1.16 g, 77%).

Scale-UP Method B: A Schlenk flask was charged with (4-methoxybenzylidene)sulfamoyl fluoride (**1a**) (1.09 g, 5.0 mmol, 1.0 equiv.) and 3-F-TX (115 mg, 0.10 eq, 0.5 mmol). The flask was capped with a septum and then evacuated and backfilled with N_2 thrice. $(CH_2Cl)_2$ (25 ml, 0.20 M) and 2-ethyl-1-butene (1.9 ml, 15 mmol, 3.0 equiv.) were added sequentially *via* syringe and the reaction was stirred under irradiation with 390 nm light for 16 h. The reaction was then concentrated under reduced pressure and the crude residue was redissolved in CH_2Cl_2 (25 ml), before cooling to 0 °C and *m*-CPBA (225 mg, 0.2 equiv., 1 mmol) was added in one portion. The reaction mixture was warmed to rt and stirred for 1 h. Following completion, the reaction mixture was quenched with aq. sat. $NaHSO_3$ and the layers partitioned. The aqueous layer was extracted with CH_2Cl_2 three times, combined organic layers were washed sequentially with aq. sat. $NaHCO_3$, brine, dried over anhydrous $MgSO_4$ subsequently filtered and concentrated under reduced pressure. Purification by flash column chromatography (0 – 5% Et_2O in pentane) afforded (*R**)-3,3-diethyl-2-(4-methoxyphenyl)azetidine-1-sulfonyl fluoride (**2a**) as a colourless oil (1.17 g, 77%).

R_f (10% diethyl ether in pentane) = 0.33.

^{1}H NMR (600 MHz, $CDCl_3$) δ 7.29 – 7.26 (m, 2H, C(2)*H*), 6.93 – 6.87 (m, 2H, C(1)*H*), 5.17 (d, *J* = 2.0 Hz, 1H, C(4)*H*), 3.84 (dd, *J* = 7.9, 1.1 Hz, 1H, C(6)H_a), 3.81 (s, 3H, C(11)H_3), 3.72 (dd, *J* = 8.0, 1.7 Hz, 1H, C(6)H_b), 1.80 (dq, *J* = 14.9, 7.5 Hz, 1H, C(7)H_a),

1.75 (dq, *J* = 14.6, 7.5 Hz, 1H, C(7)H_b), 1.39 (dq, *J* = 14.9, 7.4 Hz, 1H, C(9)H_a), 1.16 (dq, *J* = 14.7, 7.4 Hz, 1H, C(9)H_b), 0.94 (t, *J* = 7.5 Hz, 3H, C(8)H_3), 0.58 (t, *J* = 7.4 Hz, 3H, C(10)H_3).

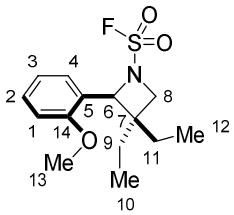
^{13}C NMR (151 MHz, $CDCl_3$) δ 159.7, 128.2, 127.4, 113.9, 75.3, 60.0, 55.4, 43.7, 29.2, 24.3, 8.1, 7.3.

^{19}F NMR (565 MHz, $CDCl_3$) δ 31.29 (s).

HRMS (ESI) *m/z* $C_{14}H_{20}FNO_3SNa^+$ requires 324.1040 ([M+Na]$^+$), found 324.1046.

IR (thin film, ν_{max} /cm^{-1}) 2971, 2940, 1749, 1615, 1516, 1423, 1305, 1254, 1215, 1178, 1035, 837, 767, 625.

(*S)-3,3-Diethyl-2-(2-methoxyphenyl)azetidine-1-sulfonyl fluoride (2b)**



Prepared according to **GP1** using (2-methoxybenzylidene)sulfamoyl fluoride (**1b**) (43.4 mg, 0.20 mmol, 1.0 equiv.), ITX (5.1 mg, 0.020 mmol, 0.10 equiv.) and 2-ethyl-1-butene (241 µl, 2.0 mmol, 10 equiv.) in $(CH_2Cl)_2$ (1.0 ml, 0.20 M). Purification by flash column chromatography (0 – 20 CH_2Cl_2 in pentane) afforded (*S**)-3,3-diethyl-2-(2-methoxyphenyl)azetidine-1-sulfonyl fluoride (**2b**) as a yellow oil (48.9 mg, 81%).

R_f (15% CH_2Cl_2 in pentane) = 0.20.

^{1}H NMR (600 MHz, $CDCl_3$) δ 7.56 (dd, *J* = 7.7, 1.7 Hz, 1H, C(4)*H*), 7.29 (td, *J* = 7.8, 1.7 Hz, 1H, C(2)*H*), 7.03 (t, *J* = 7.5 Hz, 1H, C(3)*H*), 6.84 (d, *J* = 8.2 Hz, 1H, C(1)*H*),

5.60 (d, *J* = 2.1 Hz, 1H, C(6)*H*), 3.93 (dd, *J* = 8.0, 2.0 Hz, 1H, C(8)H_a), 3.80 (s, 3H, C(13)H_3), 3.68 (dd, *J* = 8.0, 1.9 Hz, 1H, C(8)H_b), 1.85 (dq, *J* = 14.8, 7.4 Hz, 1H, C(9)H_a), 1.72 (dq, *J* = 14.7, 7.5 Hz, 1H, C(9)H_b), 1.38 (dq, *J* = 14.9, 7.7 Hz, 1H, C(11)H_a), 1.21 (dq, *J* = 14.6, 7.4 Hz, 1H, C(11)H_b), 1.02 (t, *J* = 7.5 Hz, 3H, C(10)H_3), 0.55 (t, *J* = 7.4 Hz, 3H, C(12)H_3).

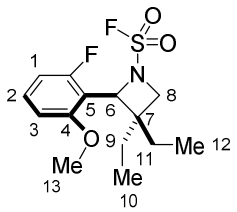
^{13}C NMR (151 MHz, $CDCl_3$) δ 156.4, 129.2, 127.9, 124.1, 120.6, 109.8, 70.1, 59.0, 55.1, 43.7, 28.6, 25.5, 8.3, 7.3.

^{19}F NMR (377 MHz, $CDCl_3$) δ 31.20 (s).

HRMS (ESI) *m/z* $C_{14}H_{20}FNO_3SNa^+$ requires 324.1040 ($[M+Na]^+$), found 324.1031.

IR (thin film, ν_{max} /cm^{-1}) 2971, 1494, 1464, 1422, 1298, 1248, 1215, 1090, 1051, 1031, 755.

(*S)-3,3-Diethyl-2-(2-fluoro-6-methoxyphenyl)azetidine-1-sulfonyl fluoride (2c)**



Prepared according to **GP1** using (2-fluoro-6-methoxybenzylidene)sulfamoyl fluoride (**S3**) (47.0 mg, 0.20 mmol, 1.0 equiv.), ITX (5.1 mg, 0.020 mmol, 0.10 equiv.) and 2-ethyl-1-butene (241 µl, 2.0 mmol, 10 equiv.) in $(CH_2Cl)_2$ (1.0 ml, 0.20 M). Purification by flash column chromatography (0 – 20% CH_2Cl_2 in pentane) afforded (*S**)-3,3-diethyl-2-(2-fluoro-6-methoxyphenyl)azetidine-1-sulfonyl fluoride (**2c**) as a colourless oil (26.8 mg, 42%).

R_f (15% CH_2Cl_2 in pentane) = 0.19.

^{1}H NMR (600 MHz, $CDCl_3$) δ 7.25 (td, *J* = 8.4, 6.2 Hz, 1H, C(2)*H*), 6.73 (dd, *J* = 10.8, 8.4 Hz, 1H, C(1)*H*), 6.68 (d, *J* = 7.9 Hz, 1H, C(3)*H*), 5.59 (s, 1H, C(6)*H*), 3.96 – 3.88 (m, 1H, C(8)H_a), 3.88 – 3.77 (m, 4H, C(13)H_3, C(8)H_b), 1.85 (dq, *J* = 14.7, 7.4 Hz, 1H, C(9)H_a), 1.76 (dq, *J* = 14.6, 7.4 Hz, 1H, C(9)H_b), 1.63 (dq, *J* = 14.8, 7.5 Hz, 1H, C(11)H_a), 1.39 (dq, *J* = 14.6, 7.4 Hz, 1H, C(11)H_b), 0.93 (t, *J* = 7.4 Hz, 3H, C(10)H_3), 0.60 (t, *J* = 7.5 Hz, 3H, C(12)H_3).

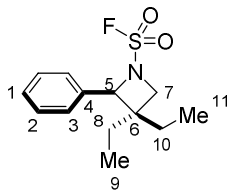
^{13}C NMR (151 MHz, $CDCl_3$) δ 162.1 (d, $^{1}J_{C\text{-}F}$ = 250.7 Hz), 158.2, 130.2 (d, $^{2}J_{C\text{-}F}$ = 11.4 Hz), 111.8 (d, $^{2}J_{C\text{-}F}$ = 11.9 Hz), 109.3, 106.3, 67.5, 60.1, 56.2, 44.3, 29.1, 24.2, 8.0, 7.5.

^{19}F NMR (565 MHz, $CDCl_3$) δ 34.08(s), -112.60(s).

HRMS (ESI) *m/z* $C_{14}H_{19}F_2NO_3SNa^+$ requires 342.0946 ($[M+Na]^+$), found 343.09301.

IR (thin film, ν_{max} /cm^{-1}) 2973, 1616, 1587, 1475, 1420, 1275, 1241, 1217, 1081, 751.

(*R)-3,3-Diethyl-2-phenylazetidine-1-sulfonyl fluoride (2d)**



Prepared according to **GP1** using benzylidenesulfamoyl fluoride (**1d**) (37.4 mg, 0.20 mmol, 1.0 equiv.), 3-F-TX (4.6 mg, 0.020 mmol, 0.10 equiv.) and 2-ethyl-1-butene (241 µl, 2.0 mmol, 10 equiv.) in $(CH_2Cl)_2$ (1.0 ml, 0.20 M). Purification by flash column chromatography (0 – 20% CH_2Cl_2 in pentane) afforded (*R**)-3,3-diethyl-2-phenylazetidine-1-sulfonyl fluoride (**2d**) as a colourless oil (40.9 mg, 75%).

R_f (20% CH_2Cl_2 in pentane) = 0.17.

^{1}H NMR (600 MHz, $CDCl_3$) δ 7.40 – 7.34 (m, 4H, C(2)*H*, C(3)*H*), 7.33 – 7.30 (m, 1H, C(1)*H*), 5.24 (d, *J* = 2.1 Hz, 1H,C(5)*H*), 3.88 (ddd, *J* = 7.9, 2.1, 1.0 Hz, 1H, C(7)H_a), 3.75 (dd, *J* = 7.9, 1.8 Hz, 1H, C(7)H_b), 1.84 (dq, *J* = 14.8, 7.5 Hz, 1H, C(8)H_a), 1.77 (dq, *J* = 14.9, 7.5 Hz, 1H, , C(8)H_b), 1.36 (dq, *J* = 14.9, 7.5 Hz, 1H, C(10)H_a), 1.15 (dq, *J* = 14.6, 7.4 Hz, 1H, C(10)H_b), 0.97 (t, *J* = 7.5 Hz, 3H, C(9)H_3), 0.58 (t, *J* = 7.5 Hz, 3H, C(11)H_3).

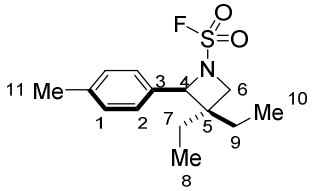
^{13}C NMR (101 MHz, $CDCl_3$) δ 135.2, 128.5, 128.3, 126.9, 75.4, 60.0, 43.7, 29.3, 24.5, 8.2, 7.3.

^{19}F NMR (565 MHz, $CDCl_3$) δ 31.51(s).

HRMS (ESI) *m/z* $C_{13}H_{22}FN_2O_2S^+$ requires 289.1381 ($[M+NH_4]^+$), found 289.1381.

IR (thin film, ν_{max} /cm^{-1}) 2971, 1456, 1425, 1217,1095, 761.

(*R)-3,3-Diethyl-2-(p-tolyl)azetidine-1-sulfonyl fluoride (2e)**



Prepared according to **GP1** using (4-methylbenzylidene)sulfamoyl fluoride (**1e**) (40.2 mg, 0.20 mmol, 1.0 equiv.), ITX (5.1 mg, 0.020 mmol, 0.10 equiv.) and 2-ethyl-1-butene (241 µl, 2.0 mmol, 10 equiv.) in $(CH_2Cl)_2$ (1.0 ml, 0.20 M). Purification by flash column chromatography (0 – 20% CH_2Cl_2 in pentane) afforded (R*)-3,3-diethyl-2-(p-tolyl)azetidine-1-sulfonyl fluoride (**2e**) as a colourless oil (40.9 mg, 86%).

R_f (20% CH_2Cl_2 in pentane) = 0.33.

^{1}H NMR (600 MHz, $CDCl_3$) δ 7.27 – 7.23 (m, 2H, C(2)*H*), 7.20 – 7.16 (m, 2H, C(1)*H*), 5.20 (d, *J* = 2.0 Hz, 1H, C(4)*H*), 3.86 (dd, *J* = 7.9, 1.1 Hz, 1H, C(6)H_a), 3.74 (dd, *J* = 8.0,

1.8 Hz, 1H, C(6)H_a), 2.36 (s, 3H, C(11)H_3), 1.82 (dq, J = 13.3, 6.7 Hz, 1H, C(7)H_a), 1.76 (dq, J = 14.3, 7.3 Hz, 1H, C(7)H_a), 1.38 (dq, J = 14.4, 7.3 Hz, 1H, C(9)H_a), 1.15 (dq, J = 14.6, 7.4 Hz, 1H, C(9)H_b), 0.96 (t, J = 7.5 Hz, 3H, C(8)H_3), 0.59 (t, J = 7.5 Hz, 3H, C(10)H_3).

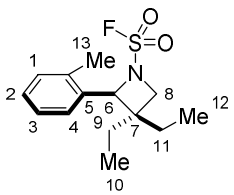
^{13}C NMR (151 MHz, $CDCl_3$) δ 138.1, 132.3, 129.2, 126.8, 75.5, 60.0, 43.7, 29.3, 24.4, 21.3, 8.1, 7.3.

^{19}F NMR (565 MHz, $CDCl_3$) δ 31.41(s).

No relevant ions were detected by ESI, APCI and EI.

IR (thin film, ν_{max} /cm^{-1}) 2971, 2939, 1763, 1517, 1424, 1216, 1096, 1055, 820, 747, 727, 626.

(*R)-3,3-Diethyl-2-(o-tolyl)azetidine-1-sulfonyl fluoride (2f)**



Prepared according to **GP1** using (2-methylbenzylidene)sulfamoyl fluoride (**1f**) (40.2 mg, 0.20 mmol, 1.0 equiv.), ITX (5.1 mg, 0.020 mmol, 0.10 equiv.) and 2-ethyl-1-butene (73 µl, 0.60 mmol, 3.0 equiv.) in $(CH_2Cl)_2$ (1.0 ml, 0.20 M). Purification by flash column chromatography (0 – 20% CH_2Cl_2 in pentane) afforded (*R**)-3,3-diethyl-2-(p-tolyl)azetidine-1-sulfonyl fluoride (**2f**) as a colourless oil (40.9 mg, 49%).

R_f (10% CH_2Cl_2 in pentane) = 0.13.

^{1}H NMR (400 MHz, $CDCl_3$) δ 7.64 (d, *J* = 7.7 Hz, 1H, C(1)*H*), 7.29 (dd, *J* = 7.4, 1.6 Hz, 1H, C(2)*H*), 7.22 (td, *J* = 7.4, 1.5 Hz, 1H, C(3)*H*), 7.13 (dd, *J* = 7.3, 1.5 Hz, 1H, C(4)*H*), 5.44 (d, *J* = 2.1 Hz, 1H, C(6)*H*), 4.00 (dd, *J* = 7.9, 2.1 Hz, 1H, C(8)H_a), 3.64 (dd, *J* = 8.0, 1.9 Hz, 1H, C(8)H_b), 2.29 (s, 3H, C(13)H_3), 1.90 (dq, *J* = 14.8, 7.5 Hz, 1H, C(9)H_a), 1.73 (dq, *J* = 14.7, 7.5 Hz, 1H, C(9)H_b), 1.46 (dq, *J* = 15.0, 7.5 Hz, 1H, C(11)H_a), 1.38 (dq, *J* = 14.6, 7.4 Hz, 1H, C(11)H_b), 1.03 (t, *J* = 7.4 Hz, 3H, C(10)H_3), 0.43 (t, *J* = 7.4 Hz, 3H, C(12)H_3).

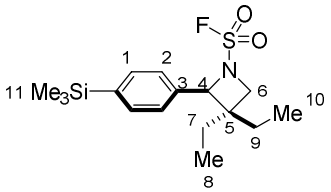
^{13}C NMR (101 MHz, $CDCl_3$) δ 134.8, 133.7, 130.4, 128.2, 127.3, 126.2, 71.6, 58.6, 44.1, 28.8, 26.0, 19.7, 8.5, 7.3.

^{19}F NMR (377 MHz, $CDCl_3$) δ 31.91(s).

HRMS (ESI) *m/z* $C_{14}H_{20}FNO_2SNa^+$ requires 308.1091 ($[M+Na]^+$), found 308.1085.

IR (thin film, ν_{max} /cm^{-1}) 2972, 2883, 1424, 1216, 1093, 1055, 1032, 918, 759, 621.

(*R)-3,3-Diethyl-2-(4-(trimethylsilyl)phenyl)azetidine-1-sulfonyl fluoride (2g)**



Prepared according to **GP1** using (4-(trimethylsilyl)benzylidene)sulfamoyl fluoride (**1g**) (51.9 mg, 0.20 mmol, 1.0 equiv.), 3-F-TX (4.6 mg, 0.020 mmol, 0.10 equiv.) and 2-ethyl-1-butene (241 µl, 2.0 mmol, 10 equiv.) in $(CH_2Cl)_2$ (1.0 ml, 0.20 M). Purification by flash column chromatography (0 – 20% CH_2Cl_2 in pentane) afforded (*R**)-3,3-diethyl-2-(4-(trimethylsilyl)phenyl)azetidine-1-sulfonyl fluoride (**2g**) as a white solid (48.1 mg, 70%).

R_f (10% CH_2Cl_2 in pentane) = 0.10.

^{1}H NMR (600 MHz, $CDCl_3$) ^{1}H NMR (500 MHz, $CDCl_3$) δ 7.55 – 7.49 (m, 2H, C(1)*H*), 7.34 – 7.29 (m, 2H, C(2)*H*), 5.22 (d, *J* = 2.0 Hz, 1H, C(4)*H*), 3.87 (d, *J* = 7.8 Hz, 1H, C(6)H_b), 3.76 (dd, *J* = 7.9, 1.8 Hz, 1H, C(6)H_b), 1.83 (dq, *J* = 14.7, 7.4 Hz, 1H, C(7)H_a), 1.77 (dq, *J* = 14.5, 7.4 Hz, 1H, C(7)H_b), 1.37 (dq, *J* = 14.9, 7.5 Hz, 1H, C(9)H_a), 1.13 (dq, *J* = 14.7, 7.6 Hz, 1H, C(9)H_b), 0.97 (t, *J* = 7.5 Hz, 3H, C(8)H_3), 0.59 (t, *J* = 7.4 Hz, 3H, C(10)H_3), 0.26 (s, 9H, C(11)H_3).

^{13}C NMR (151 MHz, $CDCl_3$) δ 140.6, 135.6, 133.5, 126.1, 75.5, 60.0, 43.7, 29.3, 24.5, 8.2, 7.3, -1.0.

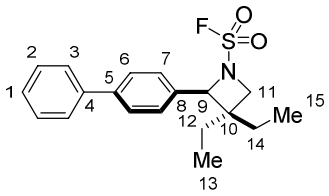
^{19}F NMR (565 MHz, $CDCl_3$) δ 31.41(s).

HRMS (ESI) *m/z* $C_{16}H_{26}FNO_2SSiNa^+$ requires 366.1330 ($[M+Na]^+$), found 366.1329.

IR (thin film, ν_{max} /cm^{-1}) 2968, 1427, 1250, 1216, 1110, 1093, 854, 842, 760.

m.p. 60 – 62 °C.

(*R)-2-([1,1'-Biphenyl]-4-yl)-3,3-diethylazetidine-1-sulfonyl fluoride (2h)**



Prepared according to **GP1** using ([1,1'-biphenyl]-4-ylmethylene)sulfamoyl fluoride (**1h**) (52.7 mg, 0.20 mmol, 1.0 equiv.), ITX (5.1 mg, 0.020 mmol, 0.10 equiv.) and 2-ethyl-1-butene (241 µl, 2.0 mmol, 10 equiv.) in $(CH_2Cl)_2$ (1.0 ml, 0.20 M). Purification by flash column chromatography (0 – 20% CH_2Cl_2 in pentane) afforded (*R**)-2-([1,1'-biphenyl]-4-yl)-3,3-diethylazetidine-1-sulfonyl fluoride (**2h**) as a white solid (48.5 mg, 70%).

R_f (20% CH_2Cl_2 in pentane) = 0.15.

^{1}H NMR (600 MHz, $CDCl_3$) δ 7.63 – 7.59 (m, 4H, Ar*H*), 7.47 – 7.42 (m, 4H, Ar*H*), 7.38 – 7.34 (m, 1H, C(1)*H*), 5.29 (d, *J* = 2.3 Hz, 1H, C(9)*H*), 3.90 (d, *J* = 8.0 Hz, 1H, C(11)H_a), 3.79 (dd, *J* = 8.0, 1.6 Hz, 1H, C(11)H_b), 1.86 (dq, *J* = 15.0, 7.6 Hz, 1H, C(12)H_a), 1.80 (dq, *J* = 14.8, 7.5 Hz, 1H, C(12)H_b), 1.43 (dq, *J* = 13.7, 6.9 Hz, 1H, C(14)H_a), 1.21 (dq, *J* = 14.6, 7.3 Hz, 1H, C(14)H_b), 1.00 (t, *J* = 7.5 Hz, 3H, C(13)H_3), 0.62 (t, *J* = 7.4 Hz, 3H, C(15)H_3).

^{13}C NMR (151 MHz, $CDCl_3$) δ 141.1, 140.5, 134.1, 128.8, 127.5, 127.2, 127.1, 75.2, 59.9, 43.7, 29.2, 24.4, 8.1, 7.2.

Note: 1 Carbon environment not observed due to signal overlap.

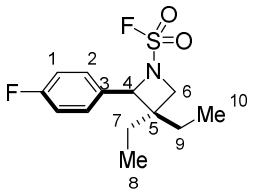
^{19}F NMR (565 MHz, $CDCl_3$) δ 31.49(s).

No relevant ions were detected by ESI, APCI and EI.

IR (thin film, ν_{max} /cm^{-1}) 2974, 2942, 1765, 1489, 1423, 1214, 1033, 763, 678.

m.p. 95 – 98 °C.

(*R)-3,3-Diethyl-2-(4-fluorophenyl)azetidine-1-sulfonyl fluoride (2i)**



Prepared according to **GP1** using (4-fluorobenzylidene)sulfamoyl fluoride (**1i**) (41.0 mg, 0.20 mmol, 1.0 equiv.), 3-F-TX (4.6 mg, 0.020 mmol, 0.10 equiv.) and 2-ethyl-1-butene (241 µl, 2.0 mmol, 10 equiv.) in $(CH_2Cl)_2$ (1.0 ml, 0.20 M). Purification by flash column

chromatography (0 – 20% CH_2Cl_2 in pentane) afforded (*R**)-3,3-diethyl-2-(4-fluorophenyl)azetidine-1-sulfonyl (**2i**) as a colourless oil (45.3 mg, 78%).

R_f (20% CH_2Cl_2 in pentane) = 0.25.

^{1}H NMR (600 MHz, $CDCl_3$) δ 7.37 – 7.30 (m, 2H, C(2)*H*), 7.11 – 7.04 (m, 2H, C(1)*H*), 5.20 (d, *J* = 2.2 Hz, 1H, C(4)*H*), 3.87 (dd, *J* = 7.9, 1.1 Hz, 1H, C(6)H_a), 3.74 (dd, *J* = 8.0, 1.7 Hz, 1H, C(6)H_b), 1.82 (dq, *J* = 14.9, 7.5 Hz, 1H, C(7)H_a), 1.76 (dq, *J* = 14.6, 7.5 Hz, 1H, C(7)H_b), 1.36 (dq, *J* = 14.9, 7.5 Hz, 1H, C(9)H_a), 1.14 (dq, *J* = 14.6, 7.4 Hz, 1H, C(9)H_b), 0.96 (t, *J* = 7.5 Hz, 3H, C(8)H_3), 0.59 (t, *J* = 7.4 Hz, 3H, C(10)H_3).

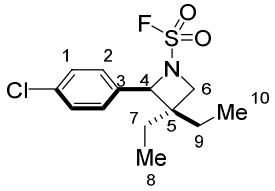
^{13}C NMR (151 MHz, $CDCl_3$) δ 162.7 (d, $^1J_{C\text{-}F}$ = 247.0 Hz), 131.1 (d, $^4J_{C\text{-}F}$ = 3.1 Hz), 128.6 (d, $^3J_{C\text{-}F}$ = 8.2 Hz), 115.5 (d, $^2J_{C\text{-}F}$ = 21.8 Hz), 74.8, 60.0, 43.7, 29.2, 24.5, 8.1, 7.3.

^{19}F(^{1}H) NMR (377 MHz, $CDCl_3$) δ 31.27(s), -113.81(s).

No relevant ions were detected by ESI, APCI and EI.

IR (thin film, ν_{max} /cm^{-1}) 2972, 1493, 1461, 1422, 1248, 1215, 1090, 1052, 1031, 755.

(*R)-2-(4-Chlorophenyl)-3,3-diethylazetidine-1-sulfonyl fluoride (2j)**



Prepared according to **GP1** using (4-chlorobenzylidene)sulfamoyl fluoride (**1j**) (44.3 mg, 0.20 mmol, 1.0 equiv.), 3-F-TX (4.6 mg, 0.020 mmol, 0.10 equiv.) and 2-ethyl-1-butene (241 µl, 2.0 mmol, 10 equiv.) in $(CH_2Cl)_2$ (1.0 ml, 0.20 M). Purification by flash column chromatography (0 – 20% CH_2Cl_2 in pentane) afforded (*R**)-2-(4-chlorophenyl)-3,3-diethylazetidine-1-sulfonyl fluoride (**2j**) as a colourless oil (45.4 mg, 74%).

R_f (20% CH_2Cl_2 in pentane) = 0.32.

^{1}H NMR (600 MHz, $CDCl_3$) δ 7.37 – 7.34 (m, 2H, C(1)*H*), 7.31 – 7.28 (m, 2H, C(2)*H*), 5.19 (s, 1H, C(4)*H*), 3.87 (ddd, *J* = 7.9, 2.0, 1.0 Hz, 1H, C(6)H_a), 3.74 (dd, *J* = 8.0, 1.7 Hz, 1H, C(6)H_b), 1.82 (dq, *J* = 14.3, 7.4 Hz, 1H, C(7)H_a), 1.76 (dq, *J* = 14.4, 7.1 Hz, 1H, C(7)H_b), 1.35 (dq, *J* = 14.9, 7.5 Hz, 1H, C(9)H_a), 1.13 (dq, *J* = 14.7, 7.4 Hz, 1H, C(9)H_b), 0.96 (t, *J* = 7.5 Hz, 3H, C(8)H_3), 0.59 (t, *J* = 7.4 Hz, 3H, C(10)H_3).

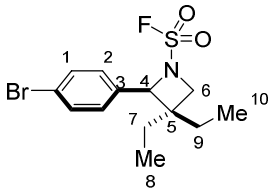
^{13}C NMR (151 MHz, $CDCl_3$) δ 134.3, 133.8, 128.8, 128.2, 74.7, 60.0, 43.7, 29.2, 24.5, 8.2, 7.3.

^{19}F NMR (565 MHz, $CDCl_3$) δ 31.42(s).

No relevant ions were detected by ESI, APCI and EI.

IR (thin film, ν_{max} /cm^{-1}) 2972, 2941, 1764, 1458, 1426, 1217, 1095, 753, 610.

(*R)-2-(4-Bromophenyl)-3,3-diethylazetidine-1-sulfonyl fluoride (2k)**



Prepared according to **GP1** using (4-bromobenzylidene)sulfamoyl fluoride (**1k**) (53.2 mg, 0.20 mmol, 1.0 equiv.), 3-F-TX (4.6 mg, 0.020 mmol, 0.10 equiv.) and 2-ethyl-1-butene (241 µl, 2.0 mmol, 10 equiv.) in $(CH_2Cl)_2$ (1.0 ml, 0.20 M). Purification by flash column chromatography (0 – 20% CH_2Cl_2 in pentane) afforded (*R**)-2-(4-bromophenyl)-3,3-diethylazetidine-1-sulfonyl fluoride (**2k**) as a colourless oil (50.7 mg, 72%).

R_f (20% CH_2Cl_2 in pentane) = 0.29.

^{1}H NMR (600 MHz, $CDCl_3$) δ 7.54 – 7.48 (m, 2H), 7.25 – 7.21 (m, 2H), 5.17 (d, J = 2.4 Hz, 1H, C(4)*H*), 3.87 (dd, J = 8.0, 1.0 Hz, 1H, C(6)H_a), 3.74 (dd, J = 8.0, 1.7 Hz, 1H, C(6)H_b), 1.82 (dq, J = 12.8, 6.4 Hz, 1H, C(7)H_a), 1.76 (dq, J = 14.4, 7.3 Hz, 1H, C(7)H_b), 1.34 (dq, J = 14.9, 7.5 Hz, 1H, C(9)H_a), 1.13 (dq, J = 14.6, 7.4 Hz, 1H, C(9)H_b), 0.96 (t, J = 7.5 Hz, 3H, C(8)H_3), 0.60 (t, J = 7.4 Hz, 3H, C(10)H_3).

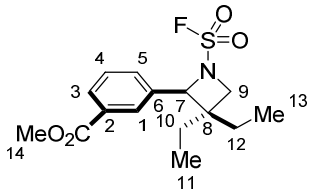
^{13}C NMR (151 MHz, $CDCl_3$) δ 134.4, 131.7, 128.6, 122.4, 74.7, 60.0, 43.7, 29.2, 24.5, 8.2, 7.3.

^{19}F NMR (565 MHz, $CDCl_3$) δ 31.44(s).

No relevant ions were detected by ESI, APCI and EI.

IR (thin film, ν_{max} /cm^{-1}) 2972, 2940, 1765, 1490, 1425, 1216, 1074, 1011, 837, 751, 623.

Methyl (*R)-3-(3,3-diethyl-1-(fluorosulfonyl)azetidin-2-yl)benzoate (2l)**



Prepared according to **GP1** using methyl 3-(((fluorosulfonyl)imino)methyl)benzoate (**1l**) (49.0 mg, 0.20 mmol, 1.0 equiv.), 3-F-TX (4.6 mg, 0.020 mmol, 0.10 equiv.) and 2-ethyl-1-butene (241 µl, 2.0 mmol, 10 equiv.) in $(CH_2Cl)_2$ (1.0 ml, 0.20 M). Purification by flash column chromatography (0 – 10% Et_2O in pentane) afforded methyl (*R**)-3-(3,3-diethyl-1-(fluorosulfonyl)azetidin-2-yl)benzoate (**2l**) as a colourless oil (41.0 mg, 62%)

R_f (10% Et_2O in pentane) = 0.30.

^{1}H NMR (400 MHz, $CDCl_3$) δ 8.01 (s, 1H, C(1)*H*), 7.99 (d, *J* = 1.6 Hz, 1H, C(3)*H*), 7.57 (dd, *J* = 7.8, 1.7 Hz, 1H, C(5)*H*), 7.46 (t, *J* = 7.9 Hz, 1H, C(4)*H*), 5.26 (s, 1H, C(7)*H*), 3.93 (s, 1H, C(14)H_3), 3.89 (d, *J* = 8.2 Hz, 1H, C(9)H_a), 3.77 (d, *J* = 7.9 Hz, 1H, C(9)H_b), 1.89 – 1.72 (m, 2H, C(10)H_2), 1.35 (dq, *J* = 14.9, 7.8 Hz, 1H, C(12)H_a), 1.10 (dq, *J* = 14.6, 7.4 Hz, 1H, C(12)H_b), 0.97 (t, *J* = 7.5 Hz, 1H, C(11)H_3), 0.56 (t, *J* = 7.4 Hz, 1H, C(13)H_3).

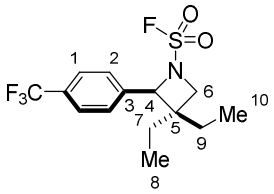
^{13}C NMR (101 MHz, $CDCl_3$) δ 166.8, 135.8, 131.3, 130.6, 129.6, 128.7, 127.9, 74.8, 59.9, 52.4, 43.7, 29.2, 24.6, 8.2, 7.3.

^{19}F NMR (377 MHz, $CDCl_3$) δ 31.20(s).

HRMS (ESI) *m/z* $C_{15}H_{21}FNO_4S^+$ requires 330.1170 ($[M+H]^+$), found 330.1158.

IR (thin film, ν_{max} /cm^{-1}) 2971, 1726, 1424, 1294, 1214, 759, 620.

(*R)-3,3-Diethyl-2-(4-(trifluoromethyl)phenyl)azetidine-1-sulfonyl fluoride (2m)**



Prepared according to **GP1** using (4-(trifluoromethyl)benzylidene)sulfamoyl fluoride (**1m**) (51.0 mg, 0.20 mmol, 1.0 equiv.), 3-F-TX (4.6 mg, 0.020 mmol, 0.10 equiv.) and 2-ethyl-1-butene (241 µl, 2.0 mmol, 10 equiv.) in $(CH_2Cl)_2$ (1.0 ml, 0.20 M). Purification by flash column chromatography (0 – 20% CH_2Cl_2 in pentane) afforded (*R**)-3,3-diethyl-2-(4-(trifluoromethyl)phenyl)azetidine-1-sulfonyl fluoride (**2m**) as a white solid (40.8 mg, 60%).

R_f (20% CH_2Cl_2 in pentane) = 0.27.

^{1}H NMR (600 MHz, $CDCl_3$) δ 7.68 – 7.63 (m, 2H, C(1)*H*), 7.51 – 7.46 (m, 2H, C(2)*H*), 5.27 (s, 1H, C(4)*H*), 3.90 (d, *J* = 8.0 Hz, 1H, C(6)H_a), 3.78 (dd, *J* = 8.0, 1.7 Hz, 1H, C(6)H_b), 1.85 (dq, *J* = 14.7, 7.4 Hz, 1H, C(7)H_a), 1.79 (dq, *J* = 14.6, 7.5 Hz, 1H, C(7)H_b), 1.33 (dq, *J* = 14.8, 7.5 Hz, 1H, C(9)H_a), 1.11 (dq, *J* = 13.6, 6.8 Hz, 1H, C(9)H_b), 0.99 (t, *J* = 7.5 Hz, 3H, C(8)H_3), 0.60 (t, *J* = 7.4 Hz, 3H, C(10)H_3).

^{13}C NMR (151 MHz, $CDCl_3$) δ 139.3, 130.6 (q, $^2J_{C-F}$ = 32.5 Hz), 127.2, 125.6 (q, $^3J_{C-F}$ = 3.8 Hz), 124.8 (q, $^1J_{C-F}$ = 272.0 Hz), 74.6, 60.0, 43.9, 29.2, 24.7, 8.2, 7.3.

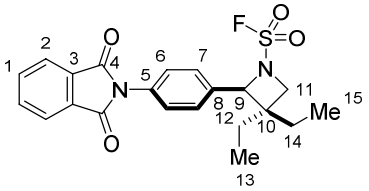
^{19}F(^{1}H) NMR (377 MHz, $CDCl_3$) δ 31.31(s), -62.60(s).

No relevant ions were detected by ESI, APCI and EI.

IR (thin film, ν_{max} /cm^{-1}) 2974, 2943, 1764, 1427, 1329, 1218, 1169, 1131, 767, 623.

m.p. 62 – 68 °C.

(*R)-2-(4-(1,3-Dioxoisoindolin-2-yl)phenyl)-3,3-diethylazetidine-1-sulfonyl fluoride (2n)**



Prepared according to **GP1** using (4-(1,3-dioxoisoindolin-2-yl)benzylidene)sulfamoyl fluoride (**1n**) (66.5 mg, 0.20 mmol, 1.0 equiv.), 3-F-TX (4.6 mg, 0.020 mmol, 0.10 equiv.) and 2-ethyl-1-butene (241 µl, 2.0 mmol, 10 equiv.) in $(CH_2Cl)_2$ (3.0 ml, 0.067 M). Purification by flash column chromatography (20% EtOAc in pentane) afforded (*R**)-2-

(4-(1,3-dioxoisoindolin-2-yl)phenyl)-3,3-diethylazetidine-1-sulfonyl fluoride (**2n**) as a yellow solid (67.4 mg, 81%).

R_f (20% ethyl acetate in pentane) = 0.16.

^{1}H NMR (600 MHz, $CDCl_3$) δ 7.95 (dd, *J* = 5.4, 3.1 Hz, 2H, C(2)*H*), 7.79 (dd, *J* = 5.4, 3.0 Hz, 2H, C(1)*H*), 7.53 – 7.46 (m, 4H, C(6)*H*, C(7)*H*), 5.28 (d, *J* = 1.6 Hz, 1H, C(9)*H*), 3.89 (d, *J* = 8.0 Hz, 1H, C(11)H_a), 3.78 (dd, *J* = 7.9, 1.3 Hz, 1H, C(11)H_b), 1.85 (dq, *J* = 14.7, 7.4 Hz, 1H, C(12)H_a), 1.79 (dq, *J* = 14.6, 7.4 Hz, 1H, C(12)H_b), 1.39 (dq, *J* = 14.8, 7.5 Hz, 1H, C(14)H_a), 1.17 (dq, *J* = 14.6, 7.4 Hz, 1H, C(14)H_b), 0.99 (t, *J* = 7.4 Hz, 3H, C(13)H_3), 0.63 (t, *J* = 7.4 Hz, 3H, C(15)H_3).

^{13}C NMR (151 MHz, $CDCl_3$) δ 167.2, 135.0, 134.6, 131.8, 127.4, 126.3, 123.9, 74.9, 60.0, 43.8, 29.2, 24.7, 8.2, 7.3.

Note: 1 Carbon environment not observed due to signal overlap.

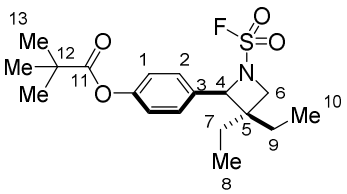
^{19}F NMR (565 MHz, $CDCl_3$) δ 31.69(s).

HRMS (ESI) *m/z* $C_{21}H_{22}FN_2O_4S^+$ requires 417.1279 ($[M+H]^+$), found 417.1288.

IR (thin film, ν_{max} /cm^{-1}) 2970, 1722, 1517, 1424, 1383, 1215, 1084, 720.

m.p. 140 °C (decomp.).

(*R)-4-(3,3-Diethyl-1-(fluorosulfonyl)azetidin-2-yl)phenyl pivalate (2o)**



Prepared according to **GP1** using 4-(((fluorosulfonyl)imino)methyl)phenyl pivalate (**1o**) (57.5 mg, 0.20 mmol, 1.0 equiv.), 3-F-TX (4.6 mg, 0.020 mmol, 0.10 equiv.) and 2-ethyl-1-butene (241 µl, 2.0 mmol, 10 equiv.) in $(CH_2Cl)_2$ (1.0 ml, 0.20 M). Purification by flash column chromatography (0 – 4% Et_2O in pentane) afforded (*R**)-4-(3,3-diethyl-1-(fluorosulfonyl)azetidin-2-yl)phenyl pivalate (**2o**) as a colourless crystalline solid (43.9 mg, 59%).

R_f (5% Et_2O in pentane) = 0.24.

^{1}H NMR (600 MHz, $CDCl_3$) δ 7.37 – 7.34 (m, 2H), 7.11 – 7.08 (m, 2H), 5.22 (d, *J* = 1.8 Hz, 1H, C(4)*H*), 3.86 (d, *J* = 7.9 Hz, 1H, C(6)H_a), 3.74 (d, *J* = 8.0 Hz, 1H, C(6)H_b), 1.82 (dq, *J* = 14.5, 7.3 Hz, 1H, C(7)H_a), 1.76 (dq, *J* = 14.6, 7.3 Hz, 1H, C(7)H_b), 1.39 – 1.32 (m, 10H, C(13)H_3, C(9)H_a), 1.14 (dq, *J* = 14.6, 7.4 Hz, 1H, C(9)H_b), 0.95 (t, *J* = 7.4 Hz, 3H, C(8)H_3), 0.58 (t, *J* = 7.4 Hz, 3H, C(10)H_3).

^{13}C NMR (151 MHz, $CDCl_3$) δ 177.0, 151.1, 132.5, 127.8, 121.6, 74.9, 60.0, 43.7, 39.2, 29.2, 27.2, 24.5, 8.1, 7.2.

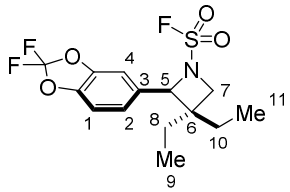
^{19}F NMR (565 MHz, $CDCl_3$) δ 31.49(s).

HRMS (ESI) *m/z* $C_{18}H_{26}FNO_4SNa^+$ requires 394.1459 ($[M+Na]^+$), found 394.1463.

IR (thin film, ν_{max} /cm^{-1}) 2973, 1755, 1509, 1425, 1215, 1168, 1120, 899, 748.

m.p. 82 – 86 °C.

(*R)-2-(2,2-Difluorobenzo[d][1,3]dioxol-5-yl)-3,3-diethylazetidine-1-sulfonyl fluoride (2p)**



Prepared according to **GP1** using ((2,2-difluorobenzo[d][1,3]dioxol-5-yl)methylene)sulfamoyl fluoride (**1p**) (53.4 mg, 0.20 mmol, 1.0 equiv.), 3-F-TX (4.6 mg, 0.020 mmol, 0.10 equiv.) and 2-ethyl-1-butene (241 µl, 2.00 mmol, 10 equiv.) in $(CH_2Cl)_2$ (1.0 ml, 0.20 M). Purification by flash column chromatography (0 – 20% CH_2Cl_2 in pentane) afforded azetidine (*R**)-2-(2,2-Difluorobenzo[d][1,3]dioxol-5-yl)-3,3-diethylazetidine-1-sulfonyl fluoride (**2p**) as a yellow oil (38.3 mg, 54 %).

R_f (10% CH_2Cl_2 in pentane) = 0.14.

^{1}H NMR (600 MHz, $CDCl_3$) δ 7.13 (s, 1H, C(4)*H*), 7.07 – 7.04 (m, 2H, C(1)*H*, C(2)*H*), 5.19 (s, 1H, C(7)*H*), 3.87 (d, *J* = 8.0 Hz, 1H, C(7)H_a), 3.74 (d, *J* = 7.9 Hz, 1H, C(7)H_b), 1.78 (m, 2H, C(8)H_2), 1.37 (dq, *J* = 14.8, 7.5 Hz, 1H, C(10)H_a), 1.14 (dq, *J* = 15.0, 7.3 Hz, 1H, C(10)H_B), 0.96 (t, *J* = 7.5 Hz, 3H, C(9)H_3), 0.61 (t, *J* = 7.4 Hz, 3H, C(11)H_3).

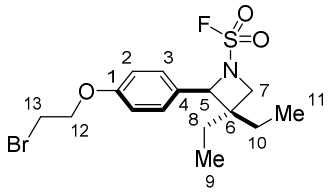
^{13}C NMR (151 MHz, $CDCl_3$) δ 144.1, 143.7, 131.8 (t, $^1J_{C\text{-}F}$ = 255.6 Hz), 131.7, 122.3, 109.5, 108.4, 74.7, 59.9, 43.9, 29.2, 24.5, 8.1, 7.3.

^{19}F NMR (565 MHz, $CDCl_3$) δ 31.34(s), -49.71(s).

HRMS (ESI) *m/z* $C_{14}H_{16}F_3NO_4SNa^+$ requires 374.0644 ($[M+Na]^+$), found 374.0645.

IR (thin film, ν_{max} /cm^{-1}) 2974, 1503, 1427, 1256, 1216, 1162, 1037, 753, 623.

(*R)-2-(4-(2-Bromoethoxy)phenyl)-3,3-diethylazetidine-1-sulfonyl fluoride (2q)**



Prepared according to **GP1** (4-(2-bromoethoxy)benzylidene)sulfamoyl fluoride **(1q**) (62.0 mg, 0.20 mmol, 1.0 equiv.), 3-F-TX (4.6 mg, 0.020 mmol, 0.10 equiv.) and 2-ethyl-1-butene (241 µl, 2.0 mmol, 10 equiv.) in $(CH_2Cl)_2$ (1.0 ml, 0.20 M). Purification by flash column chromatography (0 – 30% CH_2Cl_2 in pentane) afforded (*R**)-2-(4-(2-bromoethoxy)phenyl)-3,3-diethylazetidine-1-sulfonyl fluoride (**2q**) as a colourless oil (60.7 mg, 77%).

R_f (20% CH_2Cl_2 in pentane) = 0.12.

^{1}H NMR (600 MHz, $CDCl_3$) δ 7.30 – 7.27 (m, 2H, C(3)*H*), 6.95 – 6.89 (m, 2H, C(2)*H*), 5.17 (s, 1H, C(5)*H*), 4.29 (t, *J* = 6.2 Hz, 2H, C(12)H_2), 3.85 (d, *J* = 7.9 Hz, 1H, C(7)H_a), 3.72 (d, *J* = 8.7 Hz, 1H, C(7)H_a), 3.64 (t, *J* = 6.2 Hz, 2H, C(13)H_2), 1.80 (dq, *J* = 14.8, 7.4 Hz, 1H, C(8)H_a), 1.75 (dq, *J* = 14.6, 7.4 Hz, 1H, C(8)H_b), 1.38 (dq, *J* = 14.8, 7.5 Hz, 1H, C(10)H_a), 1.15 (dq, *J* = 15.0, 7.4 Hz, 1H, C(10)H_b), 0.94 (t, *J* = 7.4 Hz, 3H, C(9)H_3), 0.58 (t, *J* = 7.4 Hz, 3H, C(11)H_3).

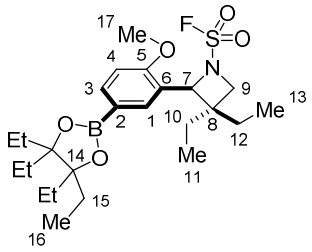
^{19}F NMR (377 MHz, $CDCl_3$) δ 31.25(s).

^{13}C NMR (151 MHz, $CDCl_3$) δ 158.2, 128.3, 128.2, 114.7, 75.2, 68.0, 60.0, 43.7, 29.2, 29.2, 24.4, 8.1, 7.3.

HRMS (ESI) *m/z* $C_{15}H_{22}{}^{79}BrFNO_3S^+$ and $C_{15}H_{22}{}^{81}BrFNO_3S^+$requires 394.0482 and 396.0462 respectively ($[M+H]^+$), found 394.0487 and 396.0435.

IR (thin film, ν_{max} /cm^{-1}) 2973, 2941, 1765, 1462, 1445, 1250, 1214, 1033, 751, 684.

(*S)-3,3-Diethyl-2-(2-methoxy-5-(4,4,5,5-tetraethyl-1,3,2-dioxaborolan-2-yl)phenyl)azetidine-1-sulfonyl fluoride (2r)**



Prepared according to **GP1** using (2-methoxy-5-(4,4,5,5-tetraethyl-1,3,2-dioxaborolan-2-yl)benzylidene)sulfamoyl fluoride (**1r**) (79.9 mg, 0.20 mmol, 1.0 equiv.), 3-F-TX (4.6 mg, 0.020 mmol, 0.10 equiv.) and 2-ethyl-1-butene (241 µl, 2.0 mmol, 10 equiv.) in $(CH_2Cl)_2$ (1.0 ml, 0.20 M). Purification by flash column chromatography (0 – 10 Et_2O in pentane) afforded (*S**)-3,3-diethyl-2-(2-methoxy-5-(4,4,5,5-tetraethyl-1,3,2-dioxaborolan-2-yl)phenyl)azetidine-1-sulfonyl fluoride (**2r**) as a white solid (40.4 mg, 42%).

R_f (10% Et_2O in pentane) = 0.26.

^{1}H NMR (400 MHz, $CDCl_3$) δ 7.94 (d, *J* = 1.6 Hz, 1H. C(1)*H*), 7.77 (dd, *J* = 8.0, 1.6 Hz, 1H, C(3)*H*), 6.82 (d, *J* = 8.2 Hz, 1H, C(4)*H*), 5.57 (d, *J* = 1.8 Hz, 1H, C(7)*H*), 3.92 (dd, *J* = 8.0, 1.8 Hz, 1H, C(9)H_a), 3.81 (s, 3H, C(17)H_3), 3.72 (dd, *J* = 8.0, 1.7 Hz, 1H, C(9)H_b), 1.90 – 1.64 (m, 10H, C(10)H_2, C(15)H_2), 1.38 (dq, *J* = 14.9, 7.5 Hz, 1H, C(12)H_a), 1.17 (dq, *J* = 14.6, 7.3 Hz, 1H, C(12)H_b), 1.04 – 0.91 (m, 15H, C(11)H_3, C(16)H_3), 0.54 (t, *J* = 7.4 Hz, 3H, C(13)H_3).

^{13}C NMR (151 MHz, $CDCl_3$) δ 158.8, 136.6, 134.3, 123.4, 109.2, 88.8, 70.2, 59.1, 55.1, 43.6, 28.7, 26.7, 26.5, 25.4, 9.1, 8.9, 8.3, 7.4.

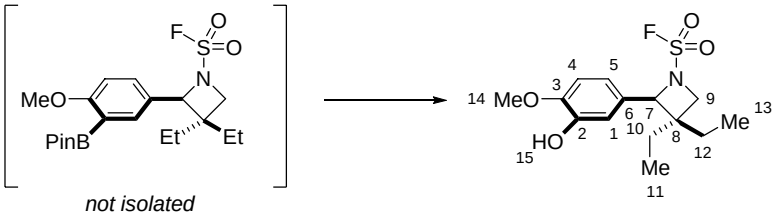
^{19}F NMR (565 MHz, $CDCl_3$) δ 32.17(s).

HRMS (ESI) *m/z* $C_{24}H_{40}BFNO_5^+$ requires 484.2699 ($[M+H]^+$), found 484.2712.

IR (thin film, ν_{max} /cm^{-1}) 2976, 1607, 1458, 1423, 1367, 1279, 1254, 1213, 1030, 924, 745.

m.p. 87 – 90 °C.

(*R)-3,3-Diethyl-2-(3-hydroxy-4-methoxyphenyl)azetidine-1-sulfonyl fluoride (2s')**



Prepared according to a modification of **GP1** using (4-methoxy-3-(4,4,5,5-tetramethyl-1,3,2-dioxaborolan-2-yl)benzylidene)sulfamoyl fluoride (**1s**) (68.6 mg, 0.20 mmol, 1.0 equiv.), 3-F-TX (4.6 mg, 0.020 mmol, 0.10 equiv.) and 2-ethyl-1-butene (241 µl, 2.0 mmol, 10 equiv.) in $(CH_2Cl)_2$ (1.0 ml, 0.20 M). Following the photochemical reaction, the reaction mixture was transferred to a round bottom flask and concentrated under reduced pressure. The crude reaction mixture was dissolved in a 1:1 mixture of THF/H_2O (3.2 ml, 0.063 M) followed by addition of $NaBO_3$ $4H_2O$ (462 mg, 3.0 mmol, 15 equiv.). The reaction mixture was stirred under air at rt for 1 h after which the reaction mixture was transferred to a separatory funnel. Brine was added and the layers partitioned. The aqueous layer was extracted three times with Et_2O, the combined organic fractions were dried over anhydrous $MgSO_4$ and concentrated under reduced pressure. Purification by flash column chromatography (0 – 30% Et_2O in pentane) afforded (*R**)-3,3-diethyl-2-(3-hydroxy-4-methoxyphenyl)azetidine-1-sulfonyl fluoride (**2s'**) as a colourless oil (39.5 mg, 62%).

R_f (30% Et_2O in pentane) = 0.19.

^{1}H NMR (500 MHz, $CDCl_3$) δ 6.91 (d, *J* = 2.0 Hz, 1H, C(1)*H*), 6.88 – 6.83 (m, 2H, C(4)*H*, C(5)*H*), 5.66 (s, 1H, O(15)*H*), 5.12 (d, *J* = 2.0 Hz, 1H, C(7)*H*), 3.88 (s, 3H, C(14)H_3), 3.83 (dd, *J* = 7.9, 1.1 Hz, 1H, C(9)H_a), 3.71 (dd, *J* = 7.8, 1.8 Hz, 1H, C(9)H_b), 1.75 (m, 2H, C(10)H_2), 1.39 (m, 1H, C(12)H_a), 1.18 (dq, *J* = 14.6, 7.6 Hz, 1H, C(12)H_b), 0.94 (t, *J* = 7.4 Hz, 3H, C(11)H_3), 0.59 (t, *J* = 7.4 Hz, 3H, C(13)H_3).

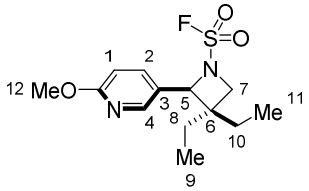
^{13}C NMR (126 MHz, $CDCl_3$) δ 146.6, 145.6, 128.5, 118.7, 113.2, 110.5, 75.2, 60.0, 56.1, 43.7, 29.2, 24.2, 8.1, 7.3.

^{19}F NMR (471 MHz, $CDCl_3$) δ 31.47(s).

HRMS (ESI) *m/z* $C_{14}H_{20}FNO_4SNa^+$ requires 340.08989 ($[M+Na]^+$), found 340.0999.

IR (thin film, ν_{max} /cm^{-1}) 3503, 2971, 1594, 1516, 1458, 1421, 1275, 1213, 1131, 1029, 762, 627.

(*S)-3,3-Diethyl-2-(6-methoxypyridin-3-yl)azetidine-1-sulfonyl fluoride (2u)**



Prepared according to **GP1** using ((6-methoxypyridin-3-yl)methylene)sulfamoyl fluoride (**1u**) (43.6 mg, 0.20 mmol, 1.0 equiv.), 3-F-TX (4.6 mg, 0.020 mmol, 0.10 equiv.) and 2-ethyl-1-butene (241 µl, 2.0 mmol, 10 equiv.) in $(CH_2Cl)_2$ (1.0 ml, 0.20 M). Purification by flash column chromatography (80 – 90 CH_2Cl_2 in pentane) afforded (*S**)-3,3-diethyl-2-(6-methoxypyridin-3-yl)azetidine-1-sulfonyl fluoride (**2u**) as a colourless oil (33.2 mg, 55%).

R_f (10% EtOAc in petrol) = 0.29.

^{1}H NMR (600 MHz, $CDCl_3$) δ 8.12 (dt, J = 2.5, 0.7 Hz, 1H, C(4)*H*), 7.61 (dd, J = 8.6, 2.5 Hz, 1H, C(2)*H*), 6.76 (d, J = 8.6 Hz, 1H, C(1)*H*), 5.16 (d, J = 2.0 Hz, 1H, C(5)*H*), 3.93 (s, 3H, C(12)H_3), 3.85 (d, J = 7.8 Hz, 1H, C(7)H_a), 3.74 (dd, J = 8.0, 1.6 Hz, 1H, C(7)H_a), 1.80 (dq, *J* = 14.8, 7.5 Hz, 1H, C(8)H_a), 1.76 (dq, *J* = 14.5, 7.4 Hz, 1H, C(8)H_b), 1.41 (dq, J = 14.8, 7.5 Hz, 1H, C(10)H_a), 1.17 (dq, J = 14.6, 7.4 Hz, 1H, C(10)H_b), 0.92 (t, J = 7.5 Hz, 3H, C(9)H_3), 0.62 (t, J = 7.4 Hz, 3H, C(11)H_3).

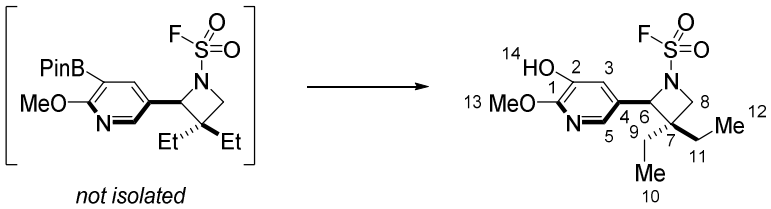
^{19}F NMR (565 MHz, $CDCl_3$) δ 31.09.

^{13}C NMR (151 MHz, $CDCl_3$) δ 164.4, 145.6, 137.4, 123.8, 110.8, 73.3, 60.1, 53.7, 43.8, 29.2, 24.4, 8.0, 7.3.

HRMS (ESI) *m/z* $C_{13}H_{20}FN_2O_3S^+$ requires 303.1173 ($[M+H]^+$), found 303.1173.

IR (thin film, ν_{max} /cm^{-1}) 2972, 1611, 1498, 1425, 1290, 1216, 1028, 834, 747.

(*S)-3,3-Diethyl-2-(5-hydroxy-6-methoxypyridin-3-yl)azetidine-1-sulfonyl fluoride (2t)**



FSI (16 µl, 0.20 mmol, 1.0 equiv.) was added dropwise to a stirred solution of 6-Methoxy-5-(4,4,5,5-tetramethyl-1,3,2-dioxaborolan-2-yl)nicotinaldehyde (**35**) (0.2 mmol, 1.0 equiv.) in dry $(CH_2Cl)_2$ (1.0 ml, 0.2 M) under N_2 at 0 °C in a tapered microwave vial. (Caution: CO_2 evolution). The reaction mixture was then heated to 55 °C and stirred for 16 h. After cooling to rt, the solvent was removed by a constant flow of N_2, before a solution of 3-F-TX in $(CH_2Cl)_2$ (0.020 M, 1.0 ml, 10 mol%) was added, followed by 2-ethyl-1-butene (241 µl, 2.0 mmol, 10 equiv.). The reaction was then stirred under purple

light irradiation (390 nm) at ambient temperature for 16 h. Following the photochemical reaction, the reaction mixture was transferred to a round bottom flask and concentrated under reduced pressure. The crude reaction mixture was dissolved in a 1:1 mixture of THF/H_2O (3.2 ml, 0.063 M) followed by addition of $NaBO_3$ $4H_2O$ (462 mg, 3.0 mmol, 15 equiv.). The reaction mixture was stirred under air at rt for 1 h after which the reaction mixture was transferred to a separatory funnel. Brine was added and the layers partitioned. The aqueous layer was extracted three times with Et_2O, the combined organic fractions were dried over anhydrous $MgSO_4$ and concentrated under reduced pressure. Purification by flash column chromatography (0 – 20 % Et_2O in pentane) afforded (*S**)-3,3-diethyl-2-(5-hydroxy-6-methoxypyridin-3-yl)azetidine-1-sulfonyl fluoride (**2t**) as a colourless oil (22.4 mg, 35%).

R_f (20% EtOAc in pentane) = 0.24.

^{1}H NMR (400 MHz, $CDCl_3$) δ 7.67 (d, *J* = 2.1 Hz, 1H, C(5)*H*), 7.17 (d, *J* = 2.1 Hz, 1H, C(3)*H*), 5.52 (s, 1H, O(14)*H*), 5.13 (d, *J* = 2.1 Hz, 1H, C(6)*H*), 4.03 (s, 3H, C(13)*H*), 3.84 (d, *J* = 7.7 Hz, 1H, C(8)H_a), 3.74 (dd, *J* = 8.0, 1.7 Hz, 1H, C(8)H_b), 1.83 – 1.72 (m, 2H, C(9)H_2), 1.42 (dq, *J* = 14.9, 7.3 Hz, 1H, C(11)H_a), 1.27 – 1.14 (m, 1H, C(11)H_b), 0.93 (t, *J* = 7.4 Hz, 3H, C(10)H_3), 0.63 (t, *J* = 7.4 Hz, 3H, C(12)H_3).

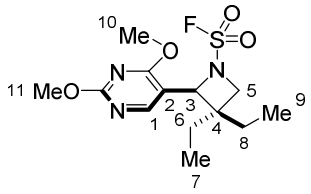
^{13}C NMR (101 MHz, $CDCl_3$) δ 153.0, 140.4, 135.7, 125.5, 119.6, 73.1, 60.2, 54.0, 43.7, 29.3, 24.4, 8.0, 7.4.

^{19}F NMR (377 MHz, $CDCl_3$) δ 31.33(s).

HRMS (ESI) *m/z* $C_{13}H_{18}FN_2O_4S^-$ requires 317.0977 ($[M-H]^-$), found 317.0991.

IR (thin film, ν_{max} /cm^{-1}) 3486, 2970, 1491, 1419, 1254, 1214, 1164, 1039, 1020, 913, 760, 622.

(*S)-2-(2,4-Dimethoxypyrimidin-5-yl)-3,3-diethylazetidine-1-sulfonyl fluoride (2v)**



FSI (16 µl, 0.20 mmol, 1.0 equiv.) was added dropwise to a stirred solution of 2,4-dimethoxypyrimidine-5-carbaldehyde (**36**) (0.2 mmol, 1.0 equiv.) in dry $(CH_2Cl)_2$ (1.0 ml, 0.2 M) under N_2 at 0 °C in a tapered microwave vial. (Caution: CO_2 evolution). The reaction mixture was then heated to 55 °C and stirred for 16 h. The reaction was then cooled to rt and the solvent removed by a constant flow of N_2.A solution of 3-F-TX in $(CH_2Cl)_2$ (0.020 M, 1.0 ml, 10 mol%) was then added followed by the addition of 2-ethyl-1-butene (241 µl, 2.0 mmol, 10 eq). The reaction was then stirred under purple light irradiation (390 nm) at ambient temperature for 16 h. The reaction mixture was diluted with CH_2Cl_2, and the solvent removed under reduced pressure. Purification by flash column chromatography (0 – 20 % Et_2O in pentane) afforded (*S**)-2-(2,4-dimethoxypyrimidin-5-yl)-3,3-diethylazetidine-1-sulfonyl fluoride (**2v**) as a white solid (43.0 mg, 64%).

R_f (20% Et_2O in pentane) = 0.20.

^{1}H NMR (600 MHz, $CDCl_3$) δ 8.40 (s, 1H, C(1)*H*), 5.31 (s, 1H, C(3)*H*), 4.00 (s, 3H, C(10)H_3 or C(11)H_3), 3.98 (s, 3H, C(10)H_3 or C(11)H_3), 3.89 (d, *J* = 8.0 Hz, 1H, C(5)H_a), 3.68 (d, *J* = 8.1 Hz, 1H, C(5)H_b), 1.81 (dq, *J* = 14.8, 7.4 Hz, 1H, C(6)H_a), 1.69 (dq, *J* =

14.6, 7.4 Hz, 1H, C(6)H_b), 1.49 – 1.40 (m, 1H, C(8)H_a), 1.27 – 1.18 (m, 1H, C(8)H_b), 0.95 (t, J = 7.5 Hz, 3H, C(7)H_3), 0.62 (t, J = 7.4 Hz, 3H, C(9)H_3).

^{13}C NMR (151 MHz, $CDCl_3$) δ 168.2, 165.4, 157.1, 109.6, 68.0, 59.4, 55.1, 54.1, 43.9, 28.7, 25.3, 8.1, 7.5.

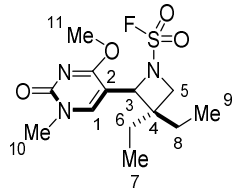
^{19}F NMR (565 MHz, $CDCl_3$) δ 30.86(s).

HRMS (ESI) *m/z* $C_{13}H_{20}FN_3O_4SNa^+$ requires 356.1051 ($[M+Na]^+$), found 356.1047.

IR (thin film, ν_{max} /cm^{-1}) 2971, 1606, 1573, 1474, 1425, 1404, 1215, 1079, 1052, 1018, 753.

m.p. 79 – 81 °C.

(*S)-3,3-Diethyl-2-(2-methoxy-1-methyl-4-oxo-1,4-dihydropyrimidin-5-yl)azetidine-1-sulfonyl fluoride (2w)**



FSI (16 µl, 0.20 mmol, 1.0 equiv.) was added dropwise to a stirred solution of 2,4-dimethoxypyrimidine-5-carbaldehyde (**36**) (0.20 mmol, 1.0 equiv.) in dry MeCN (0.20 ml, 1.0 M) under N_2 at 0 °C in a tapered microwave vial. (Caution: CO_2 evolution). The reaction mixture was then heated to 84 °C and stirred for 16 h. The reaction was then cooled to rt and the solvent removed by a constant flow of N_2. A solution of 3-F-TX in $(CH_2Cl)_2$ (0.020 M, 1.0 ml, 10 mol%) was then added followed by the addition of 2-ethyl-1-butene (241 µl, 2.0 mmol, 10 equiv.). The reaction was then stirred under purple light irradiation (390 nm) at ambient temperature for 16 h. The reaction mixture was diluted with CH_2Cl_2, and the solvent removed under reduced pressure. Purification by

flash column chromatography (50 – 70 % EtOAc in pentane) afforded (*S**)-3,3-diethyl-2-(2-methoxy-1-methyl-4-oxo-1,4-dihydropyrimidin-5-yl)azetidine-1-sulfonyl fluoride (**2w**) as a colourless oil (40.0 mg, 60%).

Note: Imine intermediate undergoes a rearrangement before photo-addition from pyrimidine to pyrimidone.

R_f (60% EtOAc in pentane) = 0.15.

^{1}H NMR (600 MHz, $CDCl_3$) δ 7.58 (s, 1H, C(1)*H*), 5.14 (s, 1H, C(3)*H*), 3.94 (s, 3H, C(11)H_3), 3.84 (d, *J* = 8.1 Hz, 1H, C(5)H_a), 3.59 (d, *J* = 8.1 Hz, 1H, C(5)H_b), 3.52 (s, 3H, C(10)H_3), 1.77 (dq, *J* = 14.8, 7.4 Hz, 1H, C(6)H_a), 1.64 (dq, *J* = 14.8, 7.5 Hz, 1H, C(6)H_b), 1.43 (dq, *J* = 14.9, 7.5 Hz, 1H, C(8)H_a), 1.28 (dq, *J* = 14.5, 7.3 Hz, 1H, C(8)H_a), 0.94 (t, *J* = 7.5 Hz, 3H, C(7)H_3), 0.67 (t, *J* = 7.4 Hz, 3H, C(9)H_3).

^{13}C NMR (151 MHz, $CDCl_3$) δ 168.6, 156.6, 146.2, 103.2, 67.4, 59.1, 54.7, 43.7, 38.5, 28.4, 25.4, 8.1, 7.5.

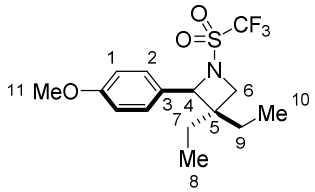
^{19}F NMR (565 MHz, $CDCl_3$) δ 30.27(s).

HRMS (ESI) *m/z* $C_{13}H_{21}FN_3O_4S^+$ requires 334.1231 ($[M+H]^+$), found 334.1228.

IR (thin film, ν_{max} /cm^{-1}) 2969, 2240, 1665, 1540, 1422, 1348, 1213, 1004, 913, 735.

m.p. 112 – 114 °C.

1,1,1-trifluoro-N-(4-methoxybenzylidene)methanesulfonamide (2x)



1,1,1-trifluoro-N-(4-methoxybenzylidene)methanesulfonamide (**1x**) (53.4 mg,, 0.20 mmol, 1.0 equiv.), ITX (5.1 mg, 0.020 mmol, 10 mol%) were added to an oven-dried tapered microwave vial equipped with a stirrer bar and a septum. The vial was evacuated and backfilled with N_2 3 times, followed by addition of anhydrous $(CH_2Cl)_2$ (1.0, 0.20 M) and 3-methylenepentane (240 µl, 2.0 mmol, 10 equiv.). The reaction was then stirred under purple light irradiation (390 nm) at ambient temperature for 16 h. The reaction mixture was diluted with CH_2Cl_2, and the solvent removed under reduced pressure. ^{19}F NMR analysis of the crude reaction mixture a total yield of 56%.

In this system the photocatalyst and product are inseparable, in order to get an analytical sample, the reaction was run with the following procedure:

1,1,1-trifluoro-N-(4-methoxybenzylidene)methanesulfonamide (**1x**) (53.4 mg, 0.20 mmol, 1.0 equiv.) and $[Ir(dFCF_3ppy)_2dtbbpy]PF_6$ (2.2 mg, 0.002 mmol, 1 mol%) were added to an oven-dried tapered microwave vial equipped with a stirrer bar and a septum. The vial was evacuated and backfilled with N_2 3 times, followed by addition of anhydrous $(CH_2Cl)_2$ (1.0 ml, 0.20 M) and 3-methylenepentane (240 µl, 2.0 mmol, 10 equiv.). The reaction was then stirred under blue light irradiation (427 nm) at ambient temperature for 16 h. The reaction mixture was diluted with CH_2Cl_2, and the solvent removed under reduced pressure. Purification by flash column chromatography (0 – 2% Et_2O in pentane) afforded (*R**)-3,3-diethyl-2-(4-methoxyphenyl)-1-((trifluoromethyl)sulfonyl)azetidine (**2x**) as a colourless oil (47.1 mg, 66%).

R_f(3% Et_2O in pentane) = 0.45.

^{1}H NMR (400 MHz, $CDCl_3$) δ 7.26 (d, *J* = 8.5 Hz, 2H, C(2)*H*), 6.94 – 6.86 (m, 2H, C(1)*H*), 5.25 (s, 1H, C(4)*H*), 3.93 (d, *J* = 7.9 Hz, 1H, C(6)H_a), 3.81 (s, 3H, C(11)H_3), 3.74 (d, *J* = 7.9 Hz, 1H, C(6)H_b), 1.87 – 1.71 (m, 2H, C(7)H_2), 1.33 (dq, *J* = 14.9, 7.3 Hz, 1H, C(9)H_a), 1.12 (dq, *J* = 14.6, 7.4 Hz, 1H, C(9)H_b), 0.93 (t, *J* = 7.4 Hz, 3H, C(8)H_3), 0.56 (t, *J* = 7.4 Hz, 3H, C(10)H_3).

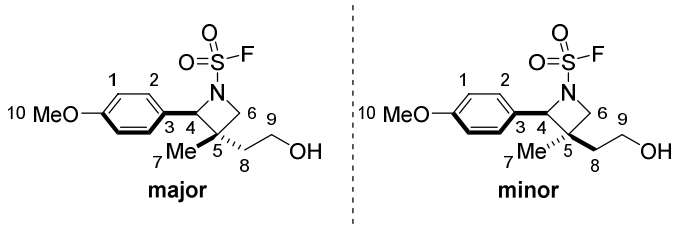
^{13}C NMR (101 MHz, $CDCl_3$) δ 159.7, 128.4, 127.8, 120.0 (q, J = 322.3 Hz), 113.8, 75.5, 60.3, 55.4, 43.6, 29.2, 24.2, 8.0, 7.3

^{19}F NMR (377 MHz, $CDCl_3$) δ -74.66(s).

HRMS (ESI) *m/z* $C_{15}H_{20}F_3NO_3SK^+$ requires 390.0748 ($[M+K]^+$), found 390.0762.

IR (thin film, ν_{max} /cm^{-1}) 2971, 1614, 1515, 1462, 1305, 1254, 1227, 1206, 1035, 837, 630.

(2*R,3*S**)-3-(2-Hydroxyethyl)-2-(4-methoxyphenyl)-3-methylazetidine-1-sulfonyl fluoride (4a) and (2*R**,3*R**)-3-(2-Hydroxyethyl)-2-(4-methoxyphenyl)-3-methylazetidine-1-sulfonyl fluoride (4a')**



Prepared according to **GP1** using (4-methoxybenzylidene)sulfamoyl fluoride (**1a)** (43.4 mg, 0.20 mmol, 1.0 equiv.), ITX (5.1 mg, 0.020 mmol, 0.10 equiv.) and 3-methylbut-3-en-1-ol (203 µl, 2.0 mmol, 10 equiv.). ^{19}F NMR analysis of the crude reaction mixture revealed a diastereomer ratio of 1.2:1. Purification by flash column chromatography (0 –

50% ethyl acetate in pentane) afforded (2*R**,3*S**)-3-(2-Hydroxyethyl)-2-(4-methoxyphenyl)-3-methylazetidine-1-sulfonyl fluoride (**4a**) and (2*R**,3*R**)-3-(2-Hydroxyethyl)-2-(4-methoxyphenyl)-3-methylazetidine-1-sulfonyl fluoride (**4a'**) as an inseparable mixture of diastereomers as a colourless oil (52.7 mg, 87%).

major

R_f (50% ethyl acetate in pentane) = 0.46.

^{1}H NMR (600 MHz, $CDCl_3$) δ 7.30 – 7.25 (m, 2H, C(2)*H*), 6.93 – 6.88 (m, 2H, C(1)*H*), 5.27 (s, 1H, C(4)*H*), 4.14 (d, *J* = 7.8 Hz, 1H, C(6)H_a), 3.80 (s, 3H, C(10)H_3), 3.83 – 3.77 (m, 1H, C(9)H_a), 3.78 – 3.70 (m, 1H, C(9)H_b), 3.68 (d, *J* = 8.0, 1H, C(6)H_a), 2.00 (ddd, *J* = 13.9, 7.8, 6.1 Hz, 1H, C(8)H_a), 1.89 (dt, *J* = 14.1, 5.6 Hz, 1H, C(8)H_b), 0.90 (s, 3H, C(9)H_3).

^{13}C NMR (151 MHz, $CDCl_3$) δ 159.7, 127.8, 127.3, 114.0, 75.8, 62.2, 59.0, 55.4, 42.3, 39.1, 20.0.

^{19}F NMR (377 MHz, $CDCl_3$) 29.98 (s).

HRMS (ESI) *m/z* $C_{13}H_{18}FNO_4SNa$ requires 326.0833 ($[M+Na]^+$), found 326.0838.

IR (thin film, ν_{max} /cm^{-1}) 3380, 2920, 1515, 1419, 1252, 1211, 1031, 840, 756.

minor

R_f (50% ethyl acetate in pentane) = 0.46.

^{1}H NMR (600 MHz, $CDCl_3$) δ 7.30 – 7.25 (m, 2H, C(2)*H*), 6.93 – 6.88 (m, 2H, C(1)*H*), 5.13 (s, 1H, C(4)*H*), 3.98 (dd, *J* = 8.0, 1.5 Hz, 1H, C(6)H_a), 3.93 (d, *J* = 8.4 Hz, 1H,

C(6)H_b), 3.80 (s, 3H, C(10)H_3), 3.54 – 3.45 (m, 2H, C(9)H_2), 1.71 (app. dt, J = 14.6, 7.5 Hz, 1H, C(8)H_a), 1.41 (s, 3H, C(9)H_3), 1.17 – 1.10 (m, 1H, C(8)H_b).

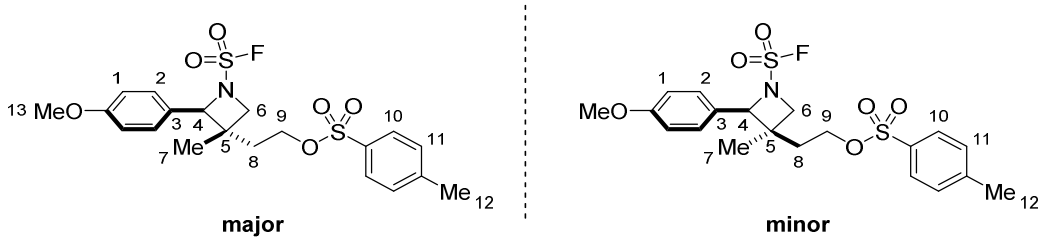
^{13}C NMR (151 MHz, $CDCl_3$) δ 159.9, 127.7, 126.9, 114.1, 77.6, 61.7, 58.9, 55.4, 39.0, 37.4, 24.6.

^{19}F NMR (377 MHz, $CDCl_3$) 30.33 (s).

HRMS (ESI) *m/z* $C_{13}H_{18}FNO_4SNa$ requires 326.0833 ($[M+Na]^+$), found 326.0838.

IR (thin film, ν_{max} /cm^{-1}) 3380, 2920, 1515, 1419, 1252, 1211, 1031, 840, 756.

2-((2*R,3*S**)-1-(Fluorosulfonyl)-2-(4-methoxyphenyl)-3-methylazetidin-3-yl)ethyl 4-methylbenzenesulfonate (4b) and 2-((2*R**,3*R**)-1-(Fluorosulfonyl)-2-(4-methoxyphenyl)-3-methylazetidin-3-yl)ethyl 4-methylbenzenesulfonate (4b')**



Prepared according to **GP1** using (4-methoxybenzylidene)sulfamoyl fluoride (**1a**) (43.4 mg, 0.20 mmol, 1.0 equiv.), 3-F-TX (4.6 mg, 0.020 mmol, 0.10 equiv.) and 3-methylbut-3-en-1-yl 4-methylbenzenesulfonate (**13**) (481 mg, 2.0 mmol, 10 equiv.) in $(CH_2Cl)_2$ (1.0 ml, 0.20 M). ^{19}F NMR analysis of the crude reaction mixture revealed a diastereomer ratio of 1.1:1. Purification by flash column chromatography (0 – 40% Et_2O in pentane) afforded a 3:1 mixture of both 2-((2*R**,3*S**)-1-(fluorosulfonyl)-2-(4-methoxyphenyl)-3-methylazetidin-3-yl)ethyl 4-methylbenzenesulfonate (**4b**) and 2-((2*R**,3*R**)-1-(fluorosulfonyl)-2-(4-methoxyphenyl)-3-methylazetidin-3-yl)ethyl 4-methylbenzenesulfonate (**4b'**) as a yellow oil (52.6 mg, 57%) and 2-((2*R**,3*R**)-1-

(fluorosulfonyl)-2-(4-methoxyphenyl)-3-methylazetidin-3-yl)ethyl 4-methylbenzenesulfonate (**4b'**) as a yellow oil (28.5 mg, 31%).

major

R_f (40% Et_2O in pentane) = 0.16.

^{1}H NMR (700 MHz, $CDCl_3$) δ 7.78 – 7.75 (m, 2H, C(10)*H*), 7.36 (d, *J* = 8.1 Hz, 2H, C(11)*H*), 7.22 (d, *J* = 8.5 Hz, 2H, C(2)*H*), 6.91 – 6.88 (m, 2H, C(1)*H*), 5.10 (s, 1H, C(4)*H*), 4.11 – 4.08 (m, 2H, C(9)H_2), 3.99 (d, *J* = 8.1 Hz, 1H, C(6)H_a), 3.80 (s, 3H, C(13)H_3), 3.63 (d, *J* = 8.1 Hz, 1H, C(6)H_b), 2.45 (s, 3H, C(12)H_3), 2.13 (dt, *J* = 14.4, 7.1 Hz, 1H, C(8)H_a), 1.95 (dt, *J* = 14.6, 5.2 Hz, 1H, C(8)H_b), 0.81 (s, 3H).

^{13}C NMR (176 MHz, $CDCl_3$) δ 159.9, 145.5, 132.6, 130.2, 128.0, 127.9, 126.4, 114.1, 75.7, 66.3, 61.7, 55.4, 38.9, 38.7, 21.8, 19.2.

^{19}F NMR (377 MHz, CDCl3) δ 30.25(s).

HRMS (ESI) *m/z*; $C_{20}H_{25}FNO_6S_2$ requires 458.1102 ($[M+H]^+$), found 458.1097.

IR (thin film, ν_{max} /cm^{-1}) 1516, 1423, 1364, 1254, 1178, 1097, 1036, 974, 919, 818, 762, 740, 666.

minor

R_f (40% Et_2O in pentane) = 0.22.

^{1}H NMR (700 MHz, $CDCl_3$) δ 7.72 – 7.68 (m, 2H, C(10)*H*), 7.34 (d, *J* = 8.0 Hz, 2H, C(11)*H*), 7.19 – 7.14 (m, 2H, C(2)*H*), 6.89 – 6.84 (m, 2H, C(1)*H*), 5.10 (s, 1H, C(4)*H*), 3.90 (d, *J* = 8.3 Hz, 1H, C(6)H_a), 3.88 – 3.84 (m, 2H, C(8)H_a, C(6)H_b), 3.82 – 3.78 (m,

4H, C(9)H_b C(13)H_3), 2.46 (s, 3H, C(12)H_3), 1.81 (ddd, J = 15.0, 8.5, 6.6 Hz, 1H, C(8)H_a), 1.35 (s, 3H, C(7)H_3), 1.22 (dt, J = 14.9, 5.4 Hz, 1H, C(8)H_b).

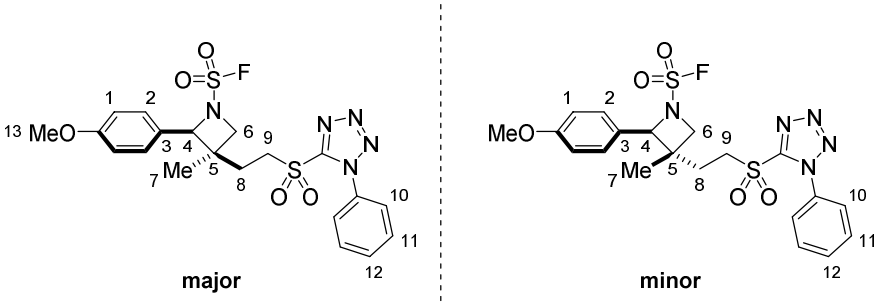
^{13}C NMR (176 MHz, $CDCl_3$) δ 160.0, 145.3, 132.7, 130.1, 127.9, 127.5, 126.3, 114.3, 77.2, 66.4, 61.2, 55.4, 38.7, 34.1, 24.2, 21.8.

^{19}F NMR (377 MHz, $CDCl_3$) δ 30.55(s).

HRMS (ESI) *m/z*; $C_{20}H_{25}FNO_6S_2$ requires 458.1102 ($[M+H]^+$), found 458.1097.

IR (thin film, ν_{max} /cm^{-1}) 1516, 1423, 1362, 1254, 1215, 1178, 1035, 969, 817, 743.

(2*R,3*R**)-2-(4-Methoxyphenyl)-3-methyl-3-(2-((1-phenyl-1H-tetrazol-5-yl)sulfonyl)ethyl)azetidine-1-sulfonyl fluoride (4c) and (2*R**,3*S**)-2-(4-methoxyphenyl)-3-methyl-3-(2-((1-phenyl-1H-tetrazol-5-yl)sulfonyl)ethyl)azetidine-1-sulfonyl fluoride (4c')**



Prepared according to **GP1** using (4-methoxybenzylidene)sulfamoyl fluoride (**1a**) (43.4 mg, 0.20 mmol, 1.0 equiv.), 3-F-TX (4.6 mg, 0.020 mmol, 0.10 equiv.) and 5-((3-methylbut-3-en-1-yl)sulfonyl)-1-phenyl-1H-tetrazole (**15**) (167 mg, 0.60 mmol, 3.0 equiv.) in $(CH_2Cl)_2$ (1.0 ml, 0.20 M). ^{19}F NMR analysis of the crude reaction mixture revealed a diastereomer ratio of 1.1:1. Purification by flash column chromatography (0 – 20% EtOAc in pentane) afforded (2*R**,3*R**)-2-(4-methoxyphenyl)-3-methyl-3-(2-((1-phenyl-1H-tetrazol-5-yl)sulfonyl)ethyl)azetidine-1-sulfonyl fluoride (**4c**) as a colourless oil (32.6 mg, 32%) and (2*R**,3*S**)-2-(4-methoxyphenyl)-3-methyl-3-(2-((1-phenyl-1H-

tetrazol-5-yl)sulfonyl)ethyl)azetidine-1-sulfonyl fluoride (**4c'**) as a white solid (39.6 mg, 30%).

Note: 107 mg (0.38 mmol) of 5-((3-methylbut-3-en-1-yl)sulfonyl)-1-phenyl-1H-tetrazole was recovered after the reaction.

major

R_f (20% EtOAc in pentane) = 0.10.

^{1}H NMR (400 MHz, $CDCl_3$) δ 7.65 – 7.55 (m, 5H, C(10)*H*, C(11)*H*, C(12)*H*), 7.29 – 7.25 (m, 2H), 6.94 – 6.90 (m, 2H), 5.16 (s, 1H, C(4)*H*), 3.98 (dd, *J* = 8.2, 1.8 Hz, 1H, C(6)H_a), 3.84 (d, *J* = 8.2 Hz, 1H, C(6)H_b), 3.80 (s, 3H, C(13)H_3), 3.42 (ddd, *J* = 14.4, 11.9, 4.2 Hz, 1H, C(9)H_a), 3.04 (ddd, *J* = 14.4, 11.9, 5.0 Hz, 1H, C(9)H_b), 2.06 (ddd, *J* = 14.0, 11.9, 4.2 Hz, 1H, C(8)H_a), 1.93 (ddd, *J* = 14.0, 11.9, 5.0 Hz, 1H, C(8)H_b), 1.48 (s, 3H, C(7)H_3).

^{13}C NMR (101 MHz, $CDCl_3$) δ 160.4, 153.2, 132.9, 131.7, 129.9, 127.6, 125.7, 125.1, 114.7, 76.0, 60.7, 55.5, 51.6, 39.4, 27.9, 24.1.

^{19}F NMR (377 MHz, $CDCl_3$) δ 30.55(s).

HRMS (ESI) *m/z*; $C_{20}H_{23}FN_5O_5S_2$ requires 496.1119 ($[M+H]^+$), found 496.1116.

IR (thin film, ν_{max} /cm^{-1}) 1420, 1311, 1243,1212, 1159, 1082, 752, 689.

minor

R_f (20% EtOAc in pentane) = 0.17.

^{1}H NMR (400 MHz, $CDCl_3$) δ 7.73 – 7.57 (m, 5H, C(10)*H*, C(11)*H*, C(12)*H*), 7.31 – 7.27 (m, 2H, C(2)*H*), 6.97 – 6.92 (m, 2H, C(1)*H*), 5.25 (s, 1H, C(4)*H*), 4.06 (dd, *J* = 8.0, 1.9 Hz, 1H, C(6)H_a), 3.82 (s, 3H, C(13)H_3), 3.81 – 3.70 (m, 1H, C(9)H_a), 3.72 (d, *J* = 7.9 Hz, 1H, C(6)H_b), 3.66 (ddd, *J* = 14.5, 10.9, 5.7 Hz, 1H, C(9)H_b), 2.45 – 2.30 (m, 2H, C(8)H_2), 0.98 (s, 3H, C(7)H_3).

^{13}C NMR (126 MHz, $CDCl_3$) δ 160.2, 153.2, 133.0, 131.8, 130.0, 127.9, 126.2, 125.0, 114.4, 75.2, 60.7, 55.5, 51.7, 39.3, 32.8, 19.7.

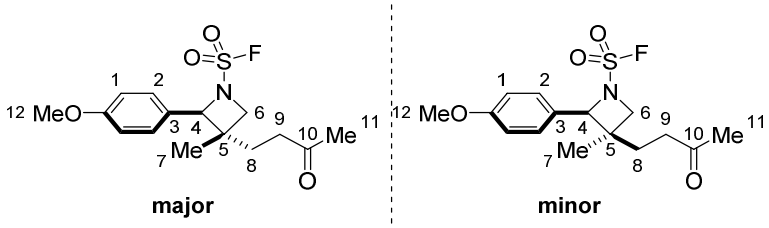
^{19}F NMR (377 MHz, $CDCl_3$) δ 31.09 (s).

HRMS (ESI) *m/z*; $C_{20}H_{23}FN_5O_5S_2$ requires 496.1119 ($[M+H]^+$), found 496.1118.

IR (thin film, ν_{max} /cm^{-1}) 1516; 1421, 1343, 1253, 1189, 1016, 689, 650.

m.p. 126 – 130 °C.

(2*R,3*S**)-2-(4-Methoxyphenyl)-3-methyl-3-(3-oxobutyl)azetidine-1-sulfonyl fluoride (4d) and (2*R**,3*R**)-2-(4-methoxyphenyl)-3-methyl-3-(3-oxobutyl)azetidine-1-sulfonyl fluoride (4d')**



Prepared according to **GP1** using (4-methoxybenzylidene)sulfamoyl fluoride (**1a**) (43.4 mg, 0.20 mmol, 1.0 equiv.), 3-F-TX (4.6 mg, 0.020 mmol, 0.10 equiv.) and 5-methylhex-5-en-2-one (258 µl, 2.0 mmol, 10 equiv.) in $(CH_2Cl)_2$ (1.0 ml, 0.20 M). ^{19}F NMR analysis of the crude reaction mixture revealed a diastereomer ratio of 1.1:1. Purification by flash column chromatography (0 – 40% Et_2O in pentane) afforded (2*R**,3*S**)-2-(4-

methoxyphenyl)-3-methyl-3-(3-oxobutyl)azetidine-1-sulfonyl fluoride (**4d**) as a colourless oil (25.4 mg, 39%) and a 10:1 mixture of ((2*R**,3*R**)-2-(4-methoxyphenyl)-3-methyl-3-(3-oxobutyl)azetidine-1-sulfonyl fluoride (**4d'**) (2*R**,3*S**)-2-(4-methoxyphenyl)-3-methyl-3-(3-oxobutyl)azetidine-1-sulfonyl fluoride (**4d**) as a colourless oil (30.1 mg, 46%).

major

R_f (50% Et_2O in pentane) = 0.41.

^{1}H NMR (700 MHz, $CDCl_3$) δ 7.25 – 7.22 (m, 2H, C(2)*H*), 6.94 – 6.89 (m, 2H, C(1)*H*), 5.12 (s, 1H, C(4)*H*), 3.97 (dd, *J* = 7.7, 1.6 Hz, 1H, C(6)H_a), 3.81 (s, 3H, C(12)H_3), 3.63 (d, *J* = 7.8 Hz, 1H, C(6)H_b), 2.49 (ddd, *J* = 17.7, 9.9, 5.6 Hz, 1H, C(9)H_a), 2.41 (ddd, *J* = 17.6, 9.9, 5.7 Hz, 1H, C(9)H_b), 2.19 (s, 3H, C(11)H_3), 2.00 (ddd, *J* = 14.3, 10.0, 5.7 Hz, 1H, C(8)H_a), 1.94 (ddd, *J* = 14.3, 9.9, 5.7 Hz, 1H, C(8)H_b), 0.84 (s, 3H, C(7)H_3).

^{13}C NMR (176 MHz, $CDCl_3$) δ 207.2, 159.8, 127.8, 127.0, 114.1, 75.5, 61.2, 55.4, 39.7, 38.2, 33.9, 30.2, 20.0.

^{19}F NMR (377 MHz, $CDCl_3$) δ 30.40(s).

HRMS (ESI) *m/z*; $C_{15}H_{20}FNO_4SNa$ requires 352.0989 ($[M+Na]^+$), found 352.0996.

IR (thin film, ν_{max} /cm^{-1}) 2968, 1716, 1615, 1515, 1420, 1305, 1252, 1211, 1177, 1085, 1033, 912, 817, 741, 641.

minor

R_f (50% Et_2O in pentane) = 0.29.

^{1}H NMR (700 MHz, $CDCl_3$) δ 7.26 (d, *J* = 2.7 Hz, 2H, C(2)*H*), 6.93 – 6.90 (m, 2H, C(1)*H*), 5.10 (d, *J* = 1.9 Hz, 1H, C(4)*H*), 3.88 (dd, *J* = 8.0, 1.7 Hz, 1H, C(6)H_a), 3.81 (s, 3H, C(12)H_3), 3.73 (d, *J* = 7.9 Hz, 1H, C(6)H_b), 2.09 (ddd, *J* = 17.2, 10.5, 5.2 Hz, 1H, C(9)H_a), 1.96 (s, 3H, C(11)H_3), 1.95 – 1.90 (m, 1H, C(9)H_b), 1.67 (ddd, *J* = 14.6, 10.5, 5.2 Hz, 1H, C(8)H_a), 1.46 (ddd, *J* = 15.0, 10.4, 5.1 Hz, 1H, C(8)H_b), 1.33 (s, 3H, C(7)H_3).

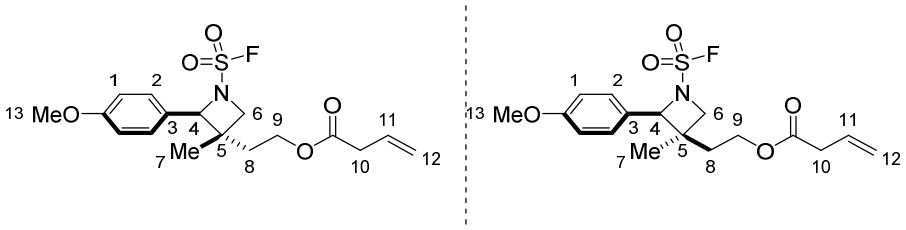
^{13}C NMR (**176 MHz, $CDCl_3$)** δ 207.4, 160.0, 127.8, 126.6, 114.2, 76.6, 61.1, 55.4, 39.6, 37.9, 30.0, 28.8, 24.5

^{19}F NMR (377 MHz, CDCl3) δ 30.17(s).

HRMS (ESI) *m/z*; $C_{15}H_{21}FNO_4S$ requires 330.1170 ($[M+H]^+$), found 330.1173.

IR (thin film, ν_{max} /cm^{-1}) 2964, 1717, 1615, 1516, 1461, 1422, 1358, 1305, 1254, 1213, 1177, 1085, 1034, 845, 816, 776, 742, 639.

2-((2*R,3*S**)-1-(Fluorosulfonyl)-2-(4-methoxyphenyl)-3-methylazetidin-3-yl)ethyl (4e) but-3-enoate and 2-((2*R**,3*R**)-1-(Fluorosulfonyl)-2-(4-methoxyphenyl)-3-methylazetidin-3-yl)ethyl but-3-enoate (4e')**



Prepared according to **GP1** using (4-methoxybenzylidene)sulfamoyl fluoride (**1a**) (43.4 mg, 0.20 mmol, 1.0 equiv.), 3-F-TX (4.6 mg, 0.020 mmol, 0.10 equiv.) and 3-methylbut-3-en-1-yl but-3-enoate (**16**) (92.5 mg, 0.60 mmol, 3.0 equiv.) in $(CH_2Cl)_2$ (1.0 ml, 0.20 M). ^{19}F NMR analysis of the crude reaction mixture revealed a diastereomer ratio of 1:1. Purification by flash column chromatography (0 – 20% EtOAc in pentane) afforded a mixture of 2-((2*R**,3*S**)-1-(fluorosulfonyl)-2-(4-methoxyphenyl)-3-methylazetidin-3-

yl)ethyl (**4e**) and but-3-enoate2-((2*R**,3*R**)-1-(fluorosulfonyl)-2-(4-methoxyphenyl)-3-methylazetidin-3-yl)ethyl but-3-enoate (**4e'**) as a colourless oil (45.9 mg, 62%).

mixture

R_f (20% Et_2O in pentane) = 0.16.

^{1}H NMR (400 MHz, $CDCl_3$) δ 7.27 – 7.21 (m, 4H, C(2)*H*), 6.94 – 6.89 (m, 4H, C(1)*H*), 5.95 – 5.77 (m, 2H, C(11)*H*), 5.22 – 5.10 (m, 6H, C(12)H_2, C(4)*H*), 4.23 (ddd, *J* = 11.6, 6.6, 5.0 Hz, 1H, C(9)H_a), 4.13 (ddd, *J* = 11.5, 8.6, 5.9 Hz, 1H, C(9)H_b), 4.07 (dd, *J* = 7.9, 1.9 Hz, 1H, C(6)H_a), 3.96 – 3.89 (m, 4H, C(9)H_2, C(6)H_2), 3.81 (s, 3H, C(13)H_3), 3.80 (s, 3H, C(13)H_3), 3.66 (dd, *J* = 7.8, 1.3 Hz, 1H, C(6)H_b), 3.10 (dt, *J* = 7.0, 1.4 Hz, 2H, C(10)H_2), 3.02 (dt, *J* = 7.0, 1.4 Hz, 2H, C(10)H_2), 2.14 (ddd, *J* = 14.9, 8.6, 6.6 Hz, 1H, C(8)H_a), 1.95 (dt, *J* = 14.3, 5.5 Hz, 1H, C(8)H_b), 1.83 – 1.74 (m, 1H, C(8)H_a), 1.41 (s, 3H, C(7)H_3), 1.20 (dt, *J* = 14.5, 5.8 Hz, 1H, C(8)H_b), 0.90 (s, 3H, C(7)H_3).

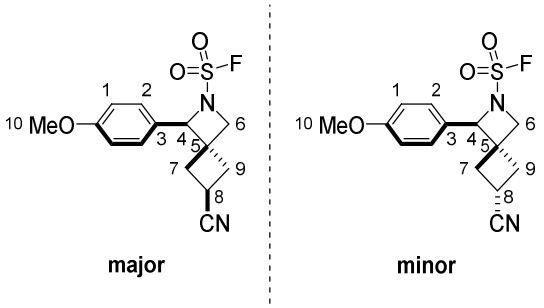
^{13}C NMR (101 MHz, $CDCl_3$) δ 171.3, 171.3, 159.9, 159.8, 129.9, 129.8, 127.7, 127.6, 126.7, 126.5, 119.2, 119.0, 114.2, 114.1, 77.4, 75.7, 61.8, 61.2, 60.8, 55.4, 39.2, 39.1, 39.0, 38.9, 38.7, 33.7, 24.4, 19.7.

^{19}F NMR (377 MHz, $CDCl_3$) δ 30.44(s), 30.08(s).

HRMS (ESI) *m/z*; $C_{17}H_{22}FNO_5SNa$ requires 394.1095 ($[M+Na]^+$), found 394.1091.

IR (thin film, ν_{max} /cm^{-1}) 1738, 1615, 1516, 1253, 1214, 1088, 1034, 993, 842, 740, 640.

(1*R,4*r**,6*R**)-6-Cyano-1-(4-methoxyphenyl)-2-azaspiro[3.3]heptane-2-sulfonyl fluoride (4f) and (1*R**,4*s**,6*S**)-6-Cyano-1-(4-methoxyphenyl)-2-azaspiro[3.3]heptane-2-sulfonyl fluoride (4f')**



Prepared according to **GP1** using (4-methoxybenzylidene)sulfamoyl fluoride (**1a**) (43.4 mg, 0.20 mmol, 1.0 equiv.), 3-F-TX (4.6 mg, 0.020 mmol, 0.10 equiv.) and 3-methylenecyclobutane-1-carbonitrile (207 µl, 2.0 mmol, 10 equiv.) in $(CH_2Cl)_2$ (1.0 ml, 0.20 M). ^{19}F NMR analysis of the crude reaction mixture revealed a diastereomer ratio of 1.1:1. Purification by flash column chromatography (0 – 50% Et_2O in pentane) afforded (1*R**,4*r**,6*R**)-6-Cyano-1-(4-methoxyphenyl)-2-azaspiro[3.3]heptane-2-sulfonyl fluoride (**4f**) as a yellow oil (22.5 mg, 37 %) and (1*R**,4*s**,6*S**)-6-Cyano-1-(4-methoxyphenyl)-2-azaspiro[3.3]heptane-2-sulfonyl fluoride (**4f'**) as a yellow oil (19.5 mg, 32%).

major

R_f (40% Et_2O in pentane) = 0.26.

^{1}H NMR (600 MHz, $CDCl_3$) δ 7.28 – 7.24 (m, 2H, C(2)*H*), 6.99 – 6.95 (m, 2H, C(1)*H*), 5.23 (s, 1H, C(4)*H*), 4.26 (d, *J* = 8.8 Hz, 1H, C(6)H_a), 4.09 (d, *J* = 8.8 Hz, 1H, C(6)H_b), 3.83 (s, 3H, C(10)H_3), 2.68 – 2.59 (m, 3H, C(8)*H*, C(9)H_2), 2.33 – 2.28 (m, 1H, C(7)H_a), 2.27 – 2.21 (m, 1H, C(7)H_b).

^{13}C NMR (101 MHz, $CDCl_3$) 160.6, 127.9, 126.3, 121.2, 114.7, 76.1, 61.1, 55.5, 42.2, 36.2, 33.0, 17.2.

^{19}F NMR (377 MHz, $CDCl_3$) δ 30.53(s).

HRMS (ESI) *m/z* $C_{14}H_{16}FN_2O_3S^+$ requires 311.0860 ($[M+H]^+$), found 311.0870.

IR (thin film, ν_{max} /cm^{-1}) 2927, 2241, 1615, 1517, 1307, 1255, 1213, 1178, 1034, 833, 768, 637.

minor

R_f (40% Et_2O in pentane) = 0.15.

^{1}H NMR (600 MHz, $CDCl_3$) δ 7.28 – 7.23 (m, 2H, C(2)*H*), 7.01 – 6.95 (m, 2H, C(1)*H*), 5.18 (s, 1H, C(4)*H*), 4.25 (d, *J* = 8.4 Hz, 1H, C(6)H_a), 4.11 (d, *J* = 8.4 Hz, 1H, C(6)H_b), 3.84 (s, 3H, C(10)H_3), 2.99 (p, *J* = 8.8 Hz, 1H, C(8)*H*), 2.65 (ddd, *J* = 12.7, 8.7, 4.0 Hz, 1H, C(9)H_a), 2.55 (dd, *J* = 12.7, 8.9 Hz, 1H, C(9)H_b), 2.31 (ddd, *J* = 12.7, 8.6, 4.1 Hz, 1H, C(7)H_a), 2.12 (dd, *J* = 12.7, 9.0 Hz, 1H, C(7)H_b).

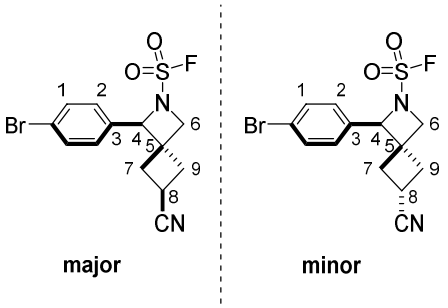
^{13}C NMR (151 MHz, $CDCl_3$) δ 160.6, 128.2, 125.9, 120.7, 114.8, 75.7, 61.9, 55.5, 42.0, 35.9, 33.6, 16.9.

^{19}F NMR (377 MHz, $CDCl_3$) δ 30.86(s).

HRMS (ESI) *m/z* $C_{14}H_{16}FN_2O_3S$ requires 311.0860 ($[M+H]^+$), found 311.0864.

IR (thin film, ν_{max} /cm^{-1}) 2942, 2847, 2240, 1614, 1517, 1422, 1308, 1255, 1212, 1178, 1032, 839, 755, 661.

(1*R,4*r**,6*R**)-6-Cyano-1-(4-bromophenyl)-2-azaspiro[3.3]heptane-2-sulfonyl fluoride (4g) and (1*R**,4*s**,6*S**)-6-Cyano-1-(4-bromophenyl)-2-azaspiro[3.3]heptane-2-sulfonyl fluoride (4g')**



Prepared according to **GP1** using (4-bromobenzylidene)sulfamoyl fluoride (**1k**) (53.2 mg, 0.20 mmol, 1.0 equiv.), 3-F-TX (4.6 mg, 0.020 mmol, 0.10 equiv.) and 3-methylenecyclobutane-1-carbonitrile (207 µl, 2.0 mmol, 10 equiv.) in $(CH_2Cl)_2$ (1.0 ml, 0.20 M). ^{19}F NMR analysis of the crude reaction mixture revealed a diastereomer ratio of 1.1:1. Purification by flash column chromatography (40 – 50% Et_2O in pentane) afforded (1*R**,4*r**,6*R**)-6-cyano-1-(4-bromophenyl)-2-azaspiro[3.3]heptane-2-sulfonyl fluoride (**4g**) as a colourless oil (27.0 mg, 27 %) and and (1*R**,4*s**,6*S**)-6-cyano-1-(4-bromophenyl)-2-azaspiro[3.3]heptane-2-sulfonyl fluoride (**4g'**) as a colourless oil (16.5 mg, 23%).

major

R_f (40% Et_2O in pentane) = 0.20.

^{1}H NMR (600 MHz, $CDCl_3$) δ 7.62 – 7.58 (m, 2H, C(1)*H*), 7.24 – 7.21 (m, 2H, C(2)*H*), 5.25 (s, 1H, C(4)*H*), 4.31 (dd, *J* = 8.8, 1.8 Hz, 1H, C(6)H_a), 4.13 (d, *J* = 8.7 Hz, 1H, C(6)H_b), 2.71 – 2.63 (m, 3H, C(8)*H*, , C(9)H_2), 2.32 (ddd, *J* = 13.3, 4.7, 2.4 Hz, 1H, C(7)H_a), 2.18 (ddd, *J* = 12.9, 4.9, 4.1 Hz, 1H, C(7)H_b).

^{13}C NMR (151 MHz, $CDCl_3$) δ 133.3, 132.7, 128.0, 123.8, 121.0, 75.5, 61.4, 42.0, 36.2, 33.0, 17.3.

^{19}F NMR (377 MHz, $CDCl_3$) δ 30.89(s).

HRMS (ESI) *m/z* $C_{13}H_{11}{}^{79}BrFN_2O_2S$ requires 356.9714 ($[M-H]^-$), found 356.9711.

minor

R_f (40% Et_2O in pentane) = 0.12.

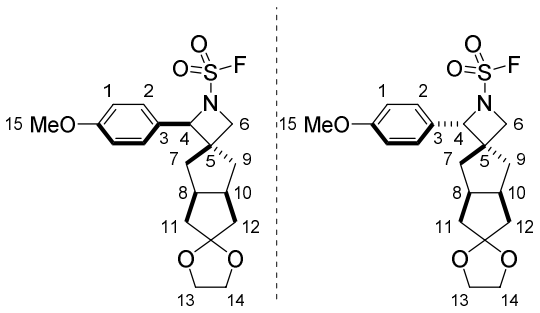
^{1}H NMR (600 MHz, $CDCl_3$) δ 7.63 – 7.60 (m, 2H, C(1)*H*), 7.25 – 7.22 (m, 2H, C(2)*H*), 5.21 (s, 1H, C(4)*H*), 4.28 (dd, *J* = 8.3, 2.0 Hz, 1H, C(6)H_a), 4.13 (d, *J* = 8.4 Hz, 1H, C(6)H_b), 3.01 (p, *J* = 8.7 Hz, 1H, , C(8)*H*), 2.69 (ddd, *J* = 12.8, 8.7, 4.1 Hz, 1H, C(9)H_a), 2.59 (dd, *J* = 12.8, 8.7 Hz, 1H, C(9)H_b), 2.31 (ddd, *J* = 13.1, 8.7, 3.8 Hz, 1H, C(7)H_a), 2.07 (dd, *J* = 12.8, 8.8 Hz, 1H, C(7)H_b).

^{13}C NMR (151 MHz, $CDCl_3$) δ 132.9, 132.7, 128.3, 123.8, 120.5, 75.1, 62.1, 41.6, 36.0, 33.6, 16.9.

^{19}F NMR (377 MHz, $CDCl_3$) δ 31.22(s).

No relevant ions were detected by ESI, APCI and EI.

(2*R,3*r**,3a'*R**,6a'*S**)-2-(4-Methoxyphenyl)tetrahydro-1'H,3'H-dispiro[azetidine-3,2'-pentalene-5',2''-[1,3]dioxolane]-1-sulfonyl fluoride (4h) and (2*S**,3*r**,3a'*R**,6a'*S**)-2-(4-Methoxyphenyl)tetrahydro-1'H,3'H-dispiro[azetidine-3,2'-pentalene-5',2''-[1,3]dioxolane]-1-sulfonyl fluoride (4h')**



Prepared according to **GP1** using (4-methoxybenzylidene)sulfamoyl fluoride (**1a**) (43.4 mg, 0.20 mmol, 1.0 equiv.), 3-F-TX (4.6 mg, 0.020 mmol, 0.10 equiv.) and 5-

methylenehexahydro-1H-spiro[pentalene-2,2'-[1,3]dioxolane] (**18**) (361 mg, 2.0 mmol, 10 equiv.) in $(CH_2Cl)_2$ (1.0 ml, 0.20 M). ^{19}F NMR analysis of the crude reaction mixture revealed a diastereomer ratio of 1.1:1. Purification by flash column chromatography (10 – 30% Et_2O in pentane) afforded an inseparable mixture of (2*R**,*3r**,3a'*R**,6a'*S**)-2-(4-methoxyphenyl)tetrahydro-1'H,3'H-dispiro[azetidine-3,2'-pentalene-5',2''-[1,3]dioxolane]-1-sulfonyl fluoride (**4h**) and (2*S**,*3r**,3a'*R**,6a'*S**)-2-(4-methoxyphenyl)tetrahydro-1'H,3'H-dispiro[azetidine-3,2'-pentalene-5',2''-[1,3]dioxolane]-1-sulfonyl fluoride (**4h'**) as a white solid (70.1 mg, 88%).

mixture

R_f (30% Et_2O in pentane) = 0.09.

^{1}H NMR (600 MHz, $CDCl_3$) δ 7.33 – 7.27 (m, 2H, C(1)*H*), 7.29 – 7.26 (m, 2H, C(1)*H*), 6.97 – 6.89 (m, 4H, C(2)*H*), 5.33 (s, 1H, C(4)*H*), 5.14 (d, *J* = 1.7 Hz, 1H, C(4)*H*), 4.19 (dd, *J* = 8.1, 1.7 Hz, 1H, C(6)H_a), 4.00 (d, *J* = 8.0 Hz, 1H, C(6)H_a), 3.94 (d, *J* = 7.8 Hz, 1H, C(6)H_b), 3.91 – 3.87 (m, 1H, C(14)H_a or C(13)H_a), 3.87 – 3.80 (m, 10H, C(6)H_b , C(15)H_3, C(14)H_2 and/or C(13)H_2, 2.57 – 2.43 (m, 3H, C(8)*H* and C(10)*H*), 2.22 (dtd, *J* = 12.8, 7.9, 1.9 Hz, 2H, C(9)H_a and C(9)H_a), 2.00 – 1.77 (m, 8H, C(8)*H* or C(10)*H*, C(9)H_b), 1.70 (dd, *J* = 12.8, 8.9 Hz, 1H, C(9)H_b), 1.58 (ddd, *J* = 13.5, 4.8, 1.6 Hz, 1H), 1.54 (ddd, *J* = 13.4, 5.1, 1.5 Hz, 1H), 1.42 (ddt, *J* = 12.4, 4.9, 2.8 Hz, 3H), 1.01 – 0.94 (m, 1H).

Note: ^{1}H NMR too complex to assign fully. A partial assignment has been given.

^{13}C NMR (151 MHz, $CDCl_3$) δ 159.9, 159.8, 128.0, 127.8, 127.7, 127.6, 119.1, 118.8, 114.1, 114.1, 77.1, 73.3, 64.6, 64.6, 64.1, 64.1, 63.4, 58.8, 55.4, 49.9, 49.7, 45.3, 44.1, 41.5, 41.1, 41.1, 41.0, 40.2, 39.5, 39.0, 38.7, 38.0, 37.7.

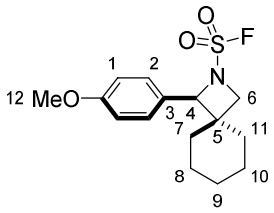
^{19}F NMR (565 MHz, $CDCl_3$) δ 30.17 (s), 30.07 (s).

HRMS (ESI) *m/z* $C_{19}H_{25}FNO_5S^+$ requires 398.1432 ($[M+H]^+$), found 398.1432.

IR (thin film, ν_{max} /cm^{-1}) 1614, 1516, 1318, 1305, 1252, 1211, 1176, 1120, 1032, 836, 741.

(*R)-1-(4-Methoxyphenyl)-2-azaspiro[3.5]nonane-2-sulfonyl fluoride (4i)**

Reaction performed by NAP, data collected by BW.



Prepared according to **GP1** using (4-methoxybenzylidene)sulfamoyl fluoride (**1a)** (43.4 mg, 0.20 mmol, 1.0 equiv.), ITX (5.1 mg, 0.020 mmol, 0.10 equiv.) and methylene cyclohexene (240 µl, 2.0 mmol, 10 equiv.) in $(CH_2Cl)_2$ (1.0 ml, 0.20 M). Purification by flash column chromatography (0 – 10% Et_2O in pentane) afforded (*R**)-1-(4-methoxyphenyl)-2-azaspiro[3.5]nonane-2-sulfonyl fluoride (**4i**) as a yellow oil (50.0 mg, 80%).

R_f (10% Et_2O in pentane) = 0.33.

^{1}H NMR (600 MHz, $CDCl_3$) δ 7.28 – 7.22 (m, 2H, C(2)*H*), 6.94 – 6.87 (m, 2H, C(1)*H*), 5.05 (s, 1H, C(4)*H*), 3.92 (d, J = 8.0 Hz, 1H, C(6)H_a), 3.81 (s, 3H, C(12)H_3), 3.79 (d, J = 7.9 Hz, 1H, C(6)H_b), 1.94 – 1.88 (m, 1H, C(11)H_a), 1.70 – 1.60 (m, 2H, C(10)H_a, C(11)H_b), 1.58 – 1.45 (m, 2H, C(7)H_a, C(9)H_a), 1.41 – 1.33 (m, 1H, C(8)H_a), 1.34 – 1.25 (m, 1H, C(10)H_b), 1.19 – 1.06 (m, 2H, C(7)H_b, C(8)H_b), 0.93 – 0.85 (m, 1H, C(9)H_b).

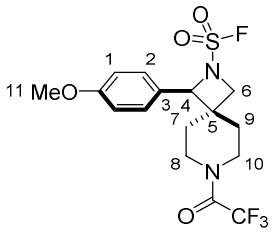
^{13}C NMR (101 MHz, $CDCl_3$) δ 159.7, 127.8, 127.0, 113.9, 76.6, 60.7, 55.4, 41.2, 37.5, 31.7, 25.2, 23.0, 22.0.

^{19}F NMR (377 MHz, $CDCl_3$) δ 30.18 (s).

HRMS (ESI) *m/z* $C_{15}H_{21}FNO_3S$ requires 314.1221 ($[M+H]^+$), found 321.1226.

IR (thin film, ν_{max} /cm^{-1}) 2933, 1615, 1515, 1450, 1420, 1212, 1176, 1033, 734.

(*R)-1-(4-Methoxyphenyl)-7-(2,2,2-trifluoroacetyl)-2,7-diazaspiro[3.5]nonane-2-sulfonyl fluoride (4j)**



Prepared according to **GP1** using (4-methoxybenzylidene)sulfamoyl fluoride (**1a**) (43.4 mg, 0.20 mmol, 1.0 equiv.), 3-F-TX (4.6 mg, 0.020 mmol, 0.10 equiv.) and 2,2,2-trifluoro-1-(4-methylenepiperidin-1-yl)ethan-1-one (**19**) (386 mg, 2.0 mmol, 10 equiv.) in $(CH_2Cl)_2$ (1.0 ml, 0.20 M). Purification by flash column chromatography (0 – 40% EtOAc in pet ether) and **Work Up A** afforded (*R**)-1-(4-methoxyphenyl)-7-(2,2,2-trifluoroacetyl)-2,7-diazaspiro[3.5]nonane-2-sulfonyl fluoride (**4j**) as a colourless oil (58.4 mg, 71%).

1.1:1 mixture of rotamers

R_f (30% Et_2O in pentane) = 0.15.

^{1}H NMR (600 MHz, $CDCl_3$) δ 7.29 – 7.24 (m, 4H, C(2)*H*), 6.95 – 6.92 (m, 4H, C(1)*H*), 5.17 (d, *J* = 1.6 Hz, 1H, C(4)*H*), 5.16 (s, 1H, C(4)*H*), 4.08 (dt, *J* = 13.7, 4.7 Hz, 1H, C(8)H_a), 4.03 (d, *J* = 8.1 Hz, 1H, C(6)H_a), 4.02 (d, *J* = 8.1 Hz, 1H, C(6)H_a), 3.90 (d, *J* =

8.2 Hz, 1H, C(6)H_b), 3.88 (d, J = 8.1 Hz, 1H, C(6)H_b), 3.82 (s, 3H, C(11)H_3), 3.81 (s, 3H, C(11)H_3), 3.80 – 3.78 (m, 1H, C(8)H_a), 3.75 (dt, J = 13.8, 4.9 Hz, 1H, C(10)H_a), 3.40 (dt, J = 14.4, 4.9 Hz, 1H, C(10)H_a), 3.30 (ddd, J = 13.9, 10.2, 3.2 Hz, 1H, C(8)H_b), 3.20 (ddd, J = 13.6, 10.0, 3.4 Hz, 1H, C(8)H_b), 3.15 (ddd, J = 13.9, 10.0, 3.2 Hz, 1H, C(10)H_b), 2.99 (ddd, J = 13.8, 10.3, 3.4 Hz, 1H, C(10)H_b), 2.07 – 1.99 (m, 2H, C(7)H_a), 1.95 – 1.88 (m, 2H, C(7)H_b), 1.64 (ddd, J = 5.2, 3.3, 1.5 Hz, 1H, C(10)H_a), 1.62 (ddd, J = 5.1, 3.2, 1.5 Hz, 1H, C(10)H_a), 1.35 – 1.24 (m, 2H, C(10)H_b).

^{13}C NMR (151 MHz, $CDCl_3$) δ 160.3, 160.3, 155.6 (q, $^2J_{C\text{-}F}$ = 35.8 Hz), 155.5 (q, $^2J_{C\text{-}F}$ = 35.8 Hz), 127.9, 127.9, 125.7, 125.6, 116.5 (q, $^1J_{C\text{-}F}$ = 288.0 Hz), 116.4 (q, $^1J_{C\text{-}F}$ = 288.0 Hz), 114.5, 75.6, 75.6, 59.7, 59.6, 55.5, 42.5 (q, $^3J_{C\text{-}F}$ = 3.6 Hz), 42.1 (q, $^3J_{C\text{-}F}$ = 3.6 Hz), 40.4, 39.9, 39.6, 39.5, 36.7, 35.8, 31.7, 30.7.

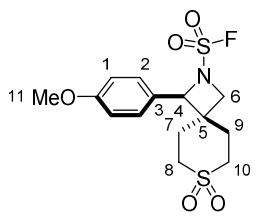
Note: 2 Carbon environments not observed due to signal overlap.

^{19}F NMR (377 MHz, $CDCl_3$) δ 31.32(s), 31.20(s), -68.96(s), -69.00(s).

HRMS (ESI) *m/z*; $C_{16}H_{18}F_4N_2O_4SNa$ requires 433.0816 ([M+Na]$^+$), found 433.0818.

IR (thin film, ν_{max} /cm^{-1}) 2932, 1694, 1614, 1516, 1467, 1304, 1255, 1214, 1129, 1034, 837, 821, 774, 738.

(*R)-1-(4-Methoxyphenyl)-7-thia-2-azaspiro[3.5]nonane-2-sulfonyl fluoride 7,7-dioxide (4k)**



Prepared according to **GP1** using (4-methoxybenzylidene)sulfamoyl fluoride (**1a**) (43.4 mg, 0.20 mmol, 1.0 equiv.), 3-F-TX (4.6 mg, 0.020 mmol, 0.10 equiv.) and 4-methylenetetrahydro-2H-thiopyran 1,1-dioxide (**21**) (292 mg, 2.0 mmol, 10 equiv.) in $(CH_2Cl)_2$ (1.0 ml, 0.20 M). Purification by flash column chromatography (0 – 40% EtOAc in pet ether) afforded (*R**)-1-(4-methoxyphenyl)-7-thia-2-azaspiro[3.5]nonane-2-sulfonyl fluoride 7,7-dioxide (**4k**) as a white solid (44.6 mg, 61%).

Note: 241 mg (1.7 mmol) of 4-methylenetetrahydro-2H-thiopyran 1,1-dioxide was recovered after the reaction.

R_f (40% EtOAc in pet ether) = 0.34.

^{1}H NMR (700 MHz, DMSO-d6) δ 7.41 – 7.35 (m, 2H, C(2)*H*), 7.03 – 6.98 (m, 2H, C(1)*H*), 5.46 (s, 1H, C(4)*H*), 4.18 (d, *J* = 8.5 Hz, 1H, C(6)H_a), 4.09 (d, *J* = 8.5 Hz, 1H, C(6)H_b), 3.77 (s, 3H, C(11)H_3), 3.24 (ddd, *J* = 15.0, 11.5, 3.5 Hz, 1H, C(8)H_a), 3.13 – 3.04 (m, 2H, C(10)H_b, C(8)H_b), 2.65 (m, 1H, C(10)H_b), 2.40 (ddd, *J* = 14.3, 5.9, 3.1 Hz, 1H, C(7)H_a), 2.22 (ddd, *J* = 14.8, 11.6, 3.5 Hz, 1H, C(7)H_b), 1.93 (ddd, *J* = 14.4, 6.0, 3.0 Hz, 1H, C(9)H_a), 1.33 (m, 1H, C(9)H_b).

^{13}C NMR (176 MHz, DMSO-d6) δ 159.5, 127.9, 126.3, 114.0, 73.6, 58.8, 55.2, 47.1, 46.3, 38.1, 33.7, 29.2.

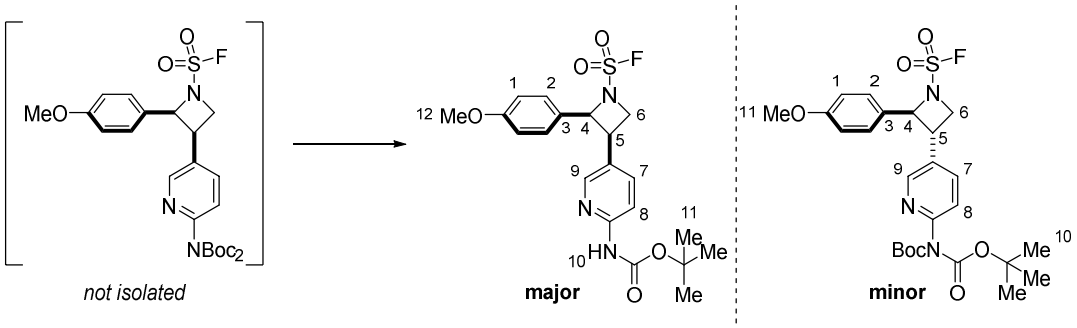
^{19}F NMR (377 MHz, DMSO-d6) δ 32.89(s).

HRMS (ESI) *m/z*; $C_{14}H_{18}FNO_5S_2Na$ requires 386.0503 ($[M+Na]^+$), found 386.0503.

IR (neat, ν_{max} /cm^{-1}) 2963, 1513, 1295, 1263, 1108, 1024, 812, 773, 753, 608.

m.p. 186 °C.

***Tert*-butyl (5-((2*S**,3*R**)-1-(fluorosulfonyl)-2-(4-methoxyphenyl)azetidin-3-yl)pyridin-2-yl)carbamate (4l') and *Tert*-butyl (*Tert*-butoxycarbonyl)(5-((2*R**,3*R**)-1-(fluorosulfonyl)-2-(4-methoxyphenyl)azetidin-3-yl)pyridin-2-yl)carbamate (4l'')**



Prepared according to **GP1** using (4-methoxybenzylidene)sulfamoyl fluoride (**1a**) (43.4 mg, 0.20 mmol, 1.0 equiv.), 3-F-TX (4.6 mg, 0.020 mmol, 0.10 equiv.) and *tert*-butyl (*tert*-butoxycarbonyl)(5-vinylpyridin-2-yl)carbamate (**23**) (640 mg, 2.00 mmol, 10 equiv.) in $(CH_2Cl)_2$ (1.0 ml, 0.20 M). ^{19}F NMR analysis of the crude reaction mixture revealed a diastereomer ratio of 1.5:1 and a total yield of both diastereomers of 52%. Purification by flash column chromatography (0 – 20% EtOAc in pentane) afforded *tert*-butyl (*tert*-butoxycarbonyl)(5-((2*R**,3*R**)-1-(fluorosulfonyl)-2-(4-methoxyphenyl)azetidin-3-yl)pyridin-2-yl)carbamate (**4l''**) as a white solid (25.3 mg, 24%). Further purification by flash column chromatography (0 – 20% Et_2O/CH_2Cl_2) yielded *tert*-butyl (5-((2*S**,3*R**)-1-(fluorosulfonyl)-2-(4-methoxyphenyl)azetidin-3-yl)pyridin-2-yl)carbamate (**4l'**) (13.3 mg, 15%) as white solid.

major (characterised as mono-Boc derivative)

^{1}H NMR (600 MHz, $CDCl_3$) δ 7.94 (s, 1H, C(9)*H*), 7.81 (s, 1H, N(10)*H*), 7.76 (s, 1H, C(7)*H*), 7.37 (d, *J* = 8.6 Hz, 1H, C(8)*H*), 7.04 – 6.99 (m, 2H, C(2)*H*), 6.74 – 6.69 (m, 2H,

C(1)*H*), 5.88 (d, *J* = 9.1 Hz, 1H, C(4)*H*), 4.72 – 4.66 (m, 1H, C(6)H_a), 4.24 (dd, *J* = 8.9, 4.7 Hz, 1H, C(6)H_b), 4.15 (td, *J* = 9.2, 4.8 Hz, 1H, C(5)*H*), 3.71 (s, 3H), 1.51 (s, 9H).

^{13}C NMR (151 MHz, $CDCl_3$) δ 159.5, 152.4, 151.5, 147.6, 138.0, 127.8, 126.2, 126.1, 114.0, 111.8, 81.3, 71.1, 55.3, 55.0, 38.1, 28.4.

^{19}F NMR (565 MHz, $CDCl_3$) δ 30.39.

HRMS (ESI) *m/z*; $C_{20}H_{25}FN_3O_5S$ requires 438.1494 ($[M+H]^+$), found 438.1499.

IR (thin film, ν_{max} /cm^{-1}) 2978, 2931, 1725, 1612, 1588, 1538, 1516, 1426, 1369, 1311, 1255, 1213, 1157, 1101, 1062, 1031, 912, 848, 809, 760, 644.

m.p. 142 °C (decomp).

minor

^{1}H NMR (600 MHz, $CDCl_3$) δ 8.34 (d, *J* = 2.5 Hz, 1H, C(9)*H*), 7.69 (dd, *J* = 8.3, 2.5 Hz, 1H, , C(7)*H*), 7.37 – 7.31 (m, 3H, C(8)*H*, C(2)*H*), 6.93 (d, *J* = 8.4 Hz, 2H, C(1)*H*), 5.27 (d, *J* = 7.8 Hz, 1H, C(4)*H*), 4.43 (t, *J* = 8.4 Hz, 1H, C(6)H_a), 4.31 (t, *J* = 8.3 Hz, 1H, C(6)H_b), 3.85 (q, *J* = 8.5 Hz, 1H, C(5)*H*), 3.81 (s, 3H, C(11)H_3), 1.47 (s, 18H, C(10)H_3).

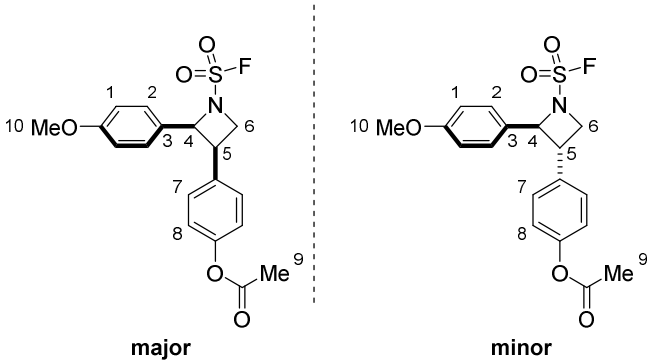
^{13}C NMR (151 MHz, $CDCl_3$) δ 160.6, 152.4, 151.5, 147.6, 136.4, 131.8, 129.1, 128.0, 121.8, 114.6, 83.7, 75.3, 55.5, 55.1, 42.1, 28.0.

^{19}F NMR (565 MHz, $CDCl_3$) δ 30.86(s).

HRMS (ESI) *m/z*; $C_{25}H_{33}FN_3O_7S$ requires 538.2018 ($[M+H]^+$), found 538.2025.

IR (thin film, ν_{max} /cm^{-1}) 2981, 1794, 1765, 1727, 1613, 1517, 1484, 1425, 1394, 1371, 1341, 1312, 1255, 1211, 1156, 1119, 1023, 913, 838, 734, 643.

4-((2*R,3*S**)-1-(Fluorosulfonyl)-2-(4-methoxyphenyl)azetidin-3-yl)phenyl acetate (4m) and 4-((2*R**,3*R**)-1-(Fluorosulfonyl)-2-(4-methoxyphenyl)azetidin-3-yl)phenyl acetate (4m')**



Prepared according to **GP1** using (4-methoxybenzylidene)sulfamoyl fluoride (**1a**) (43.4 mg, 0.20 mmol, 1.0 equiv.), ITX (5.1 mg, 0.020 mmol, 0.10 equiv.) and 4-acetoxy-styrene (295 µl, 2.0 mmol, 10 equiv.) in $(CH_2Cl)_2$ (1.0 ml, 0.20 M). ^{19}F NMR analysis of the crude reaction mixture revealed a regioisomer ratio of 17:1, a diastereomer ratio of 2.1:1 and a combined yield of 47%. Purification by flash column chromatography (10 – 18% EtOAc in pentane) afforded 4-((2*R**,3*S**)-1-(fluorosulfonyl)-2-(4-methoxyphenyl)azetidin-3-yl)phenyl acetate (**4m**) with approximately 9% minor regioisomer (30.1 mg, 40%) as a colourless oil and 4-((2*R**,3*R**)-1-(fluorosulfonyl)-2-(4-methoxyphenyl)azetidin-3-yl)phenyl acetate (**4m'**) (9.2 mg, 12%) as a colourless oil.

major

R_f (30% Et_2O in pentane) = 0.17.

^{1}H NMR (600 MHz, $CDCl_3$) δ 7.09 – 7.06 (m, 2H, C(7)*H*), 7.03 – 7.00 (m, 2H, C(1)*H*), 6.94 – 6.90 (m, 2H, C(8)*H*), 6.72 – 6.69 (m, 2H, C(2)*H*), 5.89 (app. dt, *J* = 8.9, 1.1 Hz, 1H, C(4)*H*), 4.69 (td, *J* = 9.1, 1.8 Hz, 1H, C(6)H_a), 4.33 (ddd, *J* = 9.0, 4.9, 1.1 Hz, 1H,

C(6)H_b), 4.23 (td, J = 9.2, 4.8 Hz, 1H, C(5)H), 3.72 (s, 3H, C(10)H_3), 2.26 (s, 3H, C(9)H_3).

^{13}C NMR (151 MHz, $CDCl_3$) δ 169.3, 159.4, 150.0, 133.4, 129.5, 127.9, 126.6, 121.6, 113.7, 71.3, 55.3, 55.1, 40.4, 21.2.

^{19}F NMR (377 MHz, $CDCl_3$) δ 30.27 (s).

HRMS (ESI) *m/z*; $C_{18}H_{19}FNO_5S$ requires 380.0963 ($[M+H]^+$), found 380.0959.

IR (thin film, ν_{max} /cm^{-1}) 2962, 2933, 1766, 1613, 1513, 1423, 1370, 1306, 1254, 1212, 1098, 913, 851, 807, 755, 676.

minor

R_f (30% Et_2O in pentane) = 0.30.

^{1}H NMR (600 MHz, $CDCl_3$) δ 7.39 – 7.34 (m, 2H, C(2)H), 7.29 – 7.26 (m, 2H, C(7)H), 7.12 – 7.09 (m, 2H, C(8)H), 6.94 – 6.91 (m, 2H, C(1)H), 5.29 (d, J = 7.8 Hz, 1H, C(4)H), 4.39 (t, J = 8.4 Hz, 1H, C(6)H_a), 4.31 (td, J = 8.2, 1.7 Hz, 1H, C(6)H_b), 3.85 – 3.80 (m, 4H, C(10)H_3, C(5)H), 2.31 (s, 3H, C(9)H_3).

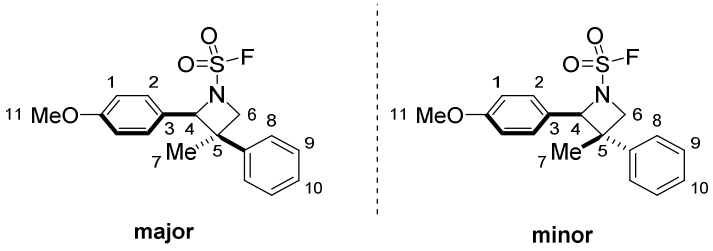
^{13}C NMR (151 MHz, $CDCl_3$) δ 169.5, 160.4, 150.5, 135.4, 129.6, 128.2, 128.1, 122.5, 114.5, 75.6, 55.6, 55.5, 44.3, 21.2.

^{19}F NMR (565 MHz, $CDCl_3$) δ 30.74 (s).

HRMS (ESI) *m/z*; $C_{18}H_{19}FNO_5S$ requires 380.0963 ($[M+H]^+$), found 380.0966.

IR (thin film, ν_{max} /cm^{-1}) 1764, 1614, 1516, 1425, 1371, 1255, 1214, 1033, 913, 838, 765, 741, 640.

(2*R,3*R**)-2-(4-Methoxyphenyl)-3-methyl-3-phenylazetidine-1-sulfonyl fluoride (4n) and (2*R**,3*S**)-2-(4-Methoxyphenyl)-3-methyl-3-phenylazetidine-1-sulfonyl fluoride (4n')**



Prepared according to **GP1** using (4-methoxybenzylidene)sulfamoyl fluoride (**1a)** (43.4 mg, 0.20 mmol, 1.0 equiv.), 3-F-TX (4.6 mg, 0.020 mmol, 0.10 equiv.) and 2-phenylpropene (260 µl, 2.00 mmol, 10 equiv.) in $(CH_2Cl)_2$ (1.0 ml, 0.20 M). ^{19}F NMR analysis of the crude reaction mixture revealed a diastereomer ratio of 2.1:1. Purification by flash column chromatography (0 – 3% Et_2O in pentane) afforded azetidine (2*R**,3*R**)-2-(4-methoxyphenyl)-3-methyl-3-phenylazetidine-1-sulfonyl fluoride (**4n**) as a white gum (23.1 mg, 34%) (and 2*R**,3*S**)-2-(4-methoxyphenyl)-3-methyl-3-phenylazetidine-1-sulfonyl fluoride (**4n'**) as a colourless oil (14.1 mg, 21%).

major

R_f (10% Et_2O in pentane) = 0.39.

^{1}H NMR (600 MHz, $CDCl_3$) δ 7.16 – 7.12 (m, 2H, C(9)*H*), 7.12 – 7.08 (m, 1H, C(10)*H*), 6.99 – 6.94 (m, 2H, C(8)*H*), 6.94 – 6.91 (m, 2H, C(2)*H*), 6.68 – 6.63 (m, 2H, C(1)*H*), 5.38 (d, *J* = 2.0 Hz, 1H, C(4)*H*), 4.69 (dd, *J* = 8.6, 1.8 Hz, 1H, C(6)H_a), 4.23 (dd, *J* = 8.5, 2.1 Hz, 1H, C(6)H_b), 3.70 (s, 3H, C(11)*H*), 1.82 (s, 3H, C(7)H_3).

^{13}C NMR (151 MHz, $CDCl_3$) δ 159.7, 139.7, 128.5, 128.2, 127.5, 126.9, 113.6, 78.8, 60.9, 55.3, 45.4, 29.3.

Note: 1 Carbon environment not observed due to signal overlap.

^{19}F NMR (377 MHz, CDCl3) δ 31.66 (s).

HRMS (ESI) *m/z*; $C_{17}H_{19}FNO_3S$ requires 336.1064 ($[M+H]^+$), found 336.1069.

IR (thin film, ν_{max} /cm^{-1}) 2918, 1614, 1586, 1516, 1424, 1306, 1254, 1215, 1178, 1034, 912, 814, 747, 702, 644.

minor

R_f (10% Et_2O in pentane) = 0.50.

^{1}H NMR (500 MHz, $CDCl_3$) δ 7.44 – 7.37 (m, 4H, C(8)*H*, C(9)*H*), 7.33 – 7.29 (m, 1H, C(10)*H*), 7.28 – 7.23 (m, 2H, C(2)*H*), 6.99 – 6.96 (m, 2H, C(1)*H*), 5.59 (s, 1H, C(4)*H*), 4.58 (dd, *J* = 7.5, 1.9 Hz, 1H, C(6)H_a), 3.97 (d, *J* = 7.5 Hz, 1H, C(6)H_b), 3.84 (s, 3H, C(11)H_3), 1.31 (s, 3H, C(7)H_3).

^{13}C NMR (126 MHz, $CDCl_3$) δ 160.1, 145.2, 129.2, 128.5, 127.4, 126.6, 125.2, 114.2, 76.4, 61.4, 55.4, 44.1, 24.3.

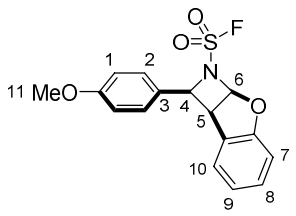
^{19}F NMR (377 MHz, CDCl3) δ 30.28 (s).

HRMS (ESI) *m/z*; $C_{17}H_{18}FNO_3S$ requires 358.0884 ($[M+Na]^+$), found 358.0901.

IR (thin film, ν_{max} /cm^{-1}) 1615, 1518, 1425, 1305, 1254, 1215, 1177, 1034, 821, 757, 737, 702, 658.

(2*S,2a*S**,7a*S**)-2-(4-Methoxyphenyl)-2a,7a-dihydrobenzofuro[2,3-*b*]azete-1(2*H*)-sulfonyl fluoride (4o)**

Reaction performed by NAP, data collected by NAP.



Prepared according to **GP1** using (4-methoxybenzylidene)sulfamoyl fluoride (**1a**) (43.4 mg, 0.20 mmol, 1.0 equiv.), 3-F-TX (4.6 mg, 0.020 mmol, 0.10 equiv.), 2,3-benzofuran (220 µl, 2.0 mmol, 10 equiv.) $(CH_2Cl)_2$ (1.0 ml, 0.20 M).^{19}F NMR analysis of the crude reaction mixture revealed a diastereomer ratio of 4.4:1. Purification by flash column chromatography (10 – 20% Et_2O in pentane) afforded (2*S**,2a*S**,7a*S**)-2-(4-methoxyphenyl)-2a,7a-dihydrobenzofuro[2,3-*b*]azete-1(2*H*)-sulfonyl fluoride (**4o**) as a white crystalline solid (40.4 mg, 60%).

^{1}H NMR (400 MHz, CDCl3) δ 7.15 (t, *J* = 7.8 Hz, 1H, C(9)*H* or C(8)*H*), 6.96 (d, *J* = 8.2 Hz, 1H, C(10)*H* or C(7)*H*), 6.84 (d, *J* = 8.3 Hz, 2H, C(2)*H*), 6.72 – 6.62 (m, 3H, C(1)*H*, C(9)*H* or C(8)*H*), 6.44 – 6.35 (m, 2H, C(6)*H*, C(10)*H* or C(7)*H*), 5.60 (d, *J* = 7.4 Hz, 1H, C(4)*H*), 4.45 (t, *J* = 6.6 Hz, 1H, C(5)*H*), 3.67 (s, 3H, C(11)H_3).

^{13}C NMR (101 MHz, CDCl3) δ 160.0, 159.9, 130.0, 128.0, 127.0, 125.7, 122.6, 122.4, 113.7, 111.4, 94.0, 69.3, 55.2, 48.1.

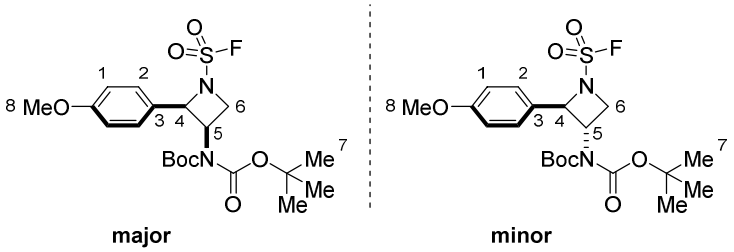
^{19}F NMR (377 MHz, CDCl3) δ 43.26(s).

HRMS (ESI) *m/z* $C_{16}H_{14}FNO_4SNa^+$ requires 358.0520 ($[M+Na]^+$), found 358.0530,

IR (thin film, ν_{max} /cm^{-1}) 2936, 1615, 1516, 1478, 1463, 1428, 1306, 1253, 1209, 1177, 1155, 1090, 1021, 948, 911, 856, 835, 796, 757, 734, 666.

m.p. 118−120 °C.

***Tert*-butyl (*tert*-butoxycarbonyl)((2*R**,3*R**)-1-(fluorosulfonyl)-2-(4-methoxyphenyl)azetidin-3-yl)carbamate (4p) and *Tert*-butyl (*tert*-butoxycarbonyl)((2*R**,3*S**)-1-(fluorosulfonyl)-2-(4-methoxyphenyl)azetidin-3-yl)carbamate (4p')**



Prepared according to **GP1** using (4-methoxybenzylidene)sulfamoyl fluoride (**1a**) (43.4 mg, 0.20 mmol, 1.0 equiv.), 3-F-TX (4.6 mg, 0.020 mmol, 0.10 equiv.), *tert*-butyl (*tert*-butoxycarbonyl)(vinyl)carbamate (**25**) (146 mg, 0.60 mmol, 3.0 equiv.) and Aldrithiol-2 (2.2 mg, 0.010 mmol, 0.050 equiv.) in $(CH_2Cl)_2$ (1.0 ml, 0.20 M). ^{19}F NMR analysis of the crude reaction mixture revealed a diastereomer ratio of 1.6:1. Purification by flash column chromatography (4 – 6% EtOAc in pentane) afforded a mixture of *tert*-butyl (*tert*-butoxycarbonyl)((2*R**,3*R**)-1-(fluorosulfonyl)-2-(4-methoxyphenyl)azetidin-3-yl)carbamate (**4p**) and *tert*-butyl (*tert*-butoxycarbonyl)((2*R**,3*S**)-1-(fluorosulfonyl)-2-(4-methoxyphenyl)azetidin-3-yl)carbamate (**4p'**) as a colourless oil (53.2 mg, 58%).

Note: compound degrades rapidly (2 – 3 days) even when stored at 0 °C.

major

^{1}H NMR (400 MHz, Acetone-d6) δ 7.40 – 7.35 (m, 2H, C(2)*H*), 6.96 – 6.92 (m, 2H, C(1)*H*), 5.76 (d, *J* = 2.2 Hz, 1H, C(4)*H*), 5.25 (ddd, *J* = 9.5, 8.4, 6.2 Hz, 1H, C(5)*H*), 4.87 (ddd, *J* = 8.9, 6.2, 2.9 Hz, 1H, C(6)H_a), 4.66 (td, *J* = 9.5, 2.3 Hz, 1H, C(6)H_b), 3.80 (s, 3H, C(8)H_3), 1.35 (s, 18H, C(7)H_3).

^{13}C NMR (151 MHz, Acetone-d6) δ 160.9, 153.0, 130.1, 126.6, 114.3, 83.5, 73.2, 55.9, 55.6, 51.4, 28.0.

^{19}F NMR (377 MHz, Acetone-d6) δ 32.82 (s).

HRMS (ESI) *m/z* $C_{20}H_{29}FN_2O_7SNa^+$ requires 483.1572 ($[M+H]^+$), found 483.1577.

IR (thin film, ν_{max} /cm^{-1}) 2983, 1818, 1740, 1704, 1614, 1517, 1480, 1461, 1425, 1396, 1371, 1354, 1307, 1276, 1255, 1213, 1179, 1126, 1035, 912, 843, 808, 777, 758, 736.

minor

^{1}H NMR (400 MHz, Acetone-d6) δ 7.50 – 7.45 (m, 2H, C(2)*H*), 7.00 – 6.96 (m, 2H, C(1)*H*), 5.78 (d, *J* = 2.4 Hz, 1H, C(4)*H*), 5.02 (q, *J* = 7.6 Hz, 1H, C(5)*H*), 4.65 – 4.60 (m, 1H, C(6)H_a), 4.37 – 4.32 (m, 1H, C(6)H_a), 3.82 (s, 3H, C(8)H_3), 1.49 (s, 18H, C(7)H_3).

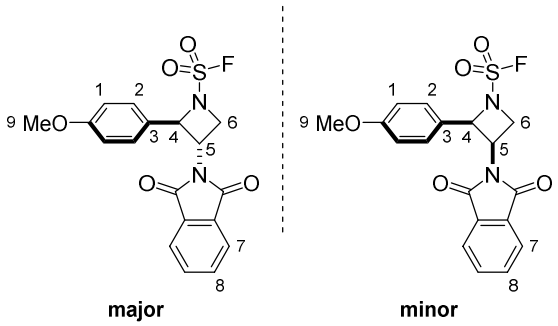
^{13}C NMR (151 MHz, Acetone-d6) δ 161.4, 153.2, 130.2, 129.6, 114.8, 84.3, 73.8, 55.9, 55.1, 54.2, 28.0.

^{19}F NMR (377 MHz, Acetone-d6) δ 33.64 (s).

HRMS (ESI) *m/z* $C_{20}H_{29}FN_2O_7SNa^+$ requires 483.1572 ($[M+H]^+$), found 483.1577.

IR (thin film, ν_{max} /cm^{-1}) 2983, 1818, 1740, 1704, 1614, 1517, 1480, 1461, 1425, 1396, 1371, 1354, 1307, 1276, 1255, 1213, 1179, 1126, 1035, 912, 843, 808, 777, 758, 736.

(2*R,3*S**)-3-(1,3-Dioxoisoindolin-2-yl)-2-(4-methoxyphenyl)azetidine-1-sulfonyl fluoride (4q) and (2*R**,3*R**)-3-(1,3-Dioxoisoindolin-2-yl)-2-(4-methoxyphenyl)azetidine-1-sulfonyl fluoride (4q')**



Prepared according to **GP1** using (4-methoxybenzylidene)sulfamoyl fluoride (**1a**) (43.4 mg, 0.20 mmol, 1.0 equiv.), 3-F-TX (4.6 mg, 0.020 mmol, 0.10 equiv.), N-vinyl phthalimide (52 mg, 0.60 mmol, 3.0 equiv.) in $(CH_2Cl)_2$ (1.0 ml, 0.20 M). ^{19}F NMR analysis of the crude reaction mixture revealed a diastereomer ratio of 2.2:1. Purification by flash column chromatography (50 – 75% CH_2Cl_2 in pentane) afforded (2*R**,3*S**)-3-(1,3-dioxoisoindolin-2-yl)-2-(4-methoxyphenyl)azetidine-1-sulfonyl fluoride (**4q**) as a white solid (20.6 mg, 26%) and a 1.4:1 mixture of (2*R**,3*R**)-3-(1,3-dioxoisoindolin-2-yl)-2-(4-methoxyphenyl)azetidine-1-sulfonyl fluoride (**4q'**) and (2*R**,3*S**)-3-(1,3-dioxoisoindolin-2-yl)-2-(4-methoxyphenyl)azetidine-1-sulfonyl fluoride (**4q**) (23.1 mg, 30%) as a yellow solid.

major

R_f (60% CH_2Cl_2 in pentane) = 0.25.

^{1}H NMR (400 MHz, CDCl3) δ 7.93 – 7.84 (m, 2H, C(7)*H*), 7.84 – 7.74 (m, 2H, C(8)*H*), 7.44 – 7.36 (m, 2H, C(2)*H*), 6.96 – 6.88 (m, 2H, C(1)*H*), 6.10 (dd, *J* = 7.4, 2.1 Hz, 1H,

C(4)*H*), 5.04 (td, *J* = 8.3, 7.4 Hz, 1H, C(5)*H*), 4.89 (td, *J* = 7.8, 2.4 Hz, 1H, C(6)H_a), 4.28 (ddd, *J* = 8.3, 6.5, 2.9 Hz, 1H, C(6)H_b), 3.81 (s, 3H, C(9)H_3).

^{13}C NMR (151 MHz, $CDCl_3$) δ 167.6, 160.7, 134.9, 131.5, 128.6, 128.1, 124.0, 114.6, 71.3, 55.5, 52.9, 47.1.

^{19}F NMR (565 MHz, $CDCl_3$) δ 32.64(s).

HRMS (ESI) *m/z*; $C_{18}H_{16}FN_2O_5S$ requires 391.0759 ($[M+H]^+$), found 391.0768.

IR (thin film, ν_{max} /cm^{-1}) 2962, 1779, 1729, 1614, 1517, 1469, 1420, 1387, 1256, 1211, 1105, 1031, 844, 814, 774, 720.

m.p. 116 – 120 °C.

minor

R_f (60% CH_2Cl_2 in pentane) = 0.19.

^{1}H NMR (600 MHz, $CDCl_3$) δ 7.69 (td, *J* = 5.1, 2.0 Hz, 2H, C(7)*H*), 7.65 (dt, *J* = 5.3, 3.5 Hz, 2H, C(8)*H*), 7.25 – 7.22 (m, 2H, C(2)*H*), 6.76 – 6.70 (m, 2H, C(1)*H*), 5.85 (d, *J* = 8.1 Hz, 1H, C(4)*H*), 5.44 – 5.35 (m, 2H, C(5)*H*, C(6)H_a), 4.71 – 4.64 (m, 1H, C(6)H_b), 3.66 (s, 3H, C(9)H_3).

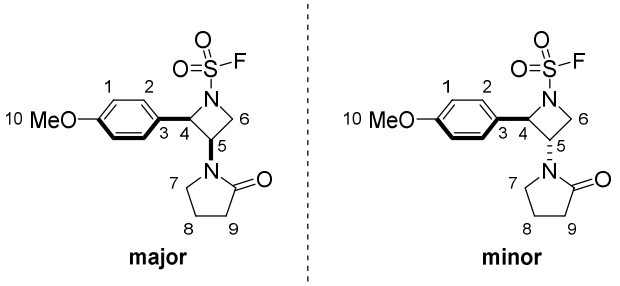
^{13}C NMR (151 MHz, $CDCl_3$) δ 167.8, 159.8, 134.5, 131.0, 127.9, 124.7, 123.5, 114.0, 72.4, 55.3, 51.9, 45.5.

^{19}F NMR (565 MHz, $CDCl_3$) δ 32.06(s).

HRMS (ESI) *m/z*; $C_{18}H_{16}FN_2O_5S$ requires 391.0759 ($[M+H]^+$), found 391.0760.

IR (thin film, ν_{max} /cm^{-1}) 2962, 2920, 1779, 1719, 1615, 1516, 1468, 1419, 1383, 1256, 1211, 1104, 843, 774, 720.

(2*R,3*R**)-2-(4-Methoxyphenyl)-3-(2-oxopyrrolidin-1-yl)azetidine-1-sulfonyl fluoride (4r) and (2*S**,3*R**)-2-(4-Methoxyphenyl)-3-(2-oxopyrrolidin-1-yl)azetidine-1-sulfonyl fluoride (4r')**



Prepared according to **GP1** using (4-methoxybenzylidene)sulfamoyl fluoride (**1a**) (43.4 mg, 0.20 mmol, 1.0 equiv.), 3-F-TX (4.6 mg, 0.020 mmol, 0.10 equiv.) and 1-vinyl-2-pyrrolidinone (214 µl, 2.0 mmol, 10 equiv.) in $(CH_2Cl)_2$ (1.0 ml, 0.20 M). ^{19}F NMR analysis of the crude reaction mixture revealed a diastereomer ratio of 3.0:1. Purification by flash column chromatography (50 – 70% EtOAc in pentane) afforded(2*R**,3*R**)-2-(4-methoxyphenyl)-3-(2-oxopyrrolidin-1-yl)azetidine-1-sulfonyl fluoride (**4r**) as a pale-yellow oil (41.2 mg, 63%) and (2*S**,3*R**)-2-(4-methoxyphenyl)-3-(2-oxopyrrolidin-1-yl)azetidine-1-sulfonyl fluoride (**4r'**) as a colourless oil (3.7 mg, 5%).

major

^{1}H NMR (500 MHz, $CDCl_3$) δ 7.23 – 7.18 (m, 2H, C(2)*H*), 6.94 – 6.89 (m, 2H, C(1)*H*), 5.77 (d, *J* = 8.4 Hz, 1H, C(4)*H*), 5.29 (td, *J* = 8.8, 4.8 Hz, 1H, C(5)*H*), 4.61 (app td, *J* = 9.6, 1.9 Hz, 1H, C(6)H_a), 4.29 (ddd, *J* = 10.0, 5.0, 1.6 Hz, 1H, C(6)H_b), 3.80 (s, 3H, C(10)H_3), 3.29 (ddd, *J* = 9.2, 7.8, 6.8 Hz, 1H, C(7)H_a), 2.93 (td, *J* = 8.8, 4.5 Hz, 1H,

C(7)H_b), 2.23 (ddd, J = 17.1, 9.2, 8.0 Hz, 1H, C(9)H_a), 2.06 (ddd, J = 17.0, 9.4, 5.3 Hz, 1H, C(9)H_b), 1.80 – 1.69 (m, 1H, C(8)H_a), 1.38 (ddtd, J = 12.7, 9.5, 8.2, 6.8 Hz, 1H, C(8)H_b).

^{13}C NMR (126 MHz, $CDCl_3$) δ 176.4, 159.7, 126.9, 125.5, 114.1, 72.2, 55.4, 53.0, 45.9, 44.8, 30.9, 18.5.

^{19}F NMR (377 MHz, $CDCl_3$) δ 30.30 (s).

HRMS (ESI) *m/z* $C_{14}H_{18}FN_2O_4S^+$ requires 329.0966 ($[M+H]^+$), found 329.0977.

IR (thin film, ν_{max} /cm^{-1}) 2959, 1691, 1614, 1515, 1464, 1422, 1294, 1253, 1211, 1177, 1112, 1031, 913, 843, 808, 755, 735, 683, 619.

minor

^{1}H NMR (400 MHz, $CDCl_3$) δ 7.40 – 7.32 (m, 2H, C(2)*H*), 6.95 – 6.89 (m, 2H, C(1)*H*), 5.43 (dd, J = 7.4, 2.1 Hz, 1H, C(4)*H*), 4.87 (q, J = 7.8 Hz, 1H, C(5)*H*), 4.34 (td, J = 8.1, 2.1 Hz, 1H, C(6)H_a), 4.22 (tt, J = 8.3, 1.1 Hz, 1H, C(6)H_b), 3.81 (s, 3H, C(10)H_3), 3.59 – 3.53 (m, 2H, C(7)H_2), 2.47 – 2.38 (m, 2H, C(9)H_2), 2.19 – 2.07 (m, 2H, C(8)H_2).

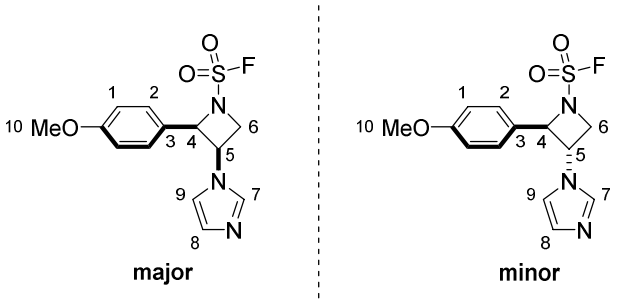
^{13}C NMR (101 MHz, $CDCl_3$) δ 175.6, 160.6, 128.4, 128.0, 114.5, 71.4, 55.5, 52.6, 49.9, 44.7, 31.2, 18.3.

^{19}F NMR (377 MHz, $CDCl_3$) δ 30.64.

HRMS (ESI) *m/z* $C_{14}H_{18}FN_2O_4S^+$ requires 329.0966 ($[M+H]^+$), found 329.0979.

IR (thin film, ν_{max} /cm^{-1}) 2921, 1667, 1613, 1515, 1493, 1465, 1422, 1398, 1294, 1250, 1207, 1178, 1071, 1032, 968, 913, 837, 737, 654.

(2*R,3*R**)-3-(1H-Imidazol-1-yl)-2-(4-methoxyphenyl)azetidine-1-sulfonyl fluoride (4s) and (2*R**,3*S**)-3-(1H-Imidazol-1-yl)-2-(4-methoxyphenyl)azetidine-1-sulfonyl fluoride (4s')**



Prepared according to **GP1** using (4-methoxybenzylidene)sulfamoyl fluoride (**1a**) (43.4 mg, 0.20 mmol, 1.0 equiv.), $[Ir(dFCF_3ppy)_2(dtbbpy)][PF_6]$ (2.2 mg, 0.002 mmol, 0.01 equiv.), Aldrithiol-2 (2.2 mg, 0.010 mmol, 0.05 equiv.) and *N*-vinyl imidazole (56 µl, 0.6 mmol, 3.0 equiv.) in $(CH_2Cl)_2$ (1.0 ml, 0.20 M). ^{19}F NMR analysis of the crude reaction mixture revealed a diastereomer ratio of 2.9:1. Purification by flash column chromatography (0 – 3% MeOH in EtOAc) afforded (2*R**,3*R**)-3-(1H-imidazol-1-yl)-2-(4-methoxyphenyl)azetidine-1-sulfonyl fluoride (**4u**) as a white solid (30.0 mg, 48%) and (2*R**,3*S**)-3-(1H-imidazol-1-yl)-2-(4-methoxyphenyl)azetidine-1-sulfonyl fluoride (**4u'**) (10.6 mg, 17%) as a colourless oil.

Note: Excess N-vinyl imidazole can be distilled off using a rotary evaporator or under high vacuum.

major

R_f(2% MeOH/EtOAc) = 0.10.

^{1}H NMR (600 MHz, $CDCl_3$) 7.41 (s, 1H, C(7)*H*), 7.08 – 7.05 (m, 2H, C(1)*H*), 6.86 (s, 1H, C(8)*H*), 6.78 – 6.74 (m, 3H, C(2)*H*, C(9)*H*), 5.85 (d, *J* = 7.8 Hz, 1H, C(4)*H*), 5.27 (td, *J* = 8.6, 4.4 Hz, 1H, C(5)*H*), 4.84 (ddd, *J* = 10.2, 8.4, 1.8 Hz, 1H, C(6)H_a), 4.42 (dd, *J* = 10.3, 4.1 Hz, 1H, C(6)H_b), 3.73 (s, 3H, C(10)H_3).

^{13}C NMR (151 MHz, $CDCl_3$) δ 160.3, 136.6, 130.1, 127.2, 123.4, 117.9, 114.3, 72.1, 56.1, 55.3, 51.5.

^{19}F NMR (565 MHz, $CDCl_3$) δ 31.68.

HRMS (ESI) *m/z* $C_{13}H_{15}FN_3O_3S^+$ requires 312.0813 ($[M+H]^+$), found 312.0802.

IR (thin film, ν_{max} /cm^{-1}) 1614, 1516, 1426, 1306, 1255, 1214, 1179, 1109, 1032, 845, 810, 764.

m.p. 230 °C (decomp.).

minor

R_f(2% MeOH/EtOAc) = 0.20.

^{1}H NMR (600 MHz, $CDCl_3$) δ 7.54 (s, 1H, C(7)*H*), 7.34 – 7.29 (m, 2H, C(1)*H*), 7.21 (s, 1H, C(8)*H*), 7.15 (d, *J* = 1.5 Hz, 1H, C(9)*H*), 6.98 – 6.92 (m, 2H, C(1)*H*), 5.41 (d, *J* = 6.7 Hz, 1H, C(4)*H*), 4.83 (q, *J* = 7.5 Hz, 1H, C(5)*H*), 4.56 (t, *J* = 8.5 Hz, 1H, C(6)H_a), 4.45 (t, *J* = 8.2 Hz, 1H, C(6)H_b), 3.82 (s, 3H, C(10)H_3).

^{13}C NMR (151 MHz, $CDCl_3$) δ 161.0, 136.7, 131.7, 127.9, 127.1, 116.5, 114.8, 76.3, 56.2, 55.5, 54.2.

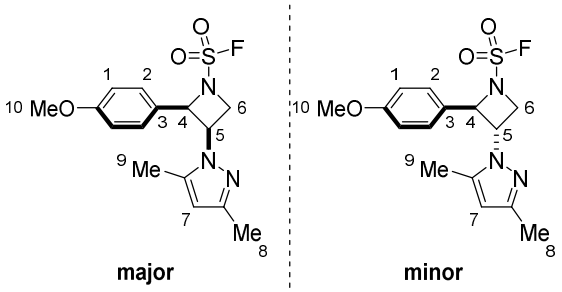
^{19}F NMR (377 MHz, $CDCl_3$) δ 31.42(s).

HRMS (ESI) *m/z* $C_{13}H_{15}FN_3O_3S^+$ requires 312.0813 ($[M+H]^+$), found 312.0810.

IR (thin film, ν_{max} /cm^{-1}) 2968, 1668, 1541, 1519, 1425, 1214, 1030, 760, 668.

m.p. 200 °C (decomp.).

(2*R,3*R**)-3-(3,5-Dimethyl-1H-pyrazol-1-yl)-2-(4-methoxyphenyl)azetidine-1-sulfonyl fluoride (4t) and (2*R**,3*S**)-3-(3,5-Dimethyl-1H-pyrazol-1-yl)-2-(4-methoxyphenyl)azetidine-1-sulfonyl fluoride (4t')**



Prepared according to **GP1** using (4-methoxybenzylidene)sulfamoyl fluoride (**1a**) (43.4 mg, 0.20 mmol, 1.0 equiv.), 3-F-TX (4.6 mg, 0.020 mmol, 0.10 equiv.) and 3,5-dimethyl-1-vinyl-1H-pyrazole (**27**) (76 µl, 0.60 mmol, 3.0 equiv.) in $(CH_2Cl)_2$ (1.0 ml, 0.20 M). ^{19}F NMR analysis of the crude reaction mixture revealed a diastereomer ratio of 1.3:1. Purification by flash column chromatography (0 – 10% EtOAc in pentane) afforded (2*R**,3*R**)-3-(3,5-dimethyl-1H-pyrazol-1-yl)-2-(4-methoxyphenyl)azetidine-1-sulfonyl fluoride (**4t**) as a white solid (30.4 mg, 45%) and (2*R**,3*S**)-3-(3,5-dimethyl-1H-pyrazol-1-yl)-2-(4-methoxyphenyl)azetidine-1-sulfonyl fluoride (**4t'**) (22.7 mg, 33%) as a colourless oil.

major

R_f (10% EtOAc in pentane) = 0.19.

^{1}H NMR (600 MHz, $CDCl_3$) δ 7.13 – 7.10 (m, 2H, C(2)*H*), 6.72 – 6.66 (m, 2H, C(1)*H*), 5.65 – 5.60 (m, 1H, C(4)*H*), 5.59 (s, 1H, C(7)*H*), 5.34 (dddd, *J* = 9.1, 4.1, 1.7, 0.9 Hz, 1H, C(6)H_a), 5.15 (ddd, *J* = 8.7, 7.5, 4.0 Hz, 1H, C(5)*H*), 4.67 (td, *J* = 8.9, 2.0 Hz, 1H, C(6)H_b), 3.74 (s, 3H, C(10)H_3), 2.15 (s, 3H, C(8)H_3 or C(9)H_3), 1.85 (d, *J* = 0.8 Hz, 3H, C(8)H_3 or C(9)H_3).

^{13}C NMR (151 MHz, $CDCl_3$) δ 160.3, 147.9, 139.5, 129.0, 124.6, 113.5, 106.8, 72.5, 55.3, 53.8, 51.8, 13.6, 10.8.

^{19}F NMR (565 MHz, $CDCl_3$) δ 31.81 (s).

HRMS (ESI) *m/z*; $C_{15}H_{19}FN_3O_3S$ requires 340.1126 ($[M+H]^+$), found 340.1125.

IR (thin film, ν_{max} /cm^{-1}) 2961, 1614, 1562, 1518, 1465, 1425, 1301, 1256, 1214, 1178, 1102, 1033, 839, 791, 771, 753.

m.p. 148 – 150 °C.

minor

R_f (10% EtOAc in pentane) = 0.26.

^{1}H NMR (600 MHz, $CDCl_3$) 7.36 – 7.32 (m, 2H, C(2)*H*), 6.94 – 6.90 (m, 2H, C(1)*H*), 5.80 (s, 1H, C(7)*H*), 5.70 (dd, *J* = 6.8, 2.2 Hz, 1H, C(4)*H*), 4.91 (td, *J* = 7.6, 2.1 Hz, 1H, C(6)H_a), 4.73 (td, *J* = 7.8, 6.7 Hz, 1H, C(5)*H*), 4.33 (t, *J* = 7.8 Hz, 1H, C(6)H_b), 3.81 (s, 3H, C(10)H_3), 2.26 (s, 3H, C(8)H_3 or C(9)H_3), 1.99 (s, 3H, C(8)H_3 or C(9)H_3).

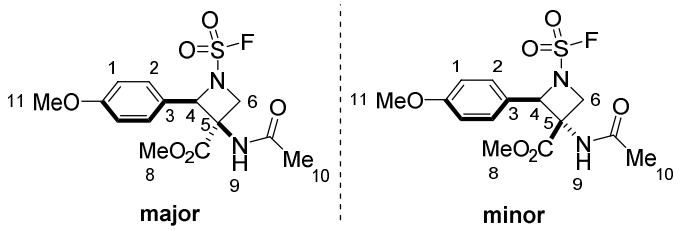
^{13}C NMR (151 MHz, $CDCl_3$) δ 160.5, 149.5, 139.7, 128.4, 128.0, 114.6, 106.5, 75.0, 55.5, 55.3, 54.6, 13.8, 10.8.

^{19}F NMR (565 MHz, $CDCl_3$) δ 32.19 (s).

HRMS (ESI) *m/z*; $C_{15}H_{19}FN_3O_3S$ requires 340.1126 ($[M+H]^+$), found 340.1128.

IR (thin film, ν_{max} /cm^{-1}) 2962, 1615, 1562, 1517, 1461, 1423, 1308, 1255, 1213, 1178, 1105, 1033, 842, 793, 679.

Methyl (2*R,3*S**)-3-acetamide-1-(fluorosulfonyl)-2-(4-methoxyphenyl)azetidine-3-carboxylate (4u) and Methyl (2*S**,3*S**)-3-acetamide-1-(fluorosulfonyl)-2-(4-methoxyphenyl)azetidine-3-carboxylate (4u')**



Prepared according to **GP1** using (4-methoxybenzylidene)sulfamoyl fluoride (**1a**) (43.4 mg, 0.20 mmol, 1.0 equiv.), ITX (5.1 mg, 0.020 mmol, 0.10 equiv.) and methyl 2-acetamidoacrylate (286.3 mg 2.0 mmol, 10 equiv.) in $(CH_2Cl)_2$ (1.0 ml, 0.20 M). ^{19}F NMR analysis of the crude reaction mixture revealed a diastereomer ratio of 4:1. Purification by flash column chromatography (50% - 67% EtOAc in petrol ether) afforded methyl (2*R**,3*S**)-3-acetamide-1-(fluorosulfonyl)-2-(4-methoxyphenyl)azetidine-3-carboxylate (**4u**) and methyl (2*S**,3*S**)-3-acetamide-1-(fluorosulfonyl)-2-(4-methoxyphenyl)azetidine-3-carboxylate (**4u'**) as an inseparable mixture of diastereomers in the form of an off-white solid (32.4 mg, 45%).

major

^{1}H NMR (500 MHz, $CDCl_3$) δ 7.38 – 7.31 (m, 2H, C(1)*H*), 7.05 – 6.98 (m, 2H, C(2)*H*), 5.61 (s, 1H, C(4)*H*), 5.44 (s, 1H, N(9)*H*), 5.03 (dd, *J* = 9.2, 1.9 Hz, 1H, C(6)H_a), 4.09 (dd, *J* = 9.2, 1.5 Hz, 1H, C(6)H_b), 3.88 (s, 3H, C(11)H_3), 3.85 (s, 3H, C(8)H_3), 1.86 (s, 3H, C(10)H_3).

^{13}C NMR (126 MHz, $CDCl_3$) δ 170.6, 169.5, 161.2, 128.8, 122.5, 115.0, 71.4, 58.9, 56.8, 55.6, 53.9, 22.8.

^{19}F NMR (377 MHz, $CDCl_3$) δ 32.96 (d, *J* = 2.4 Hz).

HRMS (ESI) *m/z* $C_{14}H_{17}FN_2O_6SNa^+$ requires 383.0684 ($[M+H]^+$), found 383.0681.

IR (thin film, ν_{max} /cm^{-1}) 3278, 2959, 1748, 1659, 1614, 1517, 1428, 1254, 1213, 1178, 1032, 912, 838, 767, 734.

minor

^{1}H NMR (500 MHz, $CDCl_3$) δ 7.25 (d, *J* = 5.7 Hz, 2H, C(1)*H*), 6.89 – 6.86 (m, 2H, C(2)*H*), 6.63 (s, 1H, N(9)*H*), 5.89 – 5.85 (m, 1H, C(4)*H*), 4.71 (dd, *J* = 8.3, 2.1 Hz, 1H, C(6)H_a), 4.67 (d, *J* = 8.3 Hz, 1H, C(6)H_b), 3.79 (s, 3H, C(11)H_3), 3.42 (s, 3H, C(8)H_3), 2.11 (s, 3H, C(10)H_3).

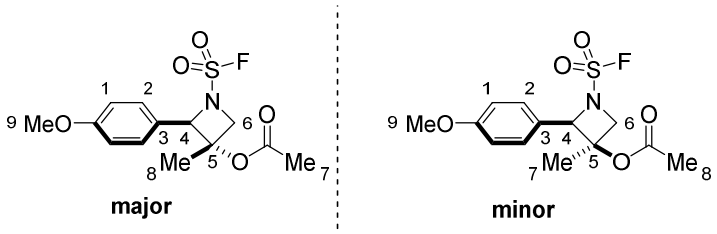
^{13}C NMR (126 MHz, $CDCl_3$) δ 170.9, 168.2, 160.5, 127.8, 125.0, 114.1, 73.0, 60.8, 57.1, 55.4, 53.1, 23.4.

^{19}F NMR (377 MHz, $CDCl_3$) δ 34.04 (d, *J* = 2.9 Hz).

HRMS (ESI) *m/z* $C_{14}H_{17}FN_2O_6SNa^+$ requires 383.0684 ($[M+H]^+$), found 383.0681.

IR (thin film, ν_{max} /cm^{-1}) 3278, 2959, 1748, 1659, 1614, 1517, 1428, 1254, 1213, 1178, 1032, 912, 838, 767, 734.

(2*R,3*S**)-1-(Fluorosulfonyl)-2-(4-methoxyphenyl)-3-methylazetidin-3-yl acetate (4v) and (2*R**,3*R**)-1-(Fluorosulfonyl)-2-(4-methoxyphenyl)-3-methylazetidin-3-yl acetate (4v')**



Prepared according to **GP1** using (4-methoxybenzylidene)sulfamoyl fluoride (**1a**) (43.4 mg, 0.20 mmol, 1.0 equiv.), 3-F-TX (4.6 mg, 0.020 mmol, 0.10 equiv.) and isopropenyl acetate (220 µl, 2.0 mmol, 10 equiv.) in $(CH_2Cl)_2$ (1.0 ml, 0.20 M). ^{19}F NMR analysis of the crude reaction mixture revealed a diastereomer ratio of 4.4:1. Purification by flash column chromatography (0 – 10% Et_2O in pentane) afforded (2*R**,3*S**)-1-(fluorosulfonyl)-2-(4-methoxyphenyl)-3-methylazetidin-3-yl acetate (**4v**) as a colourless oil (28.8 mg, 45%) and (2*R**,3*R**)-1-(fluorosulfonyl)-2-(4-methoxyphenyl)-3-methylazetidin-3-yl acetate (**4v'**) as a colourless oil (22.2 mg, 35%).

major

R_f(10% Et_2O in pentane) = 0.20.

^{1}H NMR (500 MHz, $CDCl_3$) δ 7.38 – 7.30 (m, 2H, C(2)*H*), 6.96 – 6.92 (m, 2H, C(1)*H*), 5.43 (s, 1H, C(4)*H*), 4.34 (dd, *J* = 9.3, 2.0 Hz, 1H, C(6)H_a), 4.12 (d, *J* = 9.3 Hz, 1H, C(6)H_b), 3.82 (s, 3H, C(9)H_3), 2.12 (s, 3H, C(7)H_3), 1.24 (s, 3H, C(8)H_3).

^{13}C NMR (126 MHz, $CDCl_3$) δ 169.7, 160.2, 128.4, 125.2, 114.2, 77.2, 76.6, 62.4, 55.4, 21.4, 19.1.

^{19}F NMR (470 MHz, $CDCl_3$) δ 30.60 (s).

HRMS (ESI) *m/z* $C_{13}H_{17}FNO_5S^+$ requires 318.0806 ($[M+H]^+$), found 318.0817.

IR (thin film, ν_{max} /cm^{-1}) 2940, 1747, 1616, 1517, 1427, 1372, 1306, 1252, 1213, 1177, 1148, 1123, 1081, 1031, 968, 912, 838, 817, 775, 740, 685, 607.

minor

R_f(10% Et_2O in pentane) = 0.07.

^{1}H NMR (500 MHz, $CDCl_3$) δ 7.35 – 7.29 (m, 2H, C(2)*H*), 6.95 – 6.91 (m, 2H, C(1)*H*), 5.22 (d, *J* = 2.1 Hz, 1H, C(4)*H*), 4.39 (dd, *J* = 10.2, 2.3 Hz, 1H, C(6)H_a), 4.29 (dd, *J* = 10.3, 2.1 Hz, 1H, C(6)H_b), 3.83 (s, 3H, C(9)H_3), 1.84 (s, 3H, C(7)H_3), 1.81 (s, 3H, C(8)H_3).

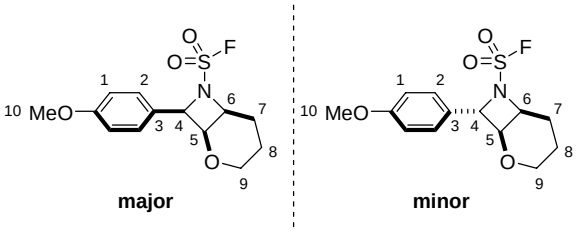
^{13}C NMR (126 MHz, $CDCl_3$) δ 169.6, 160.3, 129.2, 125.0, 113.9, 77.6, 76.5, 62.4, 55.4, 23.5, 21.3.

^{19}F NMR (470 MHz, $CDCl_3$) δ 33.41(s).

HRMS (ESI) *m/z* $C_{13}H_{17}FNO_5S^+$ requires 318.0806 ($[M+H]^+$), found 318.0821.

IR (thin film, ν_{max} /cm^{-1}) 2939, 1744, 1615, 1516, 1423, 1371, 1308, 1252, 1211, 1178, 1078, 1031, 914, 833, 778, 742, 670, 605.

(1*R,6*S**,8*R**)-8-(4-Methoxyphenyl)-2-oxa-7-azabicyclo[4.2.0]octane-7-sulfonyl fluoride (4w) and (1*R**,6*S**,8*S**)-8-(4-Methoxyphenyl)-2-oxa-7-azabicyclo[4.2.0]octane-7-sulfonyl fluoride (4w')**



Prepared according to **GP1** using (4-methoxybenzylidene)sulfamoyl fluoride (**1a**) (43.4 mg, 0.20 mmol, 1.0 equiv.), ITX (5.1 mg, 0.020 mmol, 0.10 equiv.) and 3,4-dihydro-2H-pyran (183 µl, 2.0 mmol, 10 equiv.) in $(CH_2Cl)_2$ (1.0 ml, 0.20 M). ^{19}F NMR analysis of the crude reaction mixture revealed a diastereomer ratio of 1.5:1. Purification by flash column chromatography (0 – 20% Et_2O in pentane) afforded(1*R**,6*S**,8*R**)-8-(4-methoxyphenyl)-2-oxa-7-azabicyclo[4.2.0]octane-7-sulfonyl fluoride (**4w**) as a colourless oil (15.8 mg, 26%) and (1*R**,6*S**,8*S**)-8-(4-methoxyphenyl)-2-oxa-7-azabicyclo[4.2.0]octane-7-sulfonyl fluoride (**4w'**) as a colourless oil (11.6 mg, 19%).

major

R_f (20% Et_2O in pentane) = 0.06.

^{1}H NMR (600 MHz, $CDCl_3$) δ 7.41 – 7.35 (m, 2H, C(2)*H*), 6.95 – 6.87 (m, 2H, C(1)*H*), 5.26 – 5.22 (m, 1H, C(4)*H*), 4.44 (t, *J* = 4.9 Hz, 1H, C(5)*H*), 4.40 (t, *J* = 5.0 Hz, 1H, C(6)*H*), 3.90 (ddq, *J* = 11.6, 4.3, 2.0 Hz, 1H, C(9)H_a), 3.80 (s, 3H, C(10)H_3), 3.31 (td, *J* = 11.6, 1.9 Hz, 1H, C(9)H_b), 2.33 (ddt, *J* = 15.3, 4.5, 2.3 Hz, 1H, C(7)H_a), 2.14 – 2.02 (m, 1H, C(8)H_a), 1.77 (ddt, *J* = 15.4, 12.5, 5.3 Hz, 1H, C(7)H_b), 1.58 (ddt, *J* = 13.9, 5.5, 2.5 Hz, 1H, C(8)H_b).

^{13}C NMR (151 MHz, $CDCl_3$) δ 160.1, 129.6, 124.5, 113.8, 70.2, 69.5, 64.3, 60.4, 55.4, 23.9, 20.6.

^{19}F NMR (565 MHz, $CDCl_3$) δ 28.96.

HRMS (ESI) *m/z* $C_{13}H_{17}FNO_4S^+$ requires 302.0857 ($[M+H]^+$), found 302.0864.

IR (thin film, ν_{max} /cm^{-1}) 2954, 1614, 1515, 1420, 1304, 1252, 1210, 1177, 1140, 1109, 1073, 1060, 1038, 998, 913, 835, 800, 752, 686.

minor

R_f (20% Et_2O in pentane) = 0.15.

^{1}H NMR (600 MHz, $CDCl_3$) δ 7.37 – 7.32 (m, 2H, C(2)*H*), 6.97 – 6.93 (m, 2H, C(1)*H*), 5.31 (t, *J* = 3.6 Hz, 1H, C(4)*H*), 4.69 – 4.60 (m, 1H, C(6)*H*), 4.36 (dd, *J* = 6.4, 3.9 Hz, 1H, C(5)*H*), 4.00 (dt, *J* = 11.5, 5.8 Hz, 1H, C(9)H_a), 3.84 (s, 3H, C(10)H_3), 3.65 (ddd, *J* = 11.8, 7.3, 4.9 Hz, 1H, C(9)H_b), 2.36 (ddt, *J* = 14.3, 9.9, 5.3 Hz, 1H, C(7)H_a), 2.18 (dddd, *J* = 14.2, 7.8, 6.3, 4.7 Hz, 1H, C(7)H_b), 2.03 (dtt, *J* = 14.9, 7.6, 5.1 Hz, 1H, C(8)H_a), 1.61 (dddd, *J* = 14.0, 9.0, 6.3, 4.6 Hz, 1H, C(8)H_b).

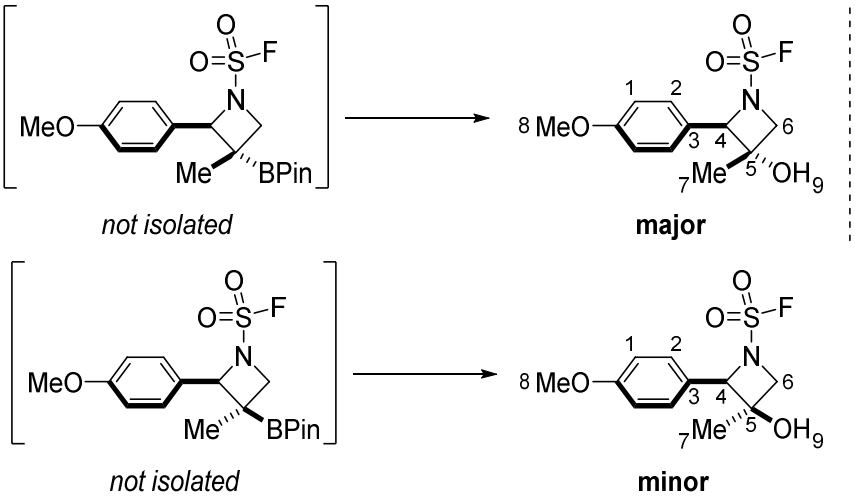
^{13}C NMR (101 MHz, CDCl3) δ 160.3, 128.6, 127.5, 114.4, 74.1, 72.7, 63.3, 62.1, 55.5, 22.2, 19.5.

^{19}F NMR (377 MHz, $CDCl_3$) δ 49.73(s).

HRMS (ESI) *m/z* $C_{13}H_{17}FNO_4S^+$ requires 302.0857 ($[M+H]^+$), found 302.0855.

IR (thin film, ν_{max} /cm^{-1}) 2957, 1614, 1516, 1461, 1416, 1252, 1206, 1178, 1154, 1079, 1033, 912, 837, 771, 746, 615.

(2*R,3*S**)-3-Hydroxy-2-(4-methoxyphenyl)-3-methylazetidine-1-sulfonyl fluoride (4x') and (2*R**,3*R**)-3-Hydroxy-2-(4-methoxyphenyl)-3-methylazetidine-1-sulfonyl fluoride (4x'')**



Prepared according to **GP1** using (4-methoxybenzylidene)sulfamoyl fluoride (**1a**) (43.4 mg, 0.20 mmol, 1.0 equiv.), 3-F-TX (4.6 mg, 0.020 mmol, 0.10 equiv.) and isopropenylboronic acid pinacol ester (378 µl, 2.00 mmol, 10 equiv.) in $(CH_2Cl)_2$ (1.0 ml, 0.20 M). ^{19}F NMR analysis of the crude reaction mixture revealed a diastereomer ratio of 3.3:1 and a total yield of both diastereomers of 44% for the boronic ester. Following the photochemical reaction, the reaction mixture was dissolved in THF (9.0 ml) and cooled to 0 °C. 3M NaOH (6 ml) was added followed by dropwise addition of 30% (w/w) H_2O_2 solution (3.0 ml). Following addition reaction mixture was warmed to rt and stirred for 4 h. The reaction mixture was then cooled to 0 °C and quenched with aq. sat. $Na_2S_2O_3$ (caution: exotherm). The reaction mixture was then warmed to rt and extracted thrice with Et_2O, dried over anhydrous $MgSO_4$, filtered and concentrated under reduced pressure. Purification by flash column chromatography (0 – 20% EtOAc in pentane) afforded an inseparable mixture of (2*R**,3*S**)-3-hydroxy-2-(4-methoxyphenyl)-

3-methylazetidine-1-sulfonyl fluoride (**4x**) and (2*R**,3*R**)-3-hydroxy-2-(4-methoxyphenyl)-3-methylazetidine-1-sulfonyl fluoride (**4x'**) as a colourless oil (17.1 mg, 31%).

major

^{1}H NMR (600 MHz, $CDCl_3$) δ 7.27 (d, *J* = 8.5 Hz, 2H, C(2)*H*), 6.94 – 6.91 (m, 2H, C(1)*H*), 5.30 (s, 1H, C(4)*H*), 4.16 (dd, *J* = 8.1, 2.0 Hz, 1H, C(6)H_a), 3.89 (dd, *J* = 8.0, 1.4 Hz, 1H, C(6)H_b), 3.81 (s, 3H, C(8)H_3), 2.35 (s, 1H, O(9)*H*), 1.12 (s, 3H, C(7)H_3).

^{13}C NMR (151 MHz, $CDCl_3$) δ 160.0, 127.6, 126.0, 114.2, 79.4, 72.4, 64.0, 55.4, 22.8.

^{19}F NMR (377 MHz, $CDCl_3$) δ 29.71 (s).

HRMS (ESI) *m/z*; $C_{11}H_{15}FNO_4S$ requires 276.0700 ($[M+H]^+$), found 276.0709.

IR (thin film, ν_{max} /cm^{-1}) 3451, 2998, 1779, 1718, 1615, 1516, 1422, 1303, 1253, 1213, 1178, 1033, 831, 746, 622.

minor

^{1}H NMR (600 MHz, $CDCl_3$) δ 7.36 – 7.32 (m, 2H, C(2)*H*), 7.00 – 6.96 (m, 2H, C(1)*H*), 5.24 (d, *J* = 2.4 Hz, 1H, C(4)*H*), 4.20 (dd, *J* = 9.1, 2.0 Hz, 1H, C(6)H_a), 4.03 (dt, *J* = 9.2, 1.2 Hz, 1H, C(6)H_b), 3.82 (s, 3H, C(8)H_3), 1.75 (s, 1H, O(9)*H*), 1.58 (s, 3H, C(7)H_3).

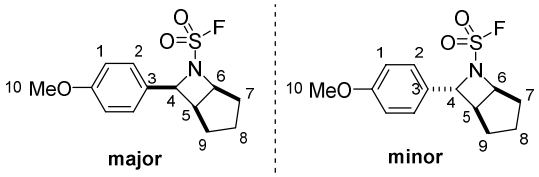
^{13}C NMR (151 MHz, $CDCl_3$) δ 160.6, 128.6, 124.4, 114.7, 77.7, 71.0, 64.5, 55.5, 26.5.

^{19}F NMR (377 MHz, $CDCl_3$) δ 31.36 (s).

HRMS (ESI) *m/z*; $C_{11}H_{15}FNO_4S$ requires 276.0700 ($[M+H]^+$), found 276.0709.

IR (thin film, ν_{max} /cm^{-1}) 3451, 2998, 1779, 1718, 1615, 1516, 1422, 1303, 1253, 1213, 1178, 1033, 831, 746, 622.

(1*R,5*S**,7*S**)-7-(4-Methoxyphenyl)-6-azabicyclo[3.2.0]heptane-6-sulfonyl fluoride (4y) and (1*R**,5*S**,7*R**)-7-(4-Methoxyphenyl)-6-azabicyclo[3.2.0]heptane-6-sulfonyl fluoride (4y')**



Prepared according to **GP1** using (4-methoxybenzylidene)sulfamoyl fluoride (**1a**) (43.4 mg, 0.20 mmol, 1.0 equiv.), ITX (5.1 mg, 0.020 mmol, 0.10 equiv.) and cyclopentene (177 µl, 2.0 mmol, 10 equiv.) in $(CH_2Cl)_2$ (1.0 ml, 0.20 M). ^{19}F NMR analysis of the crude reaction mixture revealed a diastereomer ratio of 5.5:1. Purification by flash column chromatography (0 – 6% Et_2O in pentane) afforded (1*R**,5*S**,7*S**)-7-(4-methoxyphenyl)-6-azabicyclo[3.2.0]heptane-6-sulfonyl fluoride (**4y**) as a colourless oil (24.5 mg, 43%) and a 3:1 mixture of (1*R**,5*S**,7*R**)-7-(4-methoxyphenyl)-6-azabicyclo[3.2.0]heptane-6-sulfonyl fluoride (**4y'**) and (1*R**,5*S**,7*S**)-7-(4-methoxyphenyl)-6-azabicyclo[3.2.0]heptane-6-sulfonyl fluoride (**4y**) as a colourless oil (13.3 mg, 23%).

major

R_f (5% Et_2O in pentane) = 0.20;

^{1}H NMR (600 MHz, $CDCl_3$) δ 7.22 – 7.16 (m, 2H, C(2)*H*), 6.94 – 6.89 (m, 2H, C(1)*H*), 5.56 (dd, *J* = 8.7, 2.2 Hz, 1H, C(4)*H*), 4.94 – 4.91 (m, 1H, C(6)*H*), 3.81 (s, 3H, C(10)H_3), 3.21 (td, *J* = 9.1, 6.4 Hz, 1H, C(5)*H*), 2.16 (dd, *J* = 14.1, 6.6 Hz, 1H, C(7)H_a), 1.84 – 1.69

(m, 2H, C(8)H_2), 1.48 (dddd, J = 14.1, 12.0, 7.1, 4.4 Hz, 1H, C(7)H_b), 1.41 – 1.34 (m, 2H, C(9)H_2).

^{13}C NMR (151 MHz, $CDCl_3$) δ 159.3, 127.1, 127.0, 114.1, 70.0, 67.2, 55.4, 40.1, 32.8, 25.9, 24.8.

^{19}F NMR (565 MHz, $CDCl_3$) δ 31.52(s).

HRMS (ESI) *m/z* $C_{13}H_{16}FNO_3SNa^+$ requires 308.0727 ($[M+Na]^+$), found 308.0741;

IR (thin film, ν_{max} /cm^{-1}) 2961, 2841, 1615, 1515, 1419, 1304, 1253, 1206, 1176, 1095, 1050, 1032, 1000, 912, 843, 765, 748, 695.

minor

R_f (5% Et_2O in pentane) = 0.18.

^{1}H NMR (600 MHz, $CDCl_3$) δ 7.38 – 7.35 (m, 2H, C(2)H), 6.96 – 6.94 (m, 2H, C(1)H), 4.99 (q, J = 4.9 Hz, 1H, C(6)H), 4.81 (t, J = 3.8 Hz, 1H, C(4)H), 3.84 (s, 3H, C(10)H_3), 2.97 (td, J = 6.6, 4.3 Hz, 1H, C(5)H), 2.50 (dd, J = 14.8, 5.9 Hz, 1H, C(7)H_a), 2.16 (ddd, J = 25.9, 13.5, 6.3 Hz, 1H, C(9)H_a), 2.09 (dq, J = 13.7, 7.3 Hz, 1H, C(8)H_a), 1.96 (dd, J = 13.6, 6.2 Hz, 1H, C(8)H_b), 1.66 – 1.59 (m, 2H, C(7)H_b, C(9)H_b).

^{13}C NMR (151 MHz, $CDCl_3$) δ 160.1, 128.1, 127.0, 114.4, 71.9, 69.9 (d, J = 2.4 Hz), 55.5, 45.2, 31.4, 30.5, 23.9.

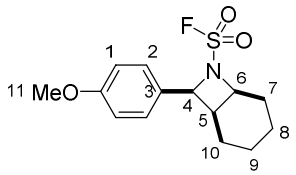
Note: Coupling between Carbon and Fluorine observed.

^{19}F NMR (565 MHz, $CDCl_3$) δ 50.56(s).

HRMS (ESI) *m/z* $C_{13}H_{17}FNO_3S^+$ requires 286.0908 ($[M+H]^+$), found 286.0911.

IR (thin film, ν_{max} /cm^{-1}) 2918, 2850, 1614, 1516, 1415, 1307, 1252, 1210, 1179, 1060, 1034, 909, 845, 774, 742, 643, 628.

(1*R,6*S**,8*S**)-8-(4-Methoxyphenyl)-7-azabicyclo[4.2.0]octane-7-sulfonyl fluoride (4z)**



Prepared according to **GP1** using (4-methoxybenzylidene)sulfamoyl fluoride (**1a**) (43.4 mg, 0.20 mmol, 1.0 equiv.), ITX (5.1 mg, 0.020 mmol, 0.10 equiv.) and cyclohexene (203 µl, 2.0 mmol, 10 equiv.) in $(CH_2Cl)_2$ (1.0 ml, 0.20 M). Purification by flash column chromatography (0 – 10% Et_2O in pentane) afforded (1*R**,6*S**,8*S**)-8-(4-methoxyphenyl)-7-azabicyclo[4.2.0]octane-7-sulfonyl fluoride (**4z**) as a colourless oil (35.5 mg, 59%).

R_f (10% Et_2O in pentane) = 0.38.

^{1}H NMR (600 MHz, $CDCl_3$) δ 7.27 – 7.22 (m, 2H, C(2)*H*), 6.96 – 6.87 (m, 2H, C(1)*H*), 5.46 (d, *J* = 7.7 Hz, 1H, C(4)*H*), 4.57 – 4.49 (m, 1H, C(6)*H*), 3.81 (s, 3H, C(11)H_3), 2.76 (p, *J* = 8.4 Hz, 1H, C(5)*H*), 2.25 – 2.15 (m, 1H, C(7)H_a), 1.65 – 1.47 (m, 4H, C(9)H_2, C(8)H_a, C(7)H_b), 1.41 – 1.22 (m, 2H, C(10)H_2), 1.13 – 1.01 (m, 1H, C(8)H_b).

^{19}F NMR (377 MHz, $CDCl_3$) δ 28.23(s).

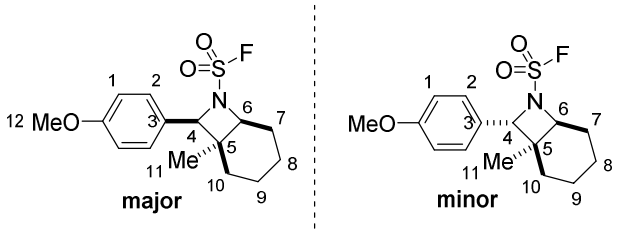
^{13}C NMR (101 MHz, $CDCl_3$) δ 159.4, 127.8, 127.2, 113.9, 68.5, 61.3, 55.4, 34.0, 26.5, 21.6, 21.3, 20.1.

HRMS (ESI) *m/z* $C_{14}H_{18}FNO_3SNa^+$ requires 322.0884 ($[M+Na]^+$), found 322.0889.

IR (thin film, ν_{max} /cm^{-1}) 2939, 1615, 1515, 1418, 1304, 1252, 1207, 1176, 1049, 1036, 835, 742, 669.

(1*R,6*S**,8*R**)-8-(4-Methoxyphenyl)-1-methyl-7-azabicyclo[4.2.0]octane-7-sulfonyl fluoride (4aa) and (1*S**,6*R**,8*R**)-8-(4-Methoxyphenyl)-1-methyl-7-azabicyclo[4.2.0]octane-7-sulfonyl fluoride (4aa')**

Reaction performed by NAP and data collected for minor diastereomer by NAP.



Prepared according to **GP1** using (4-methoxybenzylidene)sulfamoyl fluoride (**1a**) (43.4 mg, 0.20 mmol, 1.0 equiv.), ITX (5.1 mg, 0.020 mmol, 0.10 equiv.) and 1-methyl-1-cyclohexene (237 µl, 2.0 mmol, 10 equiv.) in $(CH_2Cl)_2$ (1.0 ml, 0.20 M). ^{19}F NMR analysis of the crude reaction mixture revealed a diastereomer ratio of 1.2:1. Purification by flash column chromatography (2.5 – 5% Et_2O in pentane) afforded (1*R**,6*S**,8*R**)-8-(4-methoxyphenyl)-1-methyl-7-azabicyclo[4.2.0]octane-7-sulfonyl fluoride (**4aa**) as a colourless oil (13.6 mg, 22%) and (1*S**,6*R**,8*R**)-8-(4-methoxyphenyl)-1-methyl-7-azabicyclo[4.2.0]octane-7-sulfonyl fluoride (**4aa'**) as a colourless oil (7.5 mg, 12%).

major

R_f (10% Et_2O in pentane) = 0.40.

^{1}H NMR (600 MHz, $CDCl_3$) δ 7.25 – 7.19 (m, 2H, C(2)*H*), 6.94 – 6.88 (m, 2H, C(1)*H*), 4.98 (s, 1H, C(4)*H*), 4.13 (m, 1H, C(6)*H*), 3.81 (s, 3H, C(12)H_3), 2.22 – 2.15 (m, 1H,

C(7)H_a), 1.62 – 1.47 (m, 5H, C(7)H_b C(8)H_2, C(10)H_a, C(9)H_a), 1.32 (s, 3H, C(11)H_3), 1.14 – 1.04 (m, 1H, C(9)H_b), 0.90 (dt, J = 14.1, 4.3 Hz, 1H, C(10)H_b).

^{13}C NMR (101 MHz, $CDCl_3$) δ 159.5, 127.6, 127.0, 113.9, 75.5, 68.3, 55.4, 40.1, 29.2, 25.6, 25.0, 20.5, 20.3.

^{19}F NMR (377 MHz, $CDCl_3$) δ 27.63 (s).

HRMS (ESI) *m/z* $C_{15}H_{21}FNO_3S^+$ requires 314.1221 ($[M+H]^+$), found 314.1214.

IR (thin film, ν_{max} /cm^{-1}) 2939, 1615, 1515, 1458, 1304, 1252, 1208, 1177, 1076, 1034, 994, 831, 780, 743.

minor

^{1}H NMR (600 MHz, $CDCl_3$) δ 7.24 – 7.20 (m, 2H, C(2)*H*), 6.93 – 6.89 (m, 2H, C(1)*H*), 5.17 (d, *J* = 2.9 Hz, 1H, C(4)*H*), 4.19 (q, *J* = 5.7 Hz, 1H, C(6)*H*), 3.81 (s, 3H, C(12)*H*), 2.25 – 2.16 (m, 1H, C(7)H_a), 1.97 (ddt, *J* = 14.7, 7.8, 5.4 Hz, 1H, C(7)H_b), 1.85 – 1.75 (m, 3H, , C(10)H_a, C(9)H_a, C(8)H_a), 1.58 – 1.51 (m, 2H, C(9)H_b, C(10)H_b), 1.46 – 1.38 (m, 1H, C(8)H_b), 0.79 (s, 3H, C(11)H_3).

^{13}C NMR (151 MHz, $CDCl_3$) δ 159.7, 128.1, 127.2, 114.0, 75.6, 70.2 (d, *J* = 2.4 Hz), 55.4, 39.5, 32.9, 24.2, 22.5, 19.0, 17.9.

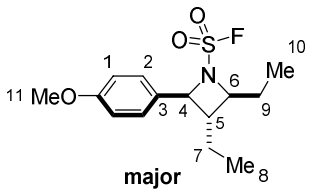
Note: Coupling between Carbon and Fluorine observed.

^{19}F NMR (377 MHz, $CDCl_3$) δ 52.39 (s).

HRMS (ESI) *m/z* $C_{15}H_{21}FNO_3S^+$ requires 314.1221 ($[M+H]^+$), found 314.1223.

IR (thin film, ν_{max} /cm^{-1}) 2959, 2873, 1615, 1516, 1416, 1254, 1206, 1036, 912, 836, 737, 616.

(2*S,3*S**,4*S**)-2,3-diethyl-4-(4-methoxyphenyl)azetidine-1-sulfonyl fluoride (*Z*-4ab)**



Prepared according to **GP1** using (4-methoxybenzylidene)sulfamoyl fluoride (**1a**) (43.4 mg, 0.20 mmol, 1.0 equiv.), 3-F-TX (4.6 mg, 0.020 mmol, 10 mol%) and Z-hex-3-ene (0.25 ml, 2.0 mmol, 10 equiv.) in $(CH_2Cl)_2$ (1.0 ml, 0.20 M). ^{19}F NMR analysis of the crude reaction mixture revealed a diastereomer ratio of 10:1.4:1:0. Purification by flash column chromatography (0 – 2% Et_2O in pentane) afforded 7.6:1 mixture of 2*S**,3*S**,4*S**)-2,3-diethyl-4-(4-methoxyphenyl)azetidine-1-sulfonyl fluoride (**4ab**) and (2*S**,3*R**,4*S**)-2,3-diethyl-4-(4-methoxyphenyl)azetidine-1-sulfonyl fluoride (**4ab'**) (38.3 mg, 64%) as a colourless oil and (2*R**,3*R**,4*S**)-2,3-diethyl-4-(4-methoxyphenyl)azetidine-1-sulfonyl fluoride as a colourless oil (**4ab''**) 6.5 mg, 11%).

Prepared according to **GP1** using (4-methoxybenzylidene)sulfamoyl fluoride (**1**) (43.4 mg, 0.20 mmol, 1.0 equiv.), 3-F-TX (4.6 mg, 0.020 mmol, 10 mol%) and E-hex-3-ene (0.25 ml, 2.0 mmol, 10 equiv.) in $(CH_2Cl)_2$ (1.0 ml, 0.20 M). ^{19}F NMR analysis of the crude reaction mixture revealed a diastereomer ratio of 7.4:1:2.5:0. Purification by flash column chromatography (0 – 2% Et_2O in pentane) afforded afforded (2*S**,3*S**,4*S**)-2,3-diethyl-4-(4-methoxyphenyl)azetidine-1-sulfonyl fluoride (**4ab**) (16.1 mg, 27%) and a 3:2:1 mixture of (2*R**,3*R**,4*S**)-2,3-diethyl-4-(4-methoxyphenyl)azetidine-1-sulfonyl fluoride (**4ab''**), (2*S**,3*R**,4*S**)-2,3-diethyl-4-(4-methoxyphenyl)azetidine-1-sulfonyl

fluoride and (2*S**,3*S**,4*S**)-2,3-diethyl-4-(4-methoxyphenyl)azetidine-1-sulfonyl fluoride (**4ab'**) (13.2 mg, 22%).

Characterisation is given for the major diastereomer only.

major

R_f(4% Et_2O in pentane) = 0.33.

^{1}H NMR (400 MHz, $CDCl_3$) δ 7.37 – 7.32 (m, 2H, C(2)*H*), 6.93 – 6.89 (m, 2H, C(1)*H*), 4.77 (dd, *J* = 7.0, 1.6 Hz, 1H, C(4)*H*), 3.97 (tdd, *J* = 7.1, 4.8, 1.5 Hz, 1H, C(6)*H*), 3.81 (s, 3H, C(11)H_3), 2.21 (p, *J* = 7.2 Hz, 1H, C(5)*H*), 2.05 – 1.93 (m, 1H, C(9)H_a), 1.93 – 1.81 (m, 1H, C(9)H_b), 1.78 – 1.65 (m, 2H, C(7)H_2), 1.02 (t, *J* = 7.5 Hz, 3H, C(10)H_3), 0.90 (t, *J* = 7.4 Hz, 3H, C(8)H_3).

^{13}C NMR (101 MHz, $CDCl_3$) δ 159.9, 131.1, 128.0, 114.3, 70.7, 69.7, 55.4, 47.7, 28.1, 26.7, 11.2, 9.0.

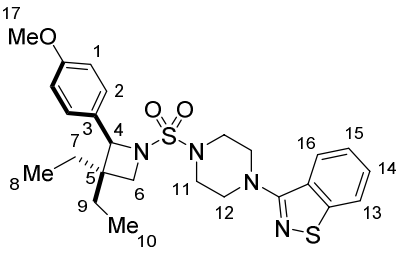
^{19}F NMR (377 MHz, $CDCl_3$) δ 31.40(s).

HRMS (ESI) *m/z* $C_{14}H_{21}FNO_3S^+$ requires 302.1221 ($[M+H]^+$), found 302.1231.

IR (thin film, ν_{max} /cm^{-1}) 2695, 2935, 1615, 1517, 1463, 1421, 1254, 1209, 1037, 840, 740.

5.2.4 Product Derivatisation

(*R)-3-(4-((3,3-Diethyl-2-(4-methoxyphenyl)azetidin-1-yl)sulfonyl)piperazin-1-yl)benzo[d]isothiazole (6)**



A solution of (*R**)-3,3-diethyl-2-(4-methoxyphenyl)azetidine-1-sulfonyl fluoride (**2a**) (0.50 ml, 0.20 M, 0.10 mmol, 1.0 equiv.) in *t*-amylOH was added to a vial containing 3-(piperazin-1-yl)benzo[d]isothiazole (43.9 mg, 0.20 mmol, 2.0 equiv.) and $Ca(NTf_2)_2$ (60.0 mg, 0.10 mmol, 1.0 equiv.) under N_2. The reaction was then heated at 90 °C for 20 h and then cooled to rt, diluted with EtOAc and partitioned over brine. The combined organic fractions were dried over anhydrous $MgSO_4$, filtered and concentrated under reduced pressure. Purification by flash column chromatography (0 – 5% Et_2O in pentane) afforded (*R**)-3-(4-((3,3-diethyl-2-(4-methoxyphenyl)azetidin-1-yl)sulfonyl)piperazin-1-yl)benzo[d]isothiazole (**6**) as a colourless oil (34.3 mg, 68%).

R_f (10% EtOAc in pentane) = 0.26.

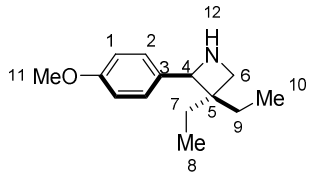
^{1}H NMR (400 MHz, $CDCl_3$) δ 7.81 (d, *J* = 8.1 Hz, 1H, C(13)*H* or C(16)*H*), 7.78 (d, *J* = 8.2 Hz, 1H, C(13)*H* or C(16)*H*), 7.47 (t, *J* = 7.5 Hz, 1H, C(14)*H* or C(15)*H*), 7.36 (t, *J* = 7.6 Hz, 1H, C(14)*H* or C(15)*H*), 7.32 (dd, *J* = 7.7, 5.7 Hz, 2H, C(2)*H*), 6.87 (d, *J* = 8.5 Hz, 2H, C(1)*H*), 4.94 (s, 1H, C(4)*H*), 3.77 (s, 3H, C(17)*H*), 3.75 (d, *J* = 7.7 Hz, 1H, C(6)H_a), 3.46 – 3.41 (m, 5H, C(6)H_b, C(11)H_2), 3.40 – 3.26 (m, 4H, C(12)H_2), 1.75 (dq, *J* = 14.5, 7.3 Hz, 1H, C(7)H_a), 1.71 (dq, *J* = 14.5, 7.3 Hz, 1H, C(7)H_b), 1.46 (dq, *J* = 14.6, 7.3 Hz, 1H, C(9)H_a), 1.17 (dq, *J* = 14.5, 7.3 Hz, 1H, C(9)H_b), 0.87 (t, *J* = 7.4 Hz, 3H, C(8)H_3), 0.55 (t, *J* = 7.4 Hz, 3H, C(10)H_3).

^{13}C NMR (101 MHz, $CDCl_3$) δ 163.2, 159.4, 152.9, 129.8, 128.8, 127.9, 127.8, 124.2, 123.7, 120.8, 113.7, 73.2, 58.7, 55.4, 49.7, 45.7, 42.5, 29.3, 24.5, 8.0, 7.5.

HRMS (ESI) *m/z*; $C_{25}H_{32}N_4O_3S_2Na$ requires 523.1808 ($[M+Na]^+$), found 523.1834.

IR (thin film, ν_{max} /cm^{-1}) 2963, 2878, 1734, 1613, 1513, 1494, 1423, 1250, 1158, 1070, 946, 911, 838, 763, 741, 648.

(*R)-3,3-Diethyl-2-(4-methoxyphenyl)azetidine (7)**



Sodium bis(2-methoxyethoxy)aluminium hydride (0.14 ml, 0.5 mmol, 60 wt% in toluene, 5.0 equiv.) was added to a stirred solution of (*R**)-3,3-diethyl-2-(4-methoxyphenyl)azetidine-1-sulfonyl fluoride (**3a**) (30.1 mg, 0.10 mmol, 1.0 equiv.) in toluene (0.25 ml, 0.40 M). The reaction was stirred at rt for 6 h, then quenched by sequential addition of 1N NaOH and brine. The product was extracted with Et_2O three times and the combined organic layers were dried over anhydrous $MgSO_4$, filtered and concentrated under reduced pressure to afford (*R**)-3,3-diethyl-2-(4-methoxyphenyl)azetidine (**5**) as a colourless oil (20.8 mg, 95%).

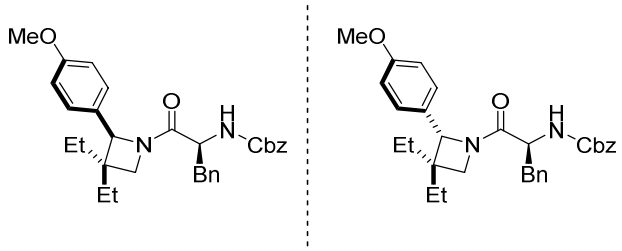
^{1}H NMR (600 MHz, $CDCl_3$) δ 7.34 – 7.28 (m, 2H, C(2)*H*), 6.89 – 6.83 (m, 2H, C(1)*H*), 4.67 (s, 1H, C(4)*H*), 3.80 (s, 3H, C(11)H_3), 3.37 (dd, *J* = 7.2, 0.9 Hz, 1H, C(6)H_a), 3.11 (d, *J* = 7.1 Hz, 1H, C(6)H_b), 2.30 – 2.12 (m, 1H, N(12)*H*), 1.74 (dq, *J* = 14.9, 7.5 Hz, 1H, C(7)H_a), 1.65 (dq, *J* = 14.9, 7.5 Hz, 1H, C(7)H_b), 1.44 (dq, *J* = 14.9, 7.5 Hz, 1H, C(9)H_a) 1.15 (dq, *J* = 14.6, 7.3 Hz, 1H, C(9)H_b), 0.88 (t, *J* = 7.5 Hz, 3H, C(8)H_3), 0.54 (t, *J* = 7.5 Hz, 3H, C(10)H_3).

^{13}C NMR (151 MHz, $CDCl_3$) δ 158.6, 134.0, 128.3, 113.4, 68.8, 55.4, 53.7, 47.3, 29.9, 24.4, 8.5, 7.5;

HRMS (ESI) *m/z*; $C_{14}H_{22}NO$ requires 220.1696 ($[M+H]^+$), found 220.1690.

IR (thin film, ν_{max} /cm^{-1}) 2964, 2937, 2863, 1614, 1515, 1459, 1423, 1301, 1251, 1213, 1180, 1037, 835, 743, 623.

Benzyl ((*S)-1-((*R**)-3,3-diethyl-2-(4-methoxyphenyl)azetidin-1-yl)-1-oxo-3-phenylpropan-2-yl)carbamate (8) and Benzyl ((*S**)-1-((*S**)-3,3-diethyl-2-(4-methoxyphenyl)azetidin-1-yl)-1-oxo-3-phenylpropan-2-yl)carbamate (8')**



Sodium bis(2-methoxyethoxy)aluminium hydride (0.14 ml, 0.50 mmol, 60 wt% in toluene, 5.0 equiv.) was added to a stirred solution of (*R**)-3,3-diethyl-2-(4-methoxyphenyl)azetidine-1-sulfonyl fluoride (**2a**) (30.1 mg, 0.10 mmol, 1.0 equiv.) in toluene (0.25 ml, 0.40 M). The reaction was stirred at rt for 6 h. The reaction was then quenched by sequential addition of 1N NaOH and brine. The reaction mixture was extracted with Et_2O three times and the combined organic layers were dried over anhydrous $MgSO_4$, filtered and concentrated under reduced pressure. The crude residue dissolved in DMF (0.25 ml) and added as a solution to a separate solution of HATU (84 mg, 0.22 mmol, 2.2 equiv.), DIPEA (58 µl, 0.33 mmol, 3.3 equiv.) and Z-Phe-OH (33 mg , 0.11 mmol, 1.1 equiv.) in DMF. The reaction was stirred at rt for 16 h, then diluted with water and extracted with EtOAc three times. The combined organic layers were dried over anhydrous $MgSO_4$, filtered and concentrated under reduced pressure. Purification by flash column chromatography (0 – 30% EtOAc in pentane) afforded an

inseparable mixture of diastereomers benzyl ((*S**)-1-((*R**)-3,3-diethyl-2-(4-methoxyphenyl)azetidin-1-yl)-1-oxo-3-phenylpropan-2-yl)carbamate (**8**) and benzyl ((*S**)-1-((*R**)-3,3-diethyl-2-(4-methoxyphenyl)azetidin-1-yl)-1-oxo-3-phenylpropan-2-yl)carbamate (**8'**) as a colourless oil (43.4 mg, 87%).

Mixture of 2 diastereomers each having 2 rotamers.

R_f (20% EtOAc in pentane) = 0.16.

^{1}H NMR (600 MHz, $CDCl_3$) δ 7.42 – 7.22 (m, 32H), 7.20 (dd, *J* = 13.1, 7.6 Hz, 2H), 7.11 (dt, *J* = 14.7, 7.2 Hz, 3H), 7.00 (d, *J* = 8.3 Hz, 2H), 6.90 (d, *J* = 8.2 Hz, 3H), 6.81 (t, *J* = 8.3 Hz, 4H), 6.76 (d, *J* = 8.2 Hz, 1H), 6.67 (d, *J* = 8.2 Hz, 1H), 6.61 (d, *J* = 7.2 Hz, 2H), 5.59 (t, *J* = 9.7 Hz, 2H), 5.56 (d, *J* = 7.0 Hz, 1H), 5.31 (s, 1H), 5.24 (d, *J* = 8.6 Hz, 1H), 5.15 (s, 1H), 5.03 (d, *J* = 12.5 Hz, 1H), 5.00 (s, 3H), 4.93 (s, 1H), 4.75 (s, 1H), 4.63 (td, *J* = 9.2, 5.5 Hz, 1H), 4.48 (td, *J* = 9.5, 5.4 Hz, 1H), 4.17 (td, *J* = 9.1, 4.9 Hz, 1H), 4.06 (d, *J* = 10.2 Hz, 2H), 3.85 (s, 1H), 3.83 (s, 3H), 3.78 (s, 4H), 3.76 (s, 3H), 3.69 (d, *J* = 8.0 Hz, 1H), 3.63 (d, *J* = 9.8 Hz, 1H), 3.55 (d, *J* = 9.8 Hz, 1H), 3.40 (d, *J* = 9.8 Hz, 1H), 3.29 (d, *J* = 8.1 Hz, 1H), 3.10 (dd, *J* = 13.2, 5.5 Hz, 1H), 3.00 (tt, *J* = 12.4, 8.0 Hz, 3H), 2.83 (dd, *J* = 22.4, 10.2 Hz, 2H), 2.77 – 2.71 (m, 2H), 2.58 (dd, *J* = 13.8, 9.5 Hz, 1H), 1.81 (s, 1H), 1.75 (h, *J* = 7.0 Hz, 2H), 1.66 (q, *J* = 7.4 Hz, 1H), 1.42 (dq, *J* = 14.4, 7.3 Hz, 1H), 1.26 (s, 4H), 1.21 – 1.08 (m, 2H), 0.97 (dq, *J* = 13.3, 6.9 Hz, 1H), 0.91 (t, *J* = 7.3 Hz, 3H), 0.87 (t, *J* = 7.6 Hz, 2H), 0.86 – 0.79 (m, 1H), 0.72 (t, *J* = 7.4 Hz, 3H), 0.62 (t, *J* = 7.3 Hz, 4H), 0.55 (t, *J* = 7.4 Hz, 3H), 0.46 (t, *J* = 7.5 Hz, 6H), 0.43 (d, *J* = 7.4 Hz, 2H).

Note: too complex to assign.

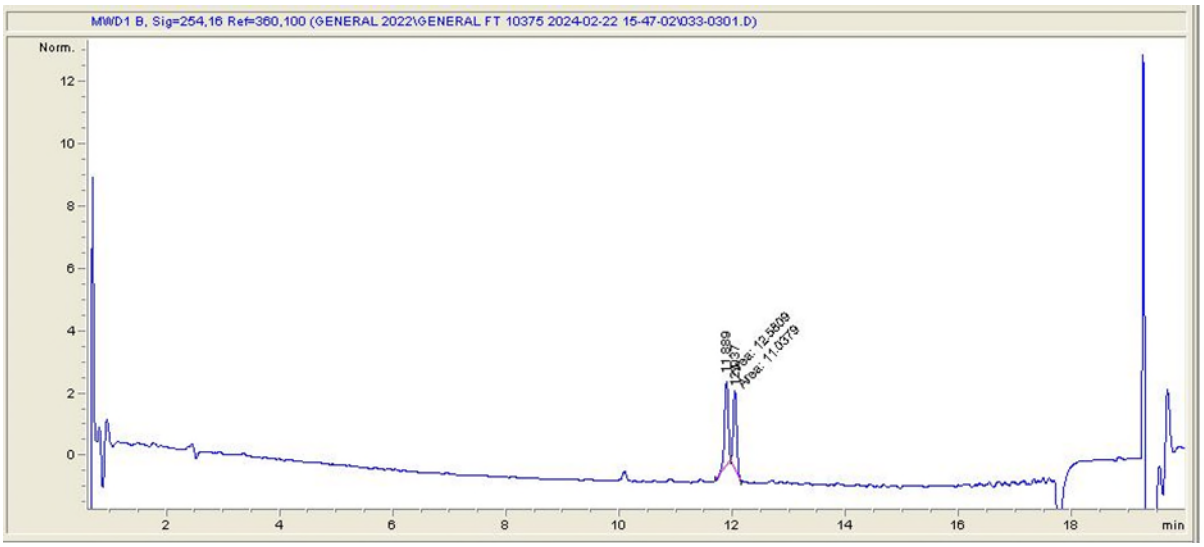
^{13}C NMR (151 MHz, $CDCl_3$) δ 173.7, 171.8, 171.6, 170.8, 159.5, 159.3, 158.8, 155.9, 155.8, 154.9, 137.0, 136.8, 136.6, 136.6, 136.6, 136.5, 136.5, 136.5, 136.4, 136.3, 130.0,

129.7, 129.5, 129.2, 128.8, 128.8, 128.8, 128.7, 128.6, 128.6, 128.5, 128.4, 128.2, 128.1, 128.0, 127.9, 127.8, 127.7, 127.4, 127.2, 127.1, 127.1, 126.7, 114.2, 114.0, 113.7, 113.6, 73.6, 72.3, 70.7, 70.6, 67.0, 66.9, 66.8, 66.5, 59.2, 58.3, 56.7, 56.4, 55.5, 55.3, 55.3, 54.2, 53.7, 52.6, 52.5, 51.8, 51.7, 43.1, 42.7, 42.5, 42.3, 41.2, 40.3, 39.6, 39.5, 38.1, 29.8, 29.3, 28.9, 28.8, 24.5, 24.3, 24.0, 24.0, 8.1, 8.1, 8.0, 8.0, 7.5, 7.4, 7.2.

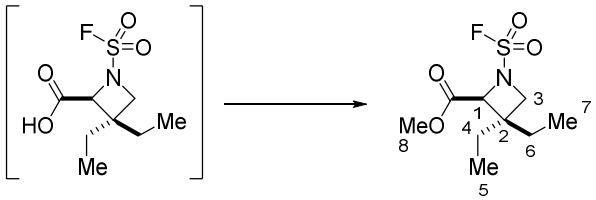
HRMS (ESI) m/z; $C_{31}H_{36}N_2O_4$ requires 501.2748 ($[M+H]^+$), found 501.2752.

IR (thin film, ν_{max} /cm^{-1}) 3271, 2964, 2876, 1719, 1648, 1514, 1456, 1251, 1177, 1033, 838, 741, 701.

HPLC(retention time) 11.9 and 12.0 minutes.



Methyl (*S)-3,3-diethyl-1-(fluorosulfonyl)azetidine-2-carboxylate (9)**



(*R**)-3,3-diethyl-2-(4-methoxyphenyl)azetidine-1-sulfonyl fluoride (**2a**) (60.3 mg, 0.2 mmol, 1.0 equiv.) was dissolved in a mixture of MeCN and EtOAc (1:1, 2.0 ml total, 0.10

M). This mixture was added to a suspension of $NaIO_4$ (830 mg, 3.80 mmol, 19.4 equiv.) in H_2O (3.0 ml) and cooled to 10 °C to which the solution of sulfamoyl fluoride was added to. $RuCl_3 \cdot xH_2O$ (2.5 mg, 0.012 mmol, 6 mol%) was then added in one portion and the solution turned dark brown. After 1 h, the reaction was slowly warmed to rt and further stirred for 2h, at which point the solution turned pale yellow. The resulting thick suspension was decanted and the white residue washed with copious EtOAc. Et_2O (5 ml) was added to the combined organic fractions and, this solution was stirred for a further 30 minutes turning the reaction mixture from pale-yellow solution to dark brown. The suspension was then filtered through Celite and washed with EtOAc. The filtrate was washed with 20% NaCl solution, dried over anhydrous $MgSO_4$, filtered and concentrated under reduced pressure to give the crude acid **9'**.

$TMSCH_2N_2$ (0.13 ml, 0.26 mmol, 2.0 M in hexane, 1.3 equiv.) was added to a solution of acid in a 4:1 mixture of toluene and MeOH (2.0 ml total, 0.10 M). The reaction was stirred for 30 minutes at rt and subsequently quenched with 10% v/v AcOH in water. The phases were then partitioned and the aqueous phase was washed with Et_2O thrice. The combined organic fractions were washed with aq. sat. $NaHCO_3$, dried over anhydrous $MgSO_4$ and concentrated under reduced pressure. Purification by flash column chromatography (0 – 5% Et_2O in pentane) afforded methyl (*S**)-3,3-diethyl-1-(fluorosulfonyl)azetidine-2-carboxylate (**9**) as a colourless oil (23.6 mg, 47%).

R_f (5% Et_2O in pentane) = 0.25.

^{1}H NMR (400 MHz, $CDCl_3$) δ 4.58 (d, *J* = 2.4 Hz, 1H, C(1)*H*), 3.80 (s, 3H, C(8)*H*), 3.78 (app. t, *J* = 2.0 Hz, 2H, C(3)H_2), 1.81 – 1.70 (m, 2H, C(4)H_2), 1.68 – 1.57 (m, 2H, C(6)H_2), 0.95 (t, *J* = 7.5 Hz, 3H, C(5)H_3), 0.80 (t, *J* = 7.4 Hz, 3H, C(7)H_3).

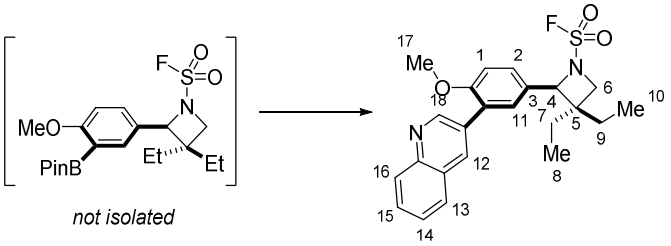
^{13}C NMR (101 MHz, $CDCl_3$) δ 167.7, 70.6, 60.0, 52.6, 43.2, 28.9, 23.8, 7.8, 7.4.

^{19}F NMR (377 MHz, $CDCl_3$) δ 36.13 (s).

HRMS (ESI) *m/z* $C_9H_{16}FNO_4SNa$ requires 276.0676 ($[M+Na]^+$), found 276.0686.

IR (thin film, ν_{max} /cm^{-1}) 2974, 1762, 1740, 1460, 1429, 1294, 1221, 1116, 758, 625.

(*R)-3,3-Diethyl-2-(4-methoxy-3-(quinolin-3-yl)phenyl)azetidine-1-sulfonyl fluoride (10)**



Prepared according to a modification of **GP1** using (4-methoxybenzylidene)sulfamoyl fluoride (**1a**) (43.4 mg, 0.20 mmol, 1.0 equiv.), 3-F-TX (4.6 mg, 0.020 mmol, 0.10 equiv.) and 2-ethyl-1-butene (241 µL, 2.0 mmol, 10 equiv.) in $(CH_2Cl)_2$ (1.0 mL, 0.20 M). Following the photochemical reaction, the mixture was transferred to a round bottom flask and concentrated under reduced pressure. $Pd(PPh_3)_4$ (4.6 mg, 0.004 mmol, 2 mol%), 3-bromoquinoline (42 µL, 0.3 mmol, 1.5 equiv.) and K_2CO_3 (415 mg, 3.0 mmol, 15 equiv.) was added to the crude reaction mixture and the vial was capped with a septum. A 2:1 MeCN/H_2O mixture was added *via* syringe (3.0 ml total, 0.067 M) and the flask was sparged with N_2 for ten minutes, then heated at 80 °C for 16 h. The reaction was then cooled to rt, filtered through celite and the filtrate was washed with aq. sat. $NaHCO_3$. The aqueous phase was then washed with EtOAc three times and the combined organic layers were dried over anhydrous $MgSO_4$, filtered and then concentrated under reduced pressure. Purification by flash column chromatography (0 – 40% Et_2O in pentane) to give

(*R**)-3,3-diethyl-2-(4-methoxy-3-(quinolin-3-yl)phenyl)azetidine-1-sulfonyl fluoride (**9**) as a mixture with pinacol.

To remove pinacol the residue obtained was redissolved in a 1:1 mixture of MeOH/H_2O (10 ml) and concentrated under reduced pressure. This process was repeated a further 4 times to remove all pinacol *via* azeotropic evaporation. This afforded (*R**)-3,3-diethyl-2-(4-methoxy-3-(quinolin-3-yl)phenyl)azetidine-1-sulfonyl fluoride (**10**) as a yellow solid (39.8 mg, 46%).

R_f (50% Et_2O in pentane) = 0.34.

^{1}H NMR δ 9.11 (s, 1H, C(18)*H*), 8.25 (d, *J* = 2.3 Hz, 1H, C(12)*H*), 8.14 (d, *J* = 8.4 Hz, 1H, C(13)*H* or C(16)*H*), 7.87 (d, *J* = 8.1 Hz, 1H, C(13)*H* or C(16)*H*), 7.76 – 7.69 (m, 1H, C(14)*H* or C(15)*H*), 7.59 – 7.53 (m, 1H, C(14)*H* or C(15)*H*), 7.41 (dd, *J* = 8.5, 2.3 Hz, 1H, C(2)*H*), 7.38 (d, *J* = 2.3 Hz, 1H, C(11)*H*), 7.04 (d, *J* = 8.5 Hz, 1H, C(1)*H*), 3.87 (d, *J* = 8.0 Hz, 1H, C(6)H_a), 3.85 (s, 3H, C(17)H_3), 3.75 (d, *J* = 7.9 Hz, 1H, C(6)H_b), 1.82 (dq, *J* = 14.6, 7.3 Hz, 1H, C(7)H_a), 1.77 (dq, *J* = 14.6, 7.4 Hz, 1H, C(7)H_b), 1.46 (dq, *J* = 14.5, 7.3 Hz, 1H, C(9)H_a), 1.28 – 1.20 (m, 1H, C(9)H_a), 0.96 (t, *J* = 7.4 Hz, 3H, C(8)H_3), 0.63 (t, *J* = 7.4 Hz, 3H, C(10)H_3).

^{13}C NMR (151 MHz, $CDCl_3$) δ 156.8, 152.0, 147.1, 135.7, 131.4, 129.5, 129.4, 129.3, 128.2, 128.1, 127.9, 127.2, 126.8, 111.3, 75.1, 60.0, 55.8, 43.8, 29.2, 24.5, 8.2, 7.4.

^{19}F NMR (565 MHz, $CDCl_3$) δ 31.42 (s).

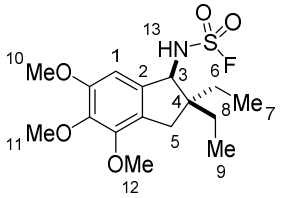
HRMS (ESI) *m/z* $C_{23}H_{26}FN_2O_3S$ requires 429.1643 ($[M+H]^+$), found 429.1647.

IR (thin film, ν_{max} /cm^{-1}) 2966, 1505, 1463, 1421, 1255, 1213, 1179, 1028, 742, 643, 622.

m.p. 120 – 122 °C.

5.2.5 Indane Preparation

(*S)-(2,2-diethyl-4,5,6-trimethoxy-2,3-dihydro-1H-inden-1-yl)sulfamoyl fluoride (12)**



Prepared according to GP1 using (3,4,5-trimethoxybenzylidene)sulfamoyl fluoride **11** (55.5 mg, 0.20 mmol, 1.0 equiv.), ITX (5.3 mg, 0.020 mmol, 0.10 equiv.), 3-methylene pentane (240 µl, 2.0 mmol, 10 equiv.) in $(CH_2Cl)_2$ (1.0 ml, 0.20 M). Purification by flash column chromatography (50 – 100% CH_2Cl_2 in pentane to 4% Et_2O in CH_2Cl_2) afforded (*S**)-(2,2-diethyl-4,5,6-trimethoxy-2,3-dihydro-1H-inden-1-yl)sulfamoyl fluoride **12** as a white crystalline solid (26.0 mg, 36%).

R_f (20% Et_2O in pentane) = 0.23.

^{1}H NMR (600 MHz, $CDCl_3$) δ 6.64 (s, 1H, C(1)*H*), 5.40 (dd, *J* = 9.8, 5.4 Hz, 1H, C(3)*H*), 4.72 (d, *J* = 9.7 Hz, 1H, N(13)*H*), 3.85 (s, 3H, C(10)H_3 or C(11)H_3 or C(12)H_3)), 3.83 (s, 3H, C(10)H_3 or C(11)H_3 or C(12)H_3), 3.82 (s, 3H, C(10)H_3 or C(11)H_3 or C(12)H_3), 2.68 (d, *J* = 16.0 Hz, 1H, C(5)H_a), 2.64 (d, *J* = 16.1 Hz, 1H, C(5)H_b), 1.62 (dq, *J* = 14.9, 7.5 Hz, 1H, C(6)H_a), 1.53 – 1.44 (m, 3H, , C(6)H_b, C(8)H_2), 0.91 (t, *J* = 7.4 Hz, 3H, C(7)H_3), 0.89 (t, *J* = 7.4 Hz, 3H, C(9)H_3).

^{13}C NMR (151 MHz, $CDCl_3$) δ 153.5, 149.5, 141.8, 135.8, 126.2, 103.2, 66.6, 61.1, 60.5, 56.1, 49.6, 37.8, 28.8, 25.7, 8.8, 8.6.

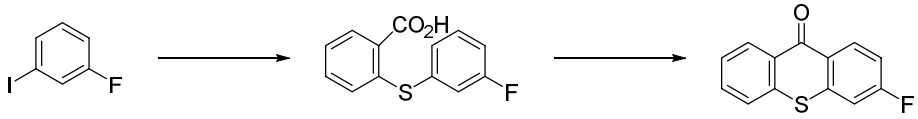
^{19}F NMR (377 MHz, $CDCl_3$) δ 55.36.

HRMS (ESI) *m/z* $C_{16}H_{23}FNO_5S$ requires 360.1286 ($[M-H]^-$), found 360.1272.

IR (thin film, ν_{max} /cm^{-1}) 3174.7, 2967.3, 2942.3, 1605.3, 1472.3, 1400.0, 1340.6, 1210.4, 1120.0, 1034.0, 760.6.

5.2.6 Photocatalyst Preparation

2-((3-fluorophenyl)thio)benzoic acid (37) and 3-fluoro-9H-thioxanthen-9-one (3-F-TX)



2-((3-fluorophenyl)thio)benzoic acid (37): 1-fluoro-3-iodobenzene (0.64 ml, 5.5 mmol, 1.1 equiv.) was added to a solution of thiosalicylic acid (771 mg, 5.0 mmol, 1.0 equiv.), K_2CO_3 (760 mg, 5.5 mmol, 1.1 equiv.) and CuI (95.3 mg, 0.5 mmol, 0.1 equiv.) in DMF (7.5 ml, 0.67 M) under N_2. The reaction was heated at 145 °C for 1 h, following this the reaction mixture was cooled to rt and poured over water. The aqueous mixture was filtered through Celite® and acidified with 1N HCl, the resulting precipitate was isolated by filtration, washed with water and dried under vacuum to give as 2-((3-fluorophenyl)thio)benzoic acid (**37**) and white solid (1.08 g, 87%).

R_f (40% EtOAc in petrol) = 0.39.

^{1}H NMR (400 MHz, DMSO) δ 13.28 (s, 1H, CO_2H), 7.91 (d, *J* = 7.7 Hz, 1H, Ar*H*), 7.53 (td, *J* = 8.1, 6.2 Hz, 1H, Ar*H*), 7.43 – 7.22 (m, 5H, Ar*H*), 6.84 (d, *J* = 8.0 Hz, 1H, Ar*H*).

^{19}F NMR (377 MHz, DMSO) δ -109.77 – -114.09 (m).

HRMS (ESI) *m/z* $C_{13}H_8FO_2S$ requires 247.0234 ($[M-H]^-$), found 247.0243.

3-fluoro-9H-thioxanthen-9-one (3-F-TX): Oxalyl chloride (0.37 ml, 4.34 mmol, 1.2 equiv.) was added to a stirred solution of 2-((3-fluorophenyl)thio)benzoic acid (**37**) (900 mg, 3.62 mmol, 1.0 equiv.) in CH_2Cl_2 (8 ml, 0.5 M) with a 4 drops of DMF added. When the reaction had reached full conversion as indicated by TLC analysis after 3 h (the reaction mixture was homogenous). The solvent was removed by sparging the reaction mixture with N_2 and the residue was redissolved in CH_2Cl_2 (12 ml, 0.3M) and cooled to 0 °C. $AlCl_3$ (579 mg, 4.34 mmol, 1.2 equiv.) was added in portion to the reaction and stirred for 1 h. The reaction was quenched with water and aqueous layer was extracted thrice with CH_2Cl_2, the combined organic extracts was washed with aq. sat. $NaHCO_3$, dried over anhydrous $MgSO_4$, filtered and concentrated under reduced pressure. Purification by flash column chromatography (60 – 80% toluene in petrol) afforded 3-fluoro-9H-thioxanthen-9-one (3-F-TX) as a white solid (646 mg, 77%).

R_f (60% PhMe in petrol) = 0.33.

^{1}H NMR (400 MHz, $CDCl_3$) δ 8.62 (dd, *J* = 9.0, 6.0 Hz, 1H, Ar*H*), 8.59 (ddd, *J* = 8.1, 1.6, 0.6 Hz, 1H, Ar*H*), 7.61 (ddd, *J* = 8.4, 7.0, 1.5 Hz, 1H, Ar*H*), 7.53 (ddd, *J* = 8.1, 1.2, 0.6 Hz, 1H, Ar*H*), 7.48 (ddd, *J* = 8.3, 7.0, 1.3 Hz, 1H, Ar*H*), 7.23 (dd, *J* = 8.7, 2.5 Hz, 1H, Ar*H*), 7.17 (ddd, *J* = 9.0, 8.0, 2.5 Hz, 1H, Ar*H*).

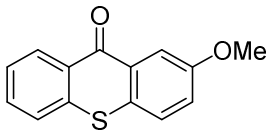
^{13}C NMR (101 MHz, $CDCl_3$) δ 179.0, 164.7 (d, *J* = 256.7 Hz), 139.7 (d, *J* = 10.1 Hz), 136.8, 133.2 (d, *J* = 10.0 Hz), 132.5, 130.0, 129.2, 126.8, 126.1 (d, *J* = 2.4 Hz), 126.0, 115.0 (d, *J* = 22.5 Hz), 111.9 (d, *J* = 24.6 Hz).

^{19}F NMR (377 MHz, $CDCl_3$) δ -104.89 (td, *J* = 8.6, 5.8 Hz).

HRMS (ESI) *m/z* $C_{13}H_7FOS$ requires 231.0274 ($[M+H]^+$), found 231.0273.

Data consistent with literature.[145]

2-Methoxy-9H-thioxanthen-9-one (2-MeO-TX)



A precatalyst solution of $Pd(OAc)_2$ (9 mg, 0.04 mmol, 2 mol%), *t*-BuBrettPhos (43 mg, 0.088 mmol, 4.4 mol%) and water (1.4 µl, 0.08 mmol, 4 mol%) in 1,4-dioxane (2 ml) was heated to 110 °C under an atmosphere of N_2 for 90 s, at which point the solution goes a dark brown colour. The precatalyst solution was transferred *via* canula to separate solution of 2-chloro-9H-thioxanthen-9-one (493 mg, 2.0 mmol, 1.0 equiv.), NaO*t*-Bu (269 mg, 2.8 mmol, 1.4 equiv.), anhydrous MeOH (0.40 ml, 10 mmol, 5 equiv.) in 1,4-dioxane (2 ml) under N_2. The combined reaction mixture was heated at 80 °C for 20 h. The reaction mixture was then cooled to rt and diluted with EtOAc and concentrated under reduced pressure. Purification by flash column chromatography (0 – 10% EtOAc in petrol) afforded 2-methoxy-9H-thioxanthen-9-one (2-MeO-TX) as a yellow solid (313 mg, 65%).

^{1}H NMR (400 MHz, $CDCl_3$) δ 8.61 (dd, *J* = 8.1, 1.5 Hz, 1H, Ar*H*), 8.05 (d, *J* = 2.9 Hz, 1H, Ar*H*), 7.62 – 7.50 (m, 2H, Ar*H*), 7.49 – 7.41 (m, 2H, Ar*H*), 7.22 (dd, *J* = 8.8, 2.9 Hz, 1H, Ar*H*), 3.92 (s, 3H, OCH_3).

^{13}C NMR (101 MHz, $CDCl_3$) δ 179.7, 158.5, 132.1, 130.3, 129.9, 129.2, 128.7, 127.4, 126.1, 126.1, 122.8, 110.4, 55.8.

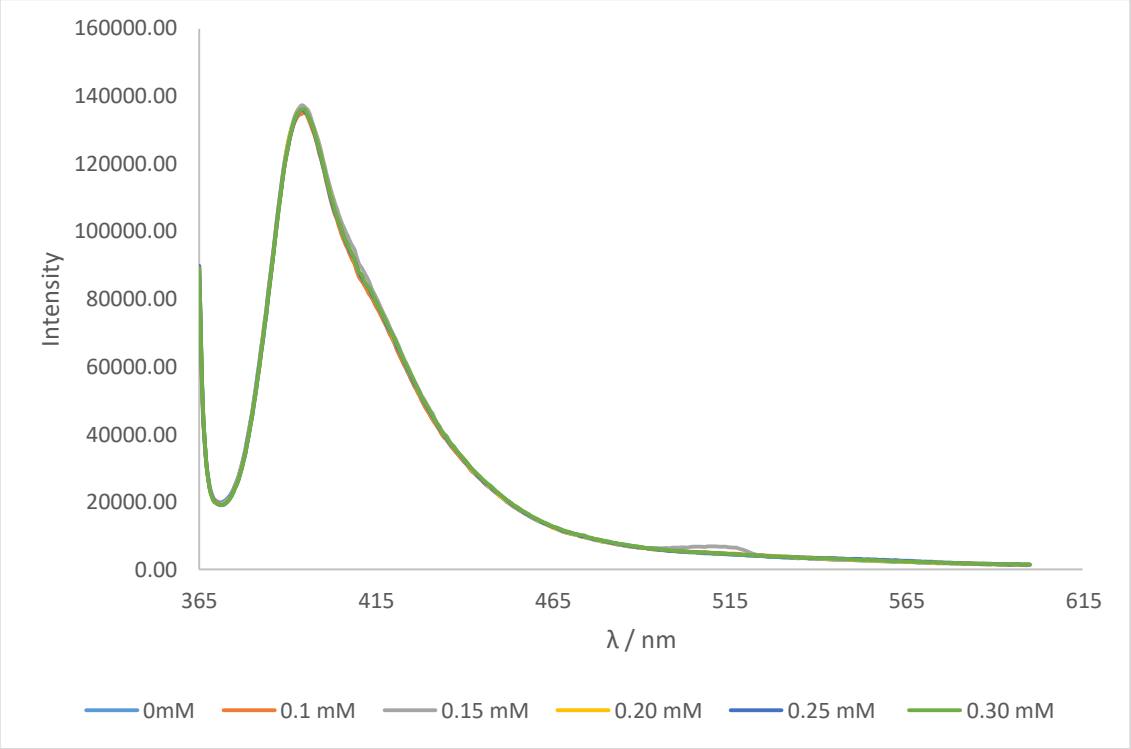
LRMS (ESI) *m/z* 243.0 ($[M+H]^+$).

Data consistent with literature.[214]

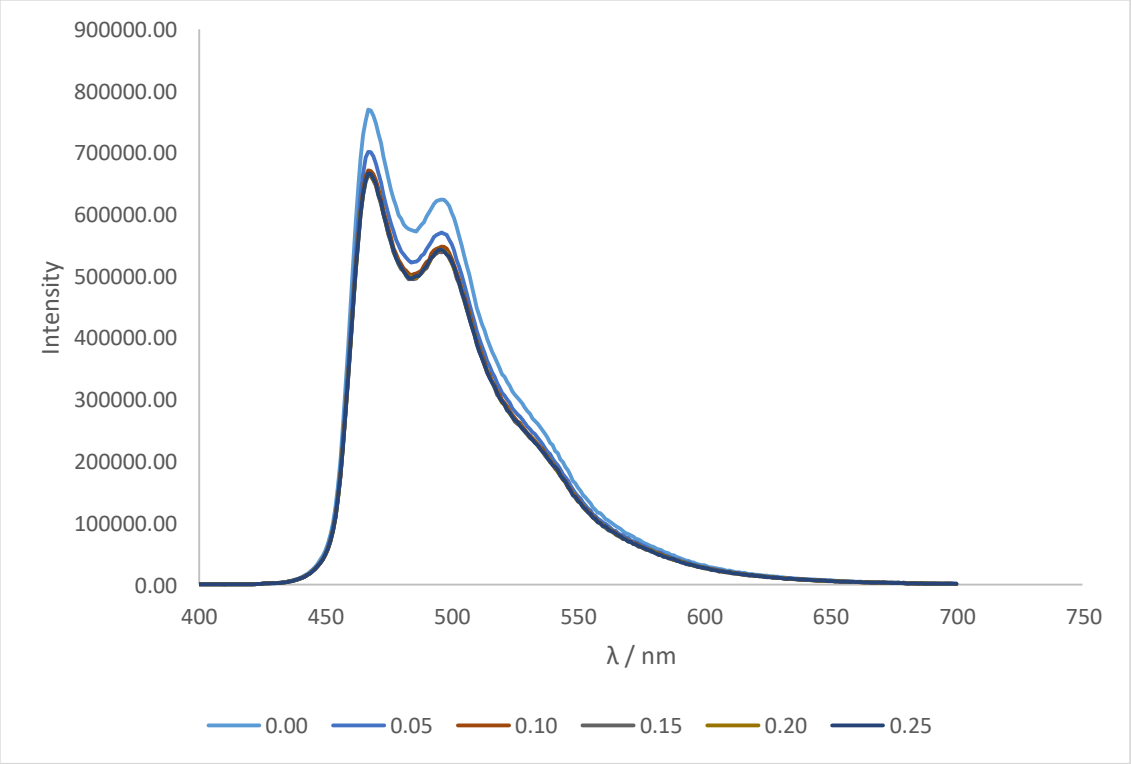
5.2.7 Stern-Volmer Data

Fluorescence spectra were acquired at 298 K using an Edinburgh Instruments FS5 spectrofluorometer operating Fluoracle® software, and equipped with a xenon arc lamp (providing 230–1000 nm excitation range), a thermostatic sample holder (SC-20) and an R13456 PMT detector (200–950 nm spectral coverage, Hamamatsu). Spectroscopic measurements were conducted using quartz cuvettes (10 mm path length, Starna Scientific Ltd).

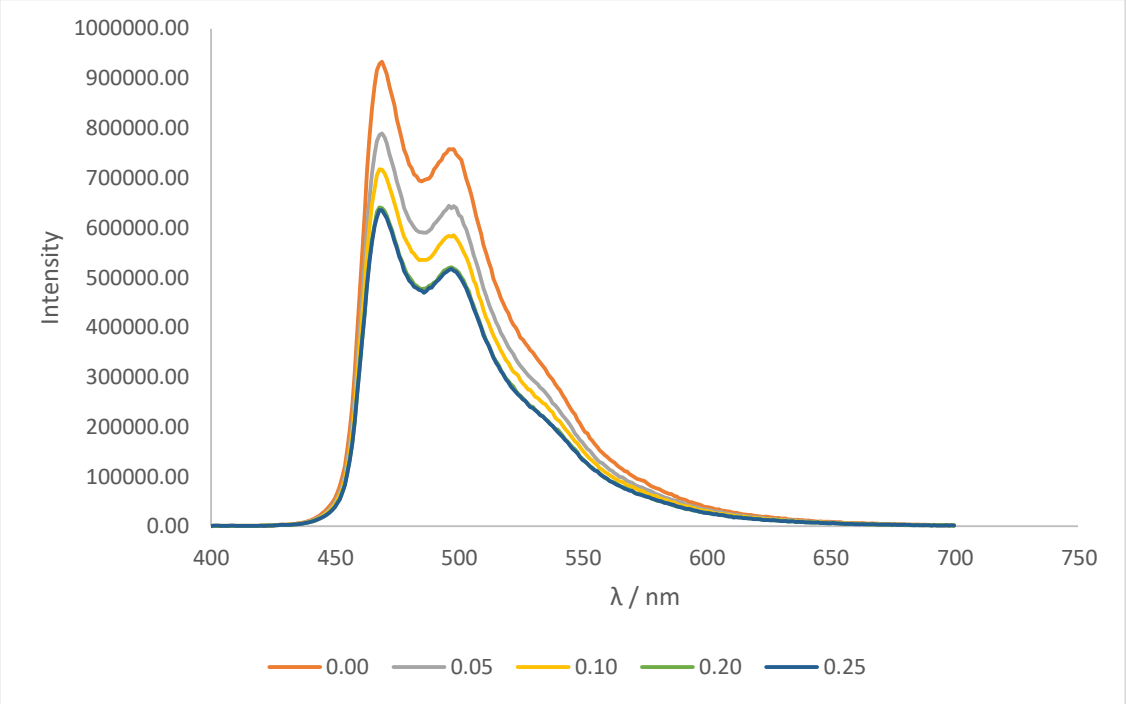
Fluorescence quenching of $[Ir(dFCF_3ppy)_2(dtbbpy)][PF_6]$ was investigated by measuring the measuring the emission spectrum of $[Ir(dFCF_3ppy)_2(dtbbpy)][PF_6]$ in the presence of the reaction components and varying the concentration under an atmosphere of N_2. A solution of $[Ir(dFCF_3ppy)_2(dtbbpy)][PF_6]$ (2 μM) was treated with (0.05 – 0.25 mM) of 3-methylene pentane and 1. The samples were irradiated at 380 nm and luminescence was measured over a range of 365 – 600 nm (at λ_{max} = 496 nm). I/I_0 in the range of 0.00 – 0.25 mM was plotted against the concentration of alkene.



Graph 5-1 Stern-Volmer quenching of 3-F-TX by 3-methylene pentane.



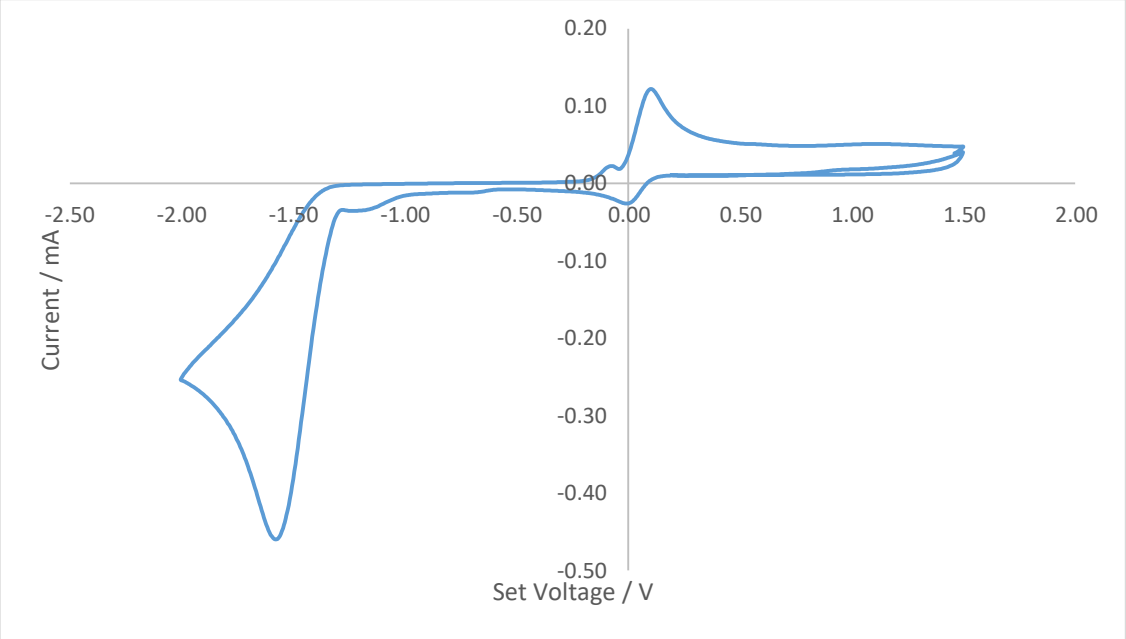
Graph 5-2 Stern-Volmer quenching of [Ir(dFCF$_3$ppy)$_2$dtbbpy][PF$_6$] by 3-methylene pentane.



Graph 5-3 Stern-Volmer quenching of [Ir(dFCF$_3$ppy)$_2$dtbbpy][PF6] by **1a**.

5.2.8 Cyclic Voltammetry

Cyclic voltammetry (CV) measurements were recorded on a Autolab Electrochemical System, using a 3-electrode setup: a glassy carbon working electrode, a platinum wire counter electrode and a Ag|AgNO$_3$ (100 mM in MeCN) reference electrode. Parameters for CV: 50 mVs^{-1} scan rate. Measurements at a concentration of 0.05 M and were performed in MeCN with tetrabutylammonium hexafluorophosphate (Bu_4NPF_6, 0.1 M) as the electrolyte. Sample solutions were deoxygenated by purging with N_2 for 2 – 3 minutes before the measurements. Ferrocene was added after the experiment and the peaks reported are reference to the Fc^+/Fc peak. The reported potentials were taken at the half-height of the cathodic peak of the compounds as all redox processes were irreversible.



Graph 5-4 Cyclic Voltammetry trace of **1a**.

5.3 Computational Data and Procedures for Chapter 3

5.3.1 Computational Methods

All calculations were carried out using the ORCA suite of programs (version 5.0.3).[173, 174] The resolution of identity chain of spheres exchange (RIJCOSX) was used to speed up the SCF process,[215-218] employing the def2/J Coulomb-fitting auxiliary basis set. The integration grid "defgrid3" was selected for energies, implicit solvation was introduced by employing the SMD explicit solvent model using default parameters for 1,2-dichloroethane.[177] Geometries of all relevant stationary points were optimized using the M06-2X functional on Ahlrich's def2-TZVP triple-zeta basis set and Grimme D3 atom-pairwise dispersion correction.[171, 172, 175, 176] M06-2X was chosen due to its high performance across a range of benchmarking studies for main group chemistry.[178-180] All energies were corrected to 1M standard state (addition of 1.89 kcal mol^{-1} to every species). Minimum energy crossing points (MECP), the point at which two potential energy surfaces cross, were calculated in ORCA[219] with the adapted frequency analysis

"SurfCrossNumFreq" to verify the MECP is at a minimum. Energies and geometries of open-shell singlet intermediates were obtained *via* (1,1) broken-symmetry DFT computations, initialized from the corresponding triplet state using ORCA's "FlipSpin" function. The absence of spin contamination was verified by using Yamaguchi's spin projection method.[220] The spin densities of the open-shell singlet intermediates were inspected to ensure that they were chemically reasonable.

Born-Oppenheimer molecular dynamics were run using ORCA 5, forces acting on all atoms were calculated using DFT, at the SMD(1,2-dichloroethane) ωB97X-D3[171, 221]/def2-SVP level of theory. Newtonian equations of motion were calculated with velocity Verlet integration algorithm. Initial velocities of each atom were assigned from a random velocity distribution where the total kinetic energy is consistent with the intended simulation temperature. In order to conserve the initial temperature of the canonical ensemble, the Nosé-Hoover thermostat with a high-order Yoshida integratorwas employed, the temperature was set at 298 K and the coupling strength of the thermostat was set at 10 fs. [189, 190] Each MD run was randomised using a stated seed. A step size of 0.5 fs and maximum simulation time of 1.5 ps were chosen as suitable for organic molecules.[188]

Natural bond orbitals (NBO) were obtained with the NBO programme (version 3.1)[222] through Gaussian16 (Revision C.01)[223] applying the SMD(1,2-DCE)-M06-2X/def2-TZVP level of theory. Various functionals and basis set sizes were tested to ensure concordant conclusions.

Molecule visualisations were created using CYLview software.[224]

A recent benchmarking study by Neese and Pantazis found that M06-2X functional in conjunction with the SMD solvent model performed comparatively with efficient local pair natural orbital (LPNO) approaches providing the smallest root-mean-square-error (RMSE) of 0.12 eV for the calculation of aqueous redox potentials of 19 small molecules.[225] This method has also been applied to the study of redox potentials in organic solvents.[226] Following this protocol, redox potentials were calculated as described previously (SMD(1,2-dichloroethane)-M06-2X-D3/def2-TZVP). Within this approach the reduction potential is calculated using the following equations.[227] The values of Faraday's constant and the Saturated Calomel Electrode (SCE) were 23.061 kcal/V and 4.429 V respectively.[228]

$$\Delta G^{\circ}_{red} = G_{A\cdot,\ solv} - G_{A+,\ solv}$$

$$E^{\circ}_{1/2} = -\frac{\Delta G^{\circ}_{red}}{nF}$$

5.3.2 Tables of Energies

Tabulated thermodynamic quantities in hartrees. E – electronic energy, ZPE – vibrational zero-point energy, H – enthalpy, S – Entropy, G- gibbs free energy. T is the temperature at 298.15 K.

Label	E(el)	ZPE	H	T.S	G(1 atm)	G(1M)
$^1PhSO_2Cl$	-1333.924254	0.125276	-1333.787545	-0.048086	-1333.835630	-1333.832618
$^3PhSO_2Cl$	-1333.813362	0.121079	-1333.680086	-0.050624	-1333.730710	-1333.727698
$^3PhSO_2Cl$-twist	-1333.813898	0.121202	-1333.680772	-0.050103	-1333.730875	-1333.727863
$^1PhSO_2CF_3$	-1211.382208	0.139136	-1211.229065	-0.053520	-1211.282584	-1211.279572
$^3PhSO_2CF_3$	-1211.274951	0.135057	-1211.125298	-0.055594	-1211.180892	-1211.177880
$^3PhSO_2CF_3$-twist	-1211.276901	0.135354	-1211.127274	-0.054728	-1211.182002	-1211.178990
$^1PhSO_2CN$	-966.534266	0.132789	-966.389306	-0.049383	-966.438689	-966.435677

$^3PhSO_2CN$	-966.423184	0.128569	-966.281688	-0.051943	-966.333631	-966.330619
$^3PhSO_2CN$-twist	-966.422074	0.128696	-966.280695	-0.051448	-966.332143	-966.329131
$^1PhSO_2F$	-973.585840	0.126728	-973.448008	-0.047859	-973.495868	-973.492856
$^3PhSO_2F$	-973.473695	0.122684	-973.339307	-0.049384	-973.388691	-973.385679
$^3PhSO_2F$-twist	-973.476056	0.123148	-973.341584	-0.048392	-973.389976	-973.386964
$^1PhSO_2Me$	-913.633782	0.162094	-913.459875	-0.048293	-913.508168	-913.505156
$^3PhSO_2Me$	-913.517718	0.157901	-913.347479	-0.050244	-913.397723	-913.394711
$^3PhSO_2Me$-twist	-913.531698	0.158265	-913.361262	-0.049940	-913.411202	-913.408190
$^1PhSO_2Bn$	-1144.683442	0.244348	-1144.422892	-0.058115	-1144.481007	-1144.477995
$^3PhSO_2Bn$	-1144.566796	0.239900	-1144.309982	-0.060535	-1144.370518	-1144.367506
$^3PhSO_2Bn$-twist	-1144.562884	0.238697	-1144.321433	-0.059627	-1144.381061	-1144.378049
$^1PhSO_2Ph$	-1105.365573	0.215605	-1105.134975	-0.055540	-1105.190516	-1105.187504
$^3PhSO_2Ph$	-1105.249258	0.211462	-1105.022240	-0.057418	-1105.079657	-1105.076645
$^3PhSO_2Ph$-twist	-1105.263722	0.212506	-1105.036248	-0.055728	-1105.091975	-1105.088963

Table 5-1 Thermodynamic quantities for photochemistry of sulfonyl aldimine

Label	**E(el)**	**ZPE**	**H**	**T.S**	**G(1 atm)**	**G(1M)**
MECP-$PhSO_2F$	-973.456493	0.12147	-973.324797	-0.04618	-973.370977	-973.367965
MECP-$PhSO_2Me$	-913.519408	0.15626	-913.352103	-0.0474	-913.399507	-913.396495
MECP-$PhSO_2Bn$	-1144.56331	0.23895	-1144.30807	-0.05899	-1144.36706	-1144.36405
MECP-$PhSO_2Ph$	-1105.25244	0.21048	-1105.02712	-0.05551	-1105.08263	-1105.07962
MECP-$PhSO_2Cl$	-1333.79669	0.11954	-1333.66547	-0.04959	-1333.71506	-1333.71205
MECP-$PhSO_2CF_3$	-1211.25716	0.13378	-1211.10931	-0.05441	-1211.16372	-1211.16071
MECP-$PhSO_2CN$	-966.401085	0.12723	-966.261472	-0.05088	-966.312352	-966.30934

Table 5-2 Thermodynamic quantities for imine MECPs.

Label	**E(el)**	**ZPE**	**H**	**T.S**	**G(1 atm)**	**G(1M)**
^{1}4-OMe-$PhSO_2F$	-1088.117713	0.159985	-1087.944246	-0.052179	-1087.996424	-1087.993412
^{3}4-OMe-$PhSO_2F$	-1088.014992	0.156965	-1087.843986	-0.054427	-1087.898413	-1087.895401
^{3}4-OMe-$PhSO_2F$-twist	-1088.004738	0.155990	-1087.834872	-0.053799	-1087.888671	-1087.885659
^{1}4-CN-$PhSO_2F$	-1065.835332	0.125555	-1065.696962	-0.050990	-1065.747952	-1065.744940
^{3}4-CN-$PhSO_2F$	-1065.835332	0.122082	-1065.594931	-0.052377	-1065.647308	-1065.644296
^{3}4-CN-$PhSO_2F$-twist	-1065.726737	0.121879	-1065.591516	-0.053040	-1065.644557	-1065.641545

Table 5-3 Themodynamic quantities for SO_2F imines with varying substituents on phenyl ring.

Label	**E(el)**	**ZPE**	**H**	**T.S**	**G(1 atm)**	**G(1M)**
^{1}A1	-973.58584	0.126728	-973.44801	-0.047859	-973.49587	-973.49286

^{1}A2	-973.57418	0.127139	-973.43619	-0.046457	-973.48265	-973.47964
^{3}A1	-973.4737	0.122684	-973.33931	-0.049384	-973.38869	-973.38568
^{3}A2	-973.47606	0.123148	-973.34158	-0.048392	-973.38998	-973.38696
^{3}A3	-973.45991	0.122761	-973.32557	-0.048801	-973.37437	-973.37136

Table 5-4 Thermodynamic quantities for imine photoisomerisation.

Label	E(el)	ZPE	H	T.S	G(1 atm)	G(1M)
TS-frag-$PhSO_2F$	-973.460615	0.121028	-973.328856	-0.047491	-973.376347	-973.373335
TS-frag-$PhSO_2Me$	-913.514728	0.156556	-913.345887	-0.050312	-913.396199	-913.393187
TS-frag-$PhSO_2Bn$	-1144.562884	0.238697	-1144.307400	-0.060476	-1144.367875	-1144.364863
TS-frag-$PhSO_2Ph$	-1105.250253	0.210357	-1105.024628	-0.056641	-1105.081269	-1105.078257
TS-frag-$PhSO_2Cl$	-1333.807900	0.119706	-1333.676168	-0.050807	-1333.726975	-1333.723963
TS-frag-$PhSO_2CF_3$	-1211.170407	0.133300	-1211.116393	-0.054014	-1211.170407	-1211.167395
TS-frag-$PhSO_2CN$	-966.410588	0.126964	-966.270777	-0.052086	-966.322863	-966.319851

Table 5-5 Thermodynamic quantities for imine N-S fragmentation.

Label	E(el)	ZPE	H	T.S	G(1 atm)	G(1M)
TS-addition-$PhSO_2Me$	-1070.734816	0.268628	-1070.448326	-0.061590	-1070.509916	-1070.506904
TS-addition-$PhSO_2Bn$	-1301.782152	0.350076	-1301.409612	-0.071422	-1301.481034	-1301.478022
TS-addition-$PhSO_2Ph$	-1262.467972	0.321414	-1262.125362	-0.068431	-1262.193793	-1262.190781

Table 5-6 Transition states for addition of sulfonyl aldimines into isobutene.

Label	E(el)	ZPE	H	T.S	G(1 atm)	G(1M)
^{3}B1	-1130.727733	0.235364	-1130.474940	-0.061088	-1130.536028	-1130.533016
^{3}B2	-1130.725981	0.235455	-1130.473235	-0.060592	-1130.533827	-1130.530815
^{1}B1	-1130.728024	0.235653	-1130.475059	-0.060077	-1130.535136	-1130.532124
^{1}B2	-1130.726106	0.235385	-1130.473377	-0.059925	-1130.533302	-1130.530290
P1a	-1130.817044	0.241192	-1130.560103	-0.056261	-1130.616364	-1130.613352
P1b	-1130.798711	0.241722	-1130.541475	-0.055574	-1130.597049	-1130.594037
^{3}C1	-1130.704660	0.235906	-1130.451567	-0.060485	-1130.512052	-1130.509040
^{3}D1	-1130.692058	0.232426	-1130.441681	-0.061867	-1130.503548	-1130.500536
^{3}E1	-1130.715876	0.235294	-1130.463363	-0.060663	-1130.524026	-1130.521014
isobutene	-157.201650	0.107929	-157.087467	-0.033559	-157.121027	-157.118015
isobutene$^{\cdot+}$	-195.027508	0.112420	-194.908402	-0.035634	-194.944036	-194.941024
TS1	-1130.690912	0.231750	-1130.441559	-0.061402	-1130.502961	-1130.499949
TS2	-1130.687536	0.234473	-1130.436103	-0.060120	-1130.496223	-1130.493211
TS3	-1130.688784	0.231739	-1130.439530	-0.061607	-1130.501137	-1130.498125
MECP1a	-1130.727461	0.233715	-1130.476724	-0.060206	-1130.536930	-1130.533918
MECP1b	-1130.725834	0.233543	-1130.475294	-0.059947	-1130.535241	-1130.532229

Table 5-7 Thermodynamic quantities for intermediates in the aza Paterno Buchi reaction of SO_2F imine.

Label	E(el)	ZPE	H	T.S	G(1 atm)	G(1M)
^{3}F1	-1168.798467	0.244808	-1168.537922	-0.057674	-1168.595595	-1168.592583
^{3}F2	-1168.788037	0.242663	-1168.528161	-0.061004	-1168.589165	-1168.586153
^{1}F2	-1168.787725	0.242641	-1168.527843	-0.059978	-1168.587821	-1168.584809
methylene cyclobutene	-195.272217	0.115259	-195.150966	-0.033707	-195.184673	-195.181661
methylene cyclobutene$^{\cdot+}$	-195.027508	0.112420	-194.908402	-0.035634	-194.944036	-194.941024
P2	-1168.889508	0.248320	-1168.625408	-0.057109	-1168.682517	-1168.679505
MECP2a	-1168.798301	0.243129	-1168.539808	-0.056875	-1168.596683	-1168.593671
MECP2b	-1168.787840	0.240757	-1168.530150	-0.060331	-1168.590480	-1168.587469

Table 5-8 Thermodynamic qunatities for intermediates in the aza Paterno Buchi reaction of SO2F imine and exocyclic alkene.

Label	E(el)	ZPE	H	T.S	G(1 atm)	G(1M)
4-OMe-PhSO$_2$F$^{\cdot-}$	-1088.229276	0.156824	-1088.058761	-0.053110	-1088.111871	-1088.108859
4-CN-PhSO$_2$F$^{\cdot-}$	-1065.835332	0.125555	-1065.696962	-0.050990	-1065.747952	-1065.744940
PhSO$_2$F$^{\cdot-}$	-973.704378	0.124031	-973.569221	-0.047752	-973.616973	-973.613961

Table 5-9 Thermodynamic quantities of imine radical anions.

Species	E(el)	ZPE	H	T.S	G(1atm)	G(1M)
ITX	-1091.556829	0.257363	-1091.283401	-0.057009	-1091.340410	-1091.337398
^{3}ITX	-1091.449412	0.253632	-1091.179288	-0.058751	-1091.238039	-1091.235027
ITX$^{\cdot+}$	-1091.329347	0.257094	-1091.056007	-0.058000	-1091.114008	-1091.110996
3-FTX	-1072.880986	0.164437	-1072.703945	-0.050217	-1072.754162	-1072.751150
^{3}FTX	-1072.767462	0.160923	-1072.593610	-0.051741	-1072.645351	-1072.642339
3-FTX$^{\cdot+}$	-1072.645148	0.164261	-1072.468229	-0.050827	-1072.519056	-1072.516044

Table 5-10 Tabulated thermodynamic quantities for photocatalyst derived species.

References

1. C. Lamberth, *Pest Manag. Sci.*, 2013, **69**, 1106-1114.
2. J. A. Joule, in *Adv. Heterocycl. Chem.*, eds. E. F. V. Scriven and C. A. Ramsden, Academic Press, 2016, vol. 119, pp. 81-106.
3. C. M. Marshall, J. G. Federice, C. N. Bell, P. B. Cox and J. T. Njardarson, *J. Med. Chem.*, 2024, **67**, 11622-11655.
4. D. R. Parmar, J. Y. Soni, R. Guduru, R. H. Rayani, R. V. Kusurkar and A. G. Vala, *Arch Pharm (Weinheim)*, 2021, **354**, e2100062.
5. D. S. Wishart, *Nucleic Acids Research*, 2006, **34**, D668-D672.
6. M. R. Bauer, P. Di Fruscia, S. C. C. Lucas, I. N. Michaelides, J. E. Nelson, R. I. Storer and B. C. Whitehurst, *RSC Med. Chem.*, 2021, **12**, 448-471.
7. R. S. Obach, E. A. LaChapelle, M. A. Brodney, M. Vanase-Frawley, G. W. Kauffman and A. Sawant-Basak, *Xenobiotica*, 2016, **46**, 1112-1121.
8. R. M. Rzasa, M. J. Frohn, K. L. Andrews, S. Chmait, N. Chen, J. G. Clarine, C. Davis, H. A. Eastwood, D. B. Horne, E. Hu, A. D. Jones, M. R. Kaller, R. K. Kunz, S. Miller, H. Monenschein, T. Nguyen, A. J. Pickrell, A. Porter, A. Reichelt, X. Zhao, J. J. S. Treanor and J. R. Allen, *Biorg. Med. Chem.*, 2014, **22**, 6570-6585.
9. A. Brown, T. B. Brown, A. Calabrese, D. Ellis, N. Puhalo, M. Ralph and L. Watson, *Bioorg. Med. Chem. Lett.*, 2010, **20**, 516-520.
10. A. Johansson, C. Löfberg, M. Antonsson, S. von Unge, M. A. Hayes, R. Judkins, K. Ploj, L. Benthem, D. Lindén, P. Brodin, M. Wennerberg, M. Fredenwall, L. Li, J. Persson, R. Bergman, A. Pettersen, P. Gennemark and A. Hogner, *J. Med. Chem.*, 2016, **59**, 2497-2511.
11. M. S. Diallo, K. Falconer and J. H. Johnson, *Environ. Sci. Technol.*, 2007, **41**, 6521-6527.
12. M. L. Sarazen and C. W. Jones, *Macromolecules*, 2017, **50**, 9135-9143.
13. X. Sun, S. Dong and E. Wang, *Macromolecules*, 2004, **37**, 7105-7108.
14. S. W. Benson, F. R. Cruickshank, D. M. Golden, G. R. Haugen, H. E. O'Neal, A. S. Rodgers, R. Shaw and R. Walsh, *Chem. Rev.*, 1969, **69**, 279-324.
15. A. Brandi, S. Cicchi and F. M. Cordero, *Chem. Rev.*, 2008, **108**, 3988-4035.
16. W. Aelterman, N. De Kimpe and J.-P. Declercq, *J. Org. Chem.*, 1998, **63**, 6-11.
17. M. C. Hillier and C.-y. Chen, *J. Org. Chem.*, 2006, **71**, 7885-7887.
18. R. A. Miller, F. Lang, B. Marcune, D. Zewge, Z. J. Song and S. Karady, *Synth. Commun.*, 2003, **33**, 3347-3353.
19. S. P. Fritz, J. F. Moya, M. G. Unthank, E. M. McGarrigle and V. K. Aggarwal, *Synthesis*, 2012, **44**, 1584-1590.
20. F. Juliá, J. Yan, F. Paulus and T. Ritter, *J. Am. Chem. Soc.*, 2021, **143**, 12992-12998.
21. H. Bräuner-Osborne, L. Bunch, N. Chopin, F. Couty, G. Evano, A. A. Jensen, M. Kusk, B. Nielsen and N. Rabasso, *Org. Biomol. Chem.*, 2005, **3**, 3926-3936.
22. A. Carlin-Sinclair, F. Couty and N. Rabasso, *Synlett*, 2003, **2003**, 0726-0728.
23. G. He, Y. Zhao, S. Zhang, C. Lu and G. Chen, *J. Am. Chem. Soc.*, 2012, **134**, 3-6.
24. M. Nappi, C. He, W. G. Whitehurst, B. G. N. Chappell and M. J. Gaunt, *Angew. Chem. Int. Ed.*, 2018, **57**, 3178-3182.

25. J. Cabral, P. Laszlo and M. T. e. Montaufier, *Tetrahedron Lett.*, 1988, **29**, 547-550.
26. A. Koldobskii, Y. N. Luzikov and V. Lunin, *Zh. Org. Khim.*, 1986, **22**, 636-638.
27. R. W. M. Aben, R. Smit and J. W. Scheeren, *J. Org. Chem.*, 1987, **52**, 365-370.
28. T. Uyehara, M. Yuuki, H. Masaki, M. Matsumoto, M. Ueno and T. Sato, *Chem. Lett.*, 1995, **24**, 789-790.
29. B. Alcaide, P. Almendros and C. Aragoncillo, *Chem. Soc. Rev.*, 2010, **39**, 783-816.
30. H. Bauman and R. O. Duthaler, *Helv. Chim. Acta*, 1988, **71**, 1025-1034.
31. T. Akiyama, K. Daidouji and K. Fuchibe, *Org. Lett.*, 2003, **5**, 3691-3693.
32. G.-L. Zhao, J.-W. Huang and M. Shi, *Org. Lett.*, 2003, **5**, 4737-4739.
33. J.-B. Denis, G. Masson, P. Retailleau and J. Zhu, *Angew. Chem.*, 2011, **123**, 5468-5472.
34. N. E. Behnke, K. Lovato, M. Yousufuddin and L. Kürti, *Angew. Chem. Int. Ed.*, 2019, **58**, 14219-14223.
35. A. G. Hortmann and D. A. Robertson, *J. Am. Chem. Soc.*, 1967, **89**, 5974-5975.
36. A. G. Hortmann and D. A. Robertson, *J. Am. Chem. Soc.*, 1972, **94**, 2758-2765.
37. R. Bartnik and A. P. Marchand, *Synlett*, 1997, **1997**, 1029-1039.
38. A. Fawcett, *Pure Appl. Chem.*, 2020, **92**, 751-765.
39. Y. Ji, L. Wojtas and J. M. Lopchuk, *ARKIVOC*, 2018, **2018**, 195-214.
40. R. Gianatassio, J. M. Lopchuk, J. Wang, C.-M. Pan, L. R. Malins, L. Prieto, T. A. Brandt, M. R. Collins, G. M. Gallego, N. W. Sach, J. E. Spangler, H. Zhu, J. Zhu and P. S. Baran, *Science*, 2016, **351**, 241-246.
41. R. Gianatassio and D. Kadish, *Org. Lett.*, 2019, **21**, 2060-2063.
42. J. L. Tyler, A. Noble and V. K. Aggarwal, *Angew. Chem. Int. Ed.*, 2022, **61**, e202214049.
43. J. L. Tyler and V. K. Aggarwal, *Chem. Eur. J.*, 2023, **29**, e202300008.
44. A. Fawcett, A. Murtaza, C. H. U. Gregson and V. K. Aggarwal, *J. Am. Chem. Soc.*, 2019, **141**, 4573-4578.
45. C. H. U. Gregson, A. Noble and V. K. Aggarwal, *Angew. Chem. Int. Ed.*, 2021, **60**, 7360-7365.
46. M. Golfmann and J. C. L. Walker, *Commun. Chem.*, 2023, **6**, 9.
47. R. I. Rodríguez, V. Corti, L. Rizzo, S. Visentini, M. Bortolus, A. Amati, M. Natali, G. Pelosi, P. Costa and L. Dell'Amico, *Nat. Catal.*, 2024, **7**, 1223-1231.
48. H. J. Dequina, C. L. Jones and J. M. Schomaker, *Chem*, 2023, **9**, 1658-1701.
49. U. K. Nadir, R. L. Sharma and V. K. Koul, *J. Chem. Soc., Perkin Trans. 1*, 1991, 2015-2019.
50. S. C. Schmid, I. A. Guzei and J. M. Schomaker, *Angew. Chem. Int. Ed.*, 2017, **56**, 12229-12233.
51. M. Dehghany, G. Pavaneli, J. W. Kailing, O. M. Duke, I. A. Guzei, C. Da Ros Montes D'Oca, I. Fernández and J. M. Schomaker, *ACS Catal.*, 2024, **14**, 5795-5803.
52. D. C. Miller, R. G. Lal, L. A. Marchetti and F. H. Arnold, *J. Am. Chem. Soc.*, 2022, **144**, 4739-4745.
53. H. J. Dequina and J. M. Schomaker, *Trends Chem.*, 2020, **2**, 874-887.
54. Y. Ning, H. Chen, Y. Ning, J. Zhang and X. Bi, *Angew. Chem. Int. Ed.*, 2024, **63**, e202318072.
55. Y. Tamaru, M. Hojo and Z. Yoshida, *J. Org. Chem.*, 1988, **53**, 5731-5741.

56. Y. Tamaru, T. Bando, Y. Kawamura, K. Okamura, Z.-i. Yoshida and M. Shiro, *J. Chem. Soc., Chem. Commun.*, 1992, 1498-1500.
57. T. Bando, H. Harayama, Y. Fukazawa, M. Shiro, K. Fugami, S. Tanaka and Y. Tamaru, *J. Org. Chem.*, 1994, **59**, 1465-1474.
58. N. Kern, A.-S. Felten, J.-M. Weibel, P. Pale and A. Blanc, *Org. Lett.*, 2014, **16**, 6104-6107.
59. N. Fu and T. T. Tidwell, *Tetrahedron*, 2008, **64**, 10465-10496.
60. R. K. Khangarot and K. P. Kaliappan, *Eur. J. Org. Chem.*, 2013, **2013**, 7664-7677.
61. B. Alcaide, P. Almendros, C. Aragoncillo and G. Gómez-Campillos, *Adv. Synth. Catal.*, 2013, **355**, 2089-2094.
62. M. Yamashita and I. Ojima, *J. Am. Chem. Soc.*, 1983, **105**, 6339-6342.
63. in *IUPAC Compendium of Chemical Terminology*, International Union of Pure and Applied Chemistry (IUPAC), 3.0.1 edn., 2019, DOI: doi:10.1351/goldbook.K03370.
64. F. H. Quina and G. T. M. Silva, *J. Photochem. Photobiol.*, 2021, **7**, 100042.
65. in *IUPAC Compendium of Chemical Terminology*, International Union of Pure and Applied Chemistry (IUPAC), 3.0.1 edn., 2019, DOI: doi:10.1351/goldbook.ET07369.
66. in *IUPAC Compendium of Chemical Terminology*, International Union of Pure and Applied Chemistry (IUPAC), 3.0.1 edn., 2019, DOI: doi:10.1351/goldbook.H02756.
67. S. Dutta, J. E. Erchinger, F. Strieth-Kalthoff, R. Kleinmans and F. Glorius, *Chem. Soc. Rev.*, 2024, **53**, 1068-1089.
68. F. Strieth-Kalthoff and F. Glorius, *Chem*, 2020, **6**, 1888-1903.
69. G. Büchi, C. G. Inman and E. S. Lipinsky, *J. Am. Chem. Soc.*, 1954, **76**, 4327-4331.
70. E. Paternò, Chieffi, G, *Gazz. Chim. Ital.*, 1909, **39**, 341-361.
71. A. C. Pratt, *Chem. Soc. Rev.*, 1977, **6**, 63-81.
72. A. Padwa, *Chem. Rev.*, 1977, **77**, 37-68.
73. D. S. Kliger and E. L. Menger, *Acc. Chem. Res.*, 1975, **8**, 81-84.
74. J. D. Coyle, *Chem. Soc. Rev.*, 1974, **3**, 329-353.
75. A. Hantzsch, *Ber. Dtsch. Chem. Ges.*, 1890, **23**, 2325-2332.
76. M. Kobayashi, M. Yoshida and H. Minato, *J. Org. Chem.*, 1976, **41**, 3322-3324.
77. A. Padwa and F. Albrecht, *J. Am. Chem. Soc.*, 1974, **96**, 4849-4857.
78. A. Padwa and F. Albrecht, *J. Org. Chem.*, 1974, **39**, 2361-2366.
79. S. K. Kandappa, L. K. Valloli, S. Ahuja, J. Parthiban and J. Sivaguru, *Chem. Soc. Rev.*, 2021, **50**, 1617-1641.
80. X. Zhang and T. Rovis, *J. Am. Chem. Soc.*, 2021, **143**, 21211-21217.
81. R. M. Rodehorst and T. H. Koch, *J. Am. Chem. Soc.*, 1975, **97**, 7298-7304.
82. T. H. Koch, R. J. Sluski and R. H. Moseley, *J. Am. Chem. Soc.*, 1973, **95**, 3957-3963.
83. D. Staveness, J. L. Collins III, R. C. McAtee and C. R. J. Stephenson, *Angew. Chem. Int. Ed.*, 2019, **58**, 19000-19006.
84. J. L. Collins, III, D. Staveness, M. J. Sowden and C. R. J. Stephenson, *Org. Lett.*, 2022, **24**, 4344-4348.
85. A. S. Harmata, T. E. Spiller, M. J. Sowden and C. R. J. Stephenson, *J. Am. Chem. Soc.*, 2021, **143**, 21223-21228.
86. N. Obata, A. Hamada and T. Takizawa, *Tetrahedron Lett.*, 1969, **10**, 3917-3920.

87. T. S. Cantrell and W. S. Haller, *Chem. Commun. (London)*, 1968, 977-978.
88. M. J. Tilby, D. F. Dewez, L. R. E. Pantaine, A. Hall, C. Martínez-Lamenca and M. C. Willis, *ACS Catal.*, 2022, **12**, 6060-6067.
89. L. Wang, Y. Yu, L. Deng and K. Du, *Org. Lett.*, 2023, **25**, 2349-2354.
90. D. Leifert and A. Studer, *Angew. Chem. Int. Ed.*, 2020, **59**, 74-108.
91. J. E. Erchinger, R. Hoogesteger, R. Laskar, S. Dutta, C. Hümpel, D. Rana, C. G. Daniliuc and F. Glorius, *J. Am. Chem. Soc.*, 2023, **145**, 2364-2374.
92. T. Matsuura and Y. Ito, *Tetrahedron Lett.*, 1973, **14**, 2283-2286.
93. Y. Ito and T. Matsuura, *Tetrahedron*, 1975, **31**, 1373-1380.
94. T. Okada, M. Kawanisi and H. Nozaki, *Bull. Chem. Soc. Jpn.*, 1969, **42**, 2981-2983.
95. S.-i. Ishikawa, H. Sakuragi, M. Yoshida, N. Inamoto and K. Tokumaru, *Chem. Lett.*, 1975, **4**, 819-822.
96. M. Yoshida, H. Sakuragi, T. Nishimura, S.-i. Ishikawa and K. Tokumaru, *Chem. Lett.*, 1975, **4**, 1125-1130.
97. H. Ohta and K. Tokumaru, *Bull. Chem. Soc. Jpn.*, 1975, **48**, 2393-2394.
98. J. C. Walton, *Molecules*, 2016, **21**, 63.
99. J. C. Walton, *Acc. Chem. Res.*, 2014, **47**, 1406-1416.
100. E. M. Scanlan, A. M. Z. Slawin and J. C. Walton, *Org. Biomol. Chem.*, 2004, **2**, 716-724.
101. R. T. McBurney and J. C. Walton, *J. Am. Chem. Soc.*, 2013, **135**, 7349-7354.
102. F. Portela-Cubillo, J. Lymer, E. M. Scanlan, J. S. Scott and J. C. Walton, *Tetrahedron*, 2008, **64**, 11908-11916.
103. C. Kolano, G. Bucher, H. H. Wenk, M. Jäger, O. Schade and W. Sander, *J. Phys. Org. Chem.*, 2004, **17**, 207-214.
104. R. T. McBurney, A. M. Z. Slawin, L. A. Smart, Y. Yu and J. C. Walton, *Chem. Commun.*, 2011, **47**, 7974-7976.
105. T. Patra, M. Das, C. G. Daniliuc and F. Glorius, *Nat. Catal.*, 2021, **4**, 54-61.
106. T. Patra, P. Bellotti, F. Strieth-Kalthoff and F. Glorius, *Angew. Chem. Int. Ed.*, 2020, **59**, 3172-3177.
107. J. Majhi, R. K. Dhungana, Á. Rentería-Gómez, M. Sharique, L. Li, W. Dong, O. Gutierrez and G. A. Molander, *J. Am. Chem. Soc.*, 2022, **144**, 15871-15878.
108. G. Tan, M. Das, H. Keum, P. Bellotti, C. Daniliuc and F. Glorius, *Nat. Chem.*, 2022, **14**, 1174-1184.
109. G. Tan, M. Das, R. Kleinmans, F. Katzenburg, C. Daniliuc and F. Glorius, *Nat. Catal.*, 2022, **5**, 1120-1130.
110. O. Tsuge, M. Tashiro and K. Oe, *Tetrahedron Lett.*, 1968, **9**, 3971-3974.
111. O. Tsuge, K. Oe and M. Tashiro, *Tetrahedron*, 1973, **29**, 41-46.
112. J. A. Hyatt and J. S. Swenton, *J. Chem. Soc., Chem. Commun.*, 1972, 1144-1145.
113. J. S. Swenton and J. A. Hyatt, *J. Am. Chem. Soc.*, 1974, **96**, 4879-4885.
114. T. H. Koch and K. H. Howard, *Tetrahedron Lett.*, 1972, **13**, 4035-4038.
115. K. A. Howard and T. H. Koch, *J. Am. Chem. Soc.*, 1975, **97**, 7288-7298.
116. T. Nishio, *J. Org. Chem.*, 1984, **49**, 827-832.
117. T. Nishio and Y. Omote, *J. Chem. Soc., Perkin Trans. 1*, 1987, 2611-2615.
118. X. Li, J. Großkopf, C. Jandl and T. Bach, *Angew. Chem. Int. Ed.*, 2021, **60**, 2684-2688.
119. C. K. Prier, D. A. Rankic and D. W. C. MacMillan, *Chem. Rev.*, 2013, **113**, 5322-5363.
120. M. R. Becker, E. R. Wearing and C. S. Schindler, *Nat. Chem.*, 2020, **12**, 898-905.

121. W. Wang and M. K. Brown, *Angew. Chem. Int. Ed.*, 2023, **62**, e202305622.
122. T. Kumagai, K. Shimizu, Y. Kawamura and T. Mukai, *Tetrahedron*, 1981, **37**, 3365-3376.
123. T. Kumagai, Y. Kawamura and T. Mukai, *Chem. Lett.*, 1983, **12**, 1357-1360.
124. Y. Kawamura, T. Kumagai and T. Mukai, *Chem. Lett.*, 1985, **14**, 1937-1940.
125. S. Futamura, H. Ohta and Y. Kamiya, *Chem. Lett.*, 1980, **9**, 655-658.
126. S. Futamura, H. Ohta and Y. Kamiya, *Bull. Chem. Soc. Jpn.*, 1982, **55**, 2190-2194.
127. R. Sakamoto, T. Inada, S. Sakurai and K. Maruoka, *Org. Lett.*, 2016, **18**, 6252-6255.
128. E. R. Wearing, Y.-C. Yeh, G. G. Terrones, S. G. Parikh, I. Kevlishvili, H. J. Kulik and C. S. Schindler, *Science*, 2024, **384**, 1468-1476.
129. D. M. Flores, M. L. Neville and V. A. Schmidt, *Nat. Commun.*, 2022, **13**, 2764.
130. X. Zeng, H. Beckers and H. Willner, *J. Am. Chem. Soc.*, 2013, **135**, 2096-2099.
131. X. Nie, T. Xu, J. Song, A. Devaraj, B. Zhang, Y. Chen and S. Liao, *Angew. Chem. Int. Ed.*, 2021, **60**, 3956-3960.
132. X. Nie, T. Xu, Y. Hong, H. Zhang, C. Mao and S. Liao, *Angew. Chem. Int. Ed.*, 2021, **60**, 22035-22042.
133. T. Guo, G. Meng, X. Zhan, Q. Yang, T. Ma, L. Xu, K. B. Sharpless and J. Dong, *Angew. Chem. Int. Ed.*, 2018, **57**, 2605-2610.
134. P. R. D. Murray, W. M. M. Bussink, G. H. M. Davies, F. W. van der Mei, A. H. Antropow, J. T. Edwards, L. A. D'Agostino, J. M. Ellis, L. G. Hamann, F. Romanov-Michailidis and R. R. Knowles, *J. Am. Chem. Soc.*, 2021, **143**, 4055-4063.
135. Y. Oe, R. Yoshida, A. Tanaka, A. Adachi, Y. Ishibashi, T. Okazoe, K. Aikawa and T. Hashimoto, *J. Am. Chem. Soc.*, 2022, **144**, 2107-2113.
136. P. Wang, L. Lin, Y. Huang, H. Zhang and S. Liao, *Angew. Chem. Int. Ed.*, 2024, **63**, e202405944.
137. W. Zhang, H. Li, X. Li, Z. Zou, M. Huang, J. Liu, X. Wang, S. Ni, Y. Pan and Y. Wang, *Nat. Commun.*, 2022, **13**, 3515.
138. P. Wang, H. Zhang, X. Nie, T. Xu and S. Liao, *Nat. Commun.*, 2022, **13**, 3370.
139. R. Graf, *Justus Liebigs Ann. Chem.*, 1963, **661**, 111-157.
140. H. Hoffmann and H. Förster, *Monatsh. Chem.*, 1968, **99**, 380-388.
141. K. Clauβ, H.-J. Friedrich and H. Jensen, *Justus Liebigs Ann. Chem.*, 1974, **1974**, 561-592.
142. F. Ahmed, M. M. Rahman, S. Chandra Sutradhar, N. S. Lopa, T. Ryu, S. Yoon, I. Choi, S. Lee and W. Kim, *Electrochim. Acta*, 2019, **298**, 709-716.
143. D. Huang, X. Wang, X. Wang, W. Chen, X. Wang and Y. Hu, *Org. Lett.*, 2016, **18**, 604-607.
144. S. Sun, B. Gao, J. Chen, K. B. Sharpless and J. Dong, *Angew. Chem. Int. Ed.*, 2021, **60**, 21195-21199.
145. L. D. Elliott, S. Kayal, M. W. George and K. Booker-Milburn, *J. Am. Chem. Soc.*, 2020, **142**, 14947-14956.
146. A. G. Griesbeck and S. Stadtmüller, *Chem. Ber.*, 1993, **126**, 2149-2150.
147. K. Poscharny, D. C. Fabry, S. Heddrich, E. Sugiono, M. A. Liauw and M. Rueping, *Tetrahedron*, 2018, **74**, 3171-3175.
148. G. E. Hilbert and T. B. Johnson, *J. Am. Chem. Soc.*, 1930, **52**, 2001-2007.
149. D. Uraguchi, Y. Tsuchiya, T. Ohtani, T. Enomoto, S. Masaoka, D. Yokogawa and T. Ooi, *Angew. Chem. Int. Ed.*, 2020, **59**, 3665-3670.

150. Y. Chen, N. McNamara, O. May, T. Pillaiyar, D. C. Blakemore and S. V. Ley, *Org. Lett.*, 2020, **22**, 5746-5748.
151. M. Nambo, K. Ghosh, J. C. H. Yim, Y. Tahara, N. Inai, T. Yanai and C. M. Crudden, *ACS Catal.*, 2022, **12**, 9526-9532.
152. A. A. Kirichok, I. O. Shton, I. M. Pishel, S. A. Zozulya, P. O. Borysko, V. Kubyshkin, O. A. Zaporozhets, A. A. Tolmachev and P. K. Mykhailiuk, *Chem. Eur. J.*, 2018, **24**, 5444-5449.
153. A. A. Kirichok, I. Shton, M. Kliachyna, I. Pishel and P. K. Mykhailiuk, *Angew. Chem.*, 2017, **129**, 8991-8995.
154. K. Hiesinger, D. Dar'in, E. Proschak and M. Krasavin, *J. Med. Chem.*, 2021, **64**, 150-183.
155. T. Ni, R. A. Caldwell and L. Melton, *J. Am. Chem. Soc.*, 1989, **111**, 457-464.
156. A. A. Lamola and G. S. Hammond, *J. Chem. Phys.*, 1965, **43**, 2129-2135.
157. P. Mukherjee, C. P. Woroch, L. Cleary, M. Rusznak, R. W. Franzese, M. R. Reese, J. W. Tucker, J. M. Humphrey, S. M. Etuk, S. C. Kwan, C. W. am Ende and N. D. Ball, *Org. Lett.*, 2018, **20**, 3943-3947.
158. S. Mahapatra, C. P. Woroch, T. W. Butler, S. N. Carneiro, S. C. Kwan, S. R. Khasnavis, J. Gu, J. K. Dutra, B. C. Vetelino, J. Bellenger, C. W. am Ende and N. D. Ball, *Org. Lett.*, 2020, **22**, 4389-4394.
159. B. Han, S. R. Khasnavis, M. Nwerem, M. Bertagna, N. D. Ball and O. M. Ogba, *Inorg. Chem.*, 2022, **61**, 9746-9755.
160. J. Dong, L. Krasnova, M. G. Finn and K. B. Sharpless, *Angew. Chem. Int. Ed.*, 2014, **53**, 9430-9448.
161. I. A. MacKenzie, L. Wang, N. P. R. Onuska, O. F. Williams, K. Begam, A. M. Moran, B. D. Dunietz and D. A. Nicewicz, *Nature*, 2020, **580**, 76-80.
162. U. Ragnarsson and L. Grehn, *Tetrahedron Lett.*, 2012, **53**, 1045-1047.
163. L. F. Audrieth and M. V. Brauchitsch, *J. Org. Chem.*, 1956, **21**, 426-428.
164. E. H. Gold and E. Babad, *J. Org. Chem.*, 1972, **37**, 2208-2210.
165. K. Miyamoto, M. M. Hoque and S. Ogasa, *J. Org. Chem.*, 2012, **77**, 8317-8320.
166. M. R. Becker, E. R. Wearing and C. S. Schindler, *Nat. Chem.*, 2020, **12**, 898-905.
167. K. A. Rykaczewski and C. S. Schindler, *Org. Lett.*, 2020, **22**, 6516-6519.
168. J. Zheng, X. Dong and T. P. Yoon, *Org. Lett.*, 2020, **22**, 6520-6525.
169. M. A. Ashley and T. Rovis, *J. Am. Chem. Soc.*, 2020, **142**, 18310-18316.
170. N. A. Romero and D. A. Nicewicz, *Chem. Rev.*, 2016, **116**, 10075-10166.
171. S. Grimme, J. Antony, S. Ehrlich and H. Krieg, *J. Chem. Phys.*, 2010, **132**, 154104.
172. S. Grimme, S. Ehrlich and L. Goerigk, *J. Comput. Chem.*, 2011, **32**, 1456-1465.
173. F. Neese, *Wiley Interdiscip. Rev. Comput. Mol. Sci.*, 2022, **12**, e1606.
174. F. Neese, *Wiley Interdiscip. Rev. Comput. Mol. Sci.*, 2012, **2**, 73-78.
175. Y. Zhao and D. G. Truhlar, *Theor. Chem. Acc.*, 2008, **120**, 215-241.
176. F. Weigend and R. Ahlrichs, *Phys. Chem. Chem. Phys.*, 2005, **7**, 3297-3305.
177. A. V. Marenich, C. J. Cramer and D. G. Truhlar, *J. Phys. Chem. B*, 2009, **113**, 6378-6396.
178. L. Goerigk and S. Grimme, *Phys. Chem. Chem. Phys.*, 2011, **13**, 6670-6688.
179. L. Goerigk, A. Hansen, C. Bauer, S. Ehrlich, A. Najibi and S. Grimme, *Phys. Chem. Chem. Phys.*, 2017, **19**, 32184-32215.
180. M. Korth and S. Grimme, *J. Chem. Theory Comput.*, 2009, **5**, 993-1003.
181. R. Kleinmans, T. Pinkert, S. Dutta, T. O. Paulisch, H. Keum, C. G. Daniliuc and F. Glorius, *Nature*, 2022, **605**, 477-482.

182. M. V. Popescu, A. Mekereeya, J. V. Alegre-Requena, R. S. Paton and M. D. Smith, *Angew. Chem. Int. Ed.*, 2020, **59**, 23020-23024.
183. M. V. Popescu and R. S. Paton, *Chem*, 2024, **10**, 3428-3443.
184. N. Münster, N. A. Parker, L. van Dijk, R. S. Paton and M. D. Smith, *Angew. Chem. Int. Ed.*, 2017, **56**, 9468-9472.
185. H. Jung, H. Keum, J. Kweon and S. Chang, *J. Am. Chem. Soc.*, 2020, **142**, 5811-5818.
186. Y. Zhang, J. Xue, Y. Gao, H.-K. Fun and J.-H. Xu, *J. Chem. Soc., Perkin Trans. 1*, 2002, 345-353.
187. P. Franceschi, S. Cuadros, G. Goti and L. Dell'Amico, *Angew. Chem. Int. Ed.*, 2023, **62**, e202217210.
188. S. Bouayad-Gervais, C. D. T. Nielsen, A. Turksoy, T. Sperger, K. Deckers and F. Schoenebeck, *J. Am. Chem. Soc.*, 2022, **144**, 6100-6106.
189. G. J. Martyna, M. E. Tuckerman, D. J. Tobias and M. L. Klein, *Mol. Phys.*, 1996, **87**, 1117-1157.
190. G. J. Martyna, M. L. Klein and M. Tuckerman, *J. Chem. Phys.*, 1992, **97**, 2635-2643.
191. A. K. Ghosh and D. R. Nicponski, *Org. Lett.*, 2011, **13**, 4328-4331.
192. C. A. Bewley, S. Ray, F. Cohen, S. K. Collins and L. E. Overman, *J. Nat. Prod.*, 2004, **67**, 1319-1324.
193. A. R. Ellwood and M. J. Porter, *Org. Biomol. Chem.*, 2011, **9**, 379-381.
194. B. M. Trost, D. Amans, W. M. Seganish and C. K. Chung, *J. Am. Chem. Soc.*, 2009, **131**, 17087-17089.
195. K. Bodenschatz, J. Stöckl, M. Winterer and R. Schobert, *Tetrahedron*, 2022, **104**, 132113.
196. J. Leonard, J. D. Hewitt, D. Ouali, L. R. Bennett, A. Mahmood and S. J. Simpson, *Tetrahedron*, 2002, **58**, 4681-4691.
197. WO2023/18781, 2023.
198. D. Yang, Y.-C. Yip, G.-S. Jiao and M.-K. Wong, *J. Org. Chem.*, 1998, **63**, 8952-8956.
199. WO2020/6296, 2020.
200. EP946508, 2009.
201. S. Chanthamath, D. T. Nguyen, K. Shibatomi and S. Iwasa, *Org. Lett.*, 2013, **15**, 772-775.
202. K. S. Rodygin, A. S. Bogachenkov and V. P. Ananikov, *Molecules*, 2018, **23**, 648.
203. E. R. Barth, D. Längle, F. Wesseler, C. Golz, A. Krupp, D. Schade and C. Strohmann, *Eur. J. Inorg. Chem.*, 2020, **2020**, 176-181.
204. J. S. Lindsey, P. A. Brown and D. A. Siesel, *Tetrahedron*, 1989, **45**, 4845-4866.
205. C. D. Díaz-Oviedo, R. Maji and B. List, *J. Am. Chem. Soc.*, 2021, **143**, 20598-20604.
206. R. n. Rubio-Presa, S. Suarez-Pantiga, M. a. R. Pedrosa and R. Sanz, *Adv. Synth. Catal.*, 2018, **360**, 2216 - 2220.
207. N. Oka, T. Yamada, H. Sajiki, S. Akai and T. Ikawa, *Org. Lett.*, 2022, **24**, 3510-3514.
208. J. Xi and Z. Gu, *Chin. J. Chem* . 2020, **38**, 1081-1085.
209. S. Hameed P, V. Patil, S. Solapure, U. Sharma, P. Madhavapeddi, A. Raichurkar, M. Chinnapattu, P. Manjrekar, G. Shanbhag, J. Puttur, V. Shinde, S. Menasinakai, S. Rudrapatana, V. Achar, D. Awasthy, R. Nandishaiah, V. Humnabadkar, A. Ghosh, C. Narayan, V. K. Ramya, P. Kaur, S. Sharma, J. Werngren, S. Hoffner,

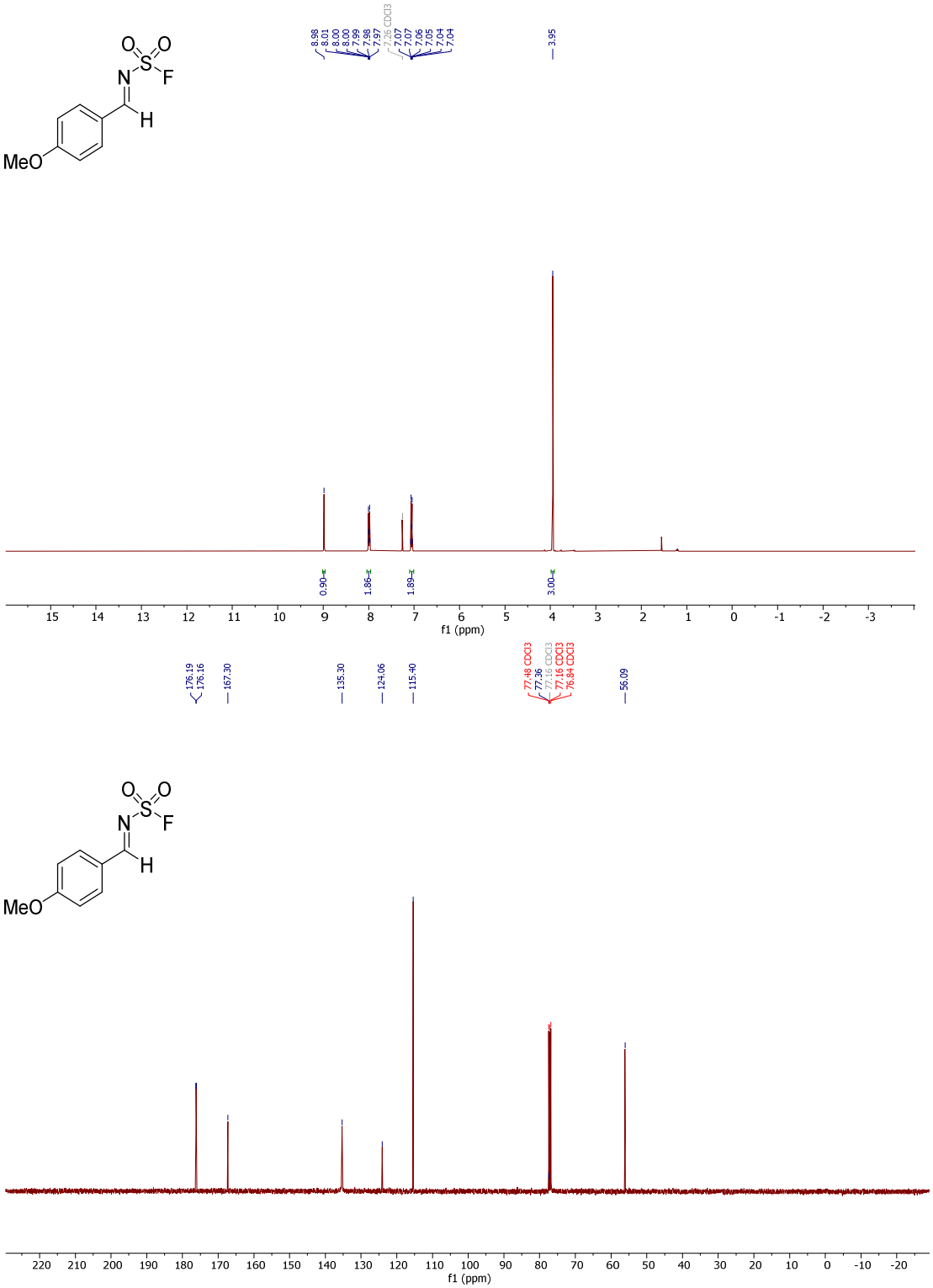
V. Panduga, C. N. N. Kumar, J. Reddy, M. Kumar Kn, S. Ganguly, S. Bharath, U. Bheemarao, K. Mukherjee, U. Arora, S. Gaonkar, M. Coulson, D. Waterson, V. K. Sambandamurthy and S. M. de Sousa, *J. Med. Chem.*, 2014, **57**, 4889-4905.
210. H. Huang, C. Yu, X. Li, Y. Zhang, Y. Zhang, X. Chen, P. S. Mariano, H. Xie and W. Wang, *Angew. Chem. Int. Ed.*, 2017, **56**, 8201-8205.
211. H. W. Roesky and S. Tutkunkardes, *Z. Anorg. Allg. Chem.*, 1970, **374**, 147-158.
212. S. Morales, F. G. Guijarro, J. L. García Ruano and M. B. Cid, *J. Am. Chem. Soc.*, 2014, **136**, 1082-1089.
213. E. C. Lee, B. L. Hodous, E. Bergin, C. Shih and G. C. Fu, *J. Am. Chem. Soc.*, 2005, **127**, 11586-11587.
214. C. W. Cheung and S. L. Buchwald, *Org. Lett.*, 2013, **15**, 3998-4001.
215. B. Helmich-Paris, B. de Souza, F. Neese and R. Izsák, *J. Chem. Phys.*, 2021, **155**.
216. R. Izsák and F. Neese, *J. Chem. Phys.*, 2011, **135**.
217. R. Izsák, F. Neese and W. Klopper, *J. Chem. Phys.*, 2013, **139**.
218. F. Neese, F. Wennmohs, A. Hansen and U. Becker, *Chem. Phys.*, 2009, **356**, 98-109.
219. J. N. Harvey, M. Aschi, H. Schwarz and W. Koch, *Theor. Chem. Acc.*, 1998, **99**, 95-99.
220. K. Yamaguchi, F. Jensen, A. Dorigo and K. Houk, *Chem. Phys. Lett.*, 1988, **149**, 537-542.
221. J.-D. Chai and M. Head-Gordon, *Phys. Chem. Chem. Phys.*, 2008, **10**, 6615-6620.
222. A. E. R. E. D. Glendening, J. E. Carpenter, F. Weihhold NBO Version 3.1.
223. M. J. Frisch, G. W. Trucks, H. B. Schlegel, G. E. Scuseria, M. A. Robb, J. R. Cheeseman, G. Scalmani, V. Barone, G. A. Petersson, H. Nakatsuji, X. Li, M. Caricato, A. V. Marenich, J. Bloino, B. G. Janesko, R. Gomperts, B. Mennucci, H. P. Hratchian, J. V. Ortiz, A. F. Izmaylov, J. L. Sonnenberg, Williams, F. Ding, F. Lipparini, F. Egidi, J. Goings, B. Peng, A. Petrone, T. Henderson, D. Ranasinghe, V. G. Zakrzewski, J. Gao, N. Rega, G. Zheng, W. Liang, M. Hada, M. Ehara, K. Toyota, R. Fukuda, J. Hasegawa, M. Ishida, T. Nakajima, Y. Honda, O. Kitao, H. Nakai, T. Vreven, K. Throssell, J. A. Montgomery Jr., J. E. Peralta, F. Ogliaro, M. J. Bearpark, J. J. Heyd, E. N. Brothers, K. N. Kudin, V. N. Staroverov, T. A. Keith, R. Kobayashi, J. Normand, K. Raghavachari, A. P. Rendell, J. C. Burant, S. S. Iyengar, J. Tomasi, M. Cossi, J. M. Millam, M. Klene, C. Adamo, R. Cammi, J. W. Ochterski, R. L. Martin, K. Morokuma, O. Farkas, J. B. Foresman and D. J. Fox, Gaussian 16 Rev. C.01, 2016.
224. C. Y. Legault, CYLview20, 2020.
225. M. Isegawa, F. Neese and D. A. Pantazis, *J. Chem. Theory Comput.*, 2016, **12**, 2272-2284.
226. J. Nugent, C. Arroniz, B. R. Shire, A. J. Sterling, H. D. Pickford, M. L. J. Wong, S. J. Mansfield, D. F. J. Caputo, B. Owen, J. J. Mousseau, F. Duarte and E. A. Anderson, *ACS Catal.*, 2019, **9**, 9568-9574.
227. J. Ho, *Phys. Chem. Chem. Phys.*, 2015, **17**, 2859-2868.
228. T. B. Demissie, K. Ruud and J. H. Hansen, *Organometallics*, 2015, **34**, 4218-4228.

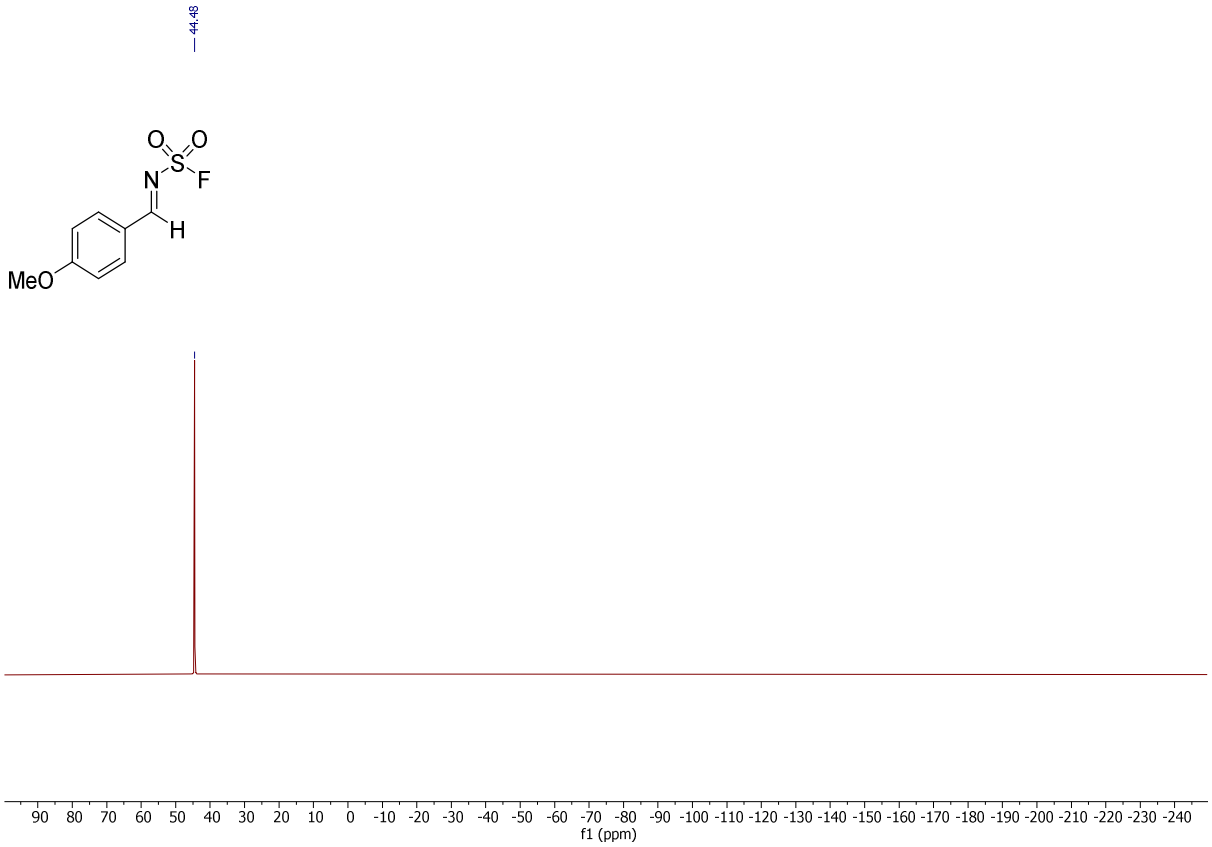
Appendix

NMR Spectra

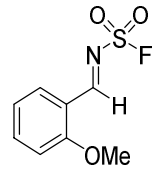
Sulfamoyl fluoride Imines

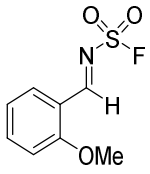
(4-Methoxybenzylidene)sulfamoyl fluoride (1a)

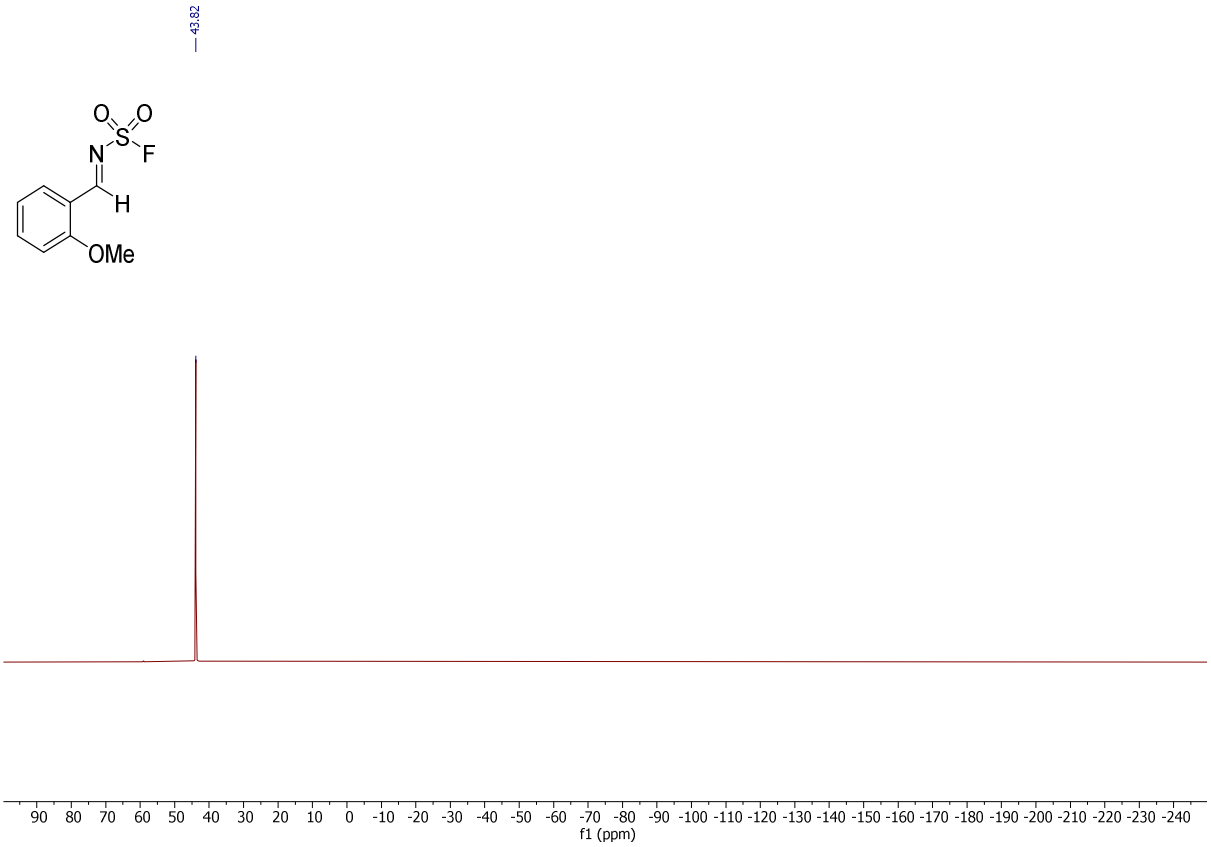



44.48
O
O
S
N
F
H
MeO
90 80 70 60 50 40 30 20 10 0 -10 -20 -30 -40 -50 -60 -70 -80 -90 -100 -110 -120 -130 -140 -150 -160 -170 -180 -190 -200 -210 -220 -230 -240
f1 (ppm)

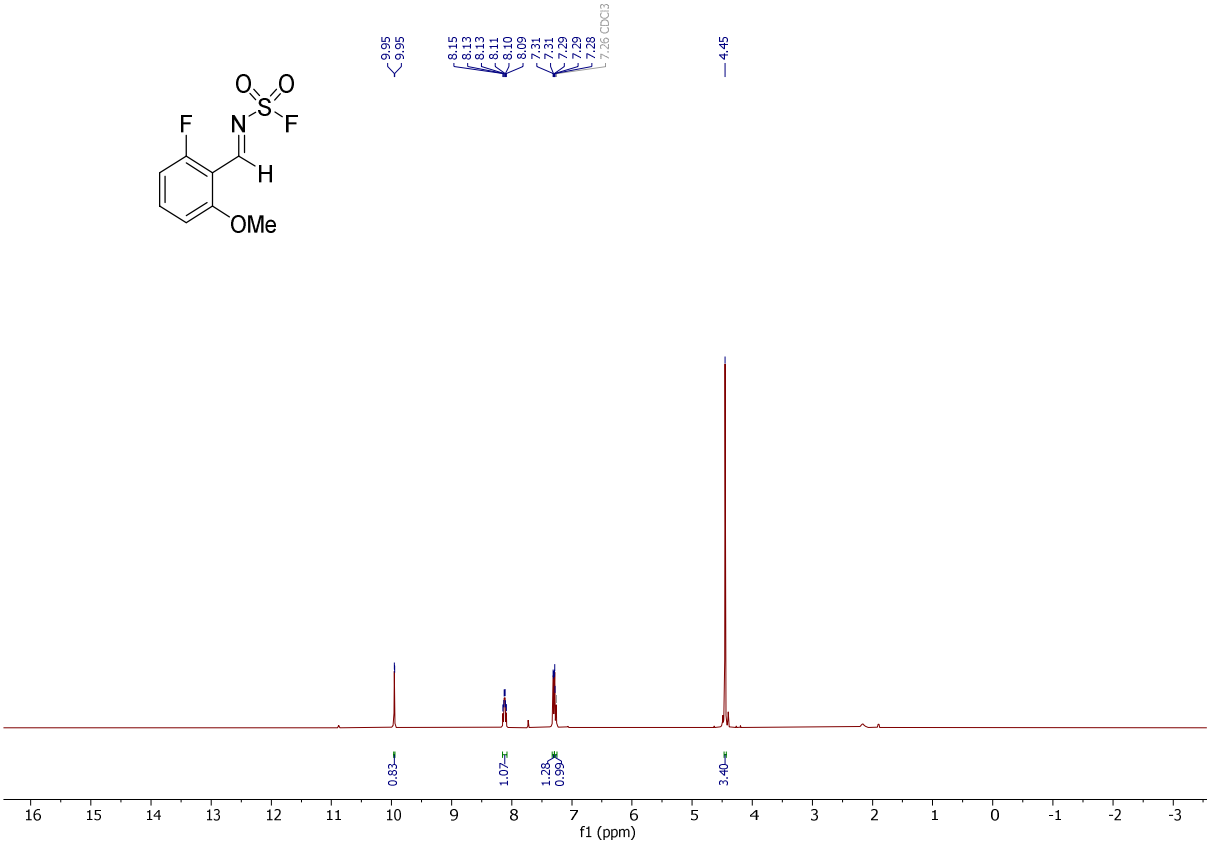
(2-Methoxybenzylidene)sulfamoyl fluoride (1b)

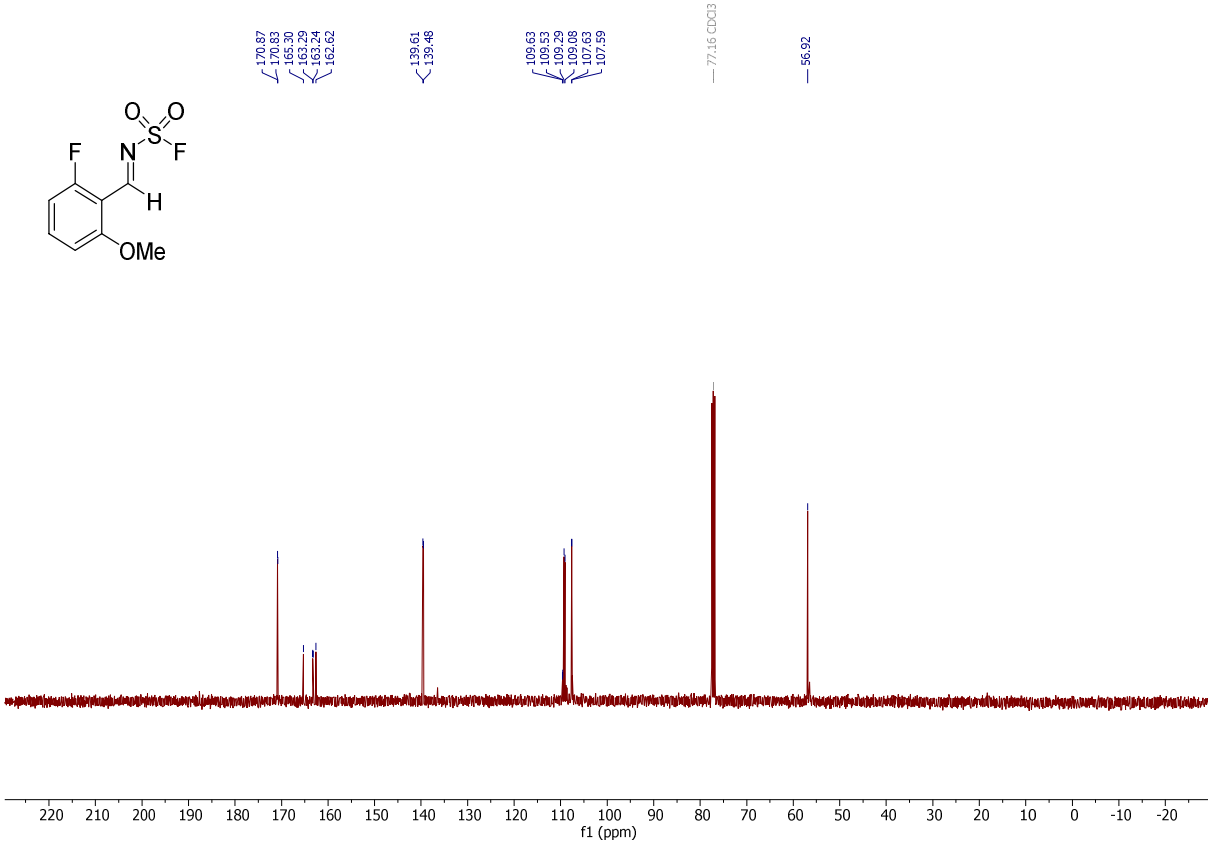


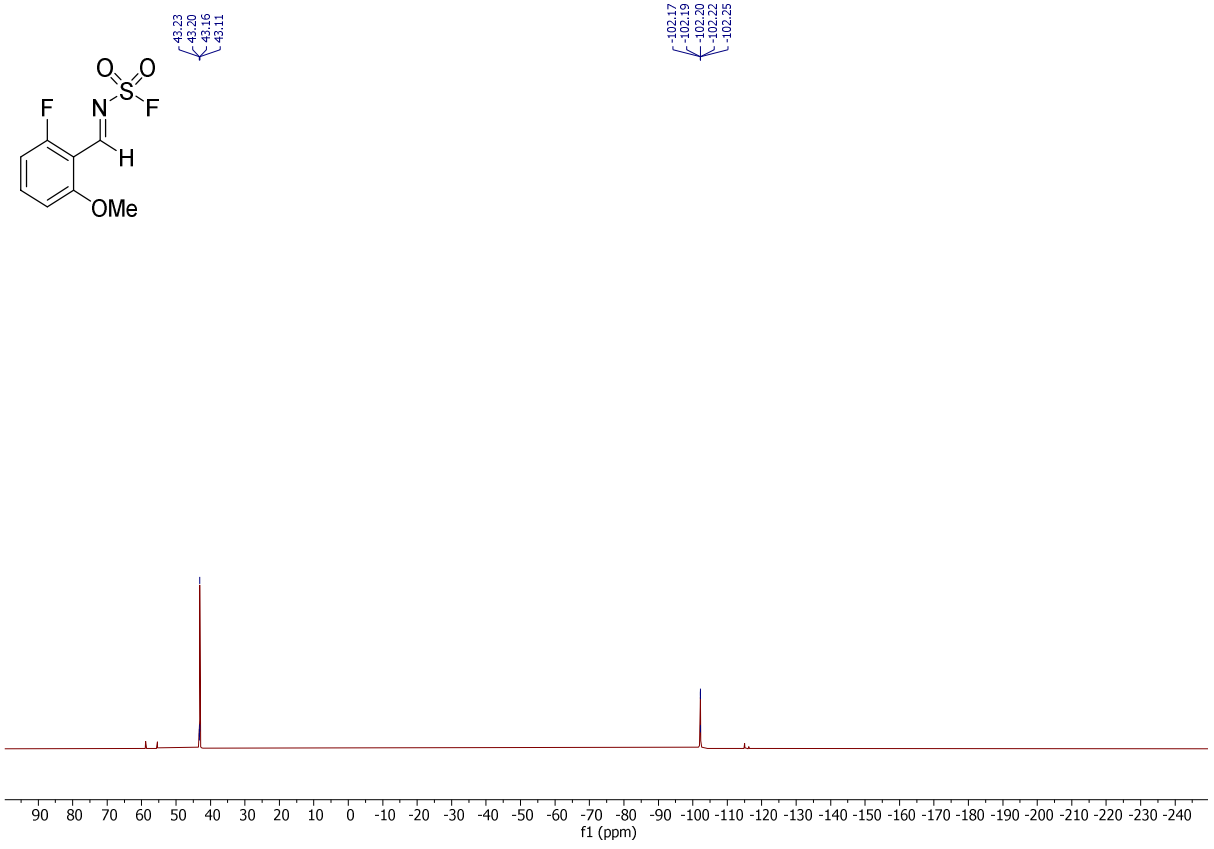




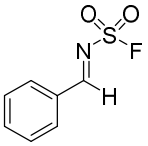
(2-Fluoro-6-methoxybenzylidene)sulfamoyl fluoride (1c)

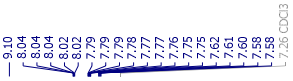


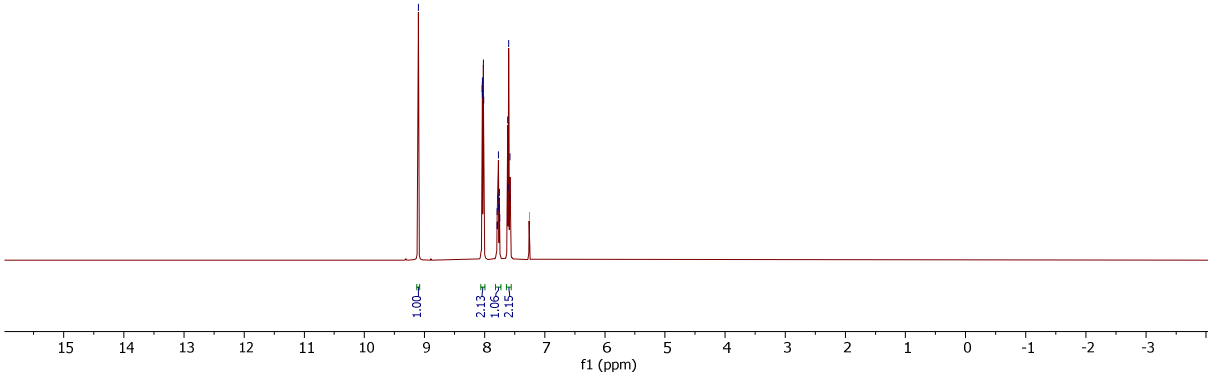

170.87
170.83
165.30
163.24
162.62
139.61
139.48
109.63
109.53
109.29
109.08
107.63
107.59
77.16 CDCl3
56.92
O
O
S
F
N
F
H
OMe
220 210 200 190 180 170 160 150 140 130 120 110 100 90 80 70 60 50 40 30 20 10 0 -10 -20
f1 (ppm)


43.23
43.20
43.16
43.11
-102.17
-102.19
-102.20
-102.22
-102.25
O
O
S
F
N
F
H
OMe
90 80 70 60 50 40 30 20 10 0 -10 -20 -30 -40 -50 -60 -70 -80 -90 -100 -110 -120 -130 -140 -150 -160 -170 -180 -190 -200 -210 -220 -230 -240
f1 (ppm)

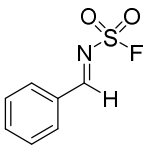
Benzylidenesulfamoyl fluoride (1d)

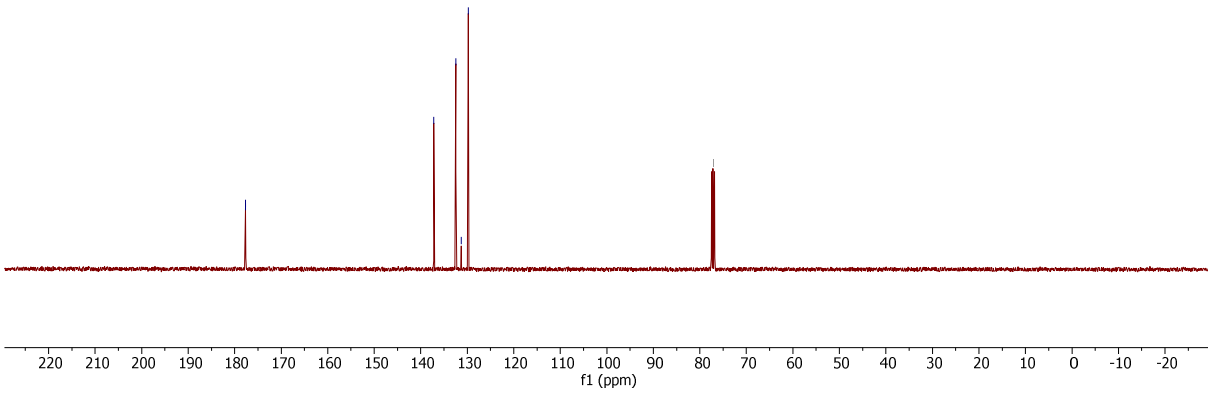


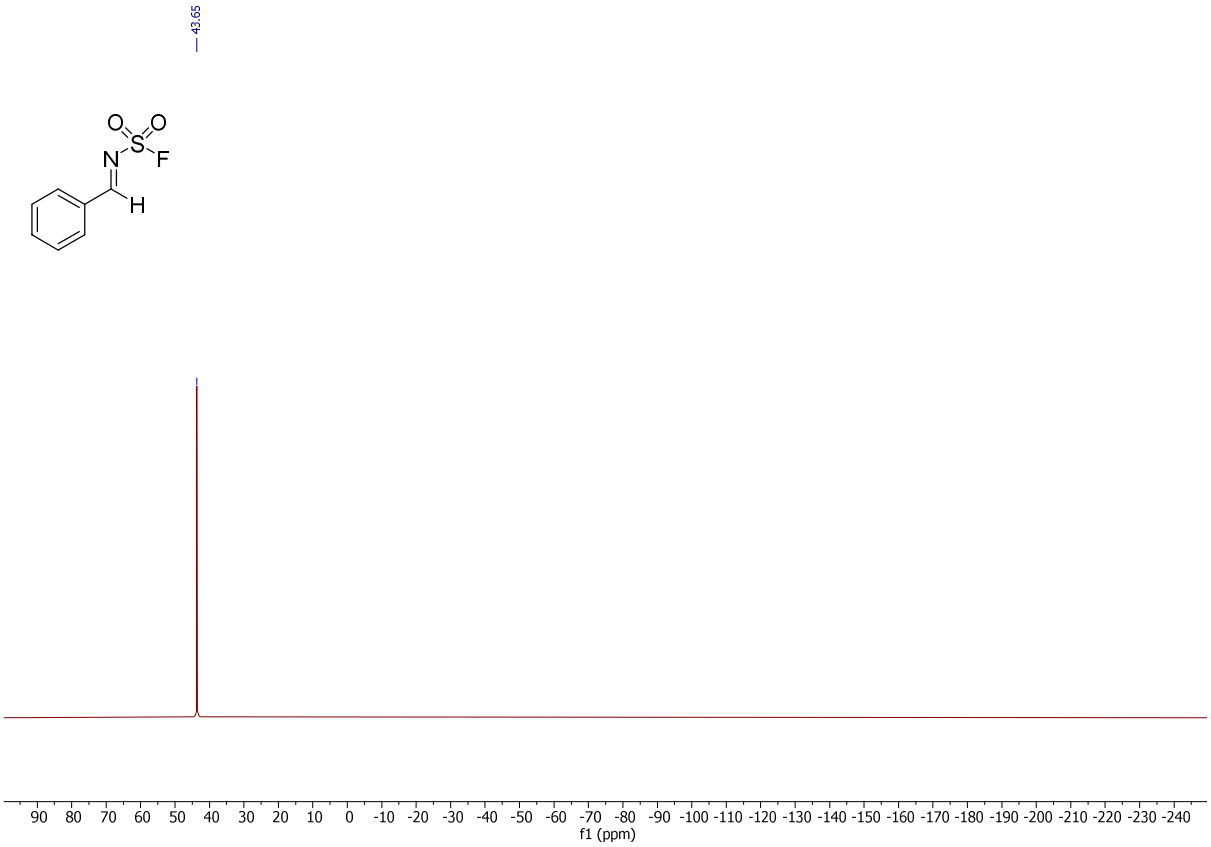




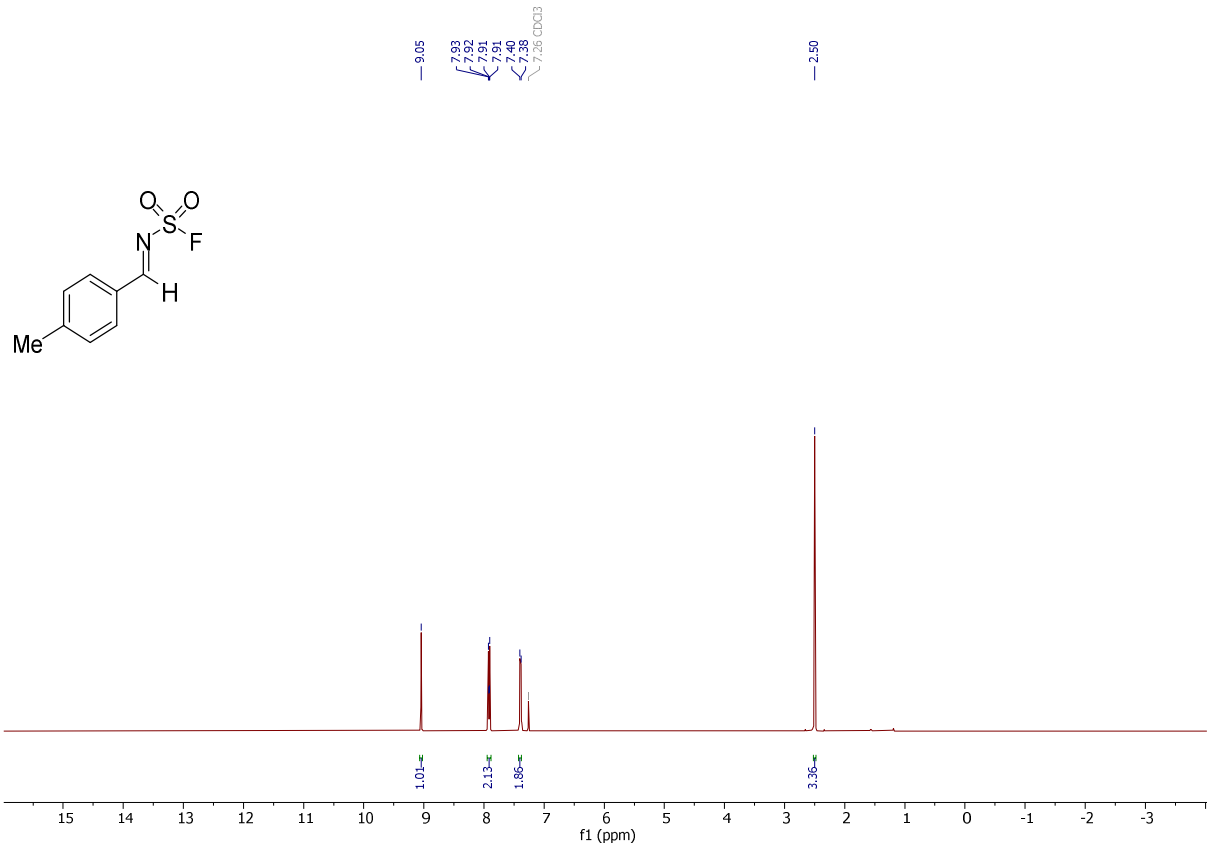


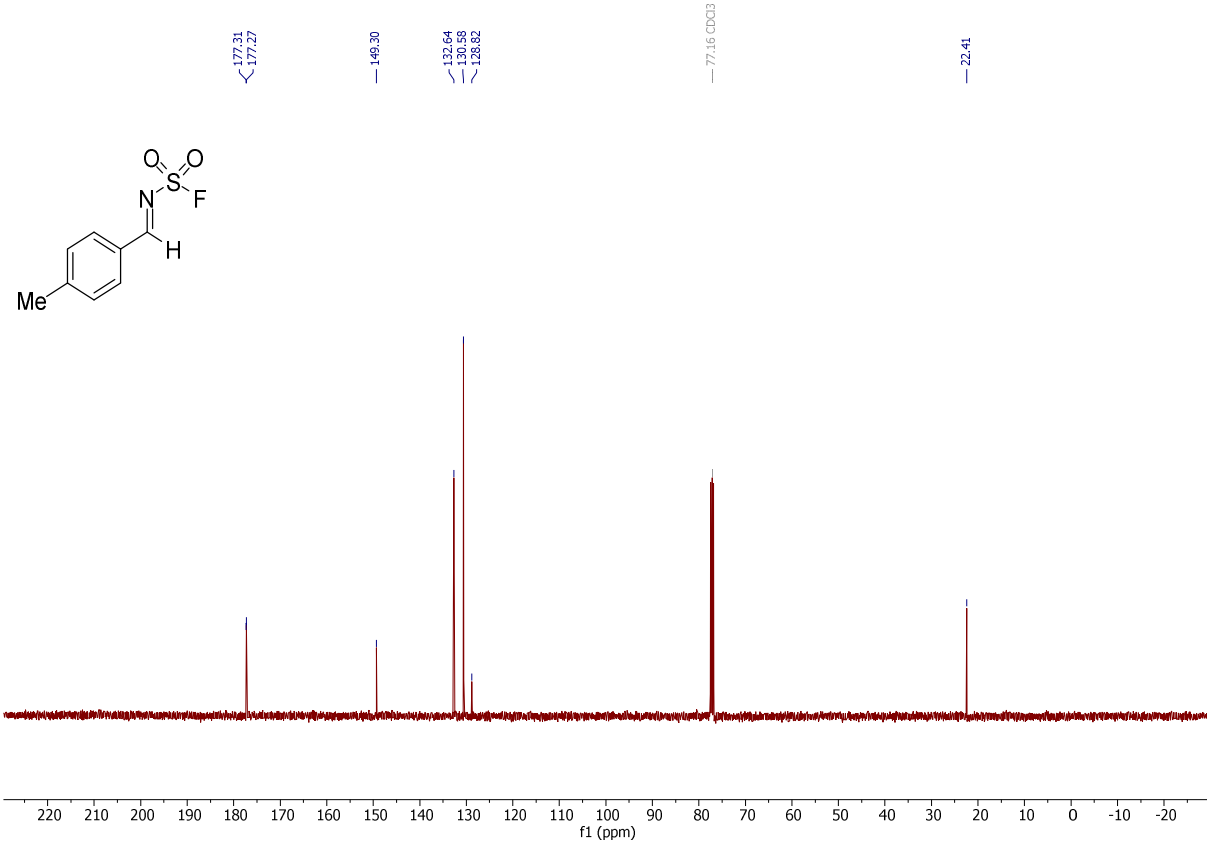


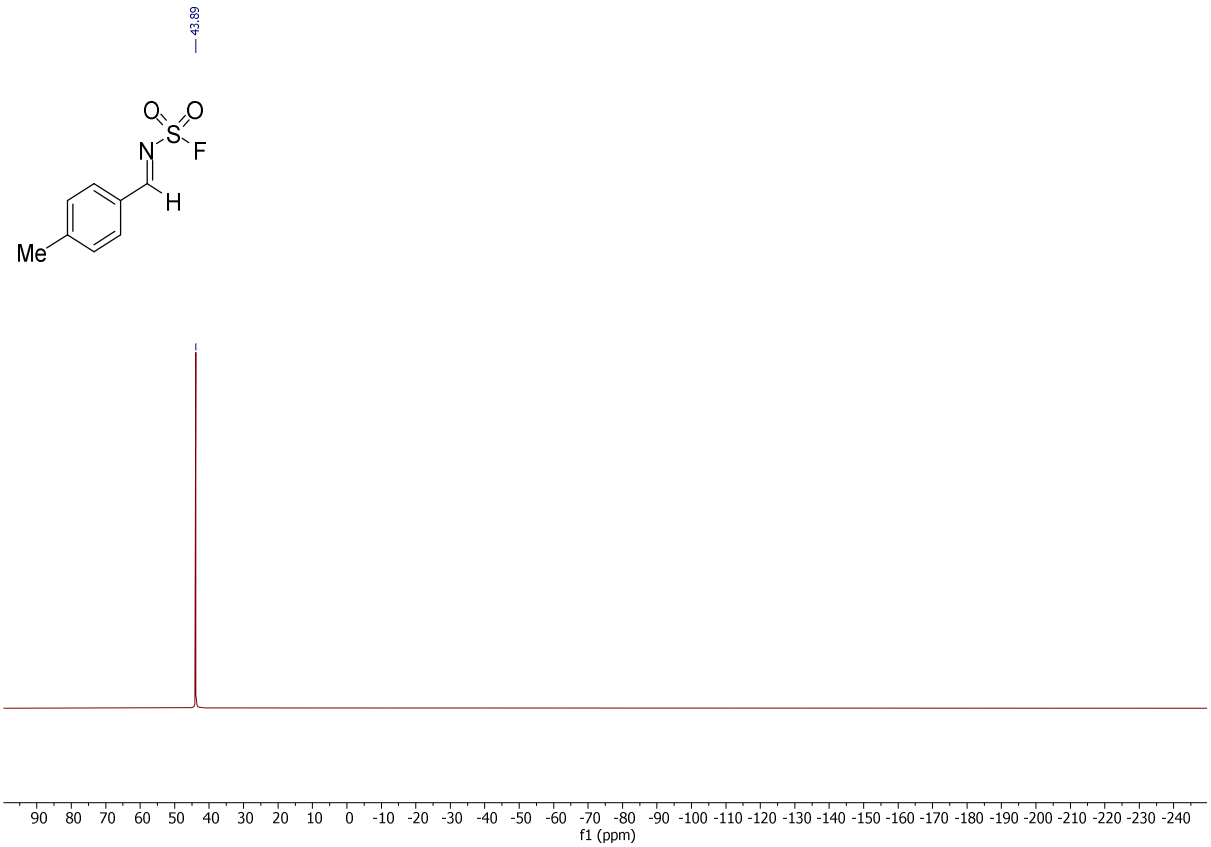




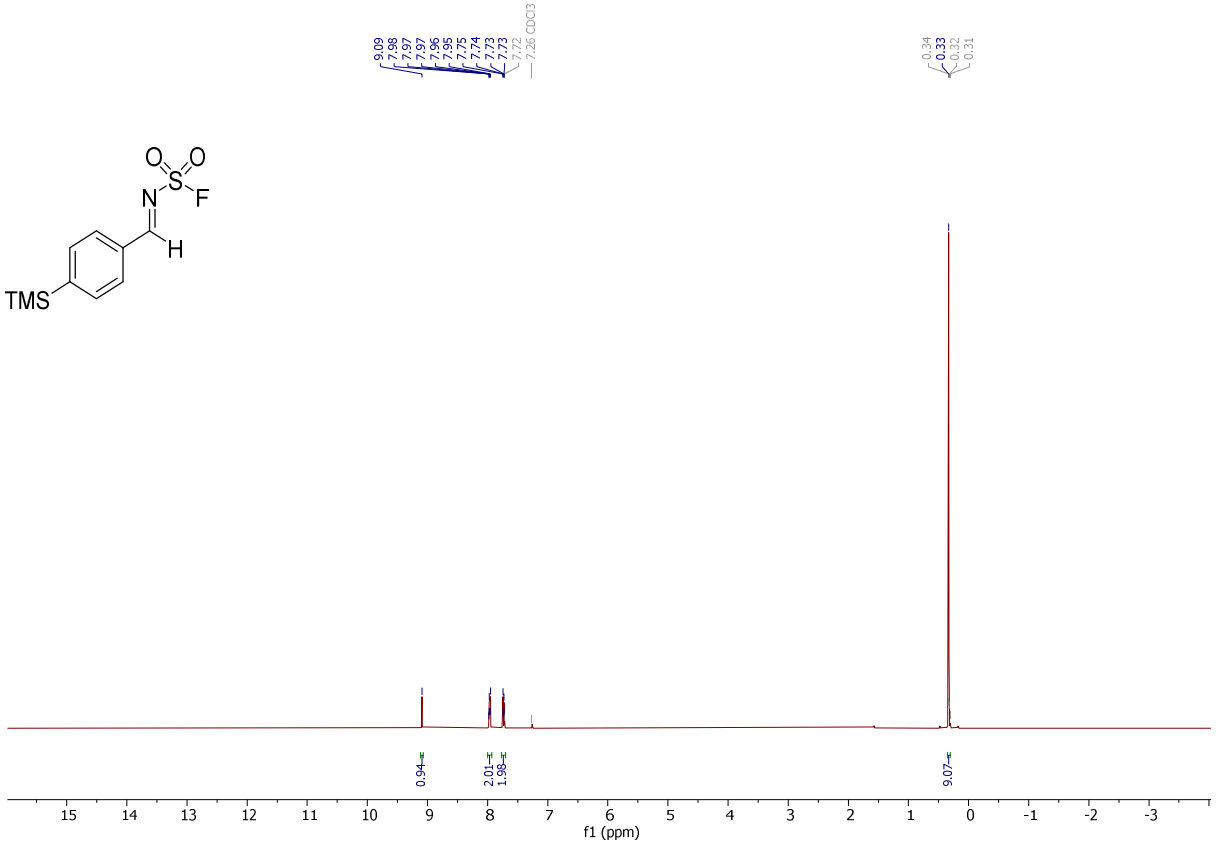
(4-Methylbenzylidene)sulfamoyl fluoride (1e)

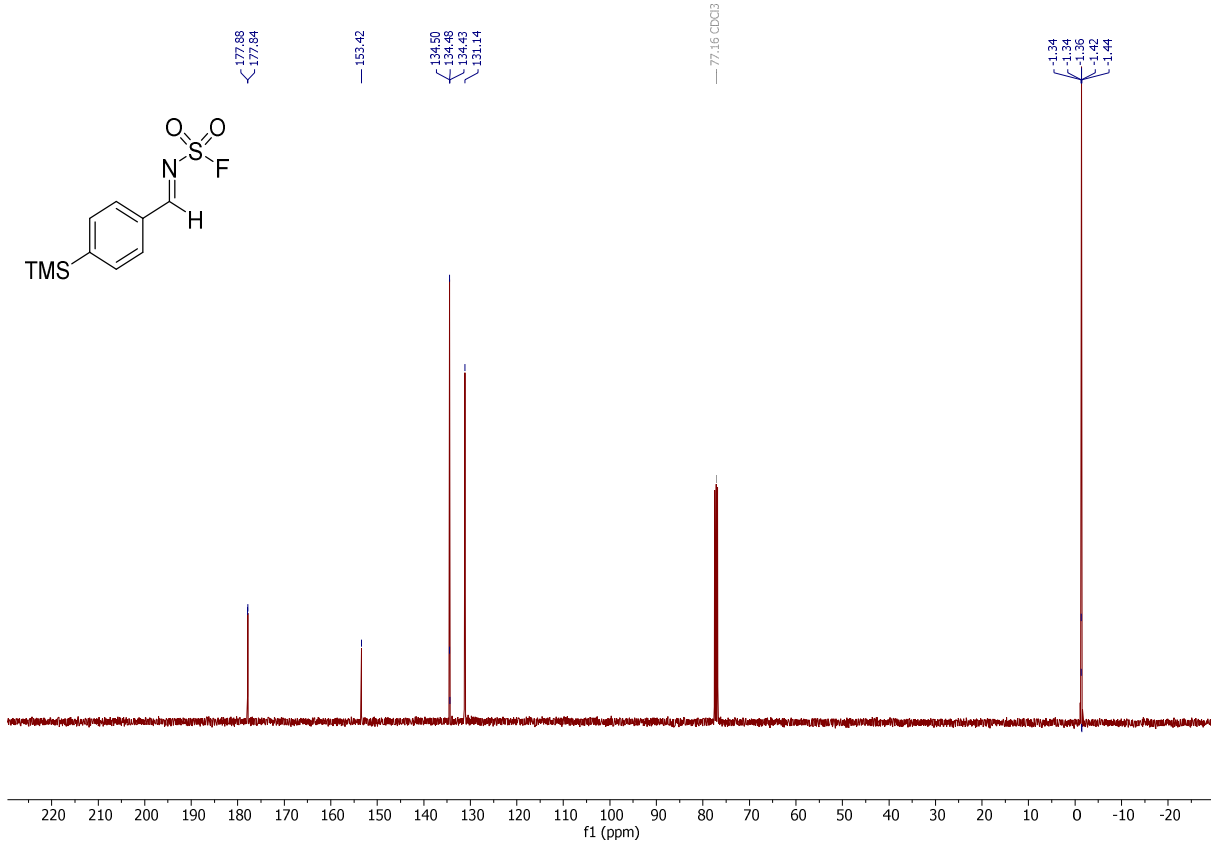


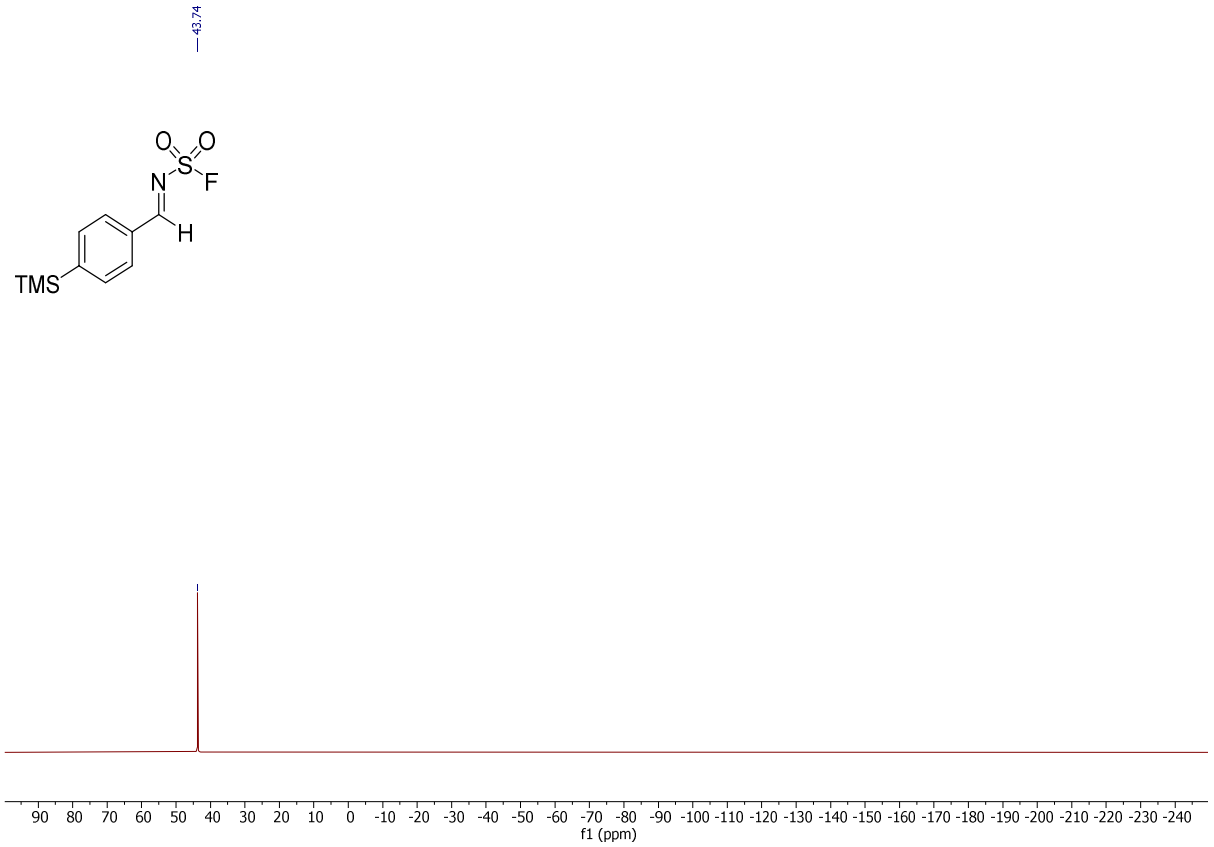

177.31
177.27
149.30
132.64
130.58
128.82
77.16 CDCl3
22.41
O
O
S
N
F
H
Me
220 210 200 190 180 170 160 150 140 130 120 110 100 90 80 70 60 50 40 30 20 10 0 -10 -20
f1 (ppm)


43.89
O
O
S
N
F
H
Me
90 80 70 60 50 40 30 20 10 0 -10 -20 -30 -40 -50 -60 -70 -80 -90 -100 -110 -120 -130 -140 -150 -160 -170 -180 -190 -200 -210 -220 -230 -240
f1 (ppm)

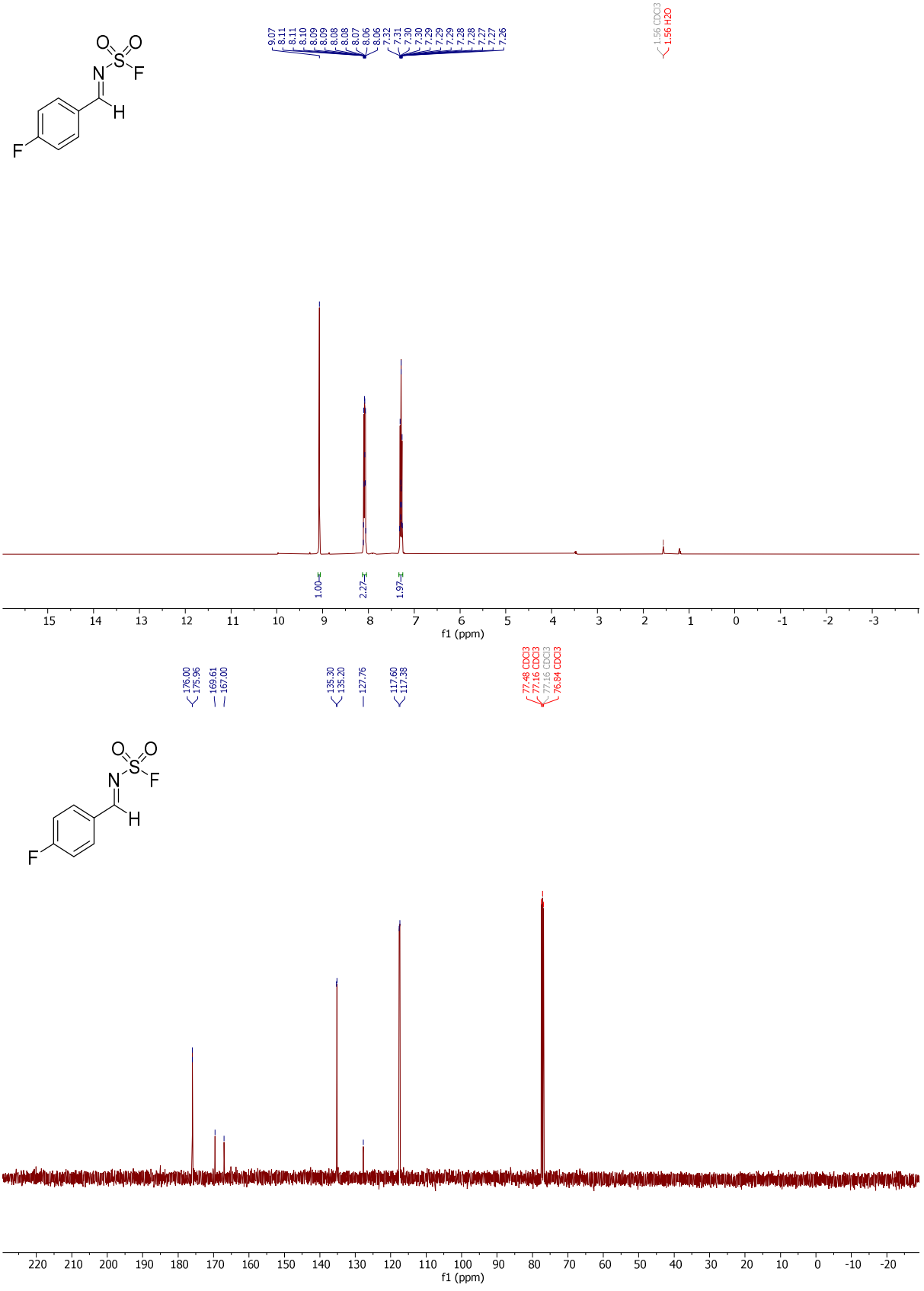
(4-(Trimethylsilyl)benzylidene)sulfamoyl fluoride (1g)

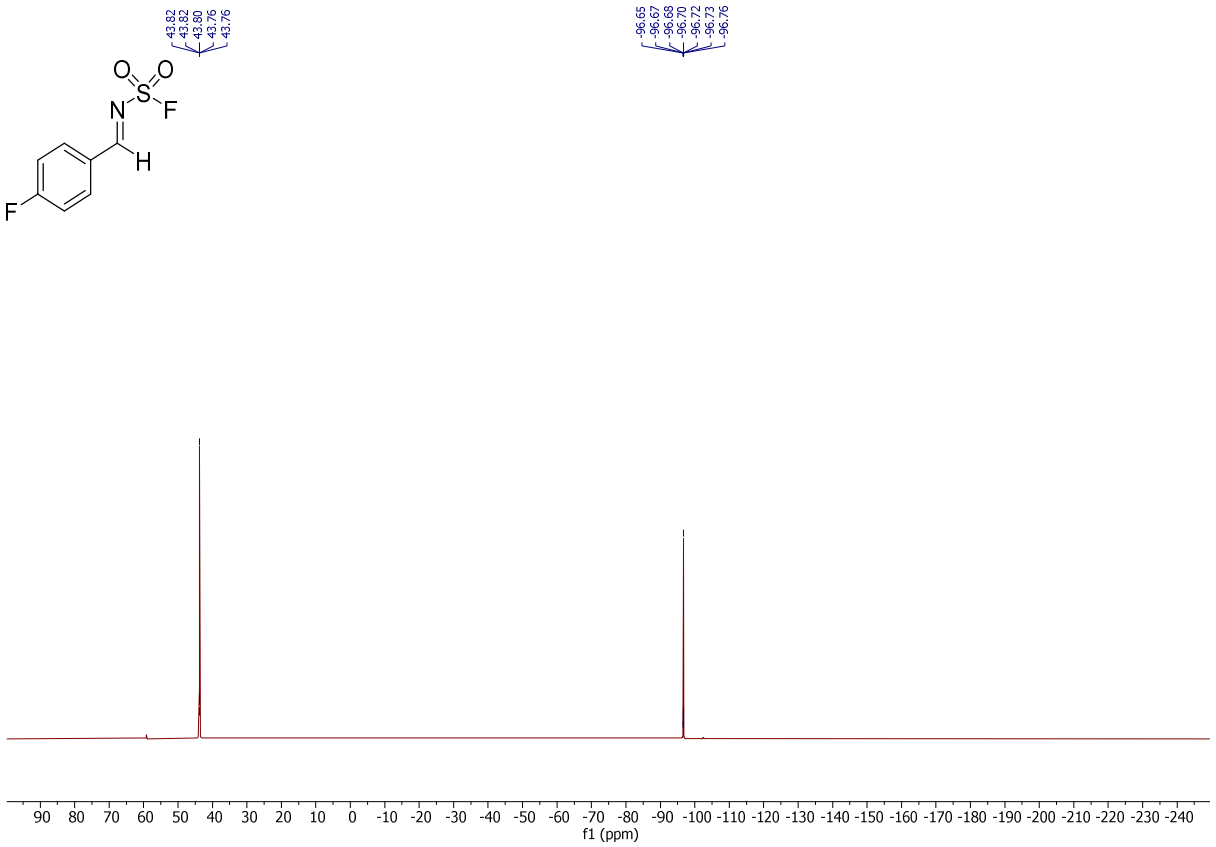

9.09
7.98
7.97
7.97
7.96
7.95
7.75
7.74
7.73
7.73
7.72
7.26 CDCl3
0.34
0.33
0.32
0.31
O
O
S
N
F
H
TMS
0.94
2.01
1.98
9.07
f1 (ppm)


177.88
177.84
153.42
134.50
134.48
134.43
131.14
77.16 CDCl3
-1.34
-1.34
-1.36
-1.42
-1.44
O
O
S
N
F
H
TMS
f1 (ppm)

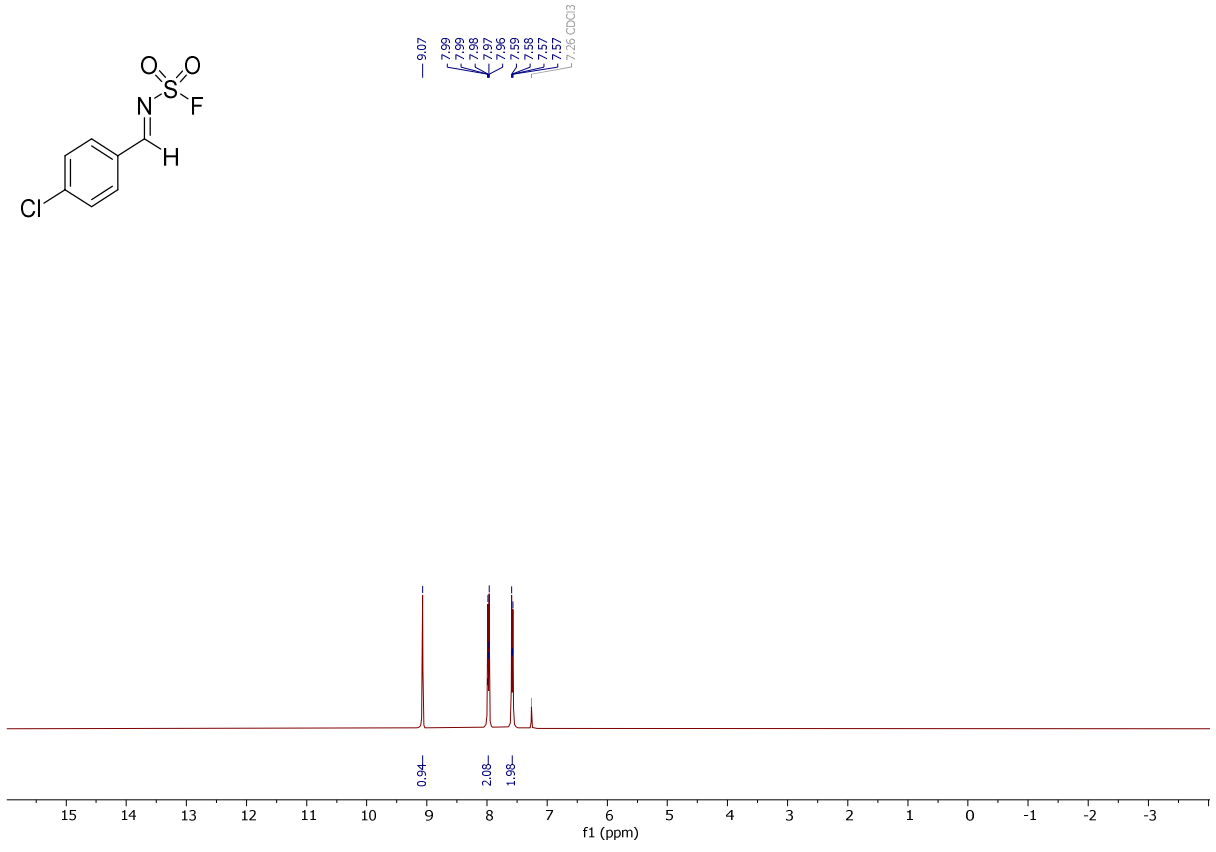

43.74
O
O
S
N
F
H
TMS
90 80 70 60 50 40 30 20 10 0 -10 -20 -30 -40 -50 -60 -70 -80 -90 -100 -110 -120 -130 -140 -150 -160 -170 -180 -190 -200 -210 -220 -230 -240
f1 (ppm)

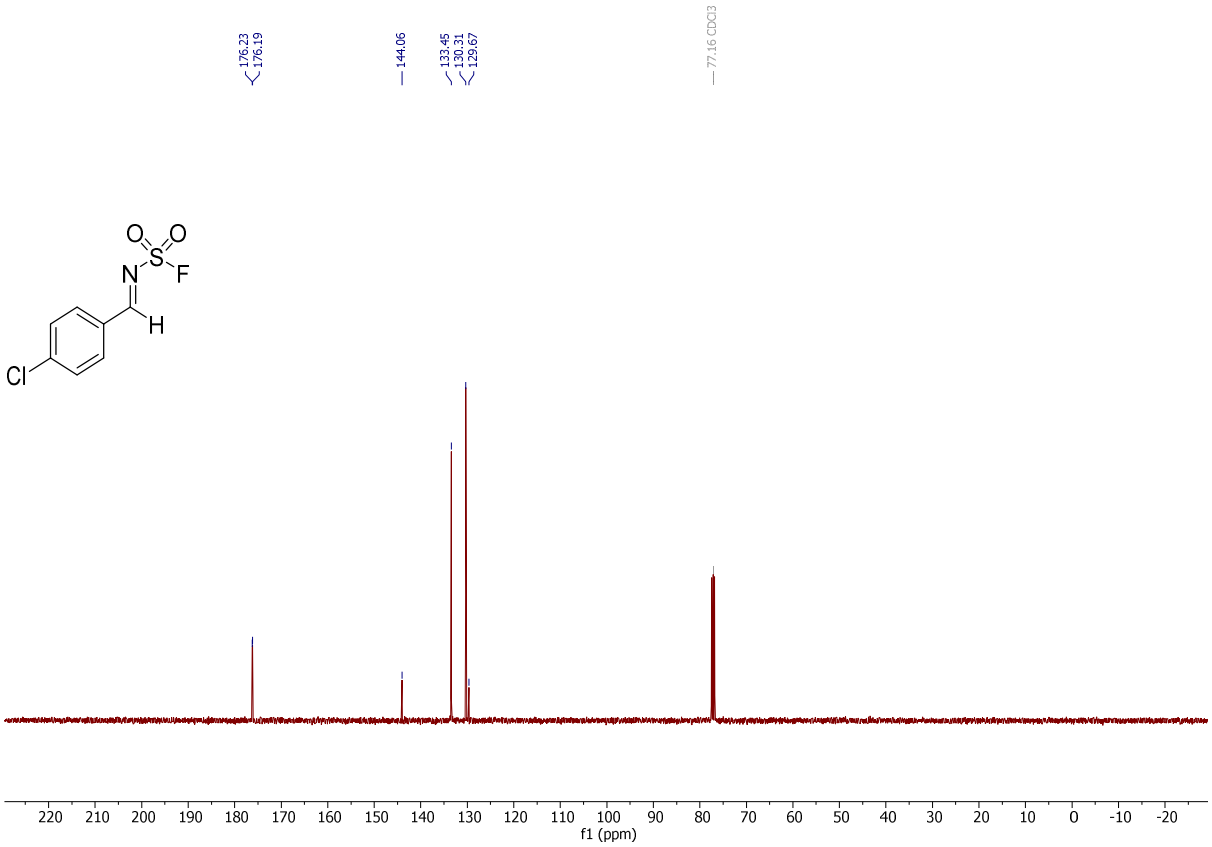
(4-Fluorobenzylidene)sulfamoyl fluoride (1i)

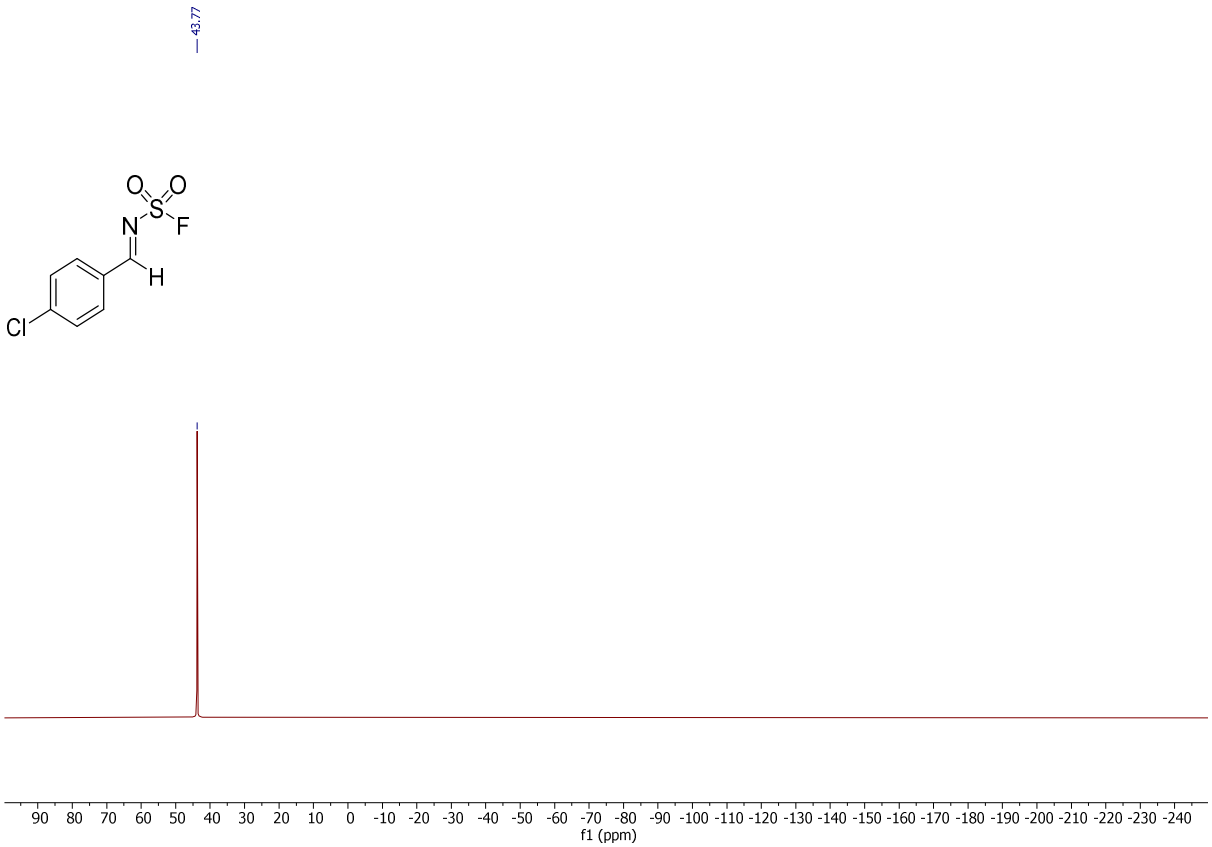




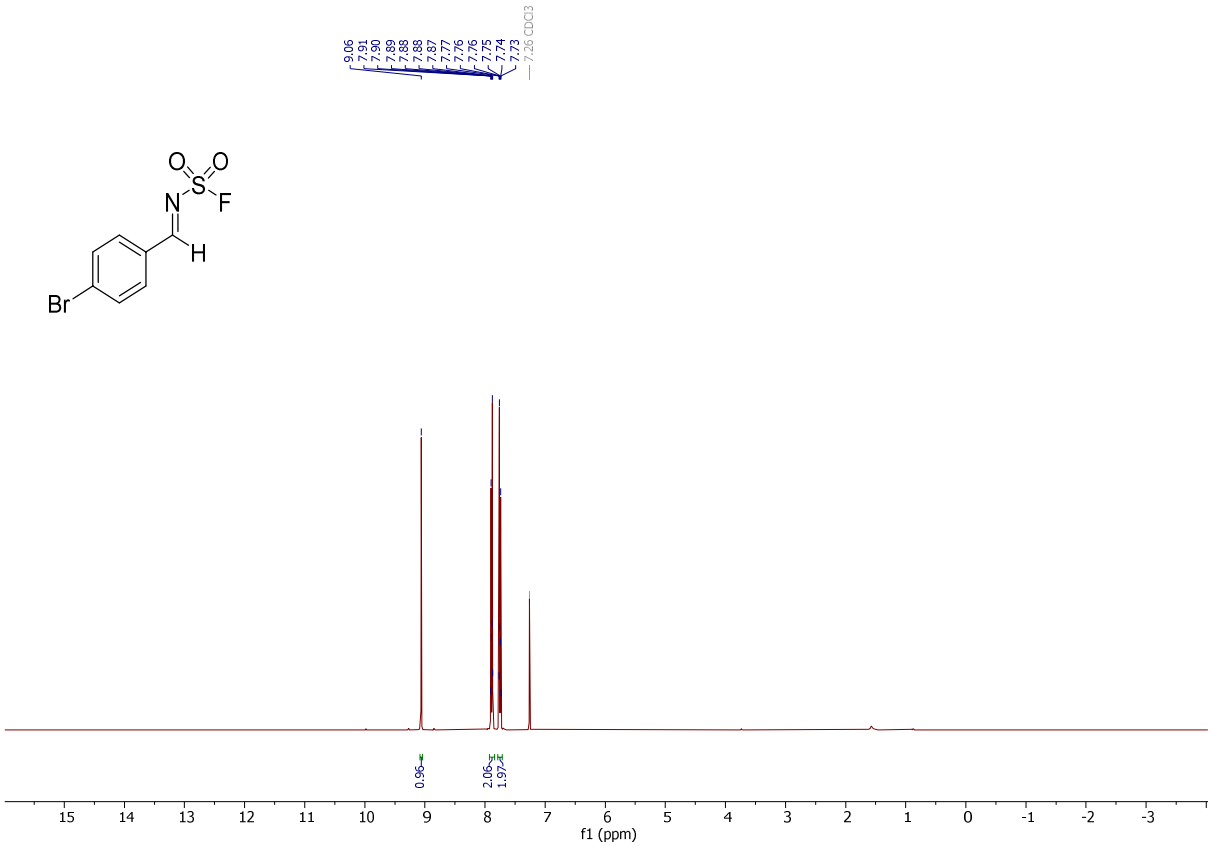
(4-Chlorobenzylidene)sulfamoyl fluoride (1j)

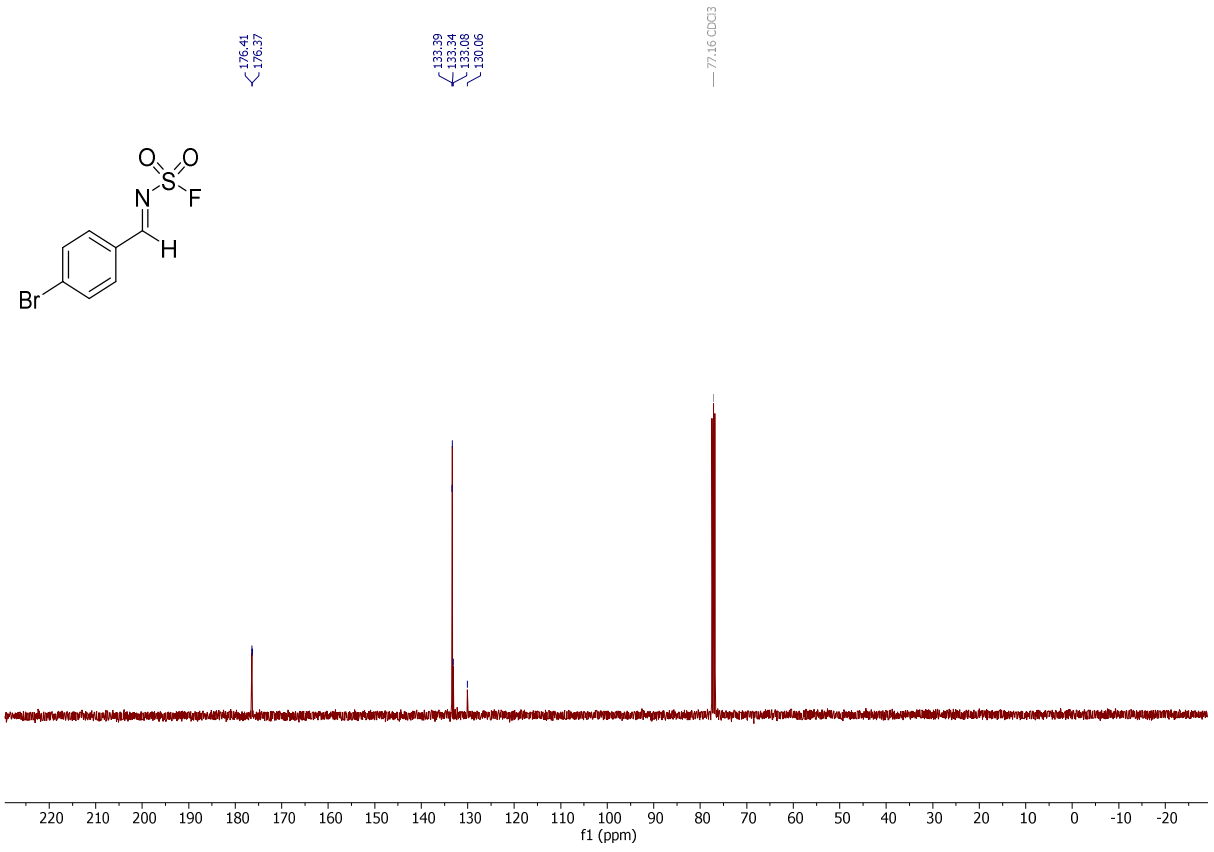


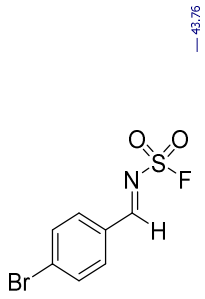


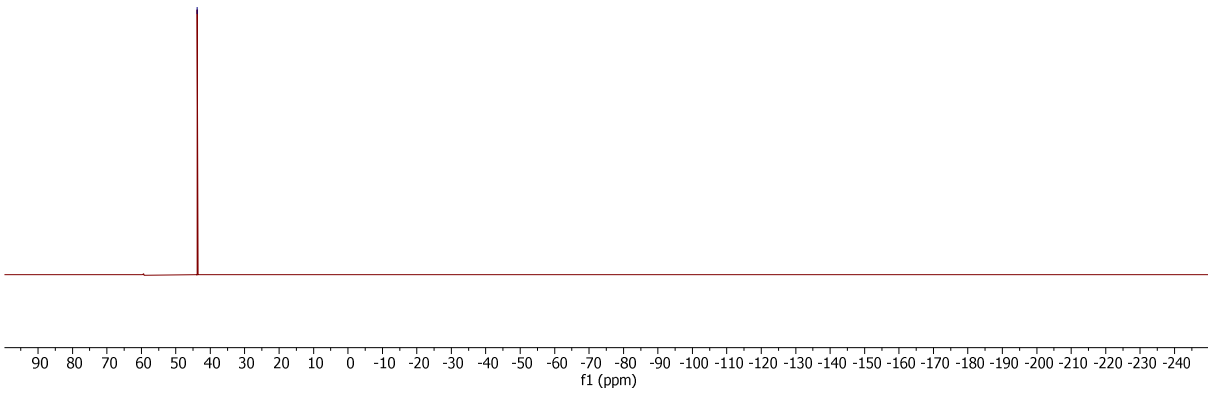


(4-Bromobenzylidene)sulfamoyl fluoride (1k)

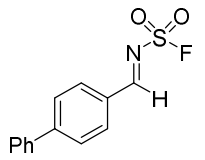

9.06
7.91
7.90
7.89
7.88
7.88
7.87
7.77
7.76
7.76
7.75
7.74
7.73
7.26 CDCl3
O
O
S
N
F
H
Br
0.96
2.06
1.97
15 14 13 12 11 10 9 8 7 6 5 4 3 2 1 0 -1 -2 -3
f1 (ppm)


176.41
176.37
133.39
133.34
133.08
130.06
77.16 CDCl3
O
O
S
N
F
H
Br
220 210 200 190 180 170 160 150 140 130 120 110 100 90 80 70 60 50 40 30 20 10 0 -10 -20
f1 (ppm)

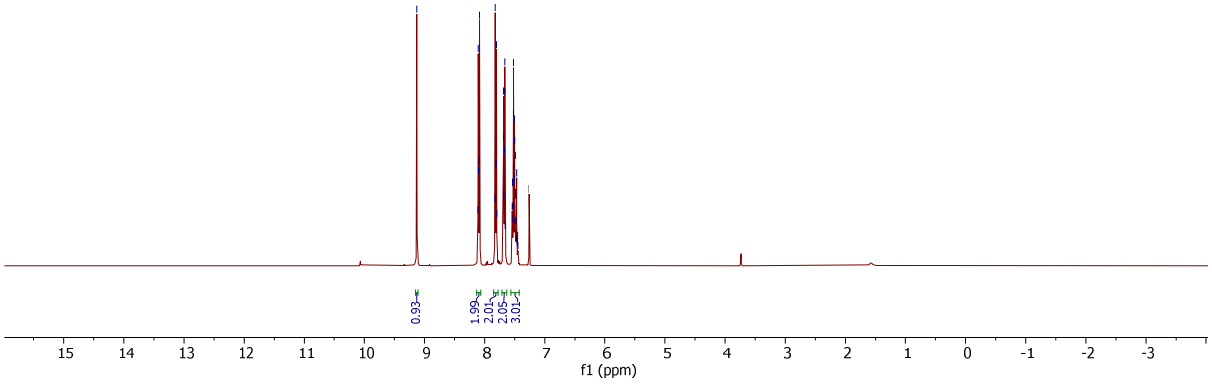


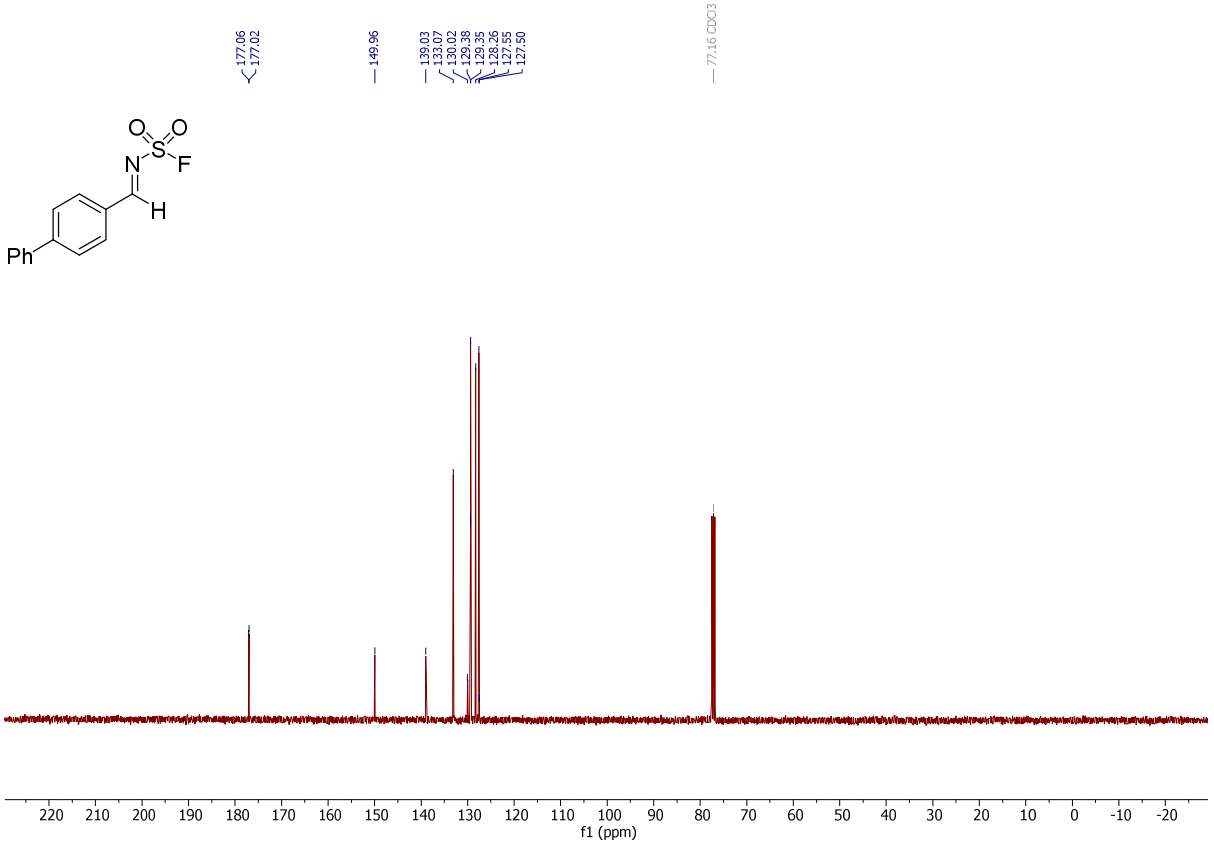


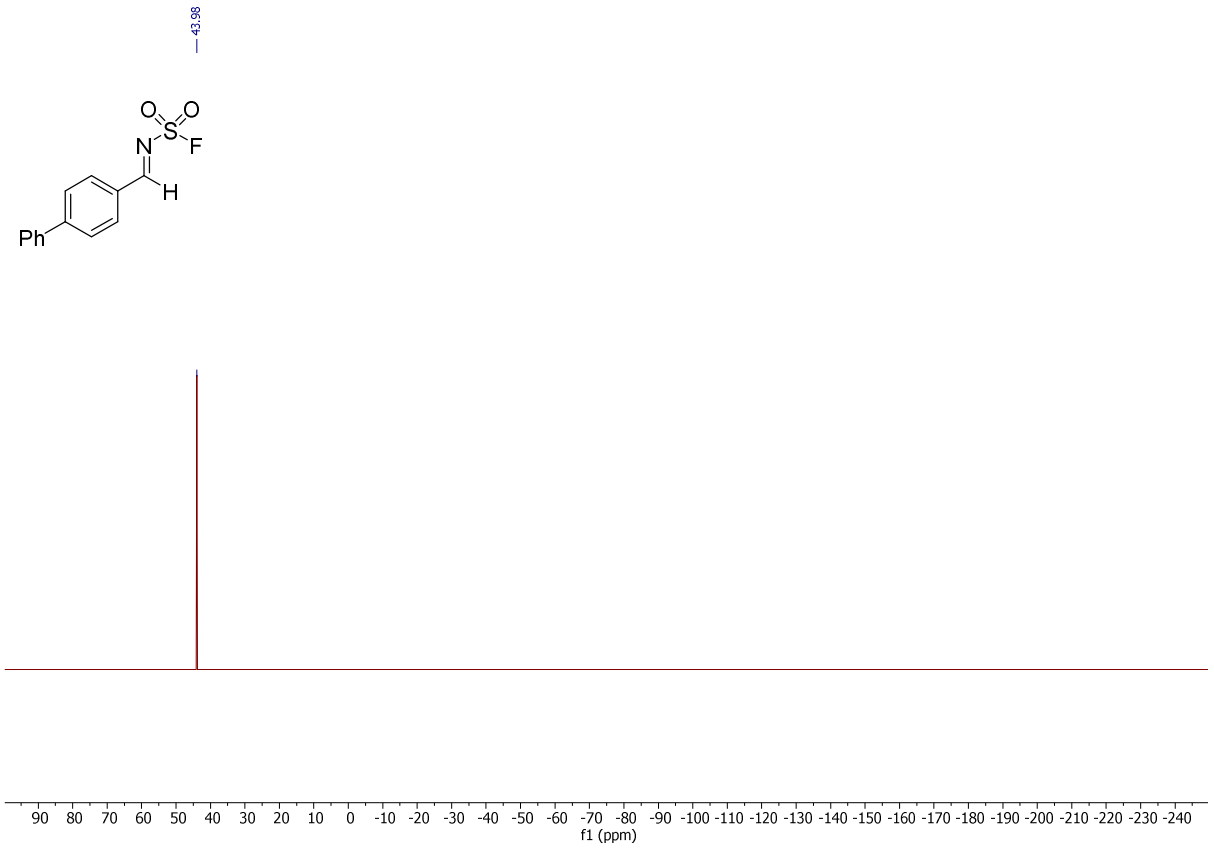
([1,1'-Biphenyl]-4-ylmethylene)sulfamoyl fluoride (1h)



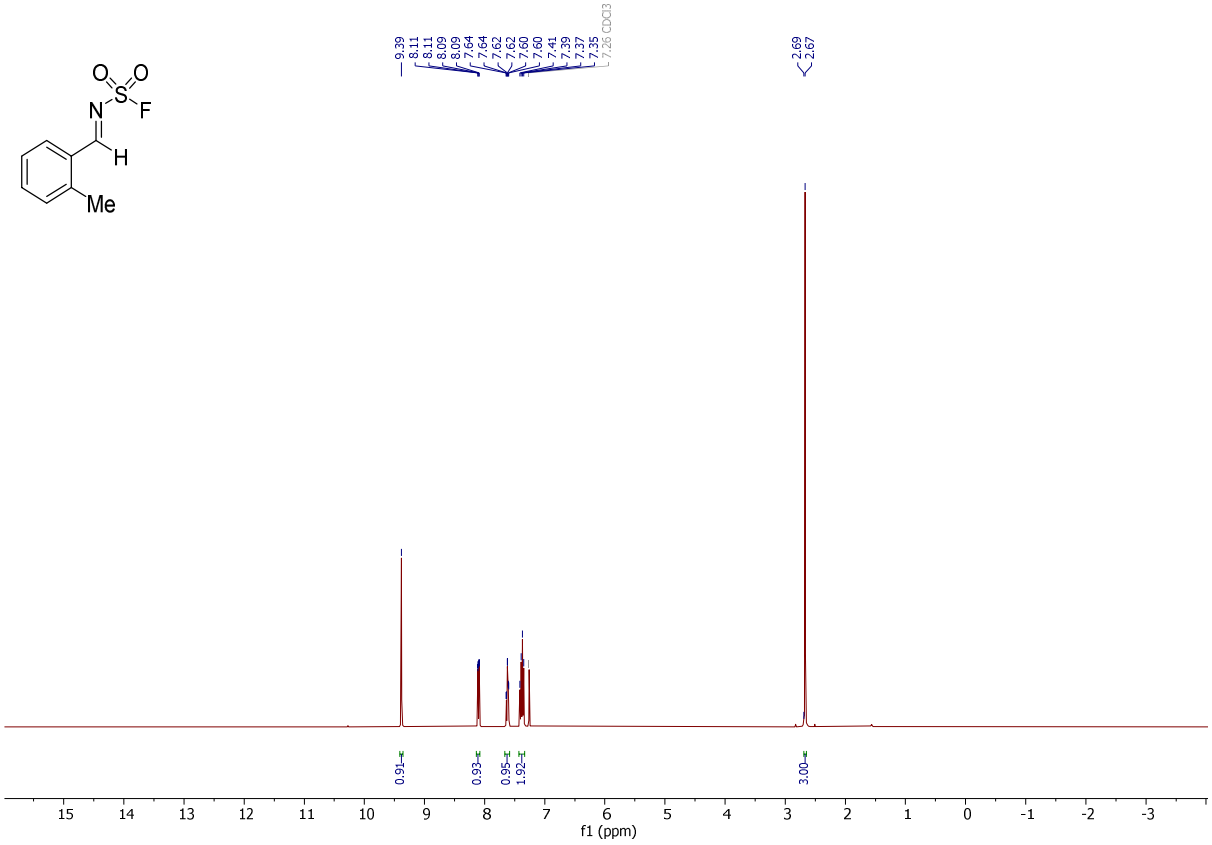


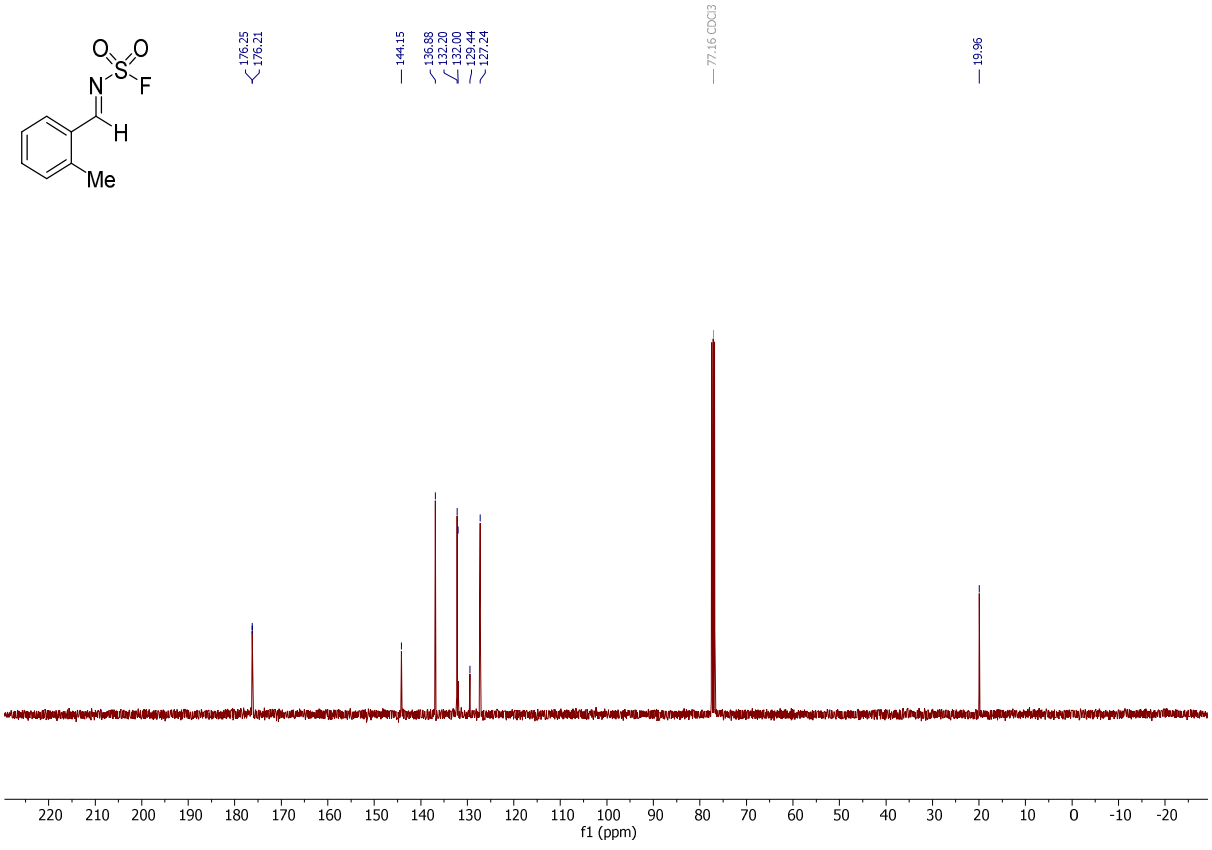


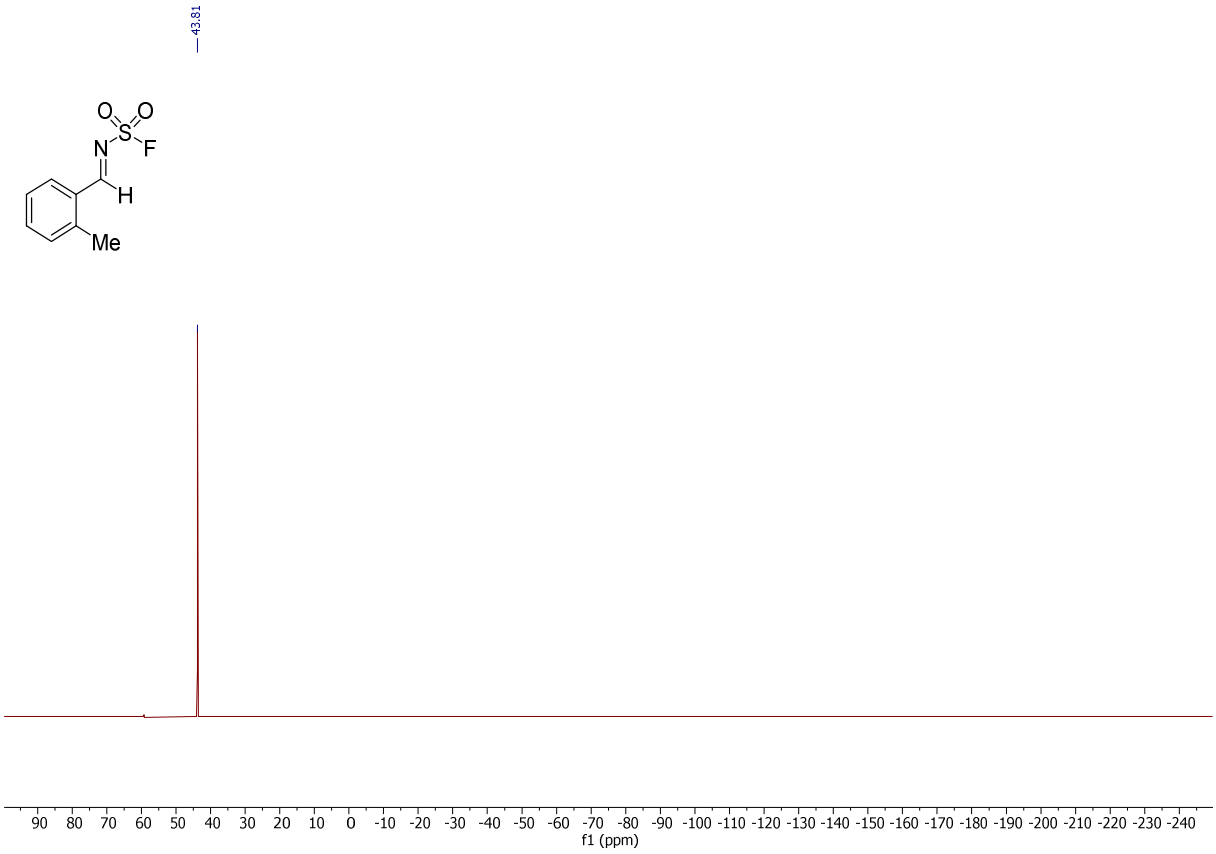

177.06
177.02
149.96
139.03
133.07
130.02
129.38
129.35
128.26
127.55
127.50
77.16 CDCl3
O
O
S
N
F
H
Ph
220 210 200 190 180 170 160 150 140 130 120 110 100 90 80 70 60 50 40 30 20 10 0 -10 -20
f1 (ppm)


43.98
O
O
S
N
F
H
Ph
90 80 70 60 50 40 30 20 10 0 -10 -20 -30 -40 -50 -60 -70 -80 -90 -100 -110 -120 -130 -140 -150 -160 -170 -180 -190 -200 -210 -220 -230 -240
f1 (ppm)

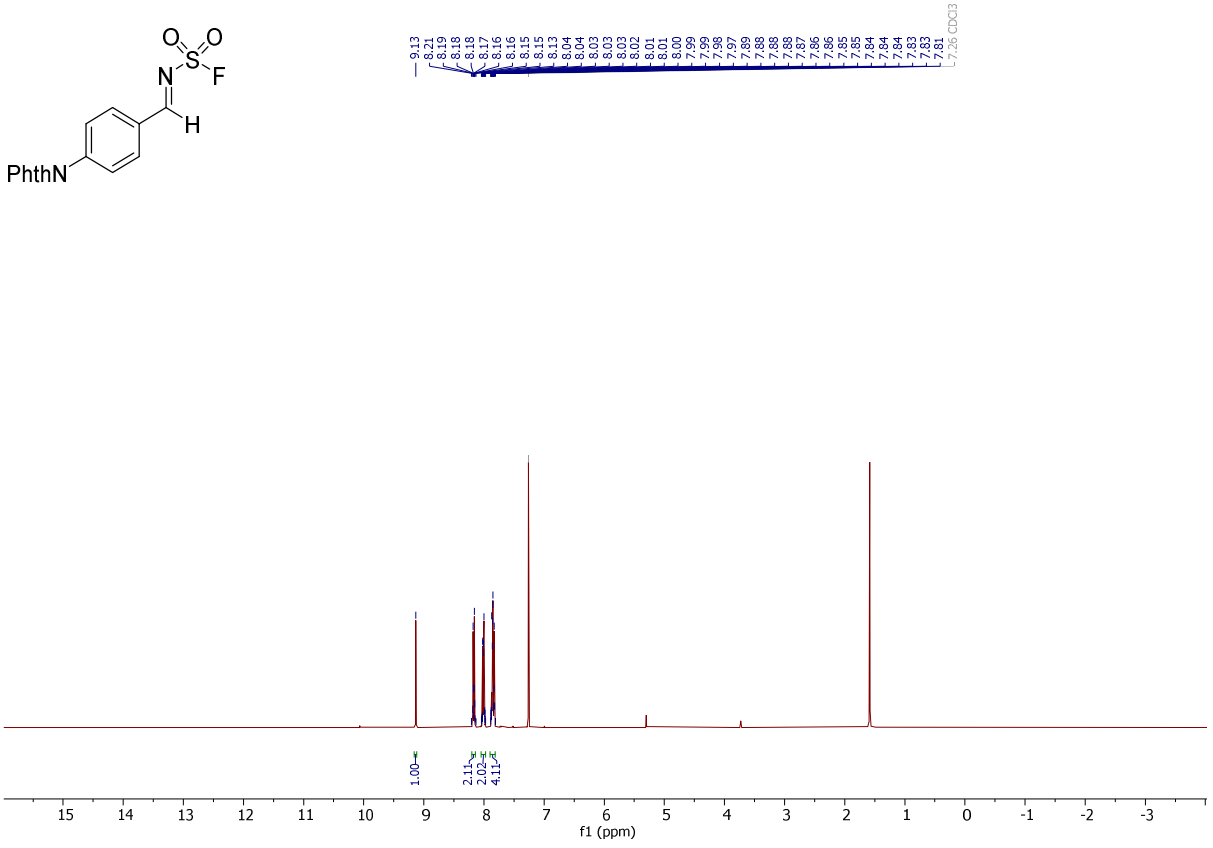
(2-Methylbenzylidene)sulfamoyl fluoride (1f)

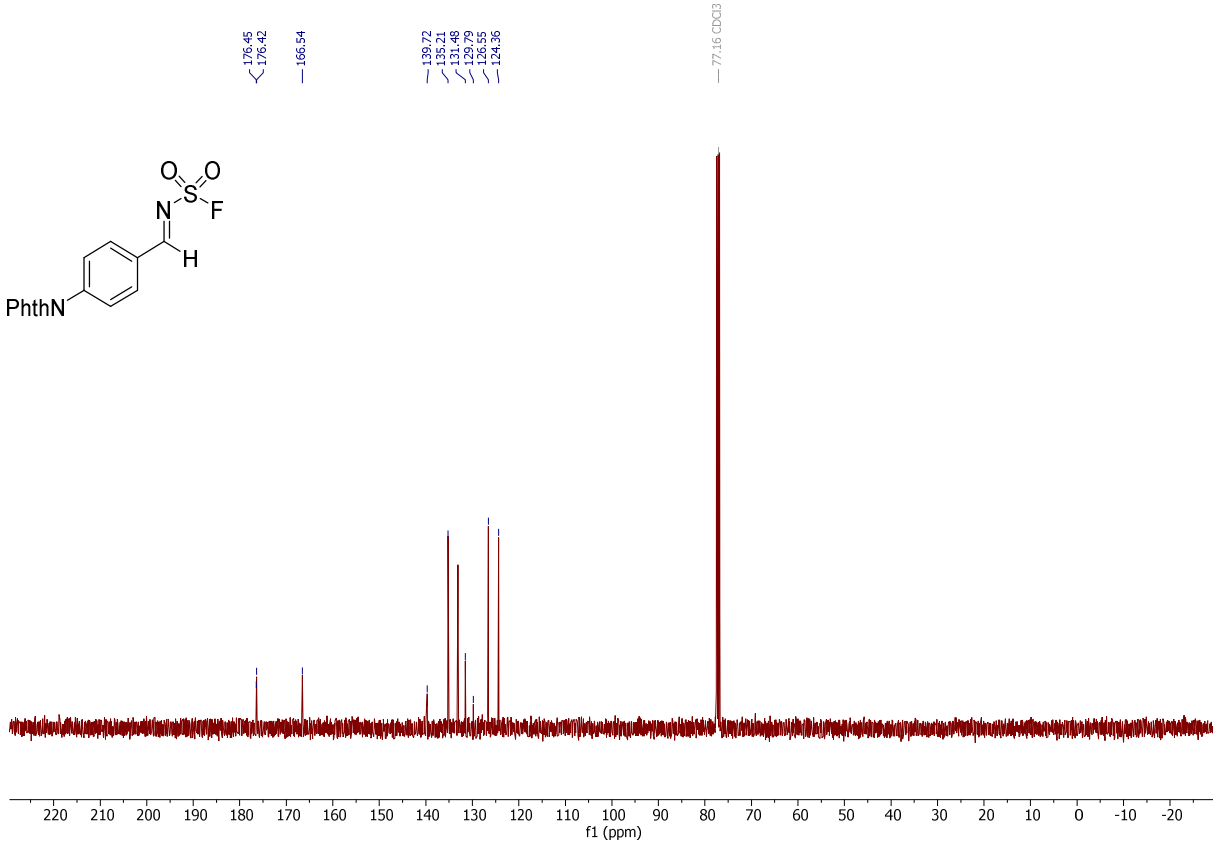


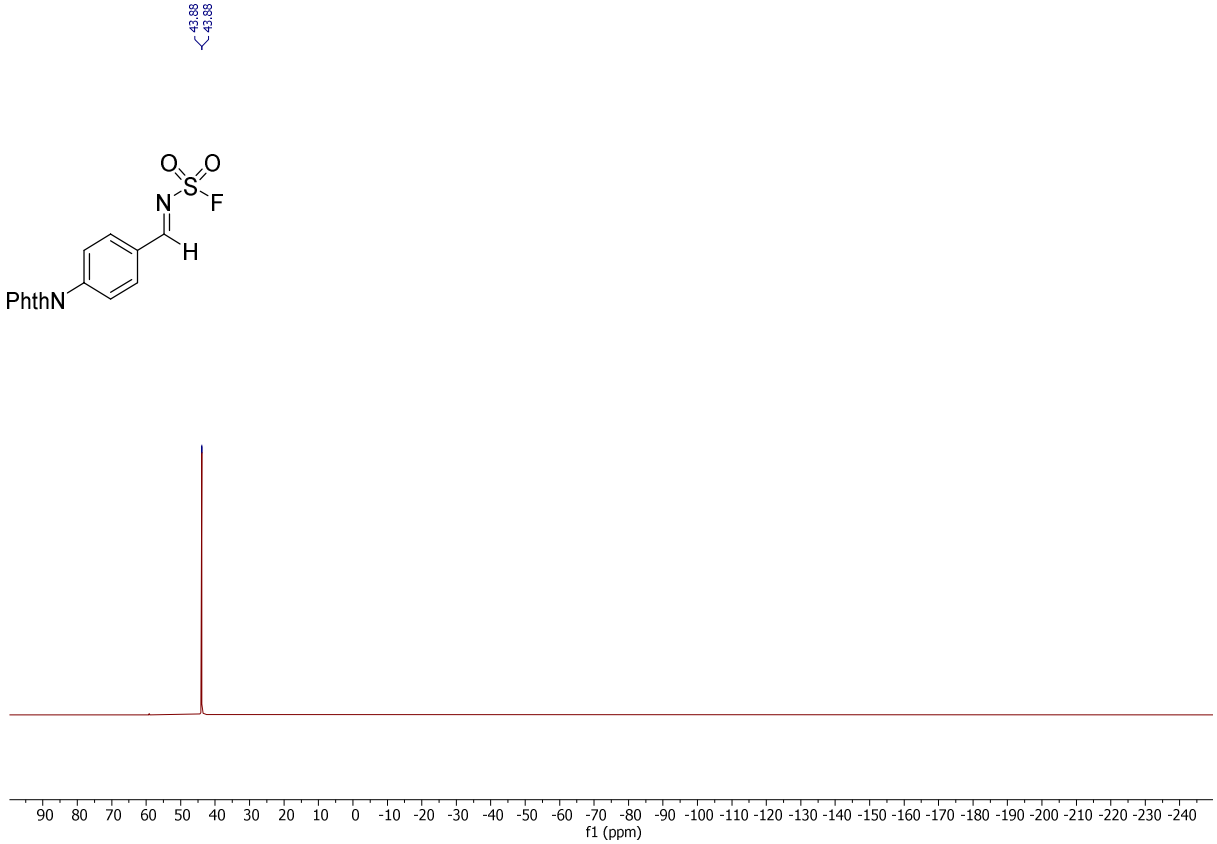




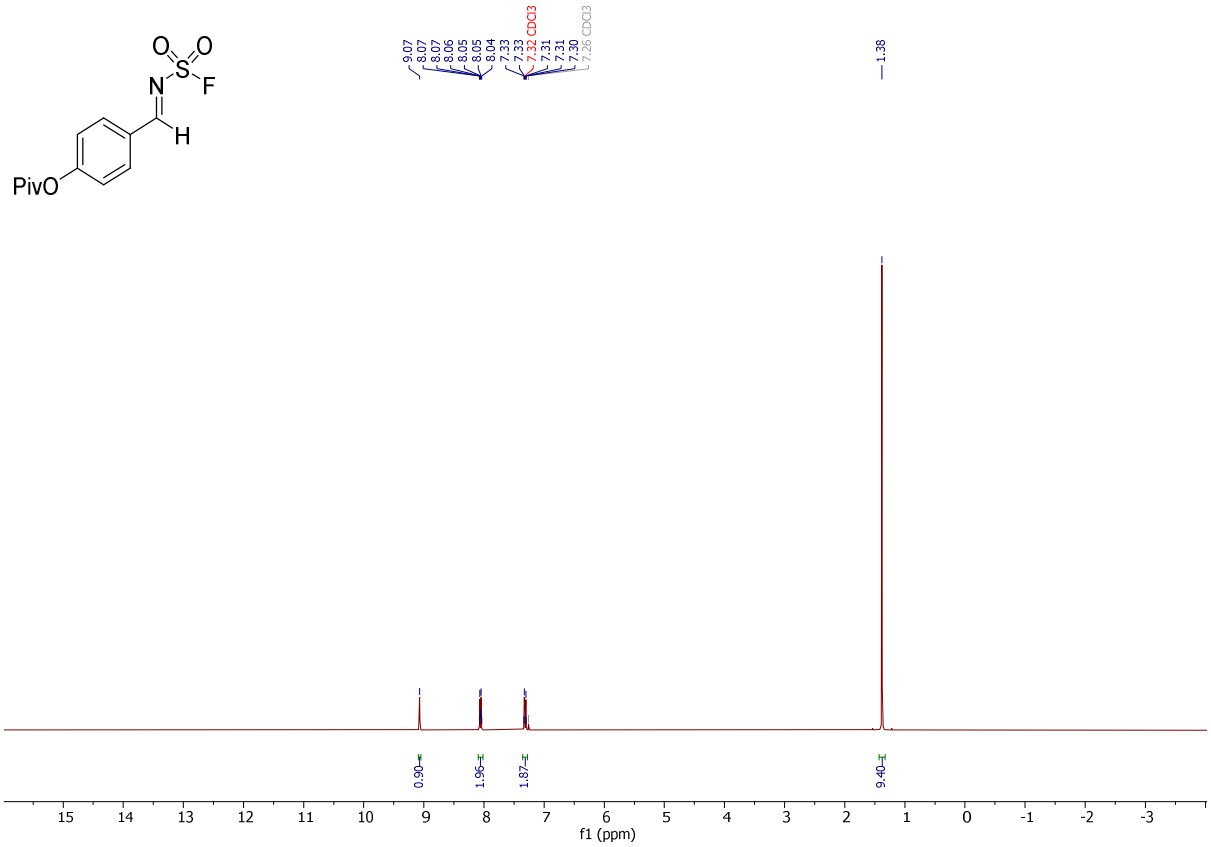
(4-(1,3-Dioxoisoindolin-2-yl)benzylidene)sulfamoyl fluoride (1n)

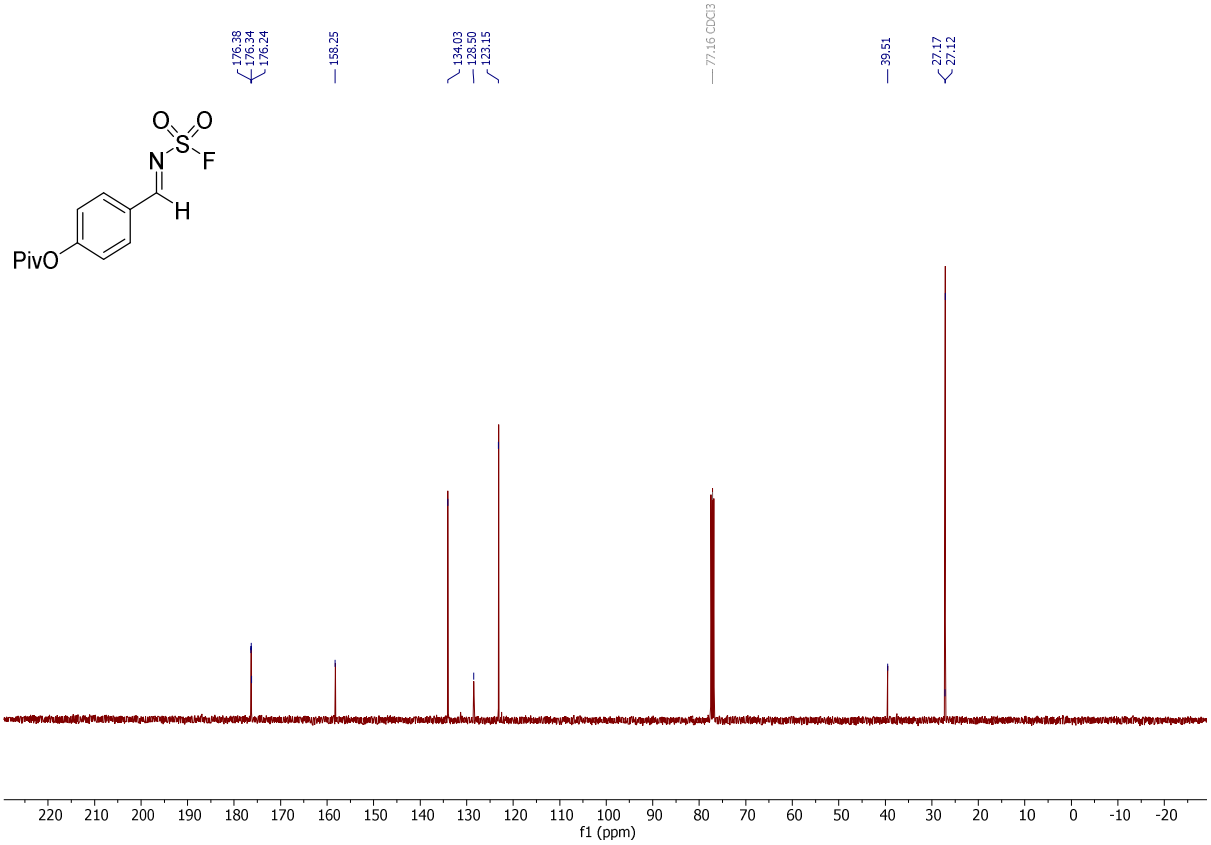


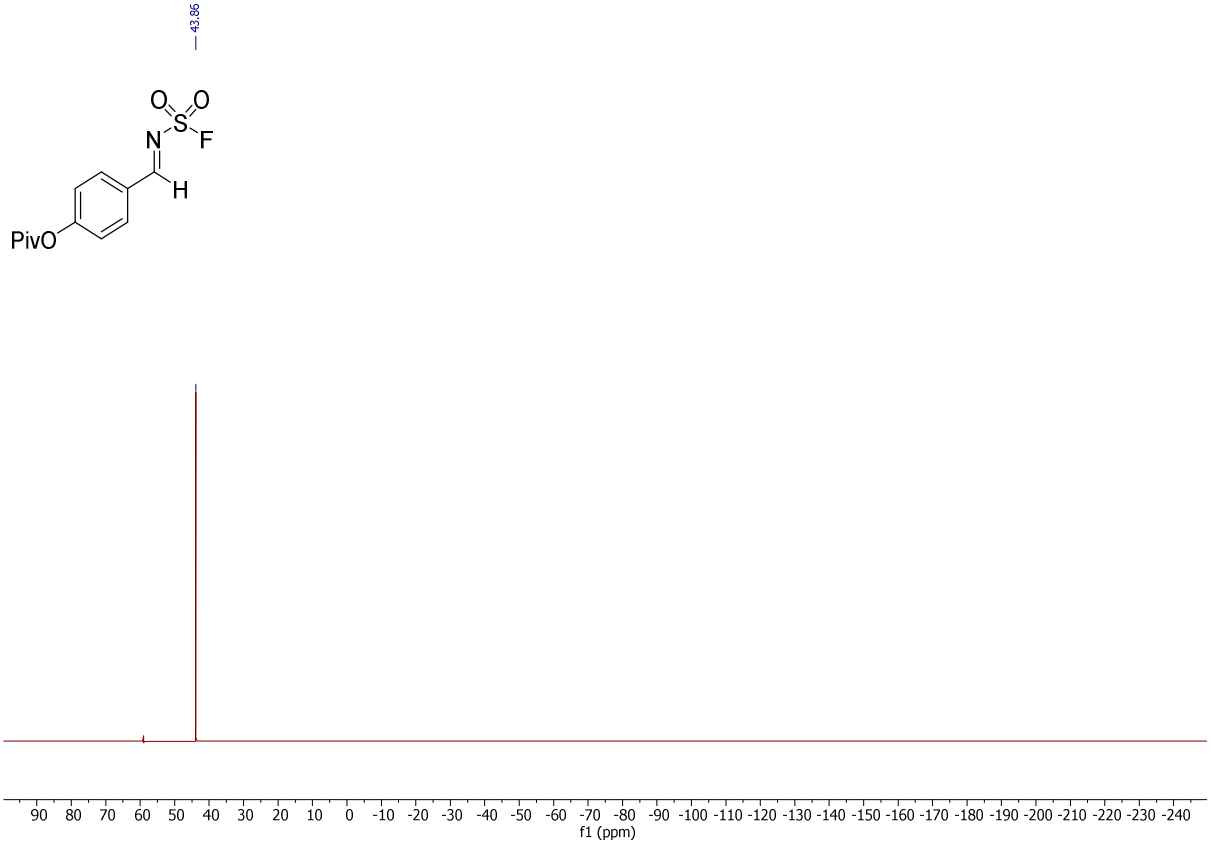




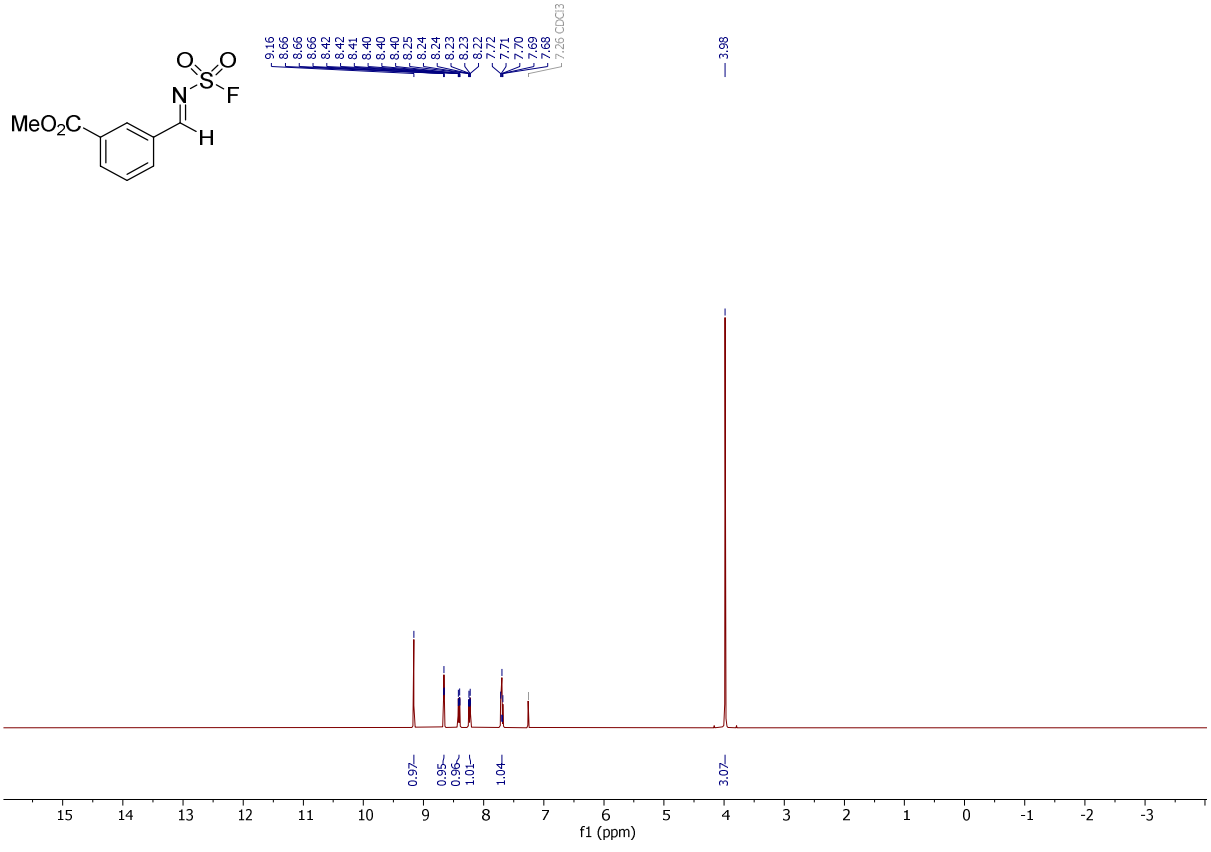
4-(((Fluorosulfonyl)imino)methyl)phenyl pivalate (1o)

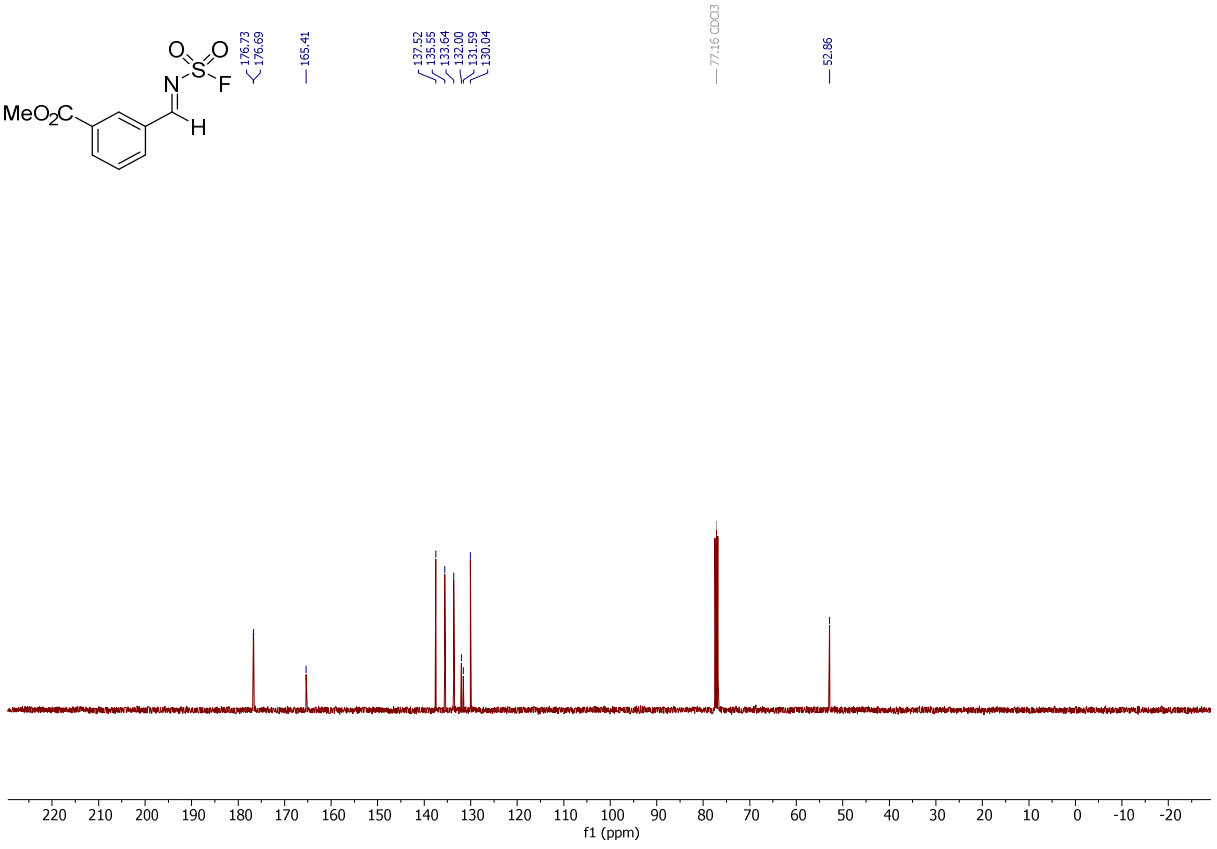

O
O
S
N
F
H
PivO
9.07
8.07
8.07
8.06
8.05
8.05
8.04
7.33
7.33
7.32 CDCl3
7.31
7.31
7.30
7.26 CDCl3
1.38
0.90
1.96
1.87
9.40
15 14 13 12 11 10 9 8 7 6 5 4 3 2 1 0 -1 -2 -3
f1 (ppm)

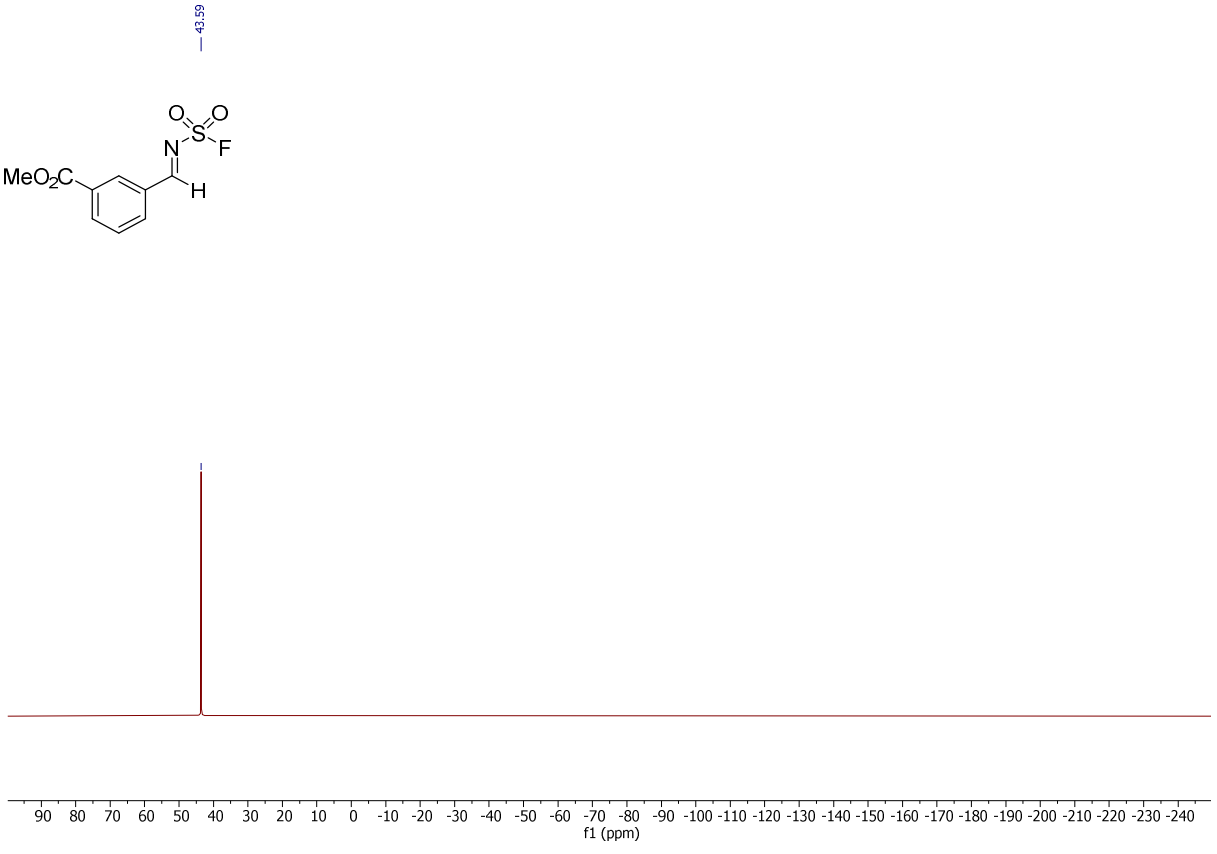

176.38
176.34
176.24
158.25
134.03
128.50
123.15
77.16 CDCl3
39.51
27.17
27.12
O
O
S
N
F
H
PivO
220 210 200 190 180 170 160 150 140 130 120 110 100 90 80 70 60 50 40 30 20 10 0 -10 -20
f1 (ppm)



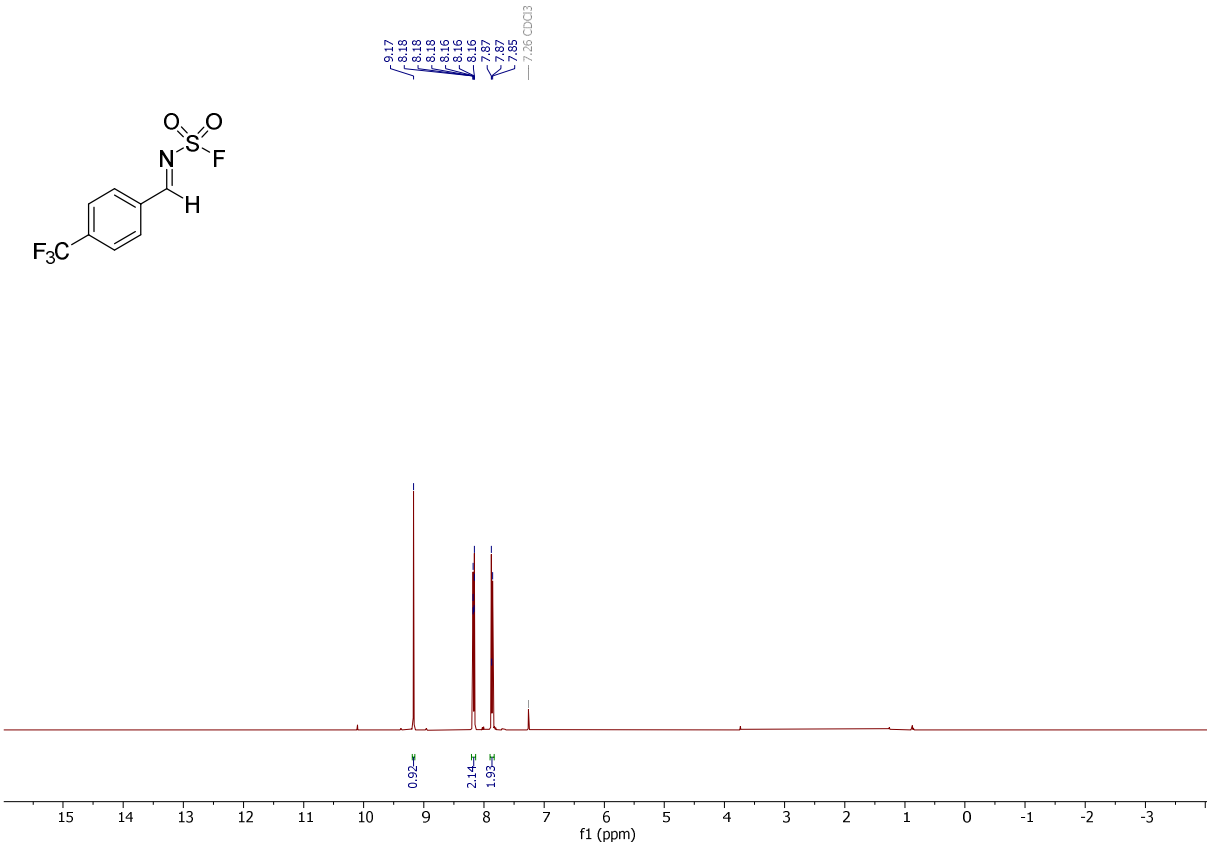
Methyl 3-(((fluorosulfonyl)imino)methyl)benzoate (1l)

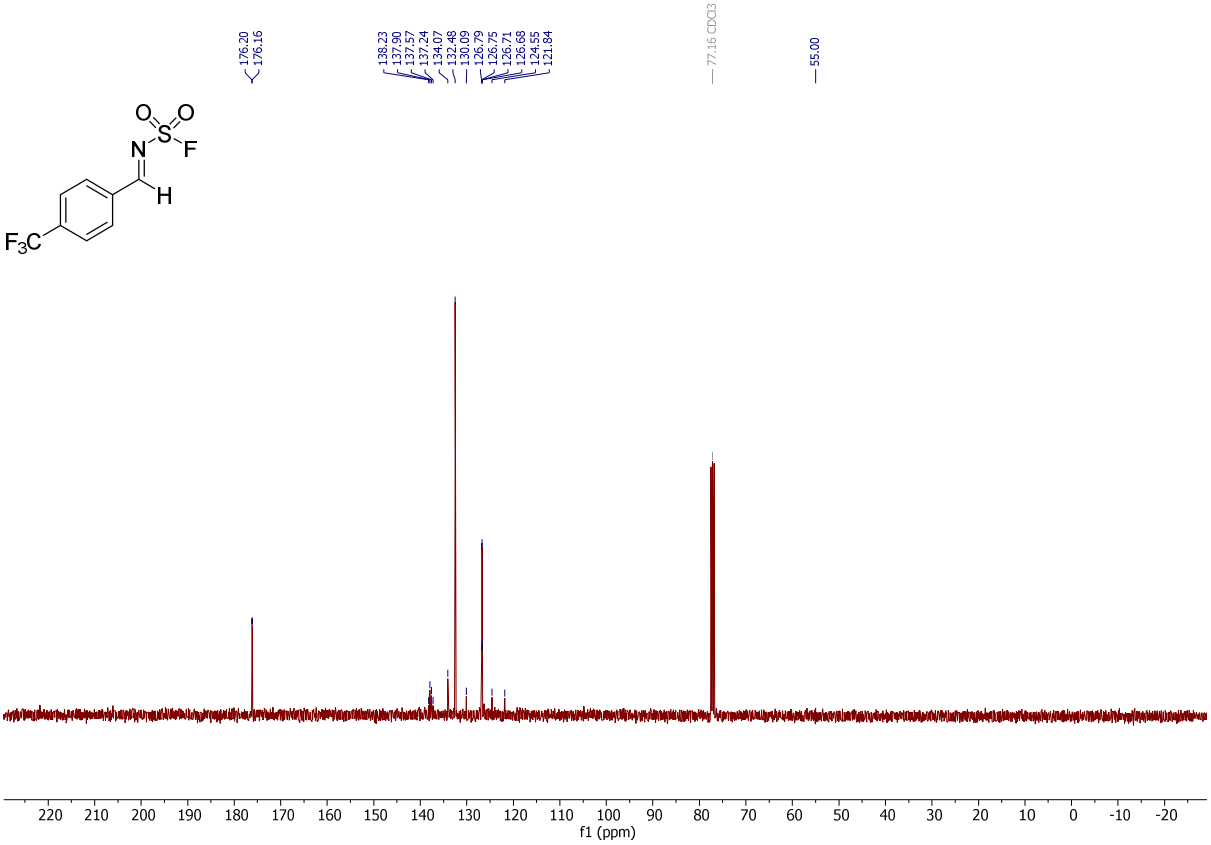


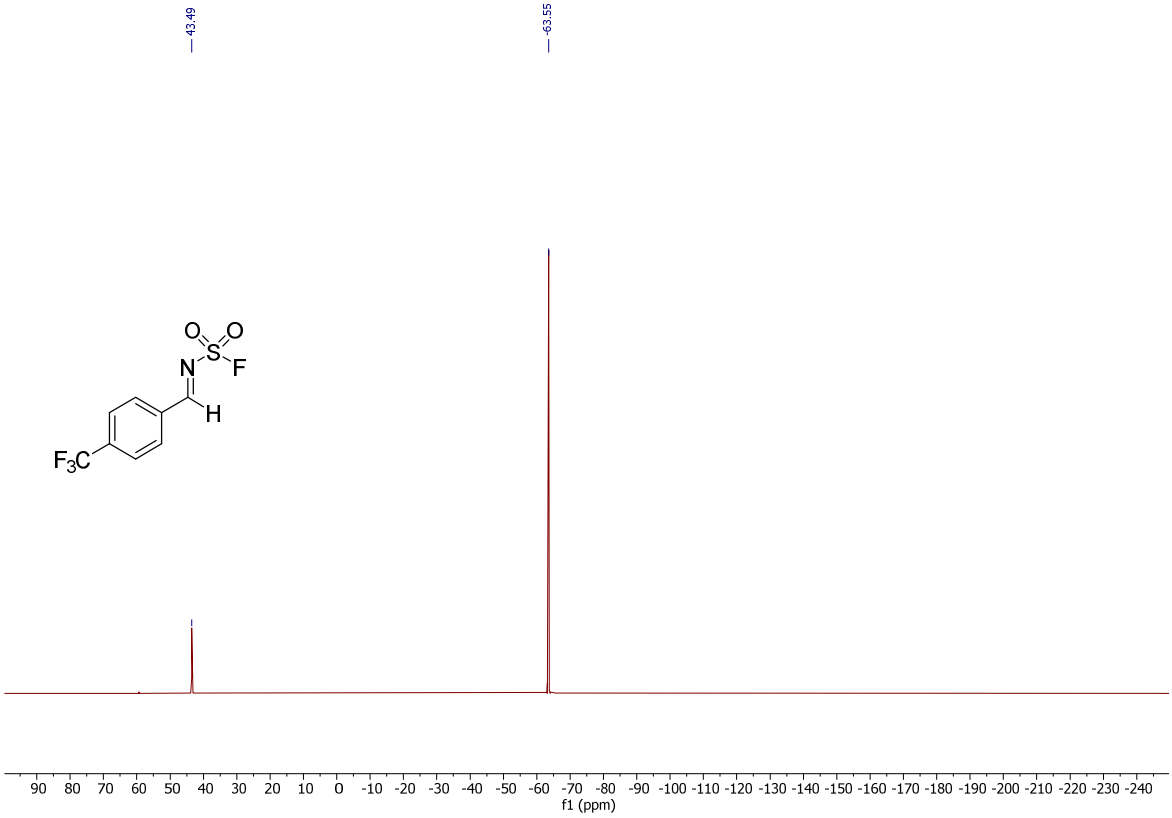

176.73
176.69
165.41
137.52
135.55
133.64
132.00
131.59
130.04
77.16 CDCl3
52.86
MeO2C
O
S
O
N
F
H
220 210 200 190 180 170 160 150 140 130 120 110 100 90 80 70 60 50 40 30 20 10 0 -10 -20
f1 (ppm)


43.59
MeO2C
O
S
O
N
F
H
90 80 70 60 50 40 30 20 10 0 -10 -20 -30 -40 -50 -60 -70 -80 -90 -100 -110 -120 -130 -140 -150 -160 -170 -180 -190 -200 -210 -220 -230 -240
f1 (ppm)

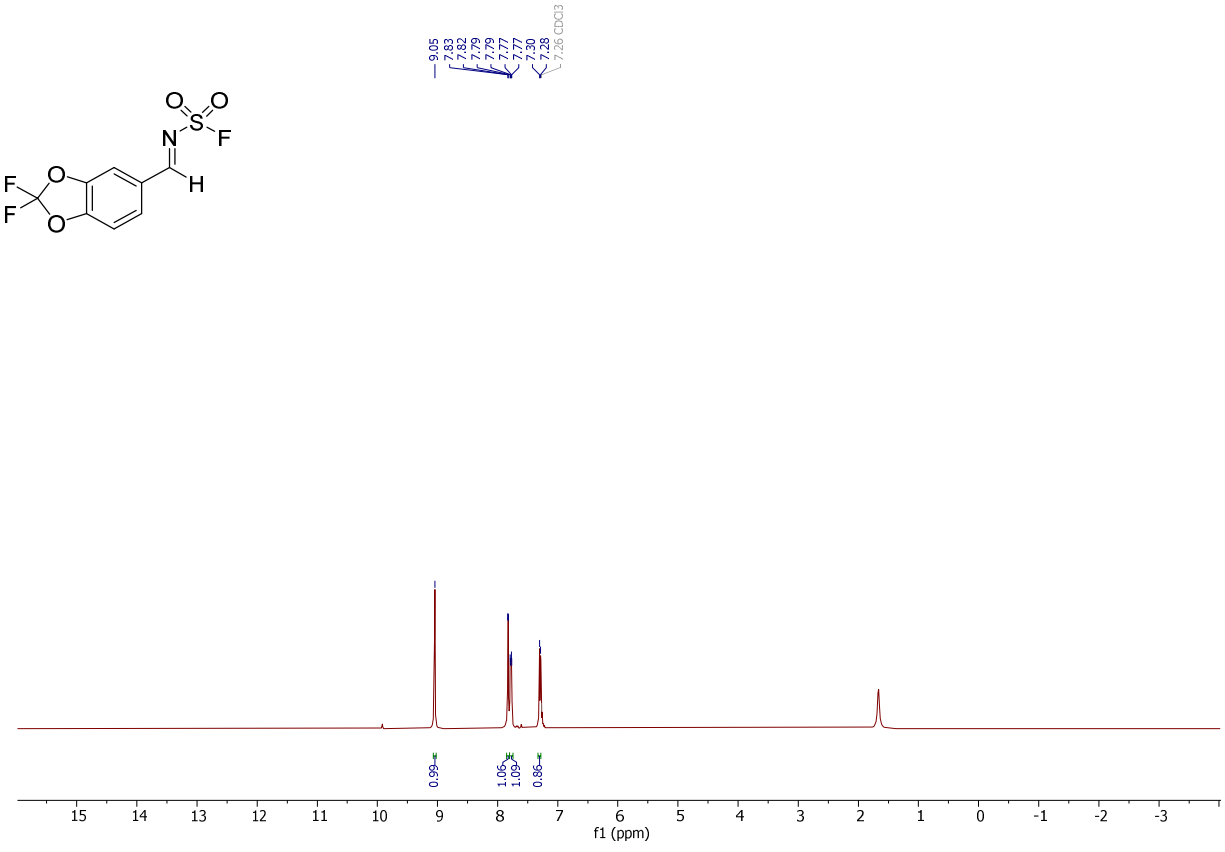
(4-(Trifluoromethyl)benzylidene)sulfamoyl fluoride (1m)

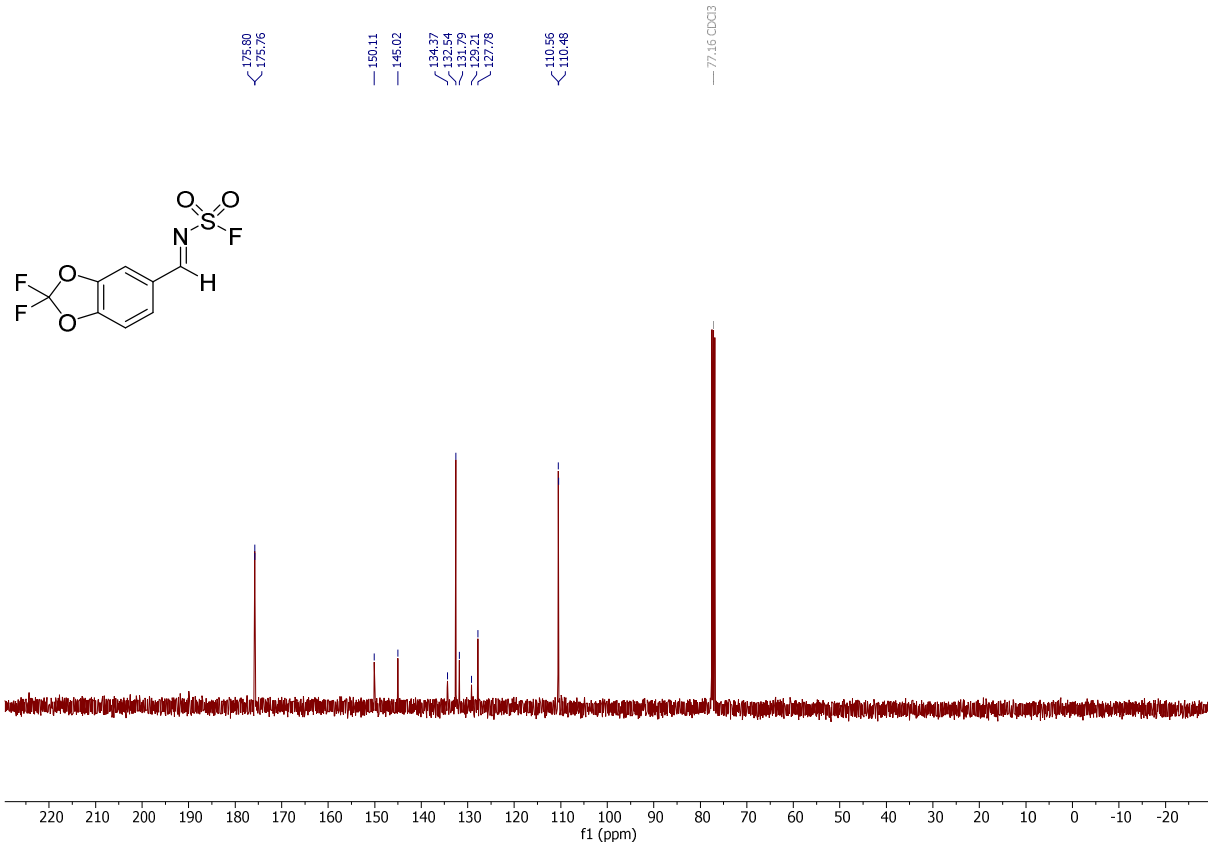

9.17
8.18
8.18
8.18
8.16
8.16
7.87
7.87
7.85
7.26 CDCl3
O
O
S
N
F
H
F3C
0.92
2.14
1.93
15 14 13 12 11 10 9 8 7 6 5 4 3 2 1 0 -1 -2 -3
f1 (ppm)

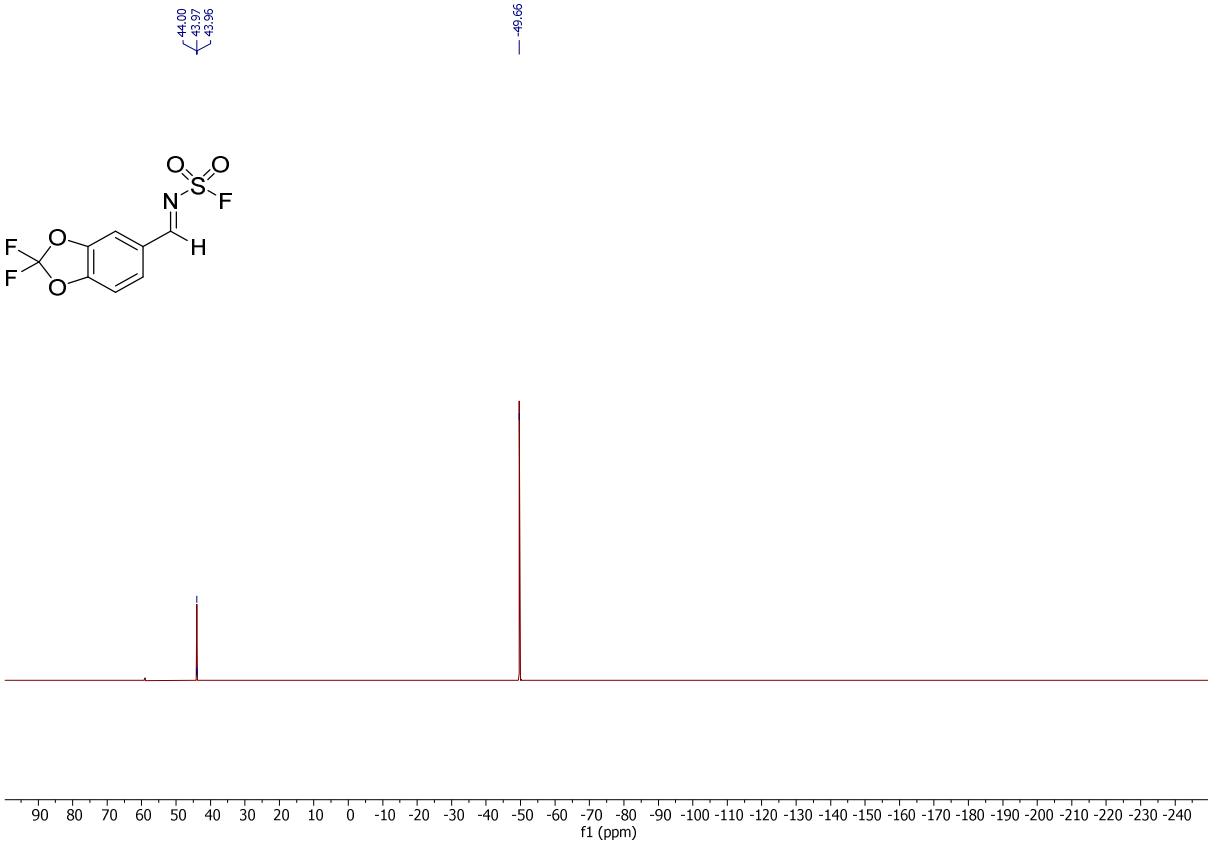

176.20
176.16
138.23
137.90
137.57
137.24
134.07
132.48
130.09
126.79
126.75
126.71
126.68
124.55
121.84
77.16 CDCl3
55.00
O
O
S
N
F
H
F3C
220 210 200 190 180 170 160 150 140 130 120 110 100 90 80 70 60 50 40 30 20 10 0 -10 -20
f1 (ppm)



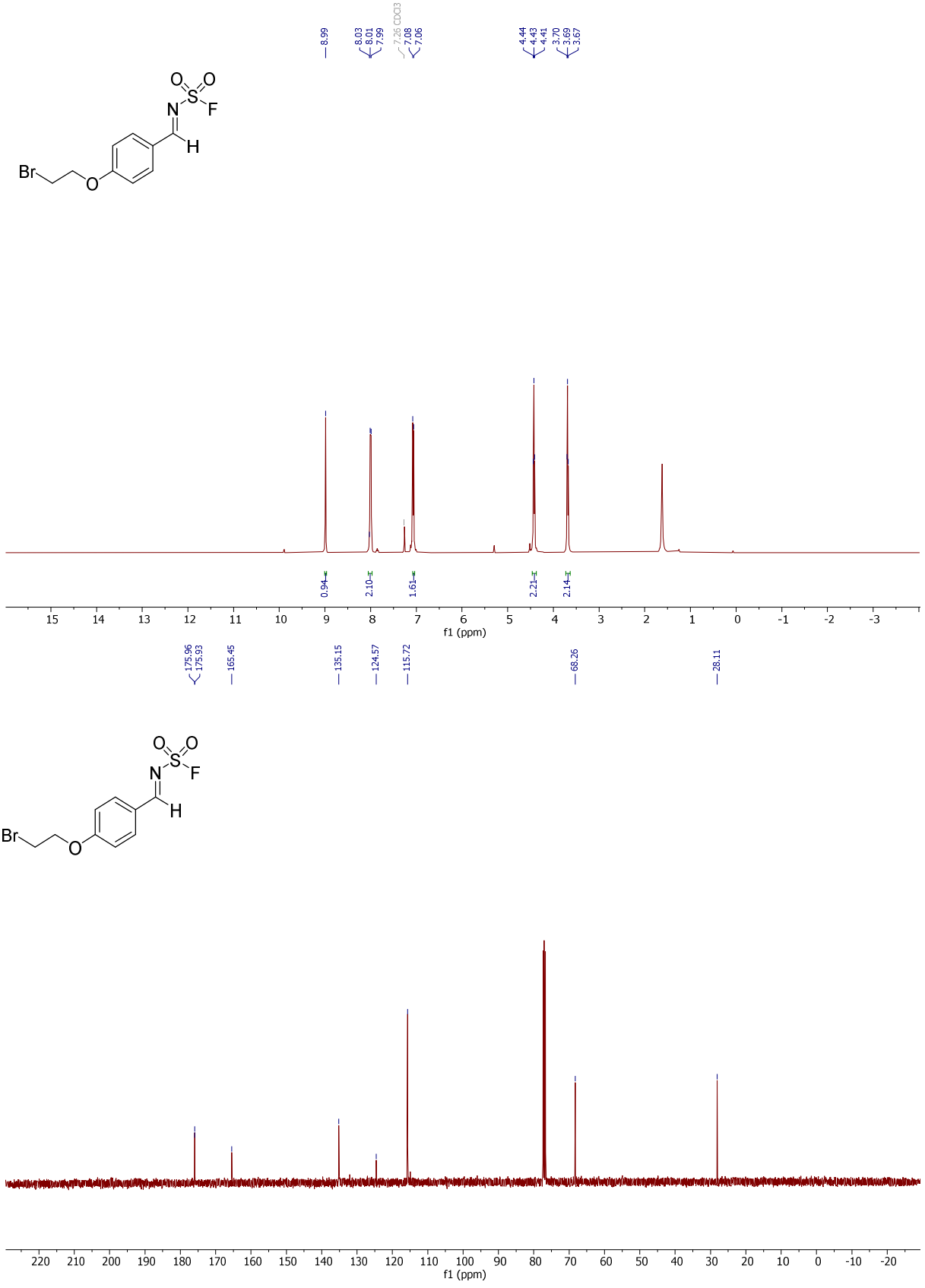
((2,2-Difluorobenzo[d][1,3]dioxol-5-yl)methylene) sulfamoyl fluoride (1p)

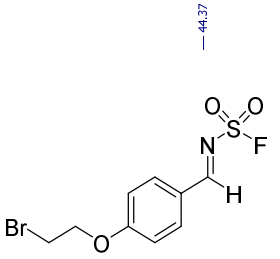


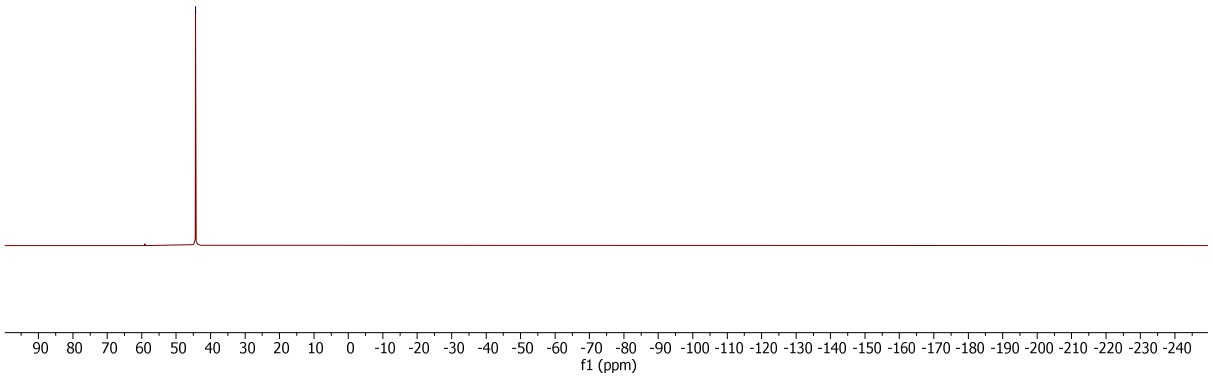

175.80
175.76
150.11
145.02
134.37
132.54
131.79
129.21
127.78
110.56
110.48
77.16 CDCl3
f1 (ppm)


44.00
43.97
43.96
-49.66
f1 (ppm)

(4-(2-Bromoethoxy)benzylidene)sulfamoyl fluoride (1q)

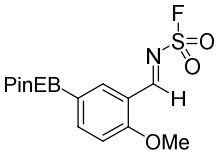


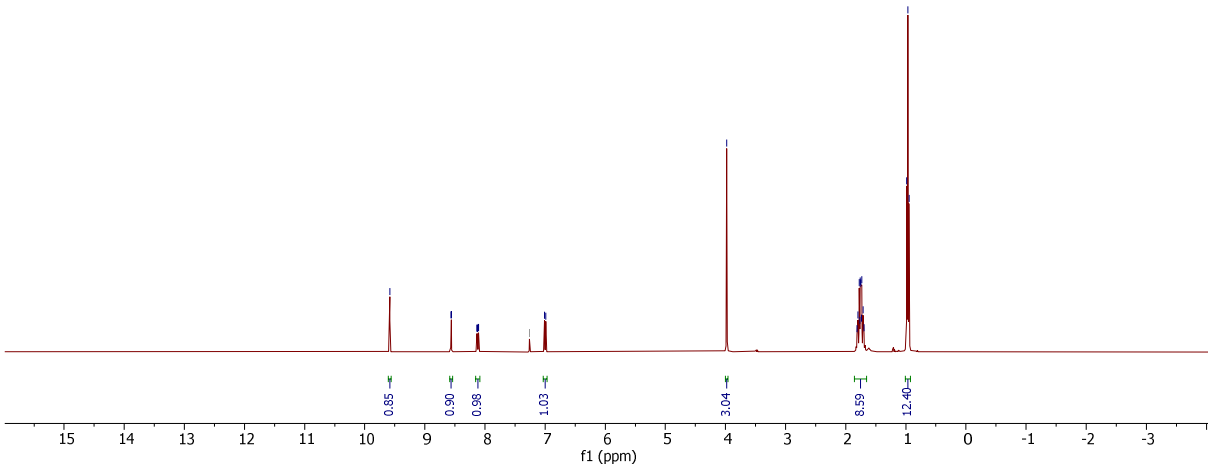


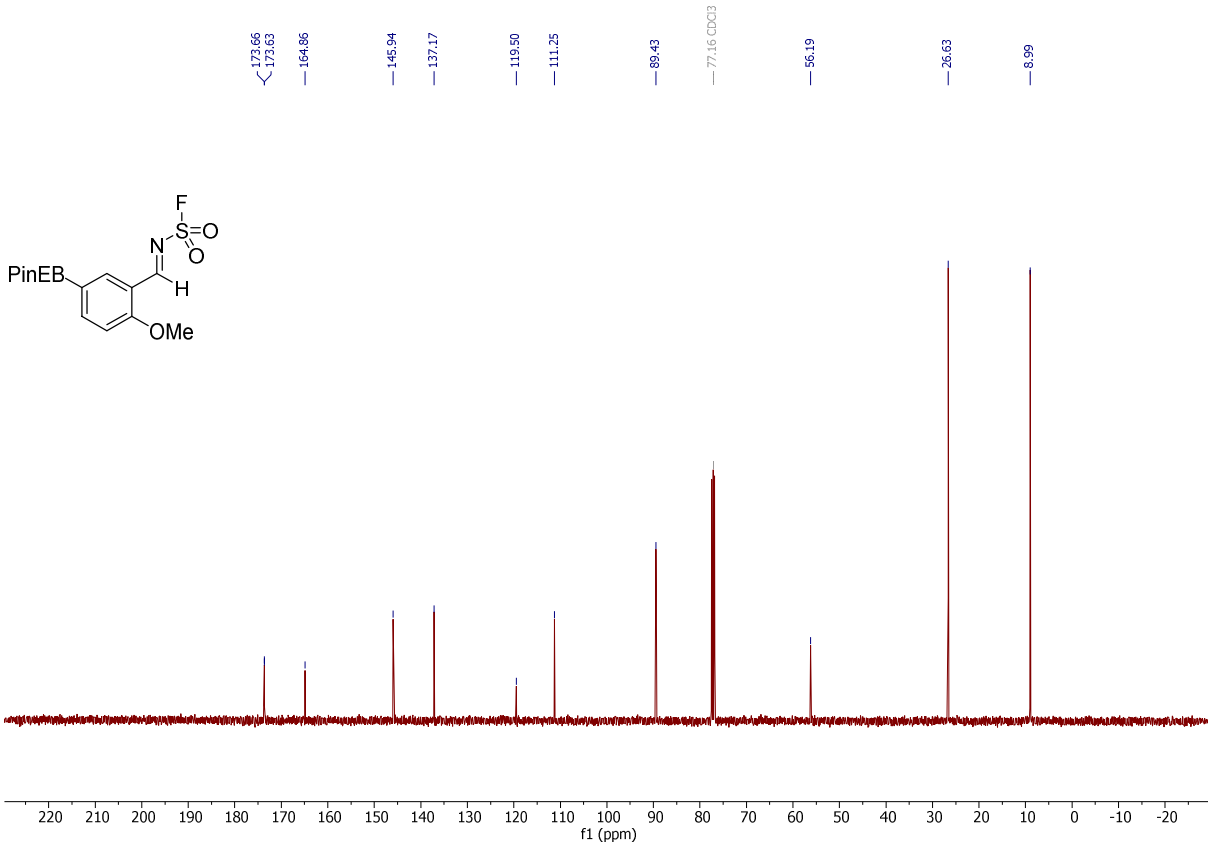


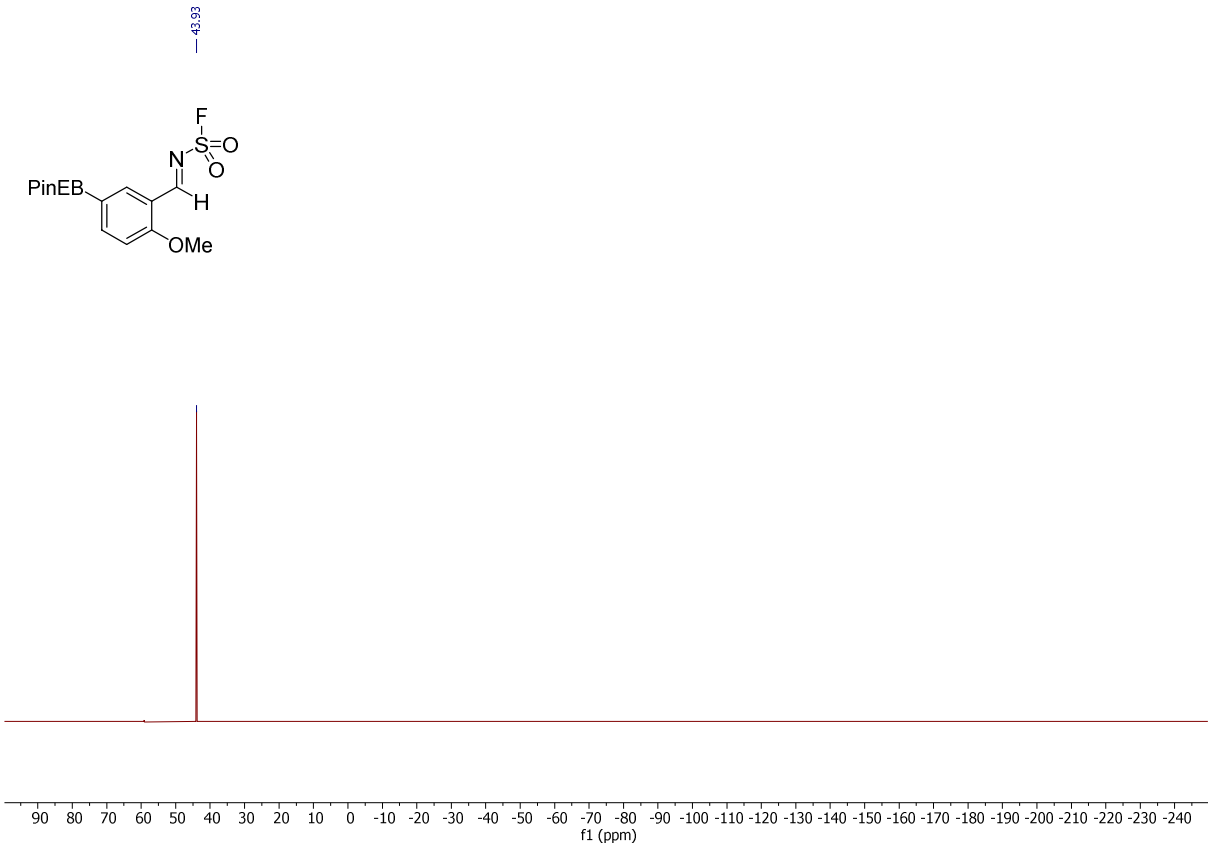
(2-Methoxy-5-(4,4,5,5-tetraethyl-1,3,2-dioxaborolan-2-yl)benzylidene)sulfamoyl fluoride (1r)



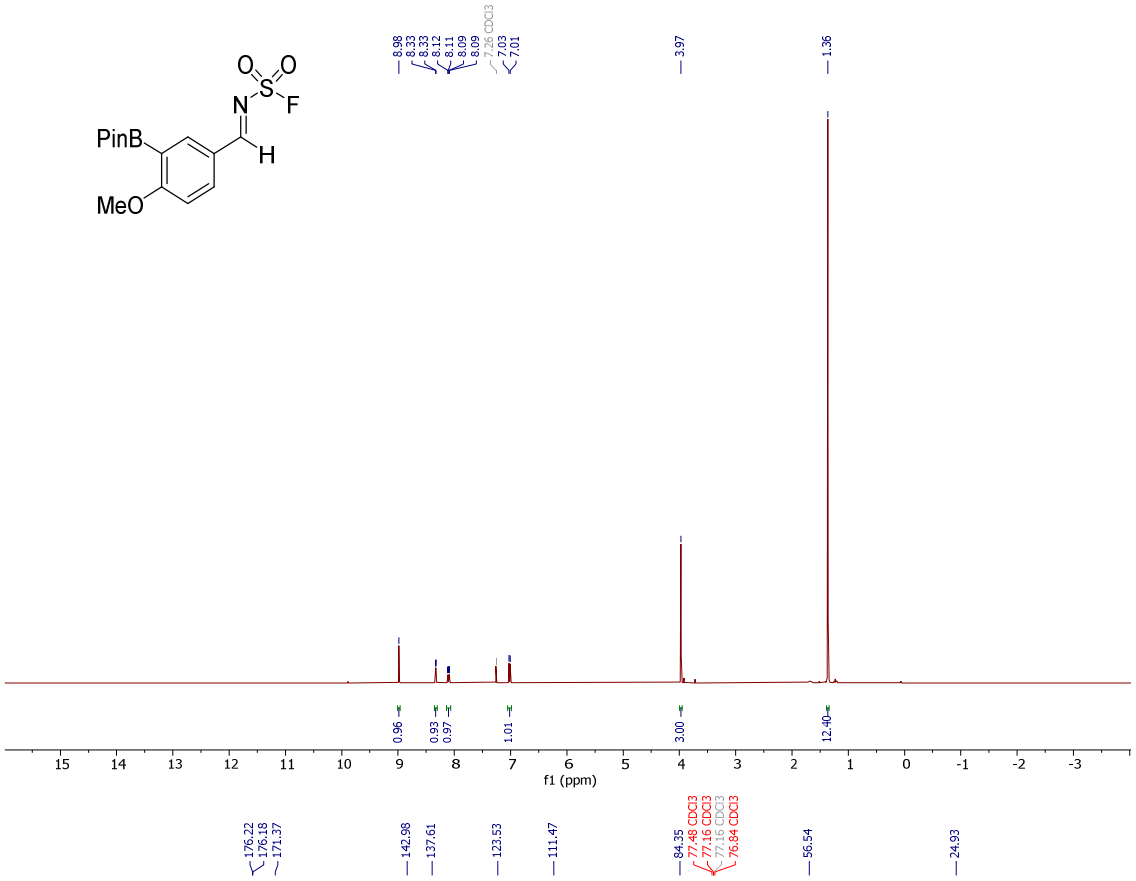


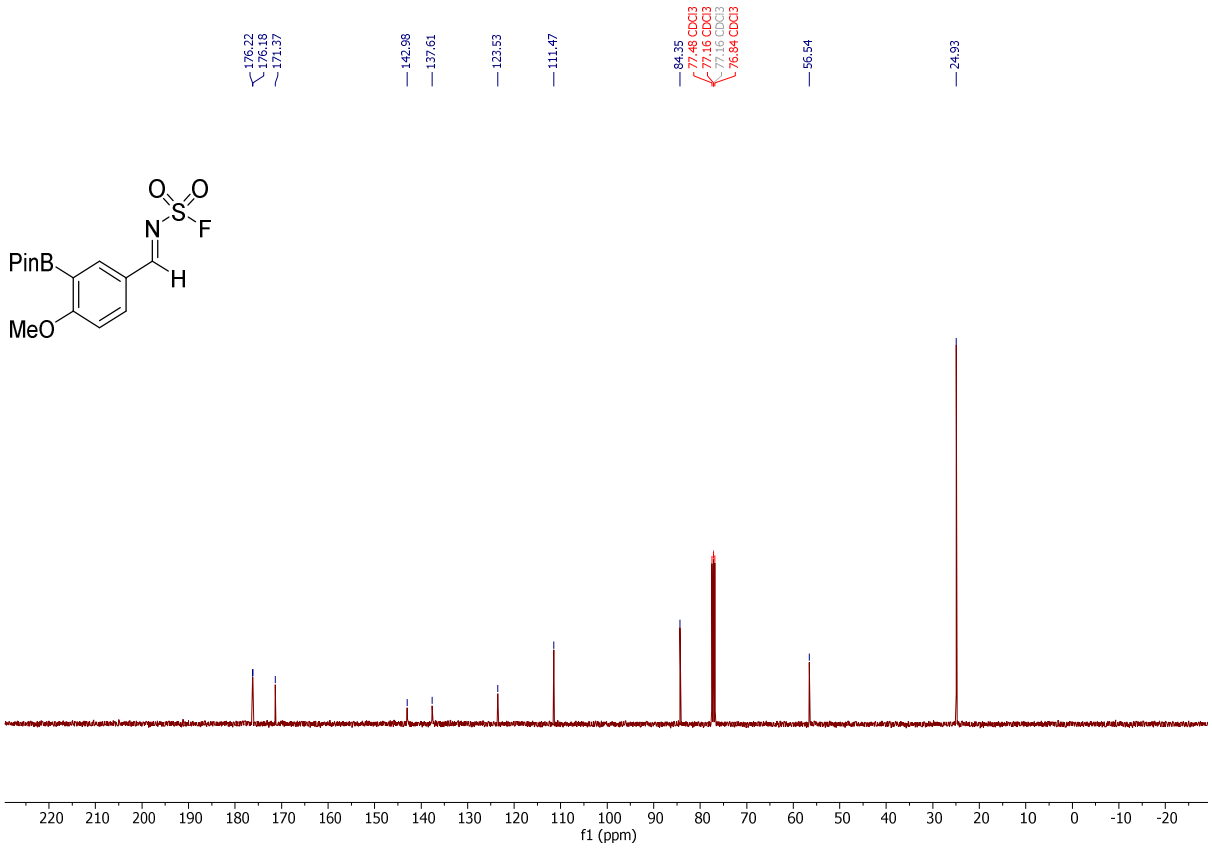


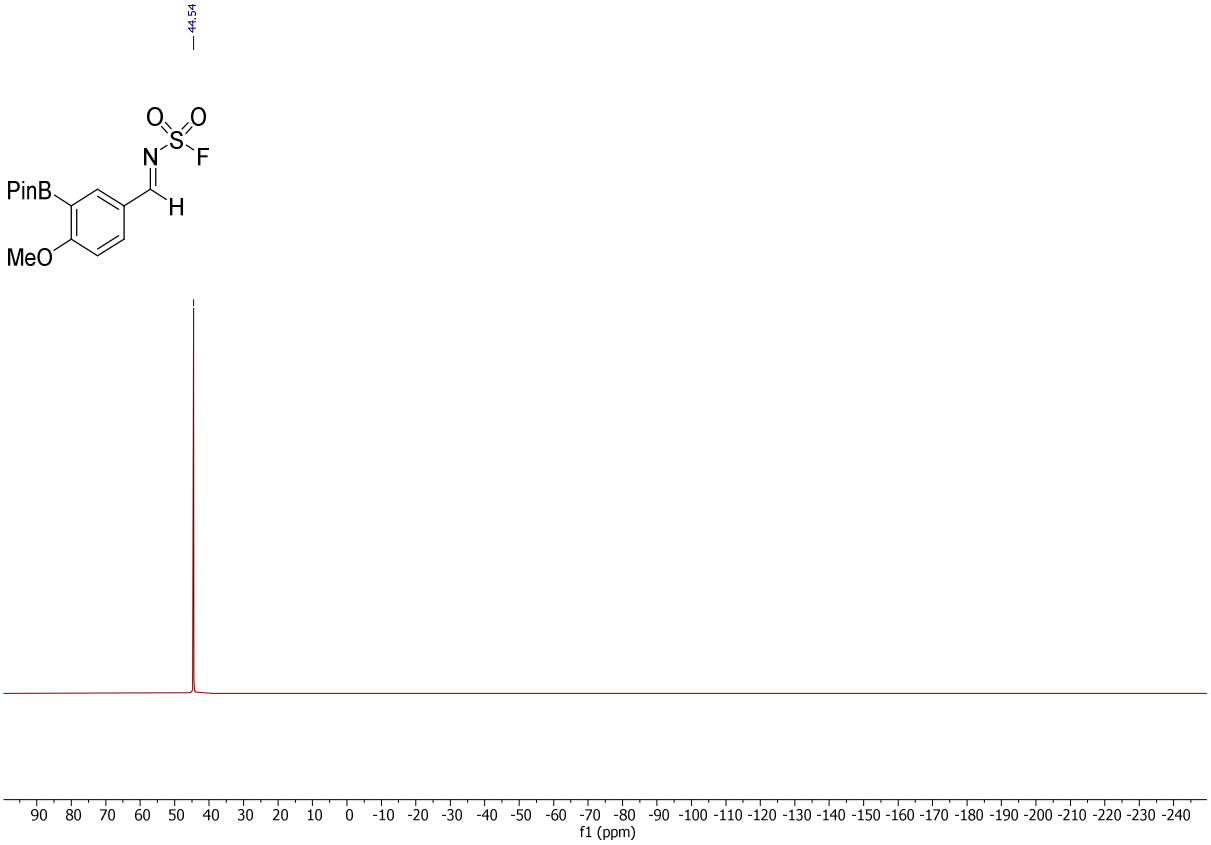

173.66
173.63
164.86
145.94
137.17
119.50
111.25
89.43
77.16 CDCl3
56.19
26.63
8.99
F
S
O
N
O
H
PinEB
OMe
220 210 200 190 180 170 160 150 140 130 120 110 100 90 80 70 60 50 40 30 20 10 0 -10 -20
f1 (ppm)


43.93
F
S
O
N
O
H
PinEB
OMe
90 80 70 60 50 40 30 20 10 0 -10 -20 -30 -40 -50 -60 -70 -80 -90 -100 -110 -120 -130 -140 -150 -160 -170 -180 -190 -200 -210 -220 -230 -240
f1 (ppm)

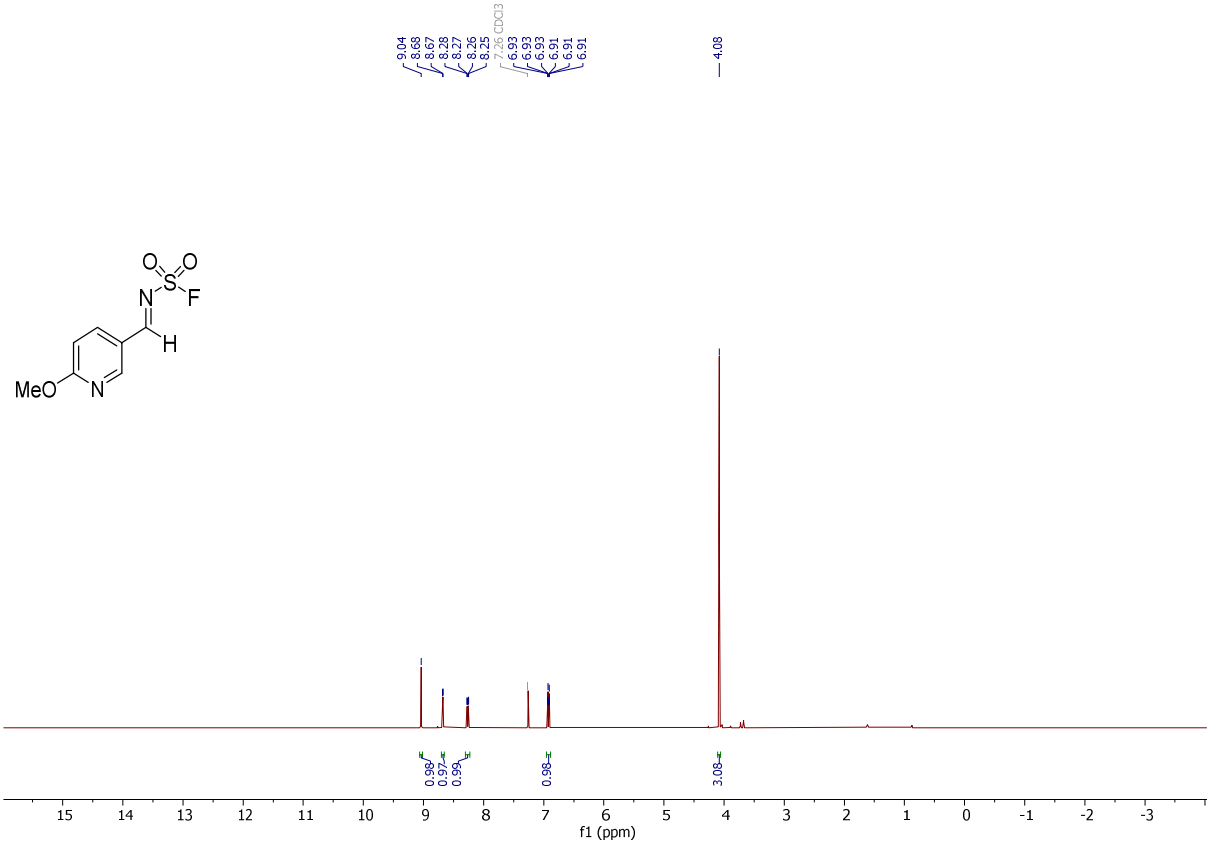
(4-Methoxy-3-(4,4,5,5-tetramethyl-1,3,2-dioxaborolan-2-yl)benzylidene)sulfamoyl fluoride (1s)

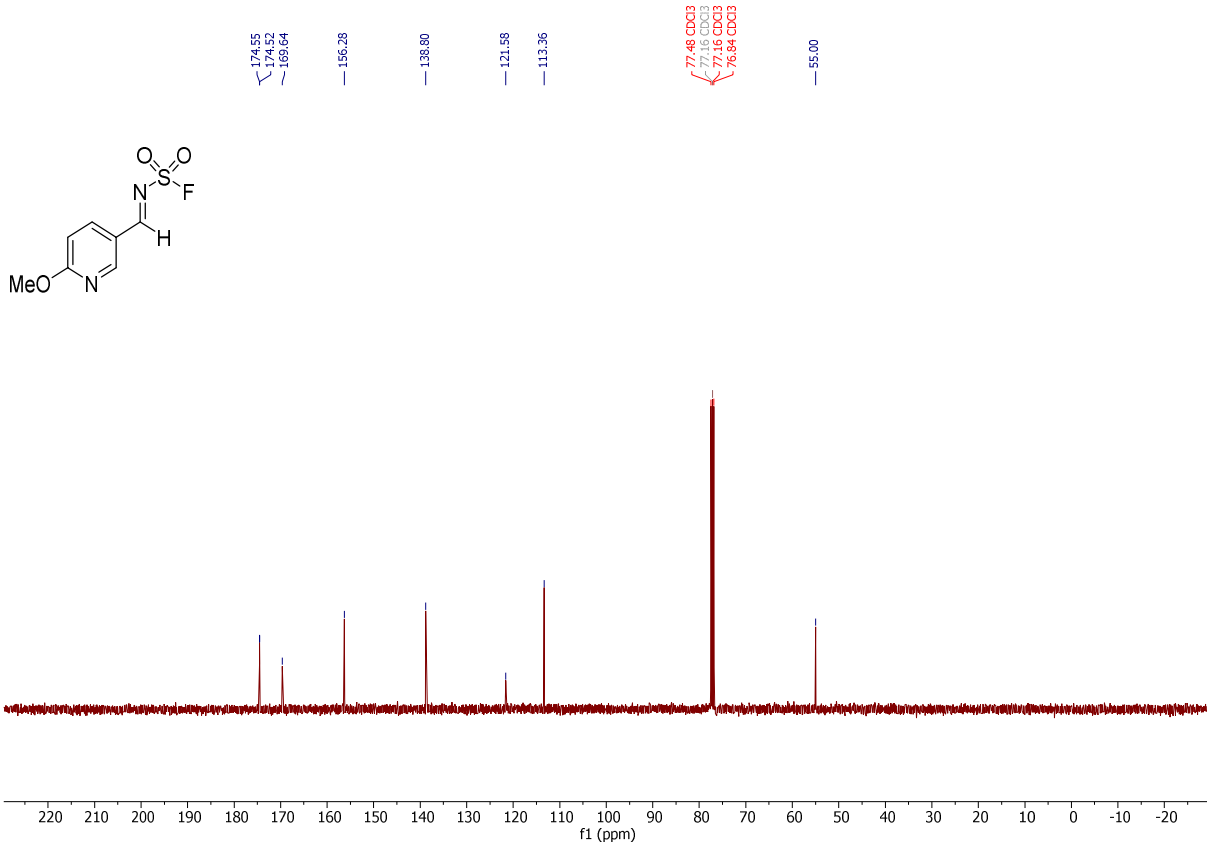


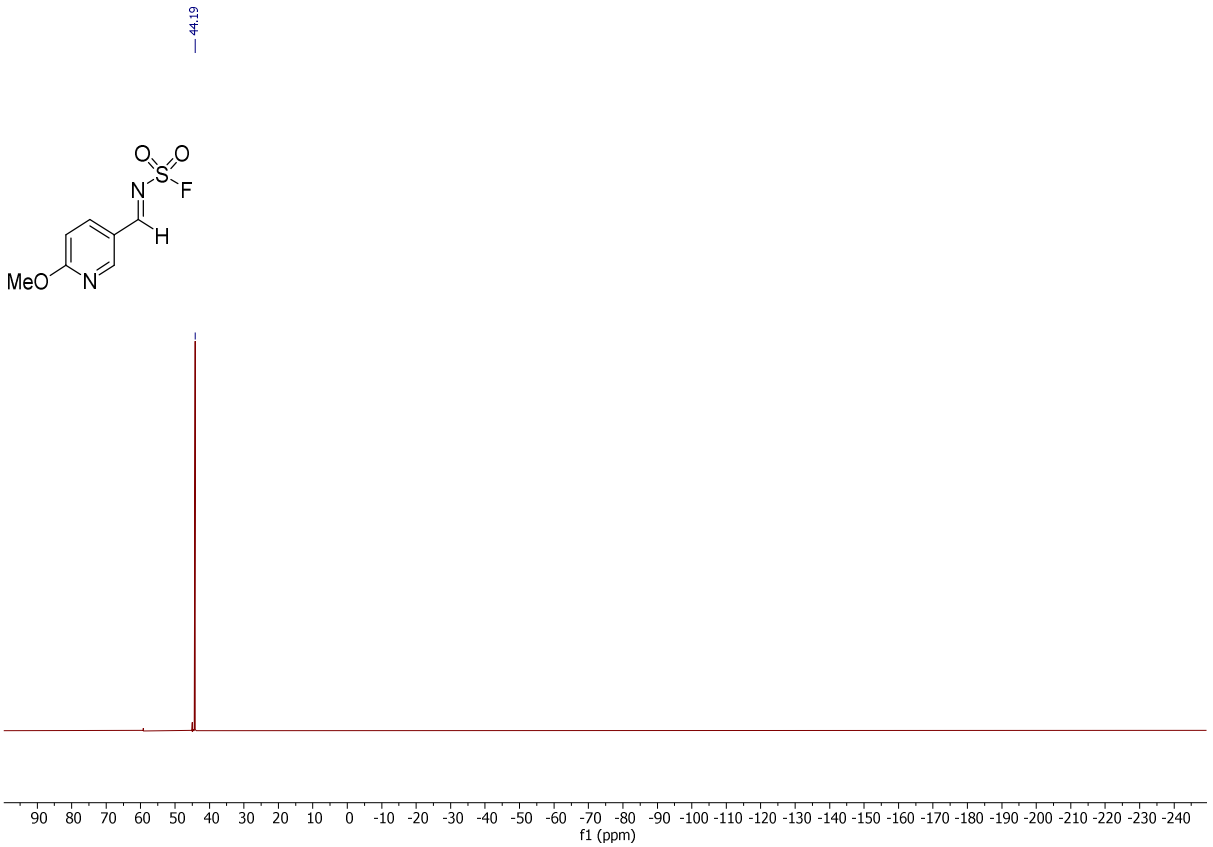




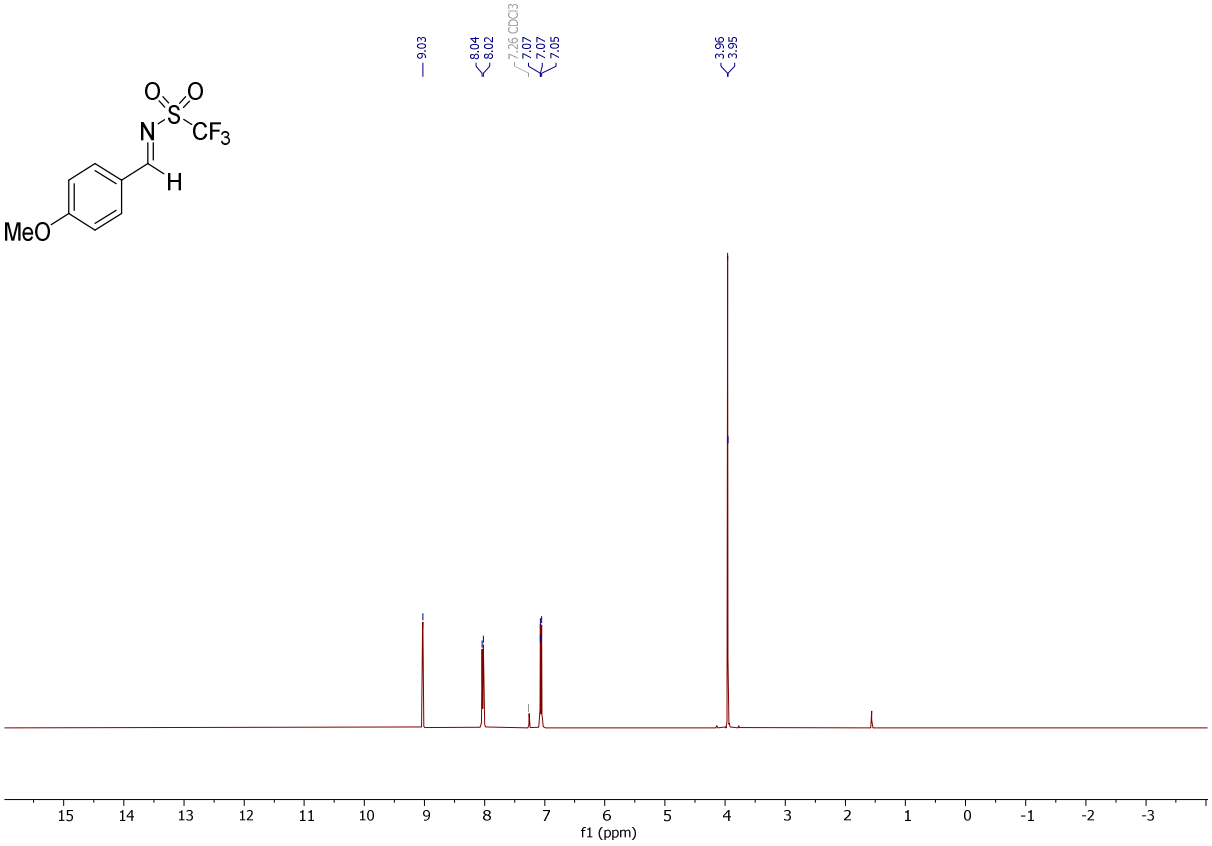
((6-Methoxypyridin-3-yl)methylene)sulfamoyl fluoride (1u)

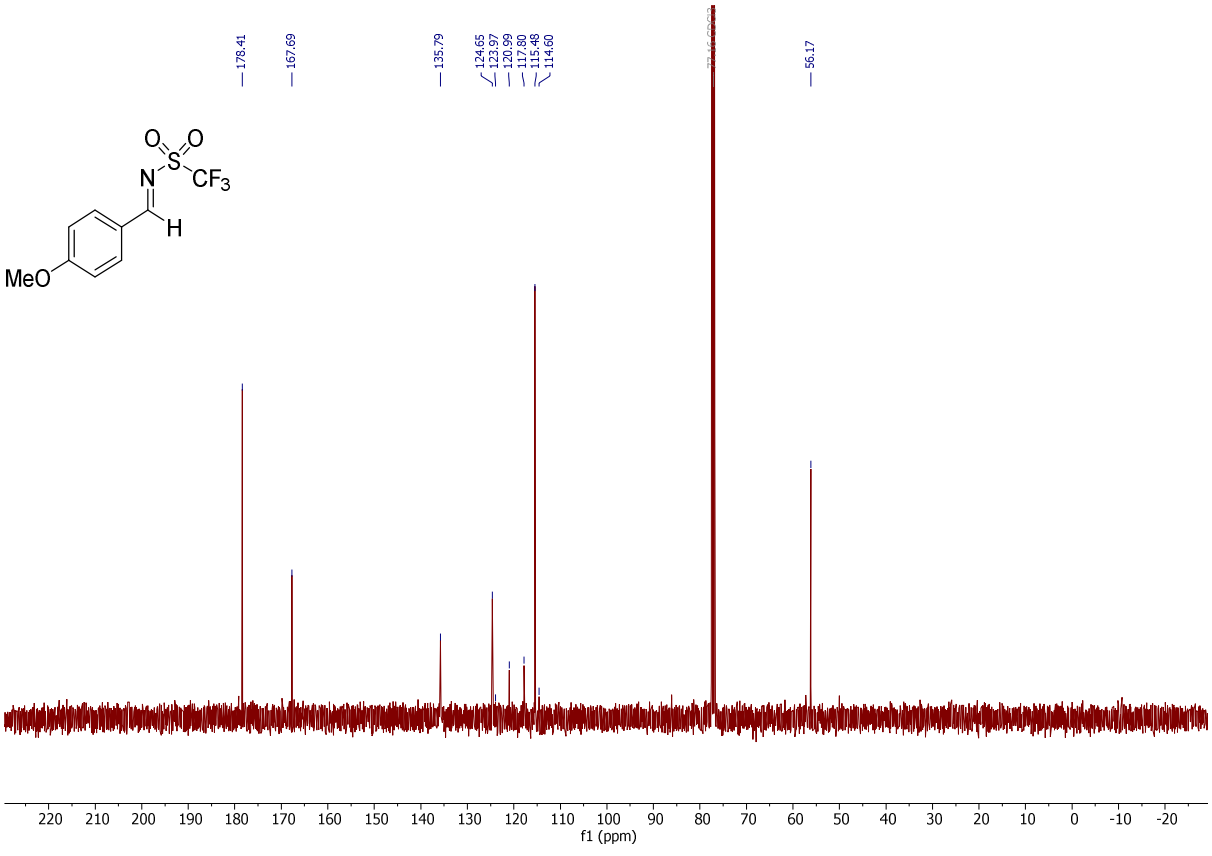


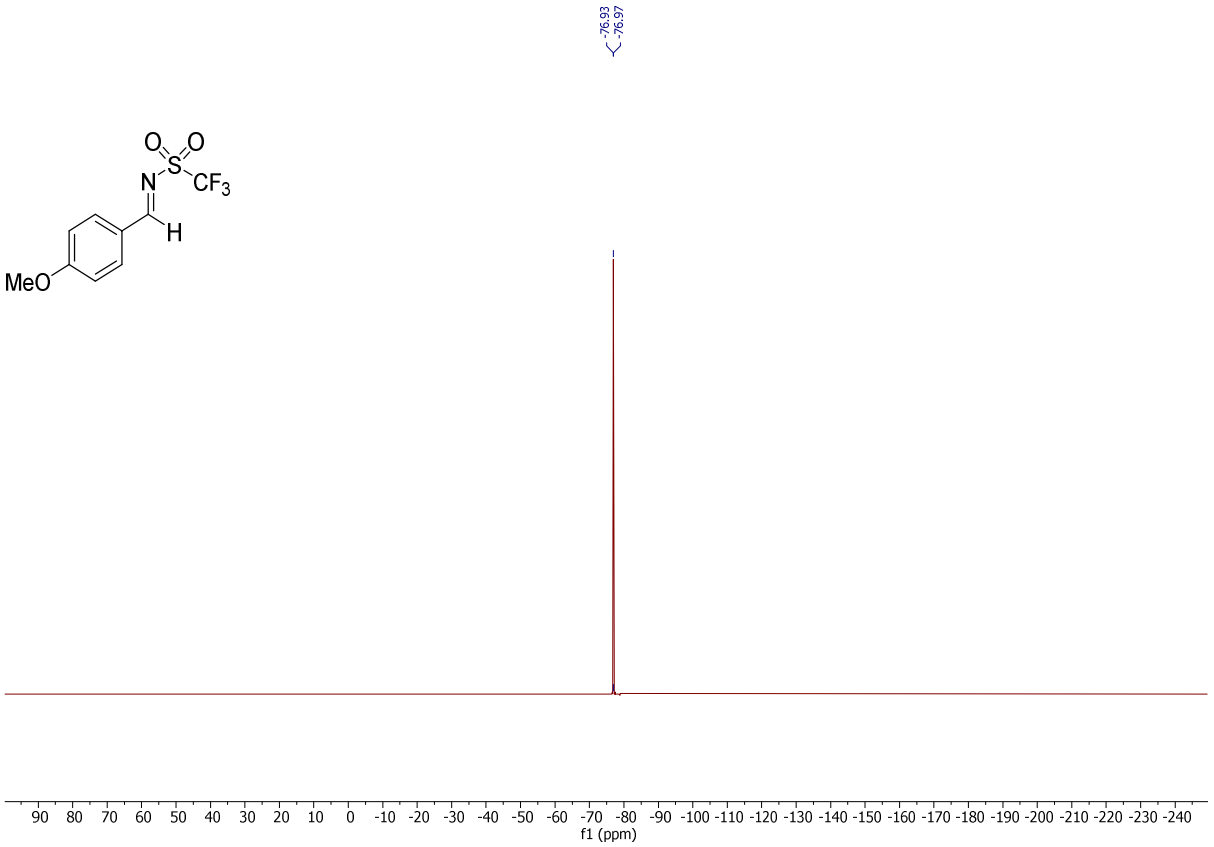

174.55
174.52
169.64
156.28
138.80
121.58
113.36
77.48 CDCl3
77.16 CDCl3
77.16 CDCl3
76.84 CDCl3
55.00
MeO
N
O
S
F
H
220 210 200 190 180 170 160 150 140 130 120 110 100 90 80 70 60 50 40 30 20 10 0 -10 -20
f1 (ppm)

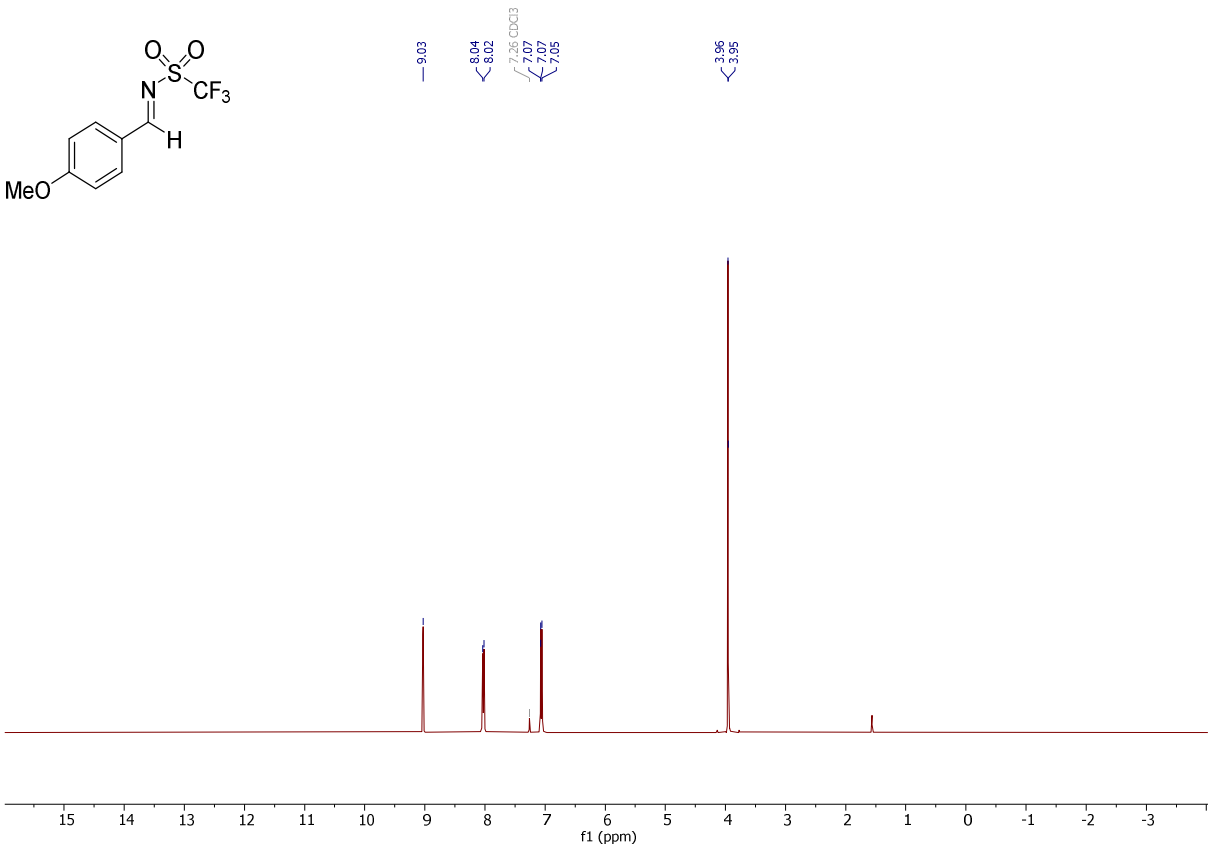

44.19
MeO
N
O
S
F
H
90 80 70 60 50 40 30 20 10 0 -10 -20 -30 -40 -50 -60 -70 -80 -90 -100 -110 -120 -130 -140 -150 -160 -170 -180 -190 -200 -210 -220 -230 -240
f1 (ppm)

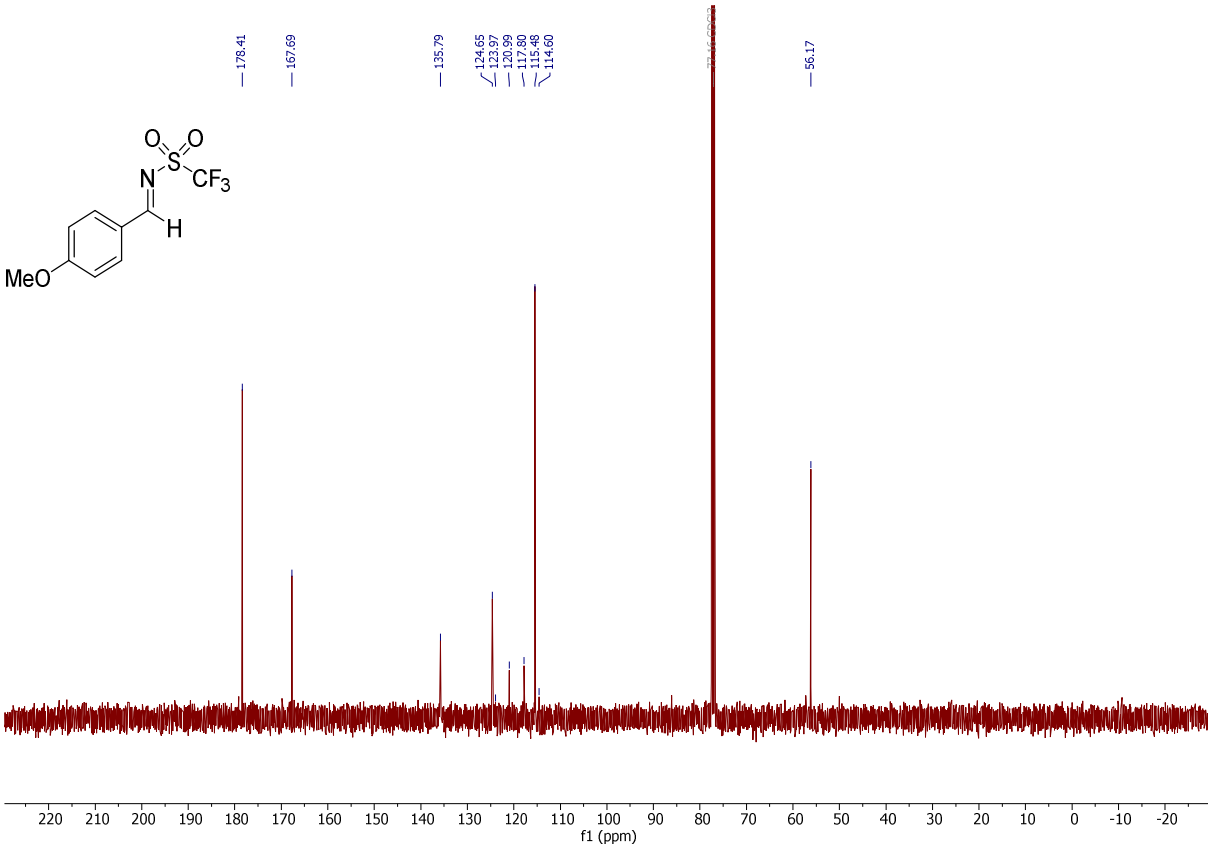
1,1,1-trifluoro-N-(4-methoxybenzylidene)methanesulfonamide (1x)

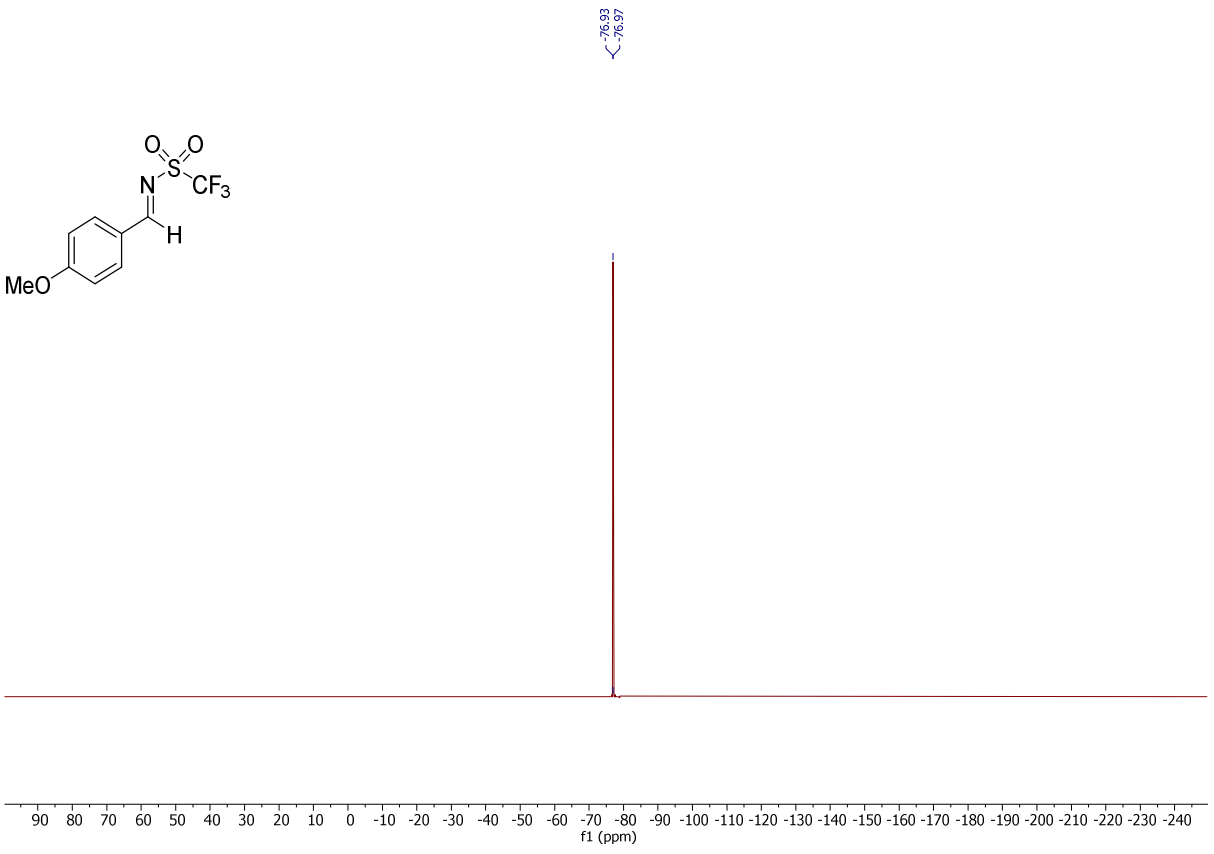





-76.93
-76.97
O
O
S
N
CF3
H
MeO
90 80 70 60 50 40 30 20 10 0 -10 -20 -30 -40 -50 -60 -70 -80 -90 -100 -110 -120 -130 -140 -150 -160 -170 -180 -190 -200 -210 -220 -230 -240
f1 (ppm)

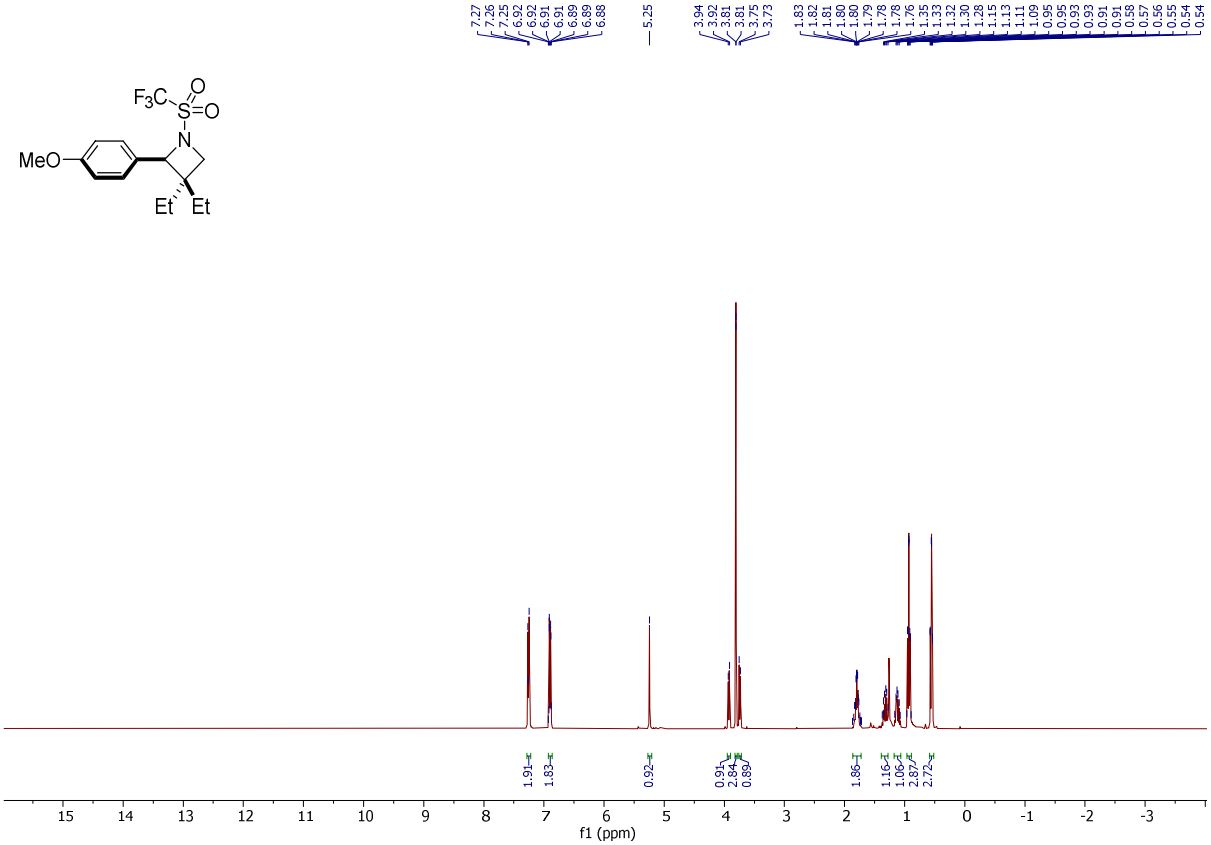

9.03
8.04
8.02
7.26 CDCl3
7.07
7.07
7.05
3.96
3.95
O
O
S
N
CF3
H
MeO
15 14 13 12 11 10 9 8 7 6 5 4 3 2 1 0 -1 -2 -3
f1 (ppm)

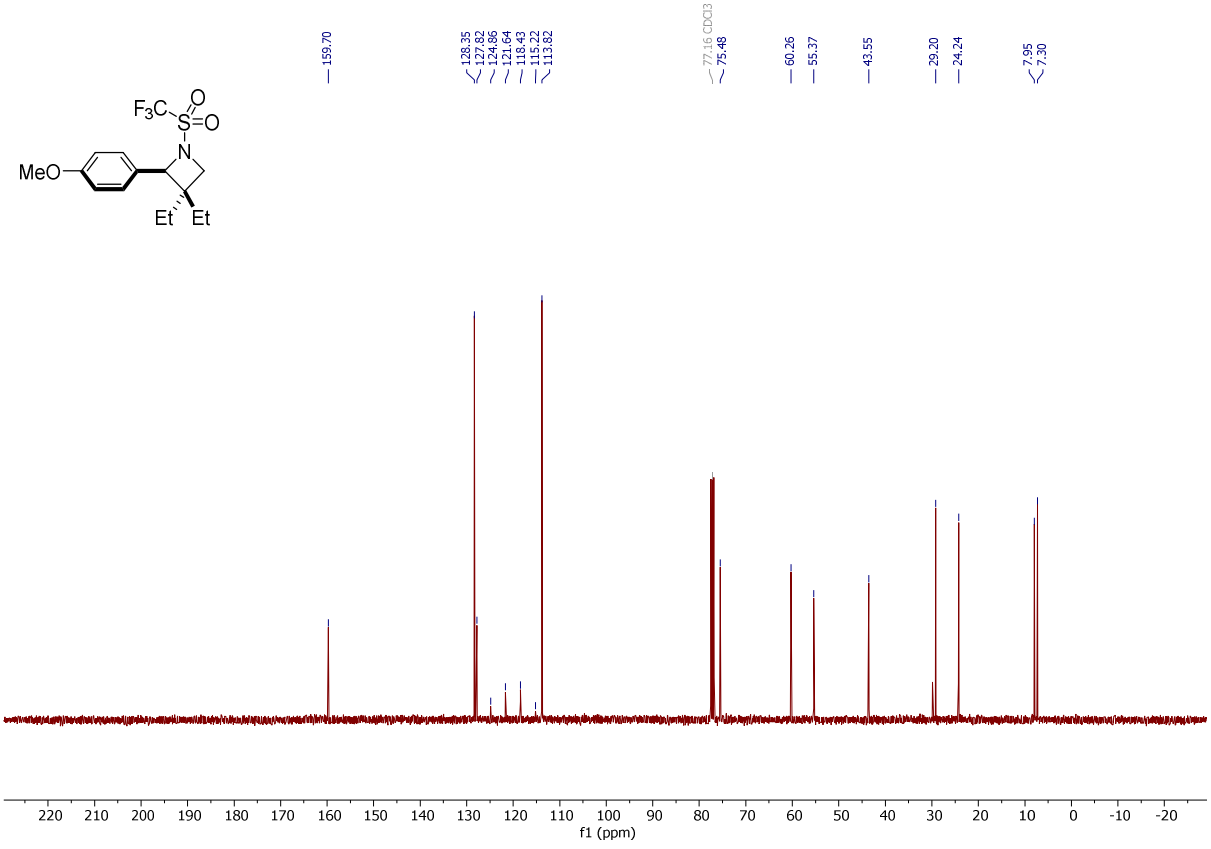

178.41
167.69
135.79
124.65
123.97
120.99
117.80
115.48
114.60
56.17
O
O
S
N
CF3
H
MeO
220 210 200 190 180 170 160 150 140 130 120 110 100 90 80 70 60 50 40 30 20 10 0 -10 -20
f1 (ppm)

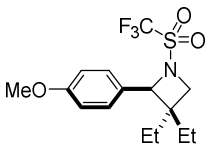

-76.93
-76.97
O
O
S
N
CF3
H
MeO
90 80 70 60 50 40 30 20 10 0 -10 -20 -30 -40 -50 -60 -70 -80 -90 -100 -110 -120 -130 -140 -150 -160 -170 -180 -190 -200 -210 -220 -230 -240
f1 (ppm)

Azetidines

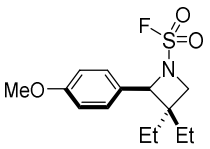
(*R**)-3,3-diethyl-2-(4-methoxyphenyl)-1-((trifluoromethyl)sulfonyl)azetidine (2x)

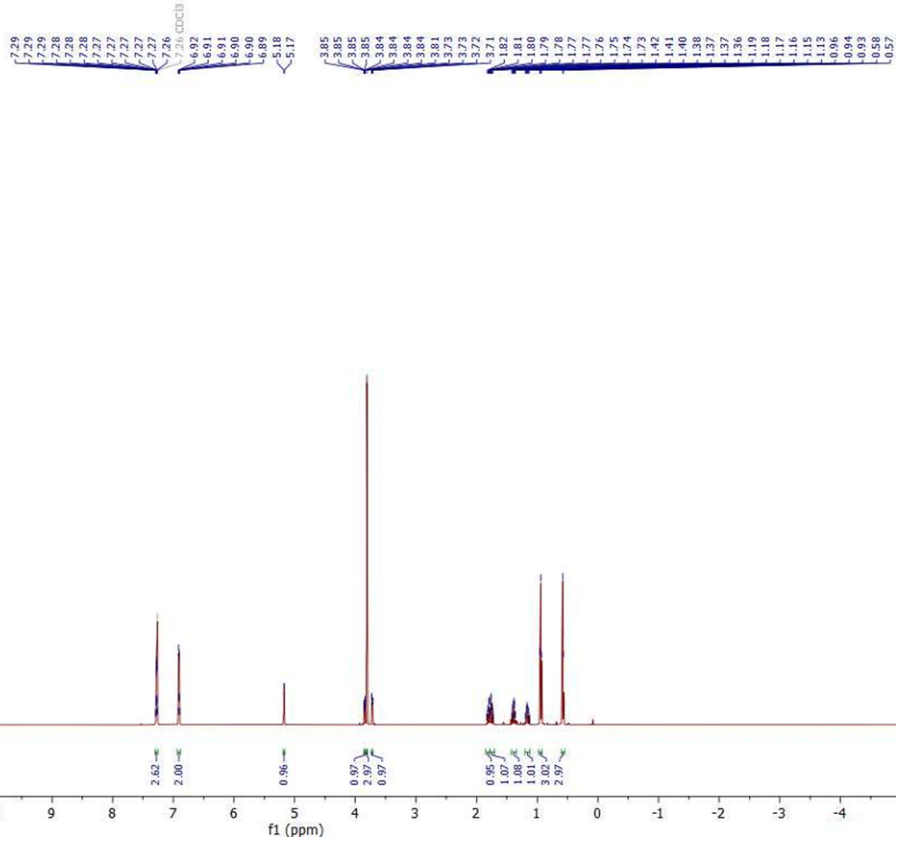


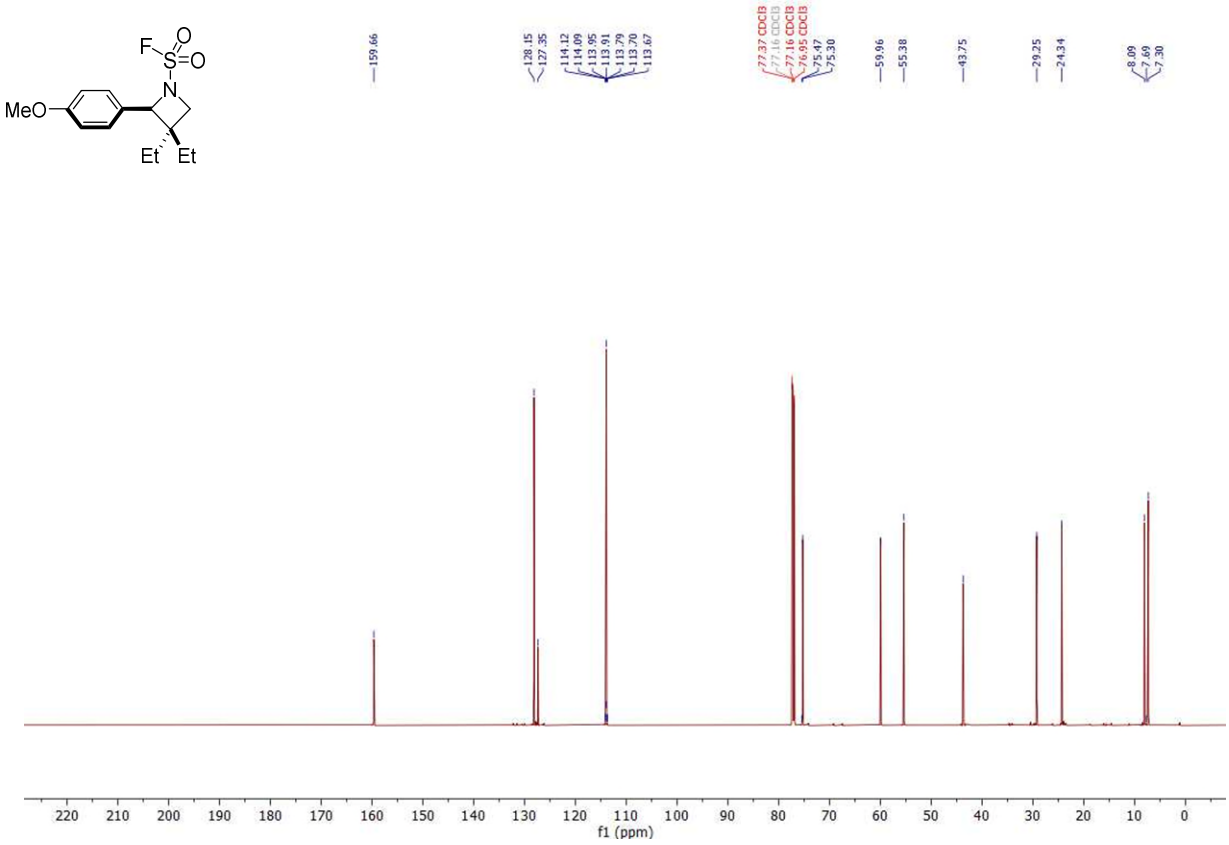


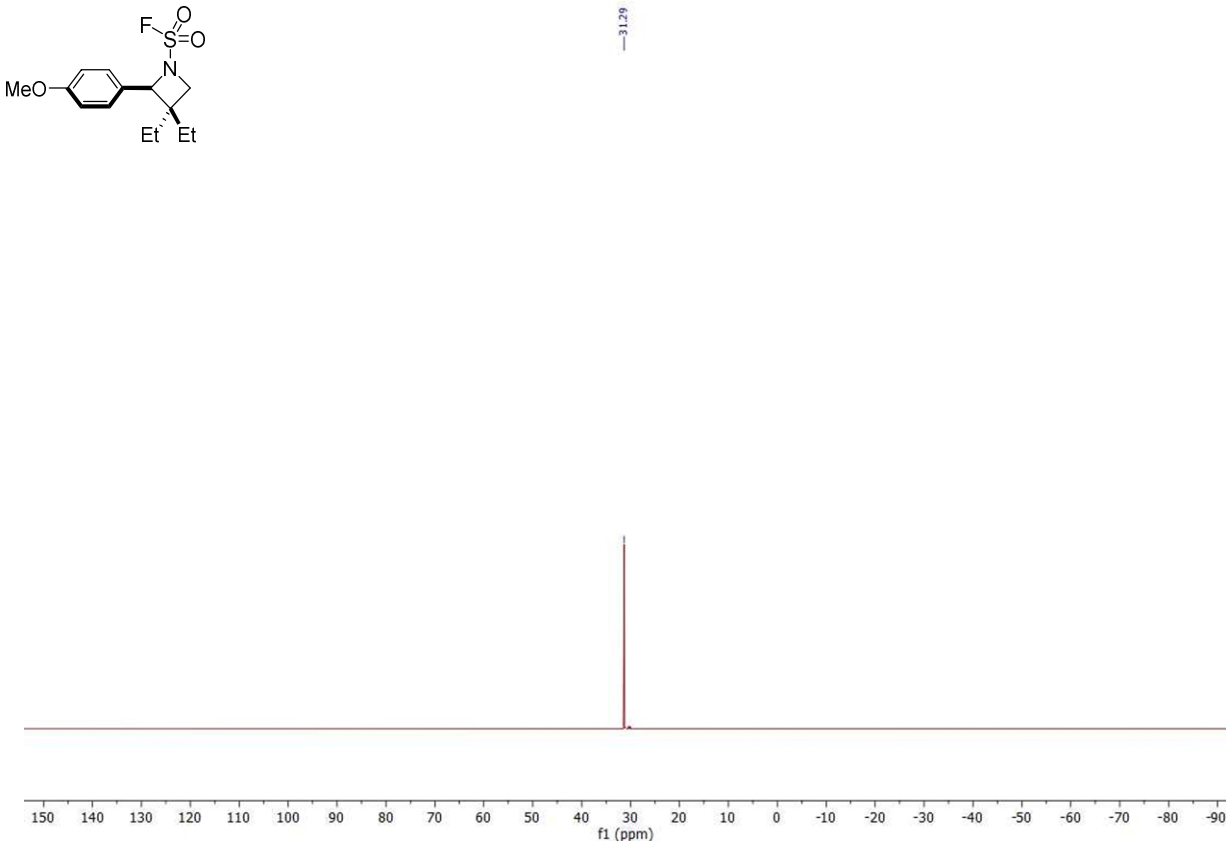


(*R**)-3,3-Diethyl-2-(4-methoxyphenyl)azetidine-1-sulfonyl fluoride (2a)

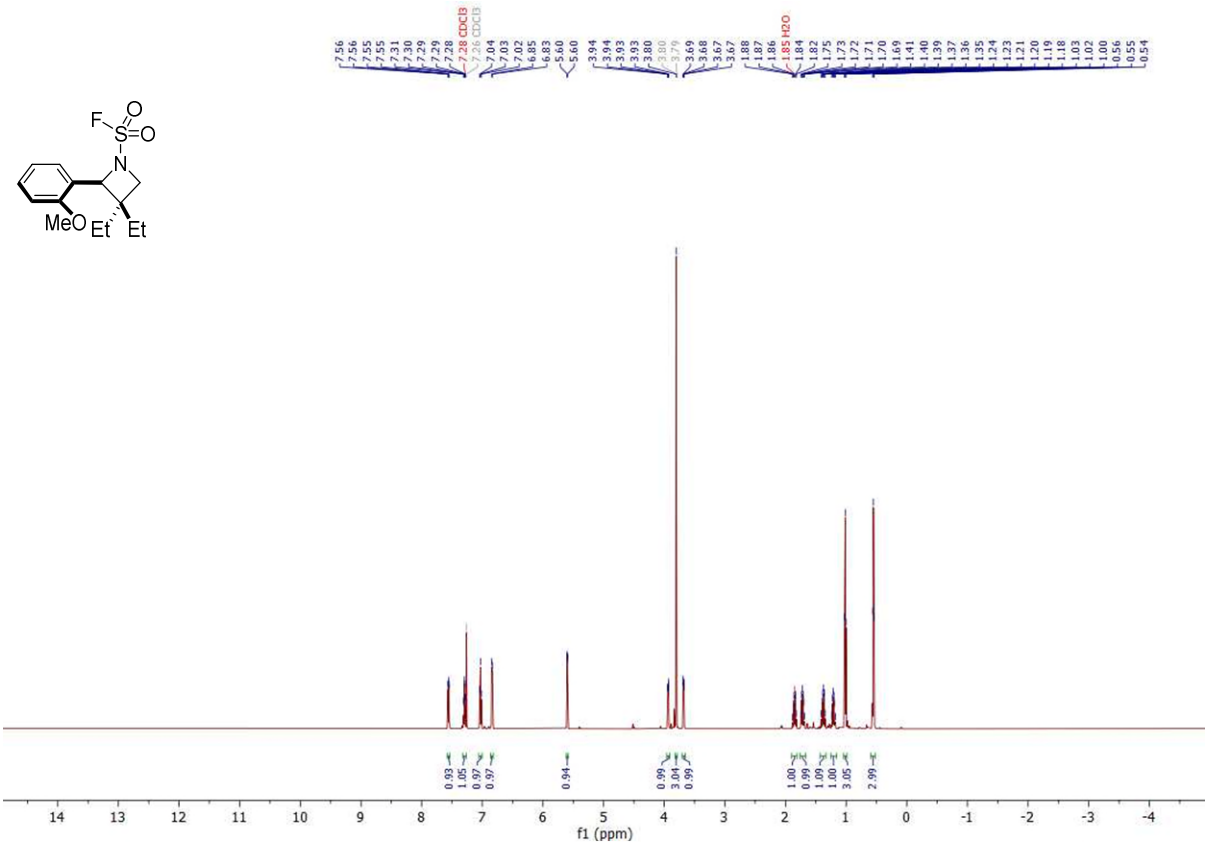


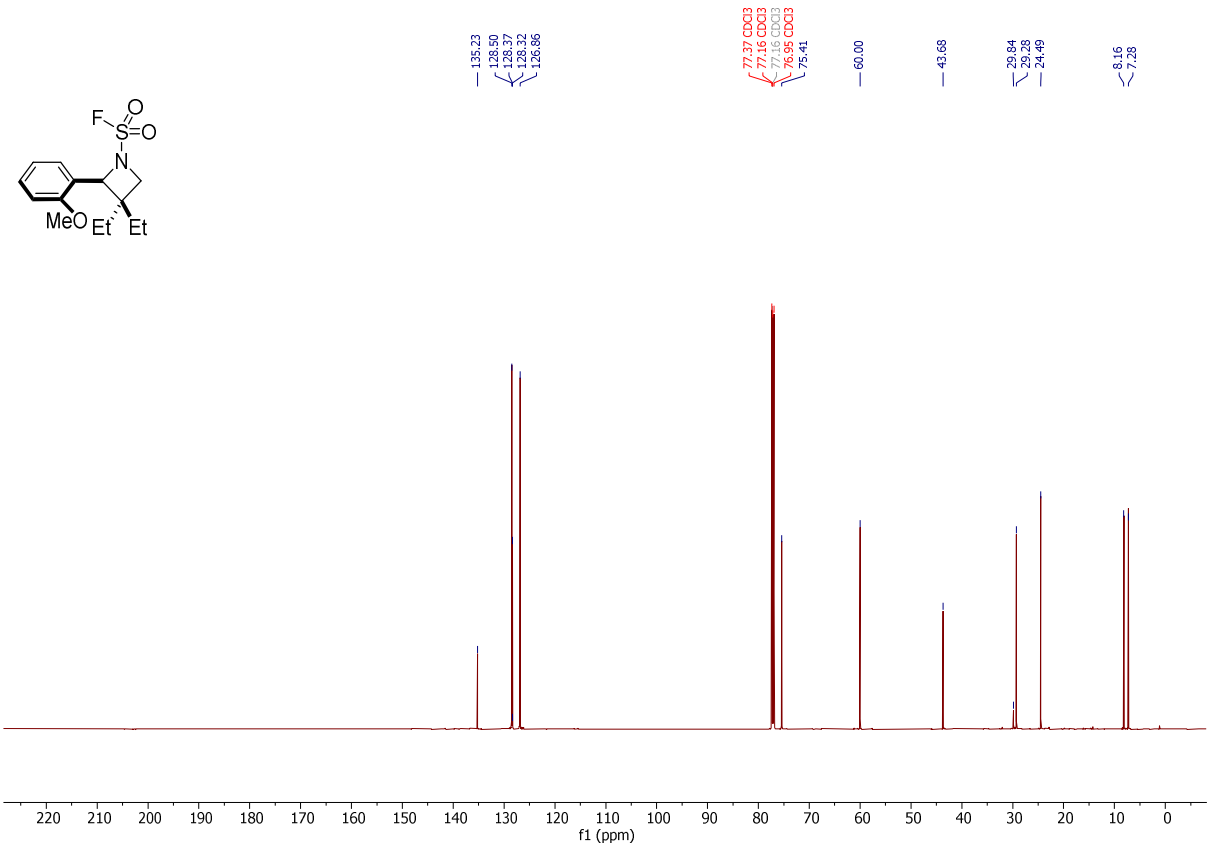


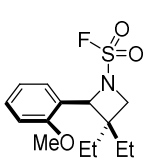

F
O
S
O
N
MeO
Et
Et
159.66
128.15
127.35
114.12
114.09
113.95
113.91
113.79
113.70
113.67
77.37 CDCl3
77.16 CDCl3
76.95 CDCl3
75.47
75.30
59.96
55.38
43.75
29.25
24.34
8.09
7.69
7.30
220 210 200 190 180 170 160 150 140 130 120 110 100 90 80 70 60 50 40 30 20 10 0
f1 (ppm)


F
O
S
O
N
MeO
Et
Et
31.29
150 140 130 120 110 100 90 80 70 60 50 40 30 20 10 0 -10 -20 -30 -40 -50 -60 -70 -80 -90
f1 (ppm)

(*S**)-3,3-Diethyl-2-(2-methoxyphenyl)azetidine-1-sulfonyl fluoride (2b)

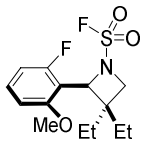


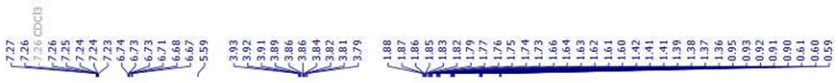


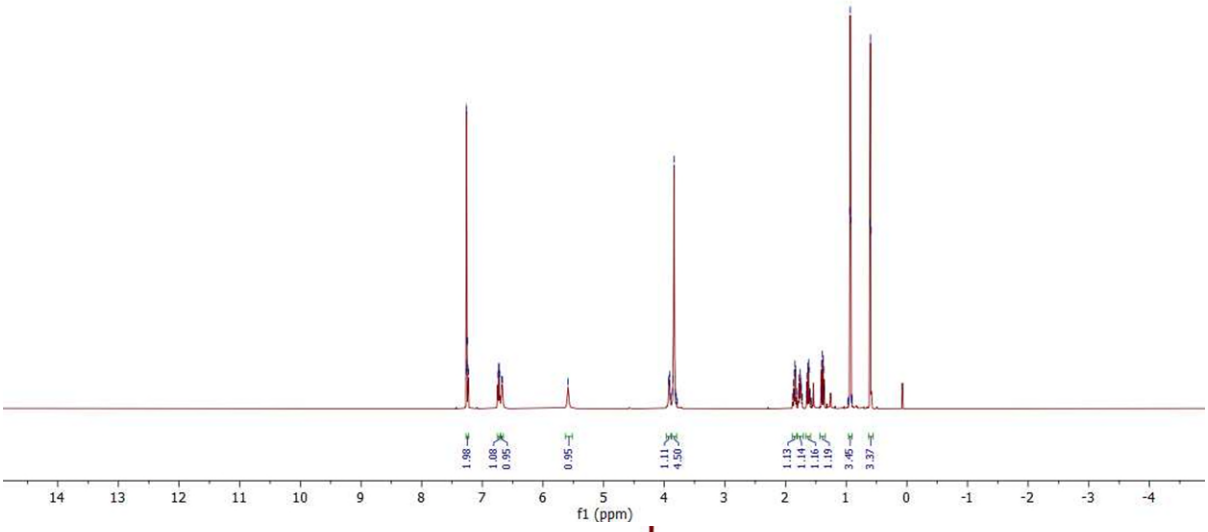

F
O
S
O
N
MeO
Et
Et

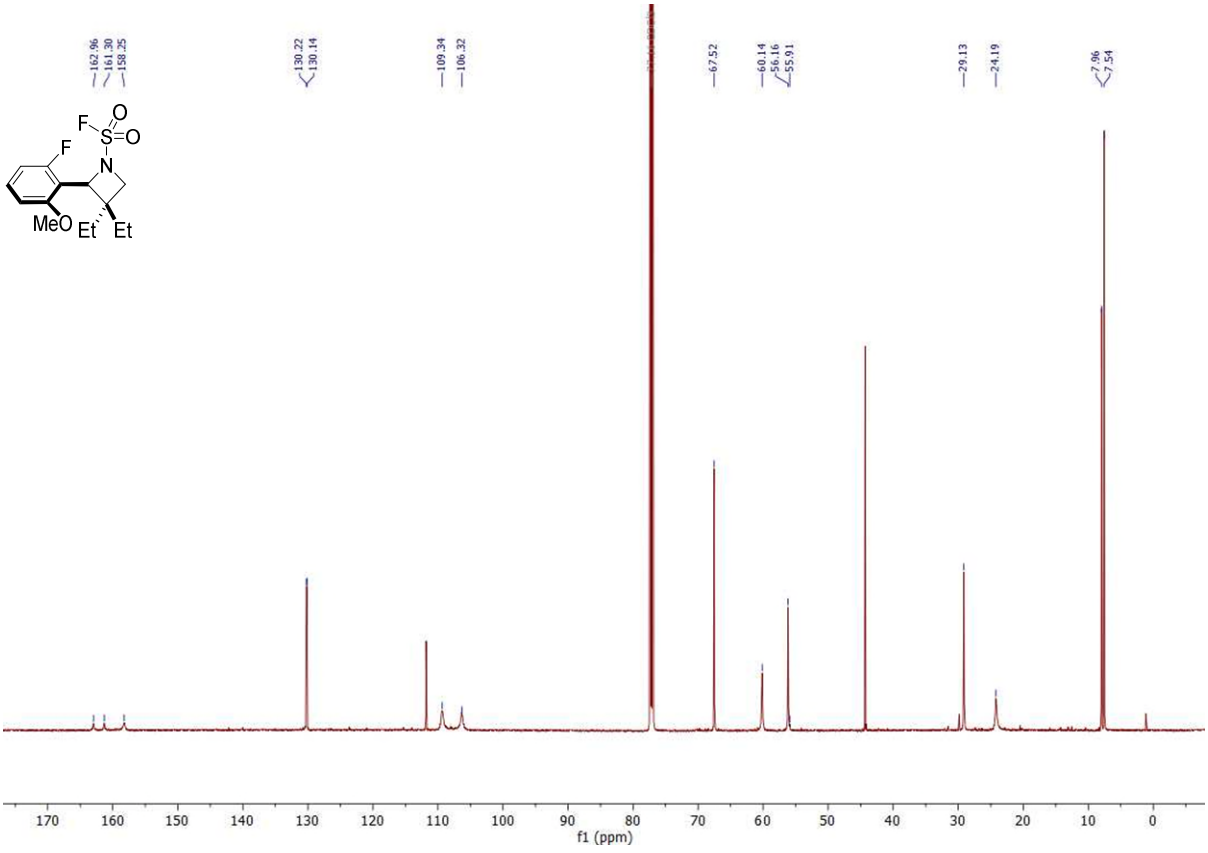
31.20
90 80 70 60 50 40 30 20 10 0 -10 -20 -30 -40 -50 -60 -70 -80 -90 -100 -110 -120 -130 -140 -150 -160 -170 -180 -190 -200 -210 -220 -230 -240
f1 (ppm)

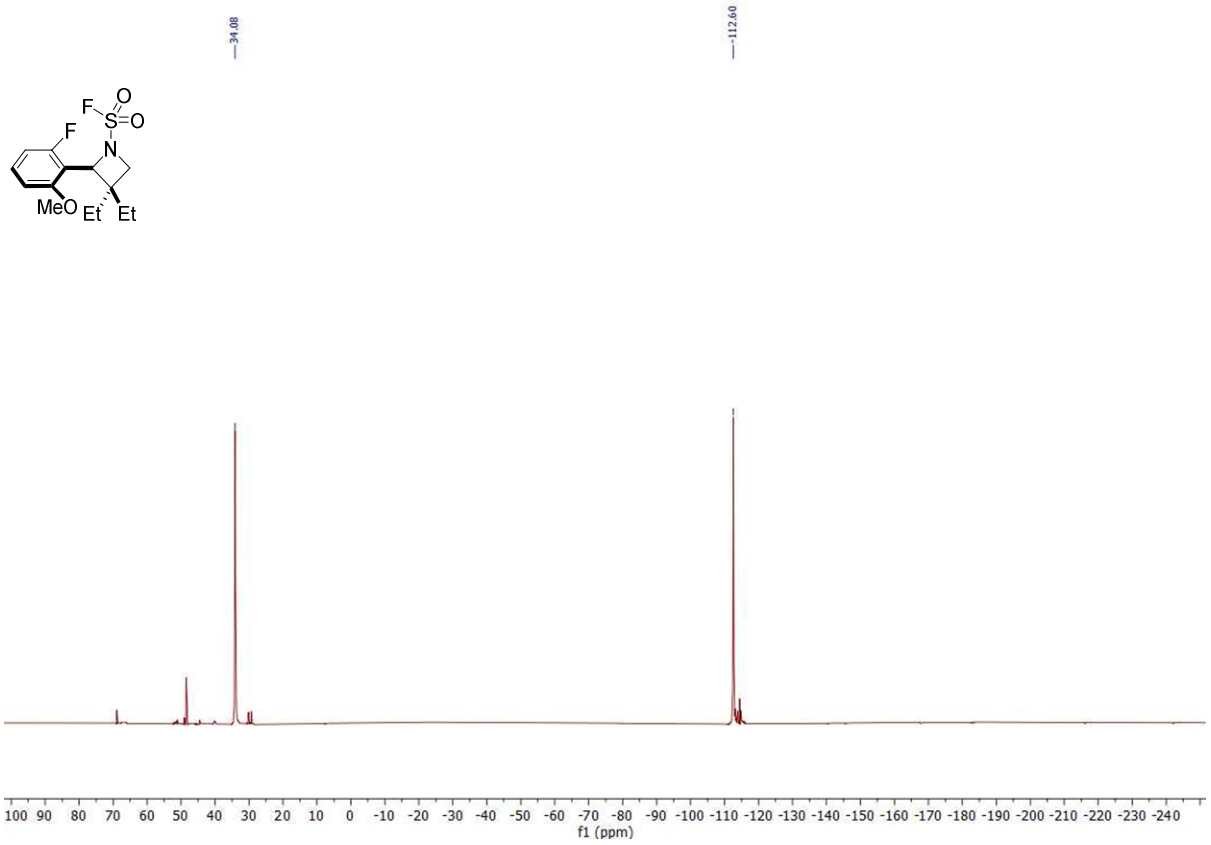
(*S**)-3,3-Diethyl-2-(2-fluoro-6-methoxyphenyl)azetidine-1-sulfonyl fluoride (2c)



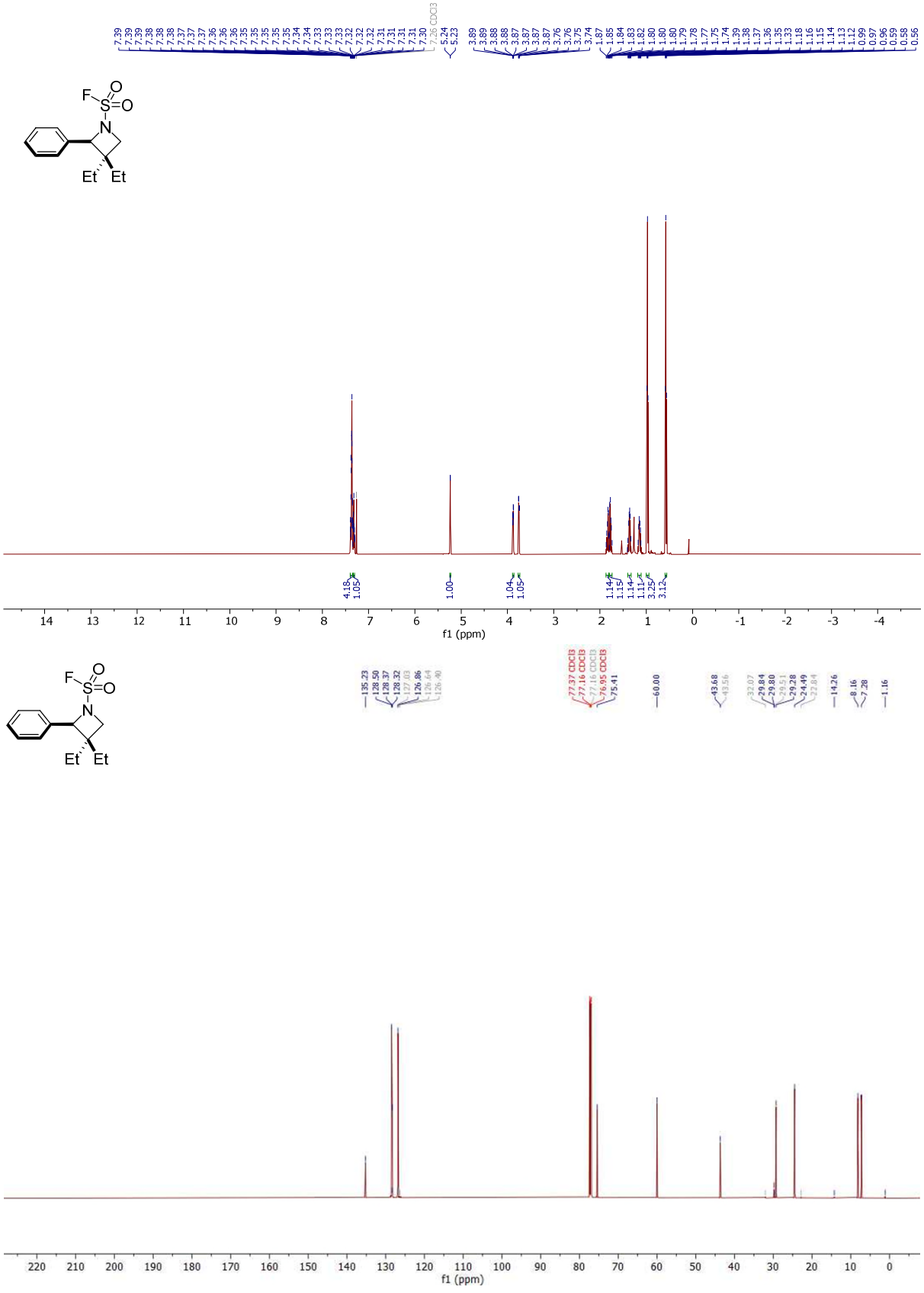


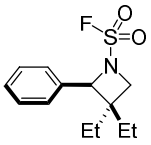




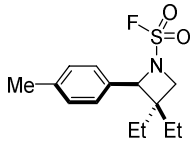

34.08
112.60
F
O
S
O
F
N
MeO
Et
Et
100 90 80 70 60 50 40 30 20 10 0 -10 -20 -30 -40 -50 -60 -70 -80 -90 -100 -110 -120 -130 -140 -150 -160 -170 -180 -190 -200 -210 -220 -230 -240
f1 (ppm)

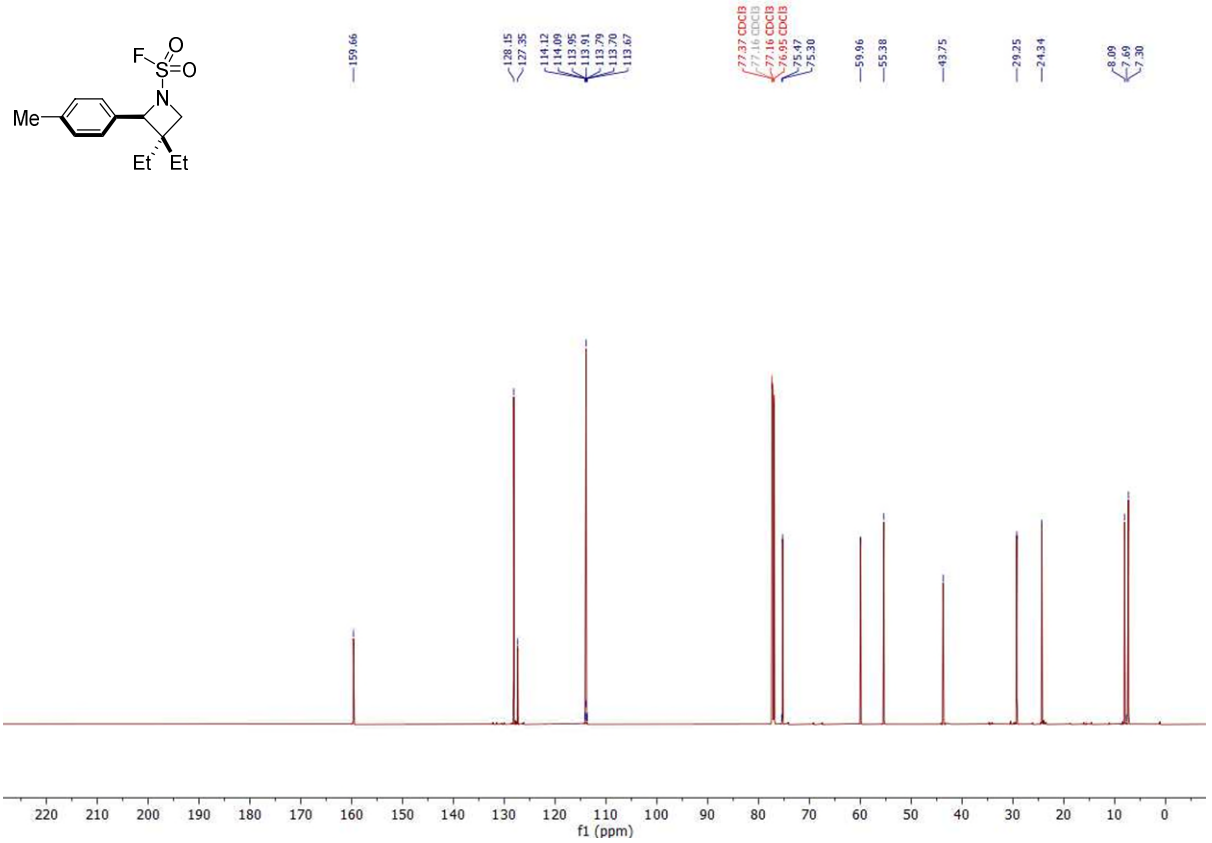
(*R**)-3,3-Diethyl-2-phenylazetidine-1-sulfonyl fluoride (2d)

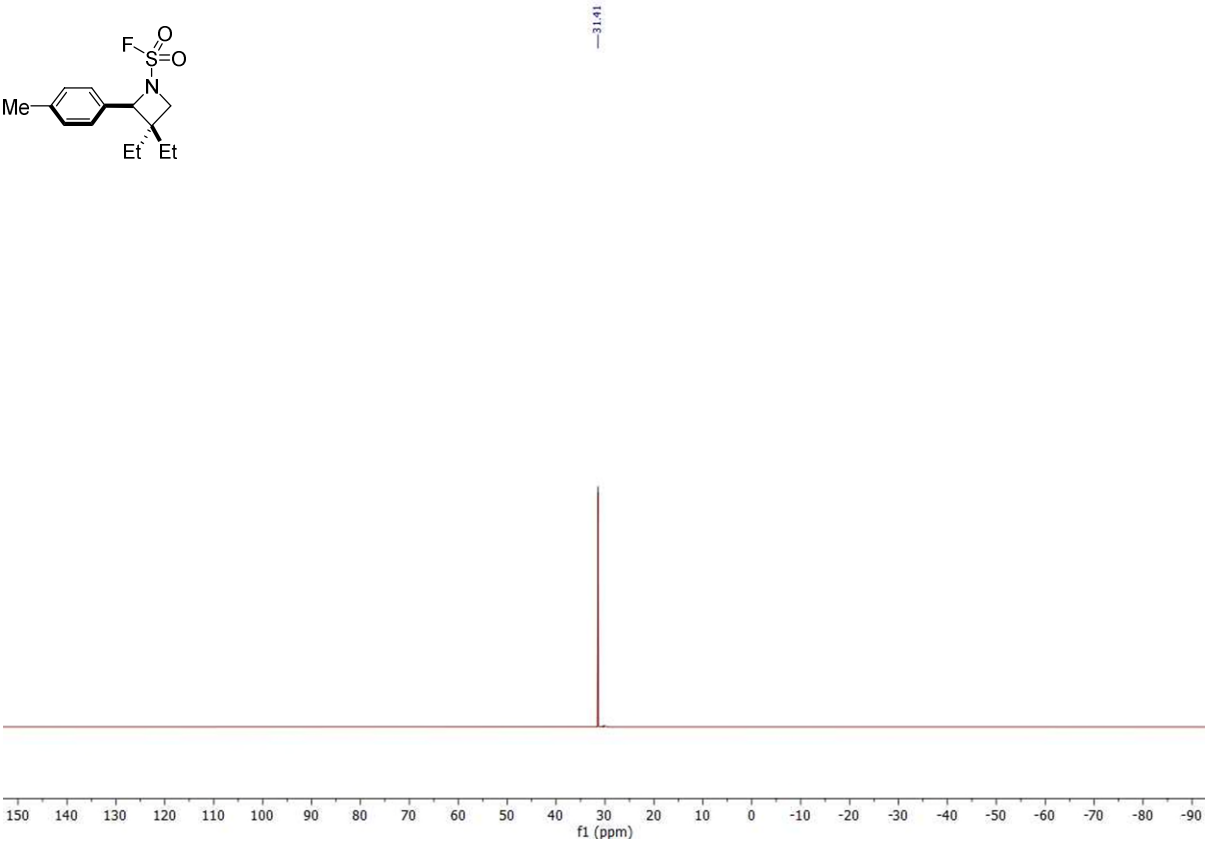




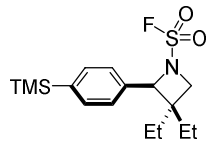
(*R**)-3,3-Diethyl-2-(p-tolyl)azetidine-1-sulfonyl fluoride (2e)



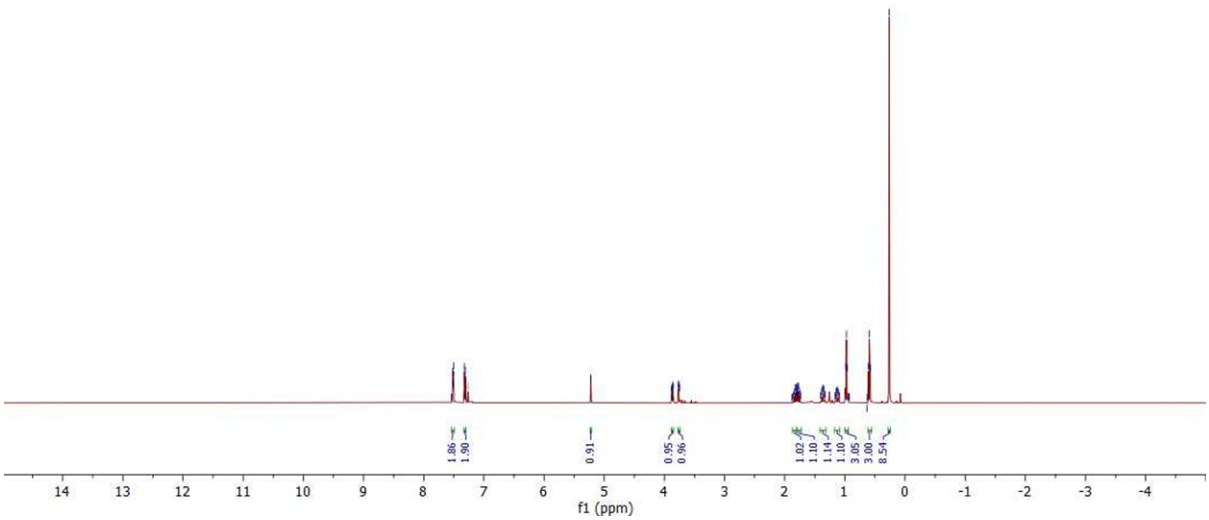

F
O
S
O
N
Me
Et
Et
159.66
128.15
127.35
114.12
114.09
113.95
113.91
113.79
113.70
113.67
77.37 CDCl3
77.16 CDCl3
76.95 CDCl3
75.47
75.30
59.96
55.38
43.75
29.25
24.34
8.09
7.69
7.30
220 210 200 190 180 170 160 150 140 130 120 110 100 90 80 70 60 50 40 30 20 10 0
f1 (ppm)

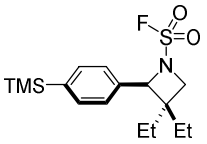

F
O
S
O
N
Me
Et
Et
31.41
150 140 130 120 110 100 90 80 70 60 50 40 30 20 10 0 -10 -20 -30 -40 -50 -60 -70 -80 -90
f1 (ppm)

(*R**)-3,3-Diethyl-2-(4-(trimethylsilyl)phenyl)azetidine-1-sulfonyl fluoride (2g)

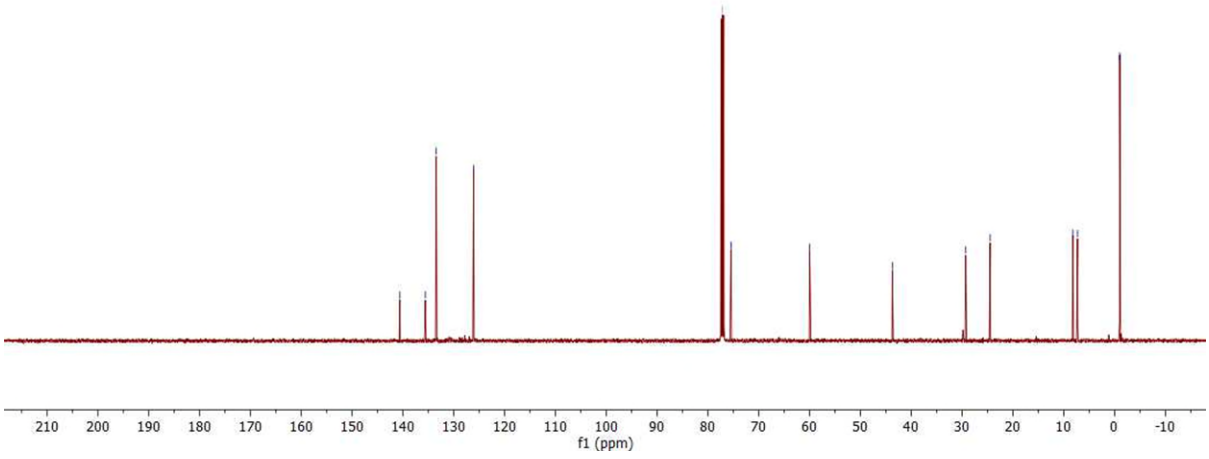


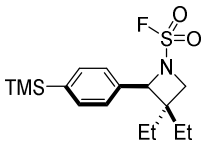






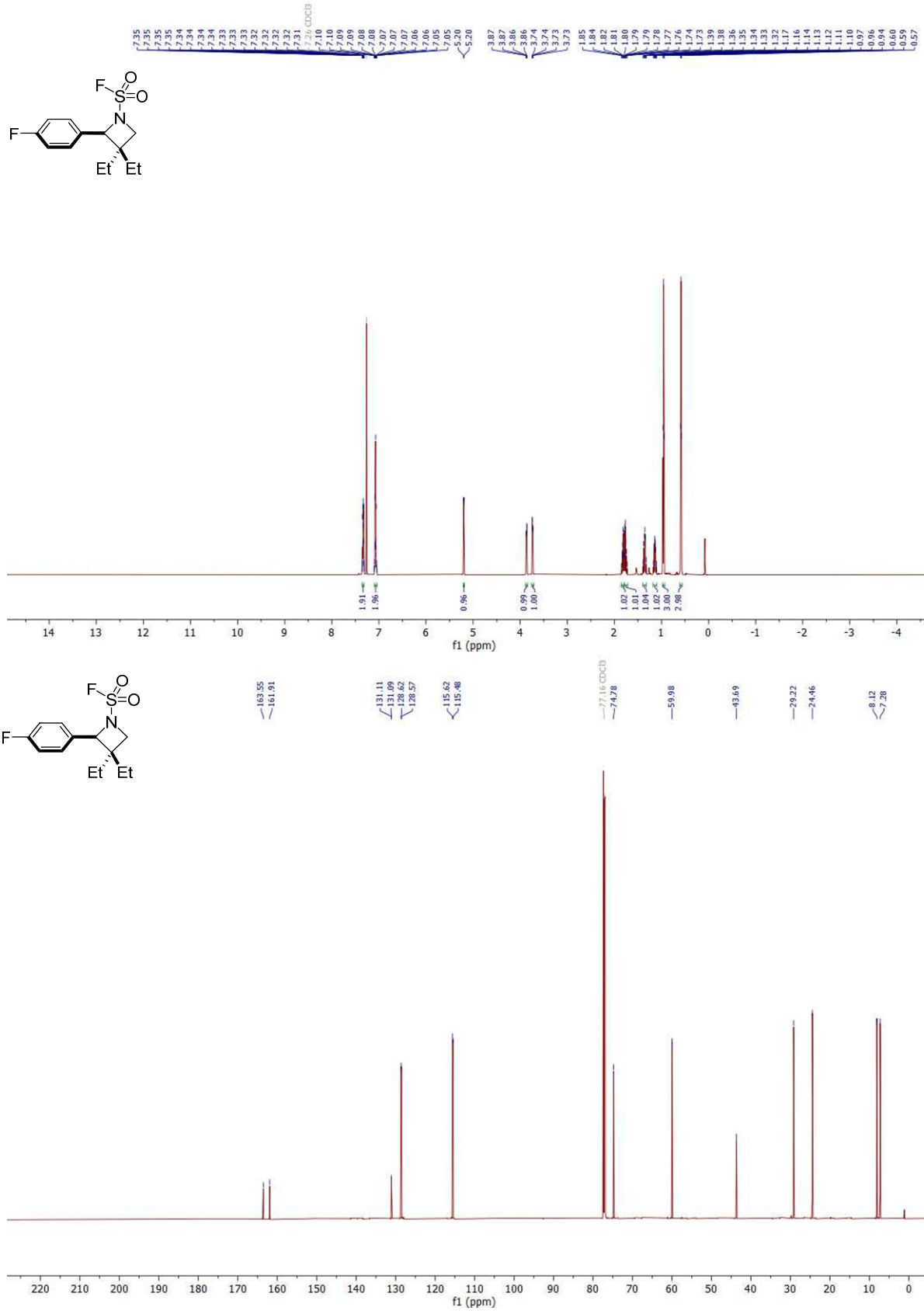


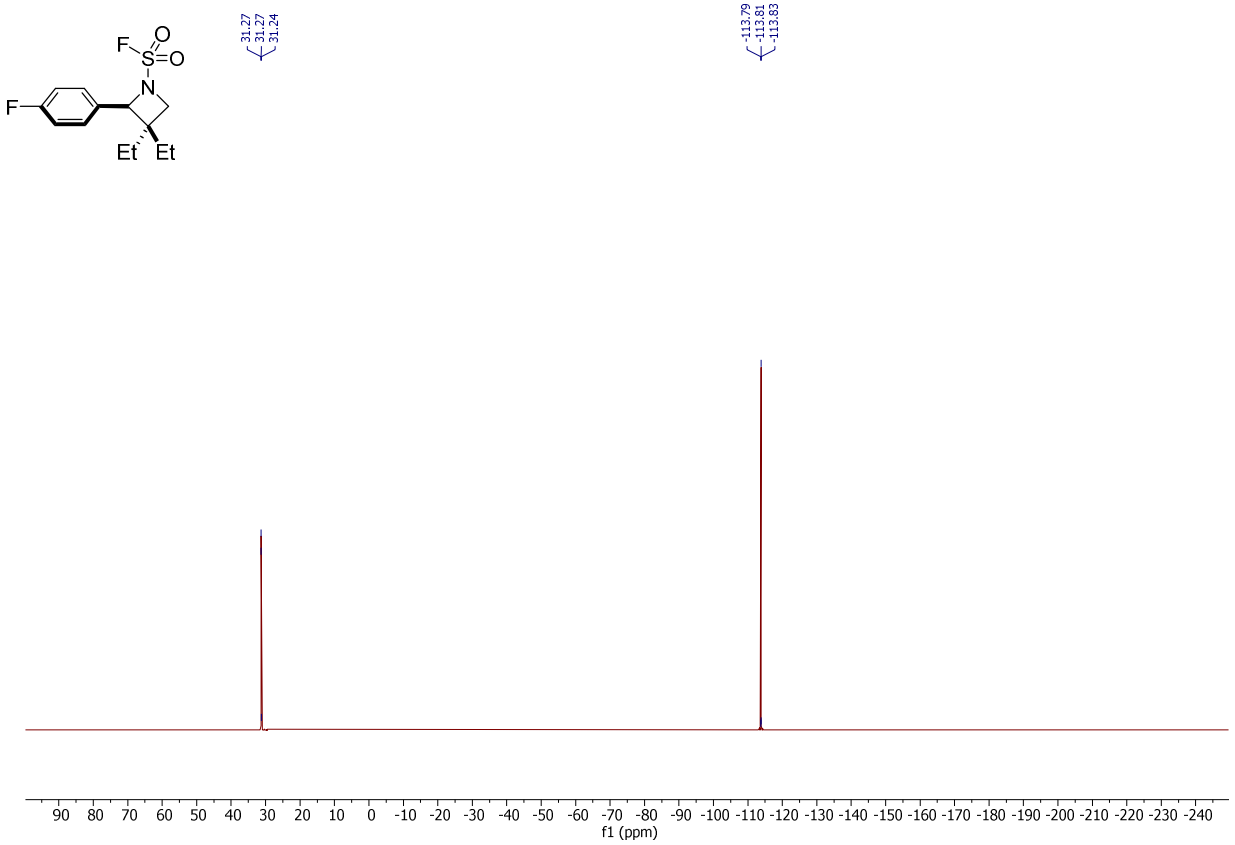



F
O
S
O
N
TMS
Et
Et

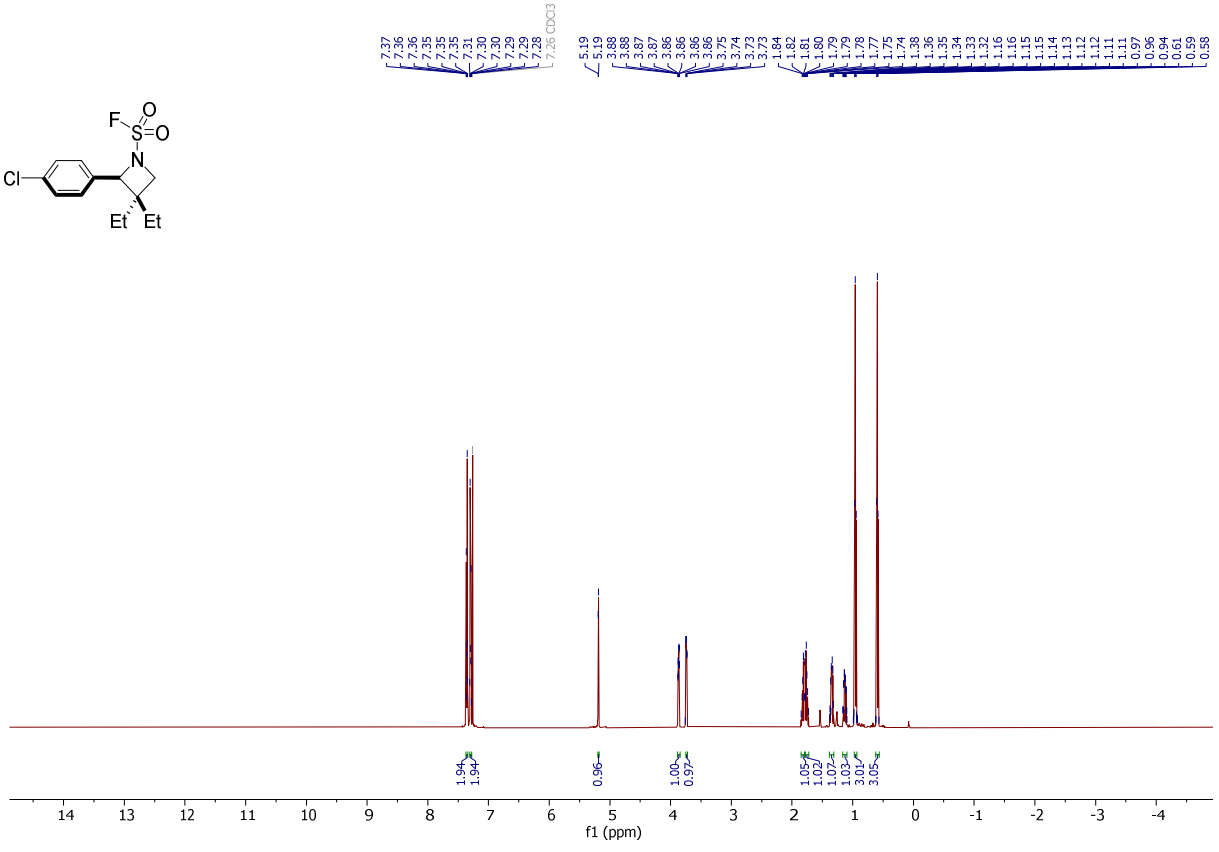
31.41
150 140 130 120 110 100 90 80 70 60 50 40 30 20 10 0 -10 -20 -30 -40 -50 -60 -70 -80
f1 (ppm)

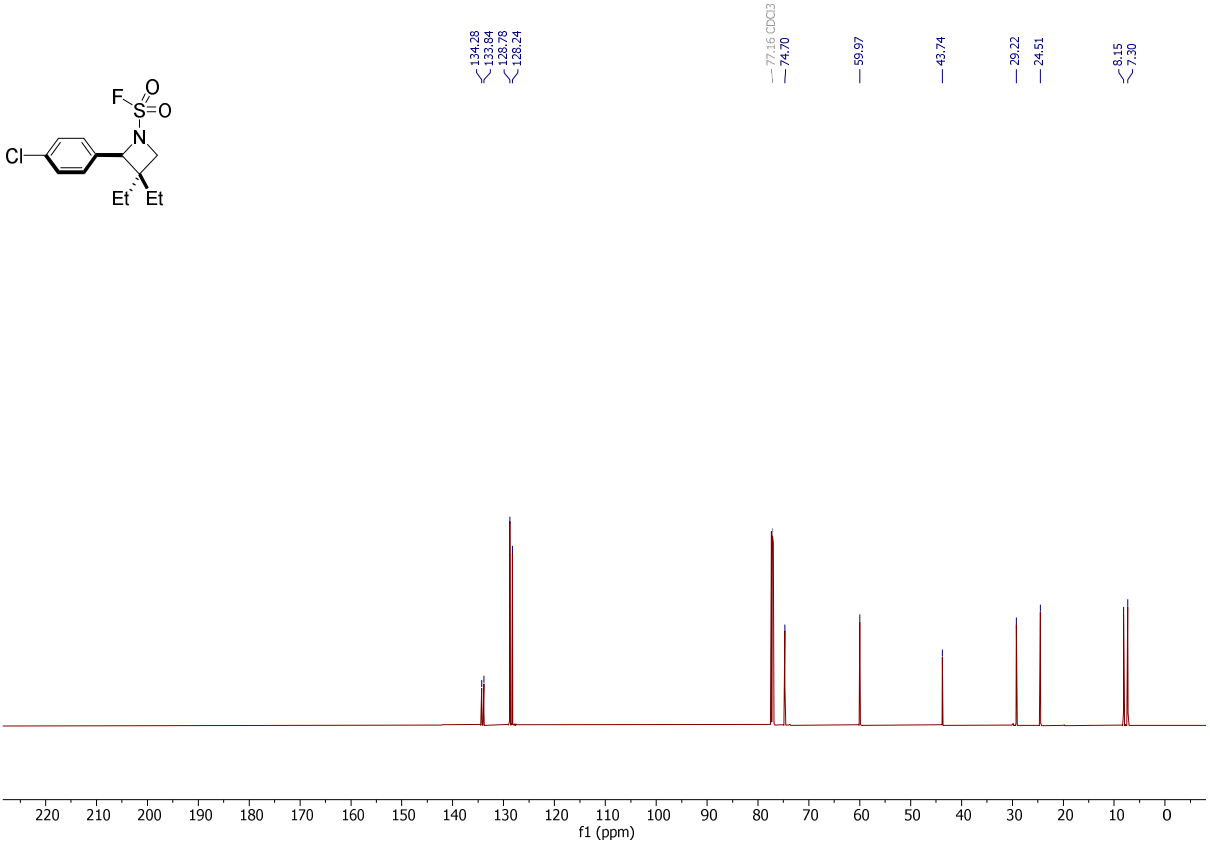
(*R**)-3,3-Diethyl-2-(4-fluorophenyl)azetidine-1-sulfonyl fluoride (2i)

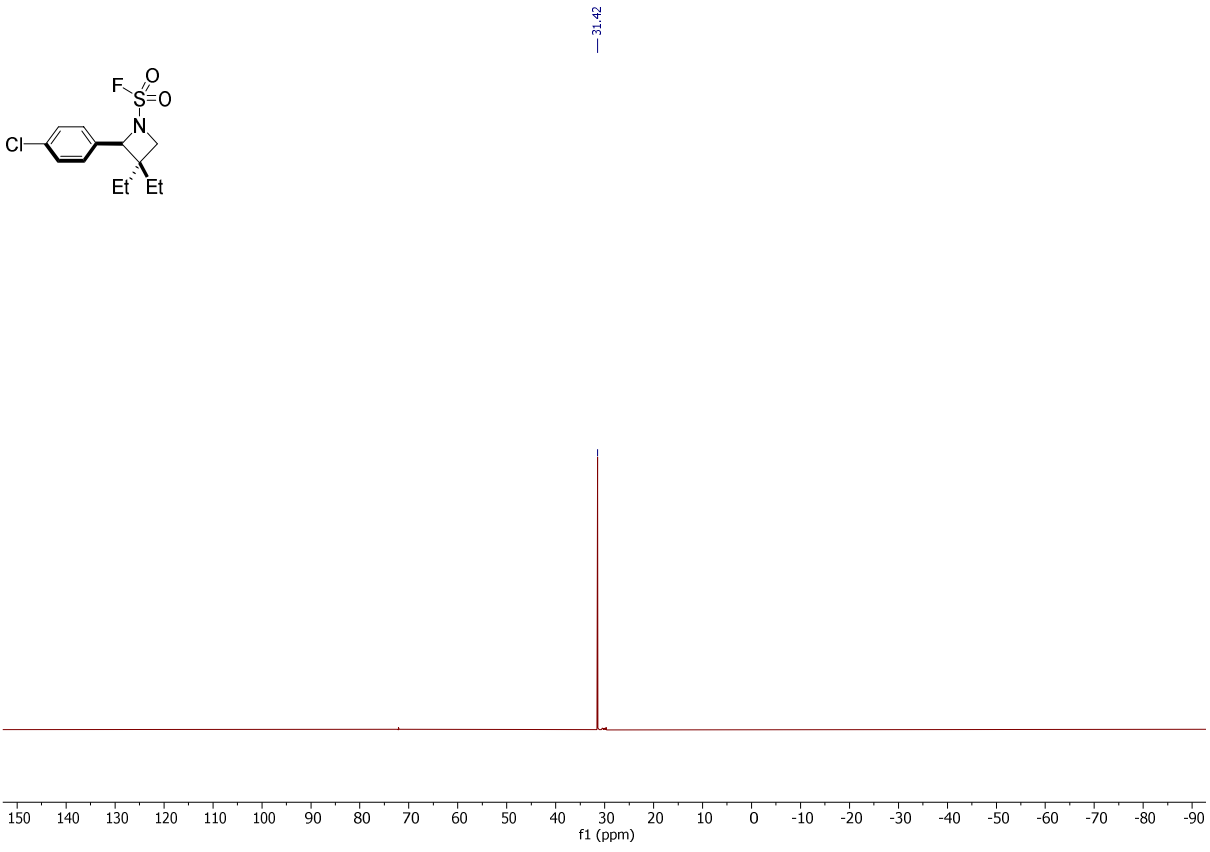




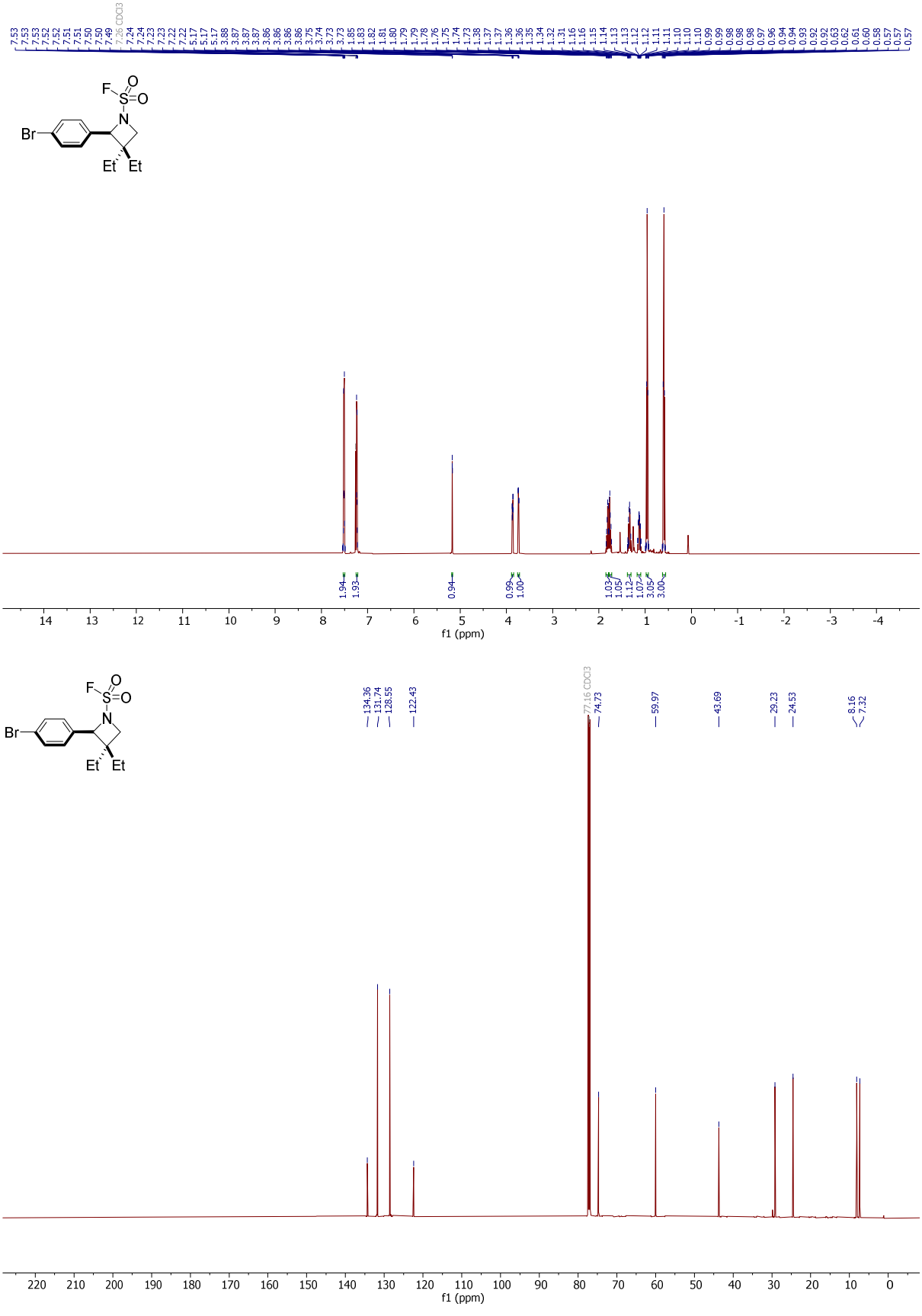
(*R**)-2-(4-Chlorophenyl)-3,3-diethylazetidine-1-sulfonyl fluoride (2j)

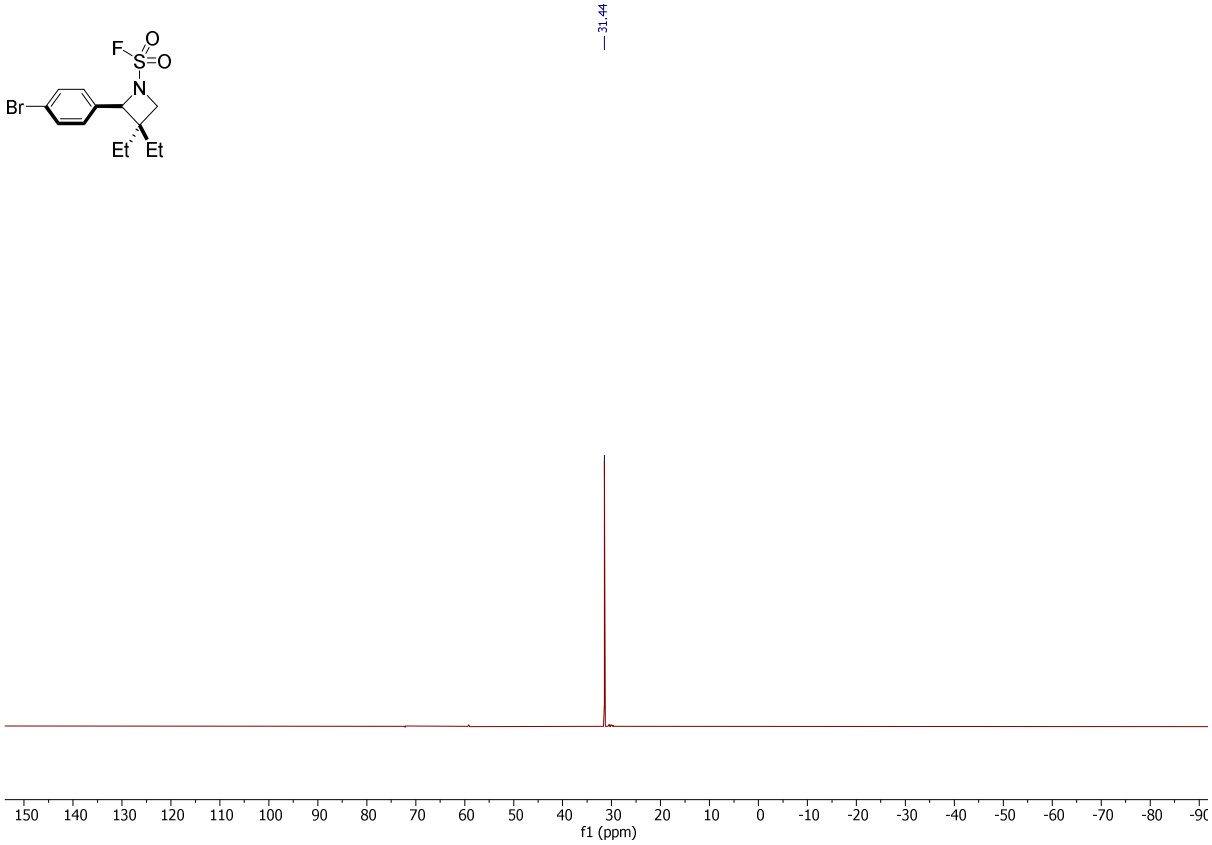



134.28
133.84
128.78
128.24
77.16 CDCl3
74.70
59.97
43.74
29.22
24.51
8.15
7.30
F
O
S
O
N
Cl
Et
Et
220 210 200 190 180 170 160 150 140 130 120 110 100 90 80 70 60 50 40 30 20 10 0
f1 (ppm)

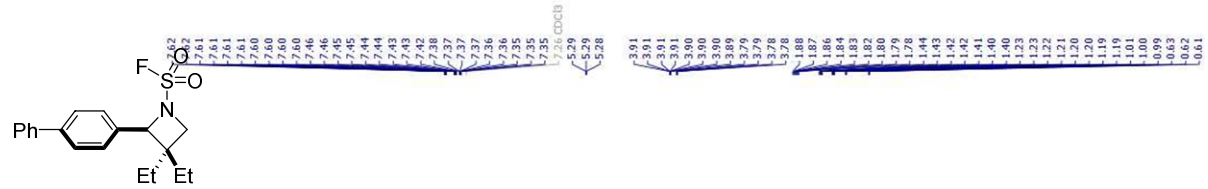

31.42
F
O
S
O
N
Cl
Et
Et
150 140 130 120 110 100 90 80 70 60 50 40 30 20 10 0 -10 -20 -30 -40 -50 -60 -70 -80 -90
f1 (ppm)

(*R**)-2-(4-Bromophenyl)-3,3-diethylazetidine-1-sulfonyl fluoride (2k)

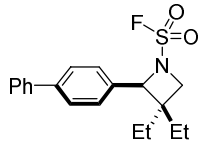



31.44
F
O
S
O
N
Br
Et
Et
150 140 130 120 110 100 90 80 70 60 50 40 30 20 10 0 -10 -20 -30 -40 -50 -60 -70 -80 -90
f1 (ppm)

(*R**)-2-([1,1'-Biphenyl]-4-yl)-3,3-diethylazetidine-1-sulfonyl fluoride (2h)

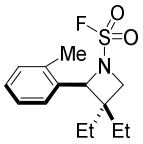




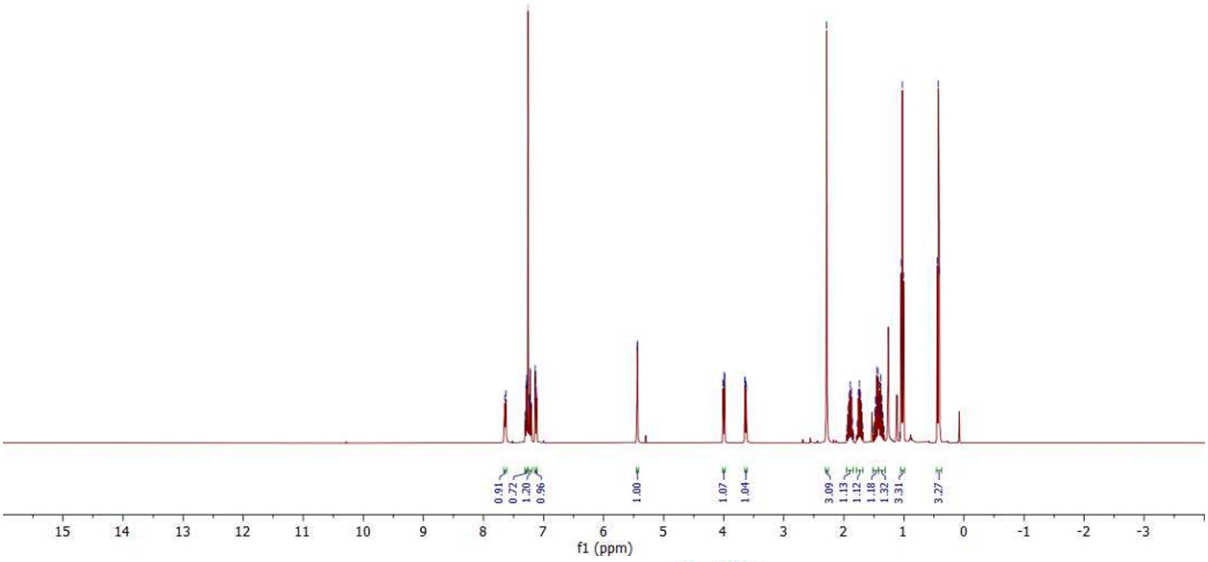

F
O
S
O
N
Ph
Et
Et

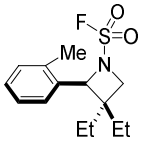
3.150
150 140 130 120 110 100 90 80 70 60 50 40 30 20 10 0 -10 -20 -30 -40 -50 -60 -70 -80 -90
f1 (ppm)

(*R**)-3,3-Diethyl-2-(o-tolyl)azetidine-1-sulfonyl fluoride (2f)

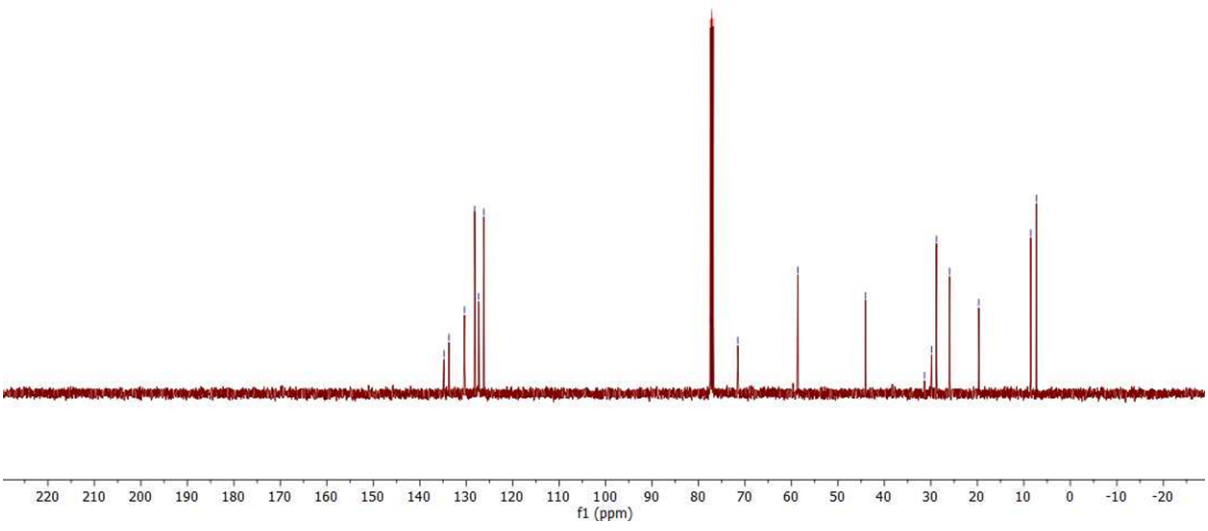


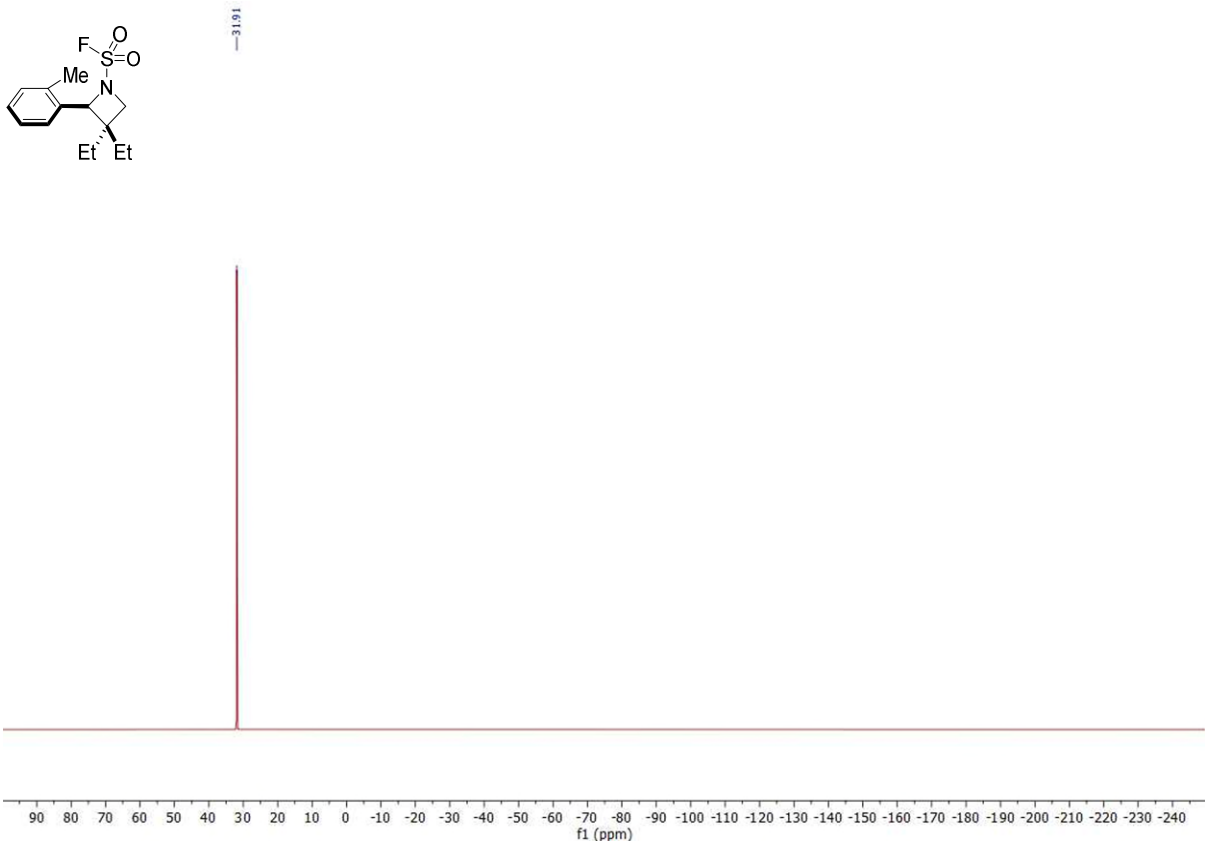




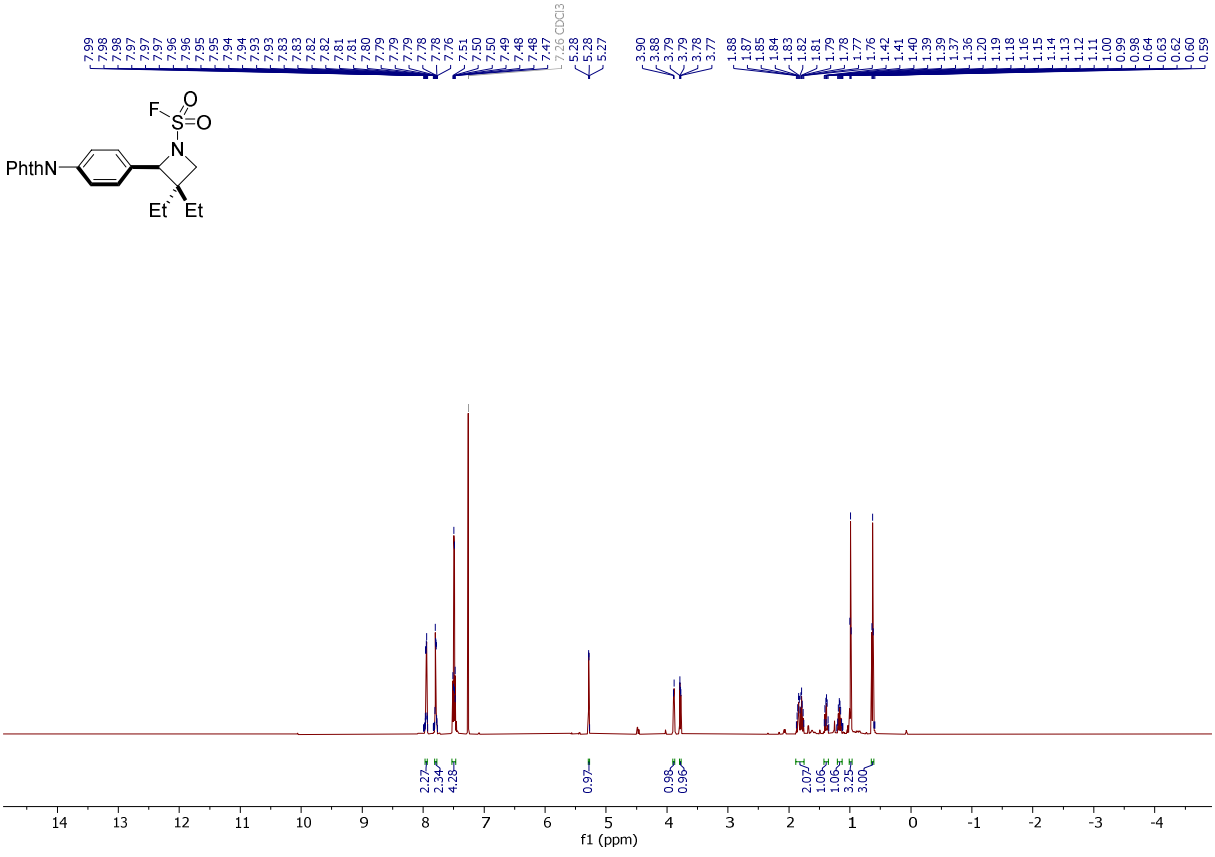


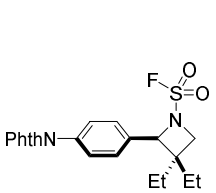




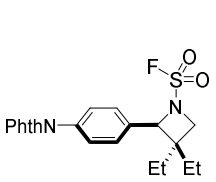


(*R**)-2-(4-(1,3-Dioxoisoindolin-2-yl)phenyl)-3,3-diethylazetidine-1-sulfonyl fluoride (2n)



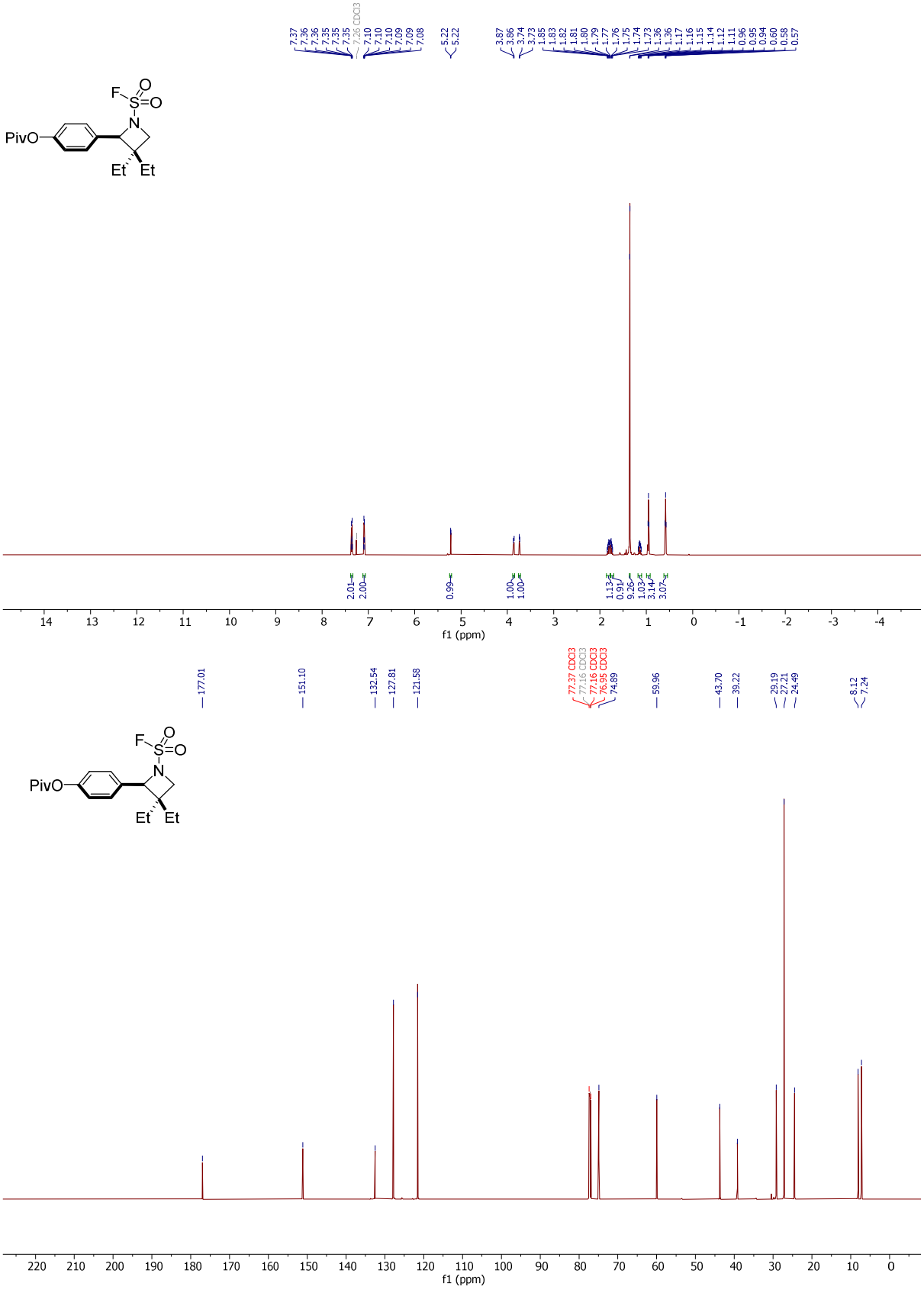

F
O
S=O
N
PhthN
Et
Et

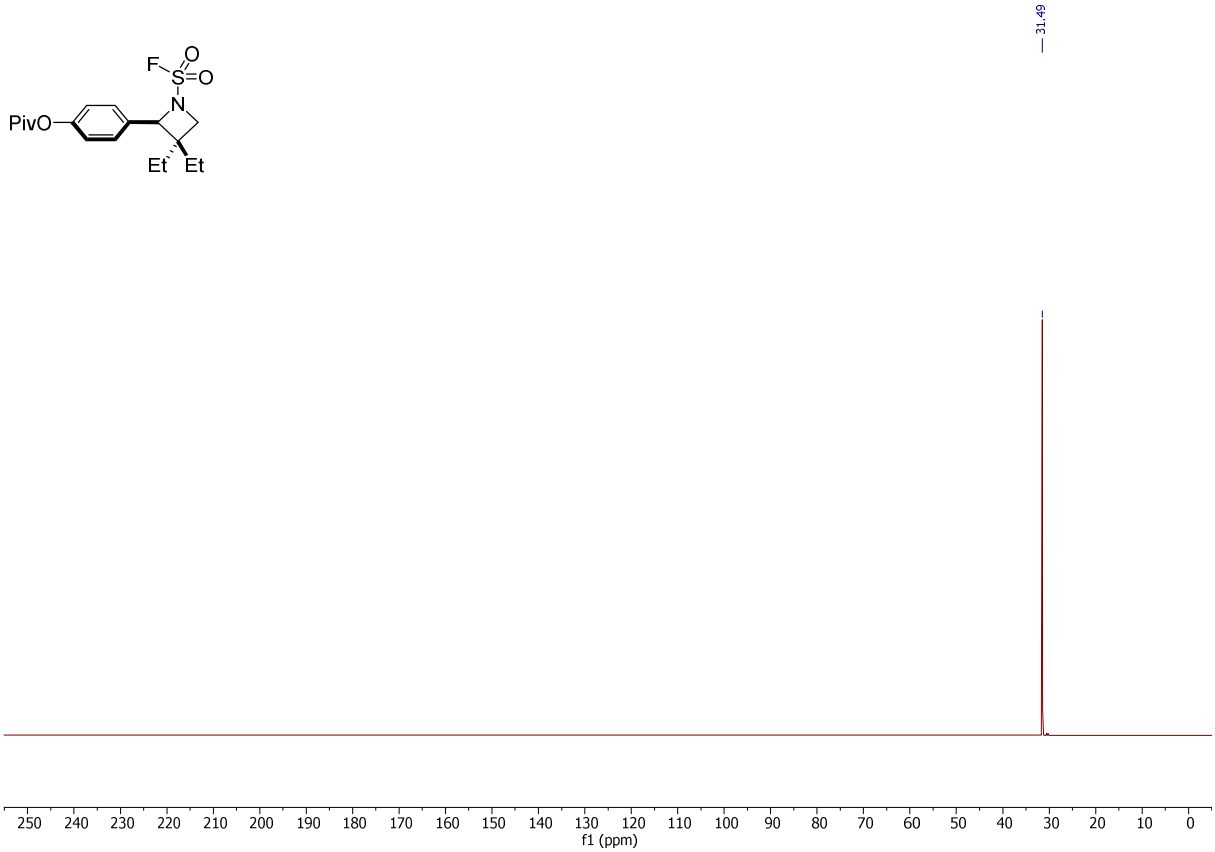
167.21
134.95
134.62
131.78
127.45
126.29
123.91
77.16 CDCl3
74.90
60.01
43.81
29.23
24.65
8.20
7.28
f1 (ppm)


F
O
S=O
N
PhthN
Et
Et

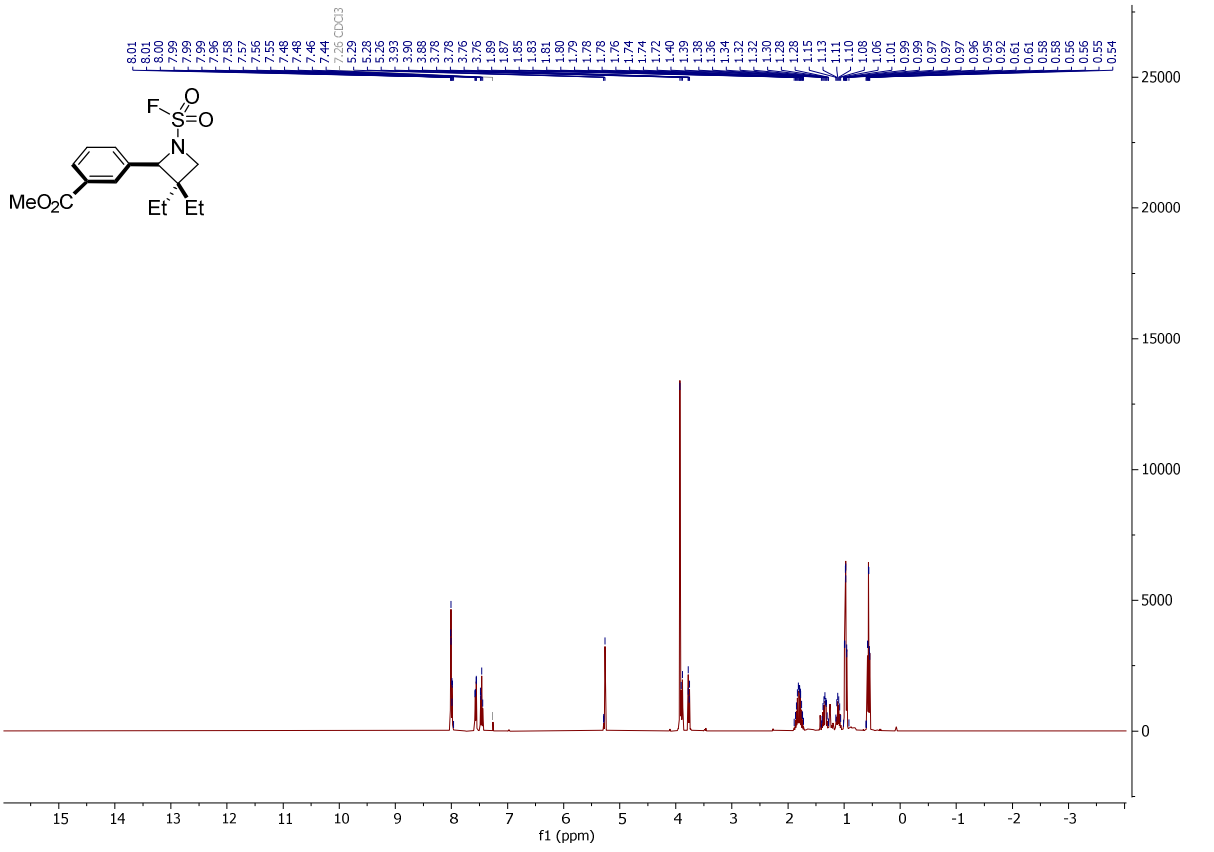
31.69
f1 (ppm)

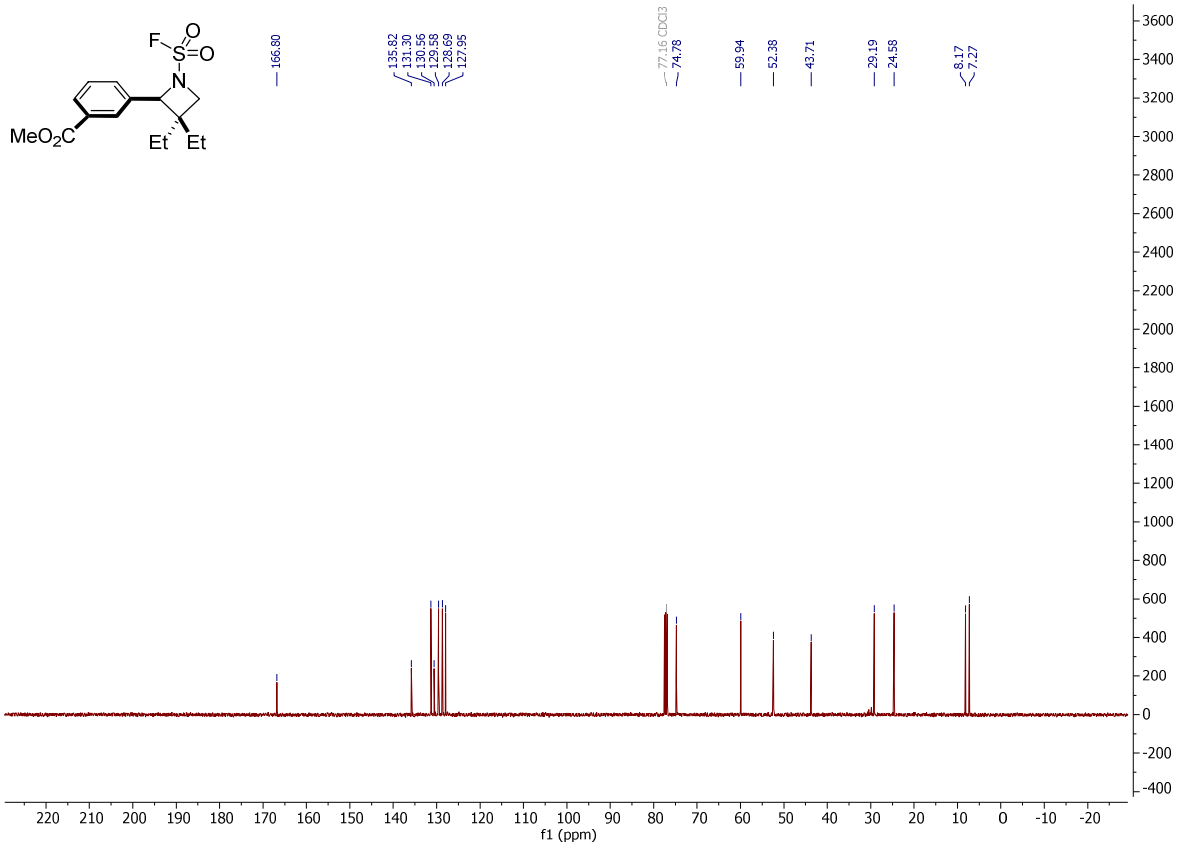
(*R**)-4-(3,3-Diethyl-1-(fluorosulfonyl)azetidin-2-yl)phenyl pivalate (2o)

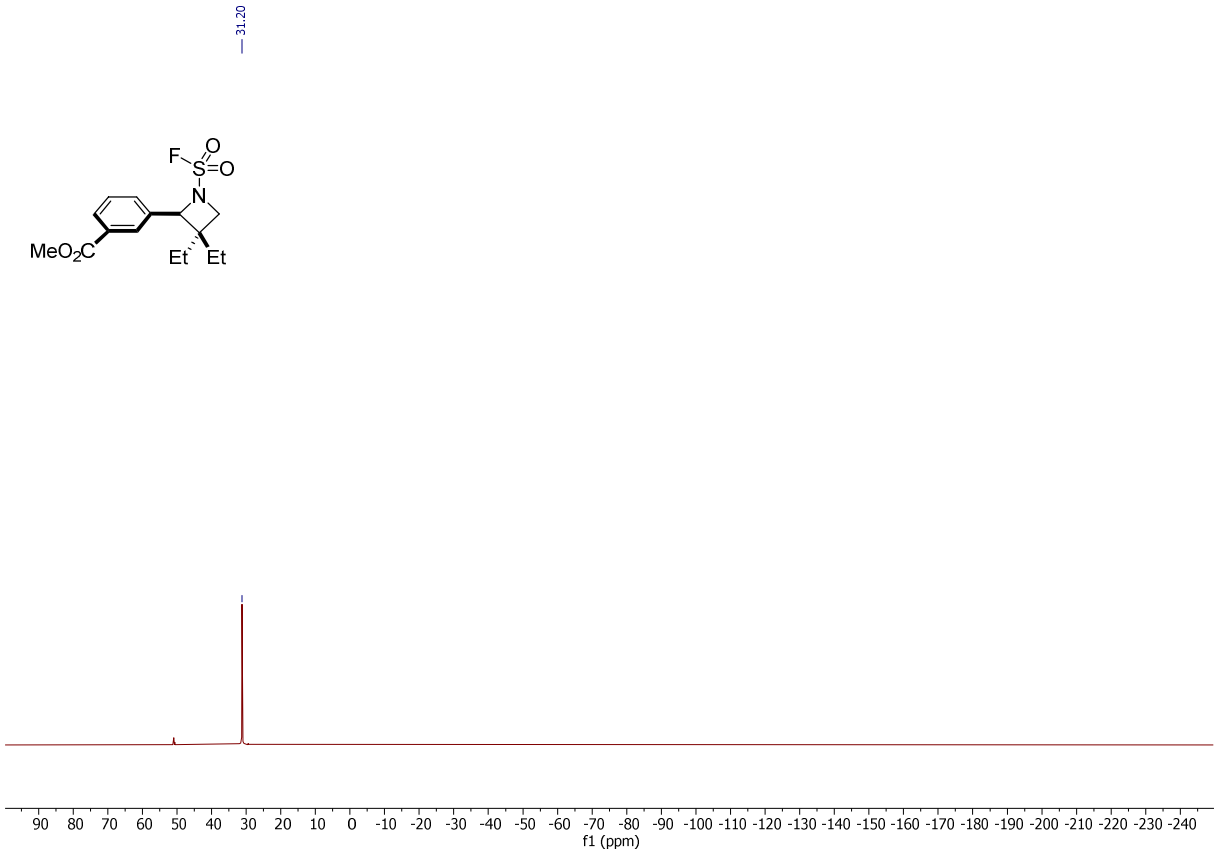




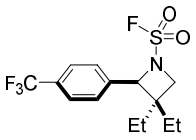
Methyl (*R**)-3-(3,3-diethyl-1-(fluorosulfonyl)azetidin-2-yl)benzoate (2l)

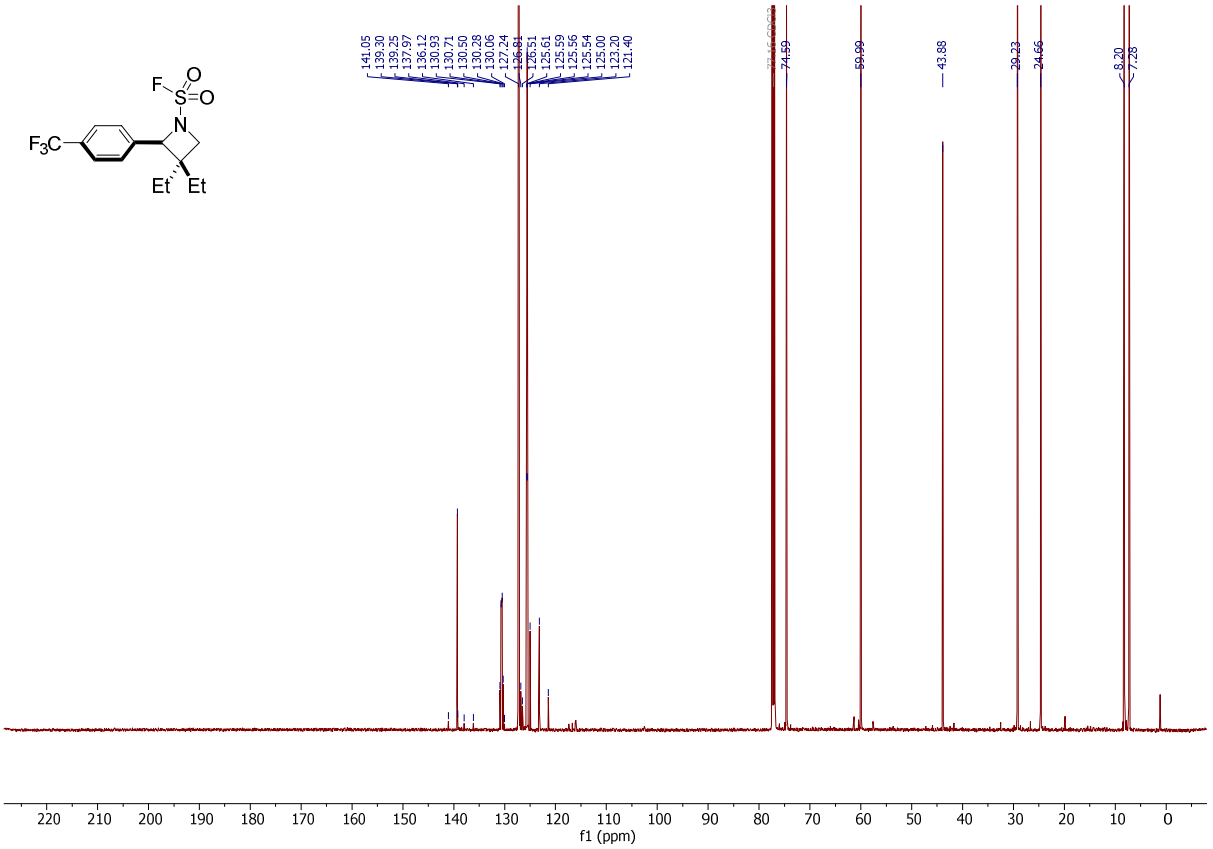


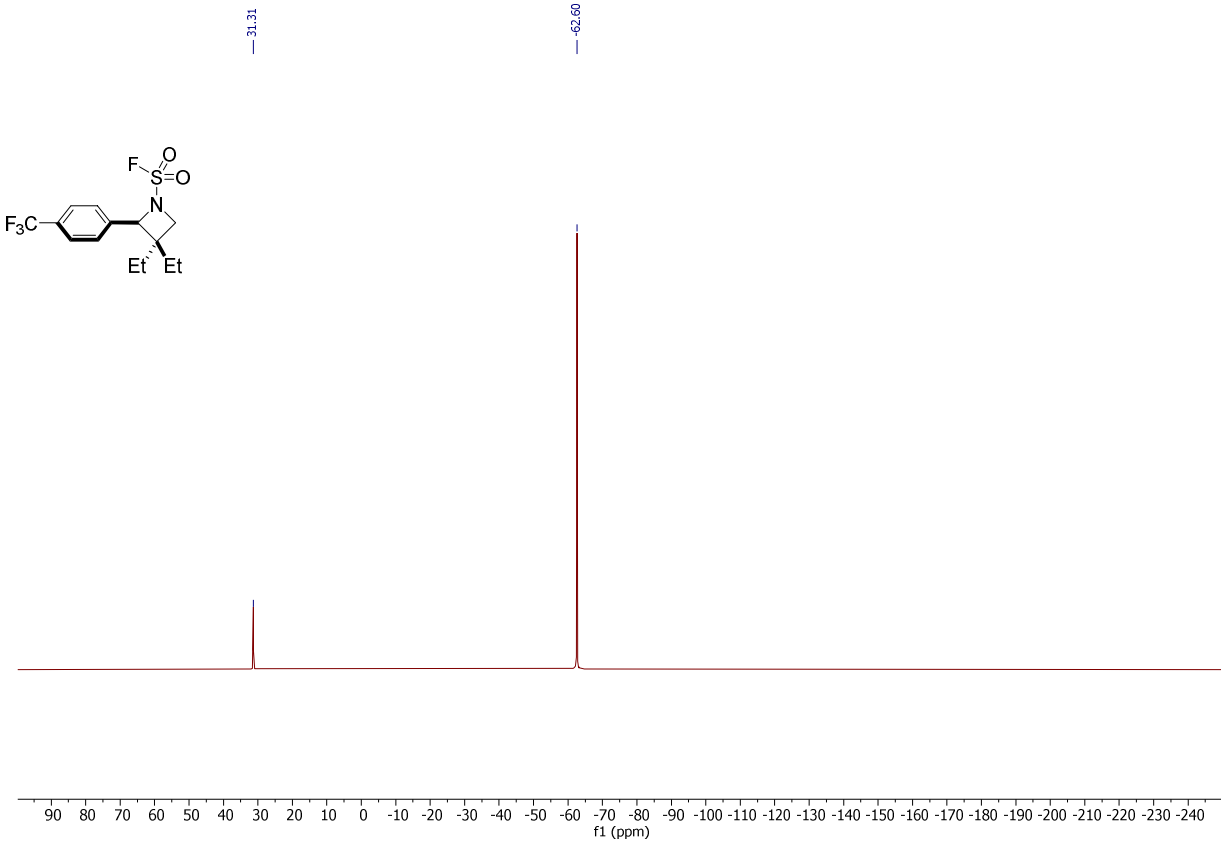

F
O
S=O
N
MeO2C
Et
Et
166.80
135.82
131.30
130.56
129.58
128.69
127.95
77.16 CDCl3
74.78
59.94
52.38
43.71
29.19
24.58
8.17
7.27
f1 (ppm)


31.20
F
O
S=O
N
MeO2C
Et
Et
f1 (ppm)

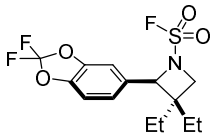
(*R**)-3,3-Diethyl-2-(4-(trifluoromethyl)phenyl)azetidine-1-sulfonyl fluoride (2m)

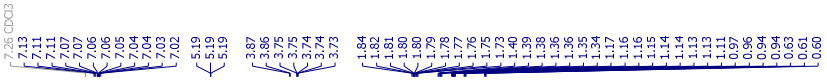


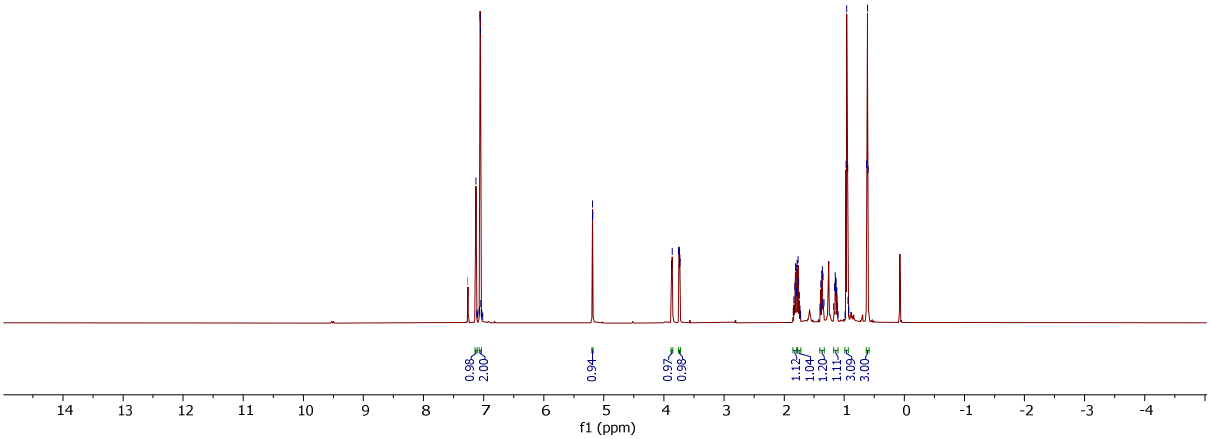

F
O
S=O
N
F3C
Et
Et
141.05
139.30
139.25
137.97
136.12
130.93
130.71
130.50
130.28
130.06
127.24
126.81
126.51
125.61
125.59
125.56
125.54
125.00
123.20
121.40
74.59
59.99
43.88
29.23
24.66
8.20
7.28
220 210 200 190 180 170 160 150 140 130 120 110 100 90 80 70 60 50 40 30 20 10 0
f1 (ppm)


31.31
-62.60
F
O
S=O
N
F3C
Et
Et
90 80 70 60 50 40 30 20 10 0 -10 -20 -30 -40 -50 -60 -70 -80 -90 -100 -110 -120 -130 -140 -150 -160 -170 -180 -190 -200 -210 -220 -230 -240
f1 (ppm)

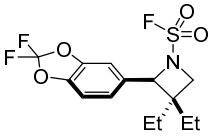
(*R**)-2-(2,2-Difluorobenzo[d][1,3]dioxol-5-yl)-3,3-diethylazetidine-1-sulfonyl fluoride (2p)

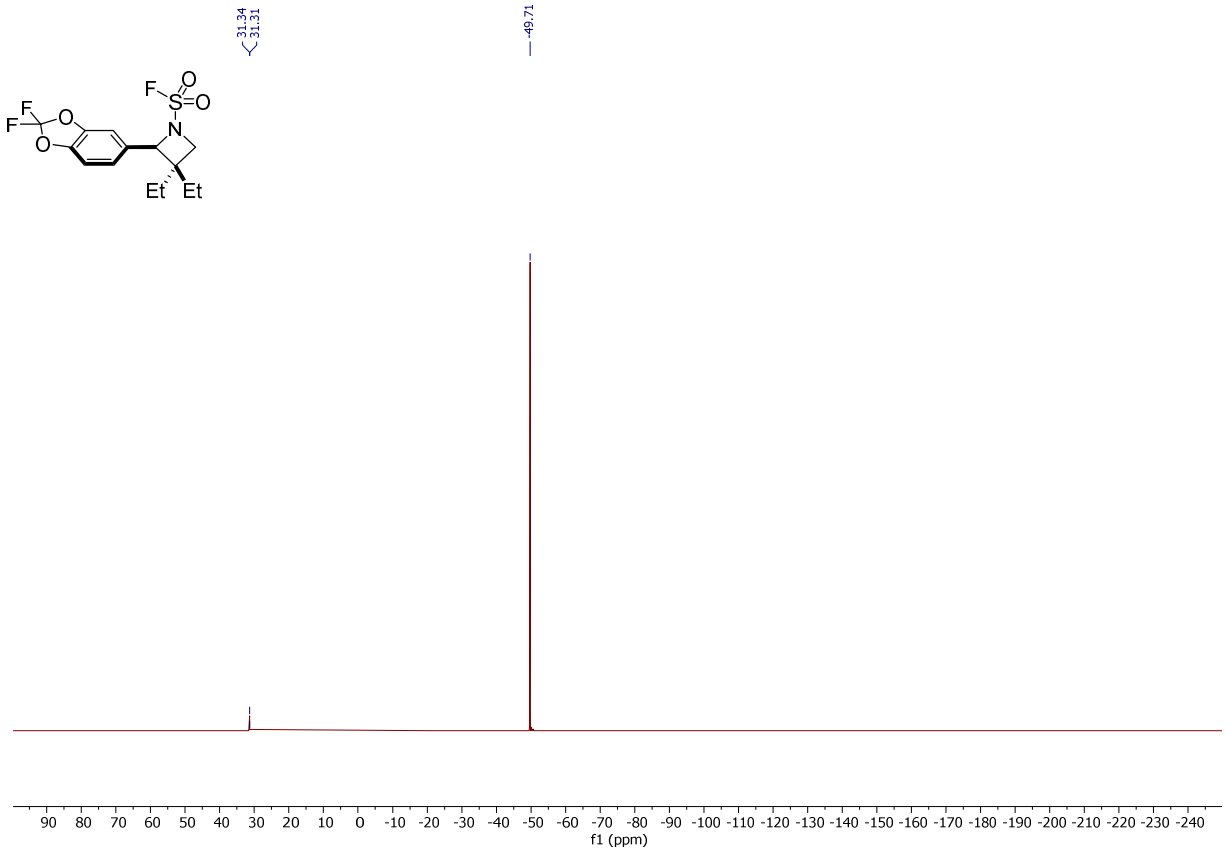




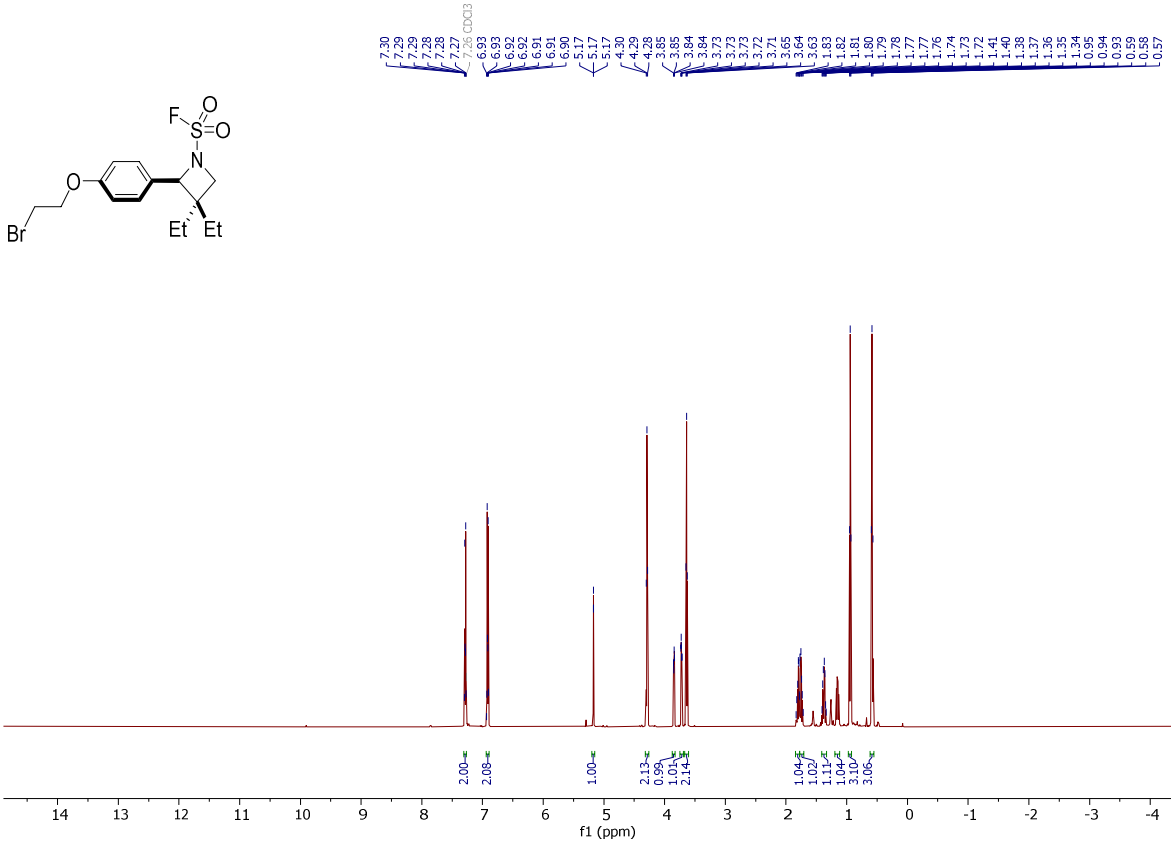


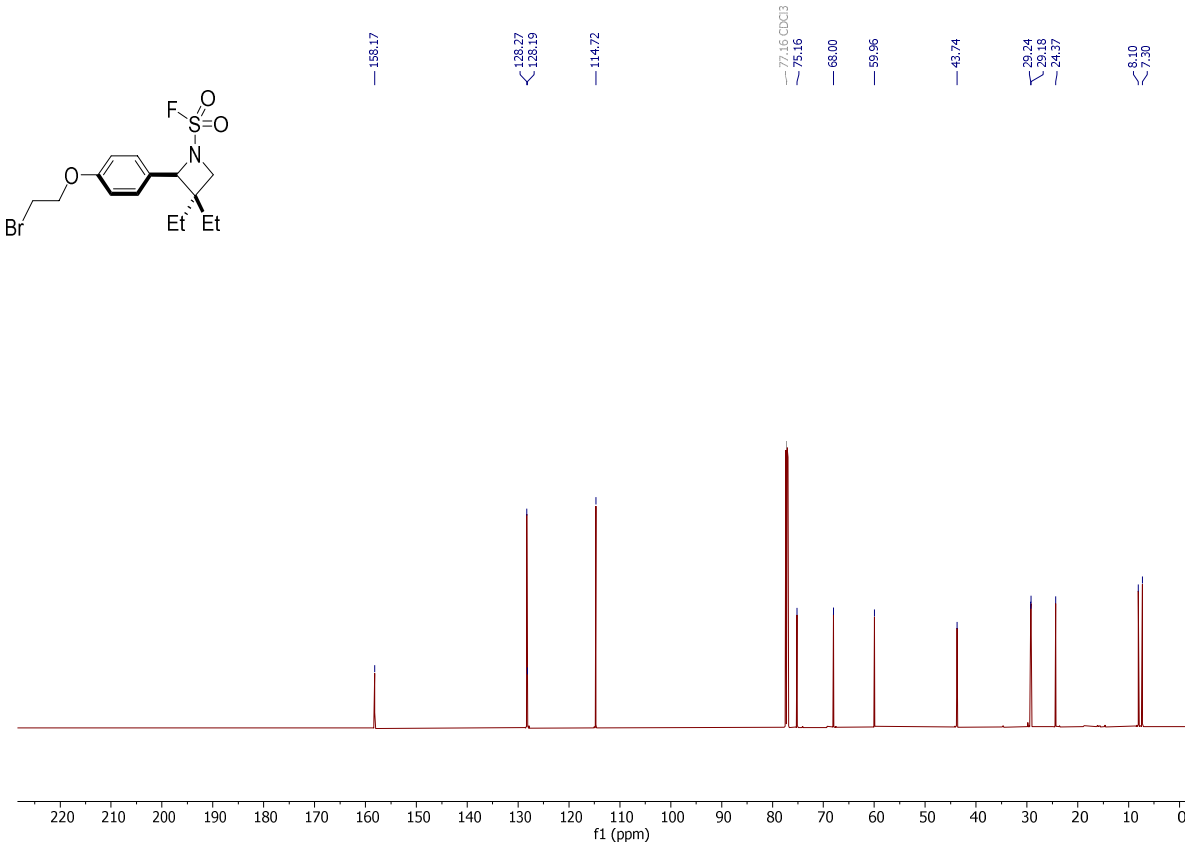


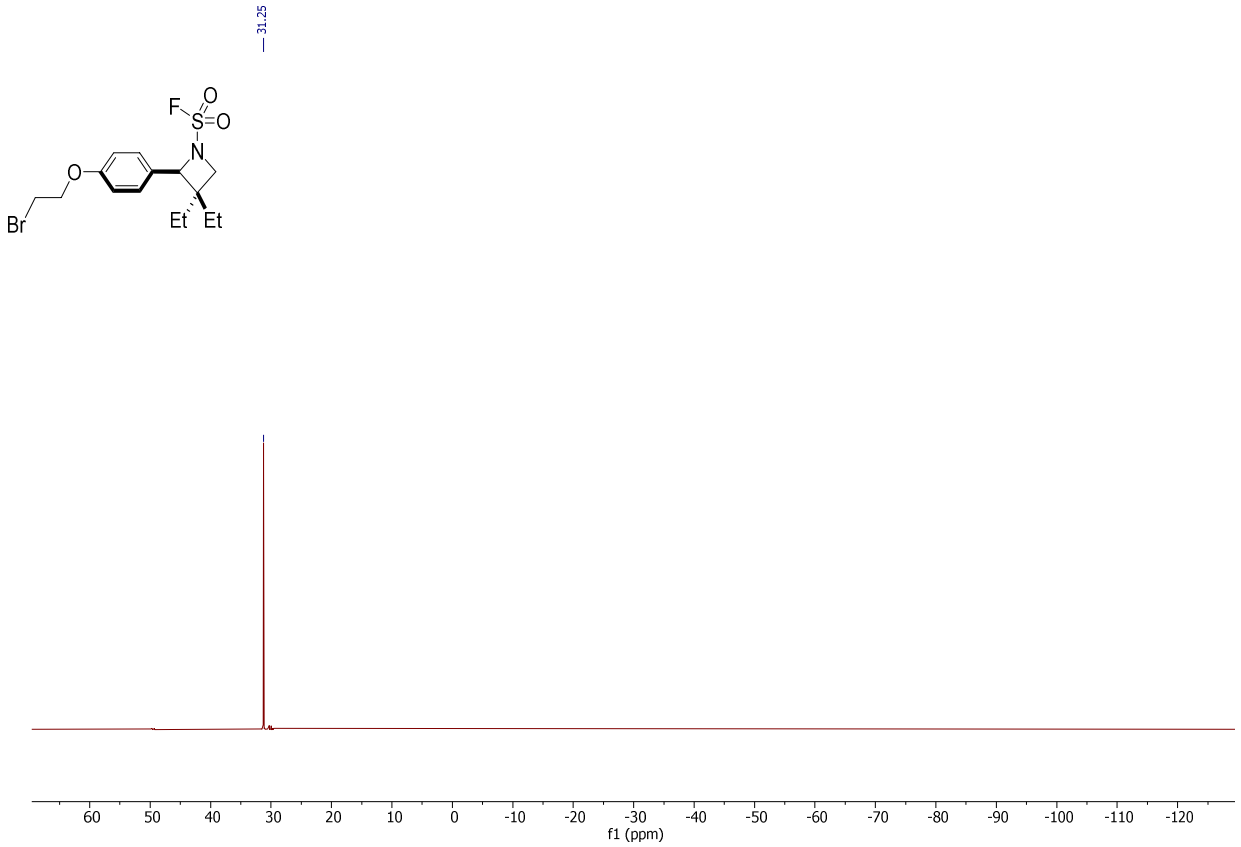



31.34
31.31
49.71
F
O
S
O
F
O
F
O
N
Et
Et
90 80 70 60 50 40 30 20 10 0 -10 -20 -30 -40 -50 -60 -70 -80 -90 -100 -110 -120 -130 -140 -150 -160 -170 -180 -190 -200 -210 -220 -230 -240
f1 (ppm)

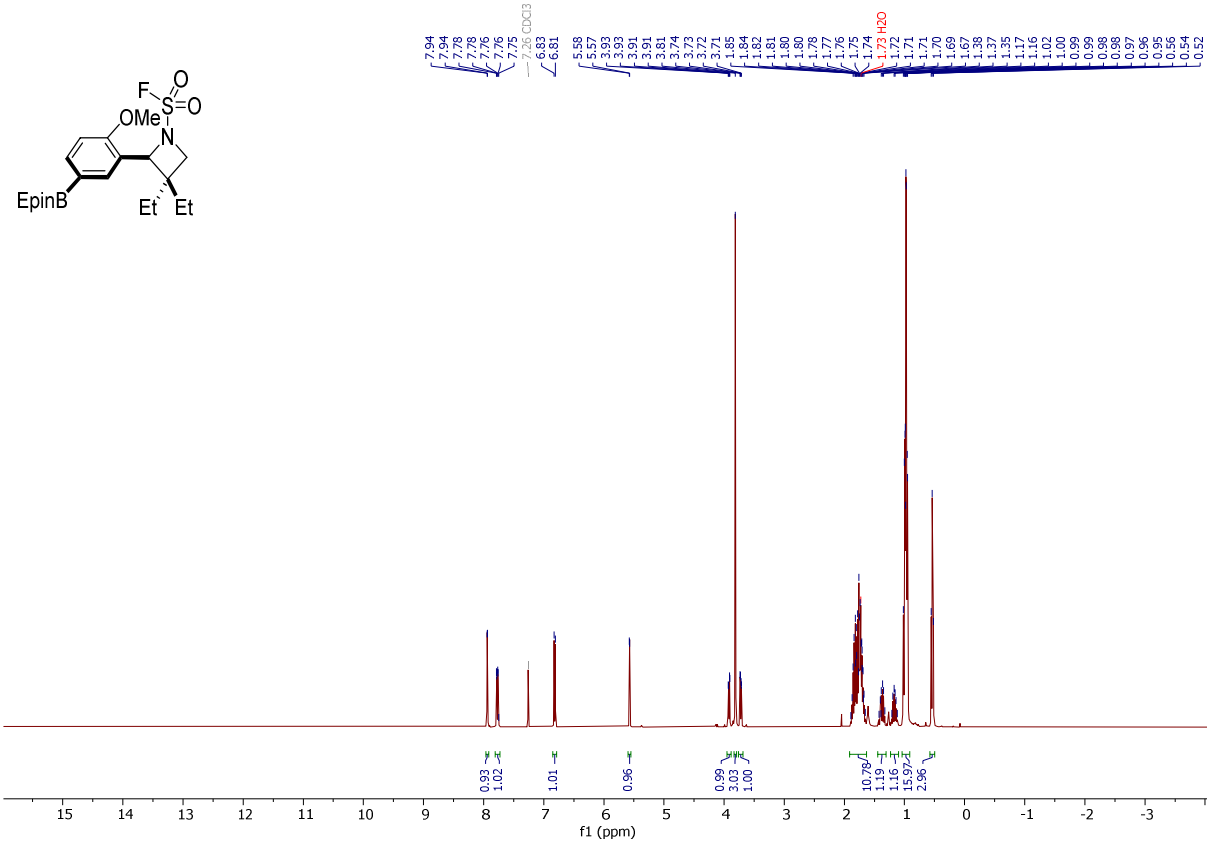
(*R**)-2-(4-(2-Bromoethoxy)phenyl)-3,3-diethylazetidine-1-sulfonyl fluoride (2q)

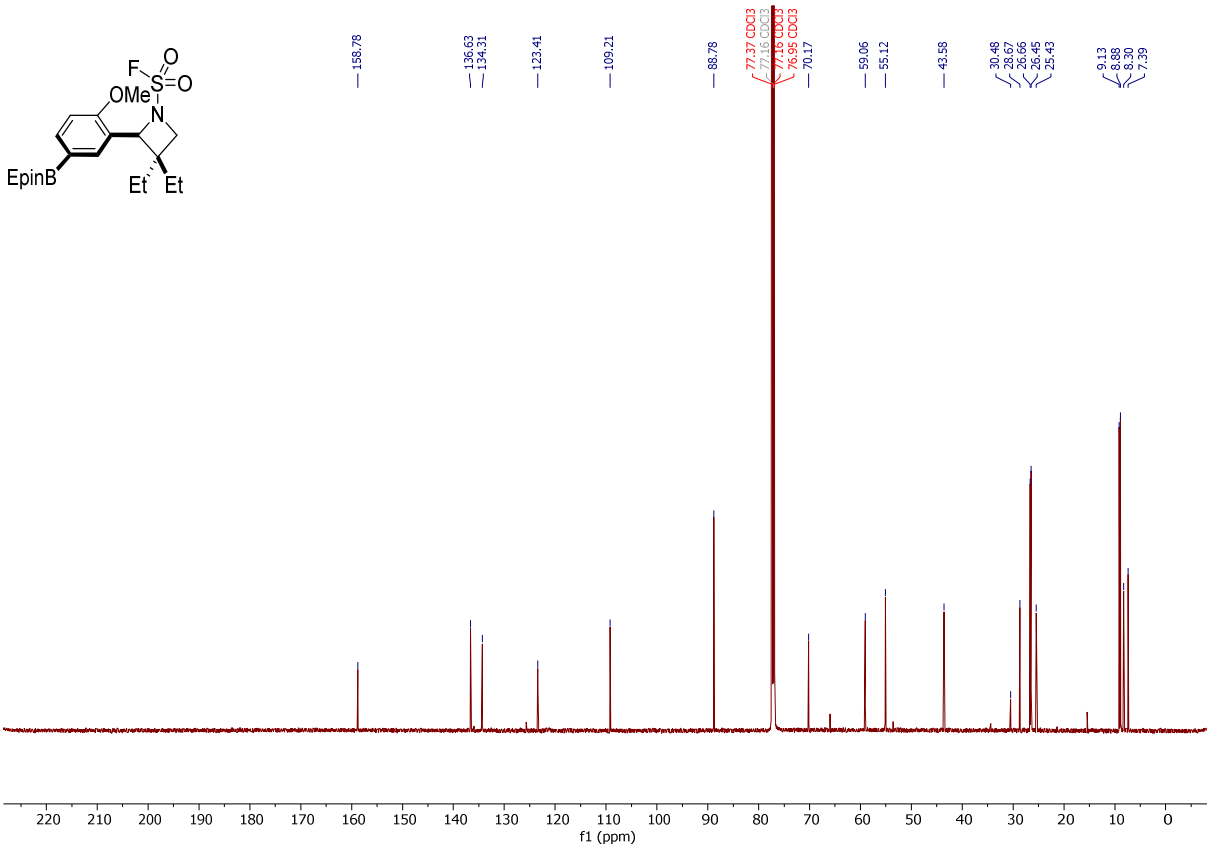


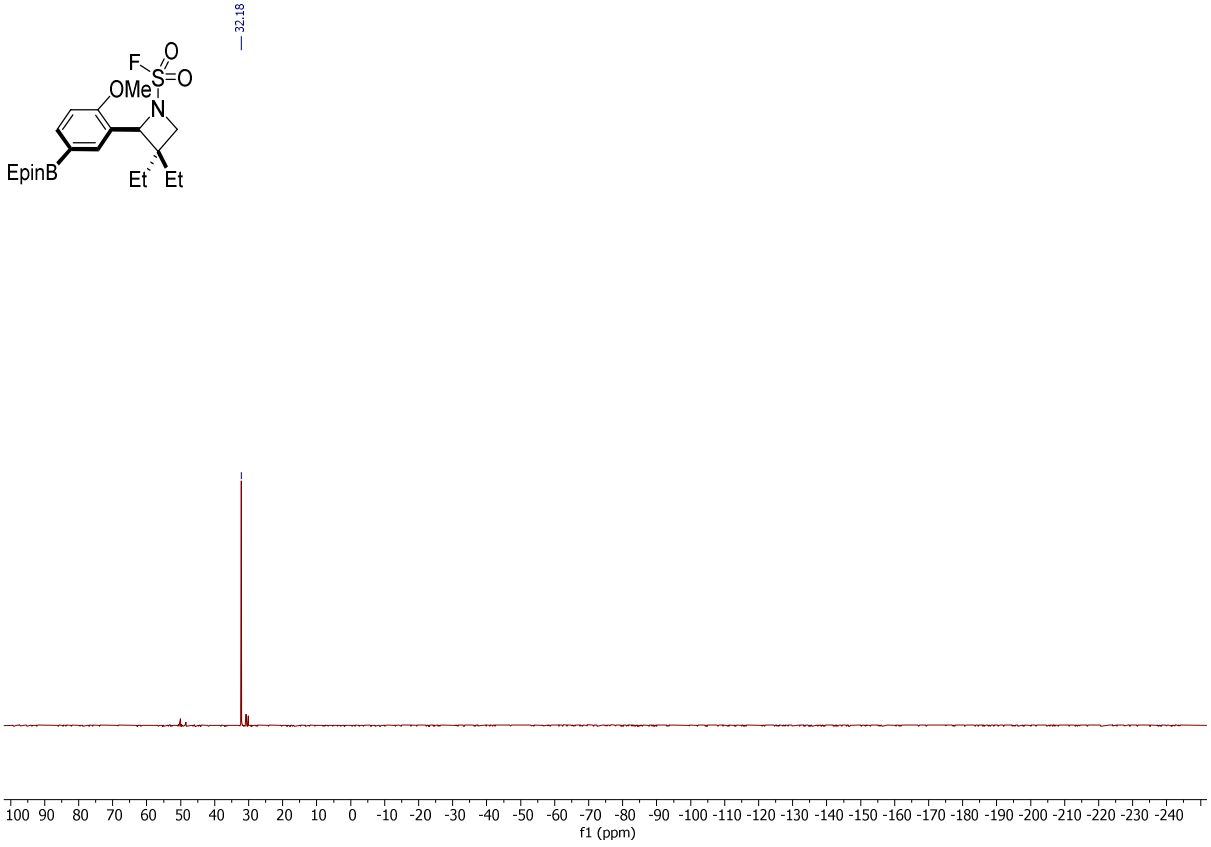



31.25
F
O
S
O
N
O
Br
Et
Et
60
50
40
30
20
10
0
-10
-20
-30
-40
-50
-60
-70
-80
-90
-100
-110
-120
f1 (ppm)

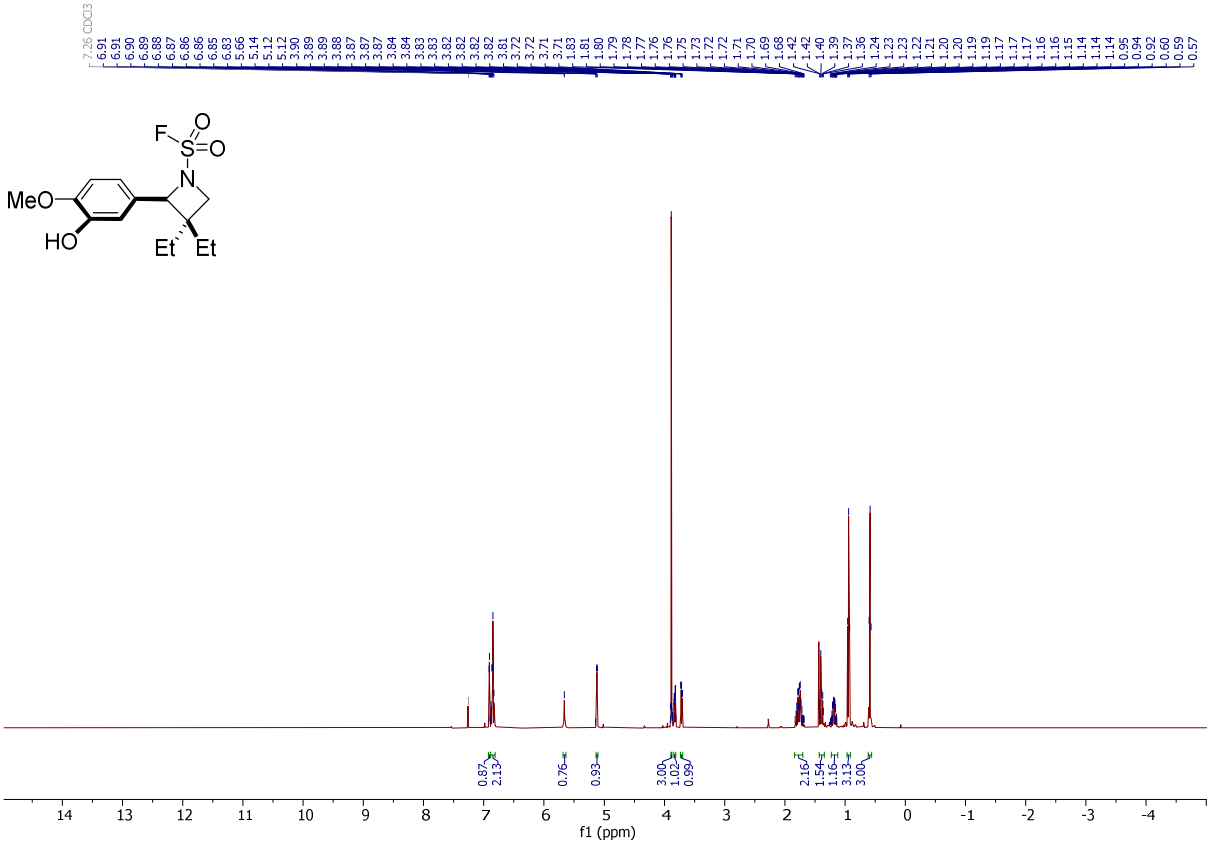
(*S**)-3,3-Diethyl-2-(2-methoxy-5-(4,4,5,5-tetraethyl-1,3,2-dioxaborolan-2-yl)phenyl)azetidine-1-sulfonyl fluoride (2r)

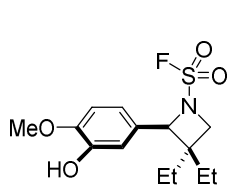






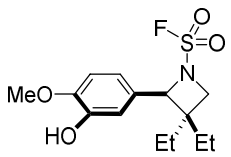
(*R**)-3,3-Diethyl-2-(3-hydroxy-4-methoxyphenyl)azetidine-1-sulfonyl fluoride (2s')

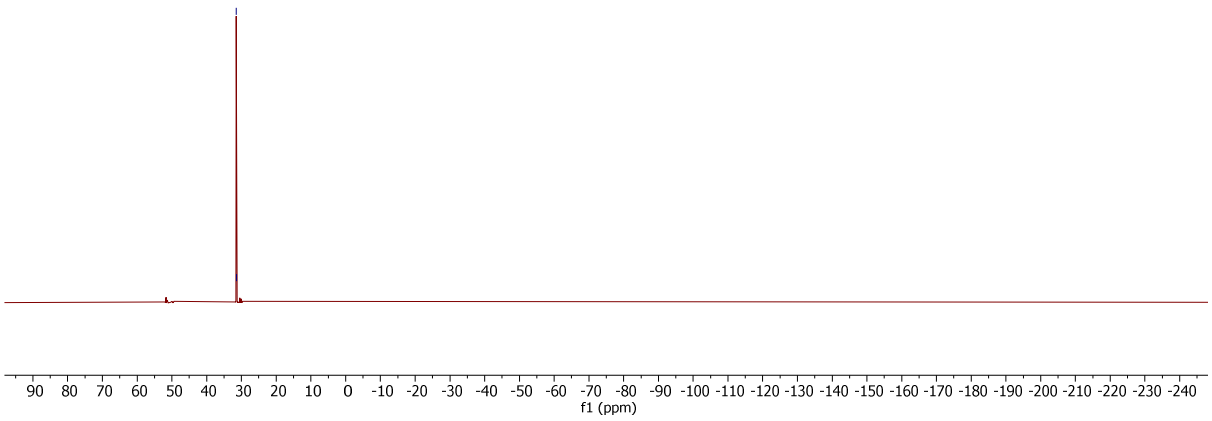



F
O
S
O
N
MeO
HO
Et
Et

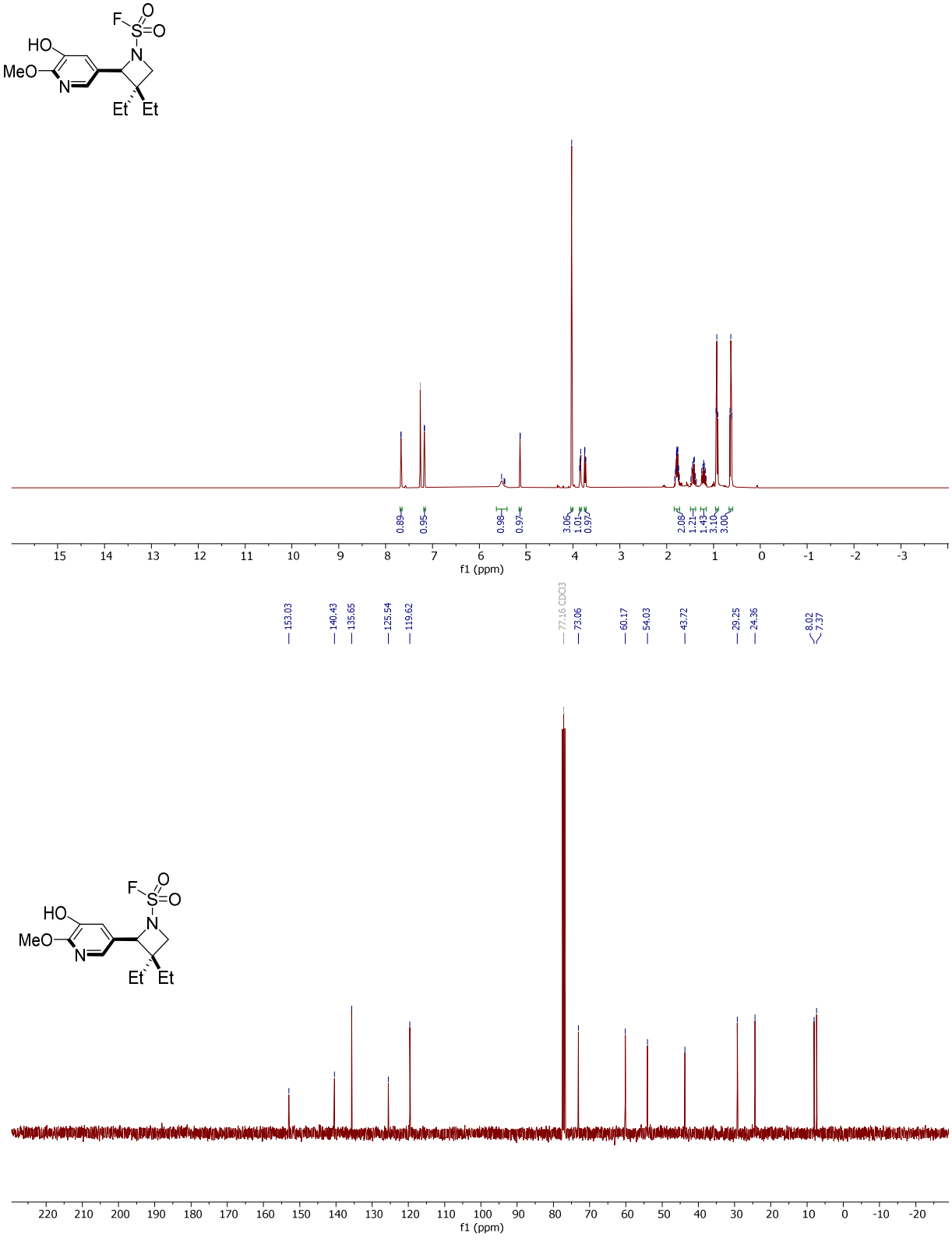
146.56
145.63
128.50
118.71
113.21
110.47
77.16 CDCl3
75.17
59.98
56.05
43.68
29.24
24.23
8.10
7.31
210 200 190 180 170 160 150 140 130 120 110 100 90 80 70 60 50 40 30 20 10 0 -10
f1 (ppm)

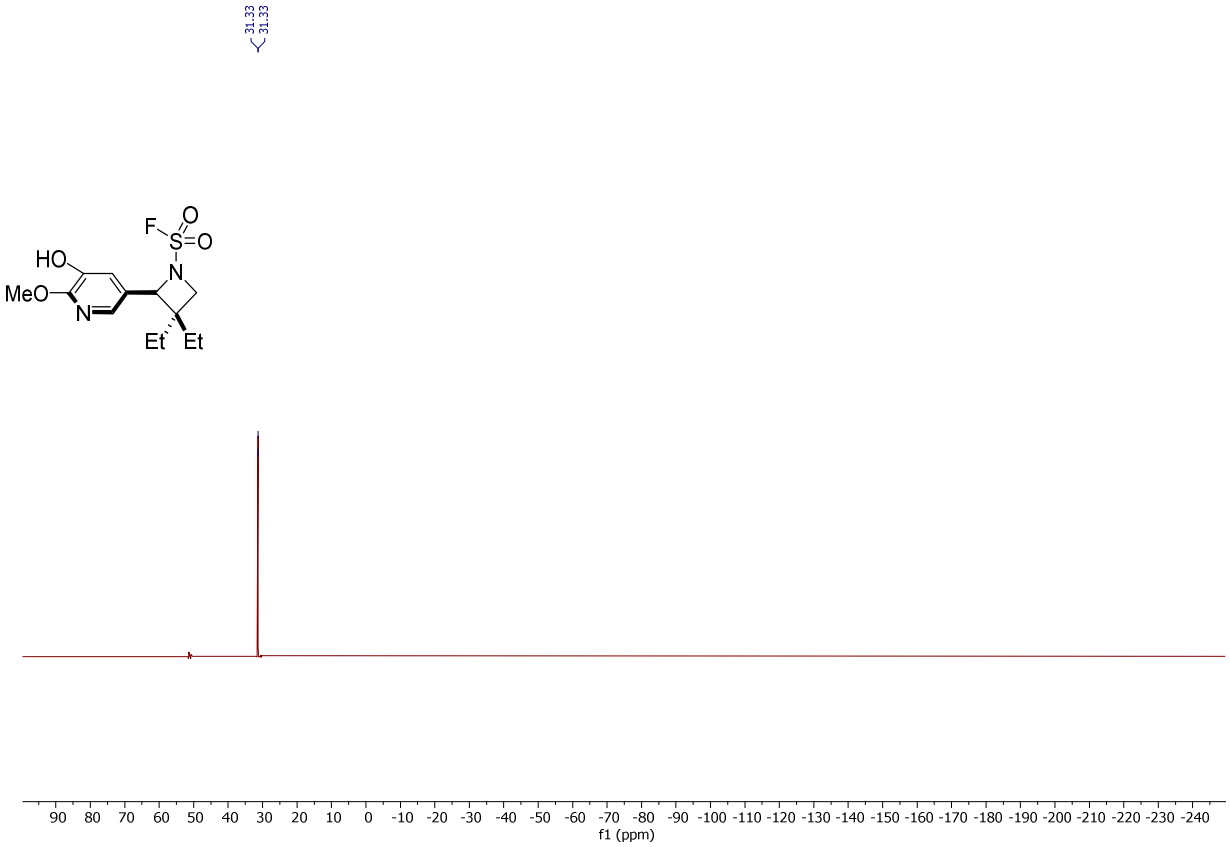

31.47
31.43


F
O
S
O
N
MeO
HO
Et
Et

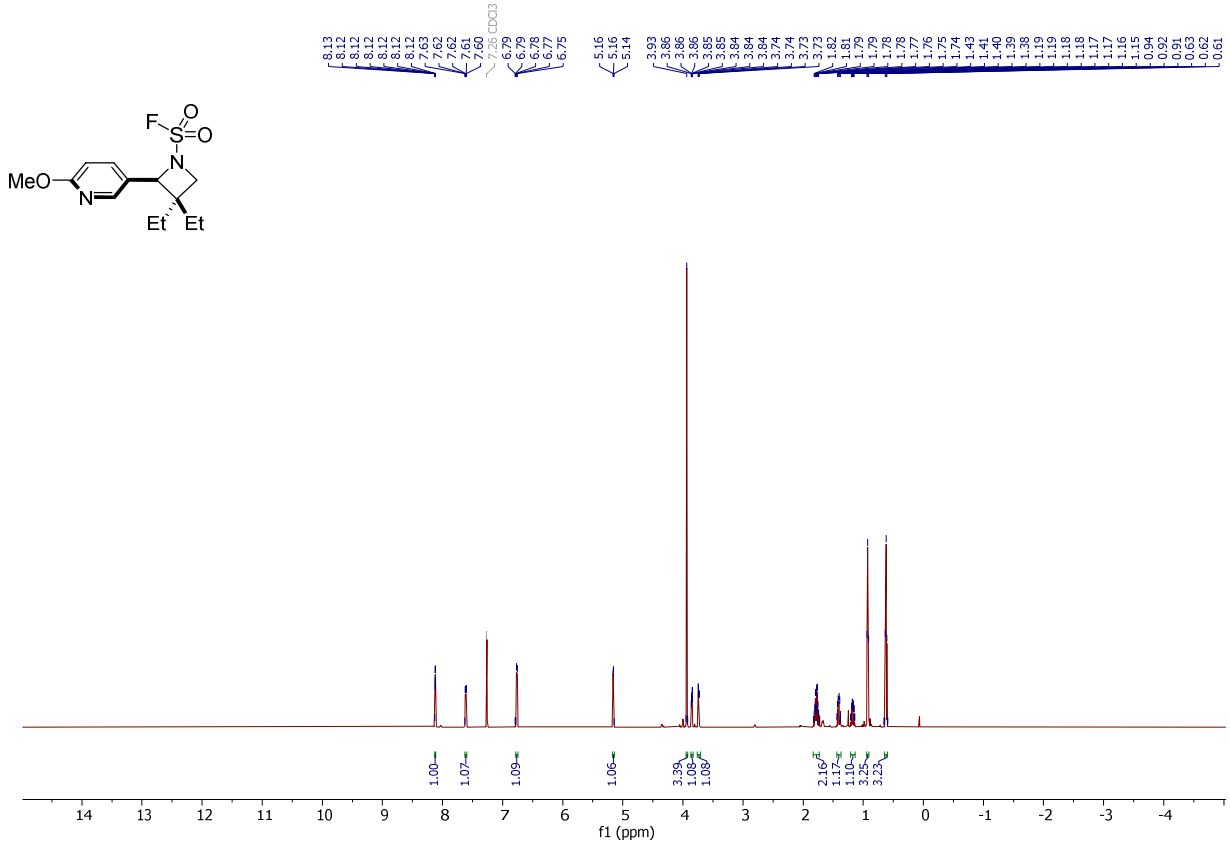

90 80 70 60 50 40 30 20 10 0 -10 -20 -30 -40 -50 -60 -70 -80 -90 -100 -110 -120 -130 -140 -150 -160 -170 -180 -190 -200 -210 -220 -230 -240
f1 (ppm)

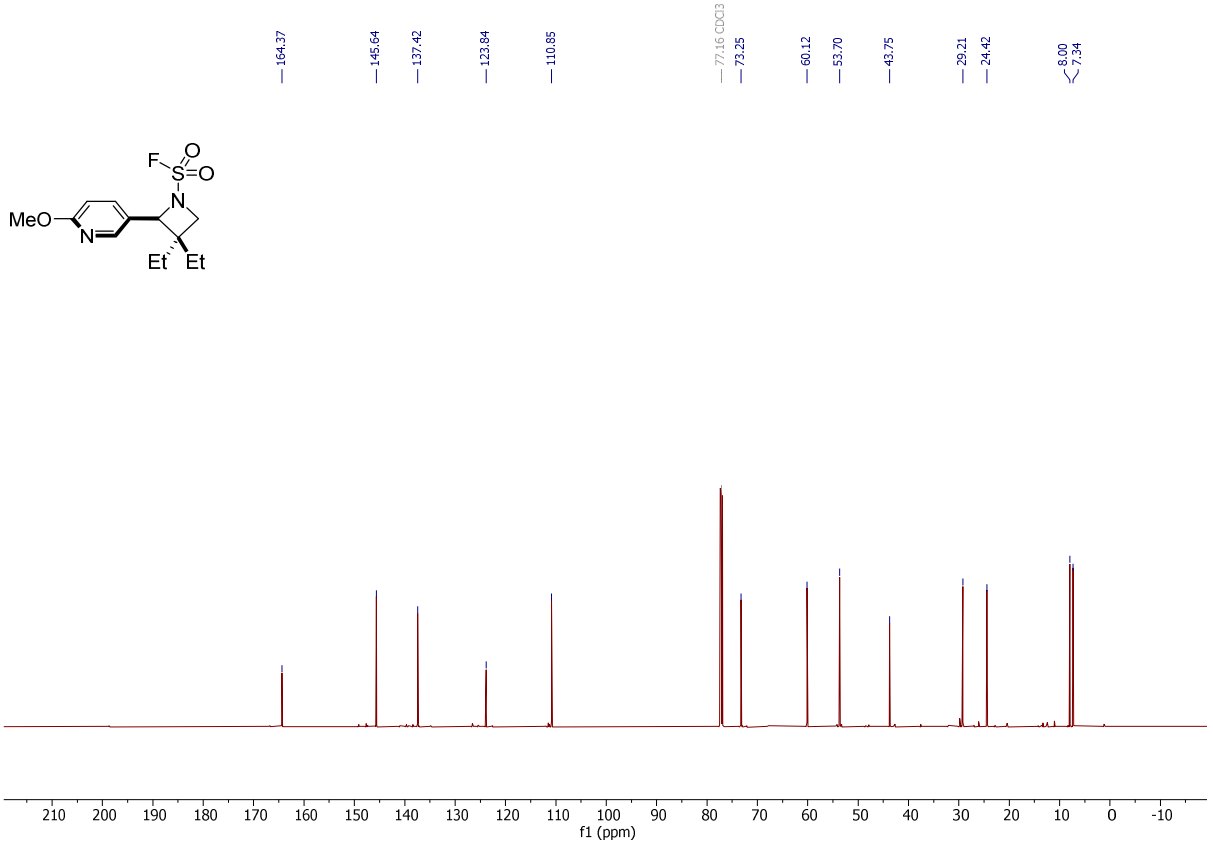
(*S**)-3,3-diethyl-2-(5-hydroxy-6-methoxypyridin-3-yl)azetidine-1-sulfonyl fluoride (2t')

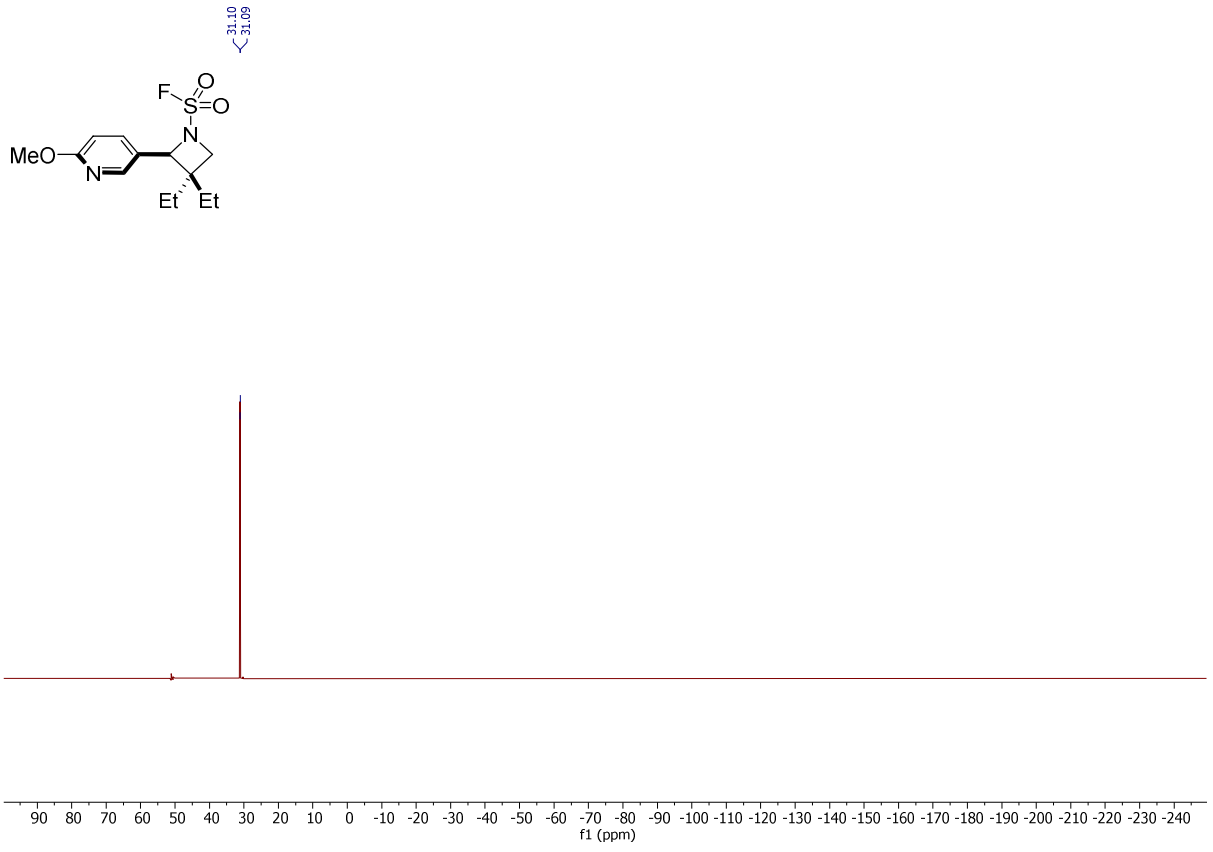




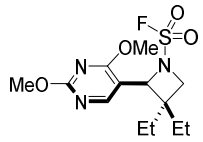
(*S**)-3,3-Diethyl-2-(6-methoxypyridin-3-yl)azetidine-1-sulfonyl fluoride (2u)

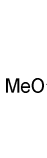


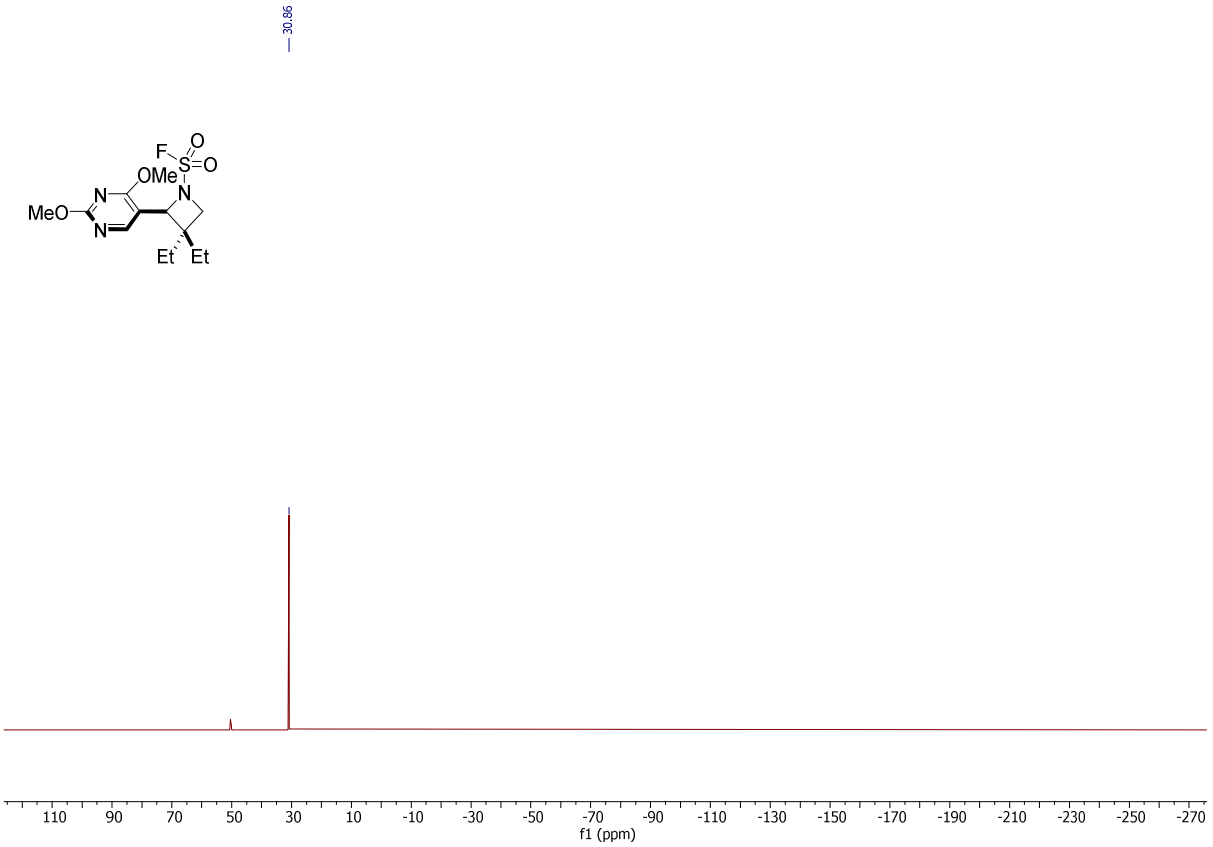

164.37
145.64
137.42
123.84
110.85
77.16 CDCl3
73.25
60.12
53.70
43.75
29.21
24.42
8.00
7.34
F
O
S
O
N
MeO
N
Et
Et
210 200 190 180 170 160 150 140 130 120 110 100 90 80 70 60 50 40 30 20 10 0 -10
f1 (ppm)


31.10
31.09
F
O
S
O
N
MeO
N
Et
Et
90 80 70 60 50 40 30 20 10 0 -10 -20 -30 -40 -50 -60 -70 -80 -90 -100 -110 -120 -130 -140 -150 -160 -170 -180 -190 -200 -210 -220 -230 -240
f1 (ppm)

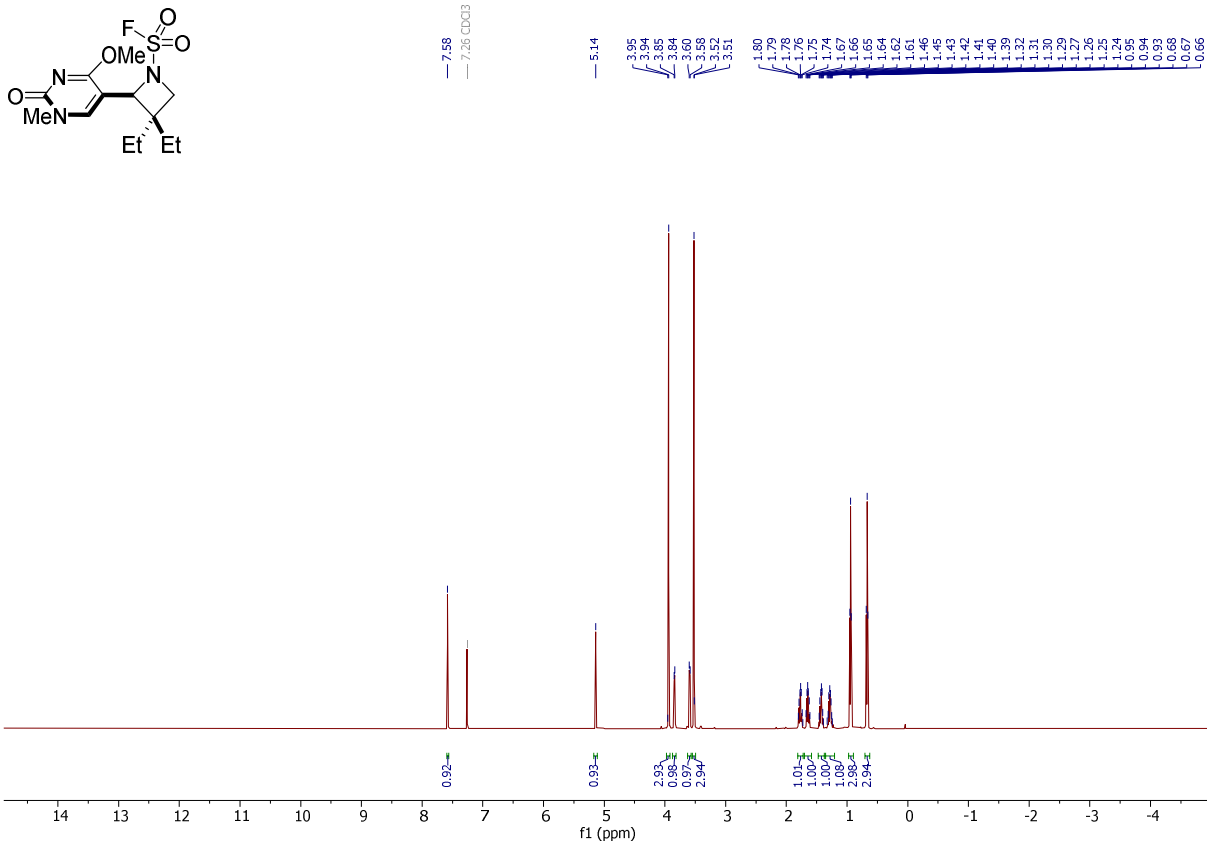
(*S**)-2-(2,4-Dimethoxypyrimidin-5-yl)-3,3-diethylazetidine-1-sulfonyl fluoride (2v)

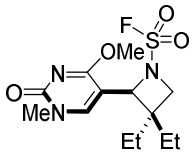




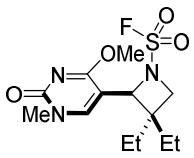


(*S**)-3,3-Diethyl-2-(2-methoxy-1-methyl-4-oxo-1,4-dihydropyrimidin-5-yl)azetidine-1-sulfonyl fluoride (2w)



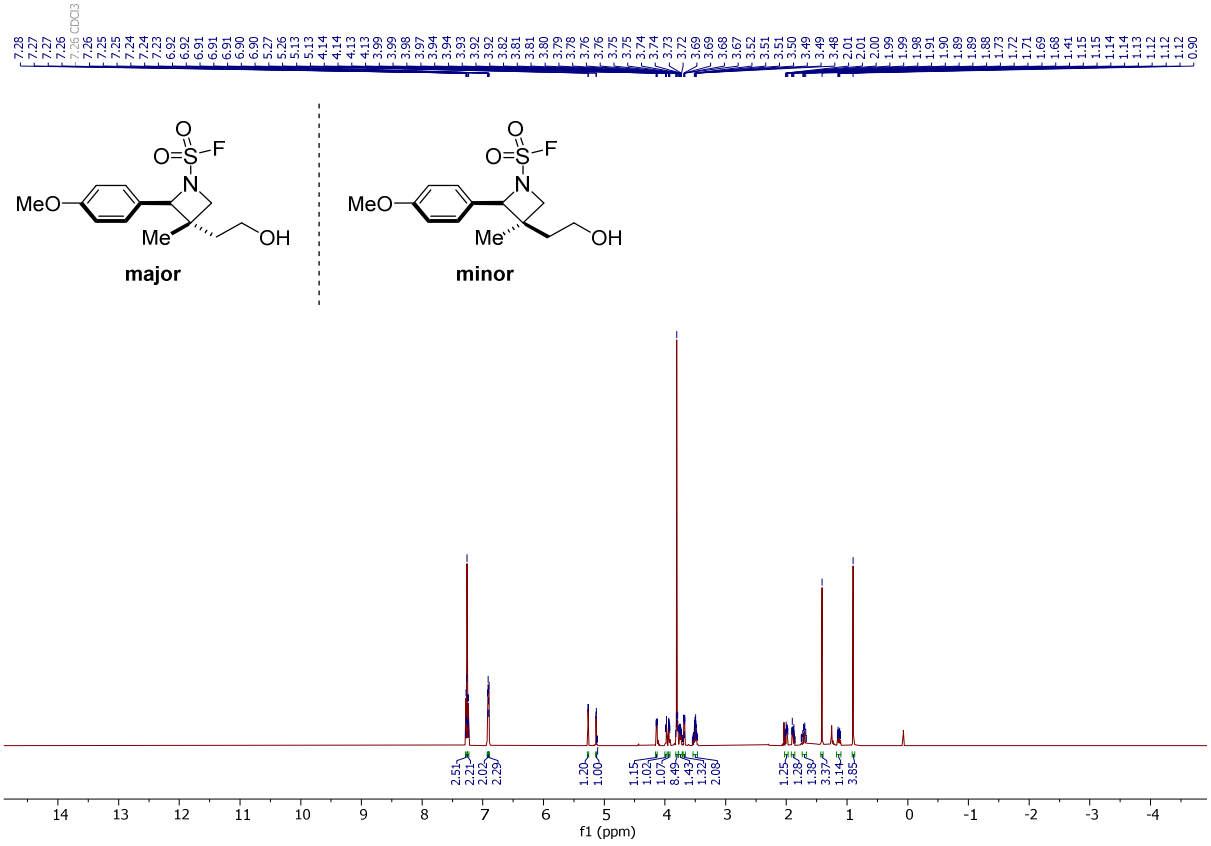

F
O
S
O
OMe
N
N
O
MeN
Et
Et

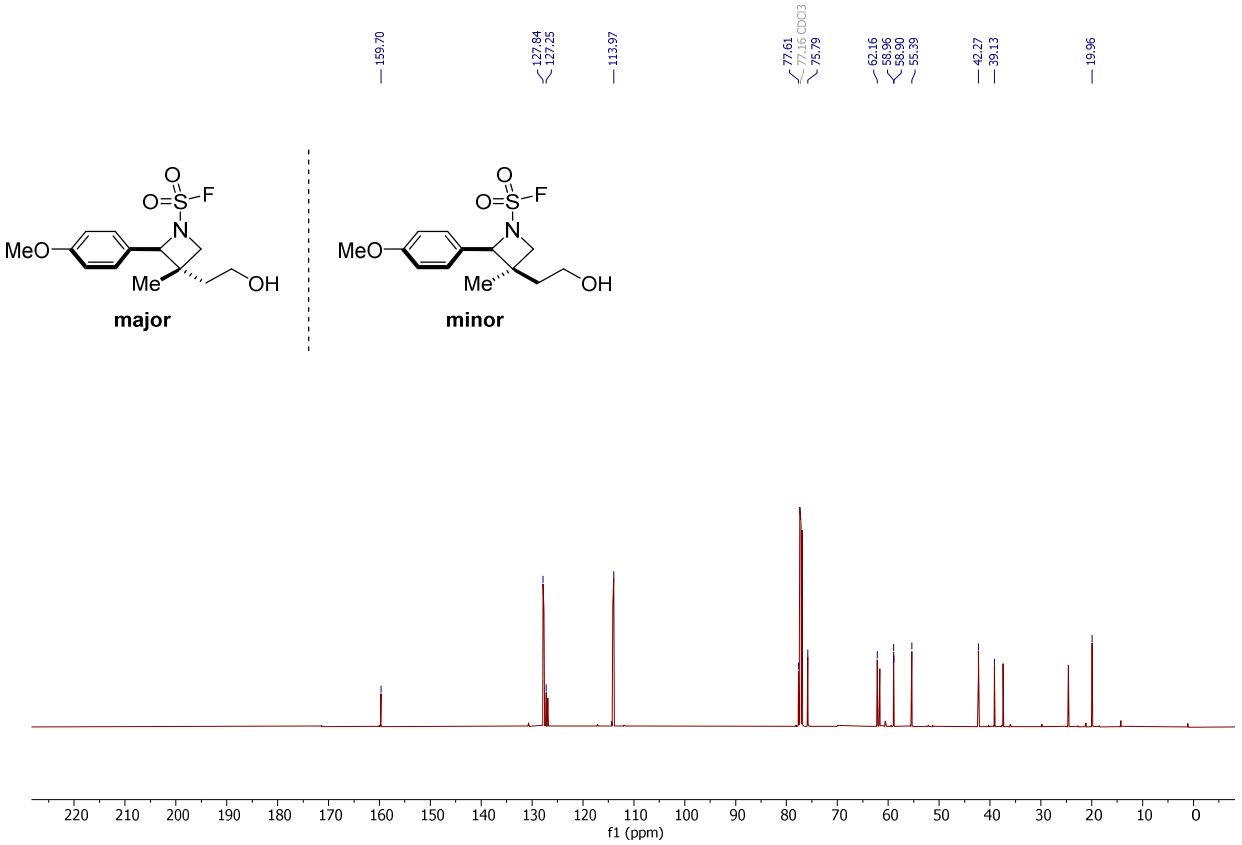
168.61
156.62
146.16
103.19
77.37 CDCl3
77.16 CDCl3
77.16 CDCl3
76.95 CDCl3
67.38
59.07
54.65
43.75
43.62
38.45
29.76
28.39
25.47
25.36
25.23
8.07
7.47
1.09
220 210 200 190 180 170 160 150 140 130 120 110 100 90 80 70 60 50 40 30 20 10 0
f1 (ppm)

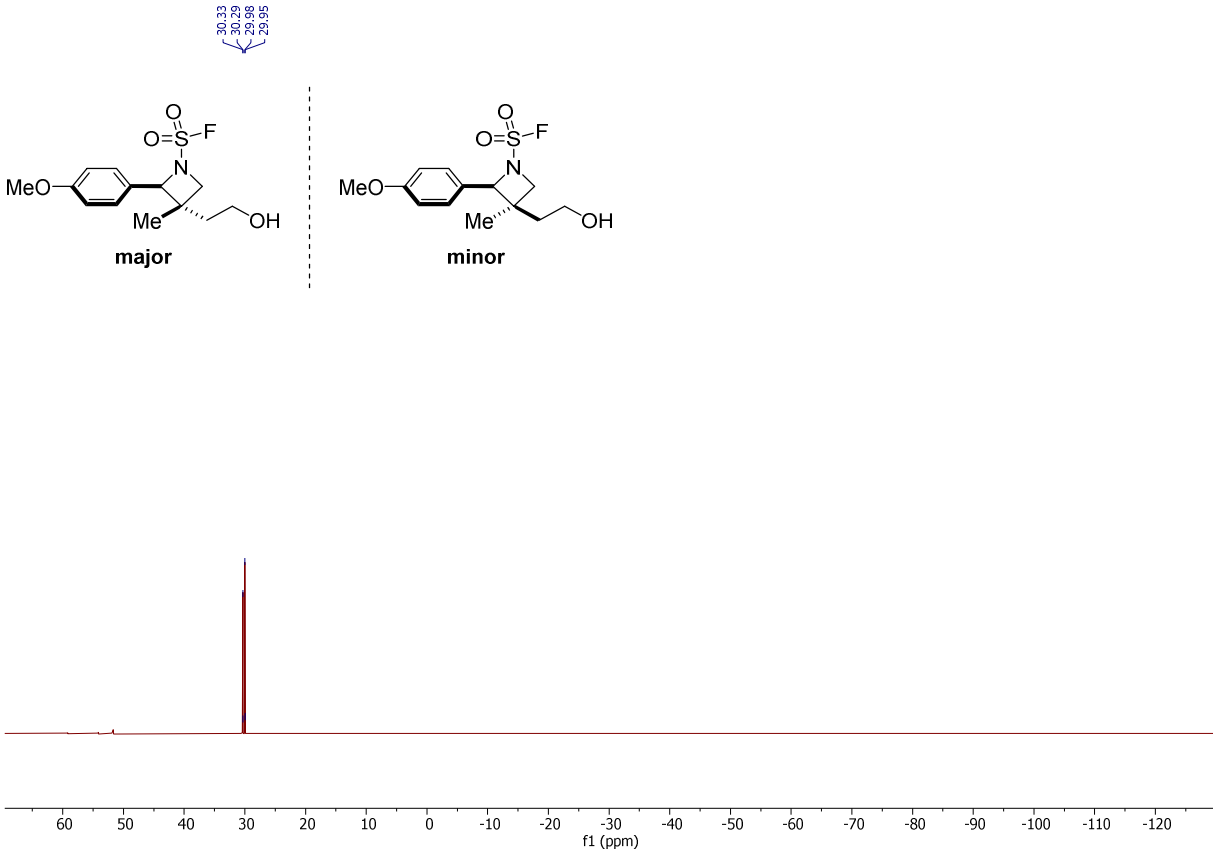

F
O
S
O
OMe
N
N
O
MeN
Et
Et

30.27
30.23
100 90 80 70 60 50 40 30 20 10 0 -10 -20 -30 -40 -50 -60 -70 -80 -90 -100 -110 -120 -130 -140 -150 -160 -170 -180 -190 -200 -210 -220 -230 -240
f1 (ppm)

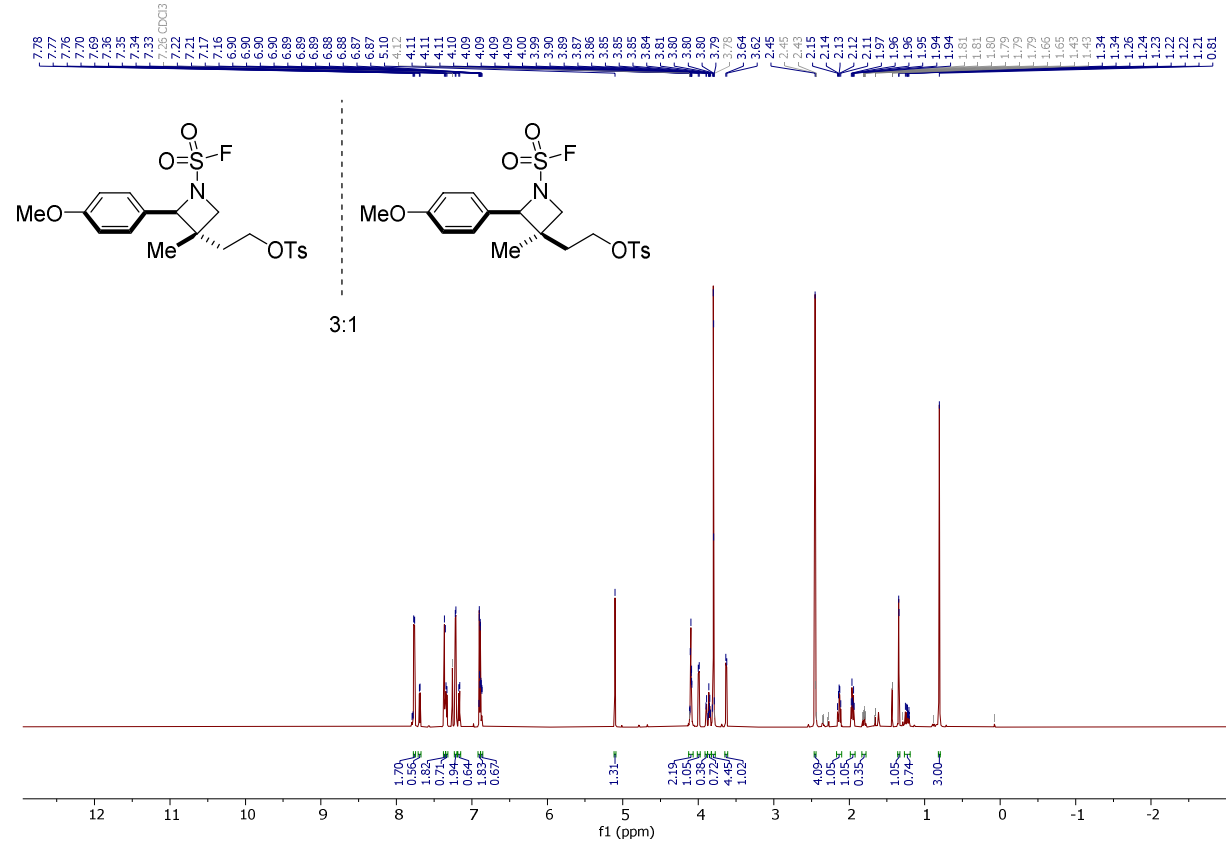
(2*R**,3*S**)-3-(2-Hydroxyethyl)-2-(4-methoxyphenyl)-3-methylazetidine-1-sulfonyl fluoride (4a) and (2*R**,3*S**)-3-(2-Hydroxyethyl)-2-(4-methoxyphenyl)-3-methylazetidine-1-sulfonyl fluoride (4a')

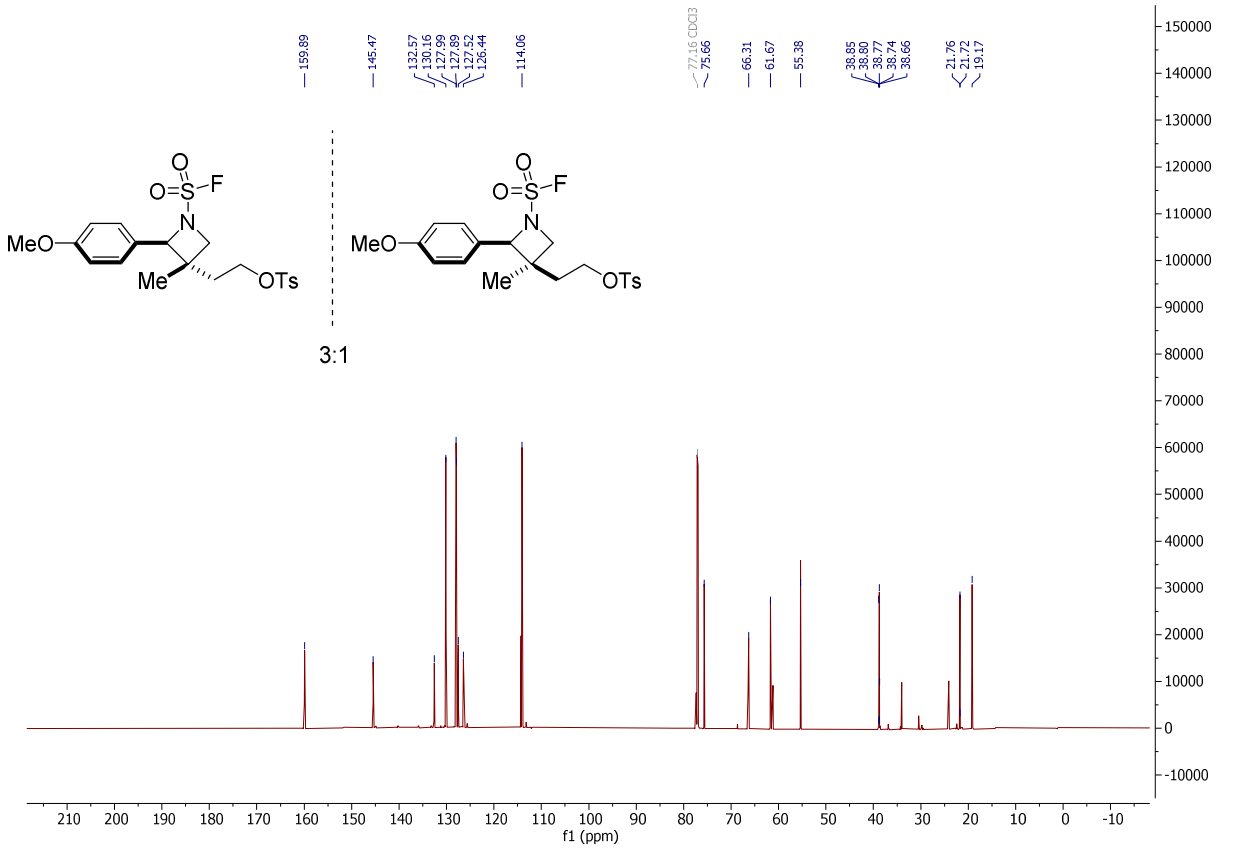


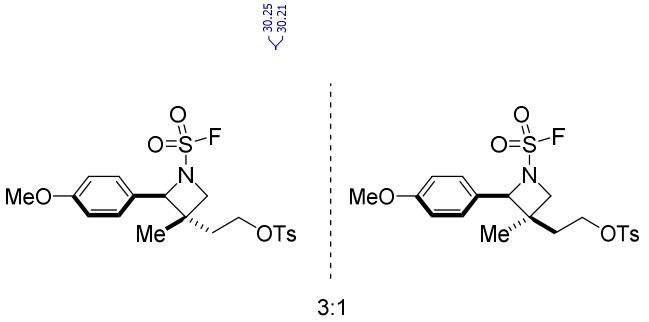

159.70
127.84
127.25
113.97
77.61
77.16
CDCl3
75.79
62.16
58.96
58.90
55.39
42.27
39.13
19.96
MeO
Me
OH
major
minor
f1 (ppm)

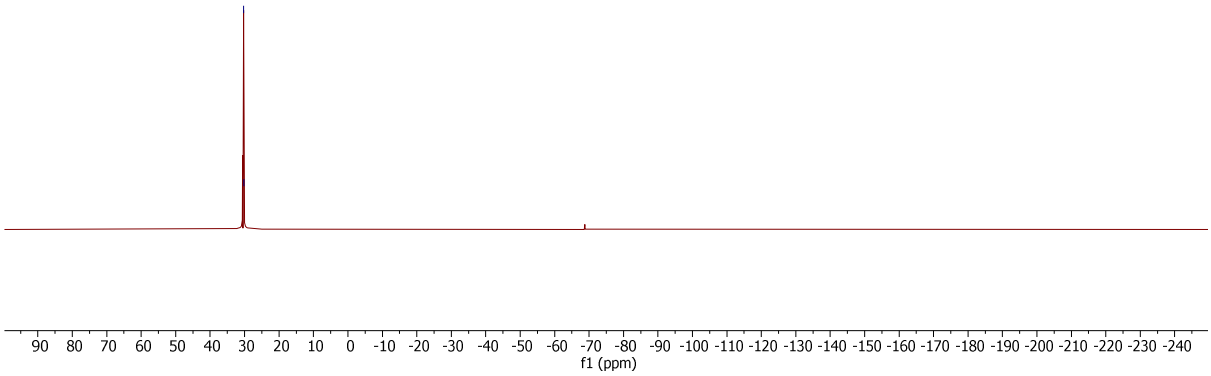

30.33
30.29
29.98
29.95
MeO
Me
OH
major
minor
f1 (ppm)

2-((2*R**,3*S**)-1-(Fluorosulfonyl)-2-(4-methoxyphenyl)-3-methylazetidin-3-yl)ethyl 4-methylbenzenesulfonate (4b)

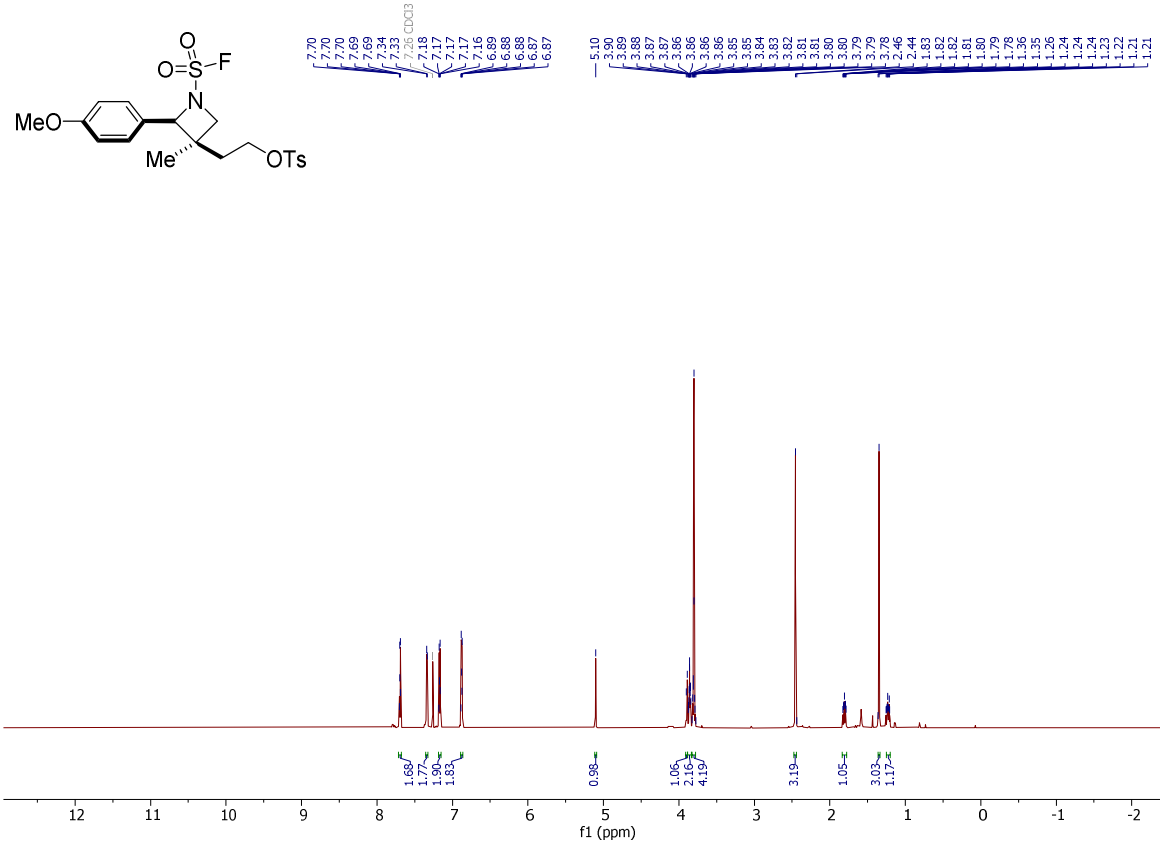


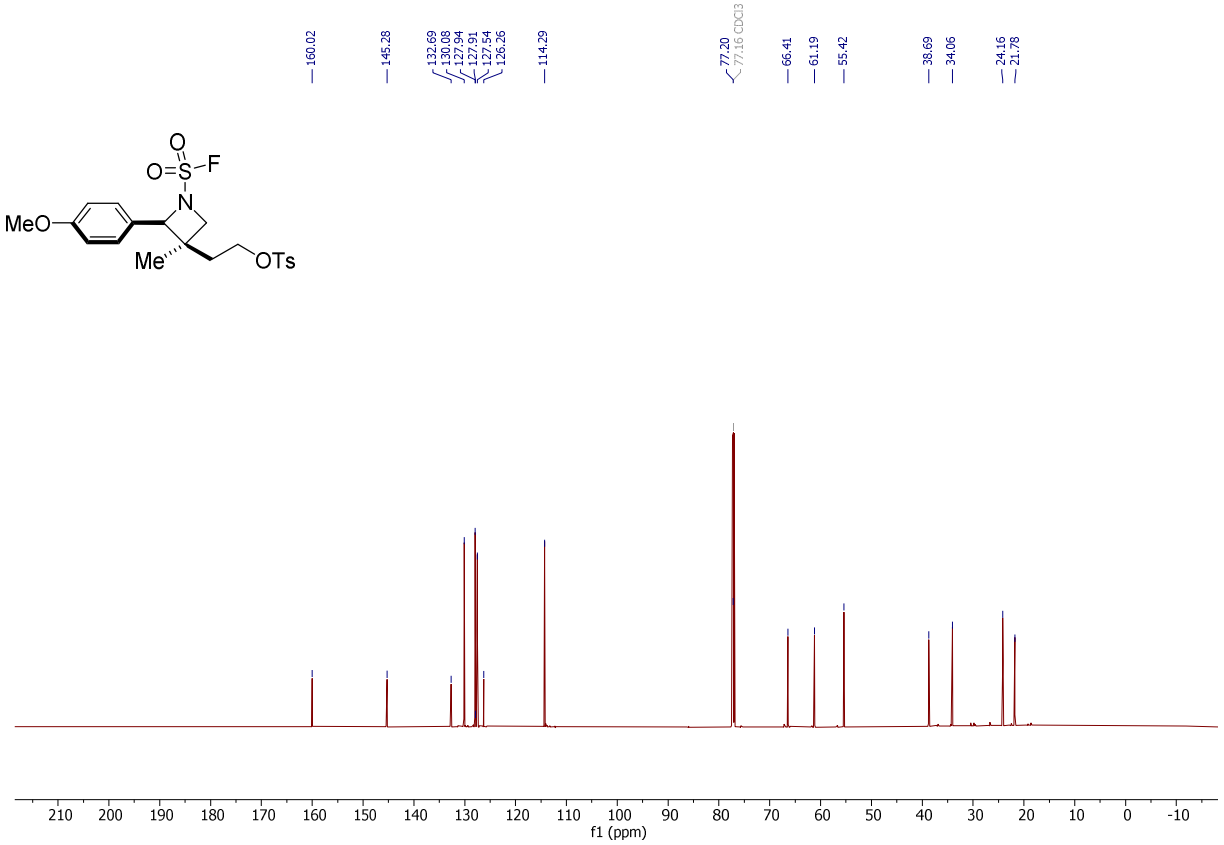


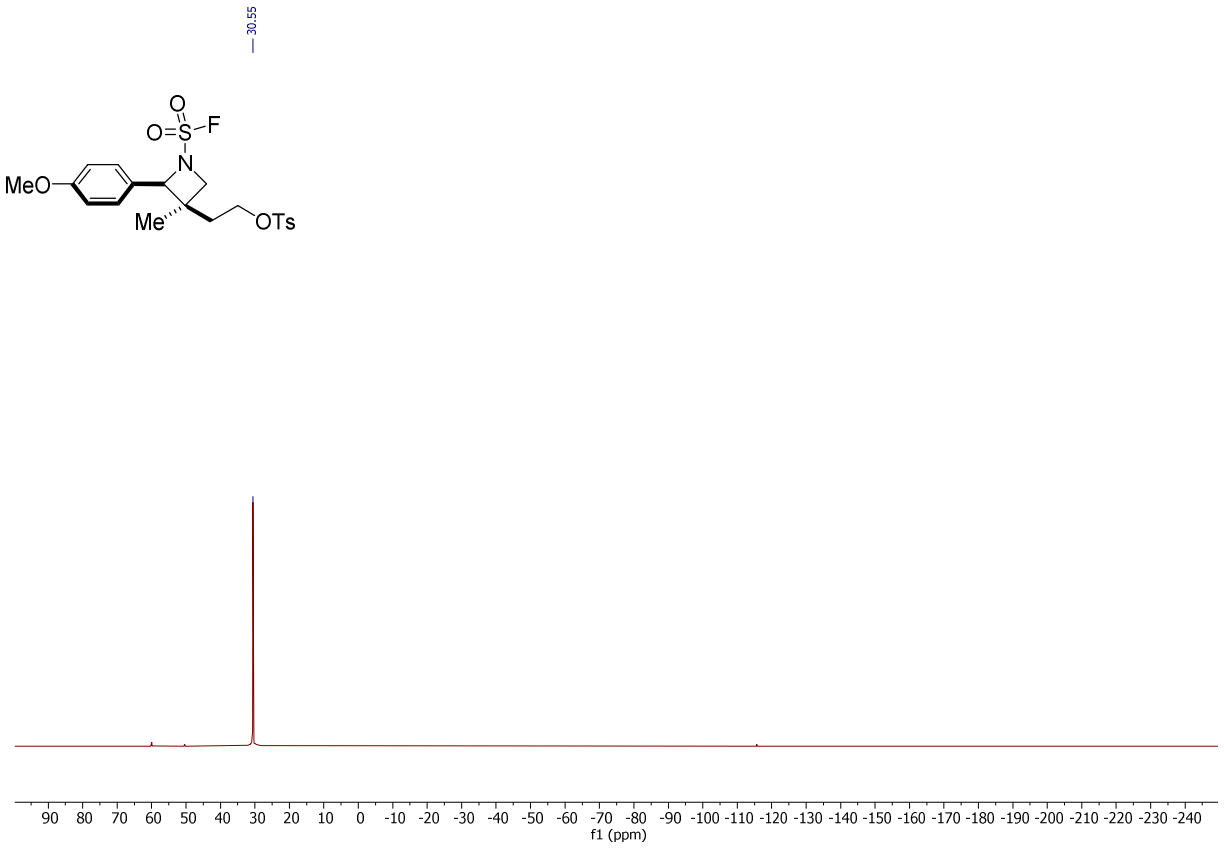




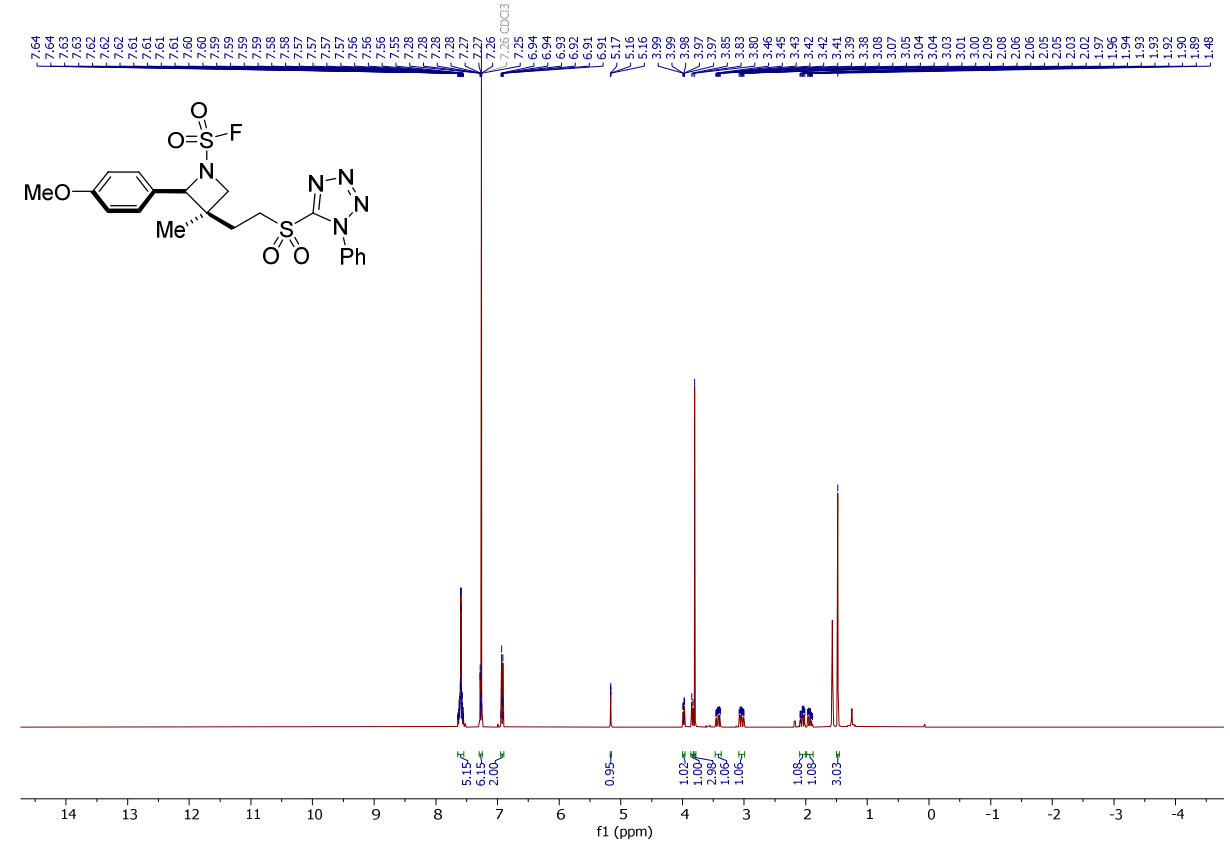
2-((2*R**,3*R**)-1-(Fluorosulfonyl)-2-(4-methoxyphenyl)-3-methylazetidin-3-yl)ethyl 4-methylbenzenesulfonate (4b')

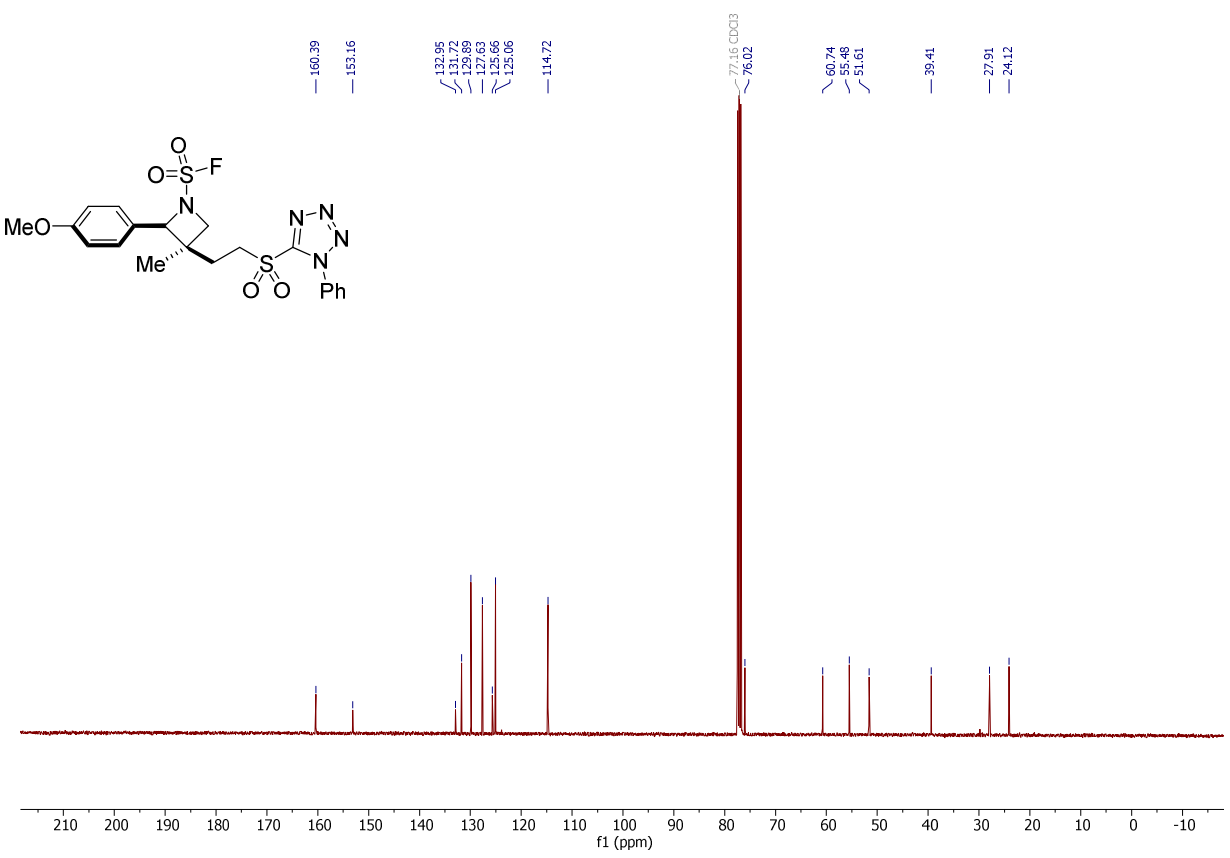


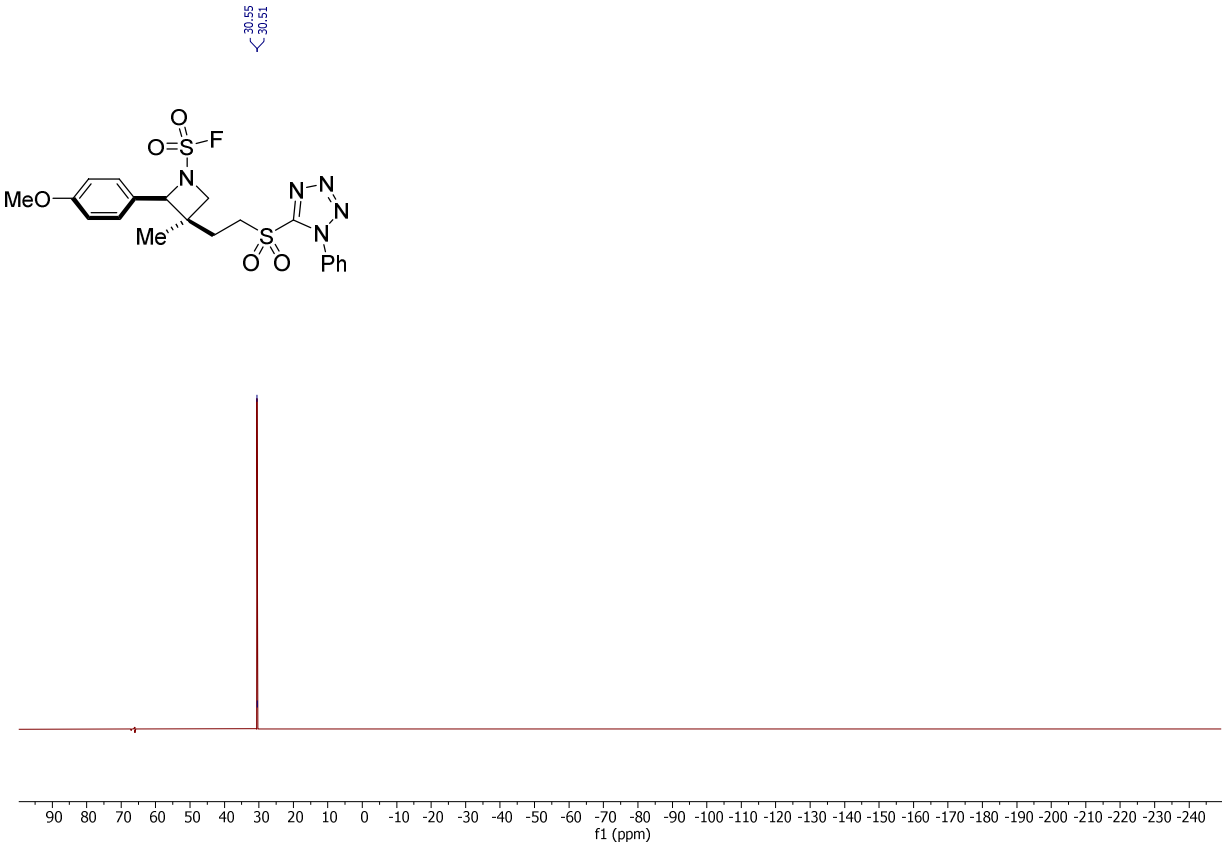

160.02
145.28
132.69
130.08
127.94
127.91
127.54
126.26
114.29
77.20
77.16 CDCl3
66.41
61.19
55.42
38.69
34.06
24.16
21.78
O
O=S–F
N
MeO
Me
OTs
210 200 190 180 170 160 150 140 130 120 110 100 90 80 70 60 50 40 30 20 10 0 -10
f1 (ppm)


30.55
O
O=S–F
N
MeO
Me
OTs
90 80 70 60 50 40 30 20 10 0 -10 -20 -30 -40 -50 -60 -70 -80 -90 -100 -110 -120 -130 -140 -150 -160 -170 -180 -190 -200 -210 -220 -230 -240
f1 (ppm)

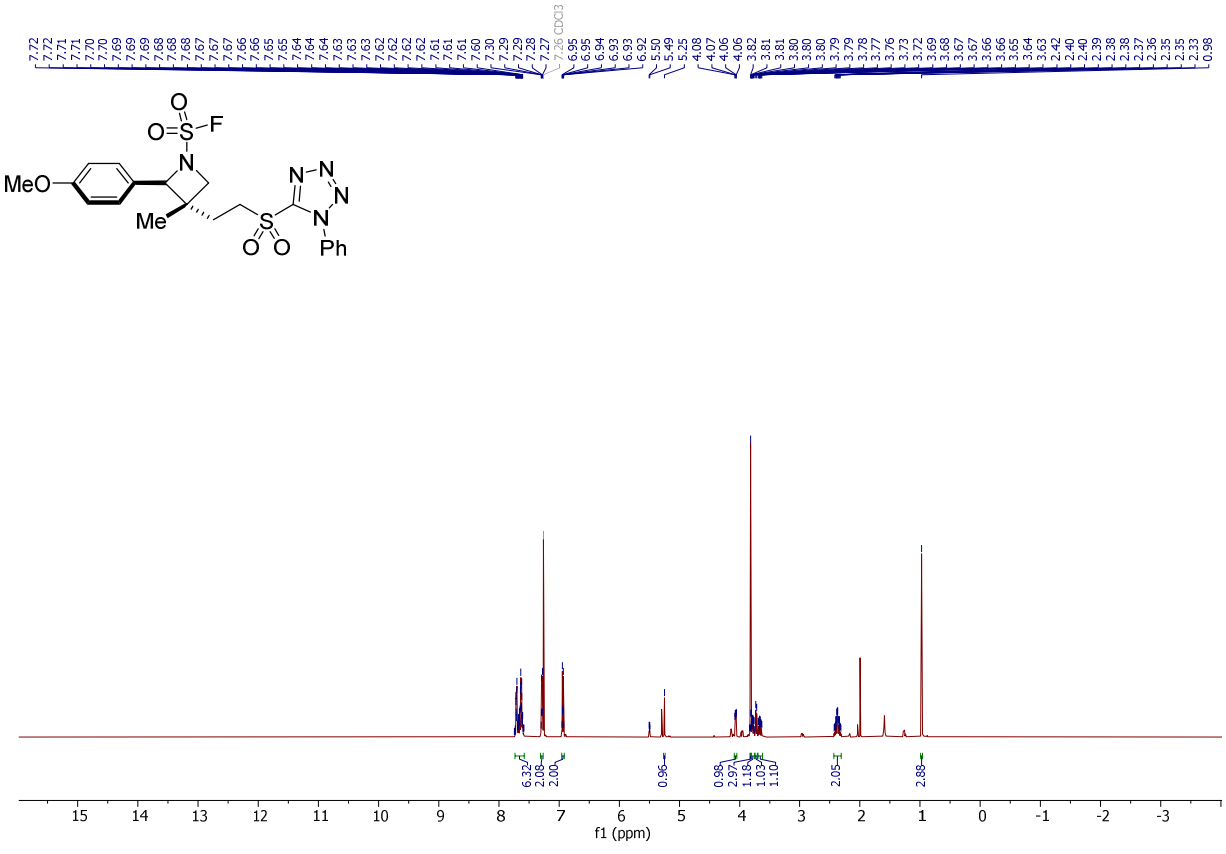
(2*R**,3*R**)-2-(4-Methoxyphenyl)-3-methyl-3-(2-((1-phenyl-1H-tetrazol-5-yl)sulfonyl)ethyl)azetidine-1-sulfonyl fluoride (4c)

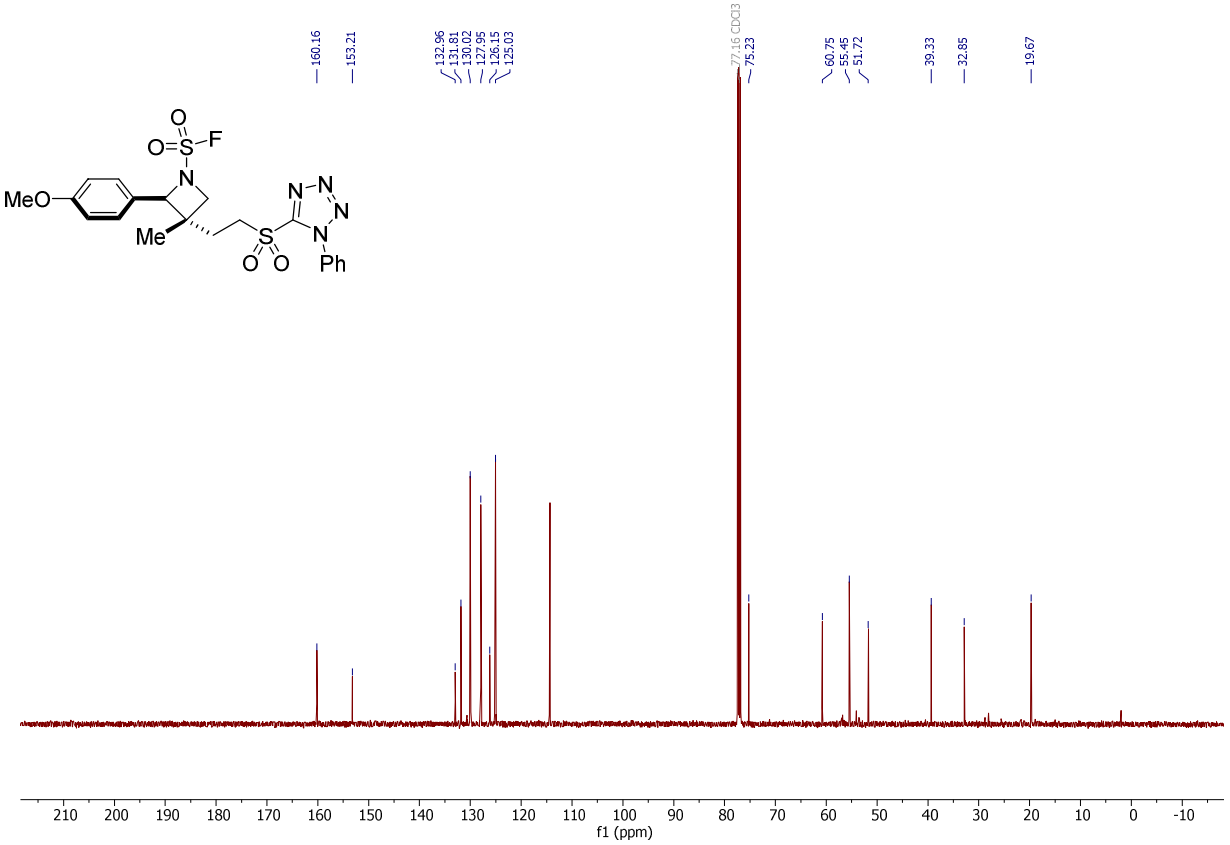


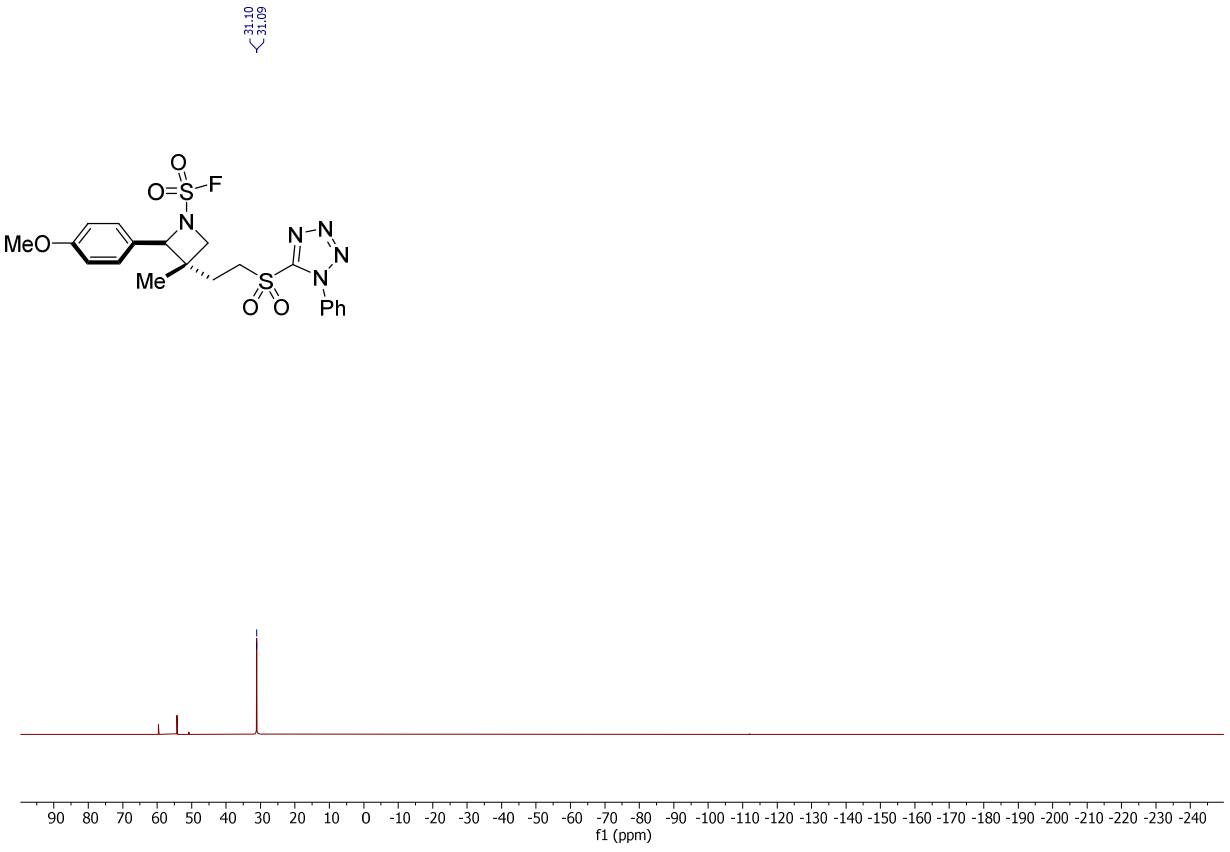




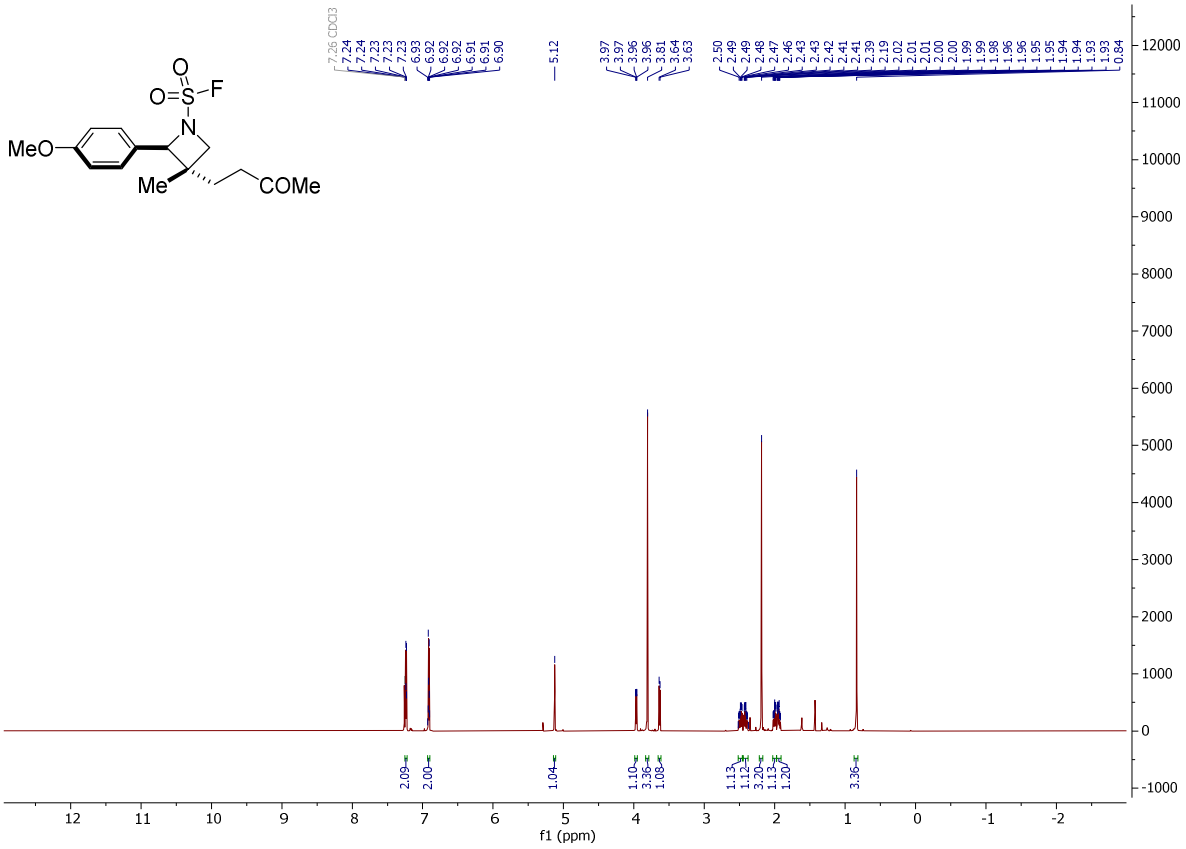
(2*R**,3*S**)-2-(4-Methoxyphenyl)-3-methyl-3-(2-((1-phenyl-1H-tetrazol-5-yl)sulfonyl)ethyl)azetidine-1-sulfonyl fluoride (4c')

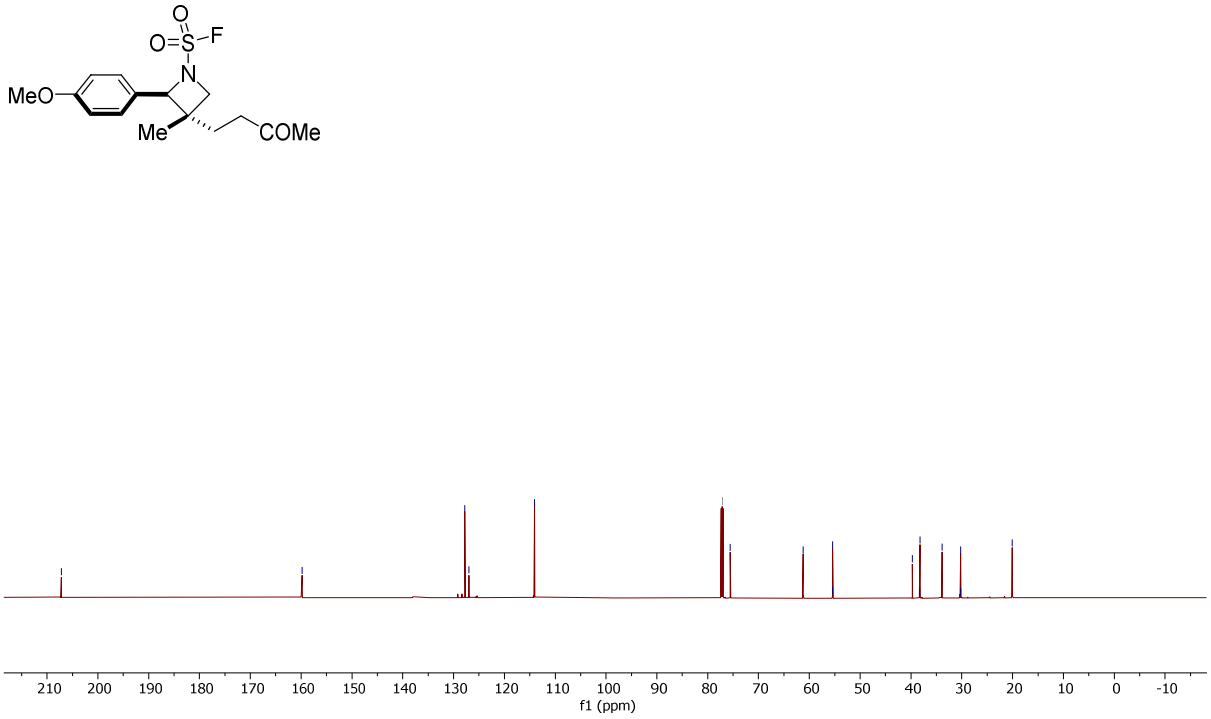


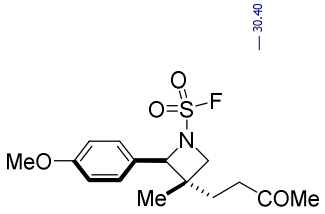

160.16
153.21
132.96
131.81
130.02
127.95
126.15
125.03
77.16 CDCl3
75.23
60.75
55.45
51.72
39.33
32.85
19.67
MeO
Me
O=S-F
N-N
N
S
O O
Ph
f1 (ppm)

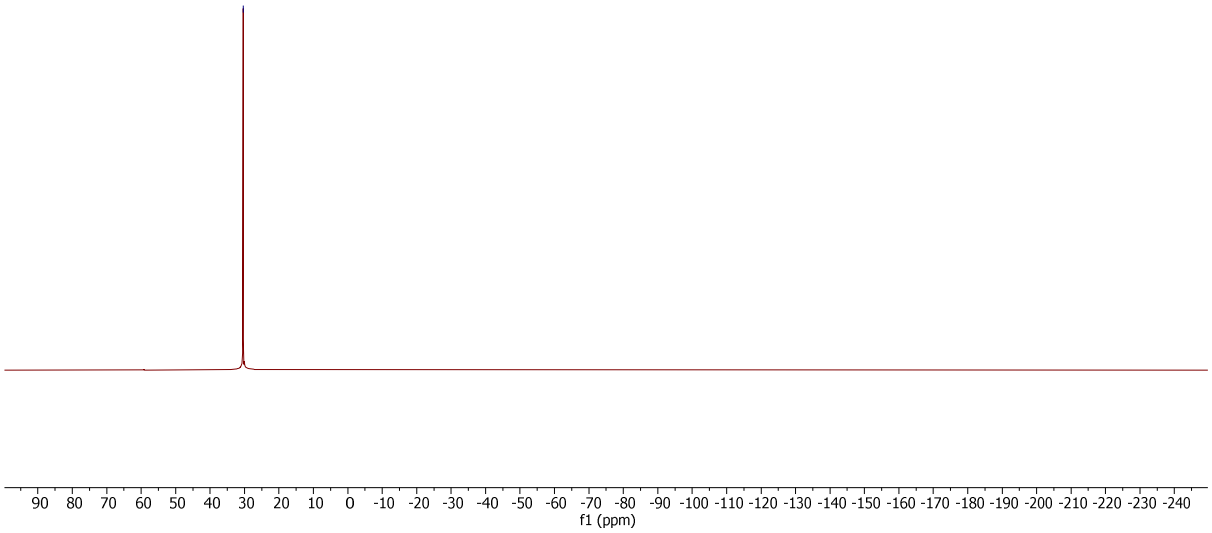

31.10
31.09
MeO
Me
O=S-F
N-N
N
S
O O
Ph
f1 (ppm)

(2*R**,3*S**)-2-(4-Methoxyphenyl)-3-methyl-3-(3-oxobutyl)azetidine-1-sulfonyl fluoride (4d)

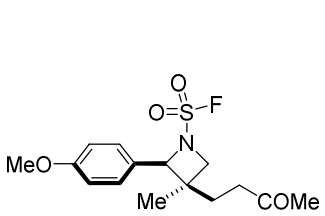




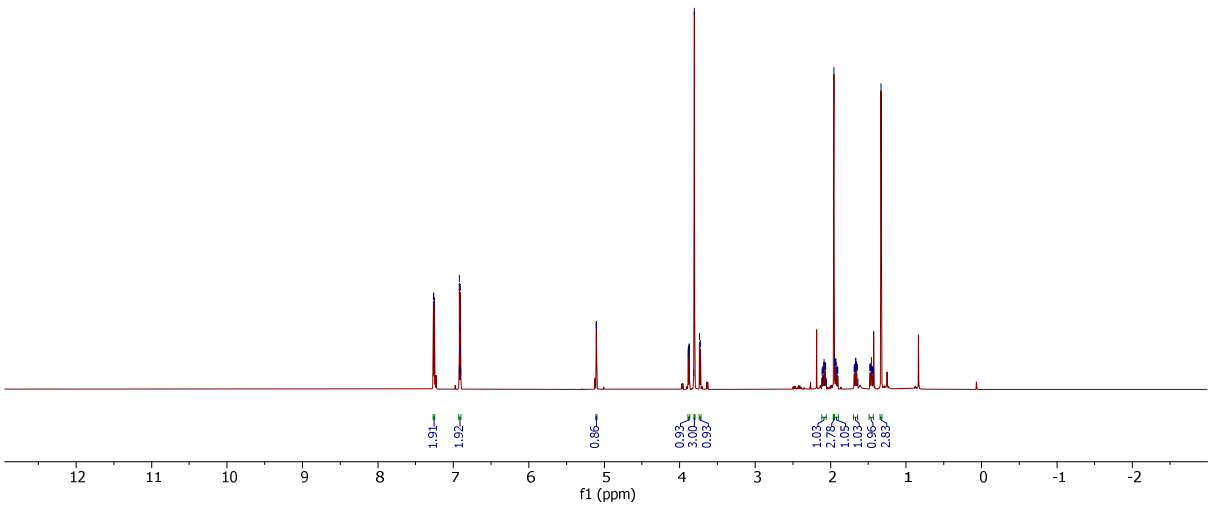


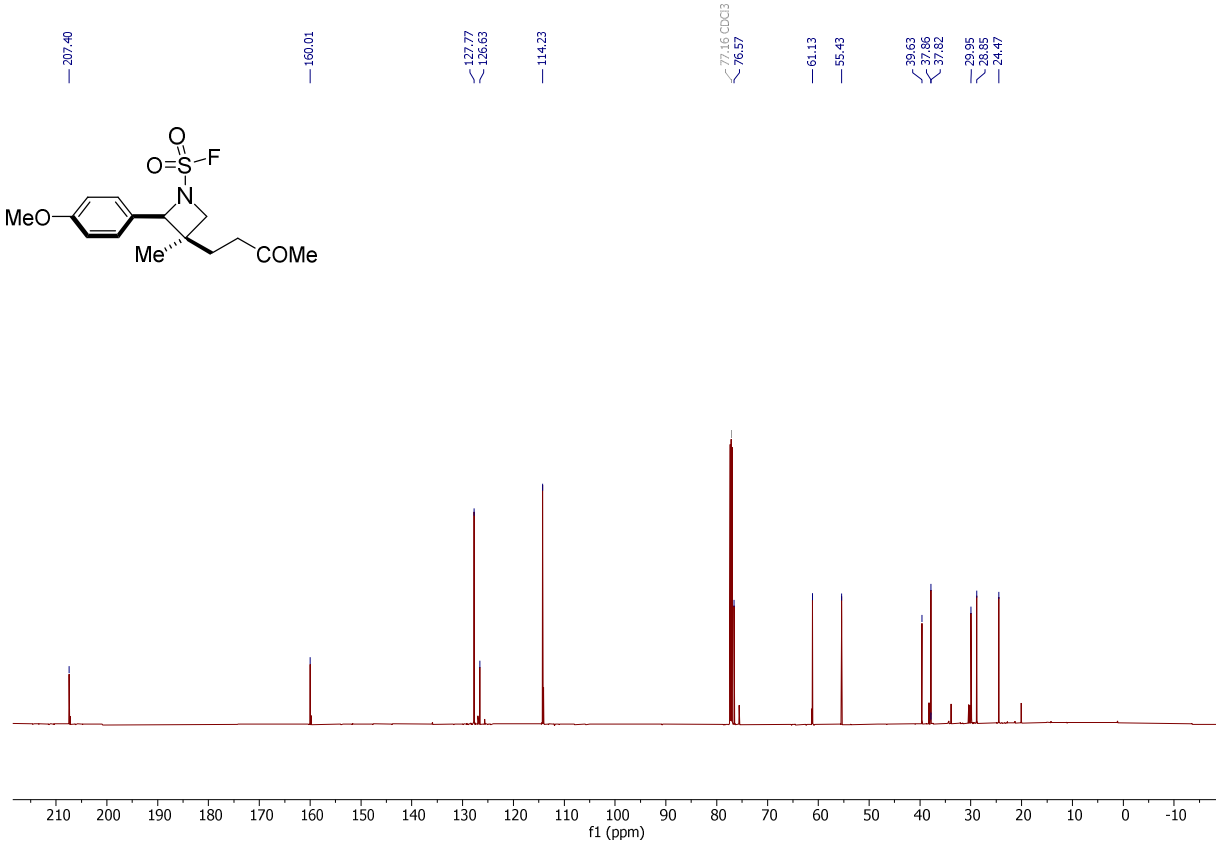


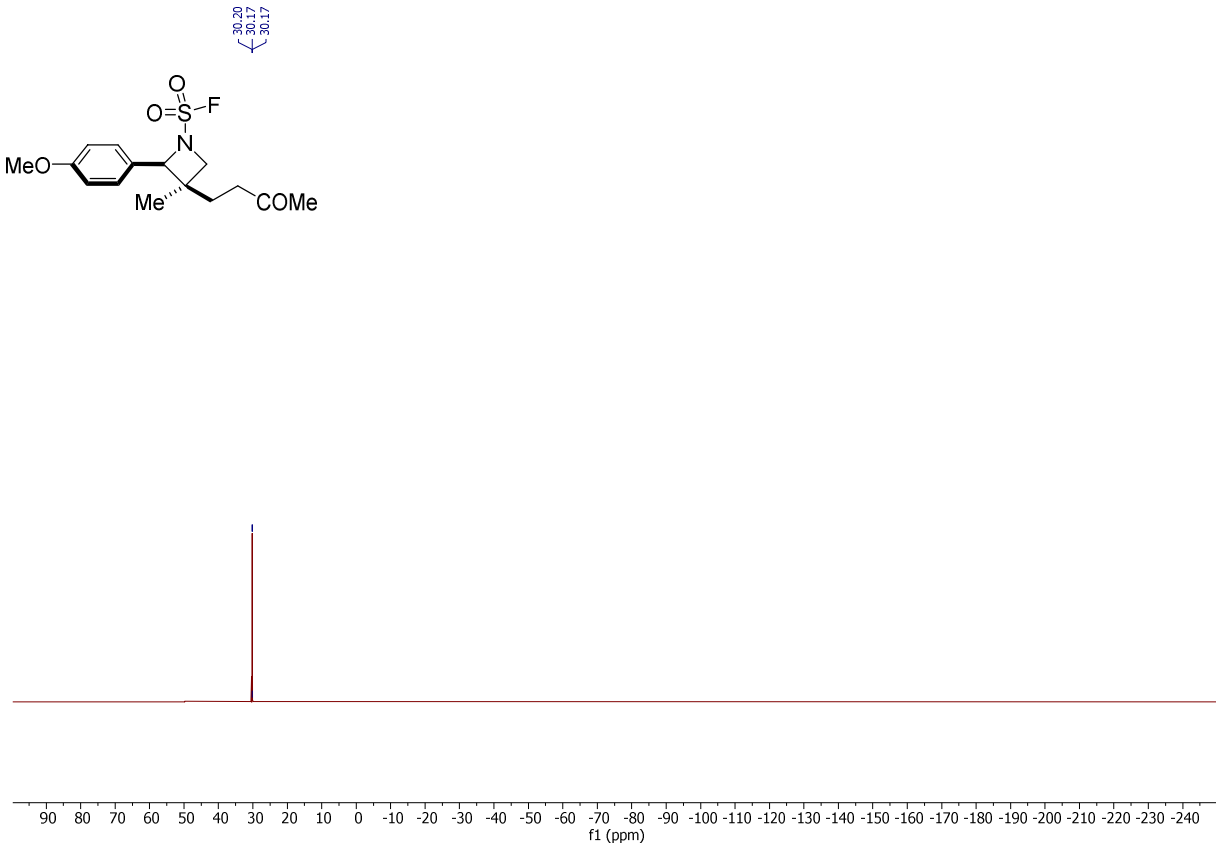
(2*R**,3*R**)-2-(4-Methoxyphenyl)-3-methyl-3-(3-oxobutyl)azetidine-1-sulfonyl fluoride (4d')



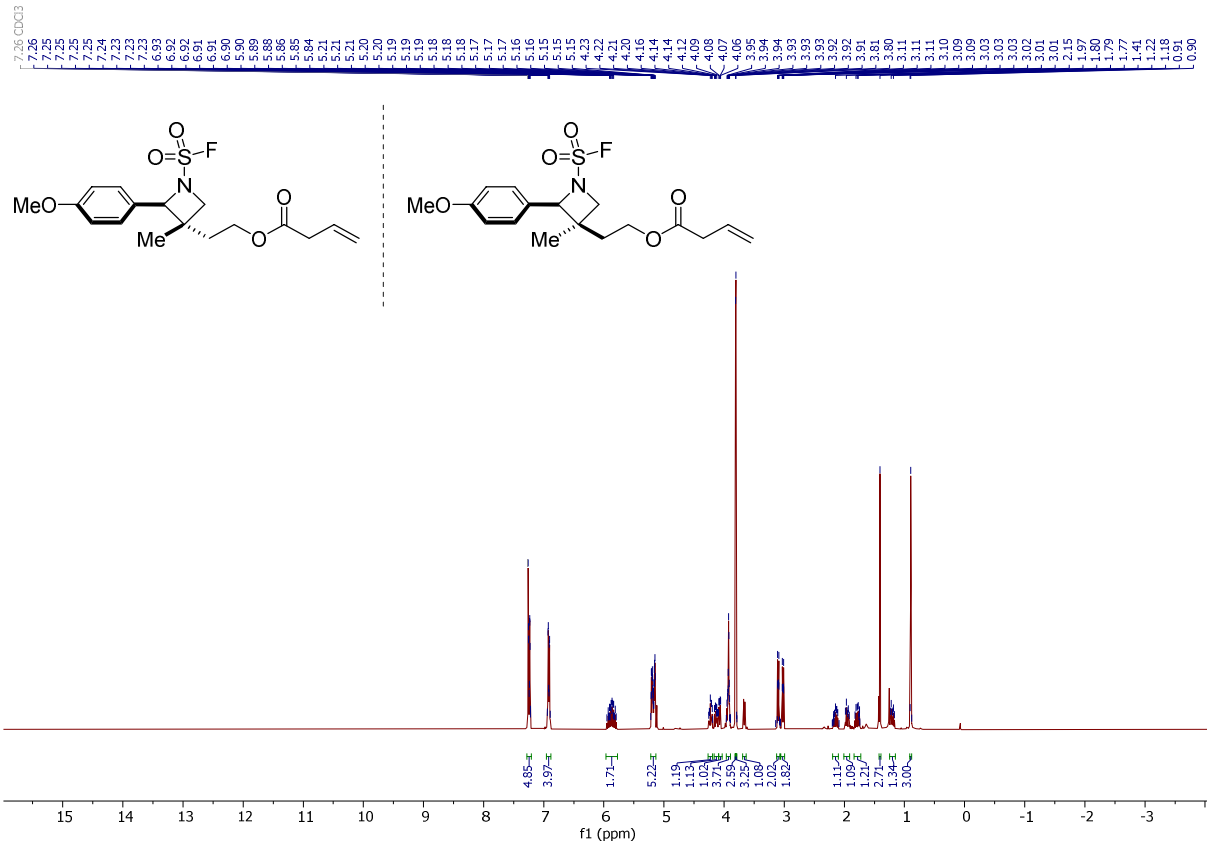


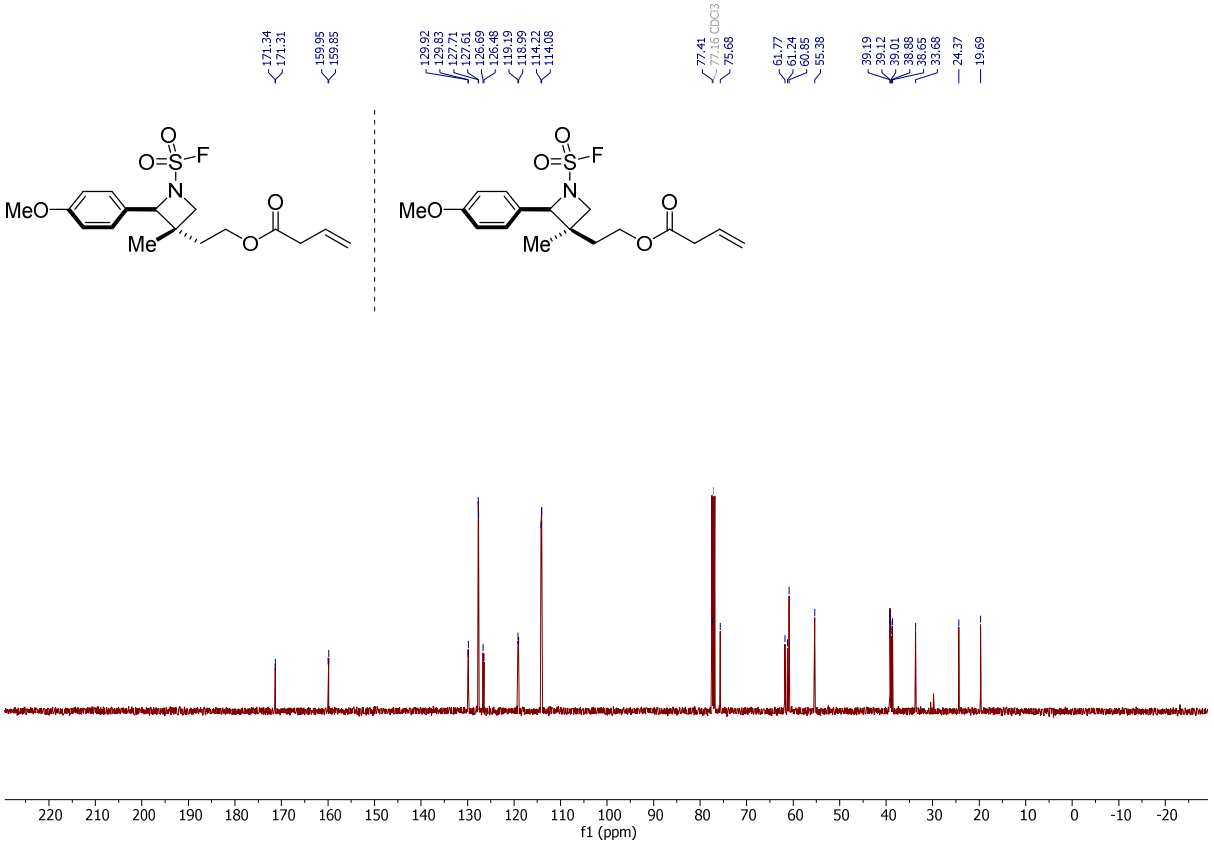


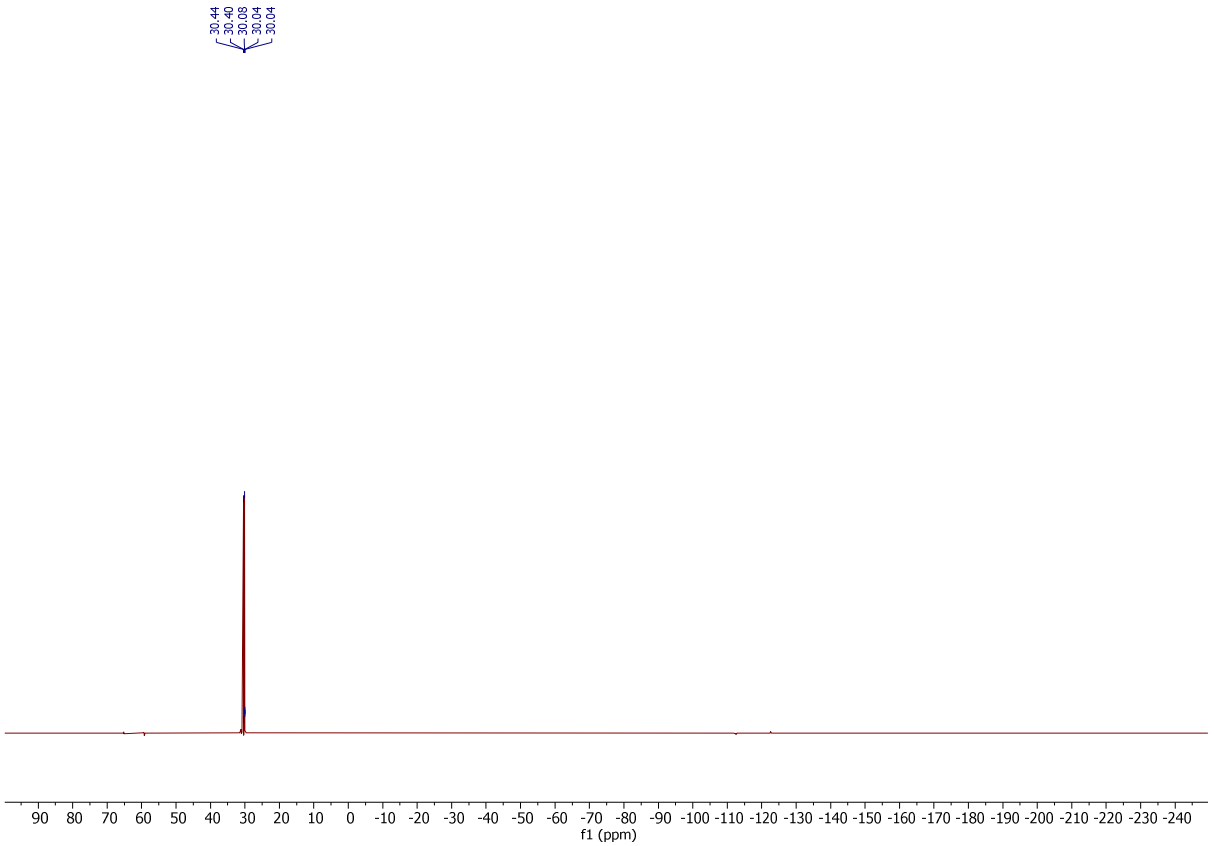

207.40
160.01
127.77
126.63
114.23
77.16 CDCl3
76.57
61.13
55.43
39.63
37.86
37.82
29.95
28.85
24.47
O
O=S–F
N
MeO
Me
COMe
210 200 190 180 170 160 150 140 130 120 110 100 90 80 70 60 50 40 30 20 10 0 -10
f1 (ppm)


30.20
30.17
30.17
O
O=S–F
N
MeO
Me
COMe
90 80 70 60 50 40 30 20 10 0 -10 -20 -30 -40 -50 -60 -70 -80 -90 -100 -110 -120 -130 -140 -150 -160 -170 -180 -190 -200 -210 -220 -230 -240
f1 (ppm)

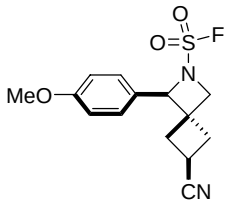
2-((2*R**,3*S**)-1-(Fluorosulfonyl)-2-(4-methoxyphenyl)-3-methylazetidin-3-yl)ethyl but-3-enoate (4e) and 2-((2*R**,3*R**)-1-(Fluorosulfonyl)-2-(4-methoxyphenyl)-3-methylazetidin-3-yl)ethyl but-3-enoate (4e')

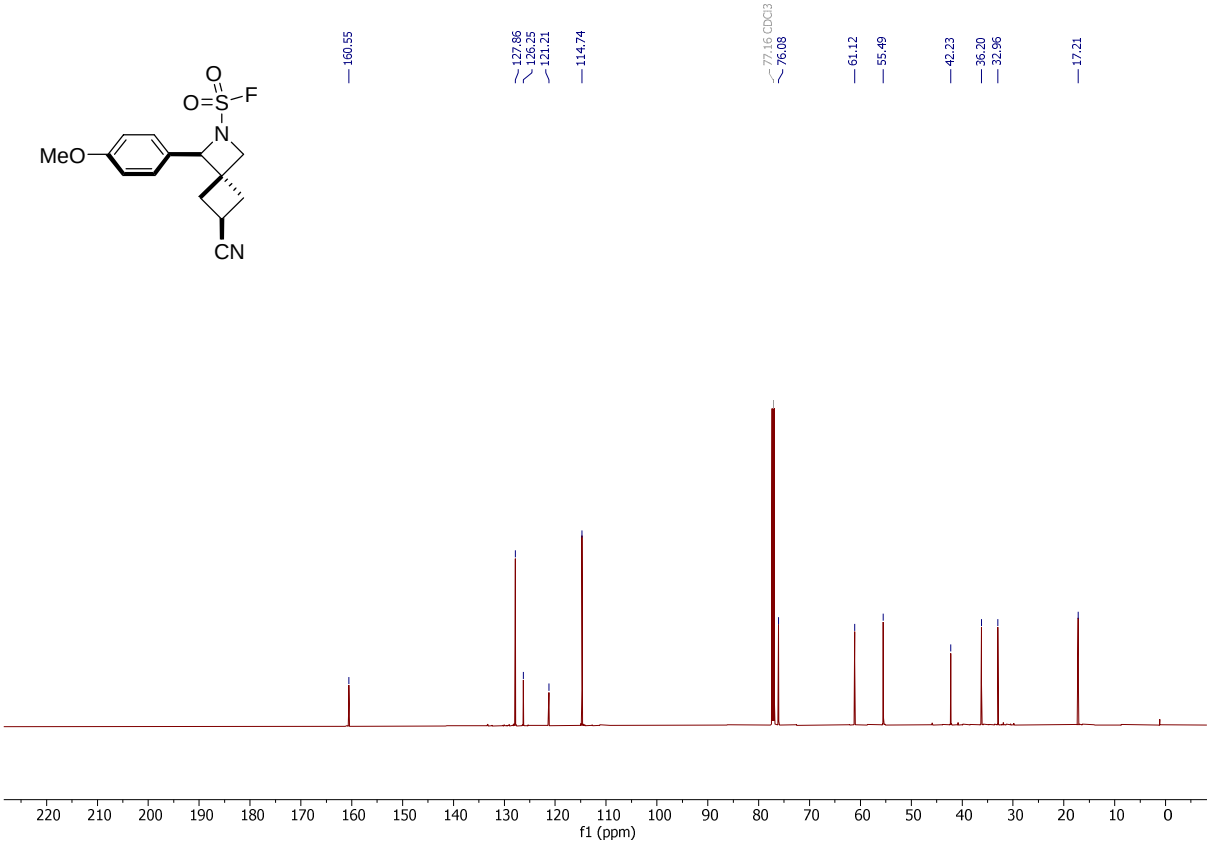


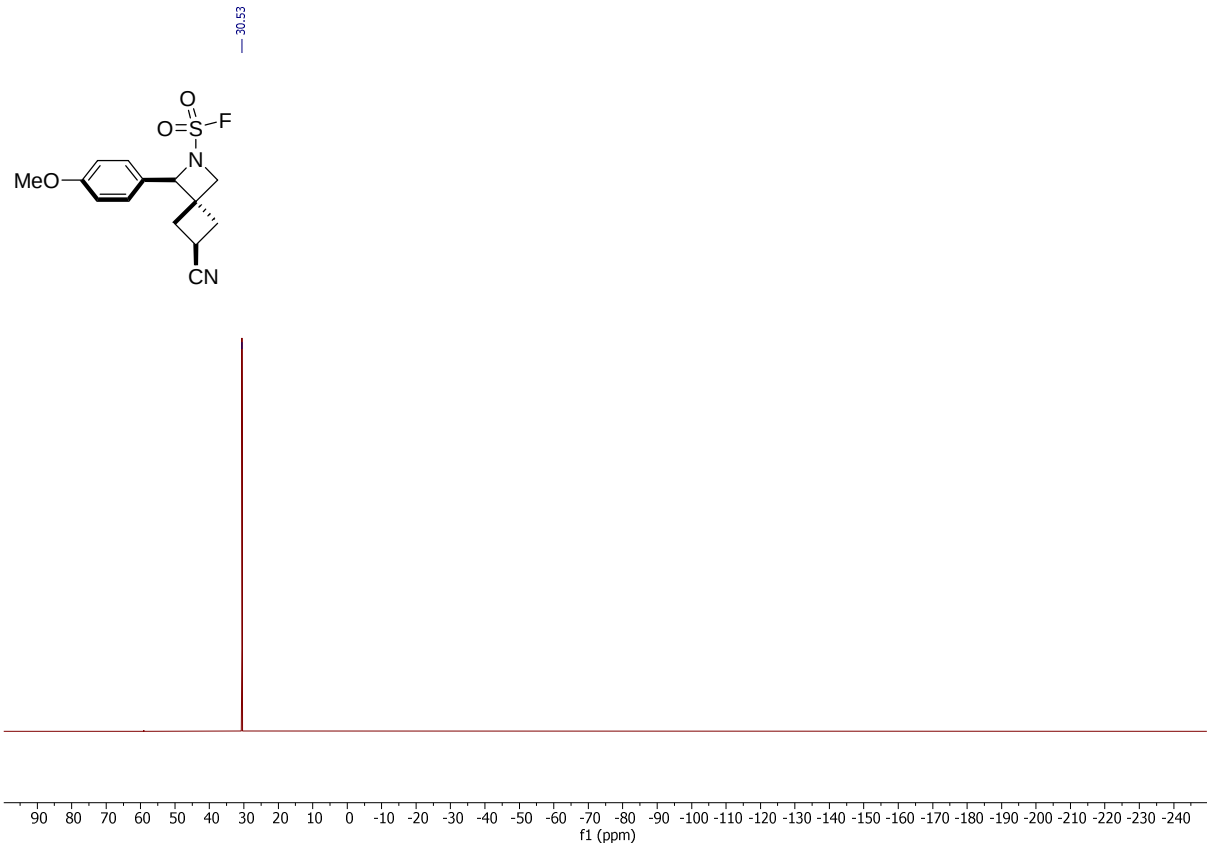

171.34
171.31
159.95
159.85
129.92
129.83
127.71
127.61
126.69
126.48
119.19
118.99
114.22
114.08
77.41
77.16 CDCl3
75.68
61.77
61.24
60.85
55.38
39.19
39.12
39.01
38.88
38.65
33.68
24.37
19.69
O=S–F
N
MeO
Me
O
O
f1 (ppm)


30.44
30.40
30.08
30.04
30.04
f1 (ppm)

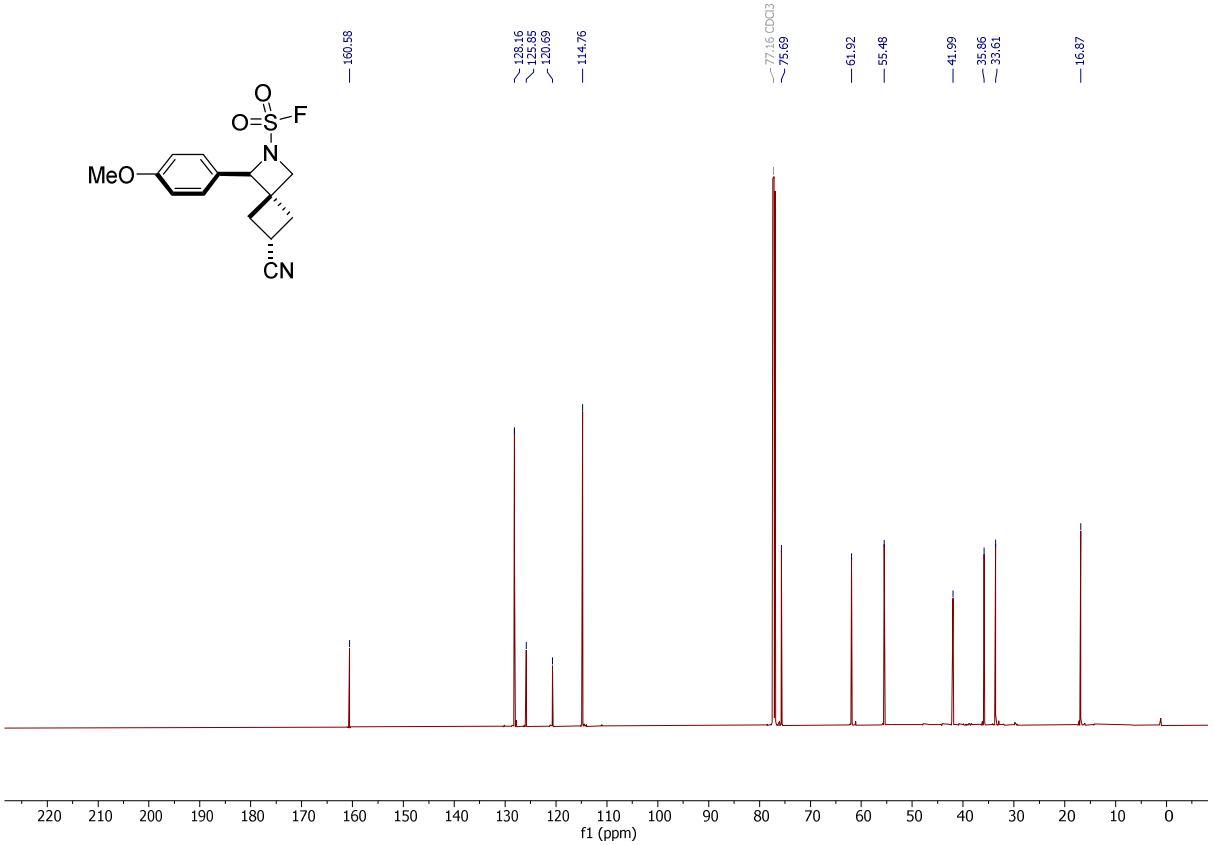
(1*R**,4*r**,6*R**)-6-Cyano-1-(4-methoxyphenyl)-2-azaspiro[3.3]heptane-2-sulfonyl fluoride (4f)

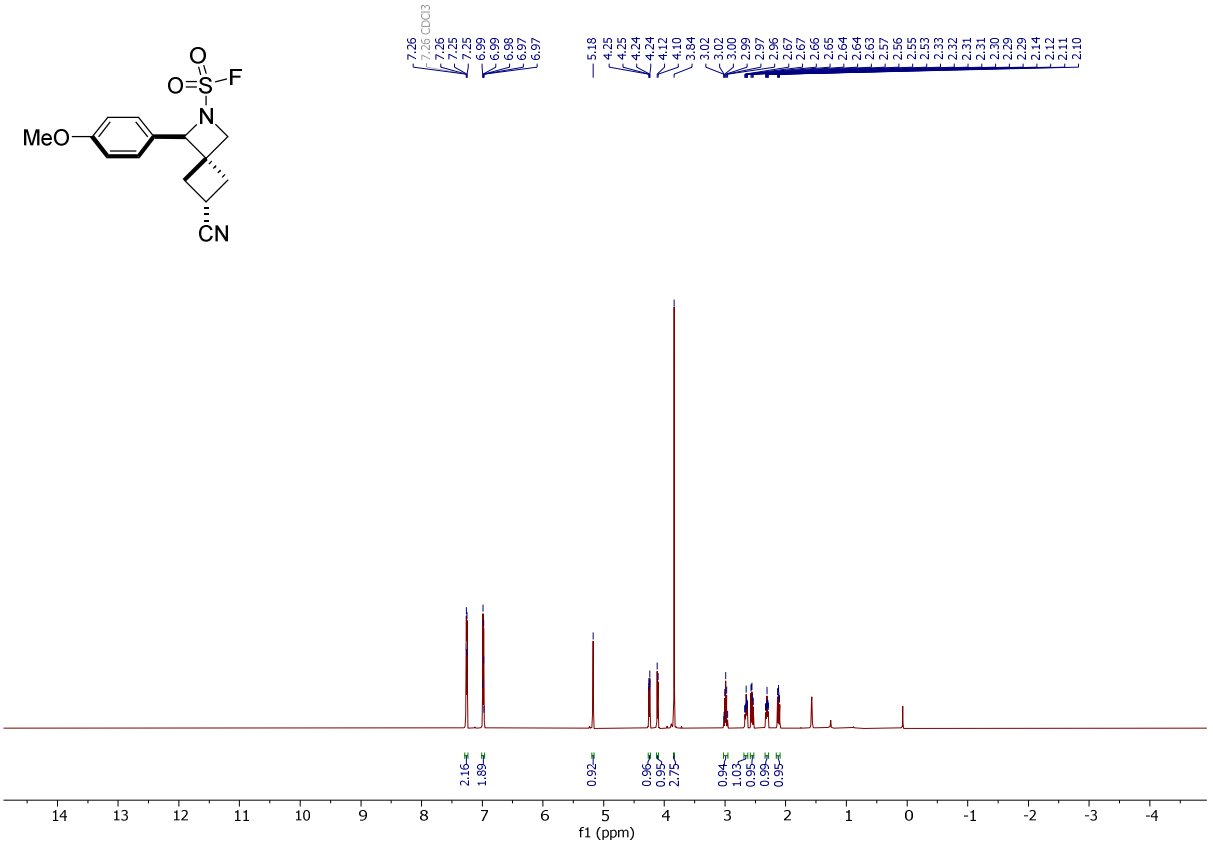


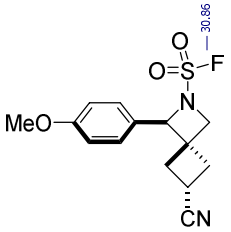

160.55
127.86
126.25
121.21
114.74
77.16 CDCl3
76.08
61.12
55.49
42.23
36.20
32.96
17.21
MeO
O
O=S
F
N
CN
220 210 200 190 180 170 160 150 140 130 120 110 100 90 80 70 60 50 40 30 20 10 0
f1 (ppm)

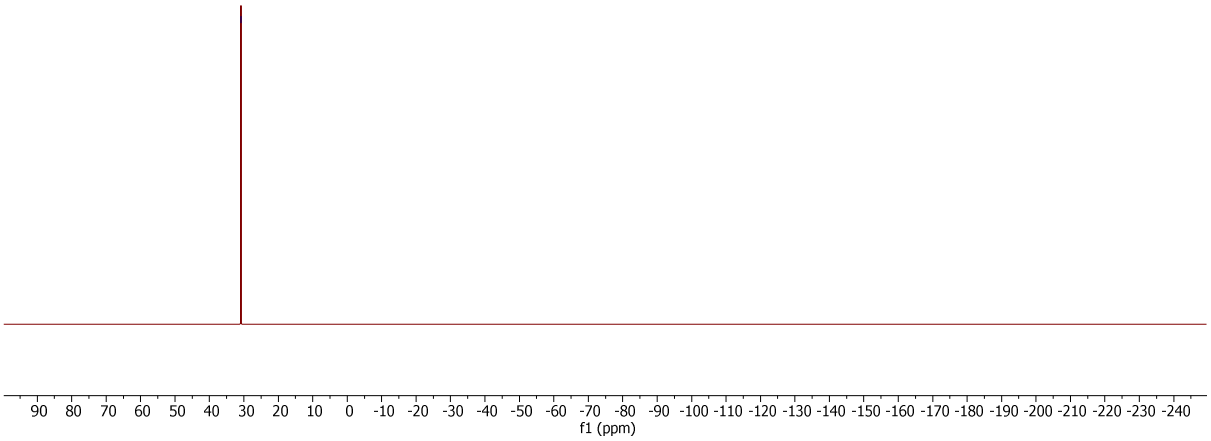

30.53
MeO
O
O=S
F
N
CN
90 80 70 60 50 40 30 20 10 0 -10 -20 -30 -40 -50 -60 -70 -80 -90 -100 -110 -120 -130 -140 -150 -160 -170 -180 -190 -200 -210 -220 -230 -240
f1 (ppm)

(1*R**,4*S**,6*S**)-6-Cyano-1-(4-methoxyphenyl)-2-azaspiro[3.3]heptane-2-sulfonyl fluoride (4f')

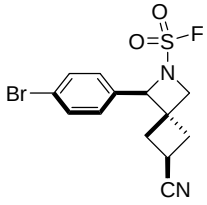


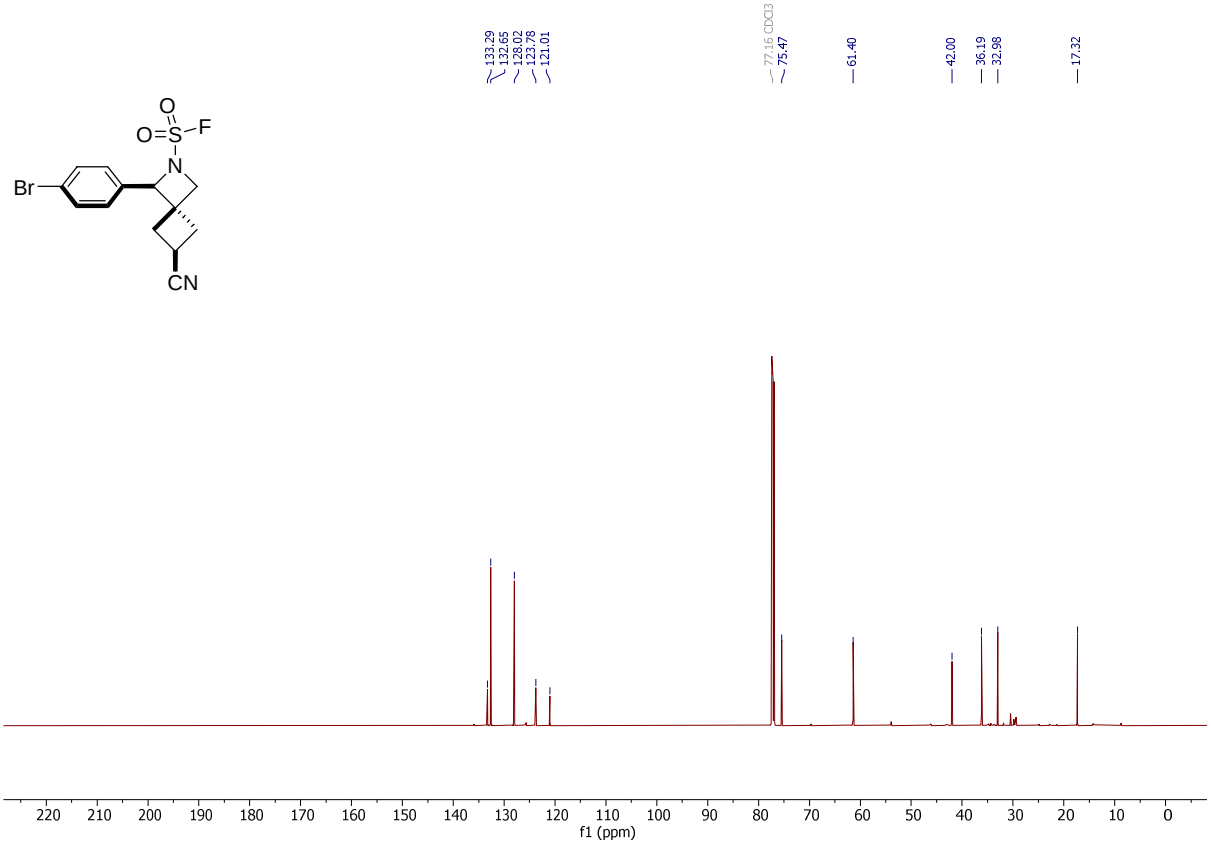


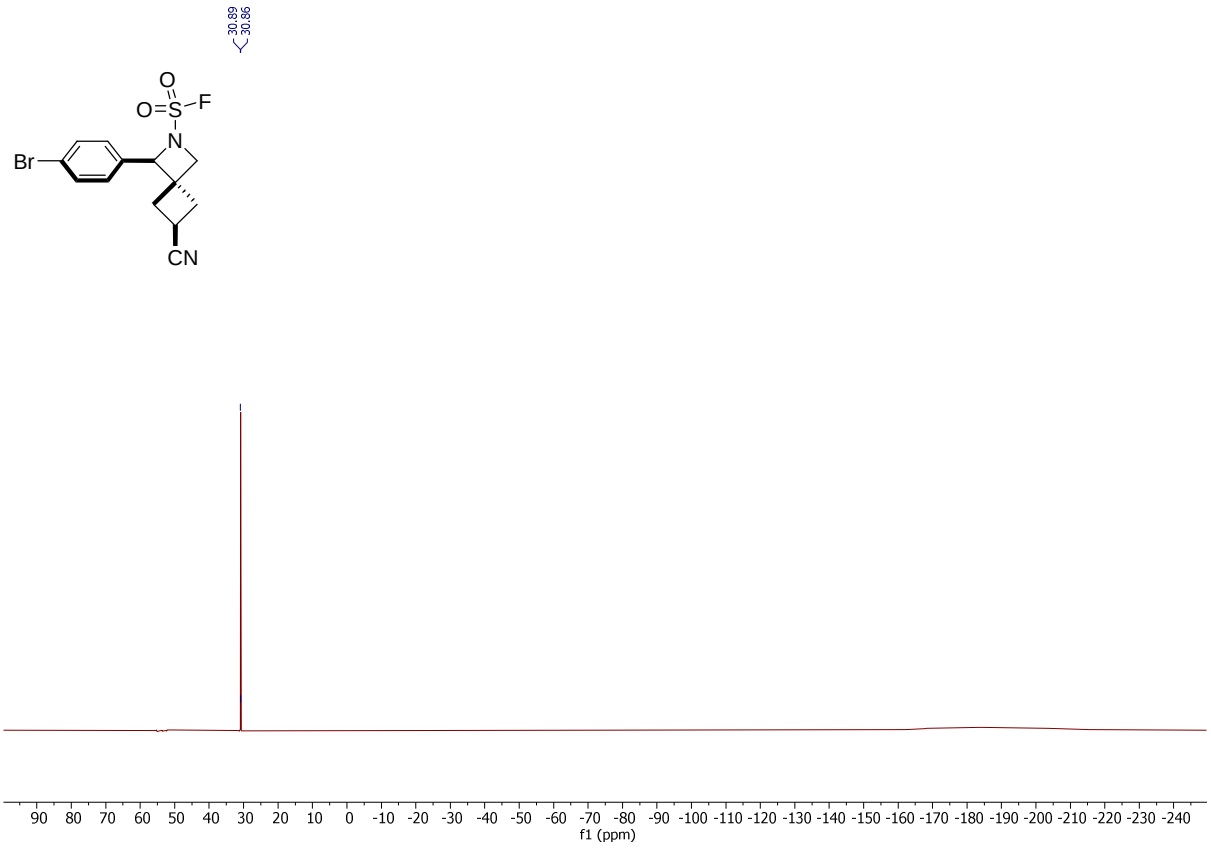




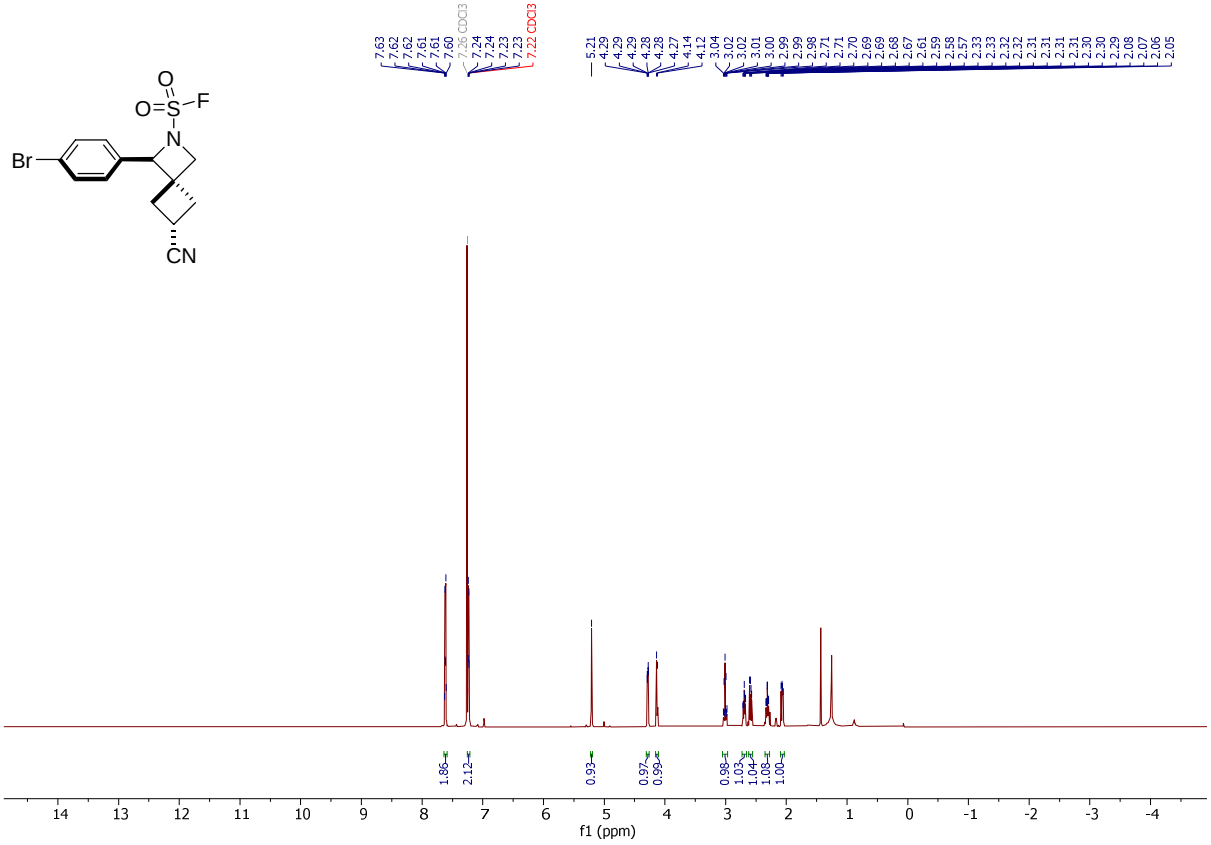
(1*R**,4*r**,6*R**)-6-Cyano-1-(4-bromophenyl)-2-azaspiro[3.3]heptane-2-sulfonyl fluoride (4g)

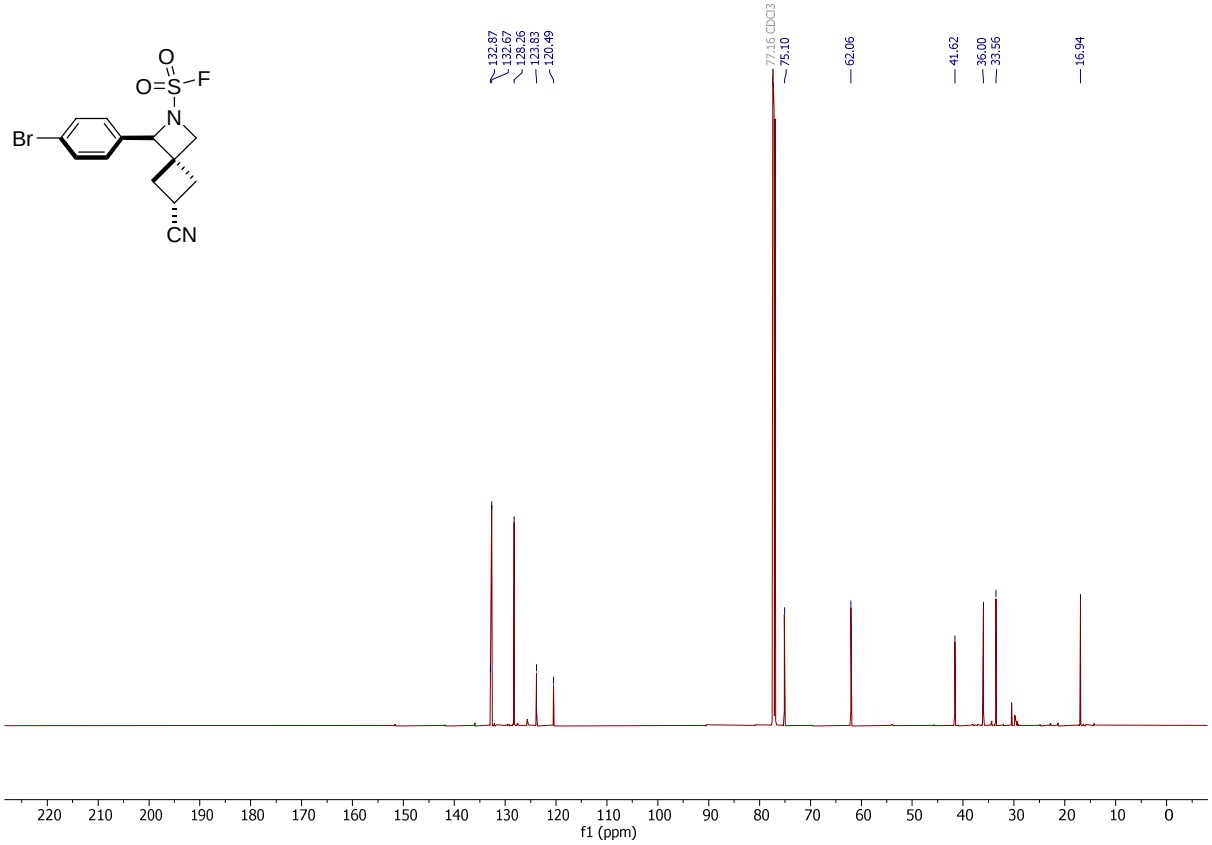


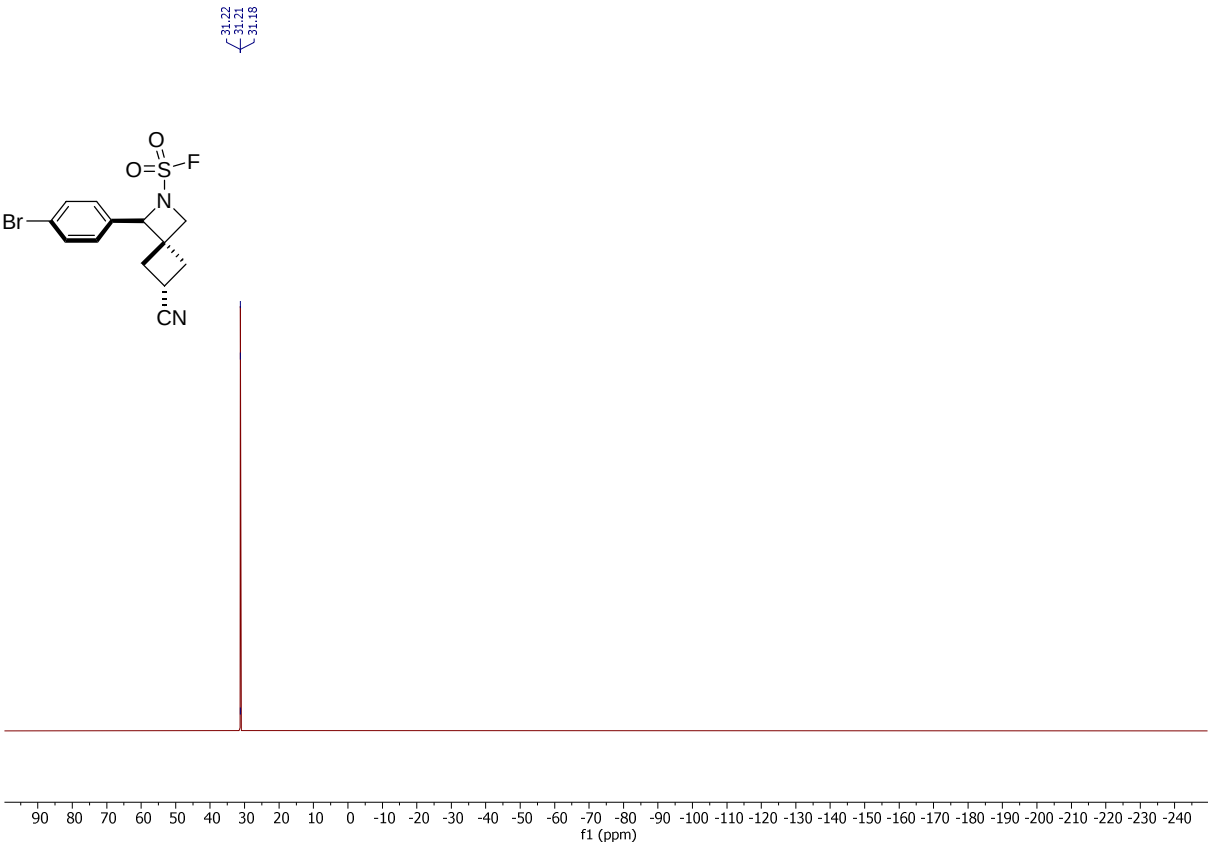

133.29
132.65
128.02
123.78
121.01
77.16 CDCl3
75.47
61.40
42.00
36.19
32.98
17.32
O
O=S–F
N
Br
CN
220 210 200 190 180 170 160 150 140 130 120 110 100 90 80 70 60 50 40 30 20 10 0
f1 (ppm)


30.89
30.86
O
O=S–F
N
Br
CN
90 80 70 60 50 40 30 20 10 0 -10 -20 -30 -40 -50 -60 -70 -80 -90 -100 -110 -120 -130 -140 -150 -160 -170 -180 -190 -200 -210 -220 -230 -240
f1 (ppm)

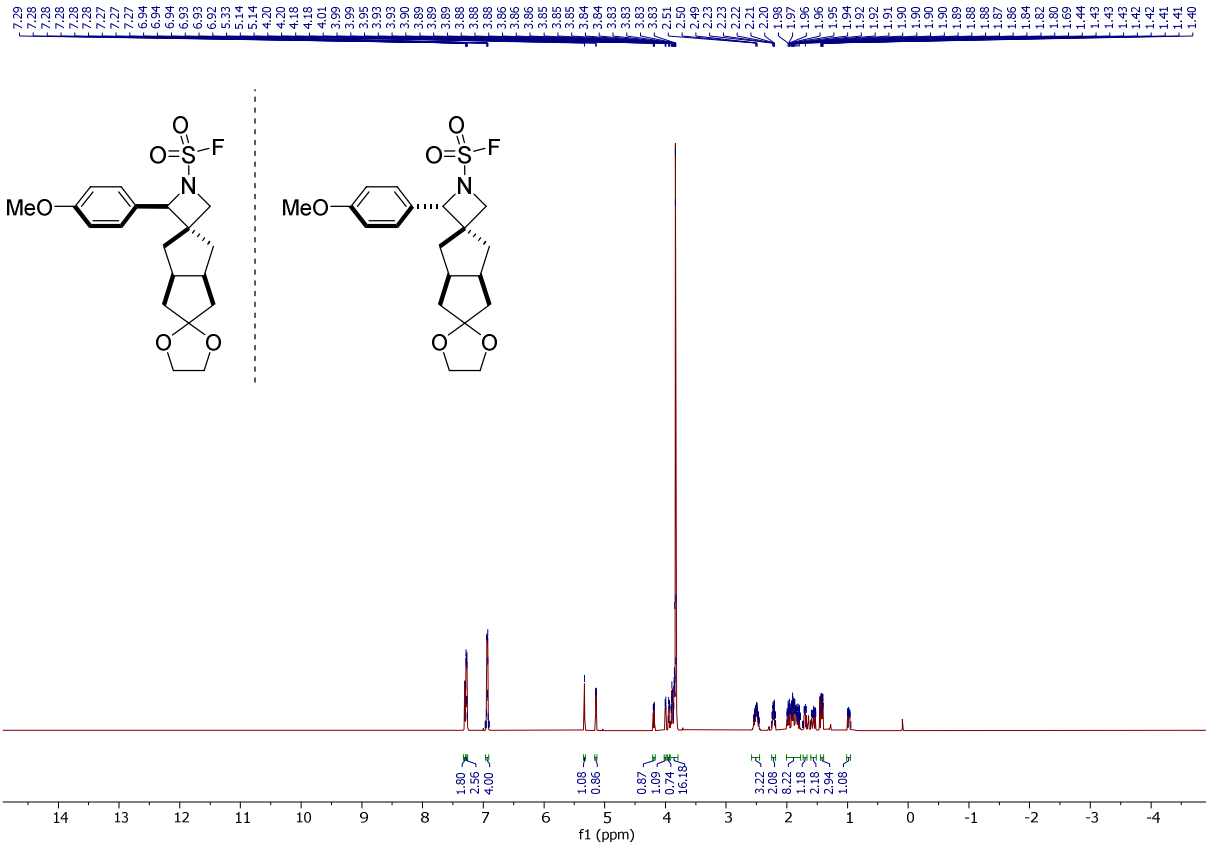
(1R*,4s*,6S*)-6-Cyano-1-(4-bromophenyl)-2-azaspiro[3.3]heptane-2-sulfonyl fluoride (4g')

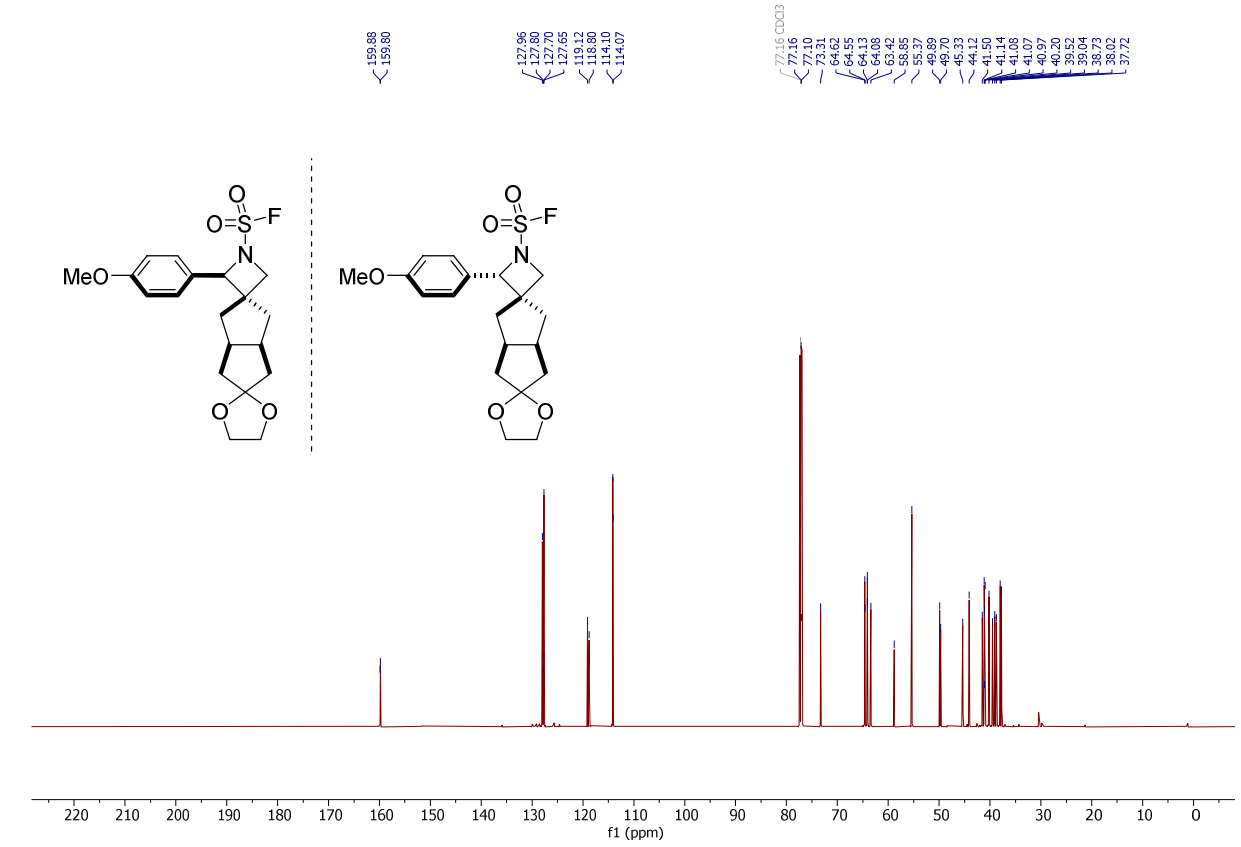


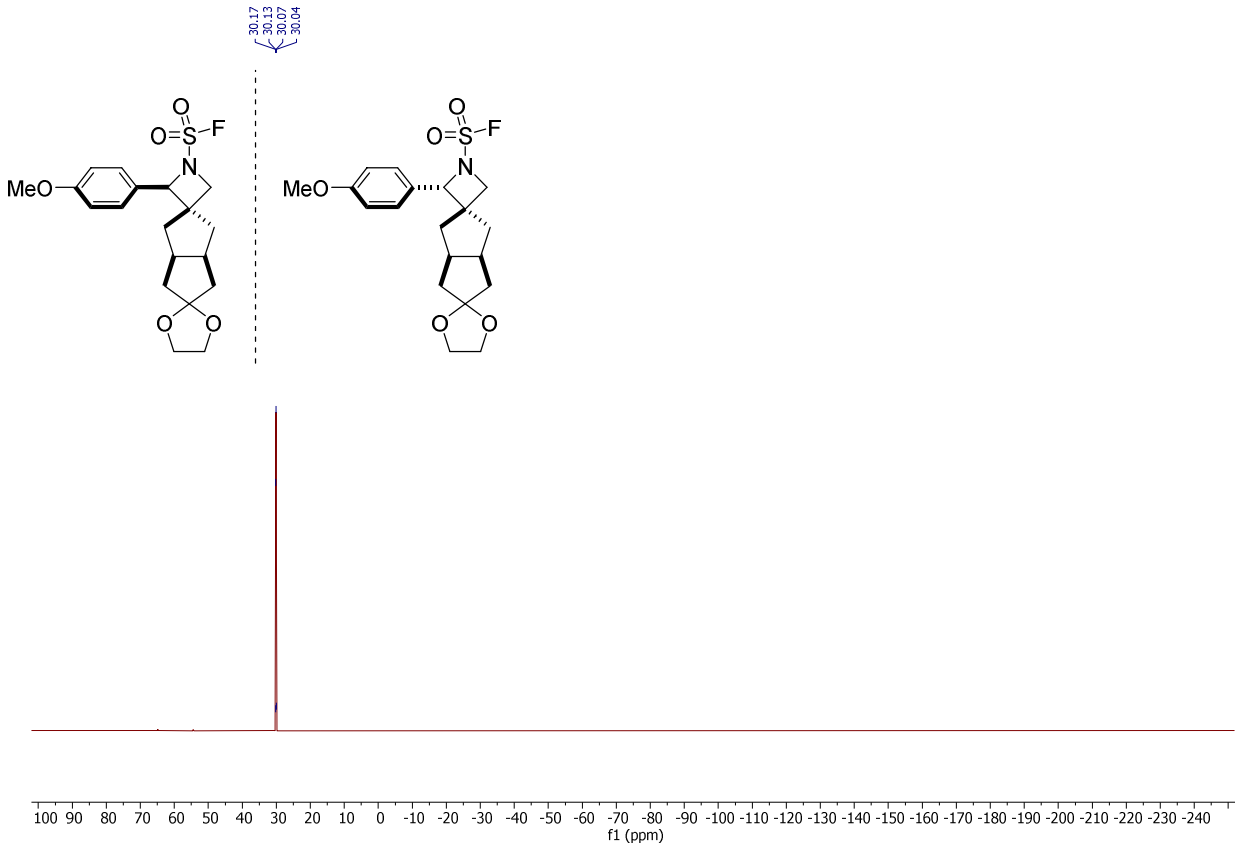

O
O=S–F
N
Br
CN
132.87
132.67
128.26
123.83
120.49
77.16 CDCl3
75.10
62.06
41.62
36.00
33.56
16.94
220 210 200 190 180 170 160 150 140 130 120 110 100 90 80 70 60 50 40 30 20 10 0
f1 (ppm)


31.22
31.21
31.18
O
O=S–F
N
Br
CN
90 80 70 60 50 40 30 20 10 0 -10 -20 -30 -40 -50 -60 -70 -80 -90 -100 -110 -120 -130 -140 -150 -160 -170 -180 -190 -200 -210 -220 -230 -240
f1 (ppm)

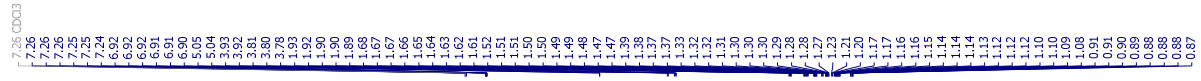
(2*R**,3*r**,3a'*R**,6a'*S**)-2-(4-Methoxyphenyl)tetrahydro-1'H,3'H-dispiro[azetidine-3,2'-pentalene-5',2''-[1,3]dioxolane]-1-sulfonyl fluoride (4h) and (2*S**,3*r**,3a'*R**,6a'*S**)-2-(4-Methoxyphenyl)tetrahydro-1'H,3'H-dispiro[azetidine-3,2'-pentalene-5',2''-[1,3]dioxolane]-1-sulfonyl fluoride (4h')

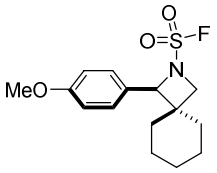


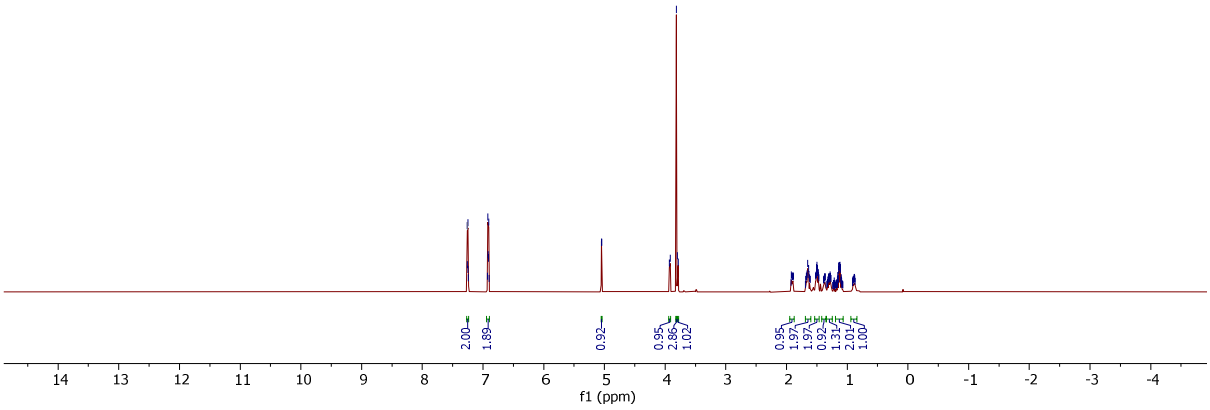

159.88
159.80
127.96
127.80
127.70
127.65
119.12
118.80
114.10
114.07
77.16 CDCl3
77.16
77.10
73.31
64.62
64.55
64.13
64.08
63.42
58.85
55.37
49.89
49.70
45.33
44.12
41.50
41.14
41.08
41.07
40.97
40.20
39.52
39.04
38.73
38.02
37.72
MeO
O=S-F
N
O
f1 (ppm)


30.17
30.13
30.07
30.04
MeO
O=S-F
N
O
f1 (ppm)

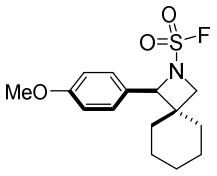
(*R**)-1-(4-Methoxyphenyl)-2-azaspiro[3.5]nonane-2-sulfonyl fluoride (4i)

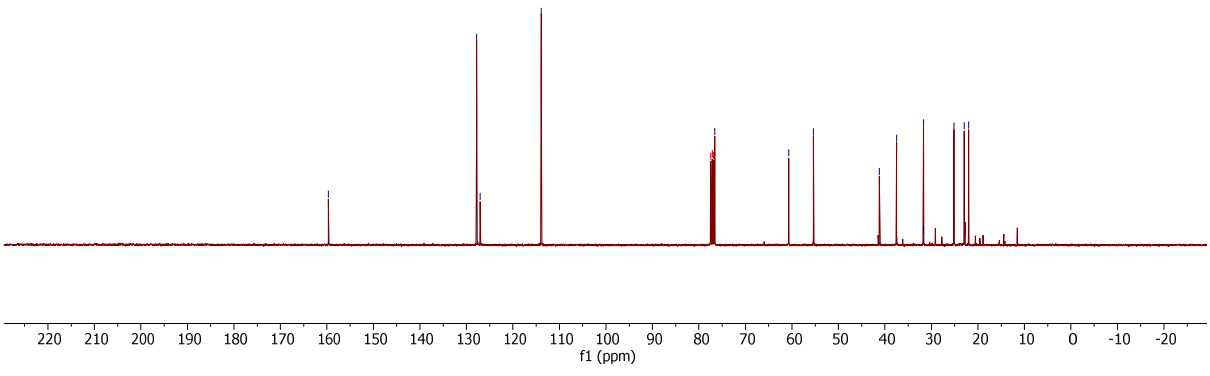


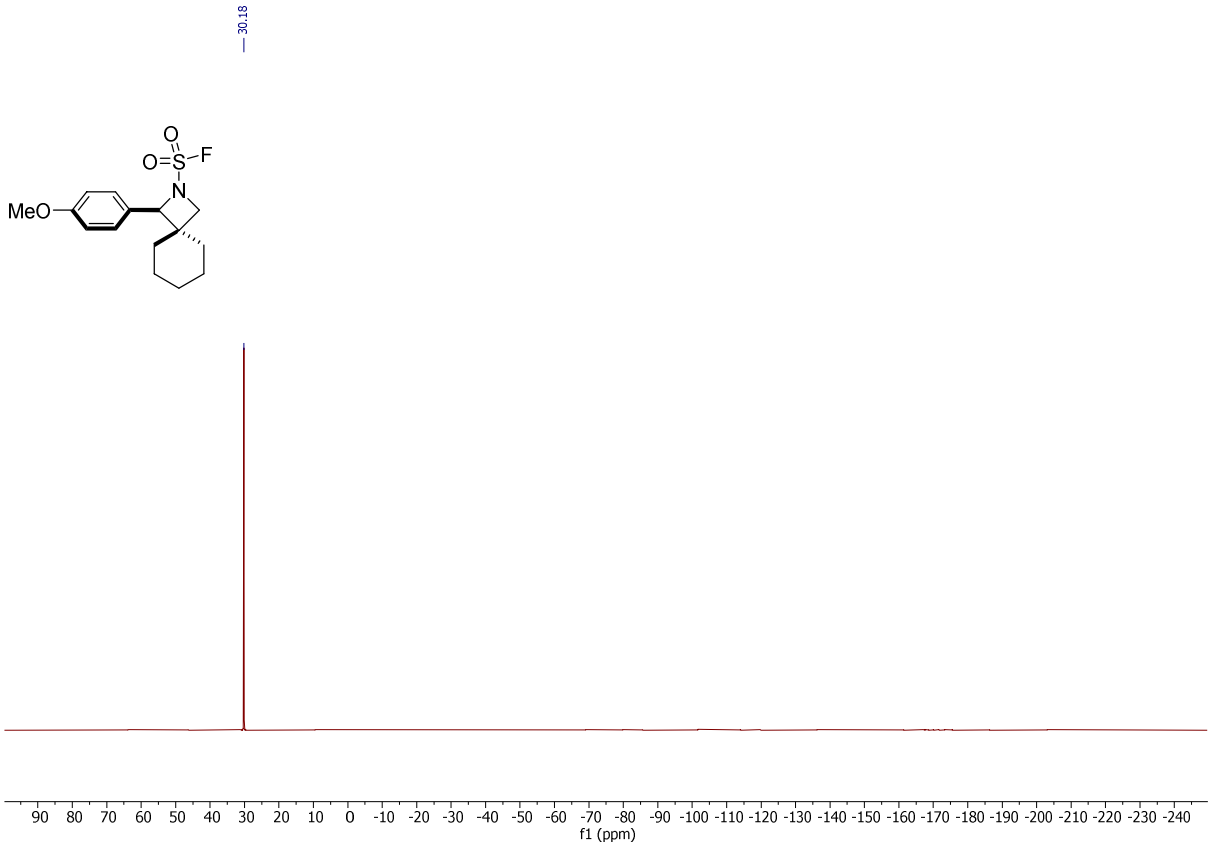




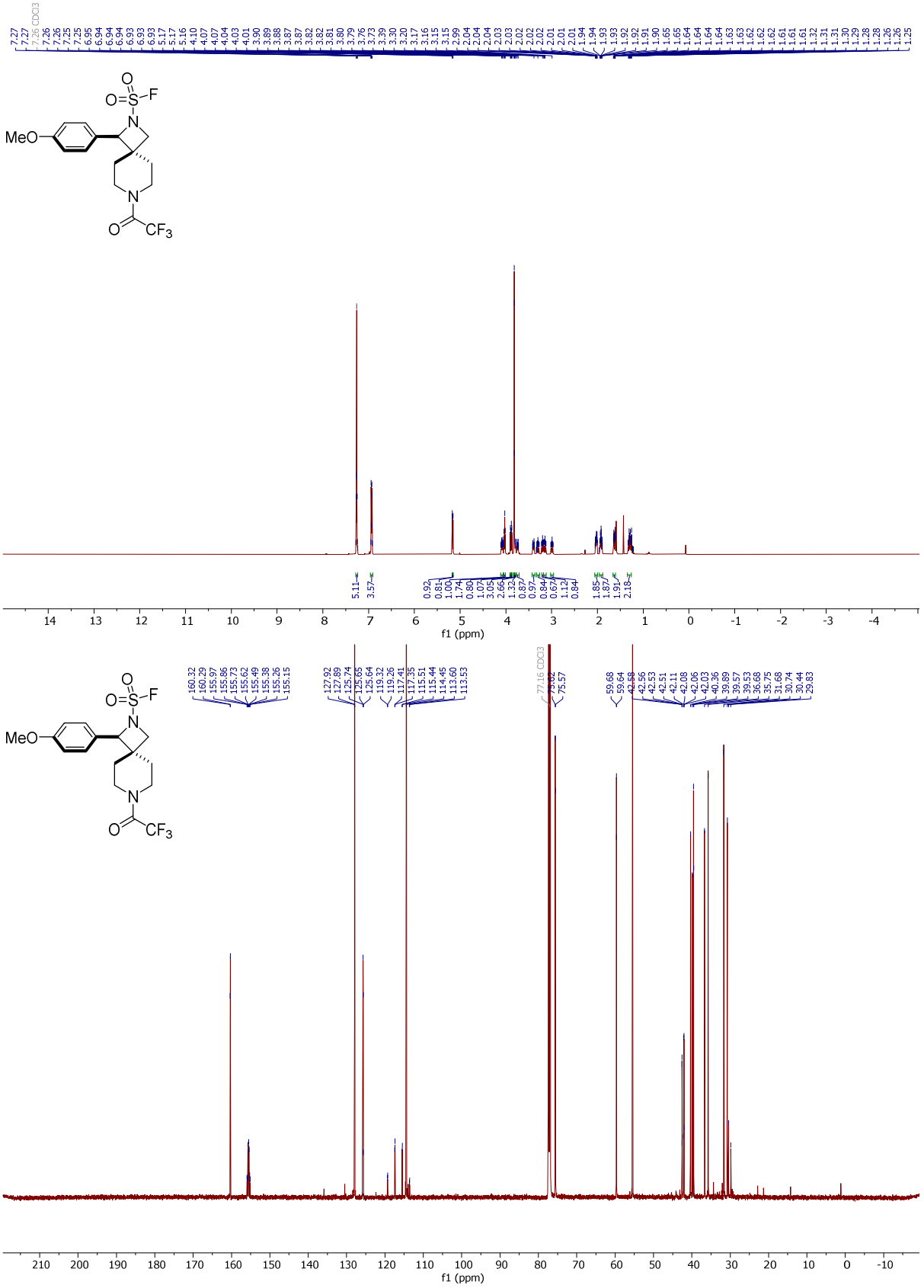


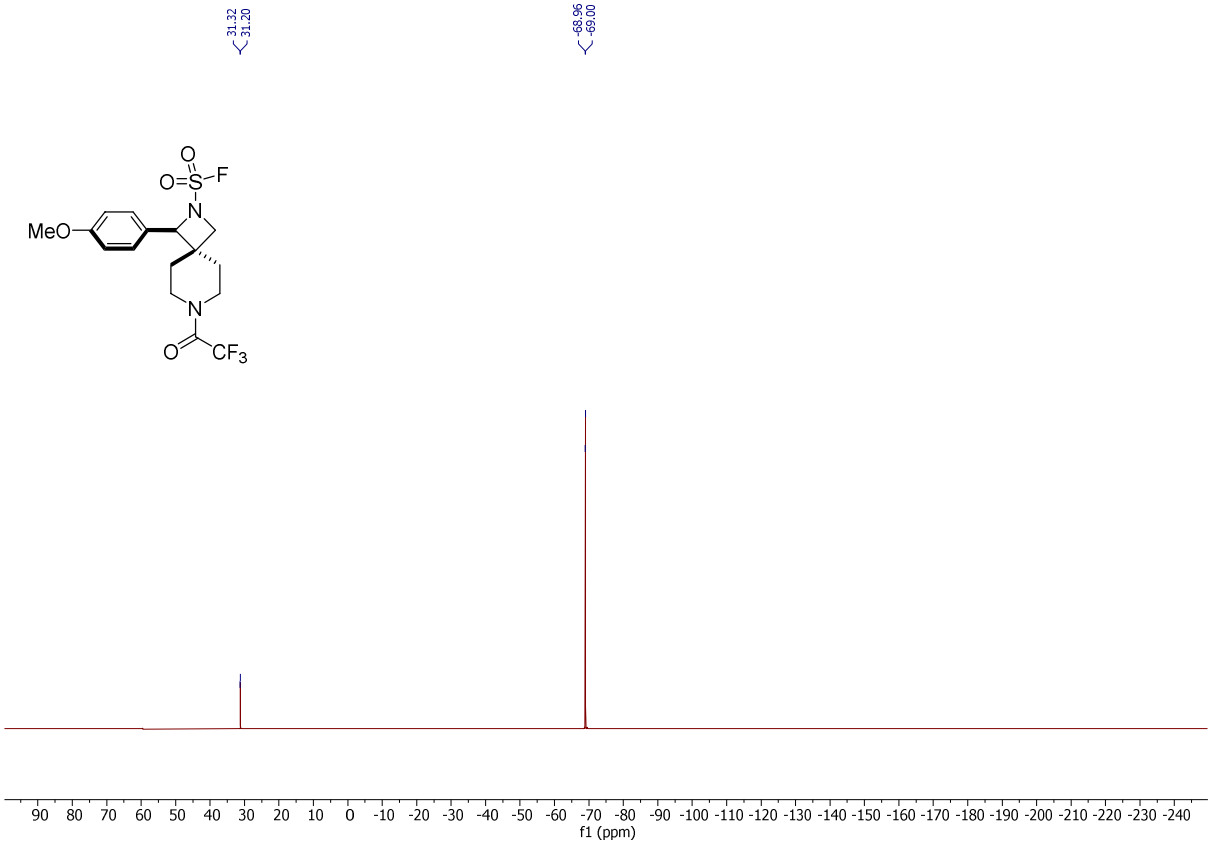




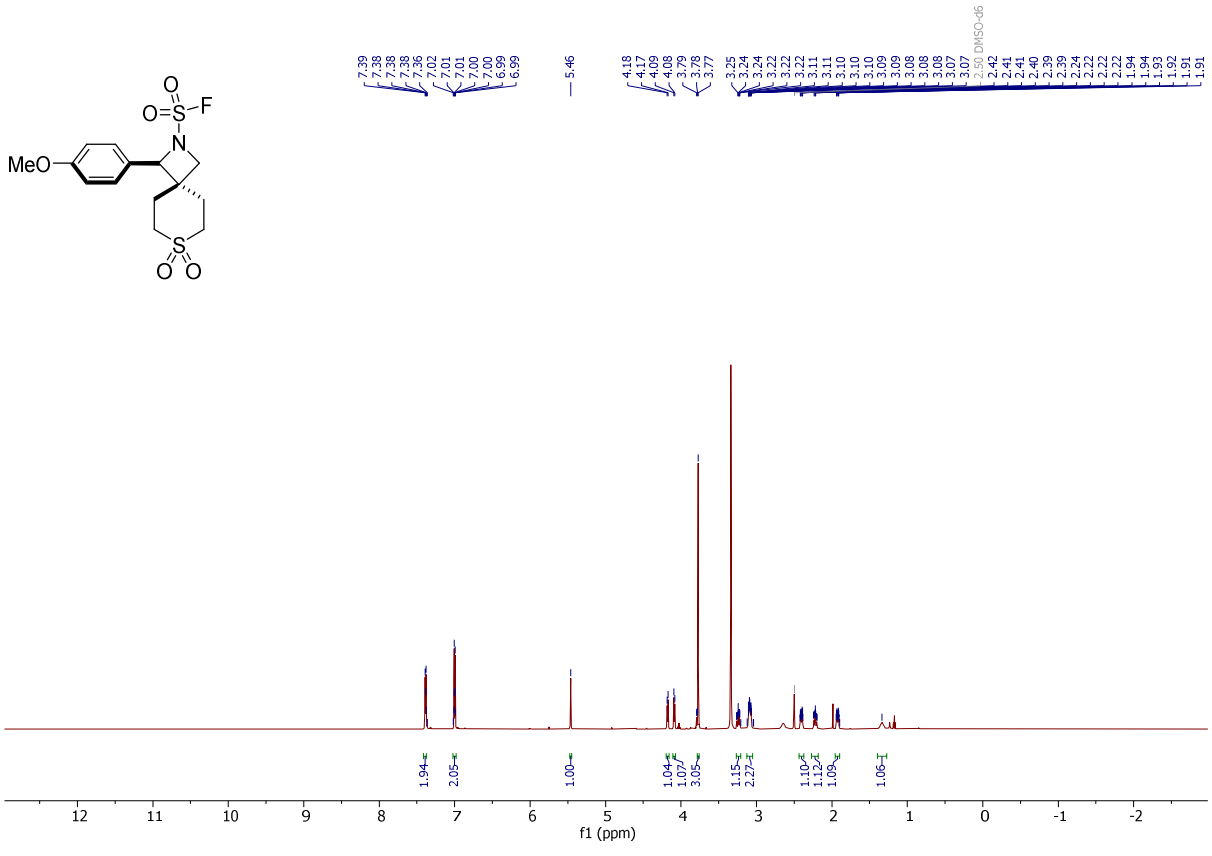

30.18
O
O=S-F
N
MeO
90 80 70 60 50 40 30 20 10 0 -10 -20 -30 -40 -50 -60 -70 -80 -90 -100 -110 -120 -130 -140 -150 -160 -170 -180 -190 -200 -210 -220 -230 -240
f1 (ppm)

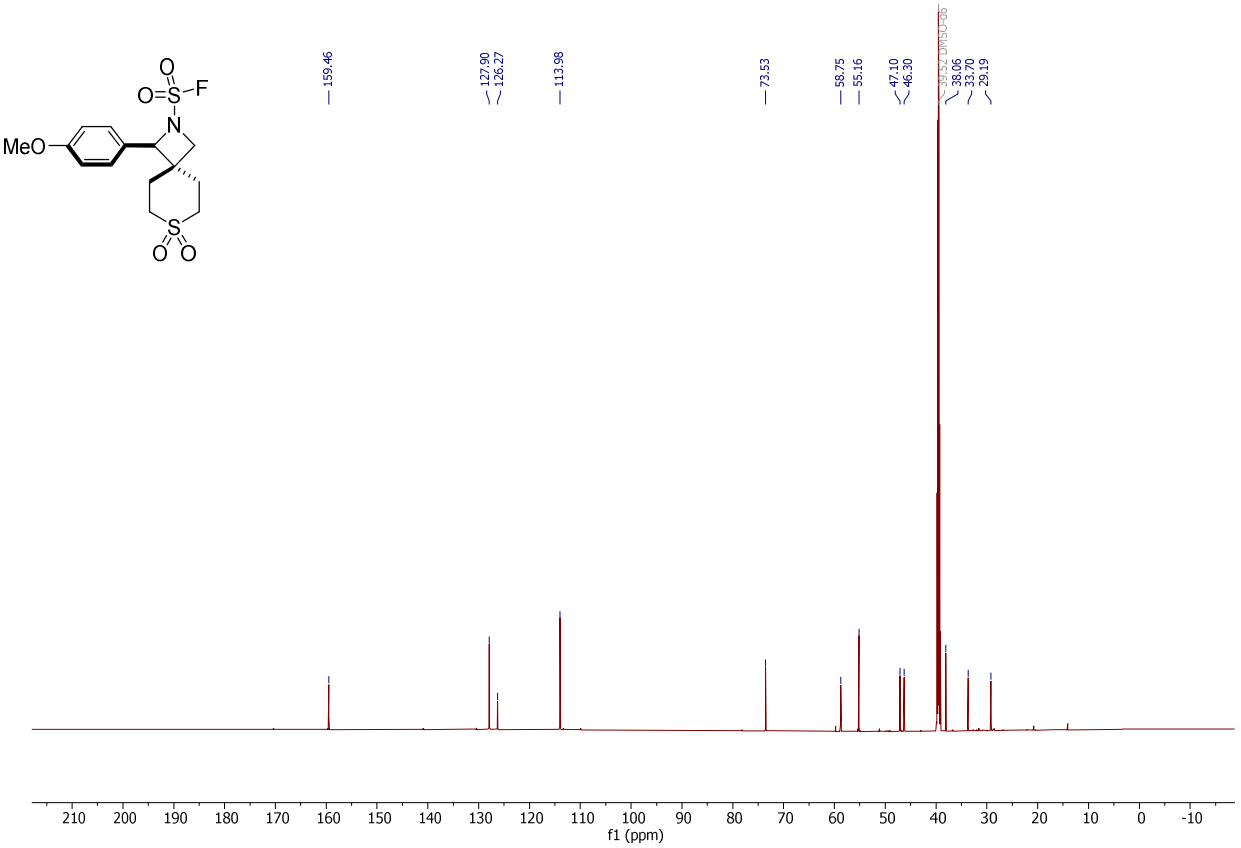
(*R**)-1-(4-Methoxyphenyl)-7-(2,2,2-trifluoroacetyl)-2,7-diazaspiro[3.5]nonane-2-sulfonyl fluoride (4j)

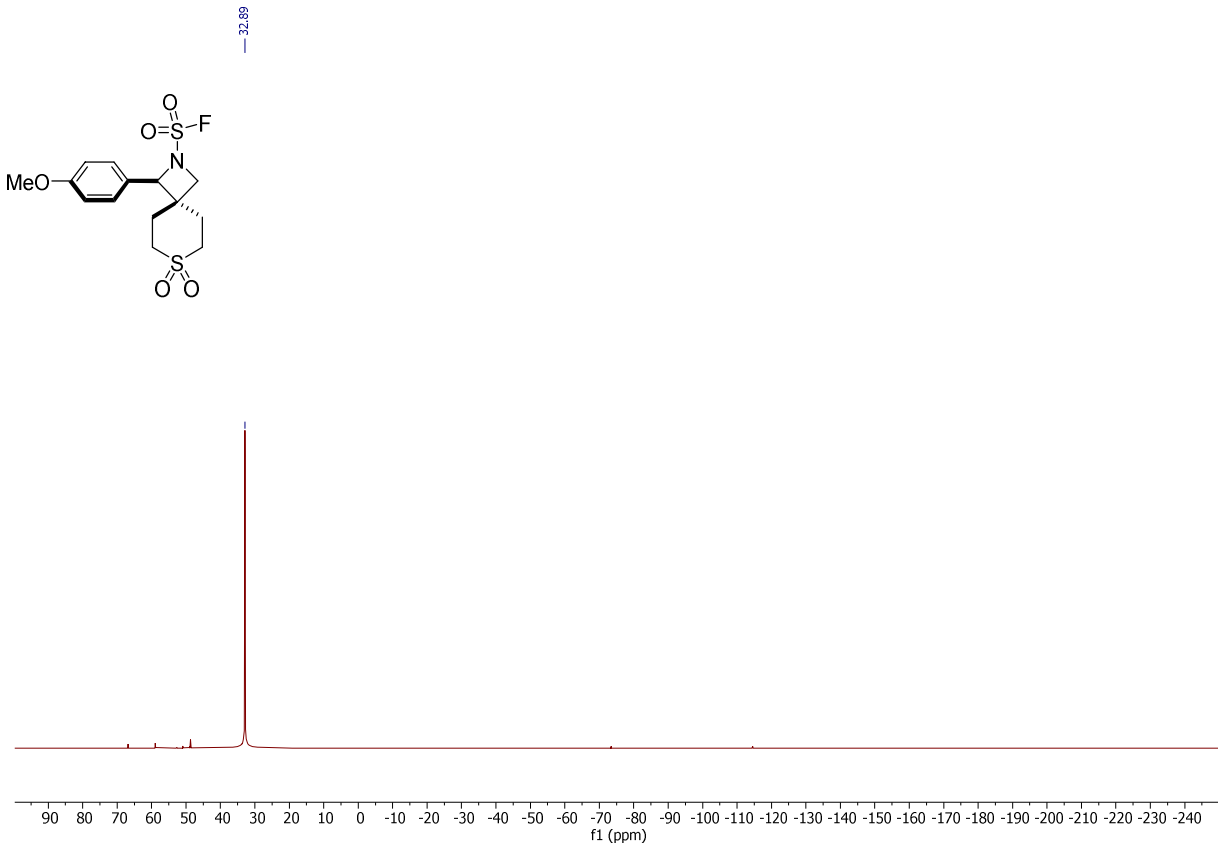




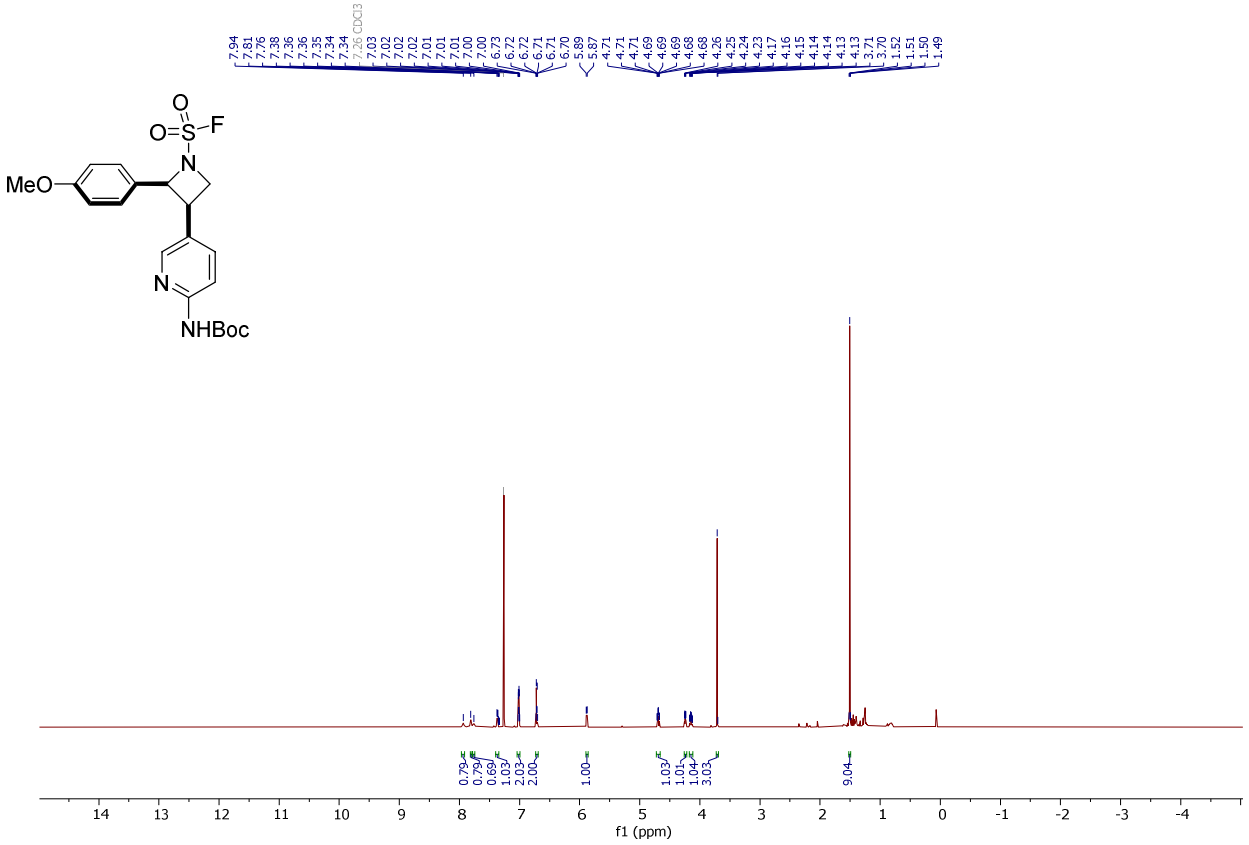
(*R**)-1-(4-Methoxyphenyl)-7-thia-2-azaspiro[3.5]nonane-2-sulfonyl fluoride 7,7-dioxide (4k)

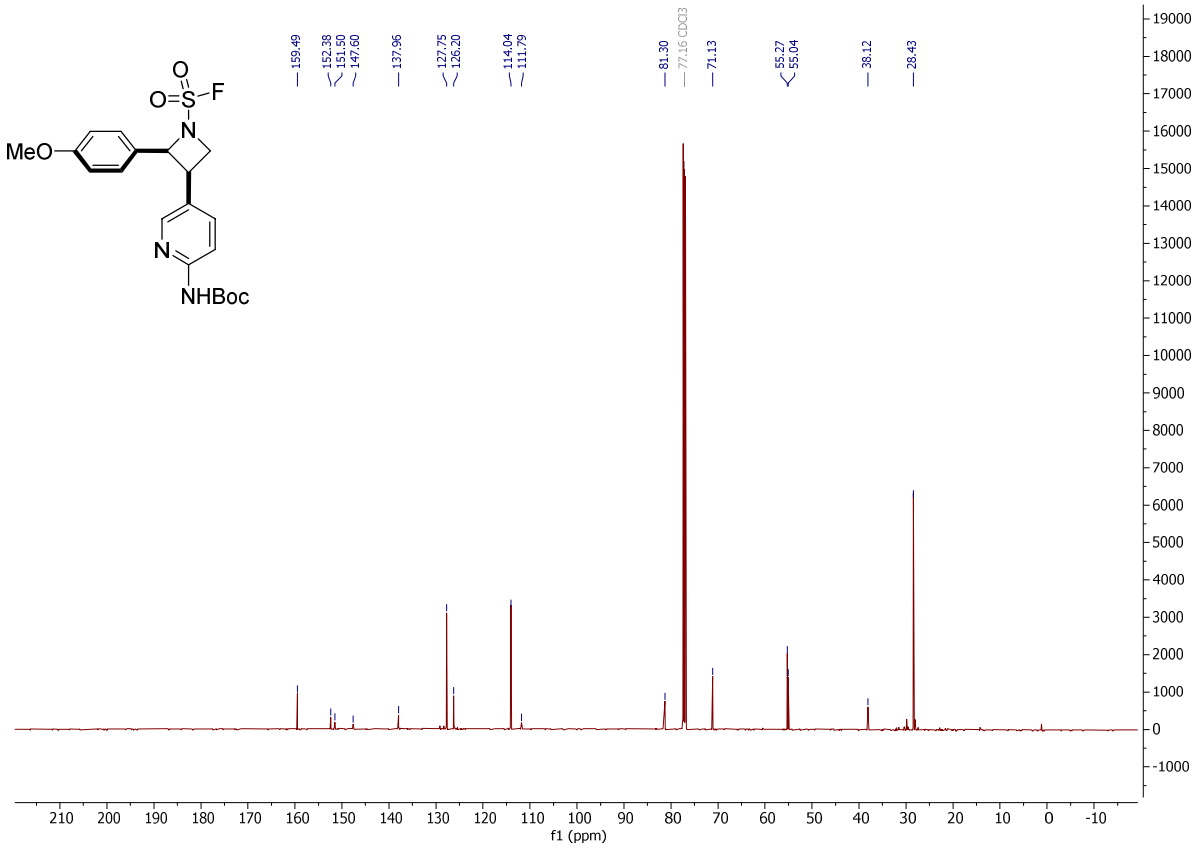


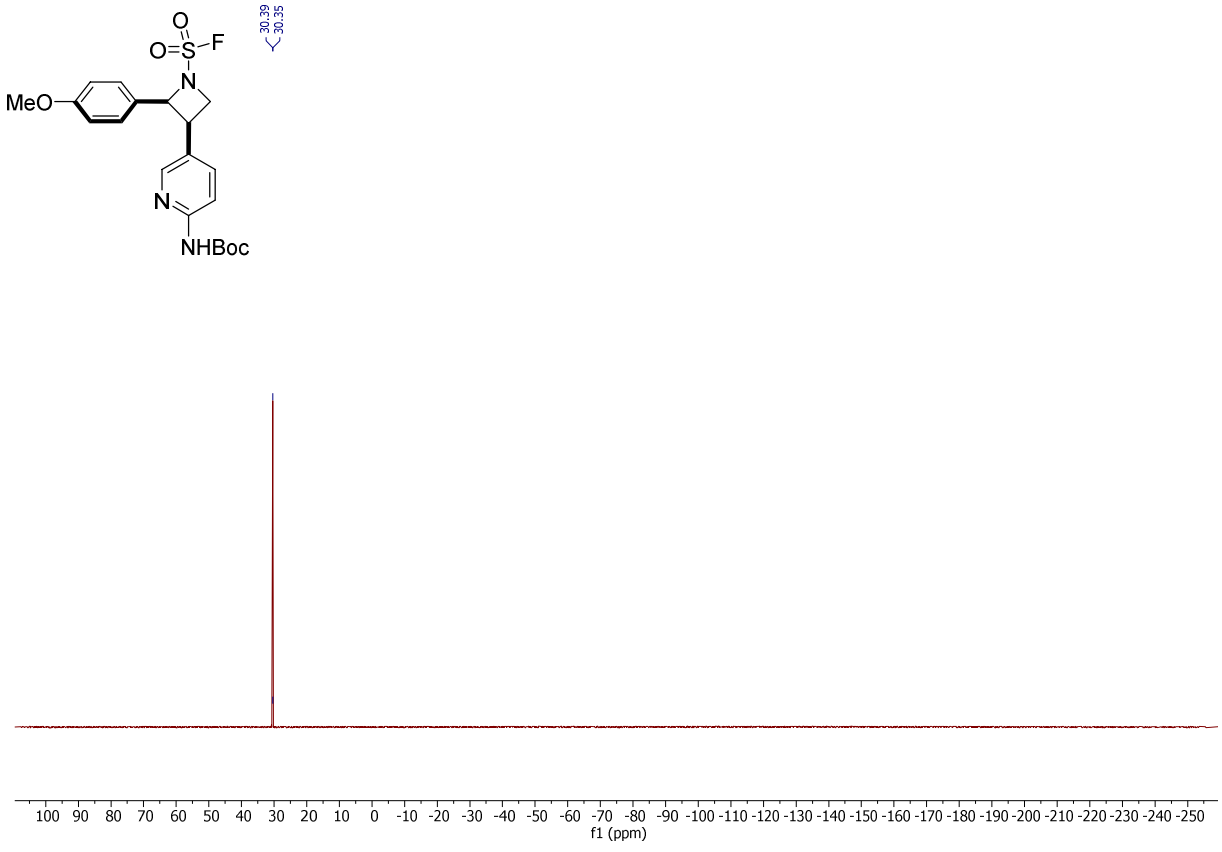

MeO
O=S-F
N
S
O O
159.46
127.90
126.27
113.98
73.53
58.75
55.16
47.10
46.30
39.52
38.06
33.70
29.19
f1 (ppm)


MeO
O=S-F
N
S
O O
32.89
f1 (ppm)

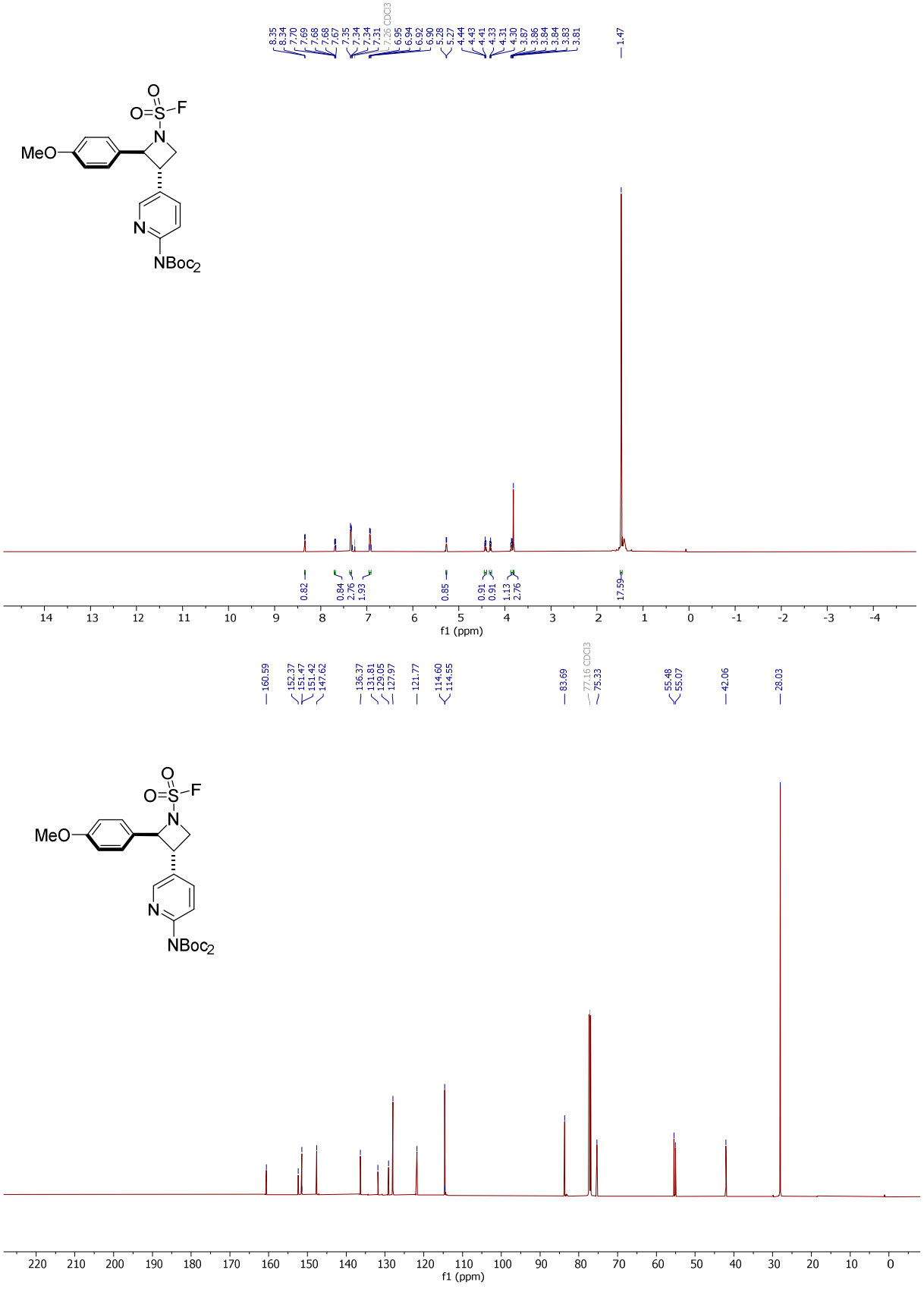
Tert-butyl (5-((2S*,3R*)-1-(fluorosulfonyl)-2-(4-methoxyphenyl)azetidin-3-yl)pyridin-2-yl)carbamate (4l')

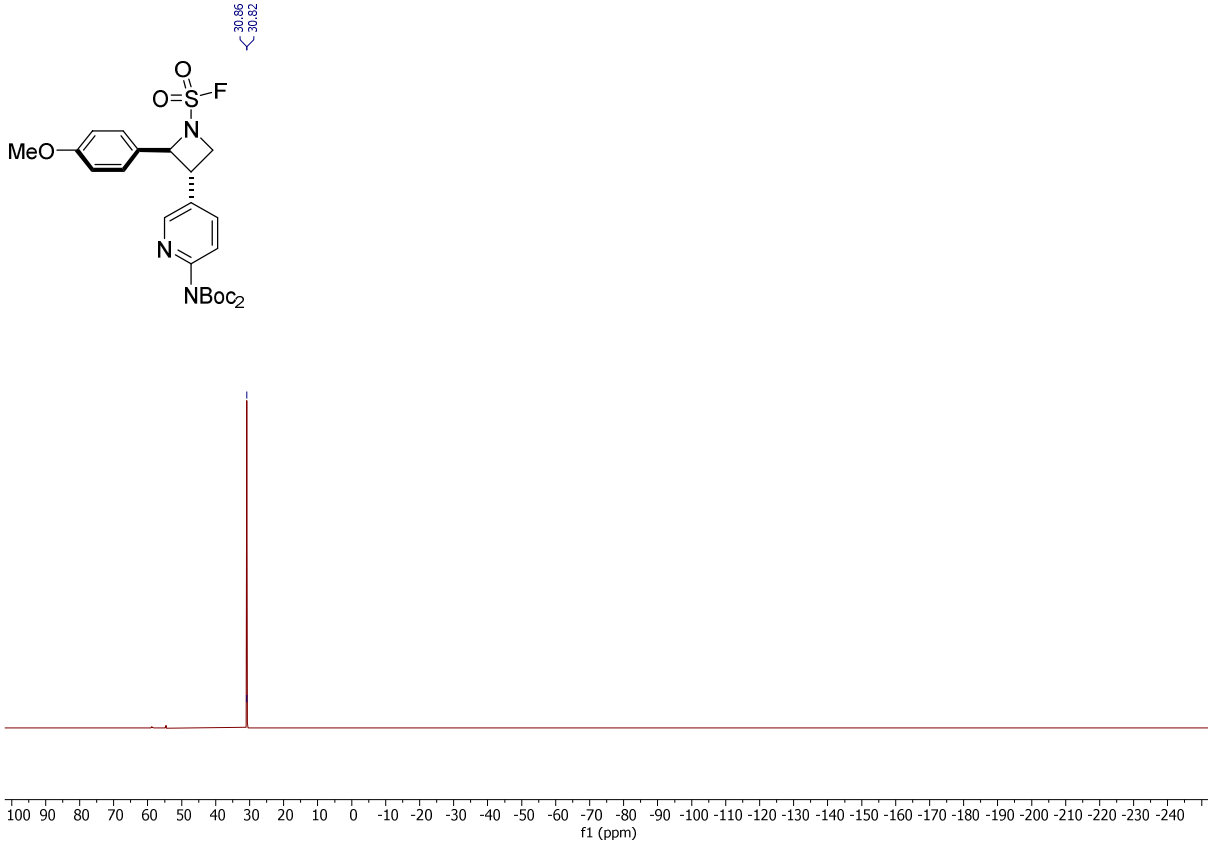



MeO
O
O=S-F
N
N
NHBoc
159.49
152.38
151.50
147.60
137.96
127.75
126.20
114.04
111.79
81.30
77.16 CDCl3
71.13
55.27
55.04
38.12
28.43
f1 (ppm)


MeO
O
O=S-F
N
N
NHBoc
30.39
30.35
f1 (ppm)

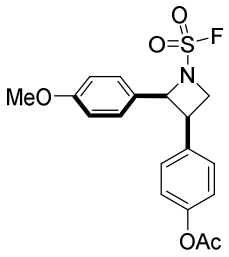
Tert-butyl (*tert*-butoxycarbonyl)(5-((2*R**,3*R**)-1-(fluorosulfonyl)-2-(4-methoxyphenyl)azetidin-3-yl)pyridin-2-yl)carbamate (4l'')

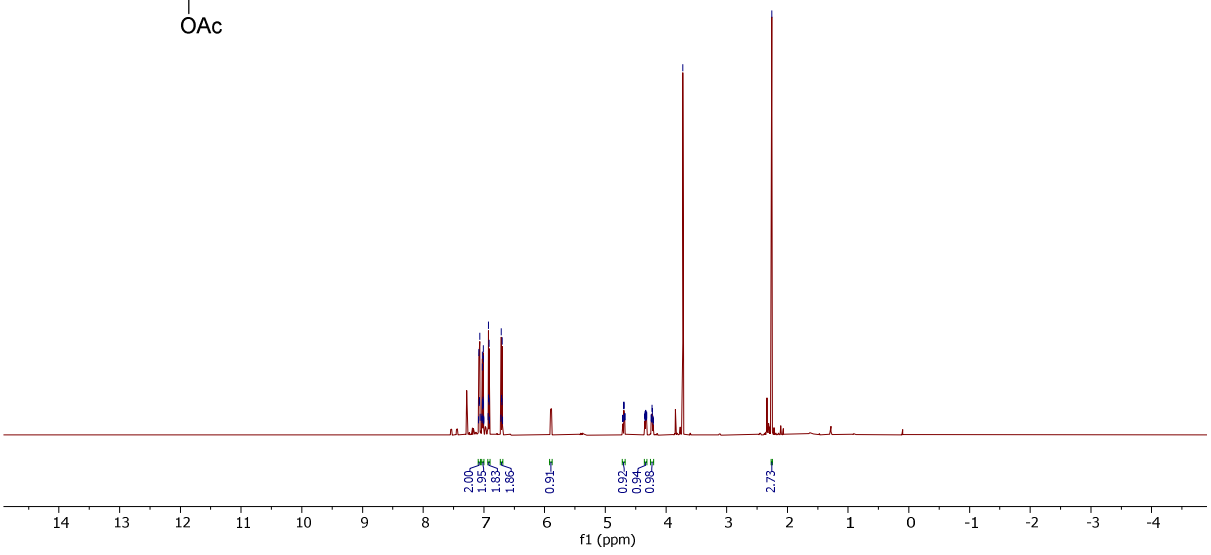



30.86
30.82
O
O=S–F
N
MeO
N
NBoc2
100 90 80 70 60 50 40 30 20 10 0 -10 -20 -30 -40 -50 -60 -70 -80 -90 -100 -110 -120 -130 -140 -150 -160 -170 -180 -190 -200 -210 -220 -230 -240
f1 (ppm)

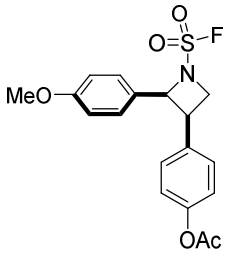
4-((2*R**,3*S**)-1-(Fluorosulfonyl)-2-(4-methoxyphenyl)azetidin-3-yl)phenyl acetate (4m)

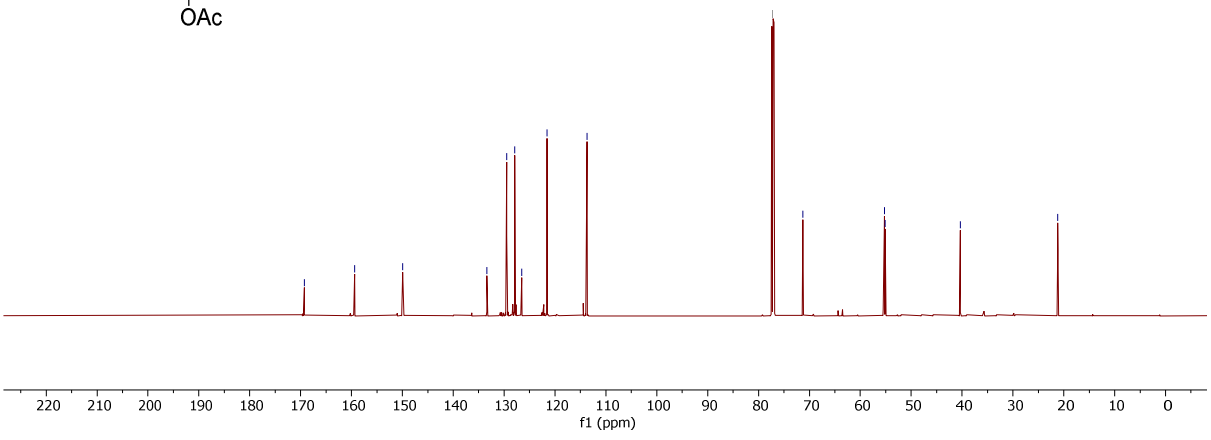


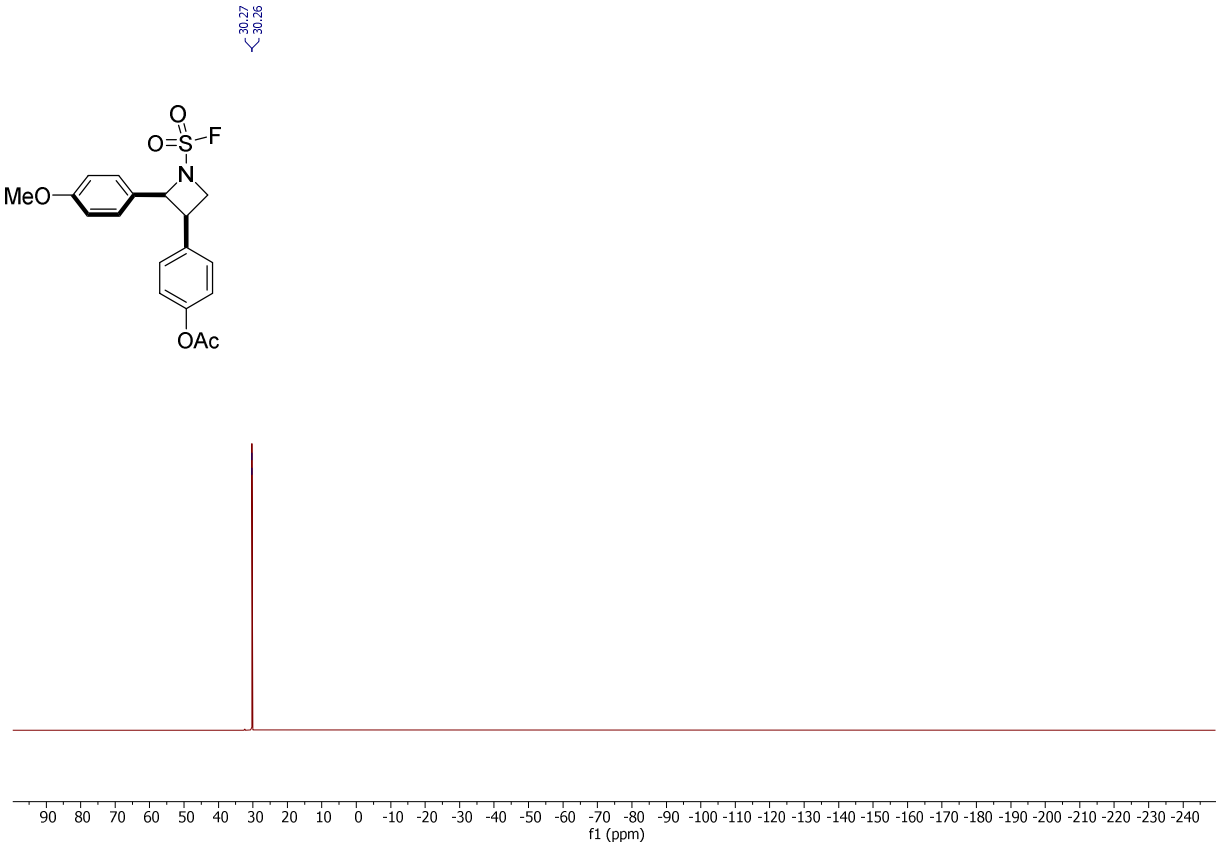




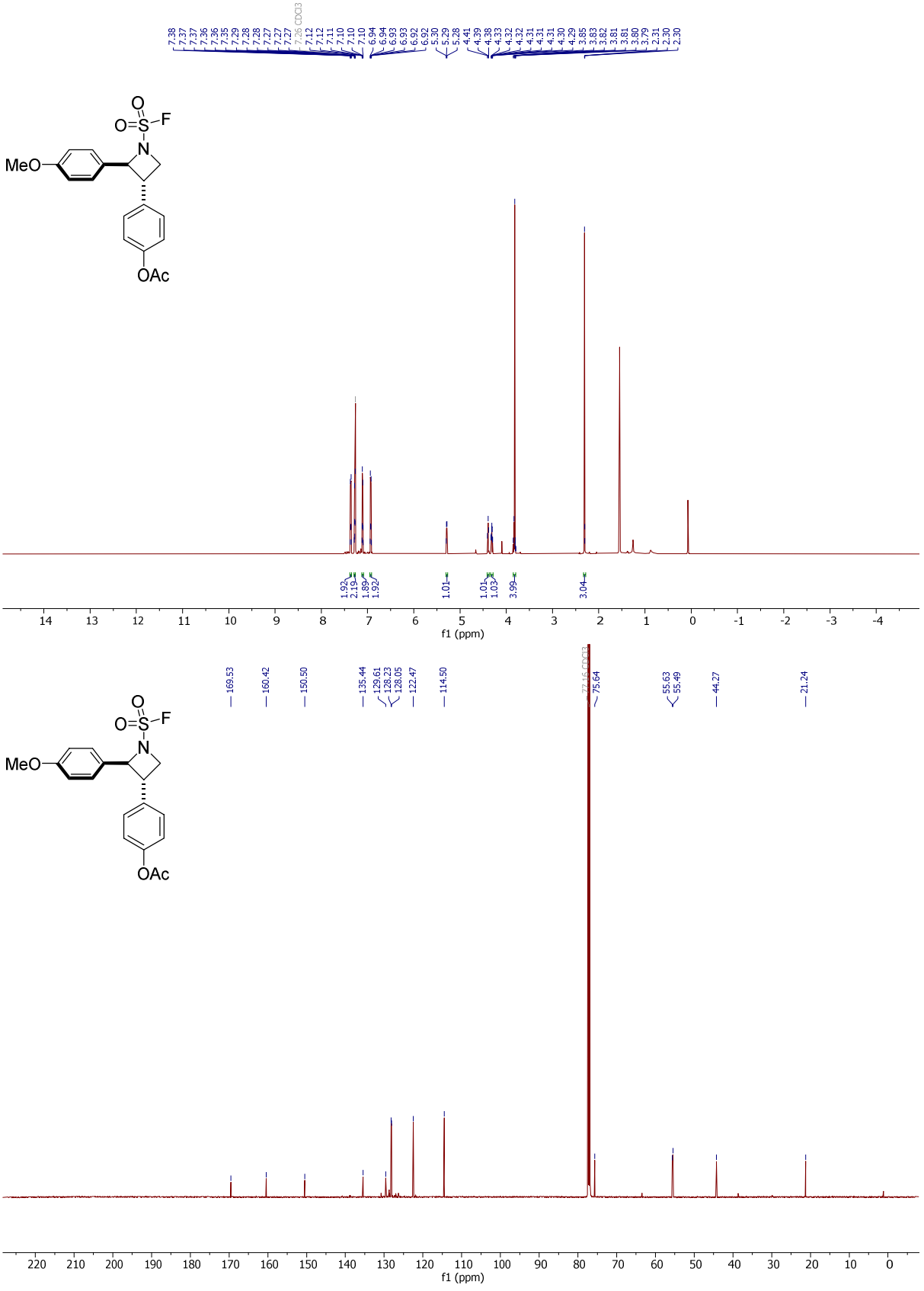






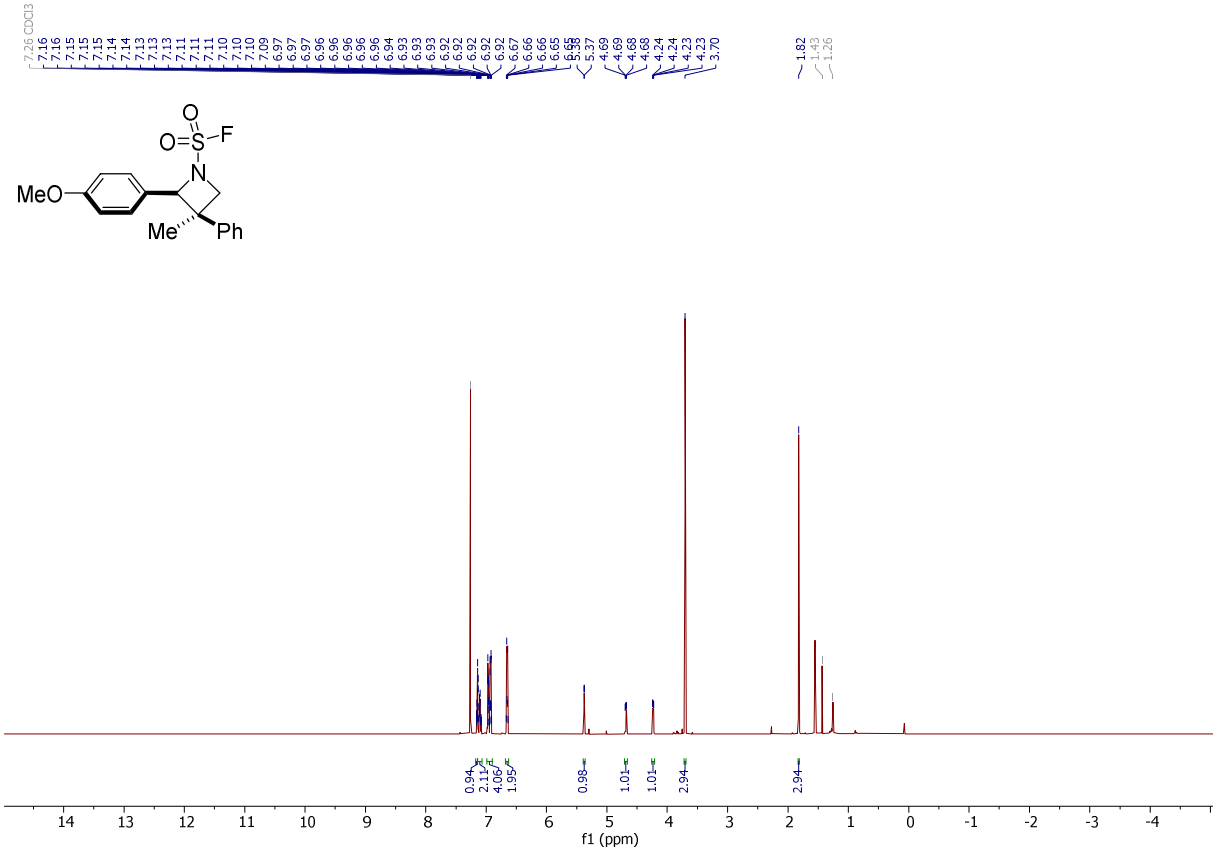

30.27
30.26
O
O=S–F
N
MeO
OAc
90 80 70 60 50 40 30 20 10 0 -10 -20 -30 -40 -50 -60 -70 -80 -90 -100 -110 -120 -130 -140 -150 -160 -170 -180 -190 -200 -210 -220 -230 -240
f1 (ppm)

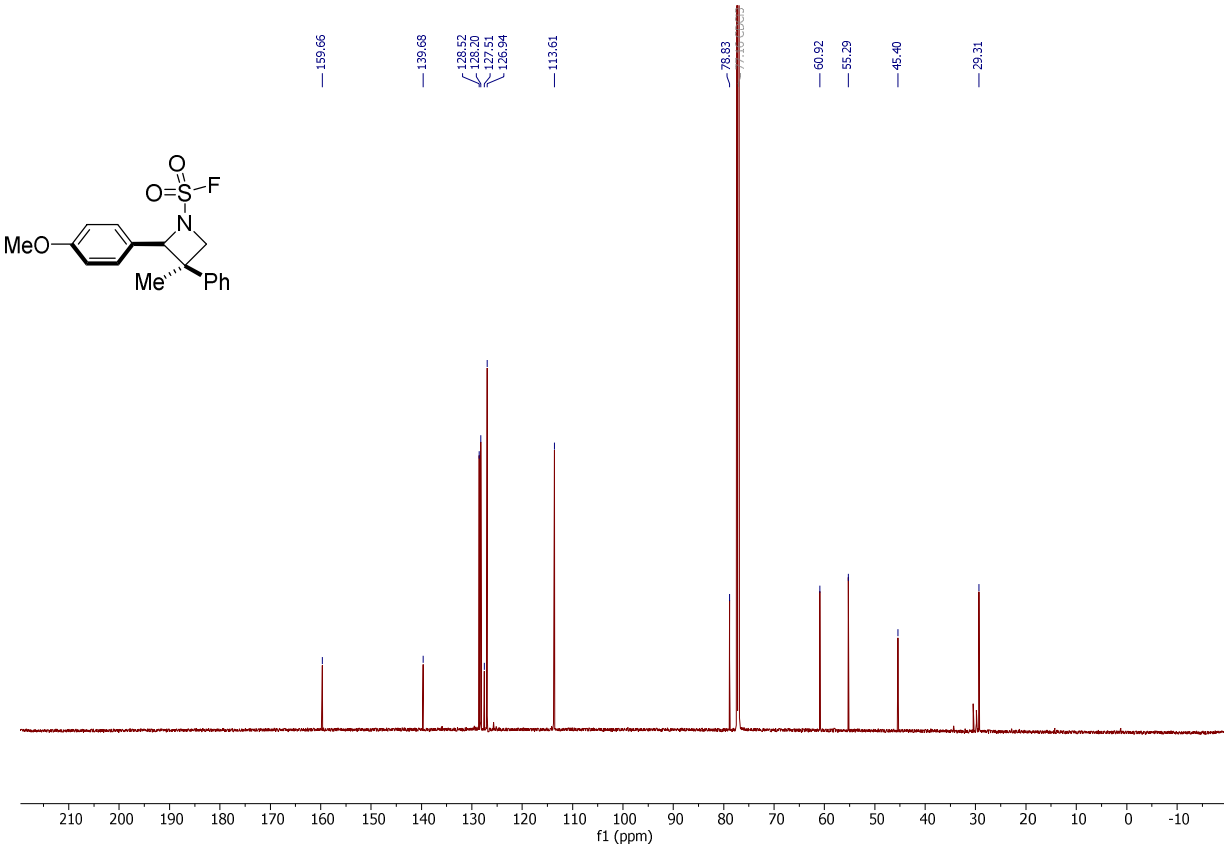
4-((2*R**,3*R**)-1-(Fluorosulfonyl)-2-(4-methoxyphenyl)azetidin-3-yl)phenyl acetate (4m')

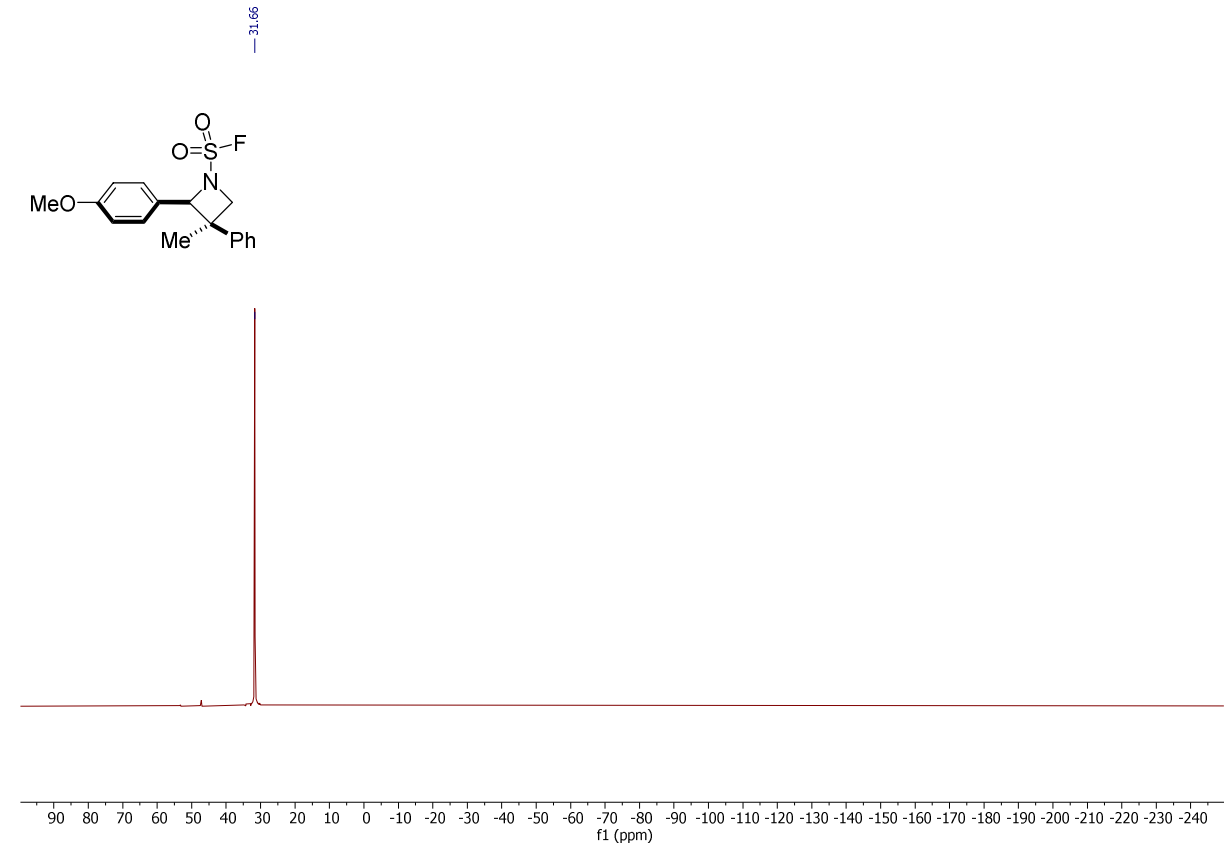




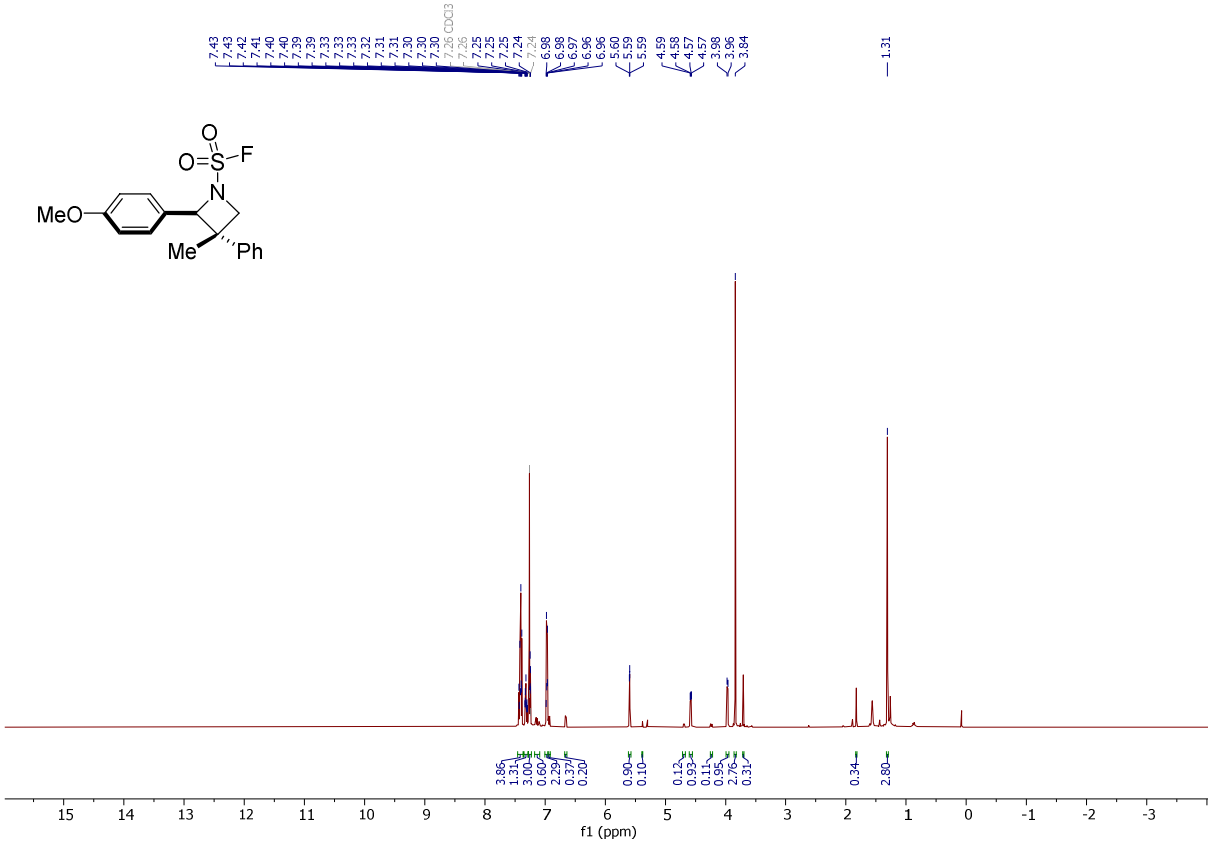
(2*R**,3*R**)-2-(4-Methoxyphenyl) -3-methyl-3-phenylazetidine-1-sulfonyl fluoride (4n)

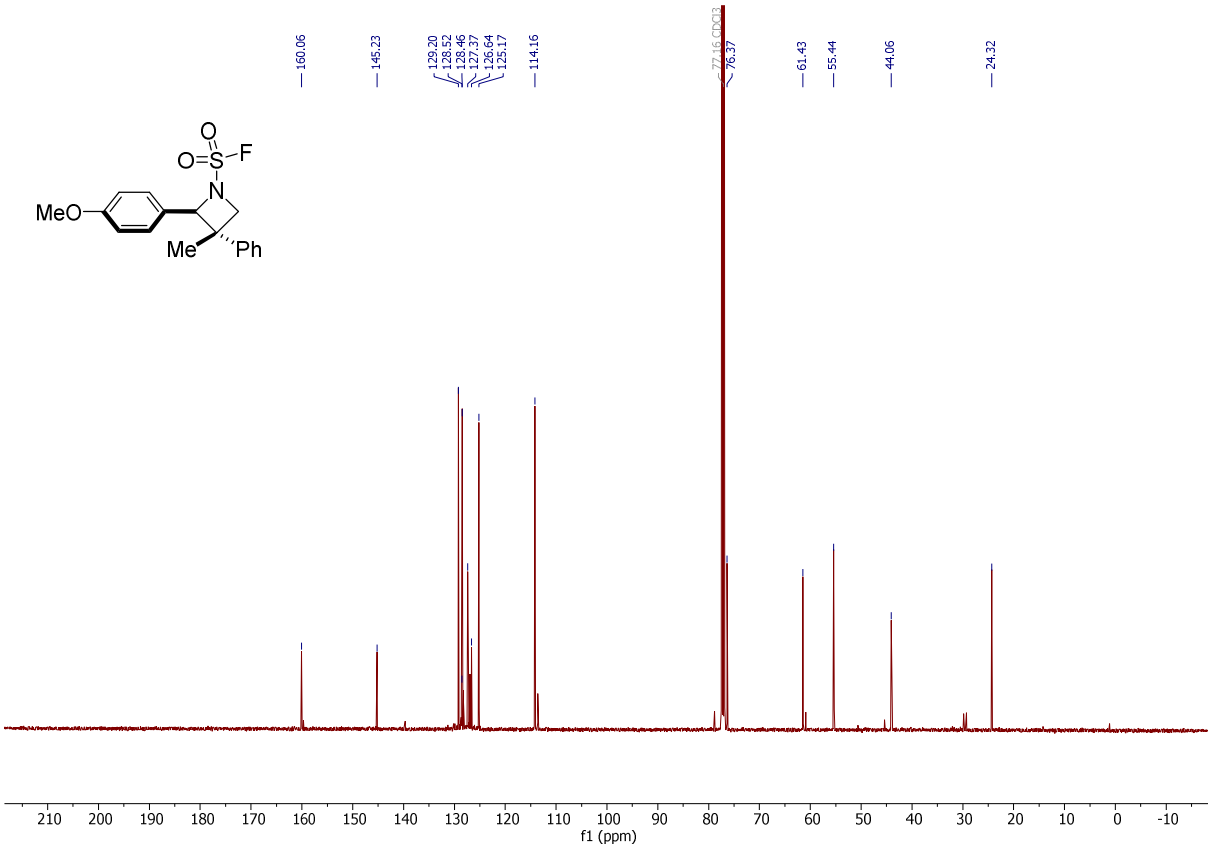


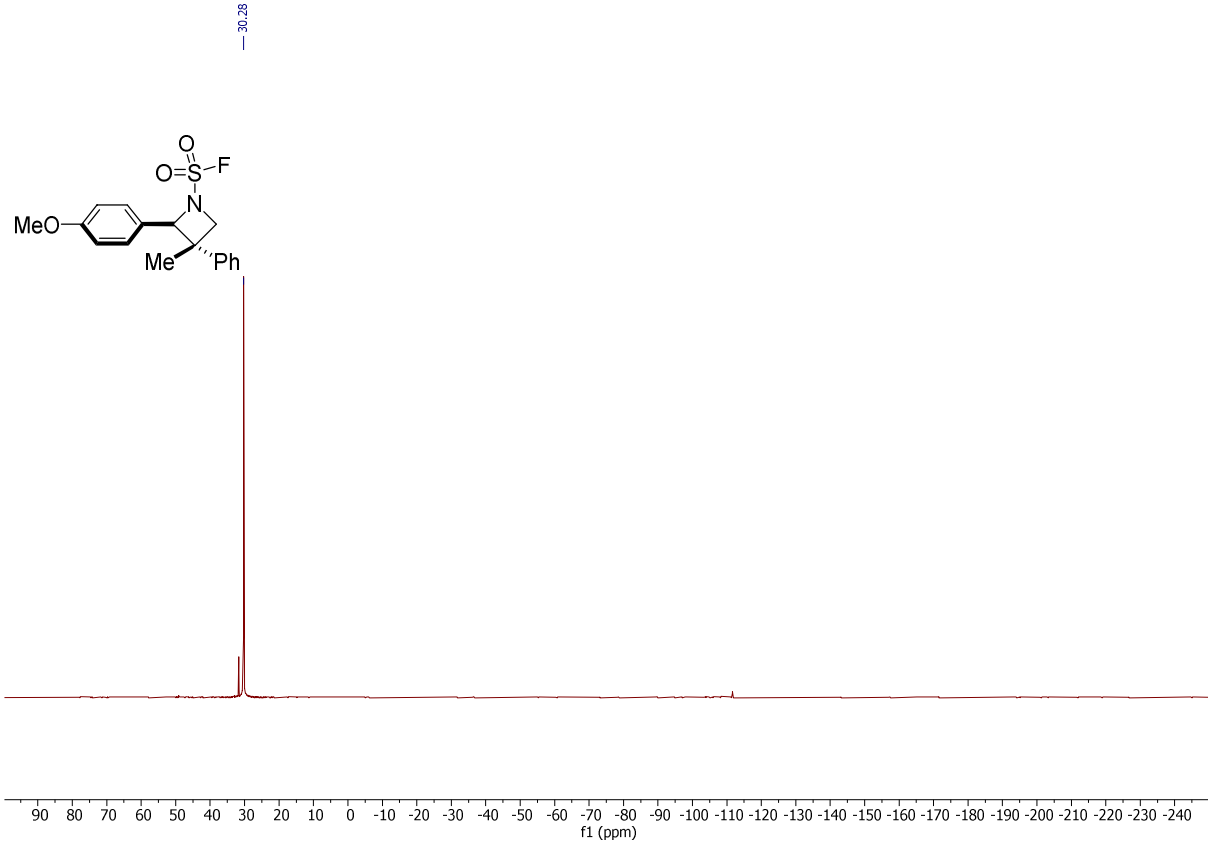

159.66
139.68
128.52
128.20
127.51
126.94
113.61
78.83
60.92
55.29
45.40
29.31
O
O=S–F
N
MeO
Me
Ph
210 200 190 180 170 160 150 140 130 120 110 100 90 80 70 60 50 40 30 20 10 0 -10
f1 (ppm)


31.66
O
O=S–F
N
MeO
Me
Ph
90 80 70 60 50 40 30 20 10 0 -10 -20 -30 -40 -50 -60 -70 -80 -90 -100 -110 -120 -130 -140 -150 -160 -170 -180 -190 -200 -210 -220 -230 -240
f1 (ppm)

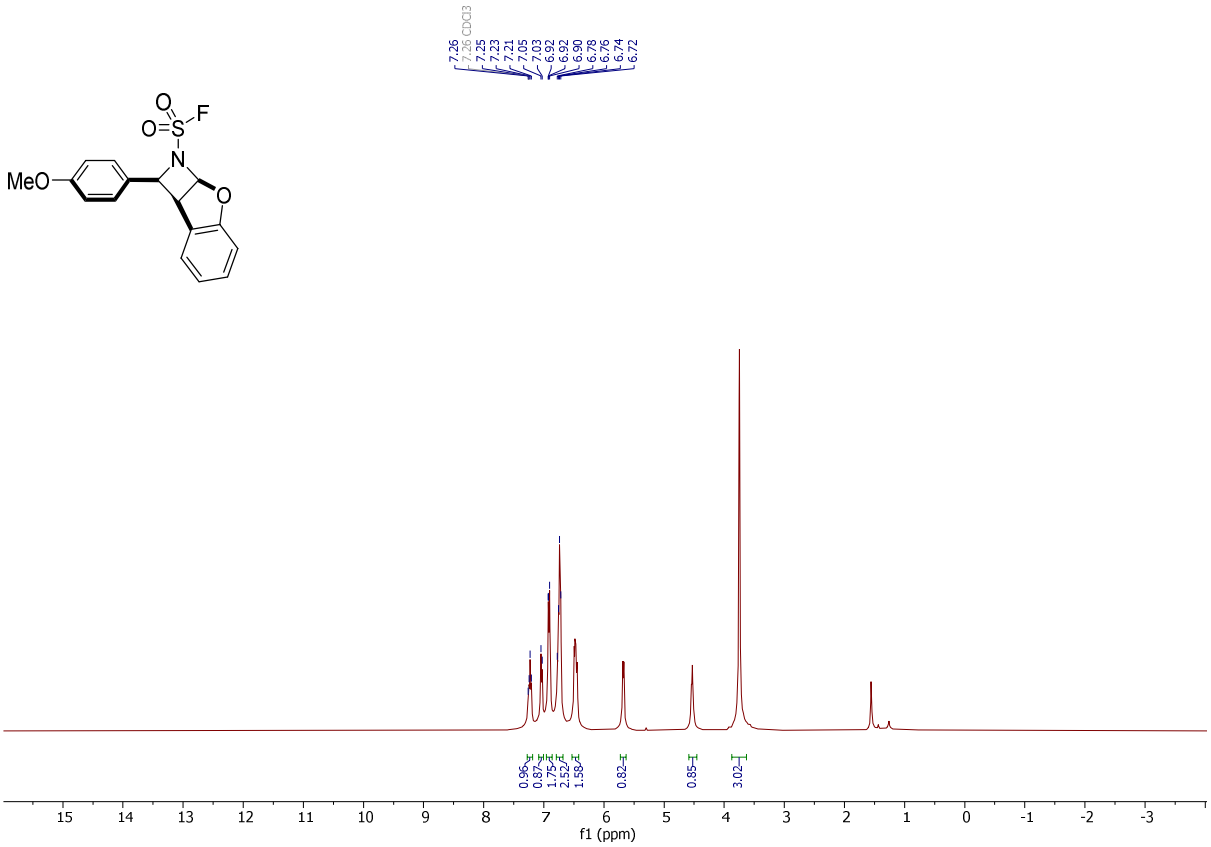
(2*R**,3*S**)-2-(4-Methoxyphenyl)-3-methyl-3-phenylazetidine-1-sulfonyl fluoride (4n')

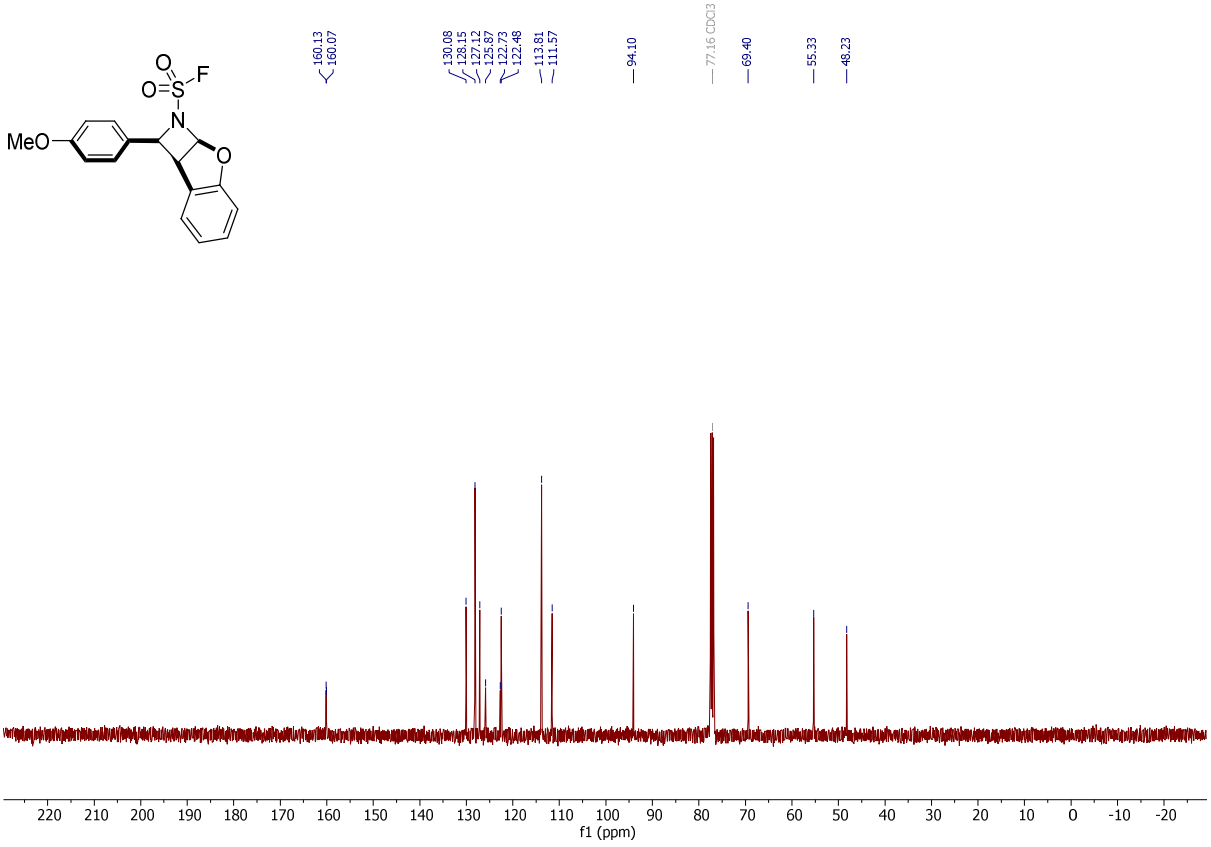


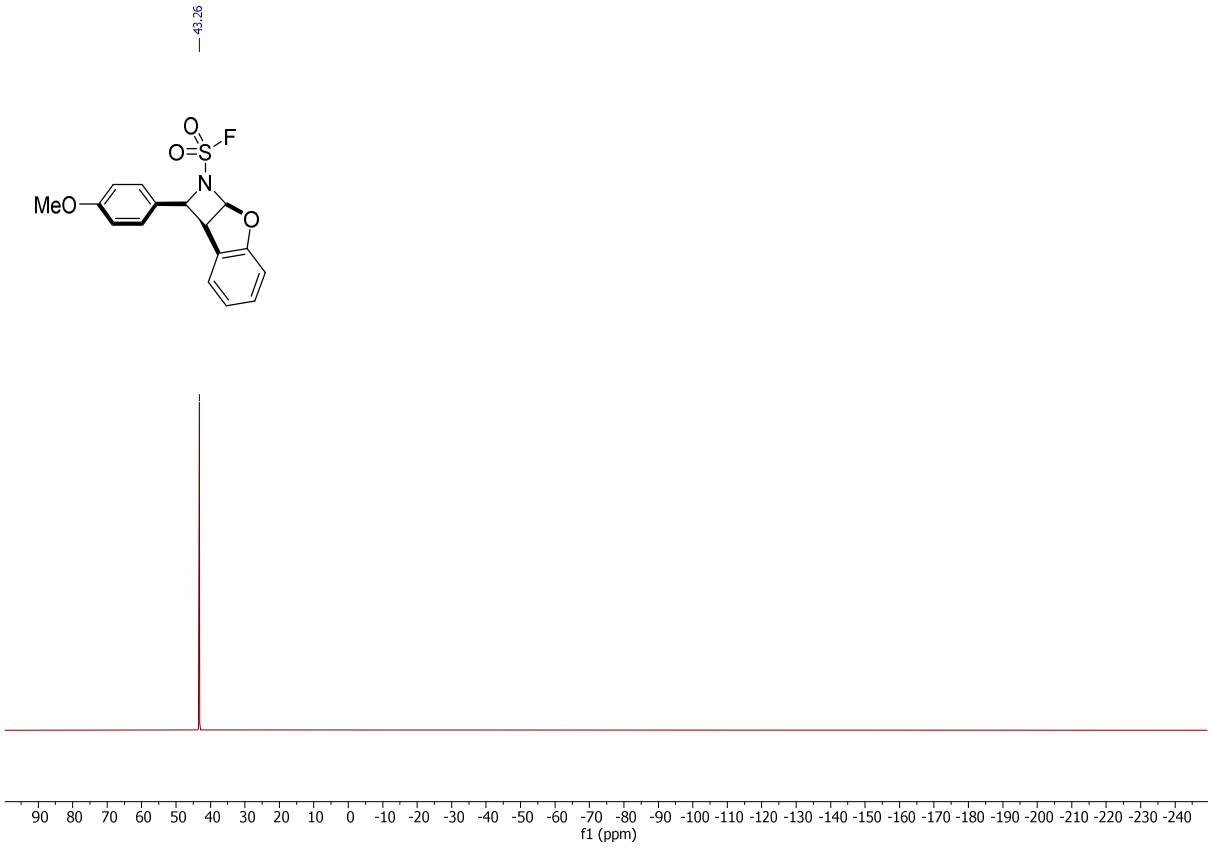

160.06
145.23
129.20
128.52
128.46
127.37
126.64
125.17
114.16
77.16 CDCl3
76.37
61.43
55.44
44.06
24.32
O
O=S–F
N
MeO
Me
Ph
210 200 190 180 170 160 150 140 130 120 110 100 90 80 70 60 50 40 30 20 10 0 -10
f1 (ppm)


30.28
O
O=S–F
N
MeO
Me
Ph
90 80 70 60 50 40 30 20 10 0 -10 -20 -30 -40 -50 -60 -70 -80 -90 -100 -110 -120 -130 -140 -150 -160 -170 -180 -190 -200 -210 -220 -230 -240
f1 (ppm)

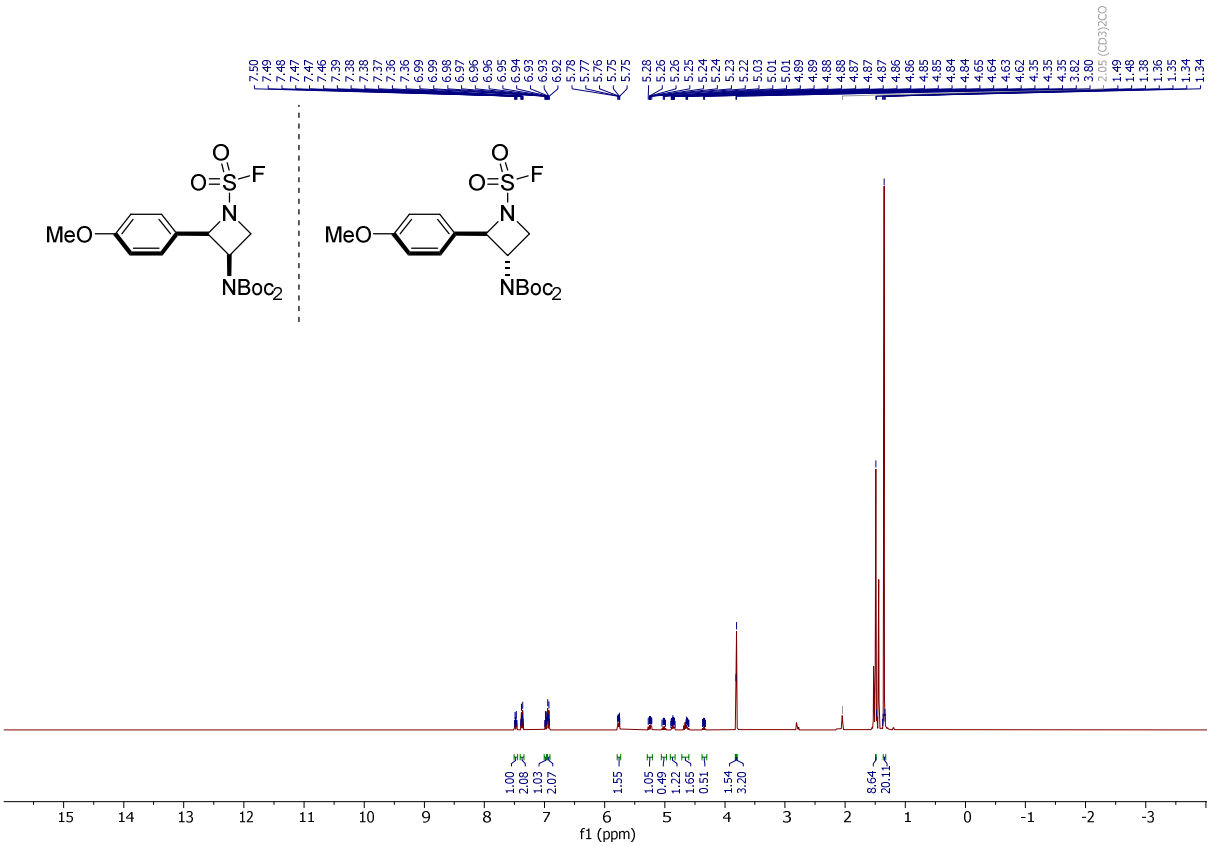
(2*S**,2a*S**,7a*S**)-2-(4-Methoxyphenyl)-2a,7a-dihydrobenzofuro[2,3-*b*]azete-1(2*H*)-sulfonyl fluoride (4o)

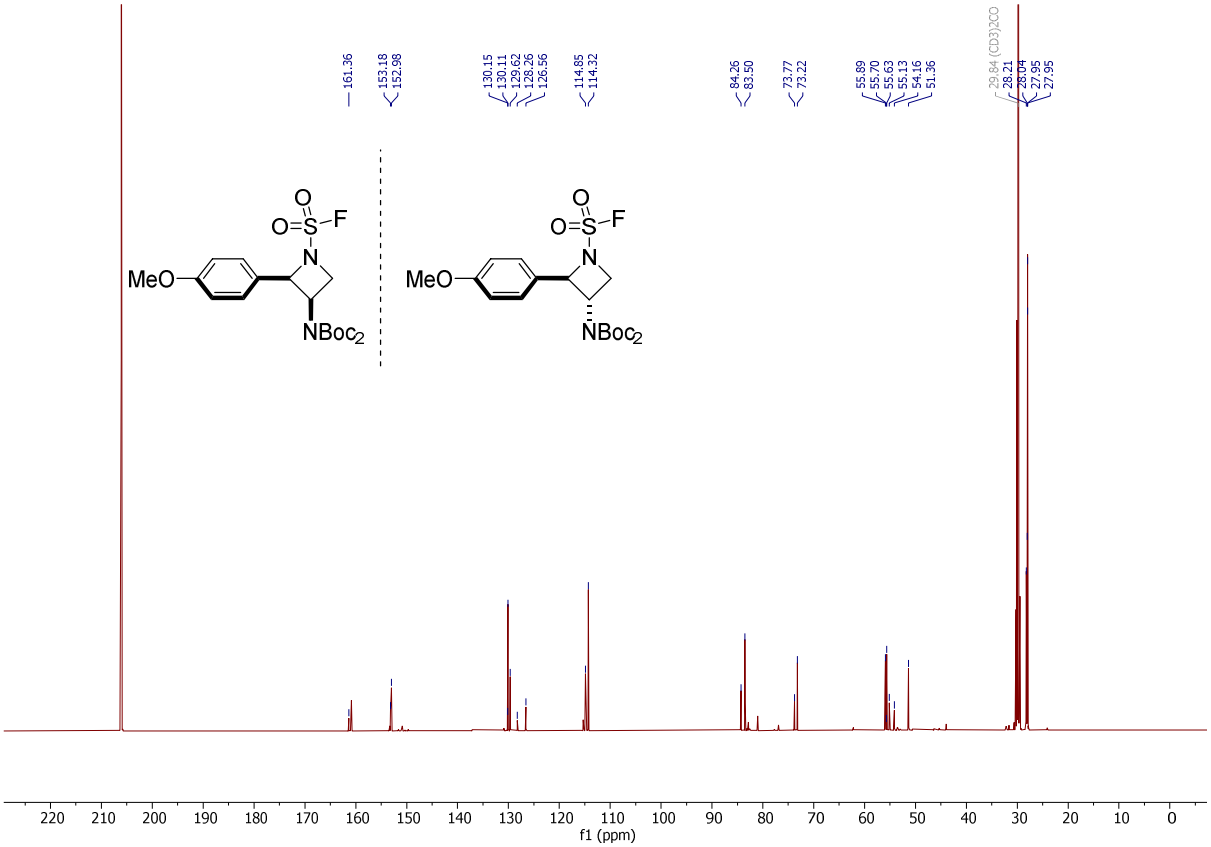

7.26
7.25 CDCl3
7.25
7.23
7.21
7.05
7.03
6.93
6.92
6.90
6.78
6.76
6.74
6.72
O
O=S
F
N
MeO
O
0.96
0.97
1.75
2.52
1.58
0.82
0.85
3.02
15 14 13 12 11 10 9 8 7 6 5 4 3 2 1 0 -1 -2 -3
f1 (ppm)

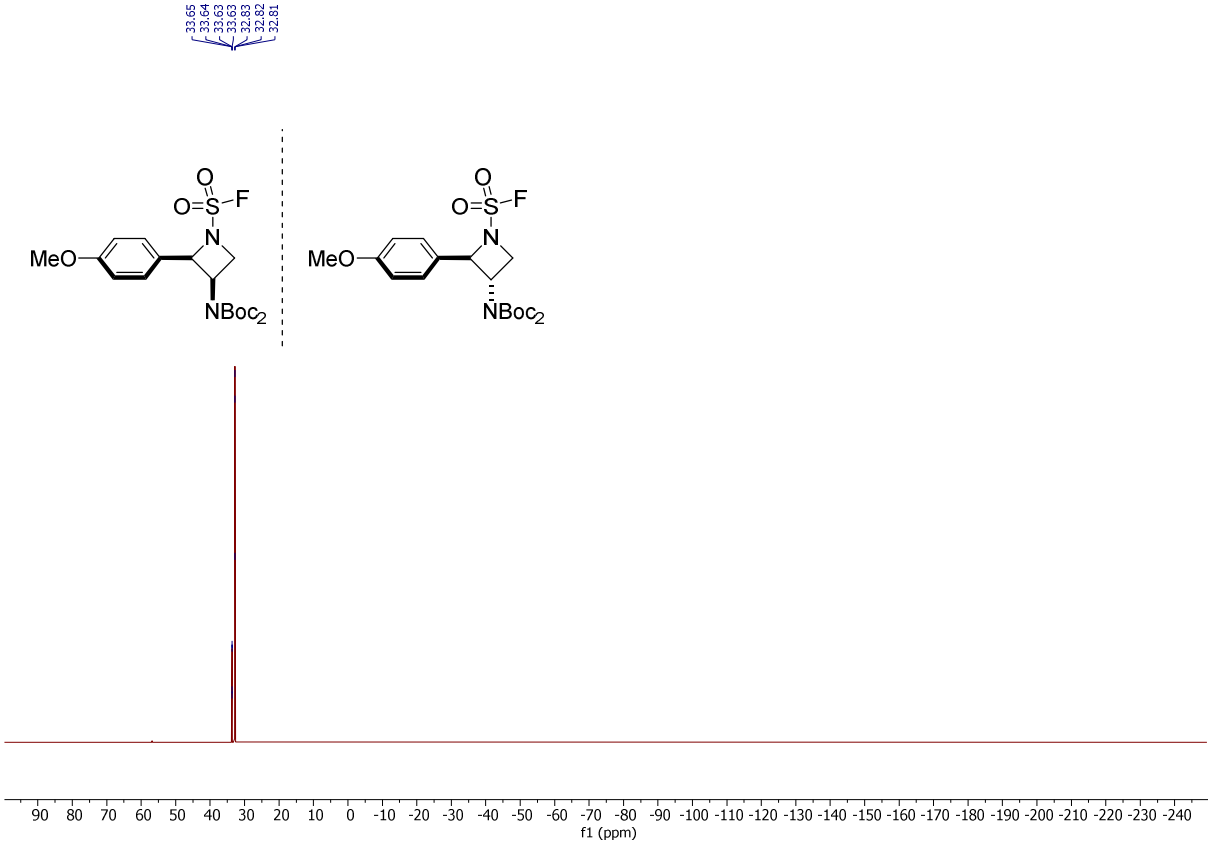

160.13
160.07
130.08
128.15
127.12
125.87
122.73
122.48
113.81
111.57
94.10
77.16 CDCl3
69.40
55.33
48.23
O
O=S
F
N
MeO
O
220 210 200 190 180 170 160 150 140 130 120 110 100 90 80 70 60 50 40 30 20 10 0 -10 -20
f1 (ppm)


43.26
O
O=S
F
N
MeO
O
90 80 70 60 50 40 30 20 10 0 -10 -20 -30 -40 -50 -60 -70 -80 -90 -100 -110 -120 -130 -140 -150 -160 -170 -180 -190 -200 -210 -220 -230 -240
f1 (ppm)

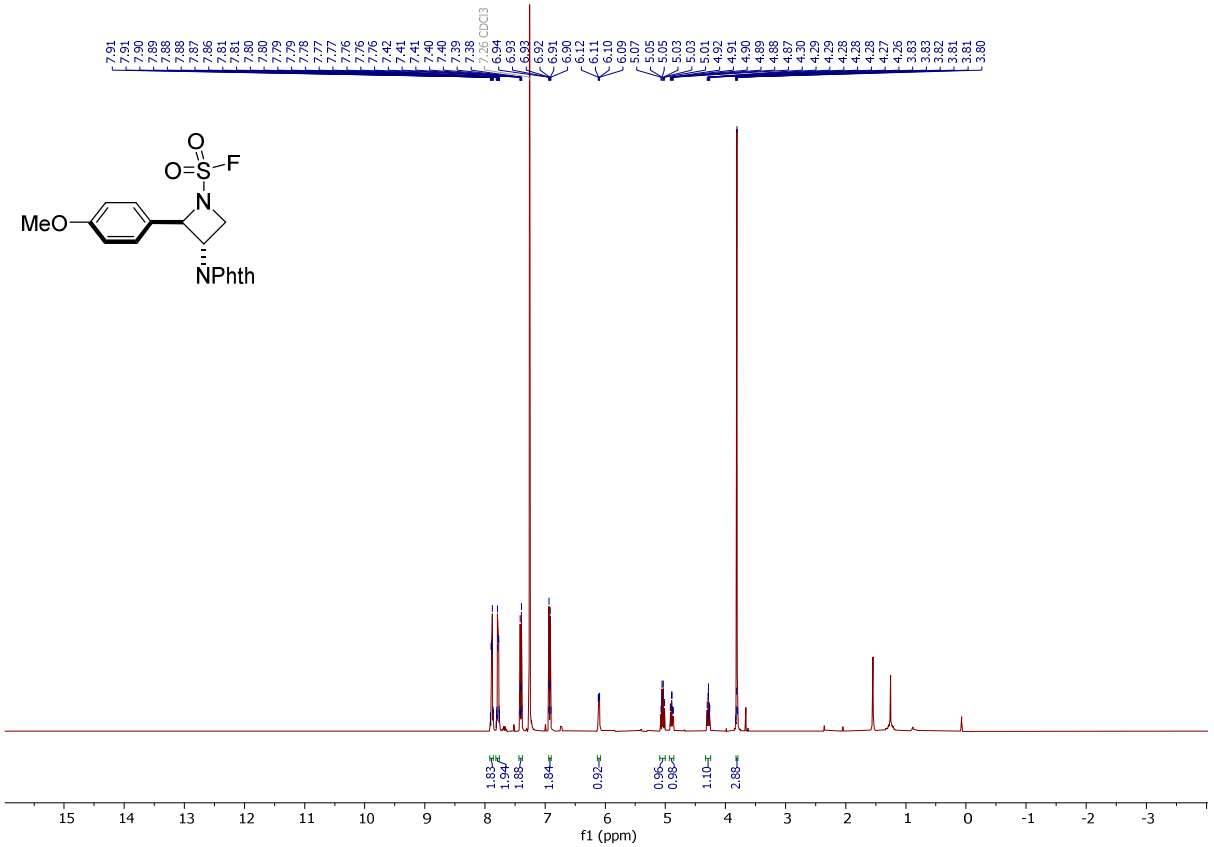
Tert-butyl (*tert*-butoxycarbonyl)((2*R**,3*R**)-1-(fluorosulfonyl)-2-(4-methoxyphenyl)azetidin-3-yl)carbamate (4p) and *Tert*-butyl (*tert*-butoxycarbonyl)((2*R**,3*S**)-1-(fluorosulfonyl)-2-(4-methoxyphenyl)azetidin-3-yl)carbamate (4p')

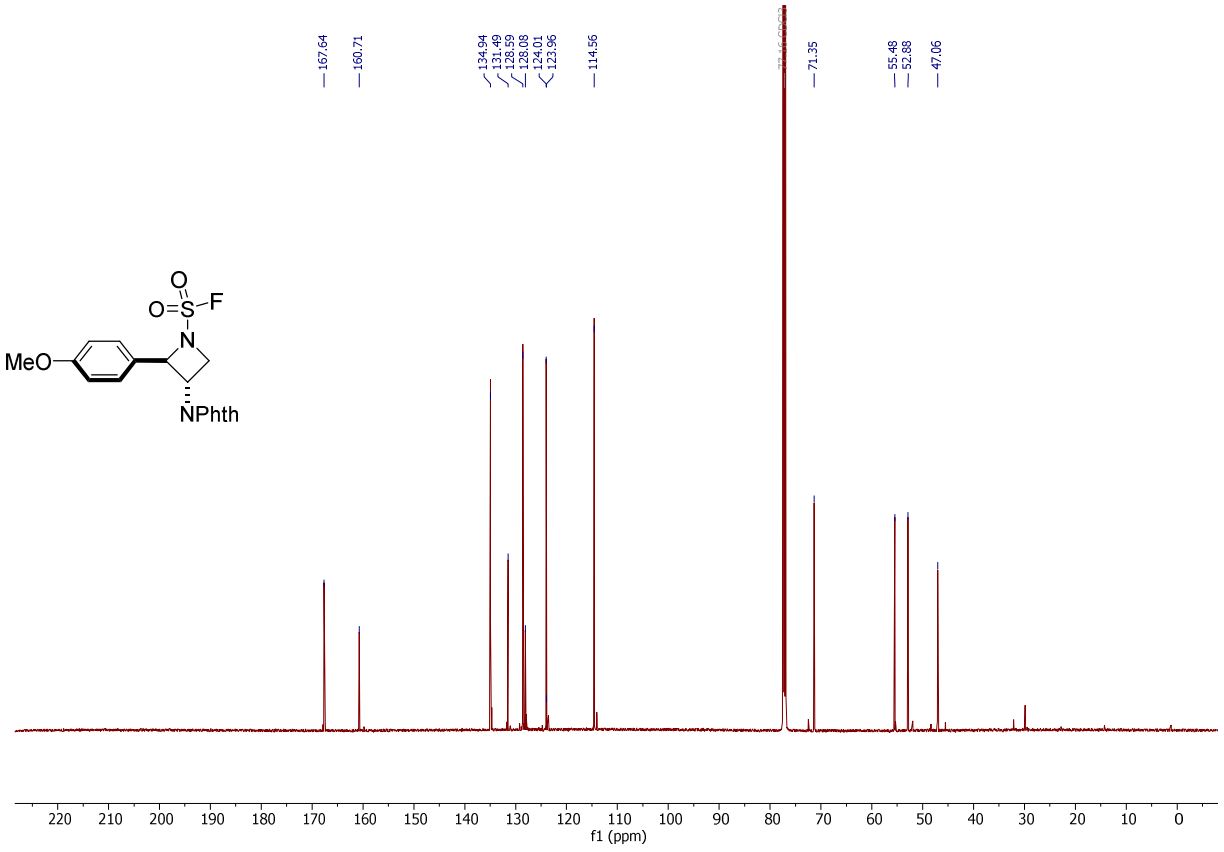

MeO
NBoc2
f1 (ppm)

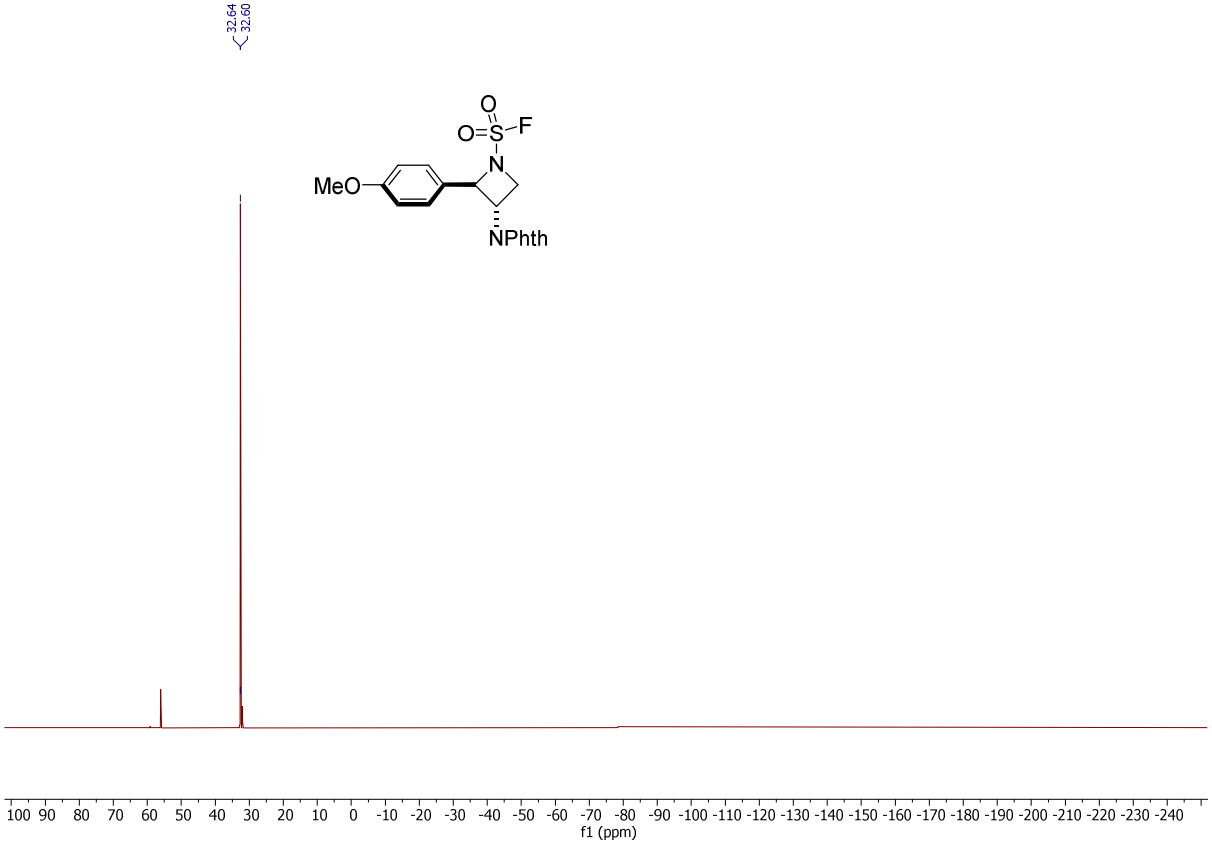

MeO
NBoc2
f1 (ppm)


33.65
33.64
33.63
33.63
32.83
32.82
32.81
O
O=S–F
N
MeO
NBoc2
O
O=S–F
N
MeO
NBoc2
90 80 70 60 50 40 30 20 10 0 -10 -20 -30 -40 -50 -60 -70 -80 -90 -100 -110 -120 -130 -140 -150 -160 -170 -180 -190 -200 -210 -220 -230 -240
f1 (ppm)

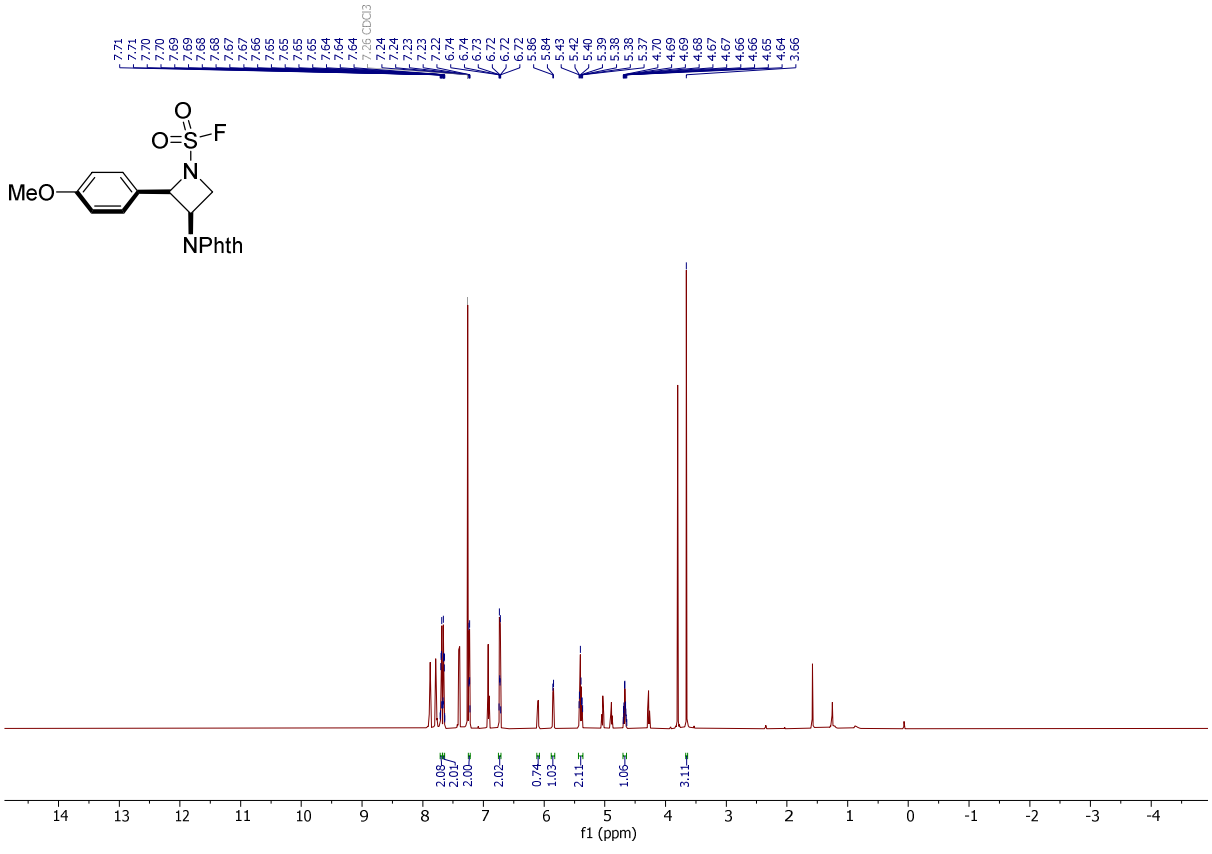
(2*R**,3*S**)-3-(1,3-Dioxoisoindolin-2-yl)-2-(4-methoxyphenyl)azetidine-1-sulfonyl fluoride (4q)

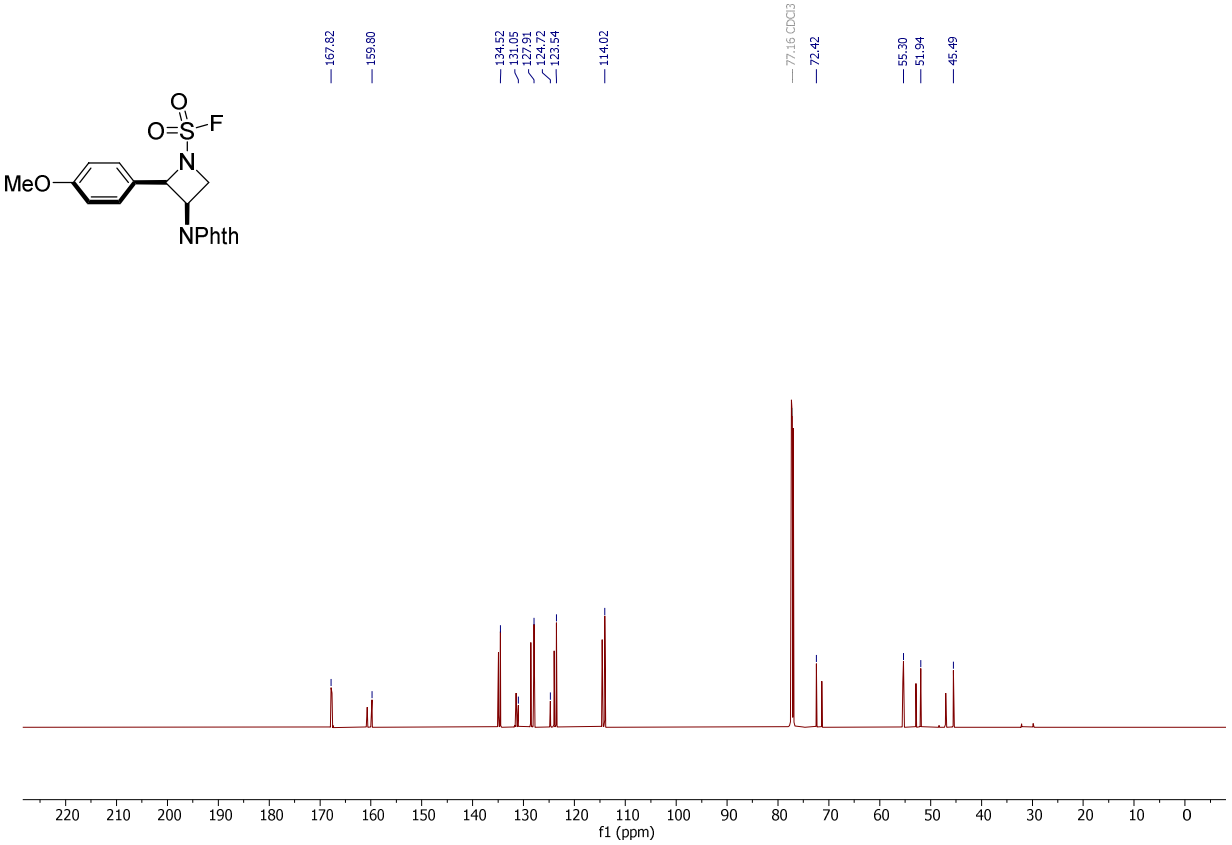


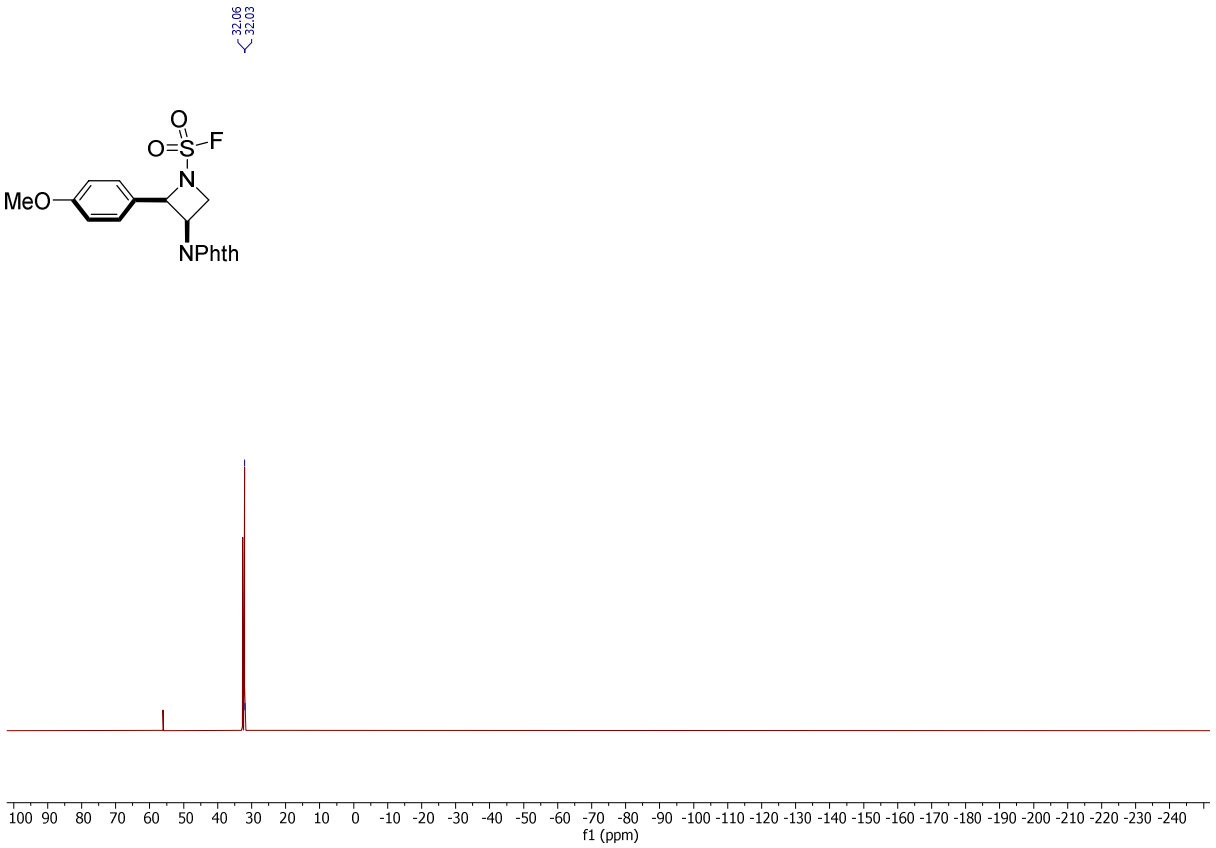




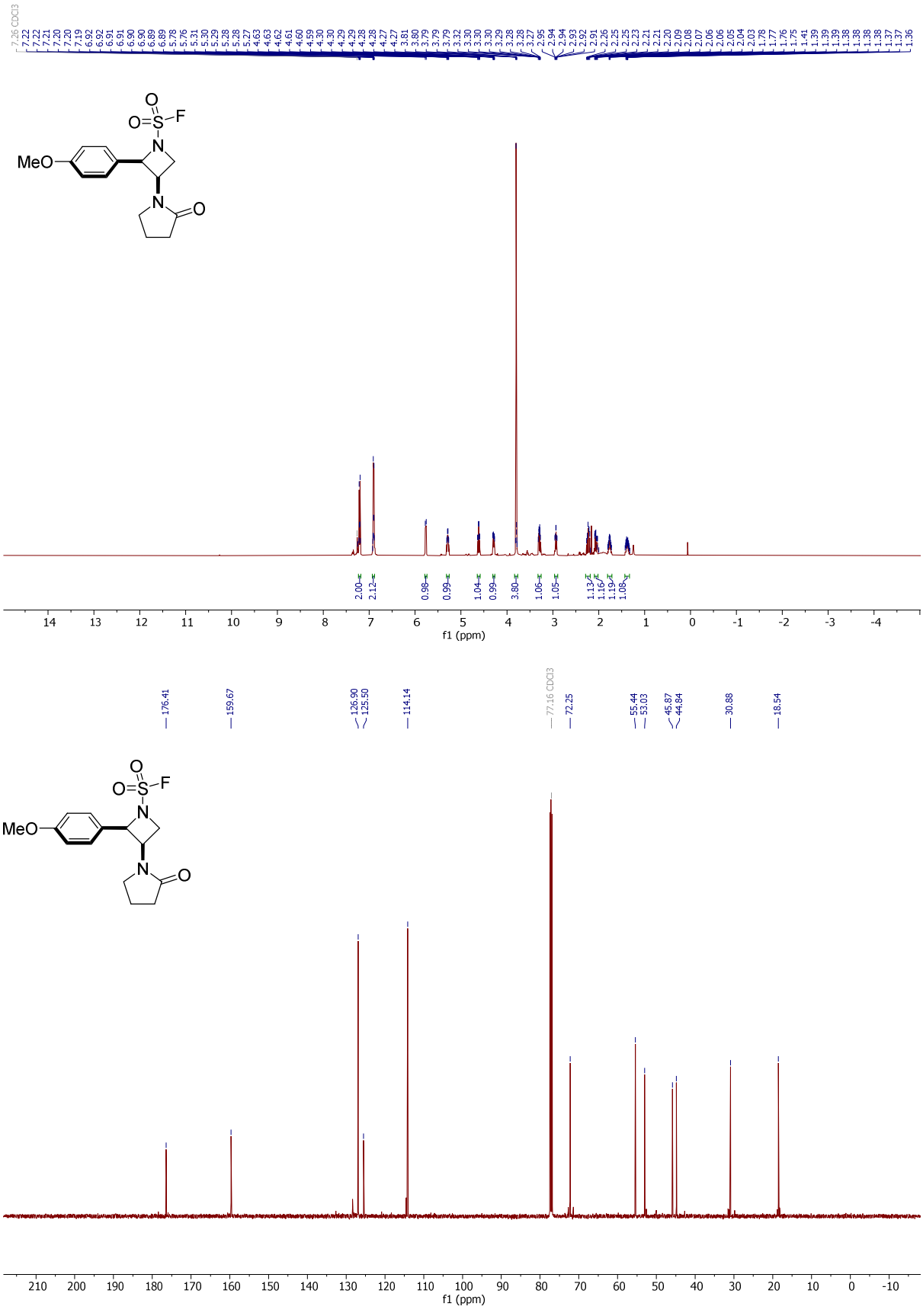
(2*R**,3*R**)-3-(1,3-Dioxoisoindolin-2-yl)-2-(4-methoxyphenyl)azetidine-1-sulfonyl fluoride (4q')

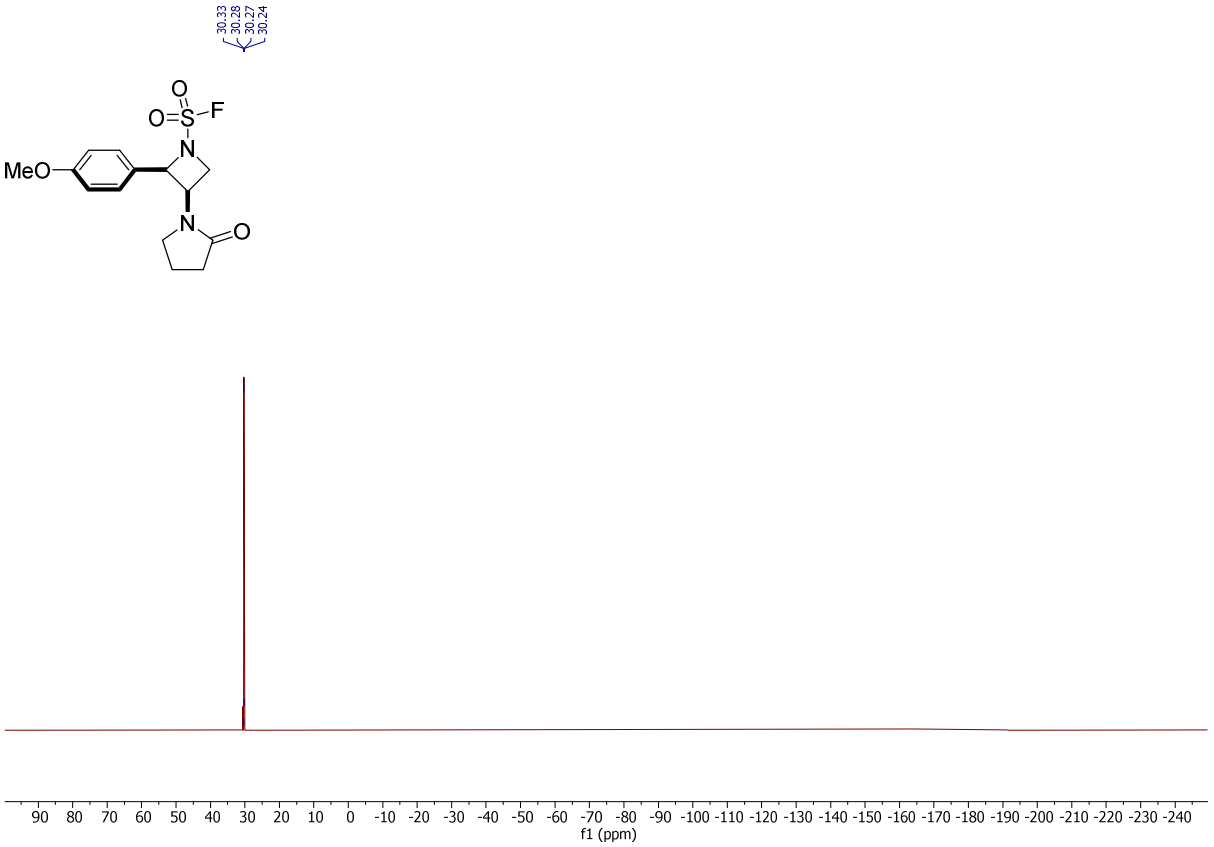



167.82
159.80
134.52
131.05
127.91
124.72
123.54
114.02
77.16 CDCl3
72.42
55.30
51.94
45.49
MeO
NPhth
f1 (ppm)

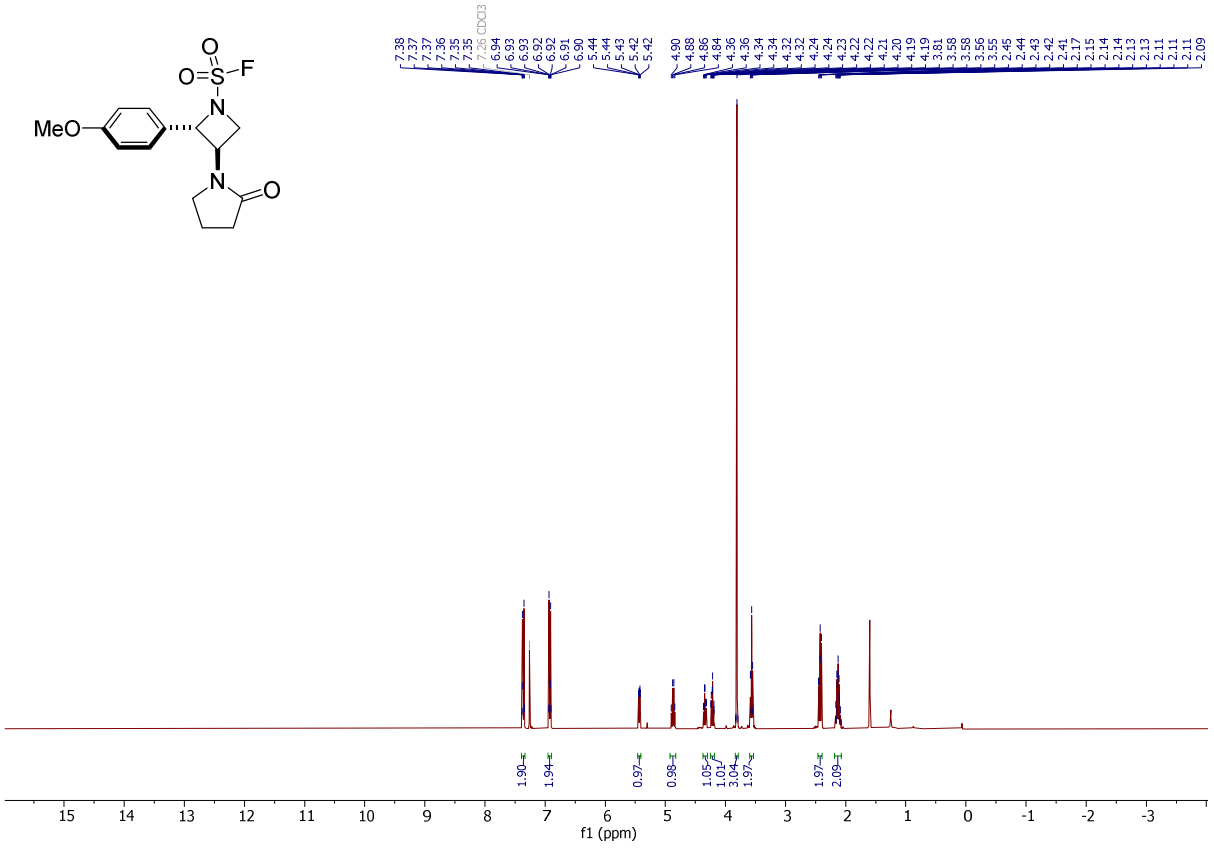

32.06
32.03
MeO
NPhth
f1 (ppm)

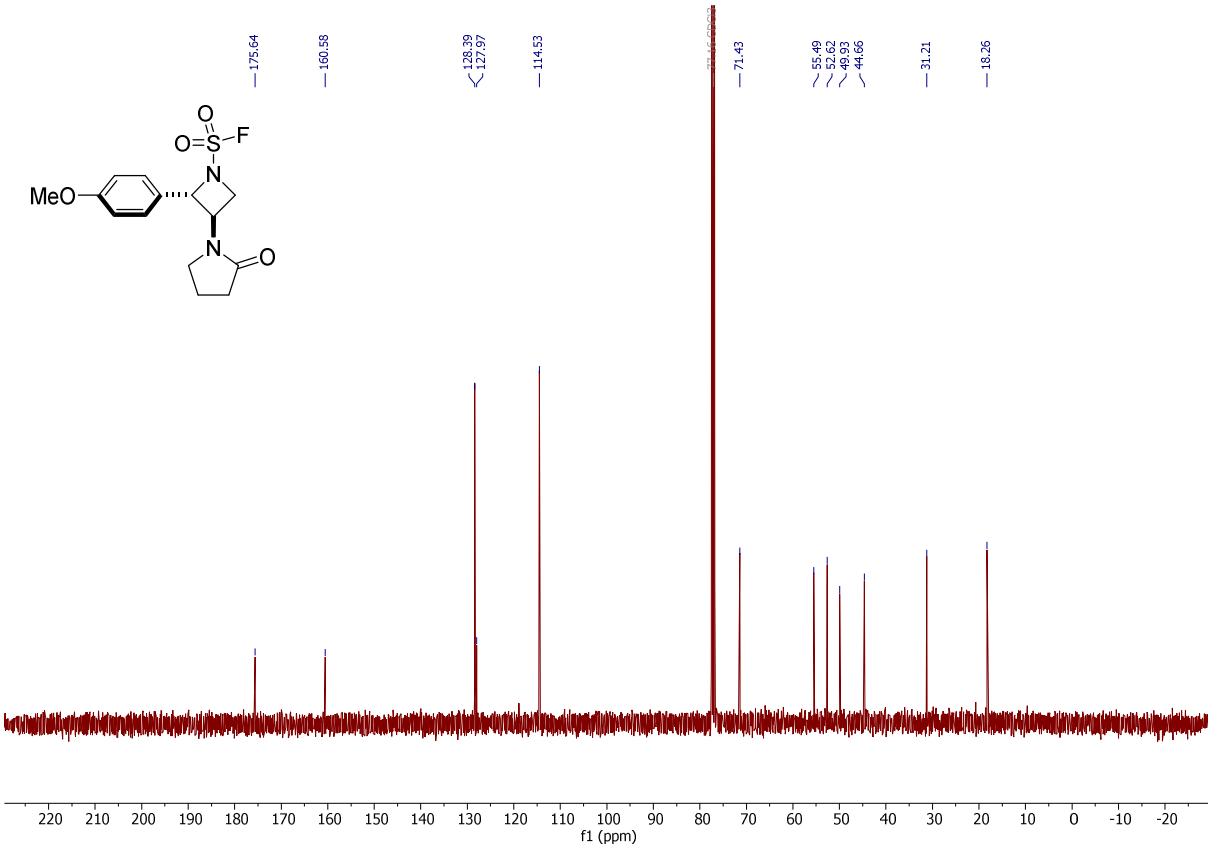
(2*R**,3*R**)-2-(4-Methoxyphenyl)-3-(2-oxopyrrolidin-1-yl)azetidine-1-sulfonyl fluoride (4r)

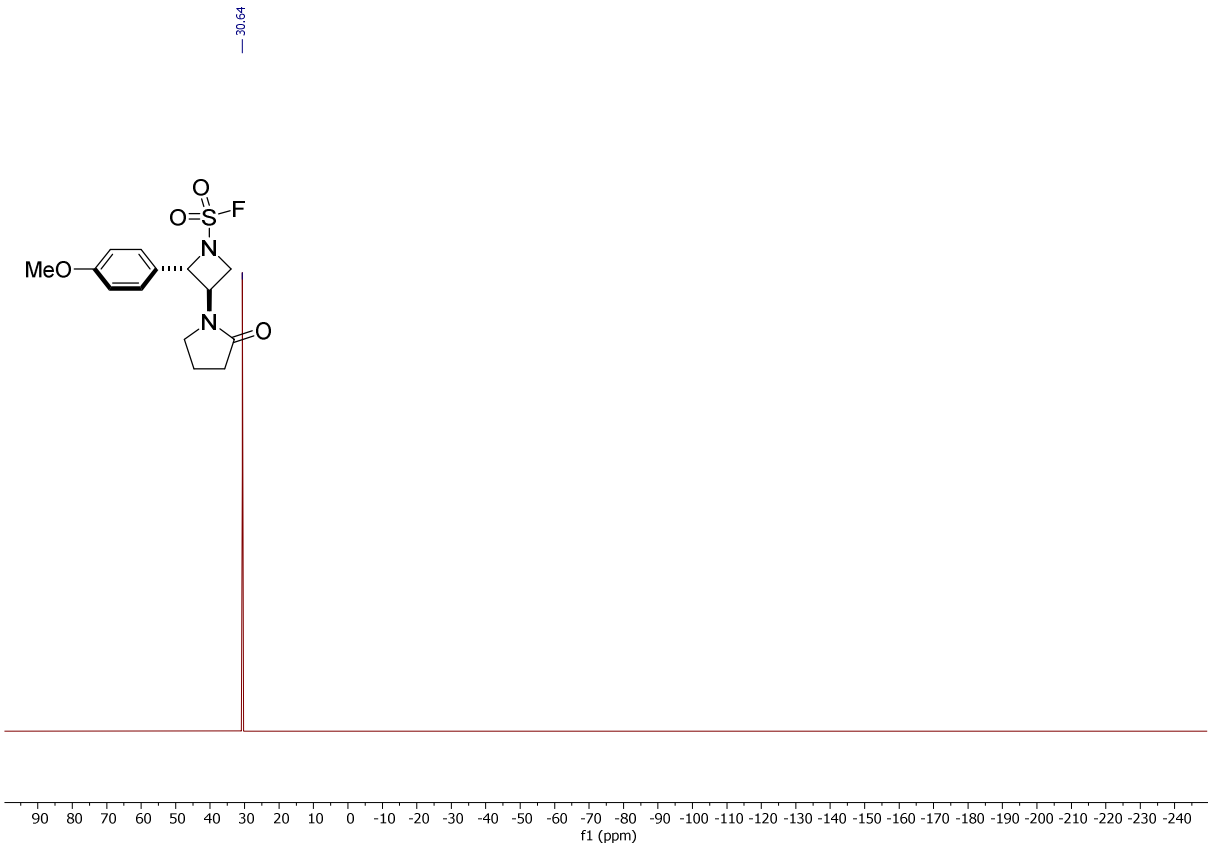




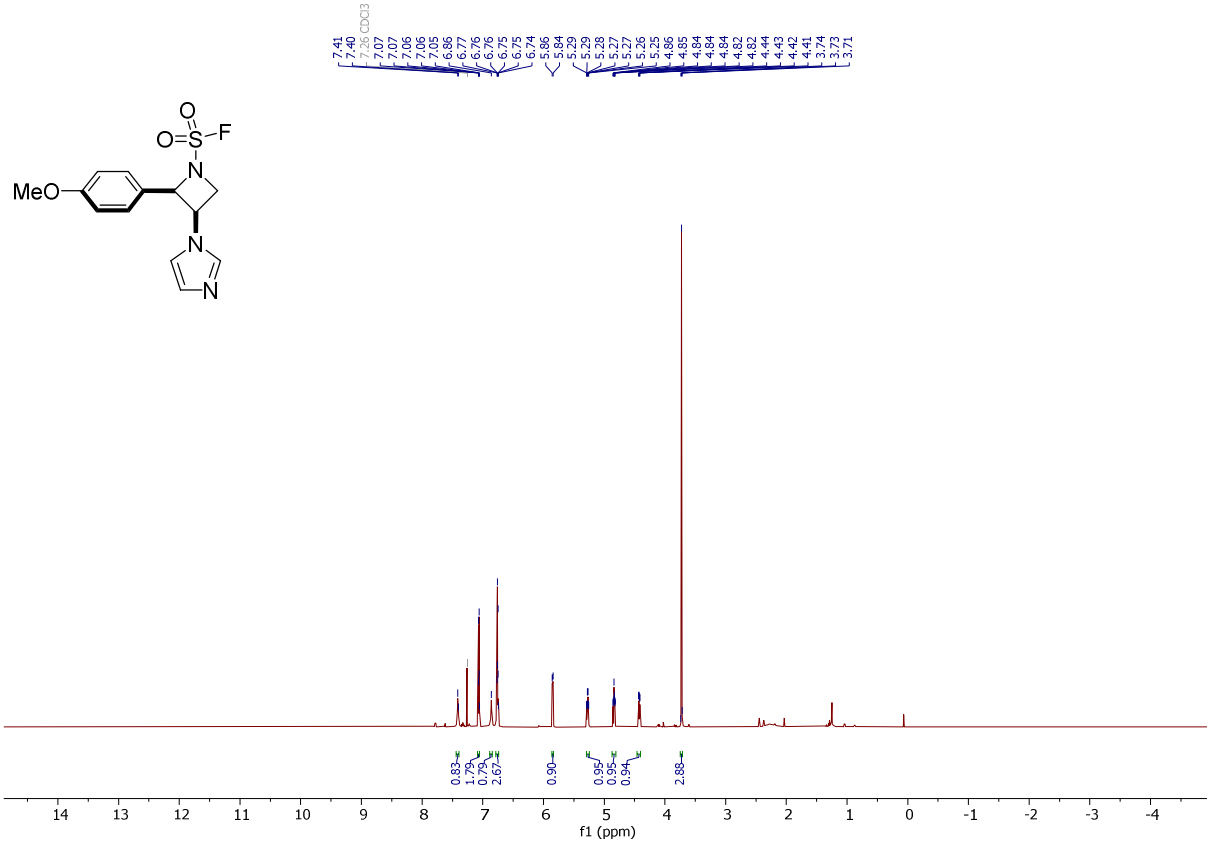
(2*S**,3*R**)-2-(4-Methoxyphenyl)-3-(2-oxopyrrolidin-1-yl)azetidine-1-sulfonyl fluoride (4r')

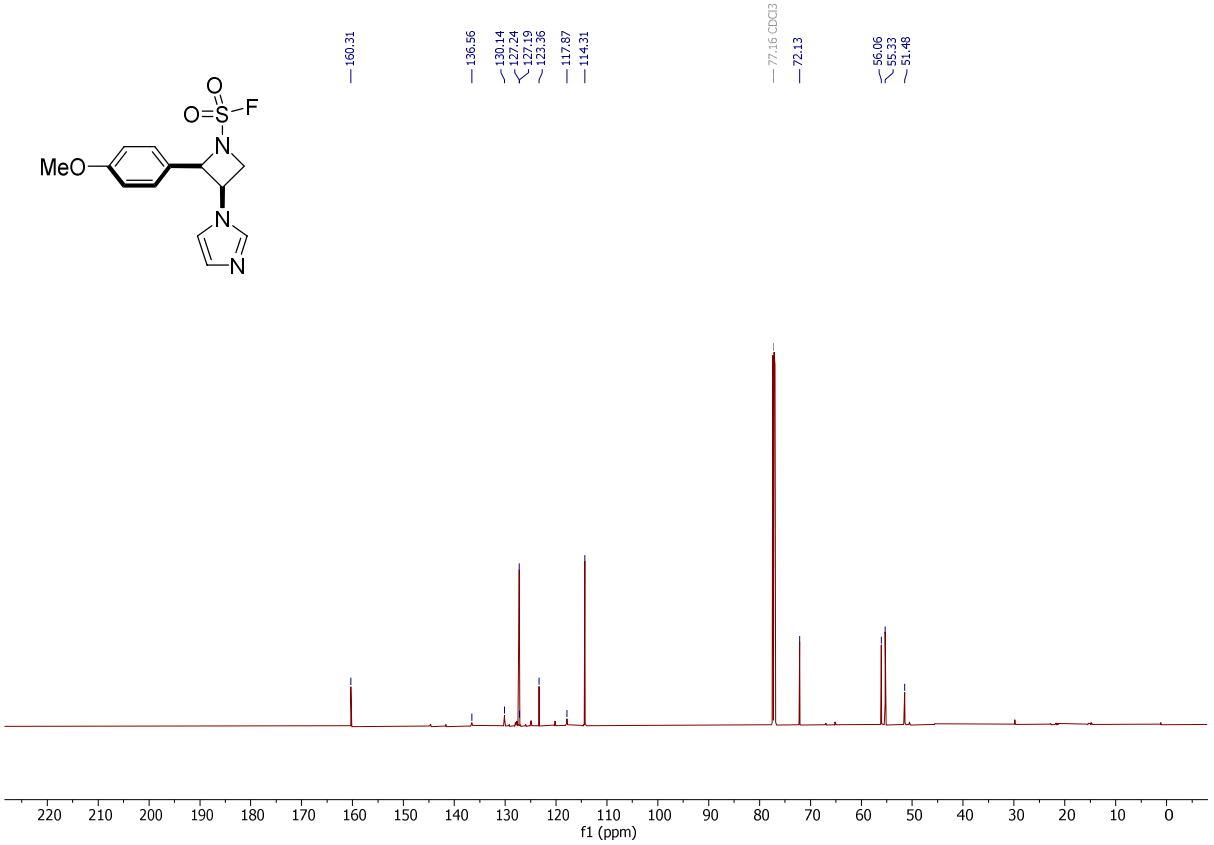


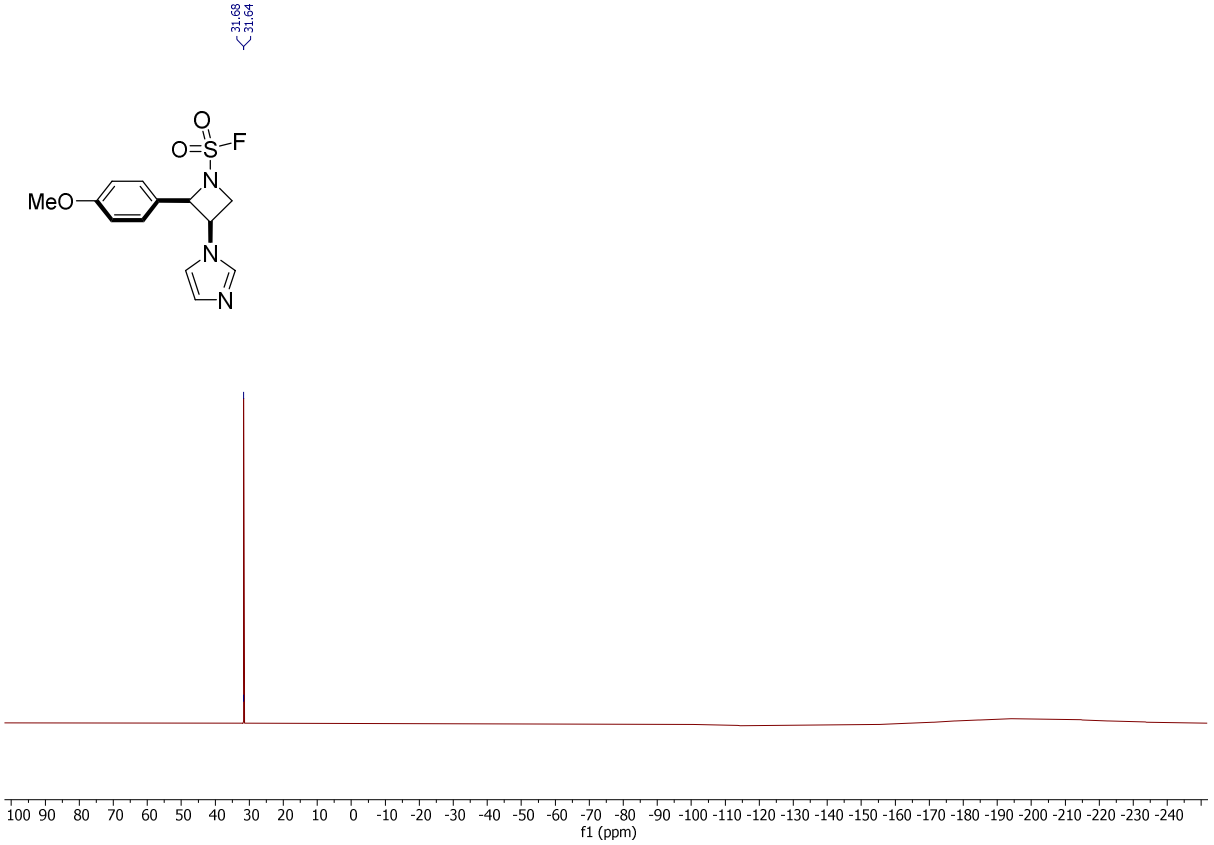

175.64
160.58
128.39
127.97
114.53
71.43
55.49
52.62
49.93
44.66
31.21
18.26
MeO
O
S
F
N
N
O
220 210 200 190 180 170 160 150 140 130 120 110 100 90 80 70 60 50 40 30 20 10 0 -10 -20
f1 (ppm)


30.64
MeO
O
S
F
N
N
O
90 80 70 60 50 40 30 20 10 0 -10 -20 -30 -40 -50 -60 -70 -80 -90 -100 -110 -120 -130 -140 -150 -160 -170 -180 -190 -200 -210 -220 -230 -240
f1 (ppm)

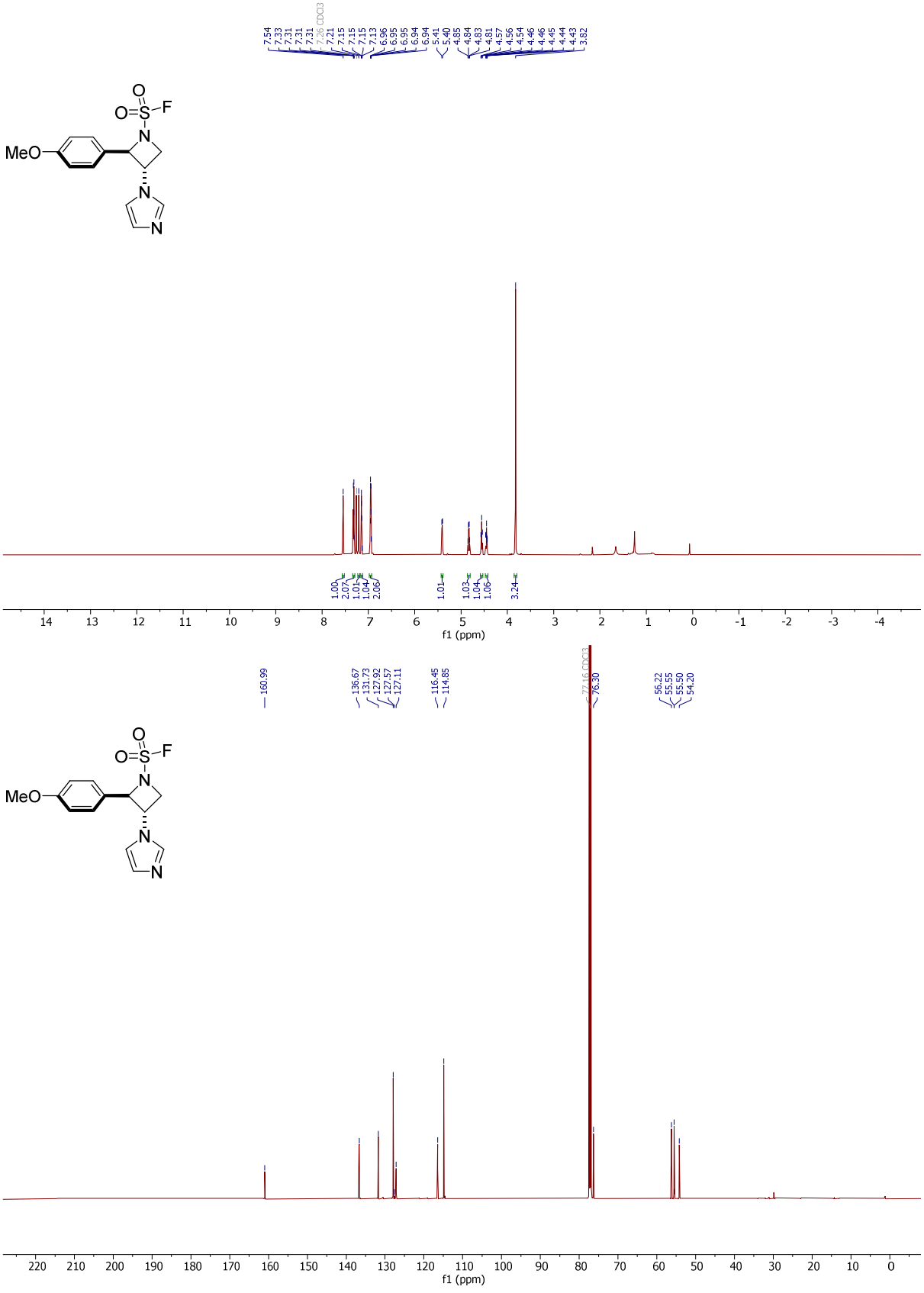
(2*R**,3*R**)-3-(1H-Imidazol-1-yl)-2-(4-methoxyphenyl)azetidine-1-sulfonyl fluoride (4s)

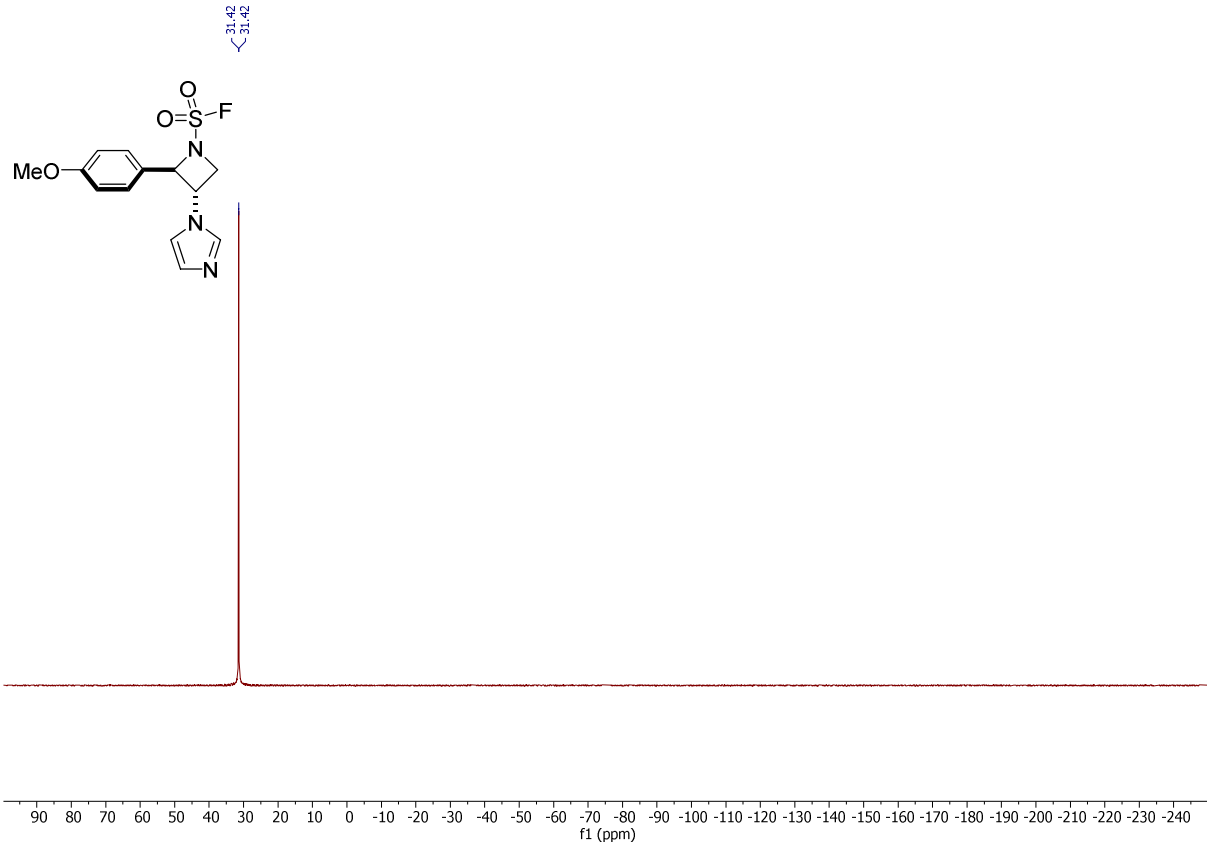



160.31
136.56
130.14
127.24
127.19
123.36
117.87
114.31
77.16 CDCl3
72.13
56.06
55.33
51.48
MeO
O
O=S
F
N
N
N
220 210 200 190 180 170 160 150 140 130 120 110 100 90 80 70 60 50 40 30 20 10 0
f1 (ppm)

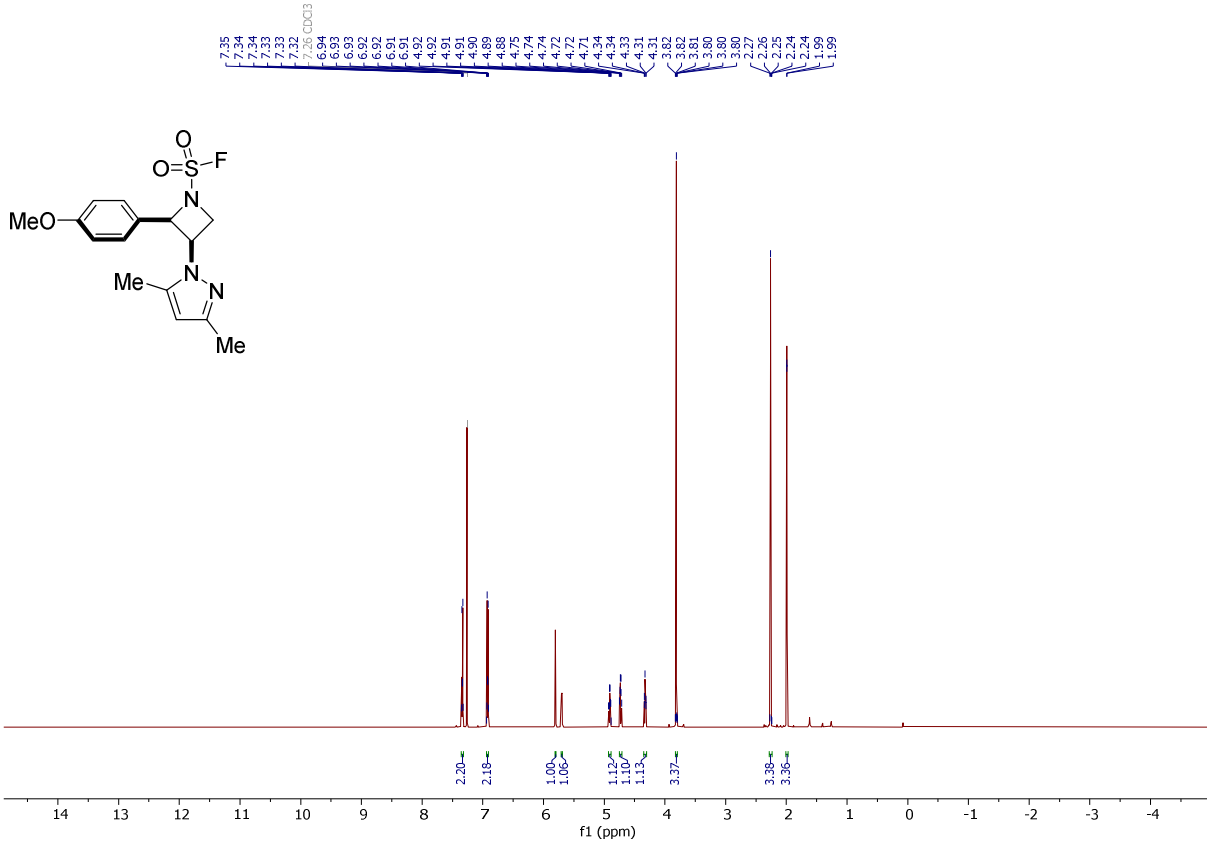

31.68
31.64
MeO
O
O=S
F
N
N
N
100 90 80 70 60 50 40 30 20 10 0 -10 -20 -30 -40 -50 -60 -70 -80 -90 -100 -110 -120 -130 -140 -150 -160 -170 -180 -190 -200 -210 -220 -230 -240
f1 (ppm)

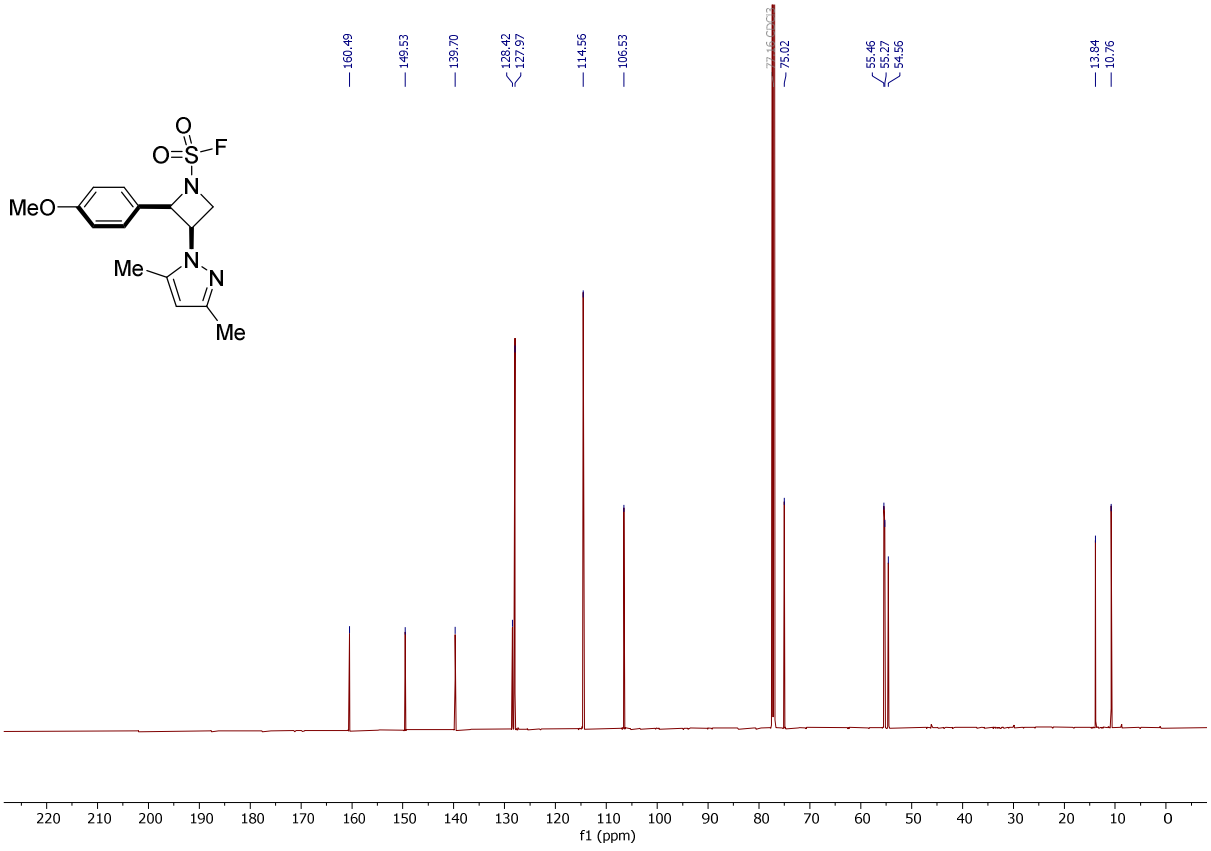
(2*R**,3*S**)-3-(1H-Imidazol-1-yl)-2-(4-methoxyphenyl)azetidine-1-sulfonyl fluoride (4s')

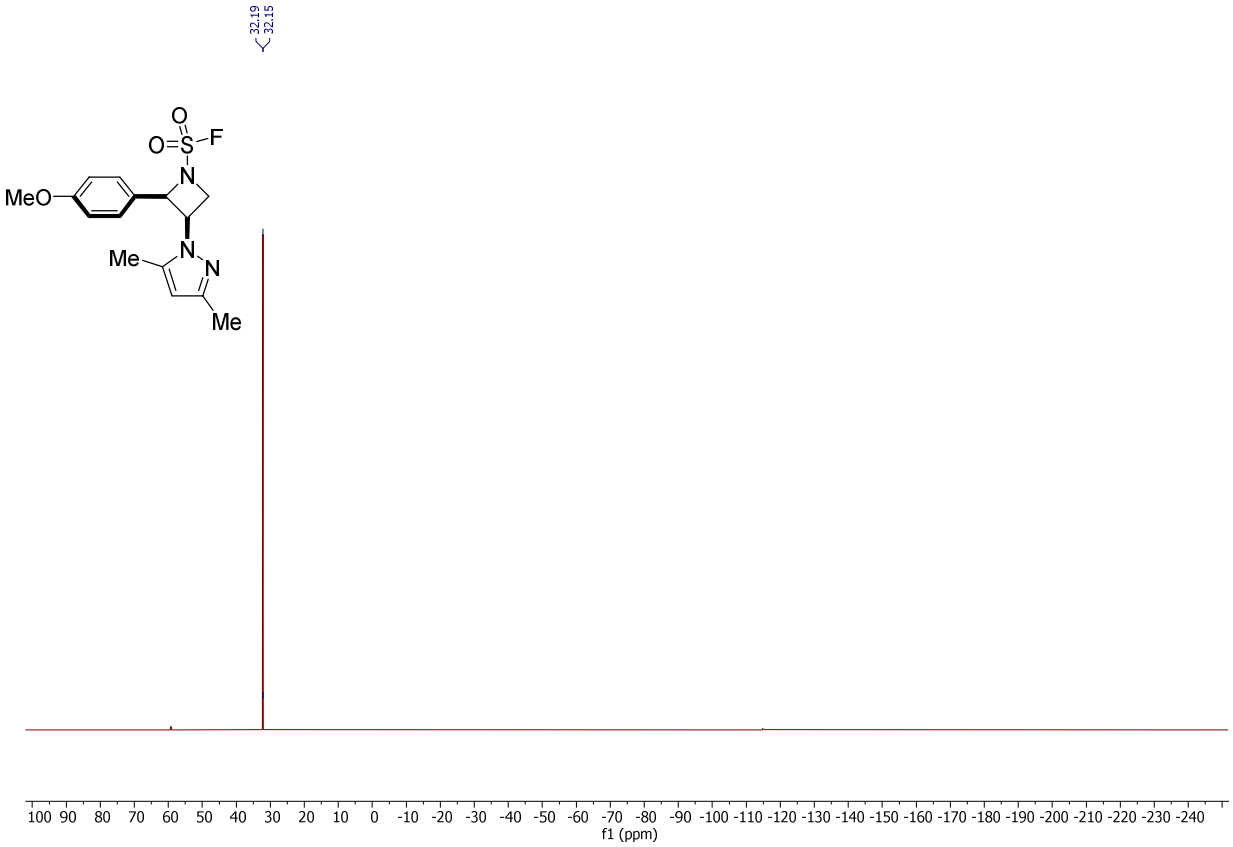



31.42
31.42
O
O=S–F
N
MeO
N
N
90 80 70 60 50 40 30 20 10 0 -10 -20 -30 -40 -50 -60 -70 -80 -90 -100 -110 -120 -130 -140 -150 -160 -170 -180 -190 -200 -210 -220 -230 -240
f1 (ppm)

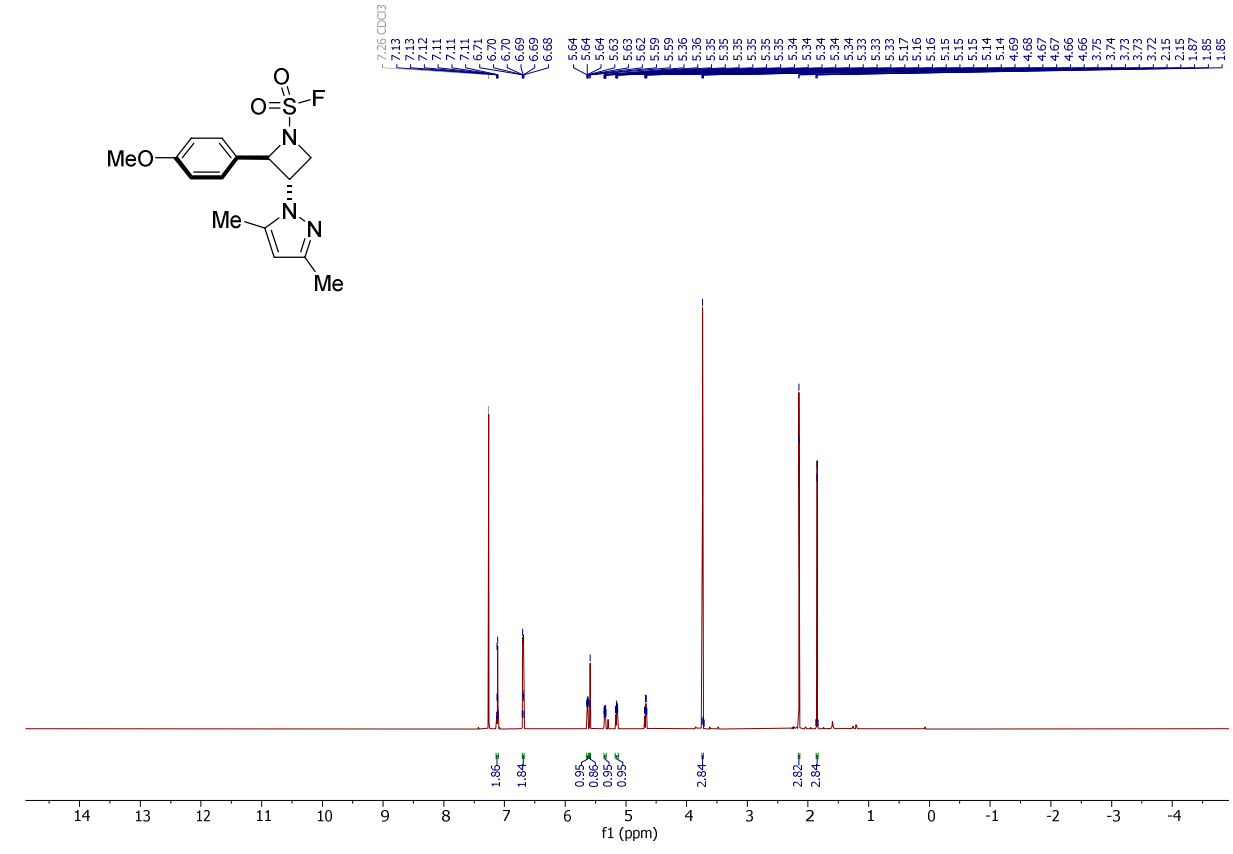
(2*S**,3*S**)-3-(3,5-Dimethyl-1H-pyrazol-1-yl)-2-(4-methoxyphenyl)azetidine-1-sulfonyl fluoride (4t)

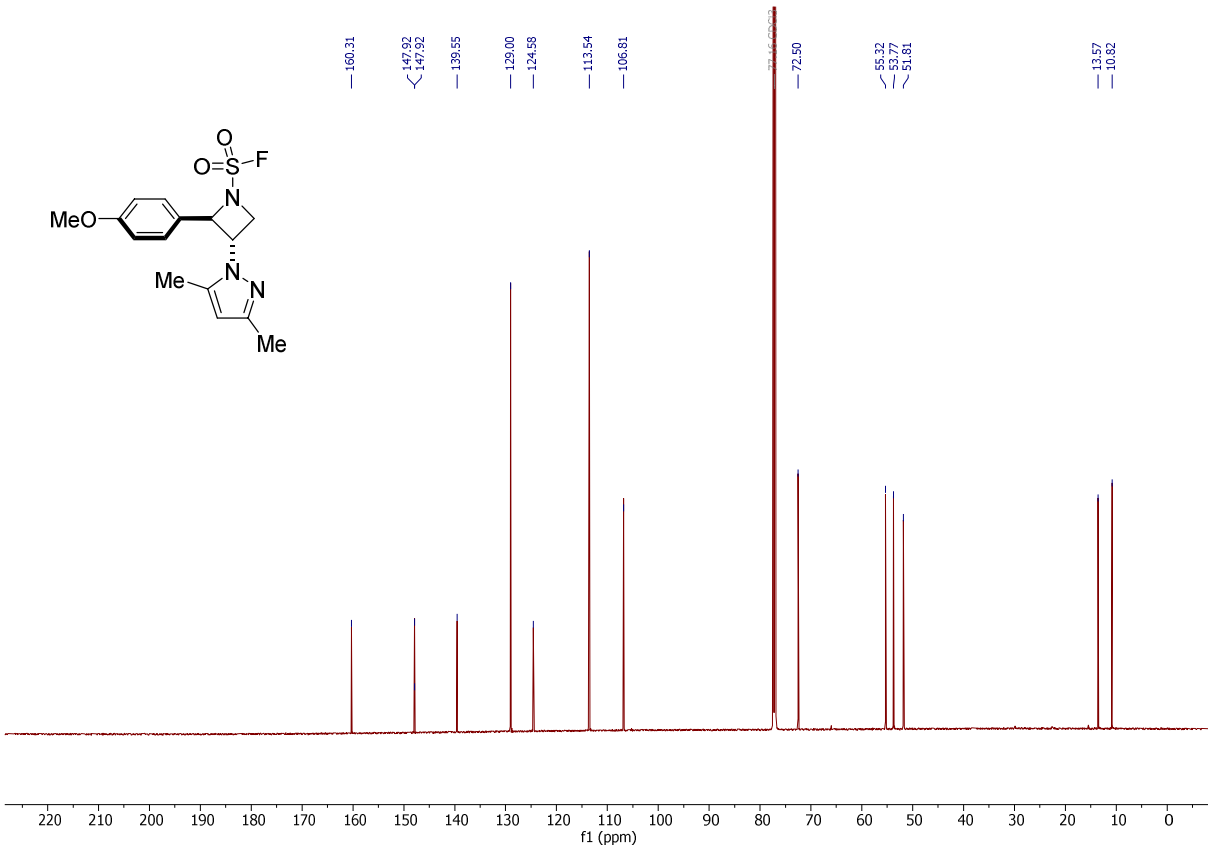


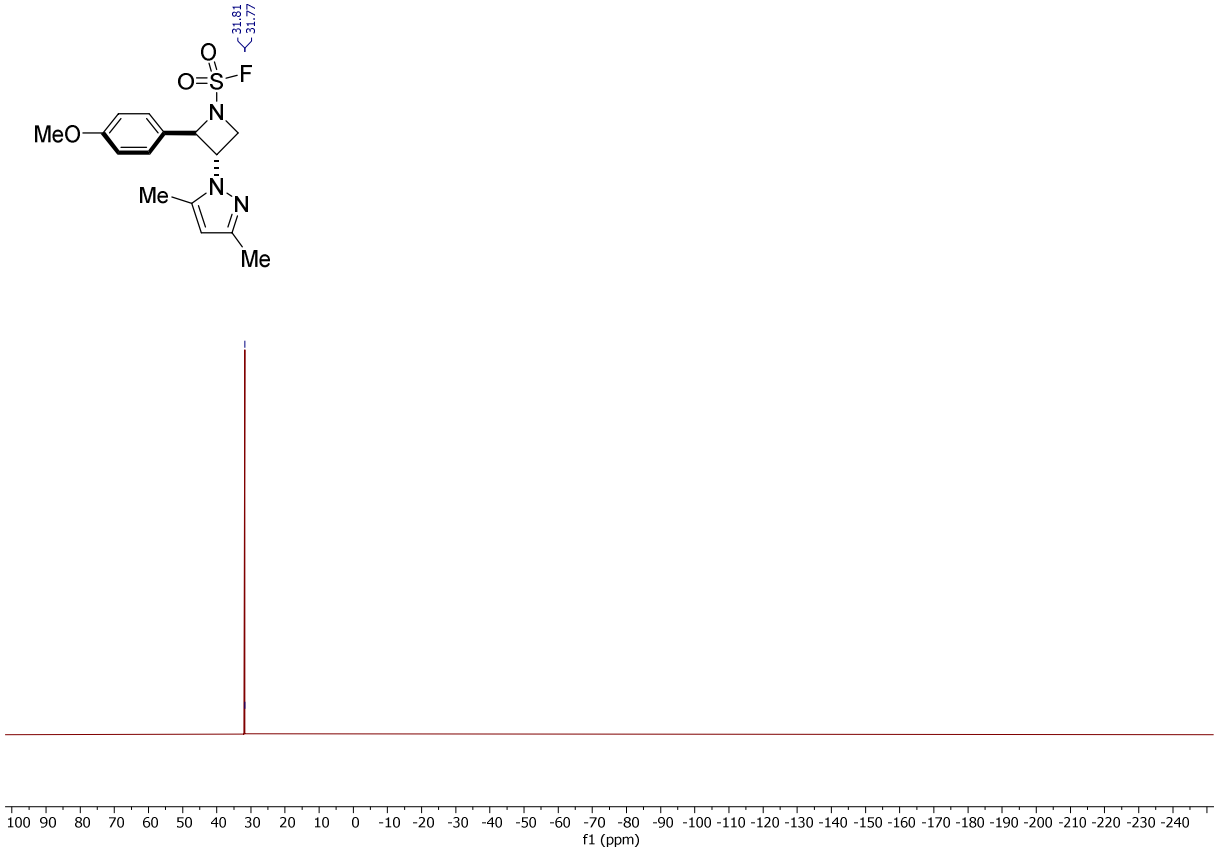




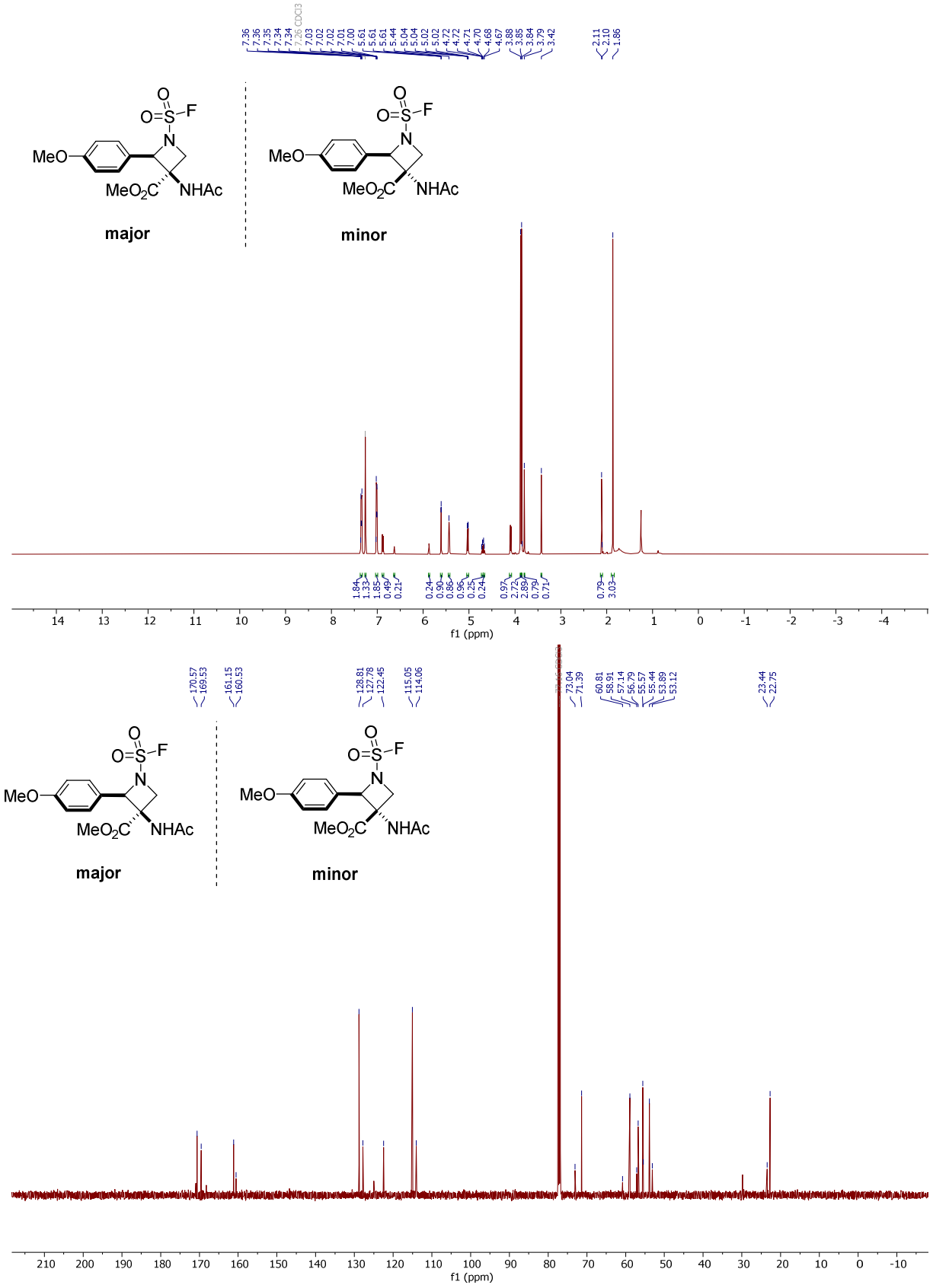
(2*S**,3*R**)-3-(3,5-Dimethyl-1H-pyrazol-1-yl)-2-(4-methoxyphenyl)azetidine-1-sulfonyl fluoride (4t')

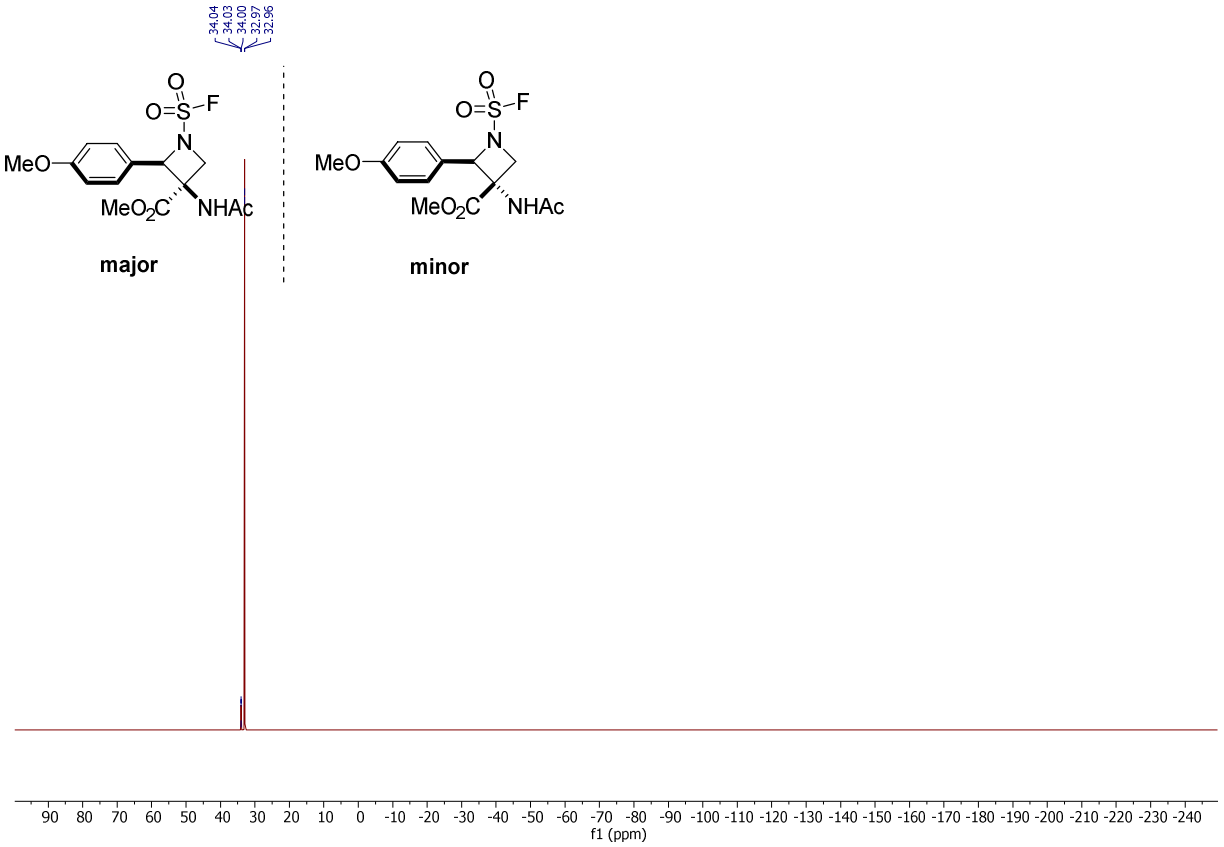



160.31
147.92
147.92
139.55
129.00
124.58
113.54
106.81
77.16
72.50
55.32
53.77
51.81
13.57
10.82
O
O=S–F
N
MeO
N
Me
N
Me
220 210 200 190 180 170 160 150 140 130 120 110 100 90 80 70 60 50 40 30 20 10 0
f1 (ppm)

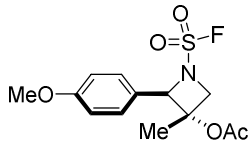

31.81
31.77
O
O=S–F
N
MeO
N
Me
N
Me
100 90 80 70 60 50 40 30 20 10 0 -10 -20 -30 -40 -50 -60 -70 -80 -90 -100 -110 -120 -130 -140 -150 -160 -170 -180 -190 -200 -210 -220 -230 -240
f1 (ppm)

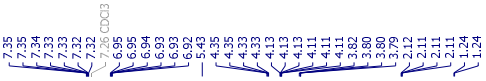
Methyl (2*R**,3*S**)-3-acetamide-1-(fluorosulfonyl)-2-(4-methoxyphenyl)azetidine-3-carboxylate and (4u) Methyl (2*S**,3*S**)-3-acetamide-1-(fluorosulfonyl)-2-(4-methoxyphenyl)azetidine-3-carboxylate (4u')

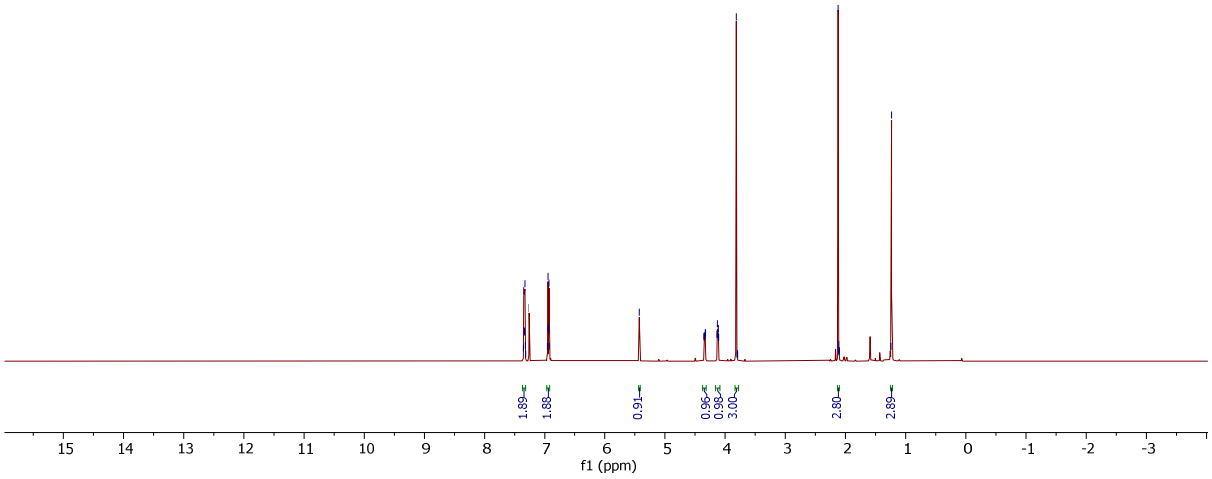



34.04
34.03
34.00
32.97
32.96
O
O=S–F
N
MeO
MeO2C
NHAc
major
minor
90 80 70 60 50 40 30 20 10 0 -10 -20 -30 -40 -50 -60 -70 -80 -90 -100 -110 -120 -130 -140 -150 -160 -170 -180 -190 -200 -210 -220 -230 -240
f1 (ppm)

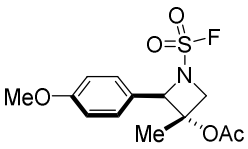
(2*R**,3*S**)-1-(Fluorosulfonyl)-2-(4-methoxyphenyl)-3-methylazetidin-3-yl acetate (4v)

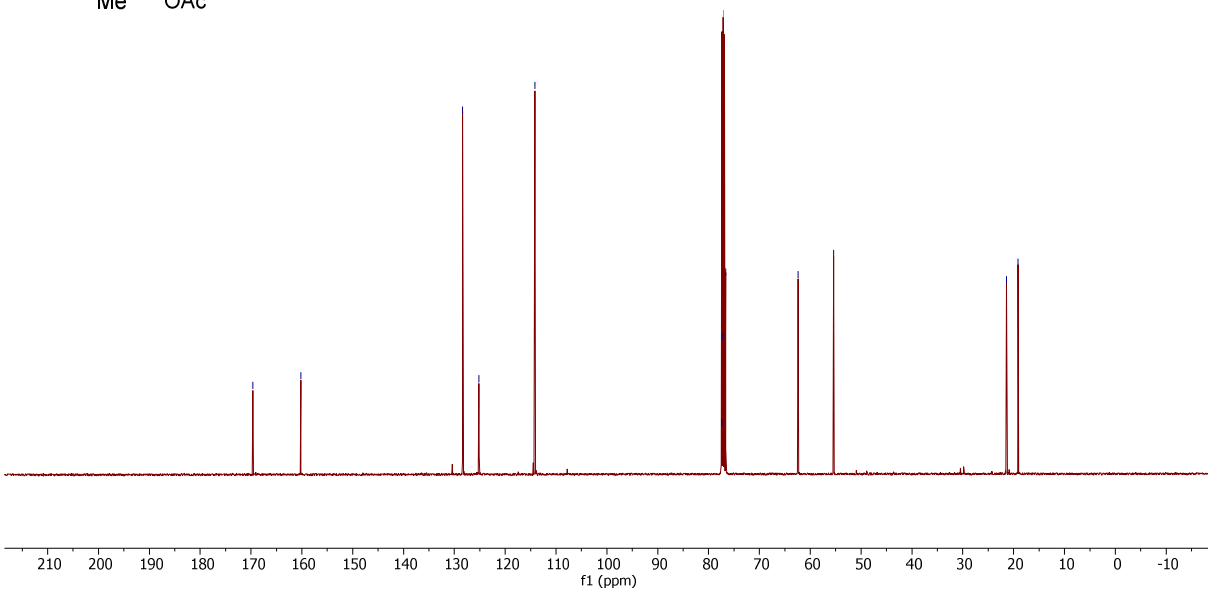


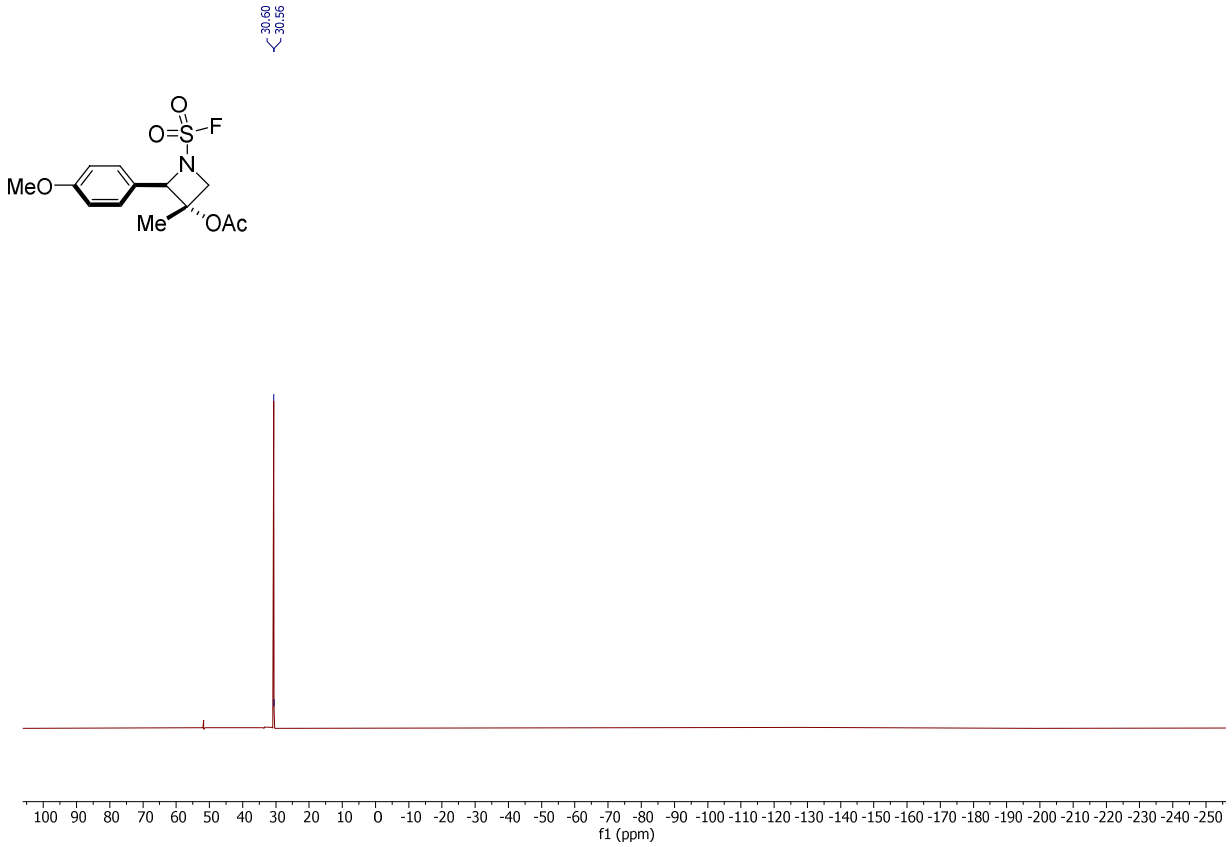




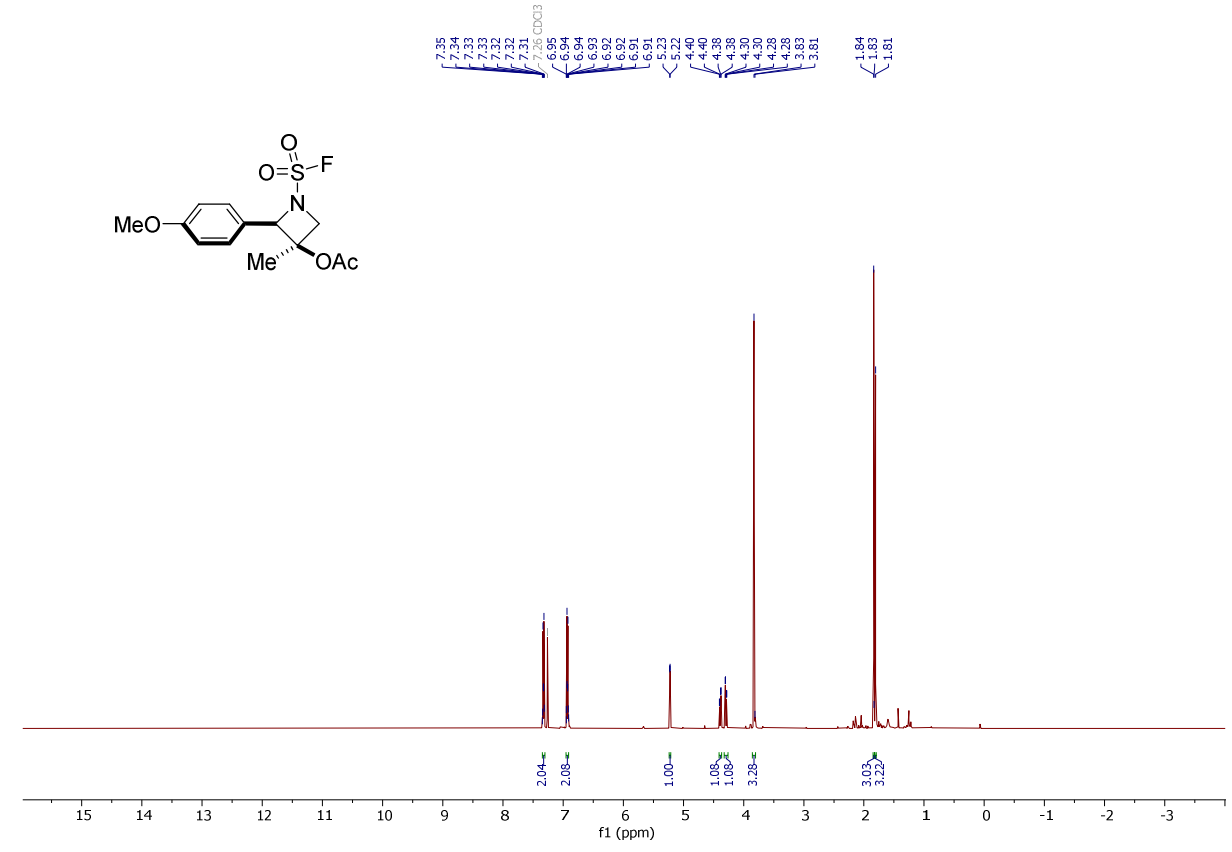


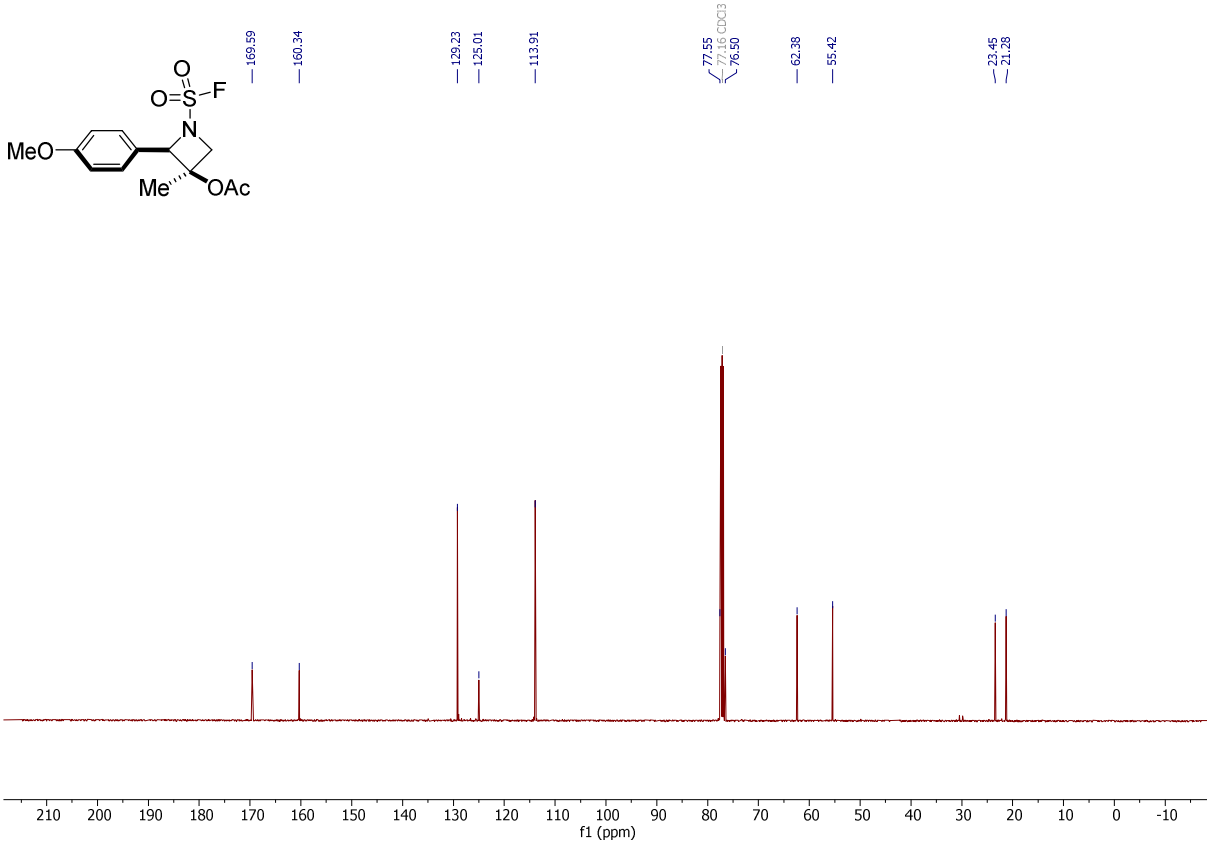


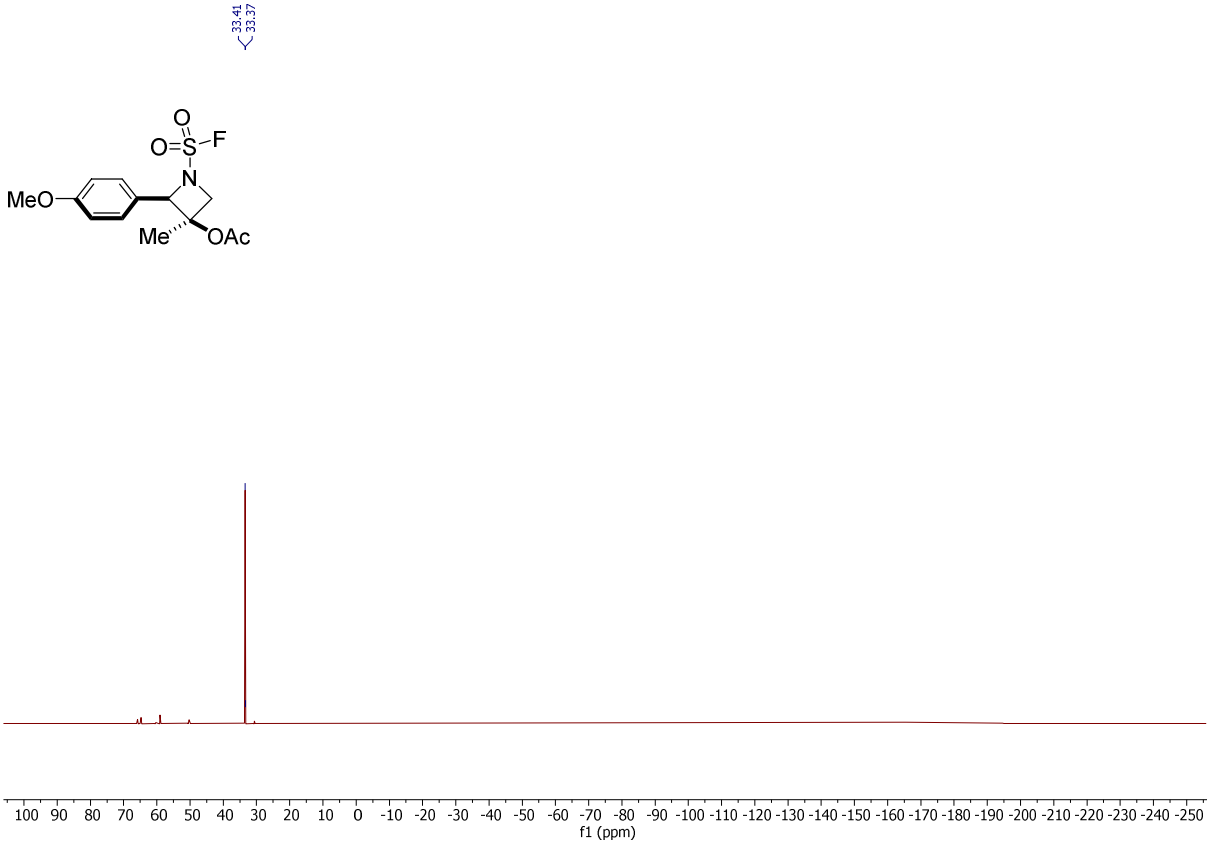




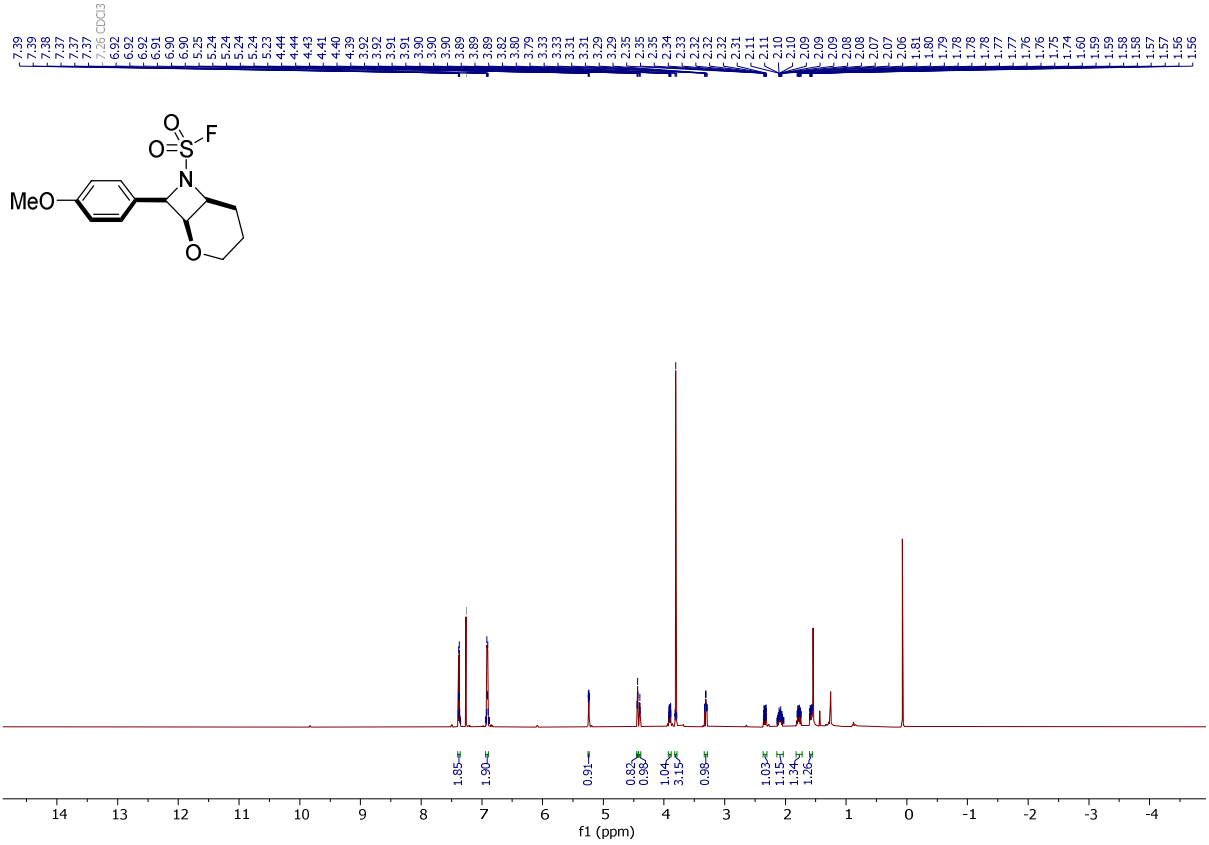
(2*R**,3*R**)-1-(Fluorosulfonyl)-2-(4-methoxyphenyl)-3-methylazetidin-3-yl acetate (4v')

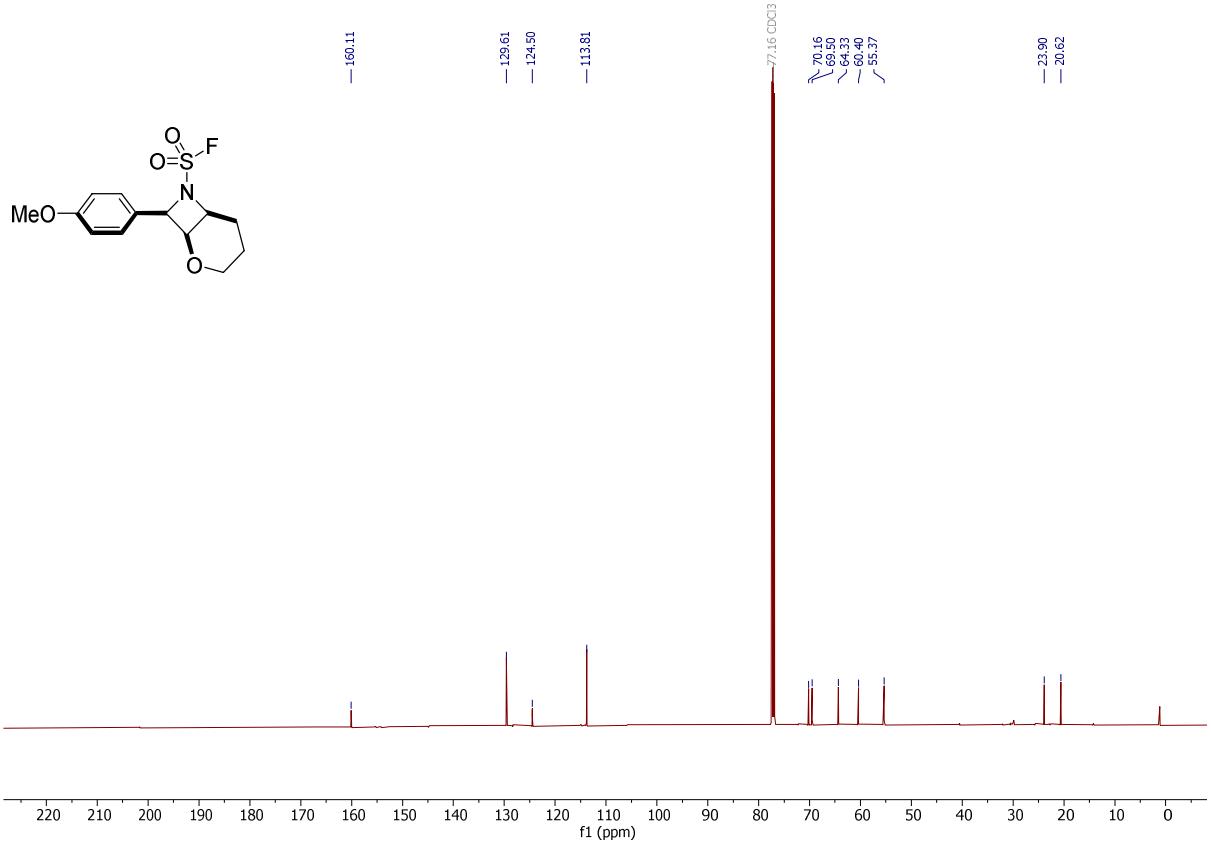


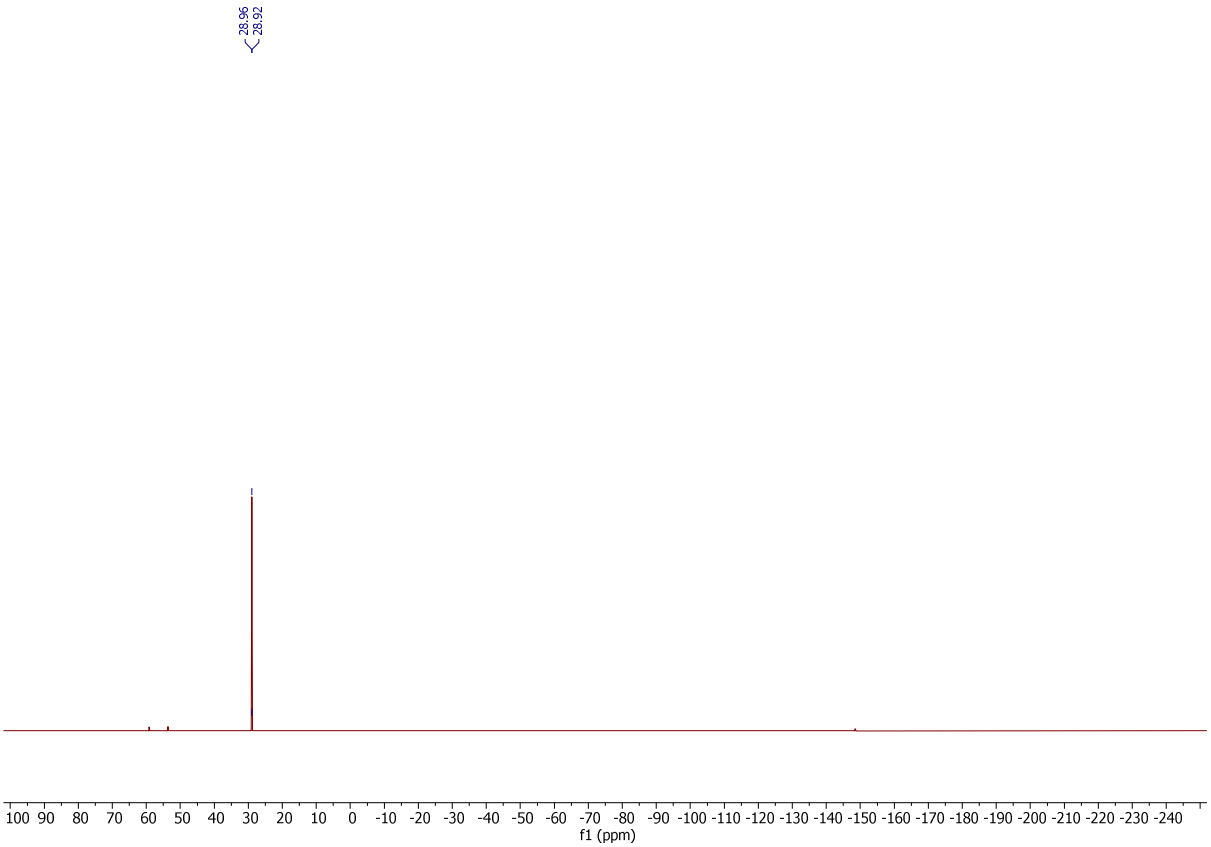

169.59
160.34
129.23
125.01
113.91
77.55
77.16 CDCl3
76.50
62.38
55.42
23.45
21.28
O
O=S–F
N
MeO
Me
OAc
210 200 190 180 170 160 150 140 130 120 110 100 90 80 70 60 50 40 30 20 10 0 -10
f1 (ppm)


33.41
33.37
O
O=S–F
N
MeO
Me
OAc
100 90 80 70 60 50 40 30 20 10 0 -10 -20 -30 -40 -50 -60 -70 -80 -90 -100 -110 -120 -130 -140 -150 -160 -170 -180 -190 -200 -210 -220 -230 -240 -250
f1 (ppm)

(1*R**,6*S**,8*R**)-8-(4-Methoxyphenyl)-2-oxa-7-azabicyclo[4.2.0]octane-7-sulfonyl fluoride (4w)

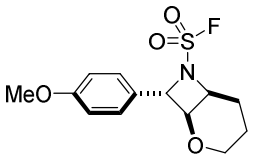


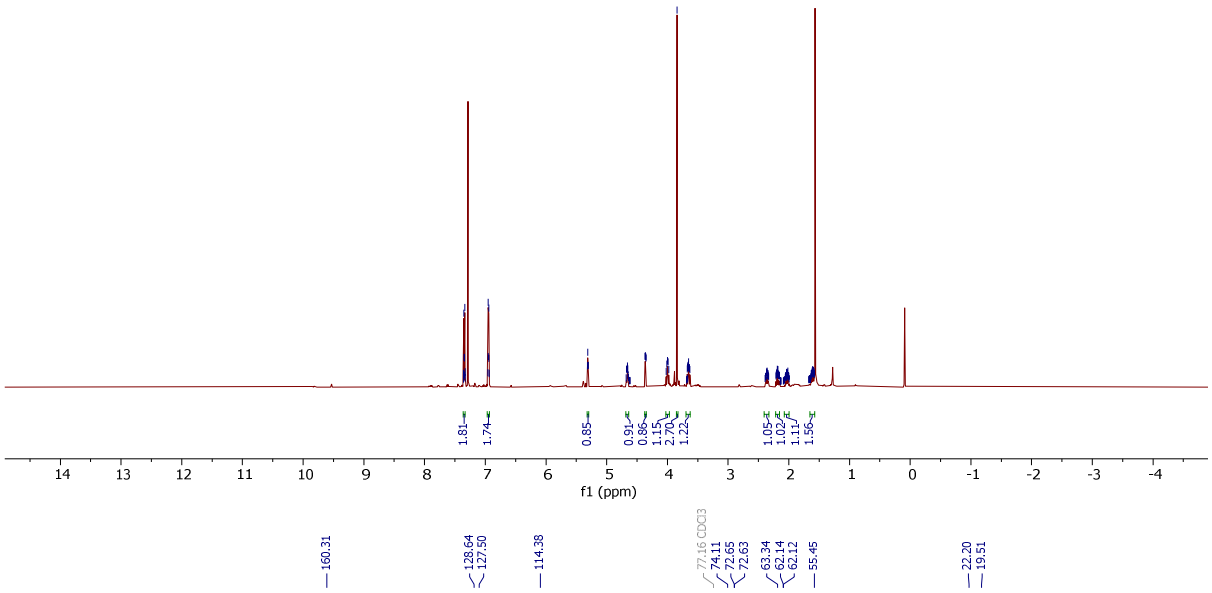

160.11
129.61
124.50
113.81
77.16 CDCl3
70.16
69.50
64.33
60.40
55.37
23.90
20.62
MeO
O
O=S
F
N
O
220 210 200 190 180 170 160 150 140 130 120 110 100 90 80 70 60 50 40 30 20 10 0
f1 (ppm)

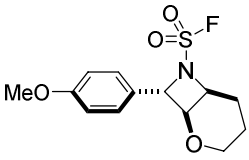

28.96
28.92
100 90 80 70 60 50 40 30 20 10 0 -10 -20 -30 -40 -50 -60 -70 -80 -90 -100 -110 -120 -130 -140 -150 -160 -170 -180 -190 -200 -210 -220 -230 -240
f1 (ppm)

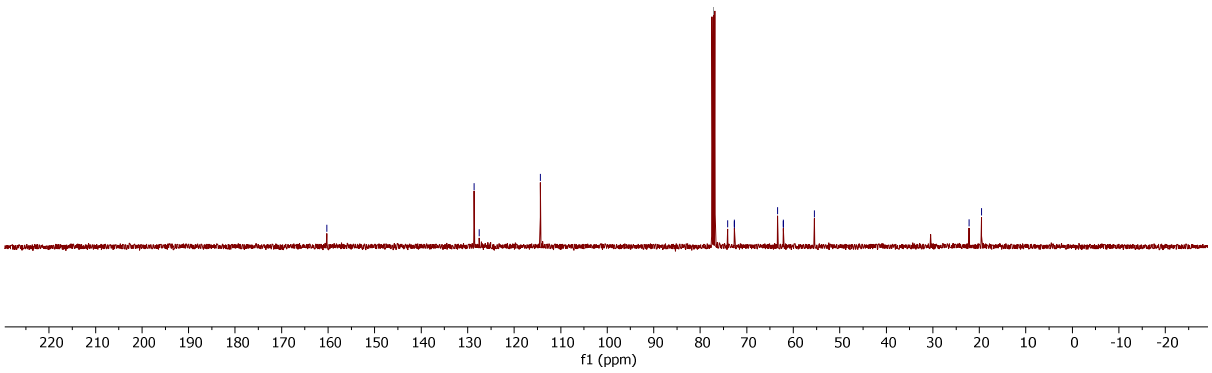
(1*R**,6*S**,8*S**)-8-(4-Methoxyphenyl)-2-oxa-7-azabicyclo[4.2.0]octane-7-sulfonyl fluoride (4w')

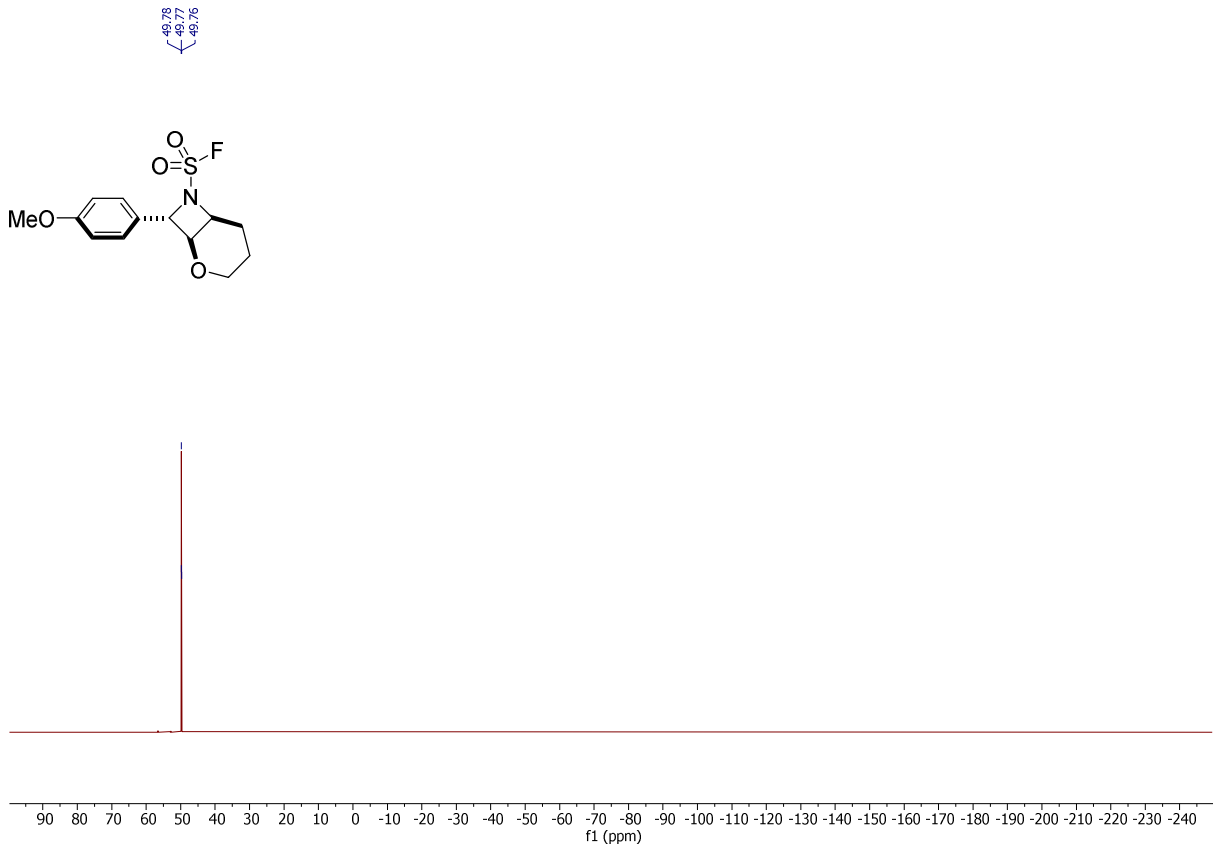




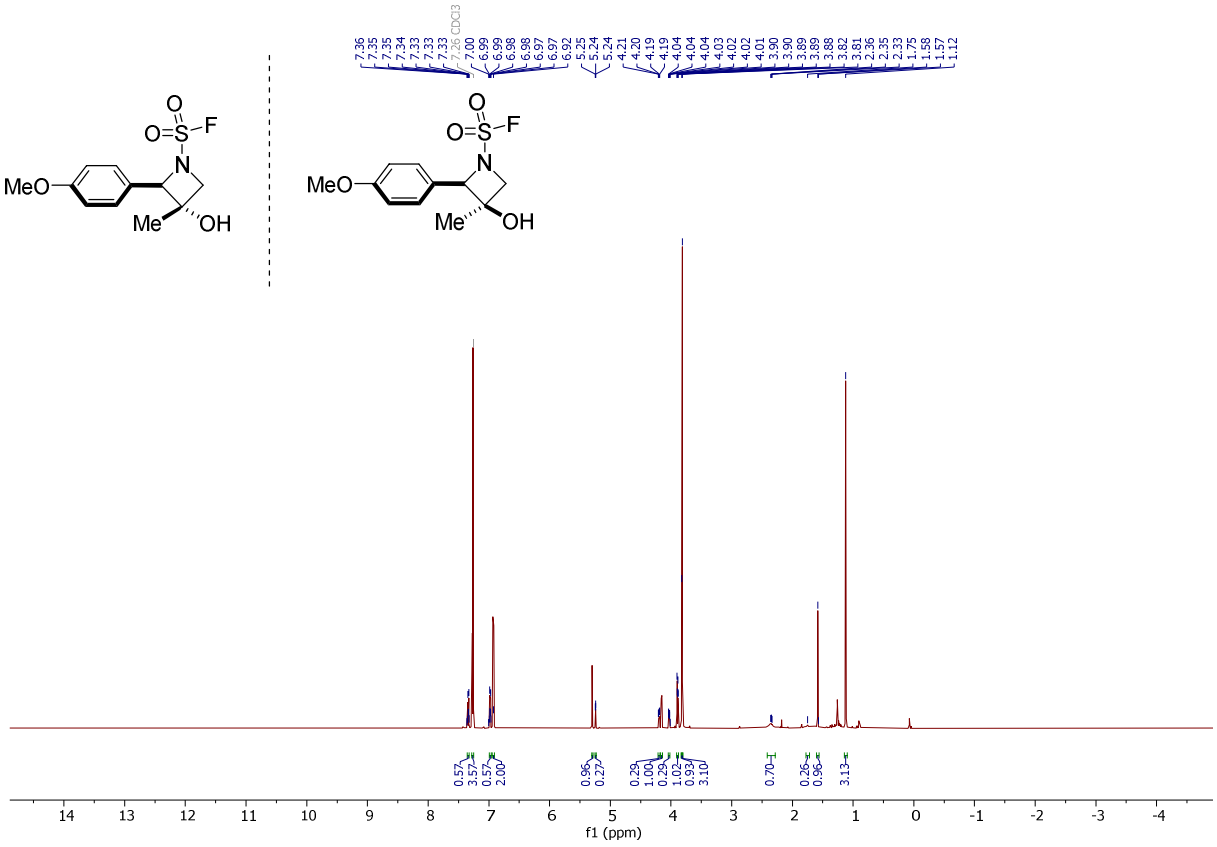


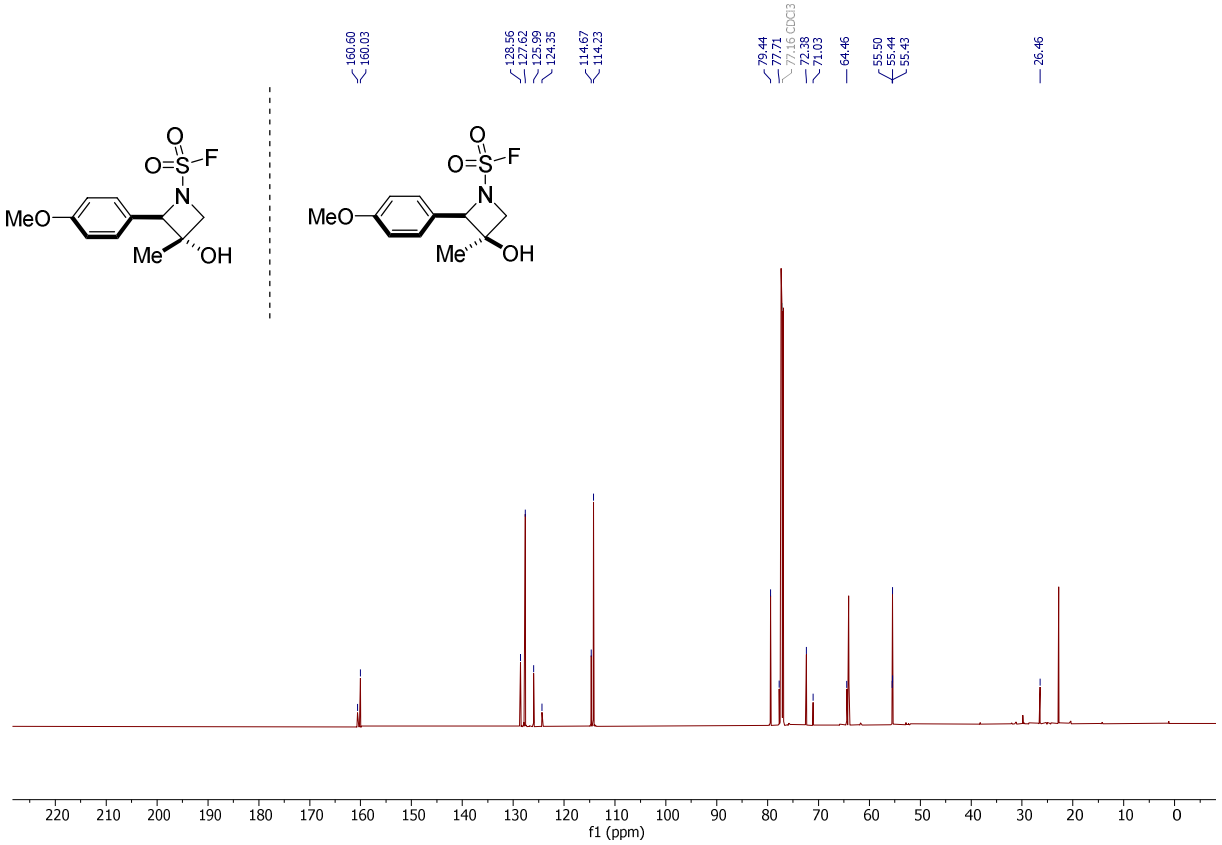


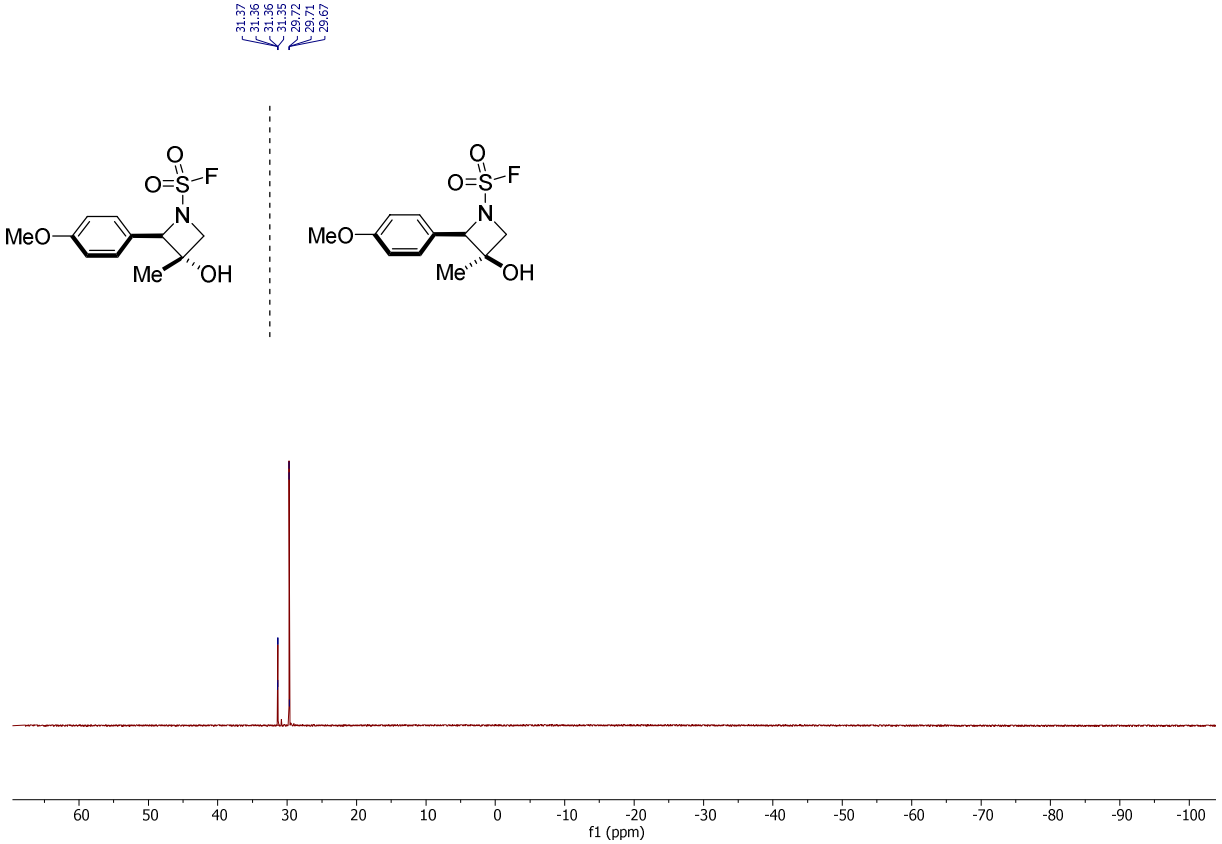



49.78
49.77
49.76
O
O=S
F
N
MeO
O
90 80 70 60 50 40 30 20 10 0 -10 -20 -30 -40 -50 -60 -70 -80 -90 -100 -110 -120 -130 -140 -150 -160 -170 -180 -190 -200 -210 -220 -230 -240
f1 (ppm)

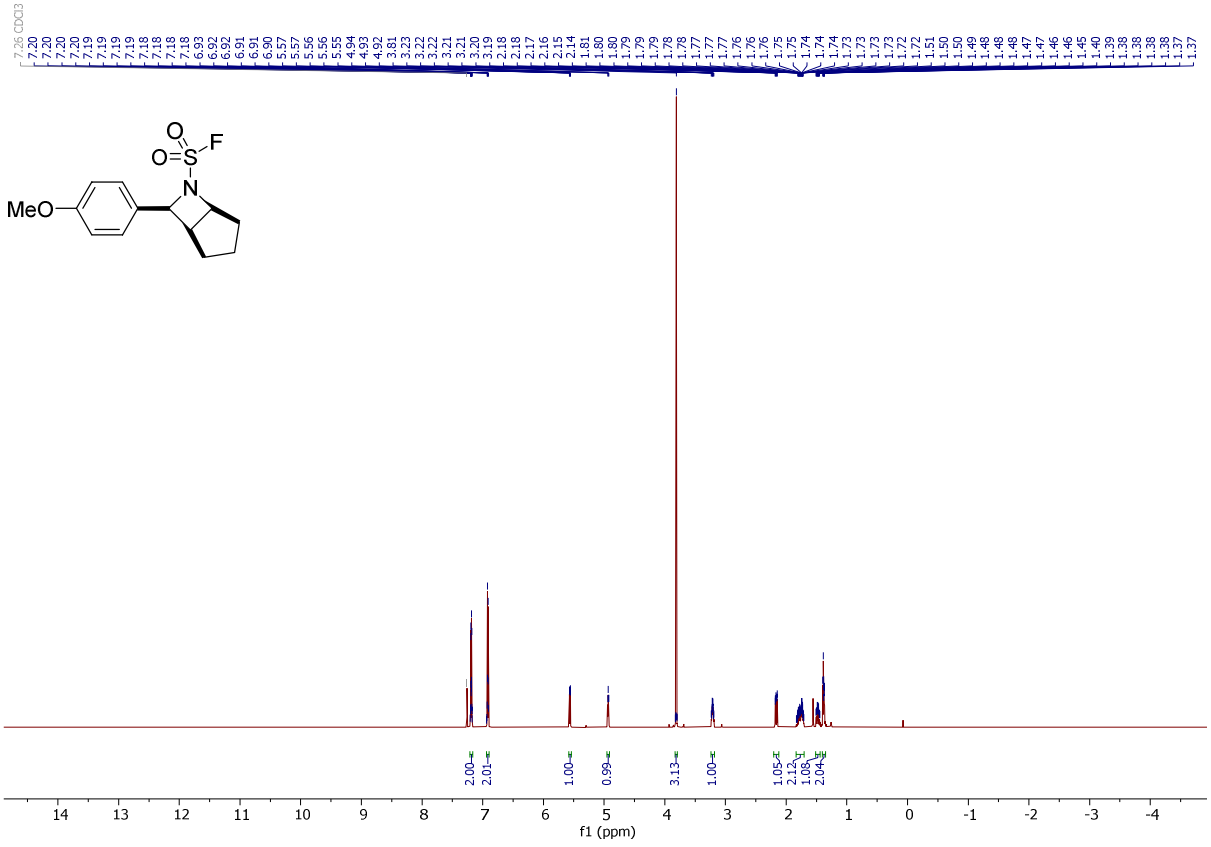
(2*R**,3*S**)-3-Hydroxy-2-(4-methoxyphenyl)-3-methylazetidine-1-sulfonyl fluoride (4x) and (2*R**,3*R**)-3-Hydroxy-2-(4-methoxyphenyl)-3-methylazetidine-1-sulfonyl fluoride (4x')

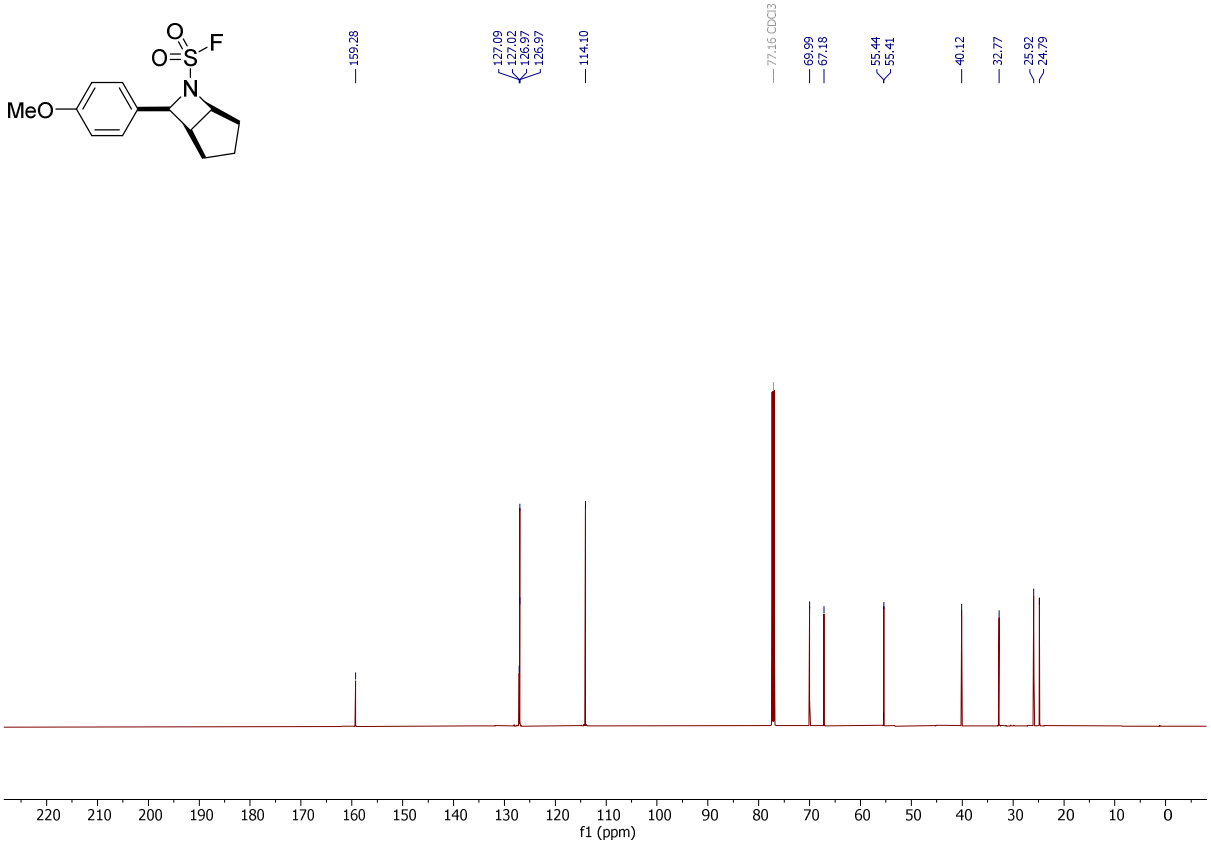


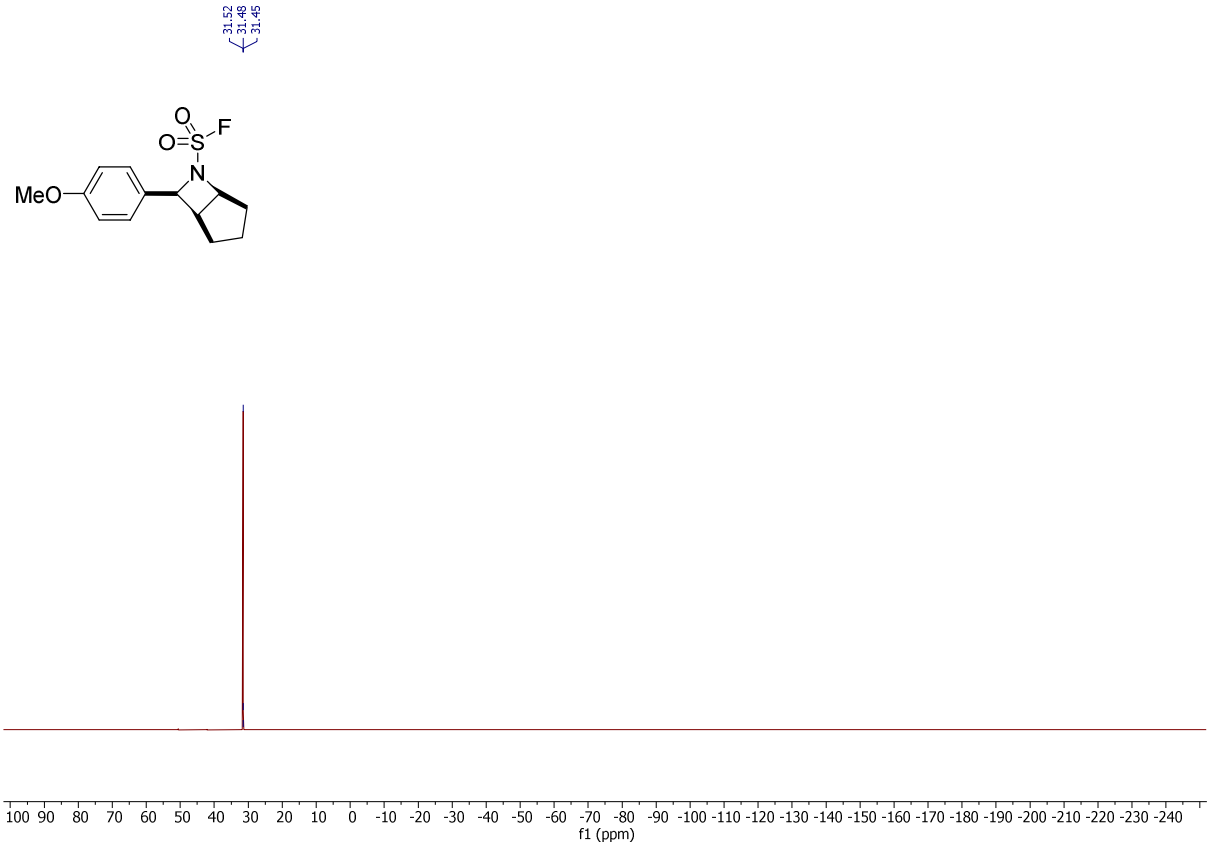

160.60
160.03
128.56
127.62
125.99
124.35
114.67
114.23
79.44
77.71
77.16 CDCl3
72.38
71.03
64.46
55.50
55.44
55.43
26.46
MeO
Me
OH
f1 (ppm)


31.37
31.36
31.36
31.35
29.72
29.71
29.67
MeO
Me
OH
f1 (ppm)

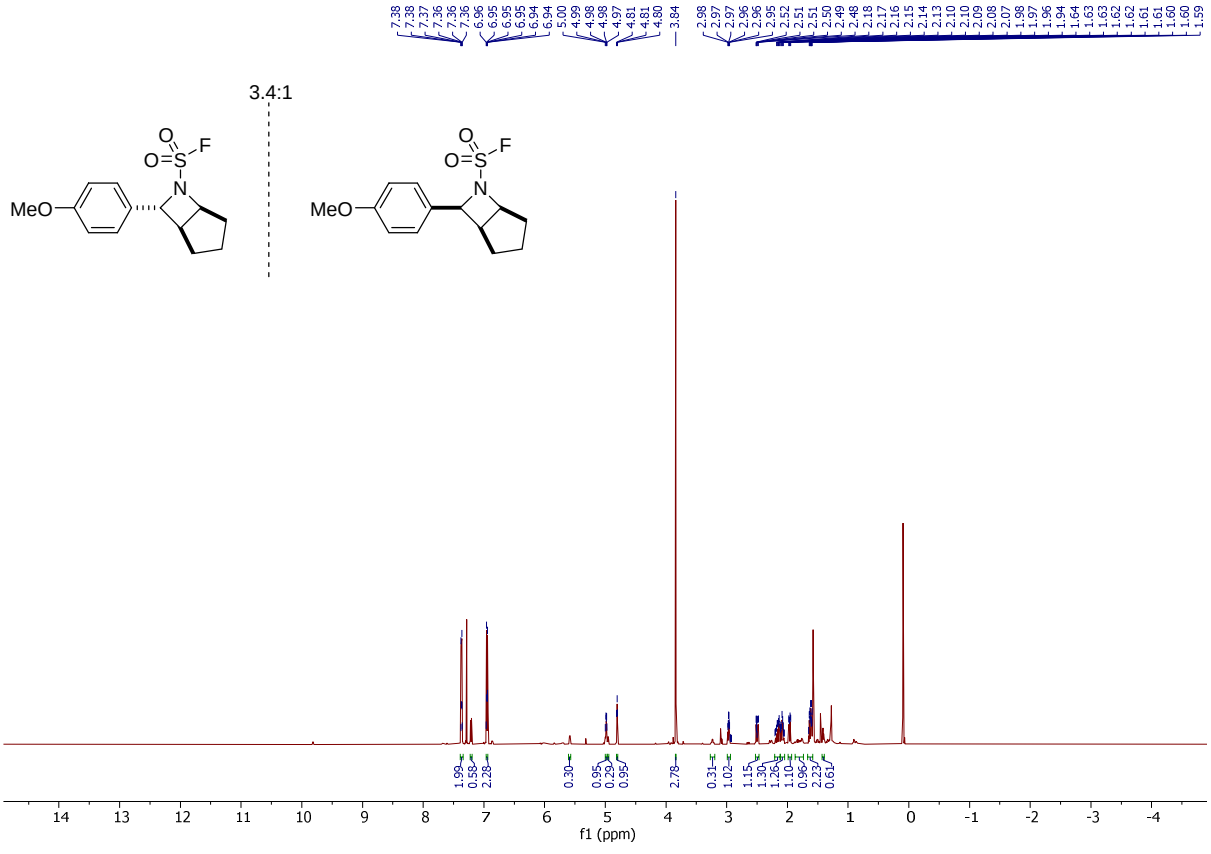
(1*R**,5*S**,7*S**)-7-(4-Methoxyphenyl)-6-azabicyclo[3.2.0]heptane-6-sulfonyl fluoride (4y)

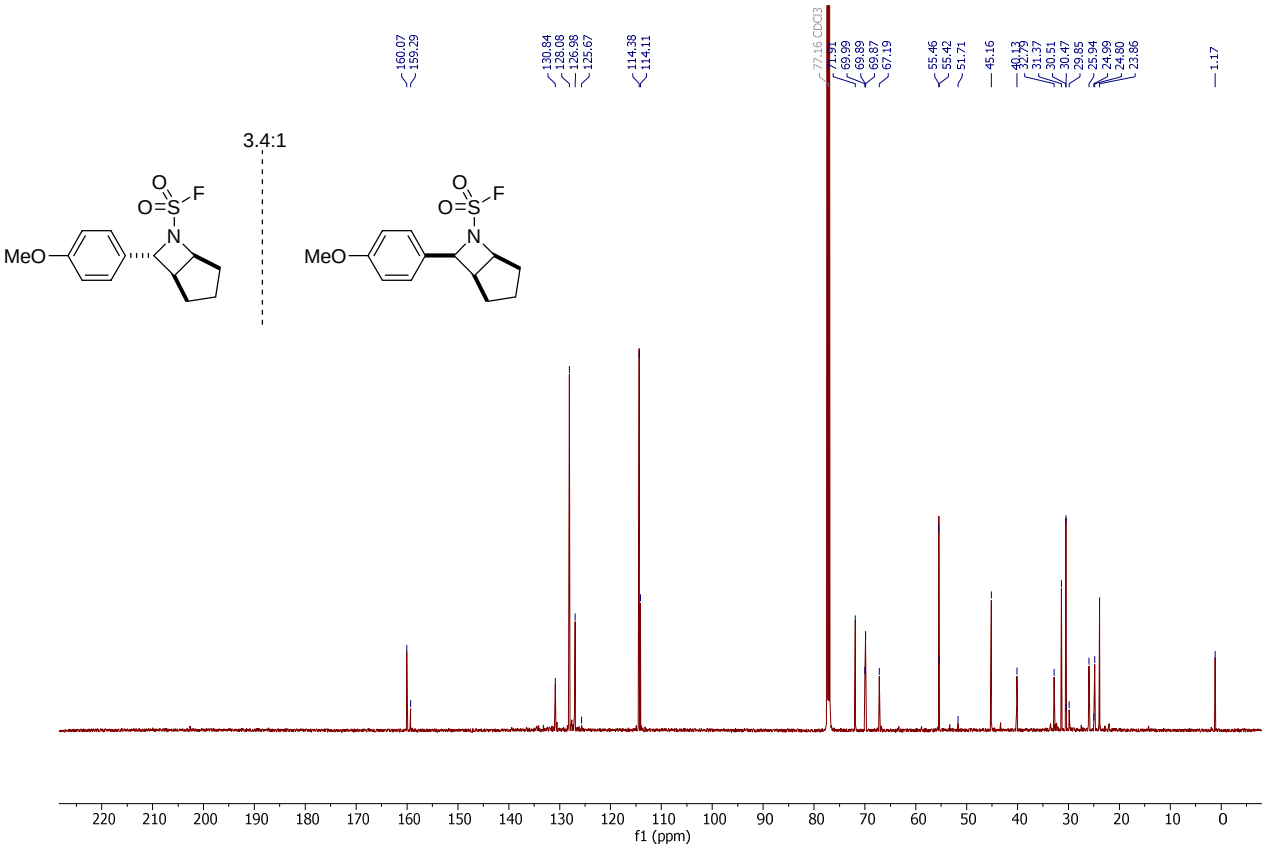


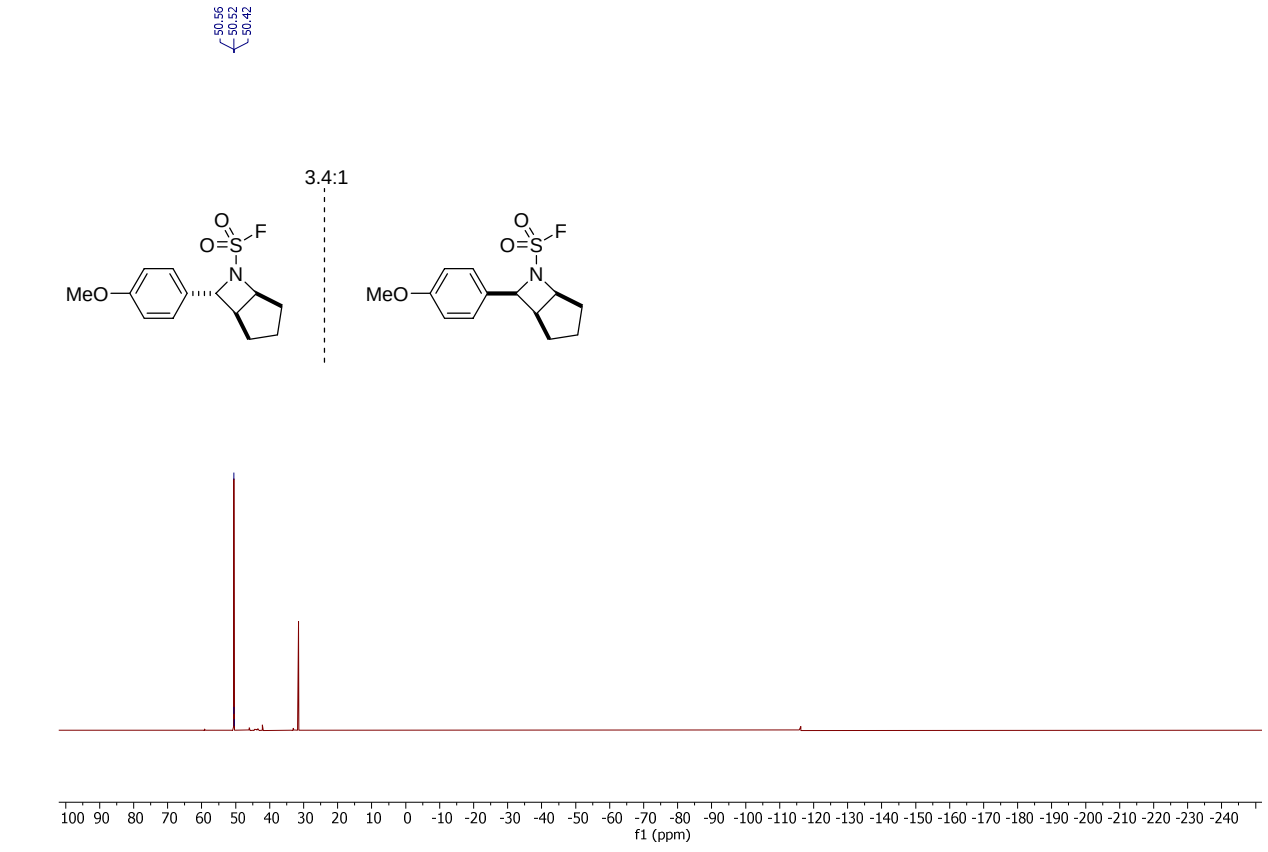




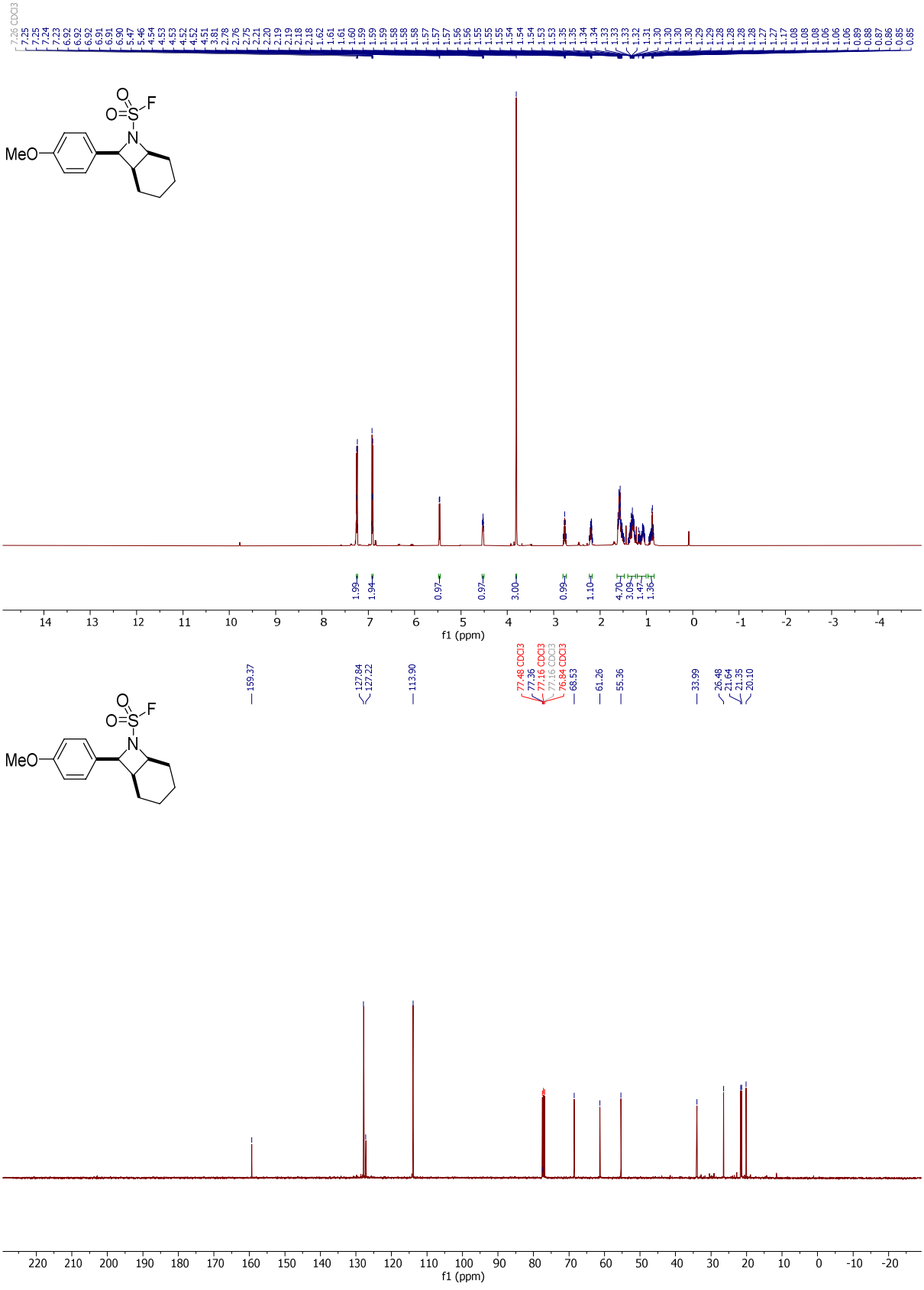
(1R*,5S*,7R*)-7-(4-Methoxyphenyl)-6-azabicyclo[3.2.0]heptane-6-sulfonyl fluoride (4y')

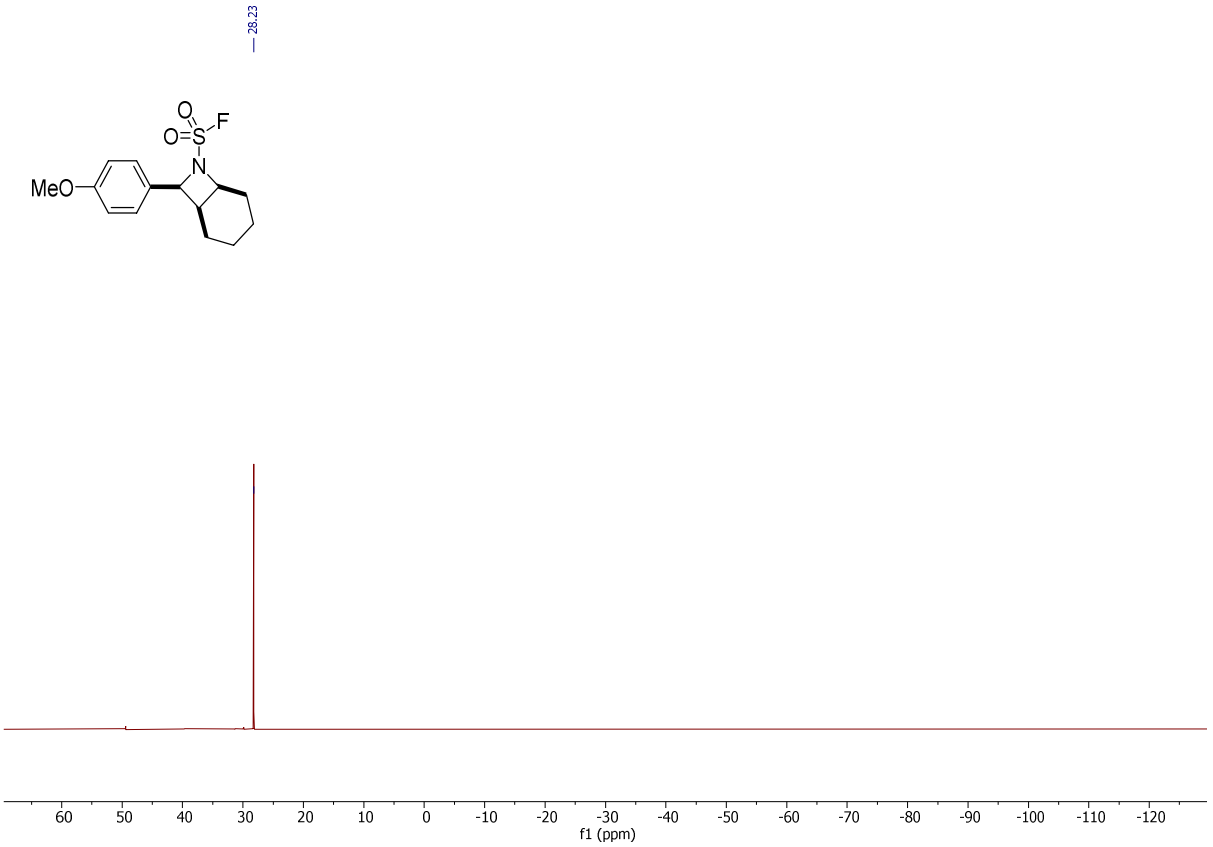



160.07
159.29
130.84
128.08
126.98
125.67
114.38
114.11
77.16 CDCl3
71.91
69.99
69.89
69.87
67.19
55.46
55.42
51.71
45.16
40.13
32.79
31.37
30.51
30.47
29.85
25.94
24.99
24.80
23.86
1.17
3.4:1
MeO
MeO
f1 (ppm)

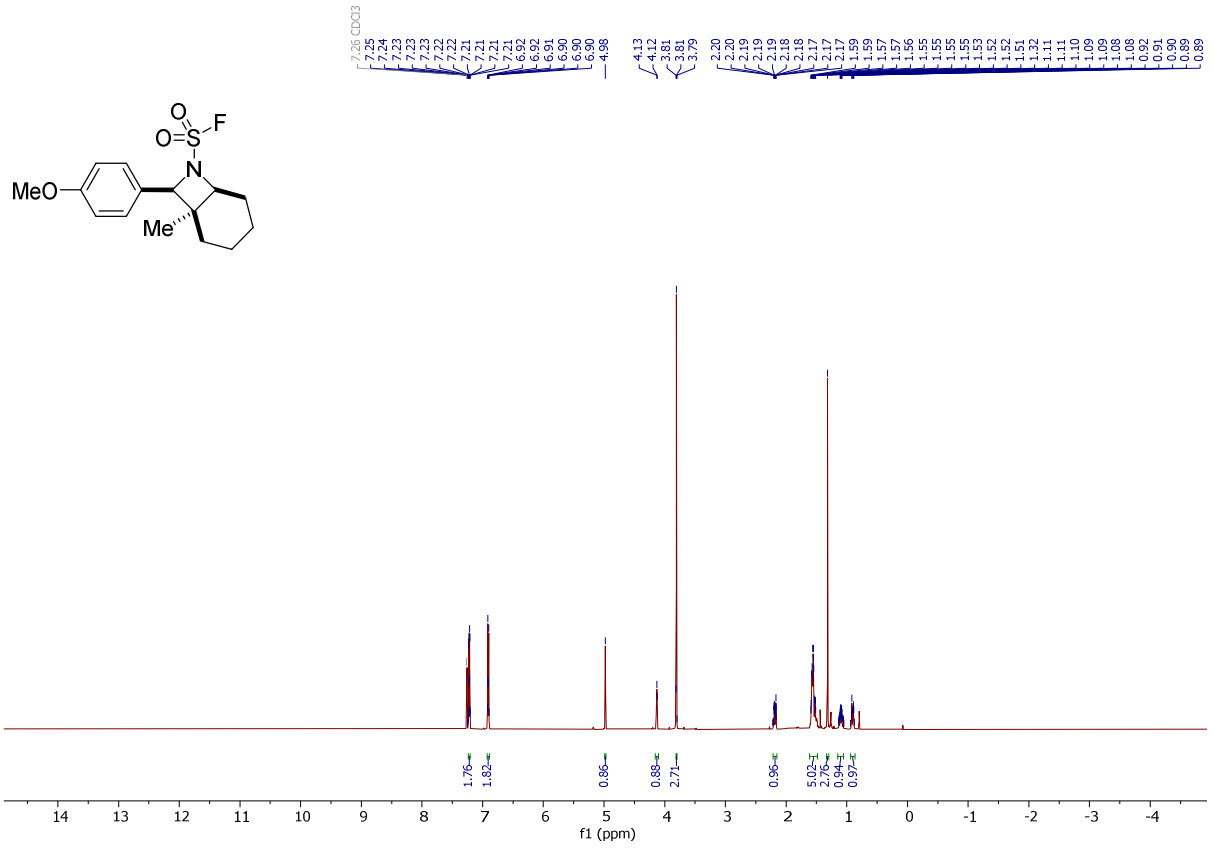

50.56
50.52
50.42
3.4:1
MeO
MeO
f1 (ppm)

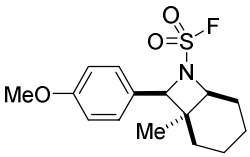
(1*R**,6*S**,8*S**)-8-(4-Methoxyphenyl)-7-azabicyclo[4.2.0]octane-7-sulfonyl fluoride (4z)



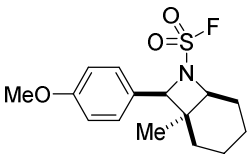


(1*R**,6*S**,8*R**)-8-(4-Methoxyphenyl)-1-methyl-7-azabicyclo[4.2.0]octane-7-sulfonyl fluoride (4aa)




O
O=S
F
N
MeO
Me

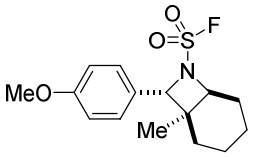
128.09
127.55
126.99
113.95
113.90
77.48 CDCl3
77.36
77.16 CDCl3
77.16 CDCl3
76.84 CDCl3
75.50
68.31
55.39
40.09
32.87
29.16
25.56
24.97
20.46
20.31
220 210 200 190 180 170 160 150 140 130 120 110 100 90 80 70 60 50 40 30 20 10 0 -10 -20
f1 (ppm)

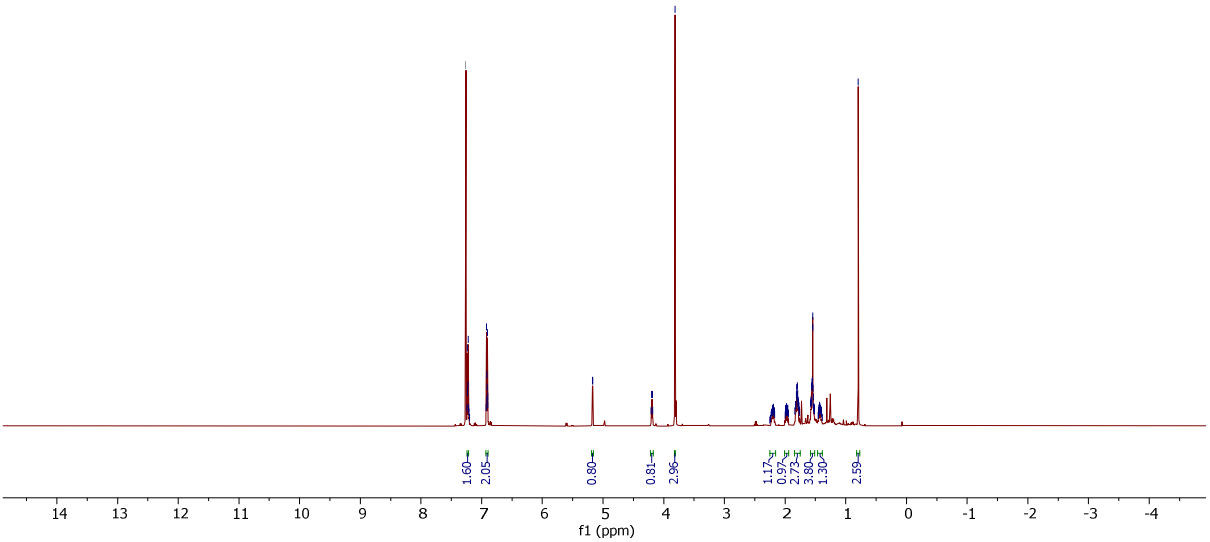

O
O=S
F
N
MeO
Me

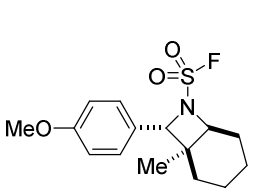
30.55
30.51
90 80 70 60 50 40 30 20 10 0 -10 -20 -30 -40 -50 -60 -70 -80 -90 -100 -110 -120 -130 -140 -150 -160 -170 -180 -190 -200 -210 -220 -230 -240
f1 (ppm)

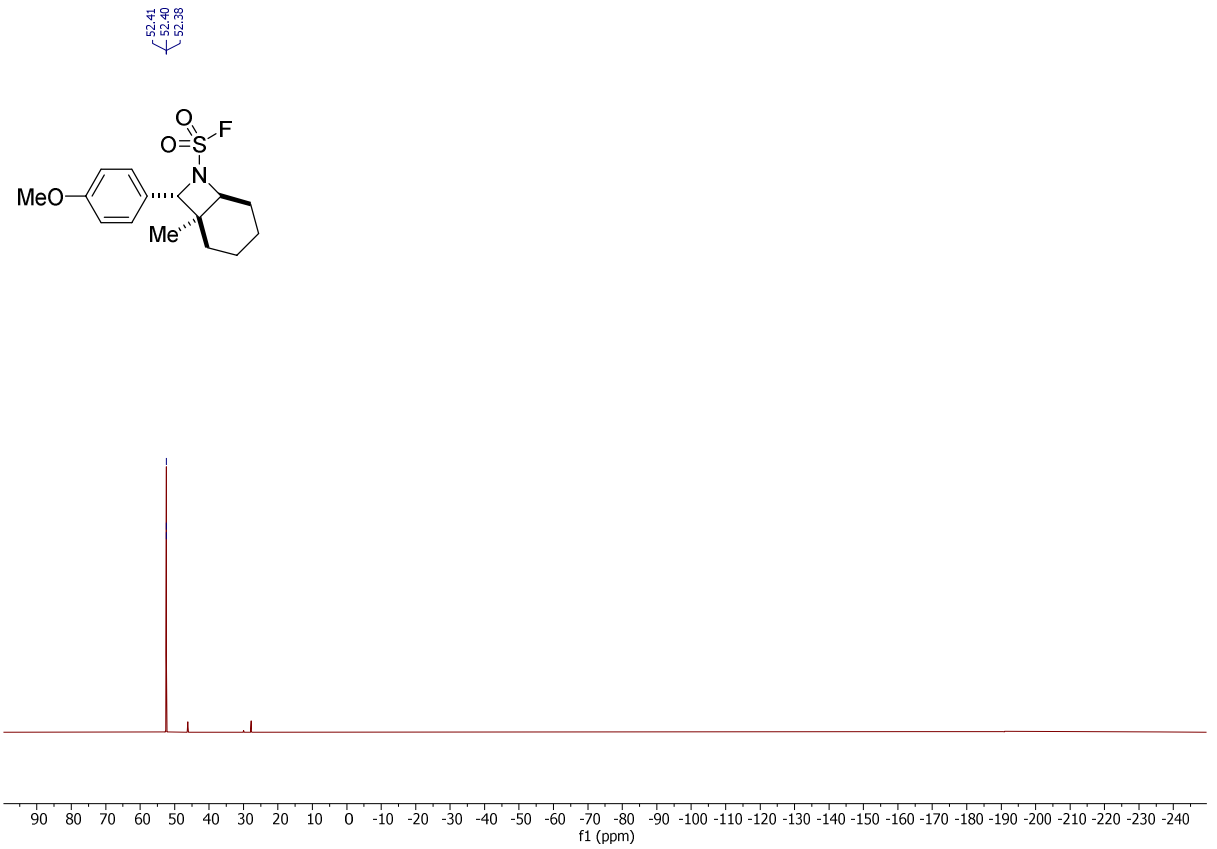
(1*S**,6*R**,8*S**)-8-(4-Methoxyphenyl)-1-methyl-7-azabicyclo[4.2.0]octane-7-sulfonyl fluoride (4aa')



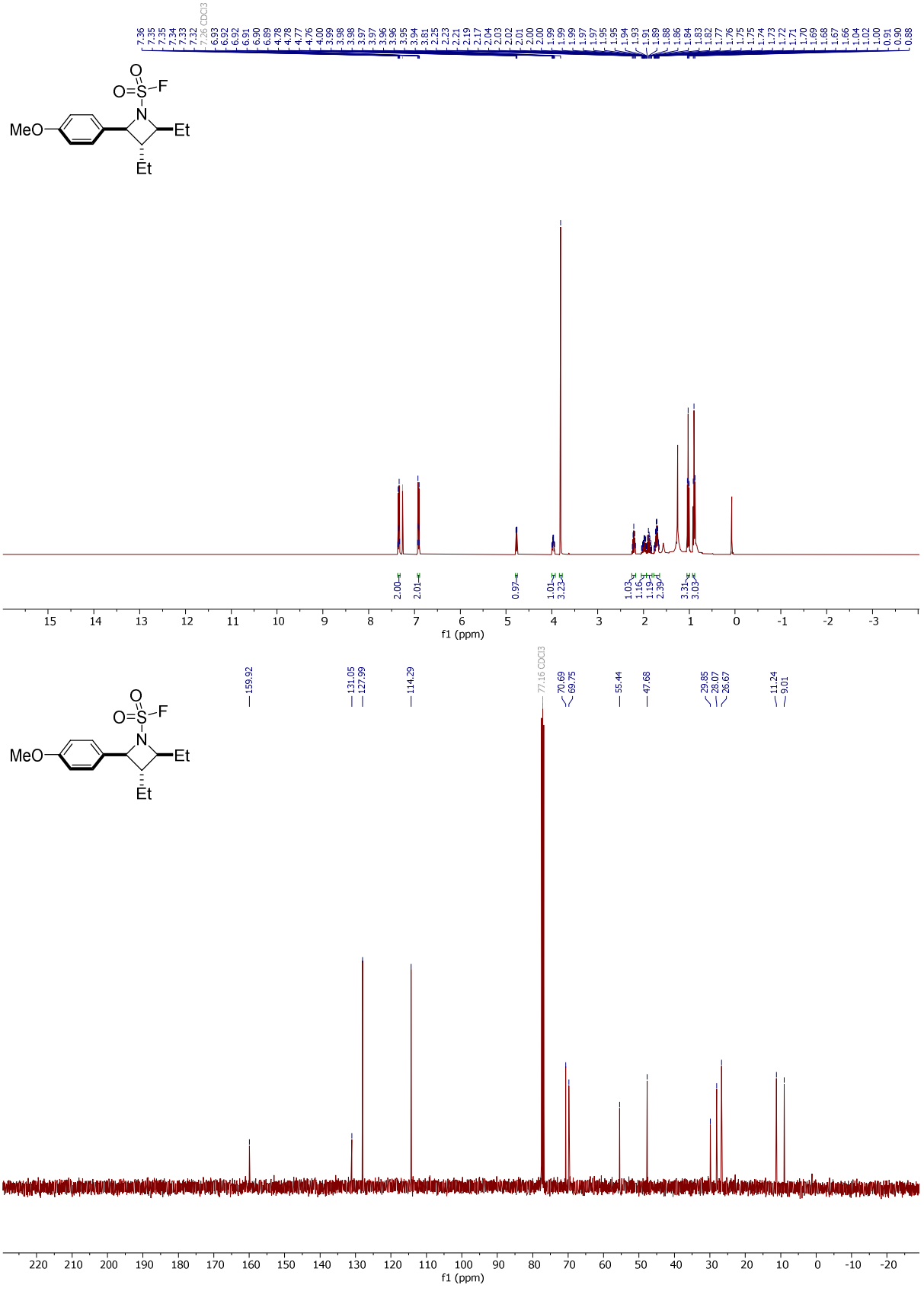


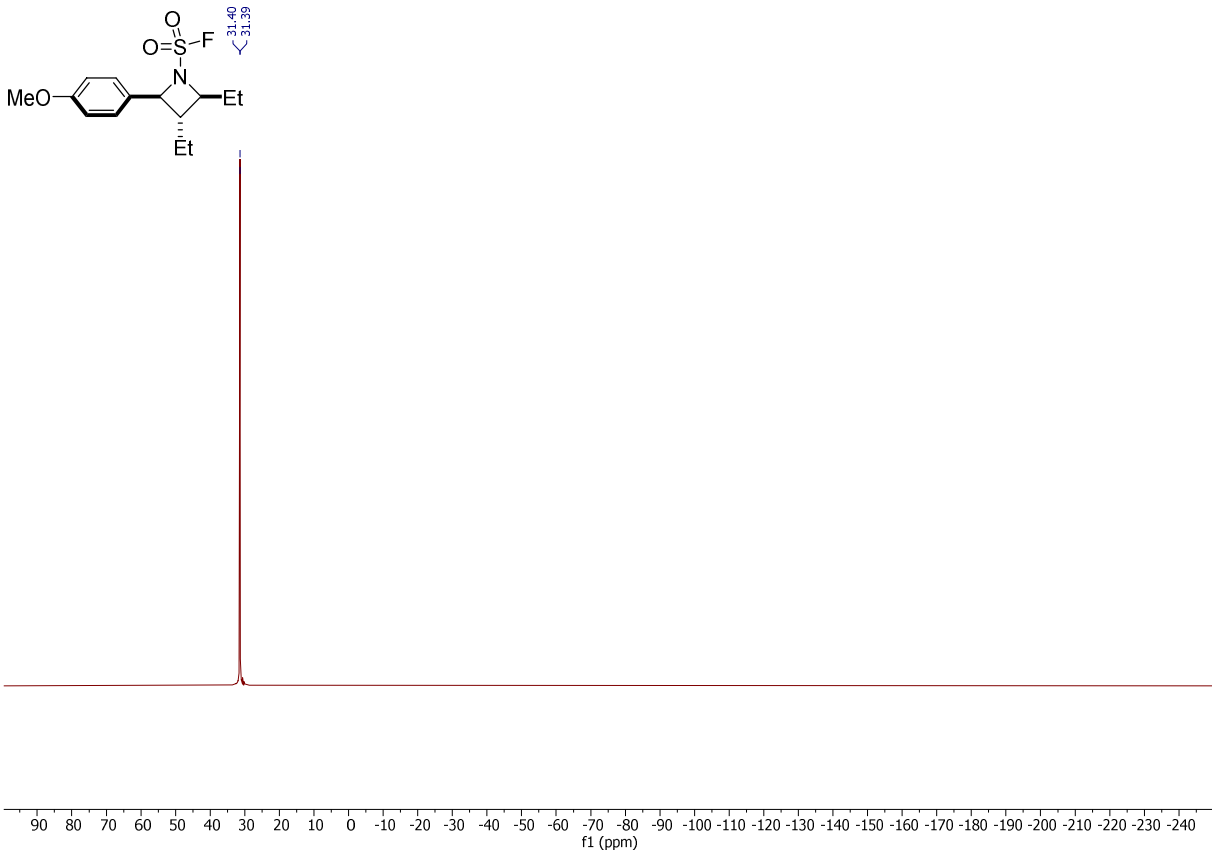





52.41
52.40
52.38
O
O=S
F
N
MeO
Me
90 80 70 60 50 40 30 20 10 0 -10 -20 -30 -40 -50 -60 -70 -80 -90 -100 -110 -120 -130 -140 -150 -160 -170 -180 -190 -200 -210 -220 -230 -240
f1 (ppm)

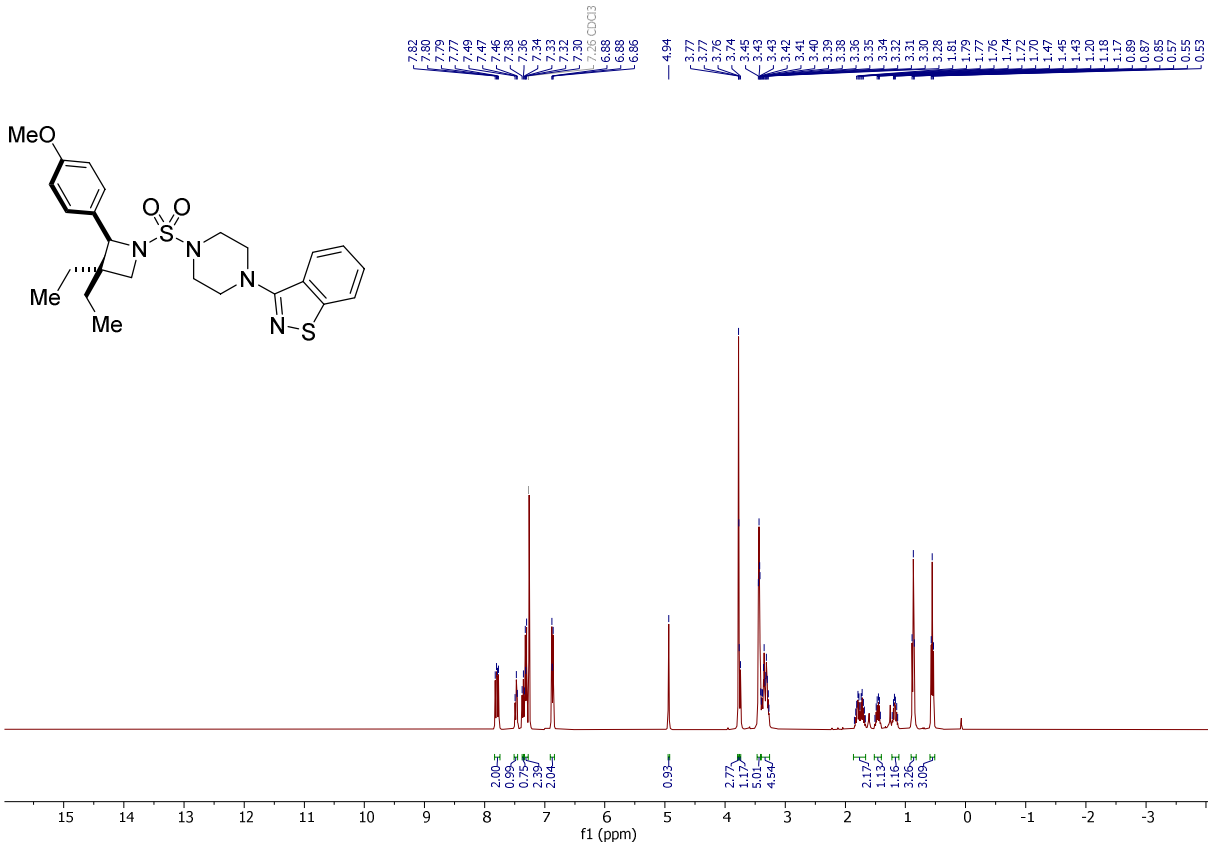
(2*S**,3*S**,4*S**)-2,3-diethyl-4-(4-methoxyphenyl)azetidine-1-sulfonyl fluoride (4ab)

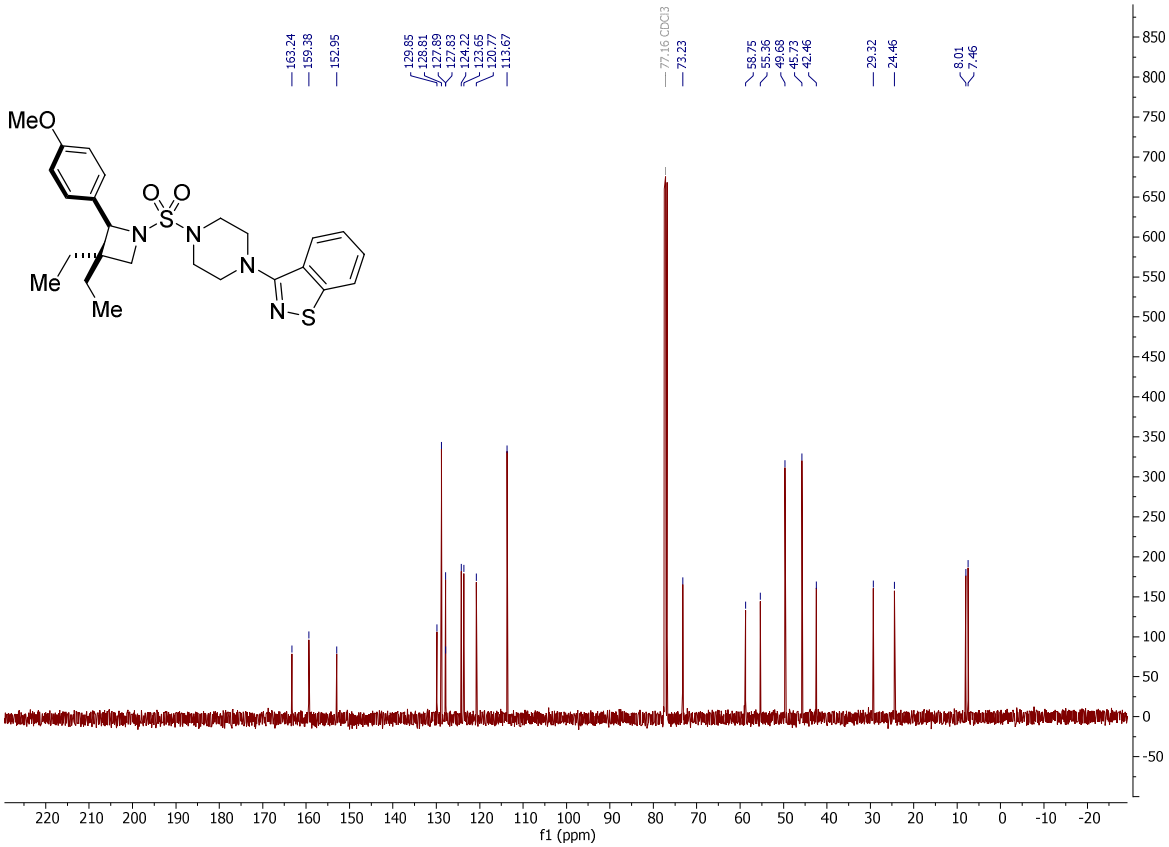



O
O=S–F
N
MeO
Et
Et
31.40
31.39
90 80 70 60 50 40 30 20 10 0 -10 -20 -30 -40 -50 -60 -70 -80 -90 -100 -110 -120 -130 -140 -150 -160 -170 -180 -190 -200 -210 -220 -230 -240
f1 (ppm)

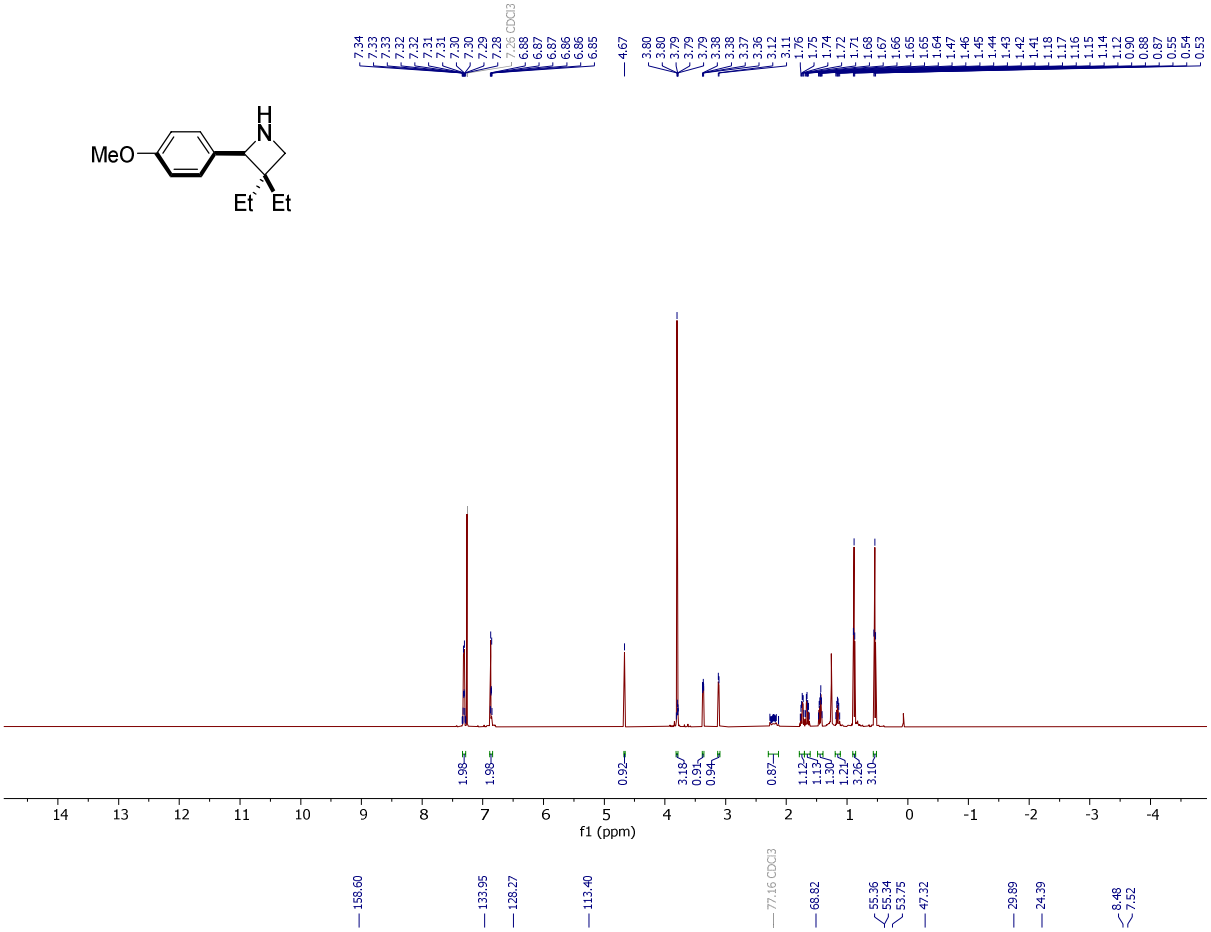
Derivitisation

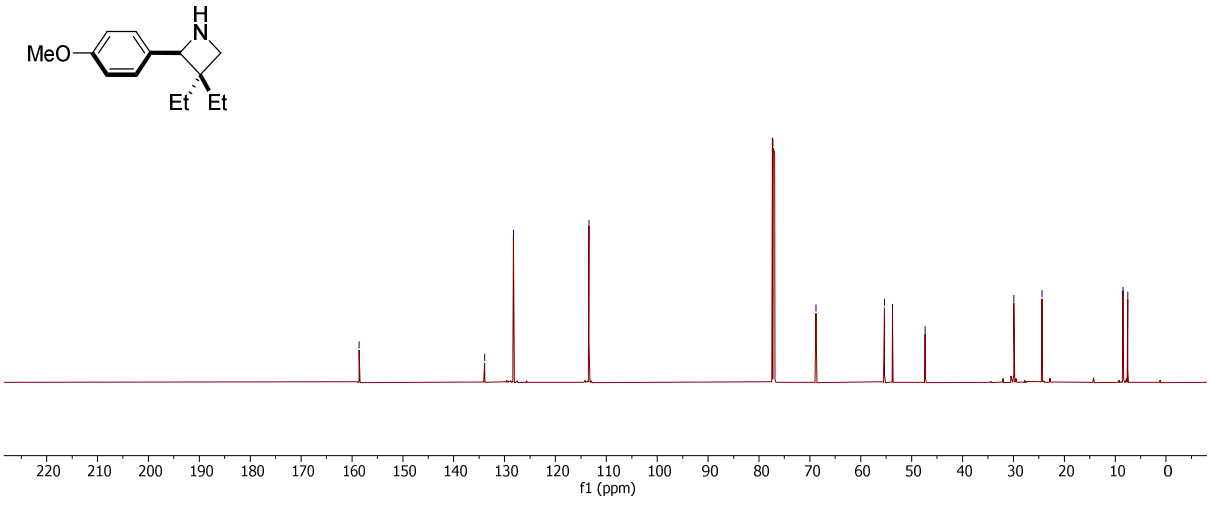
(*R**)-3-(4-((3,3-Diethyl-2-(4-methoxyphenyl)azetidin-1-yl)sulfonyl)piperazin-1-yl)benzo[d]isothiazole (6)


MeO
O O
S
N
N
N
Me
Me
N
S
f1 (ppm)

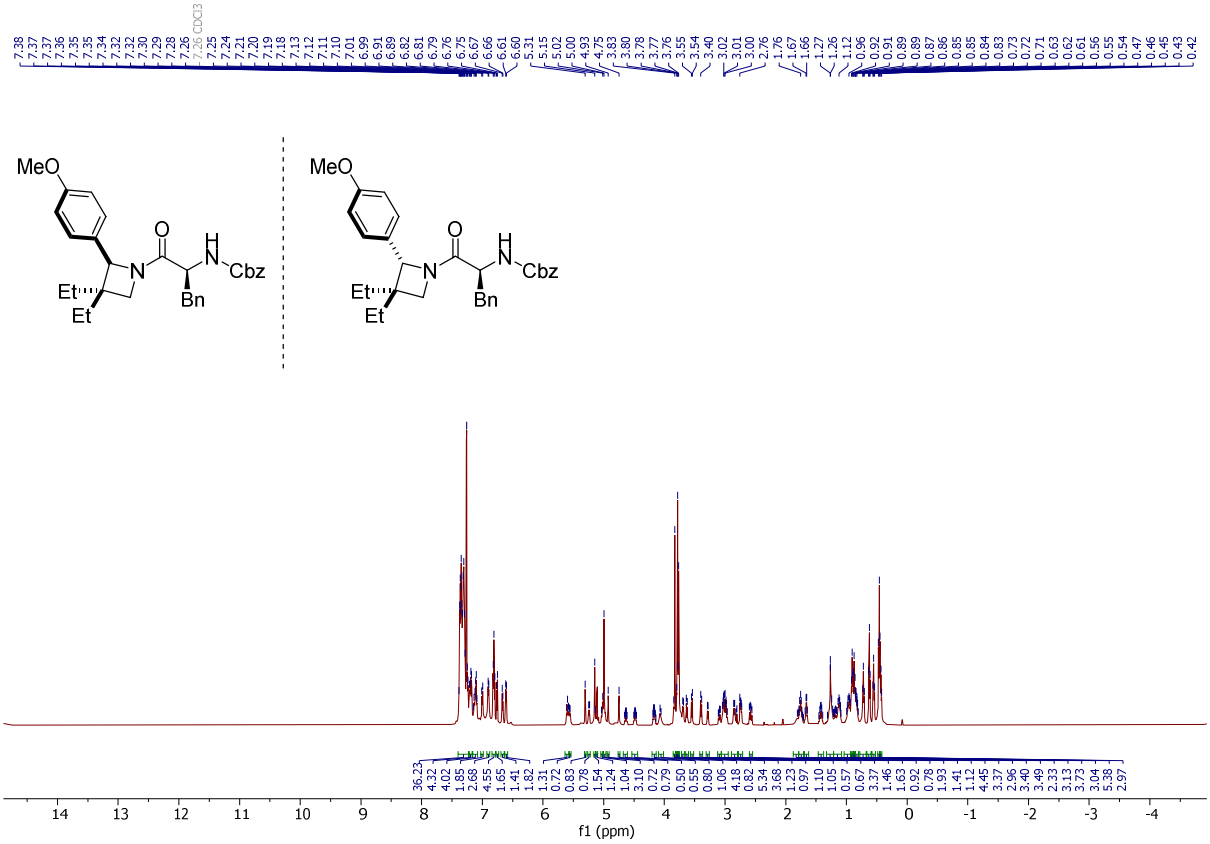

MeO
O O
S
N
N
N
Me
Me
N
S
f1 (ppm)

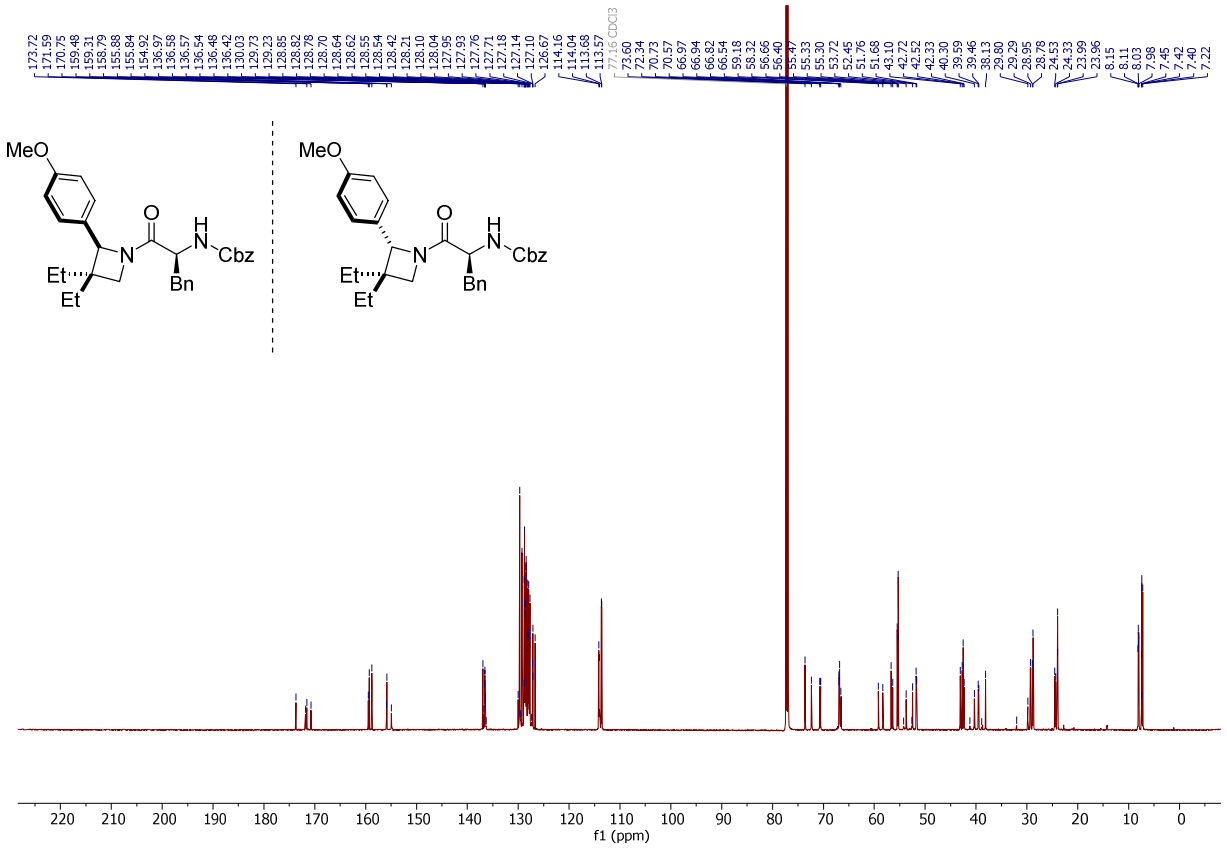
(*R**)-3,3-Diethyl-2-(4-methoxyphenyl) azetidine (7)



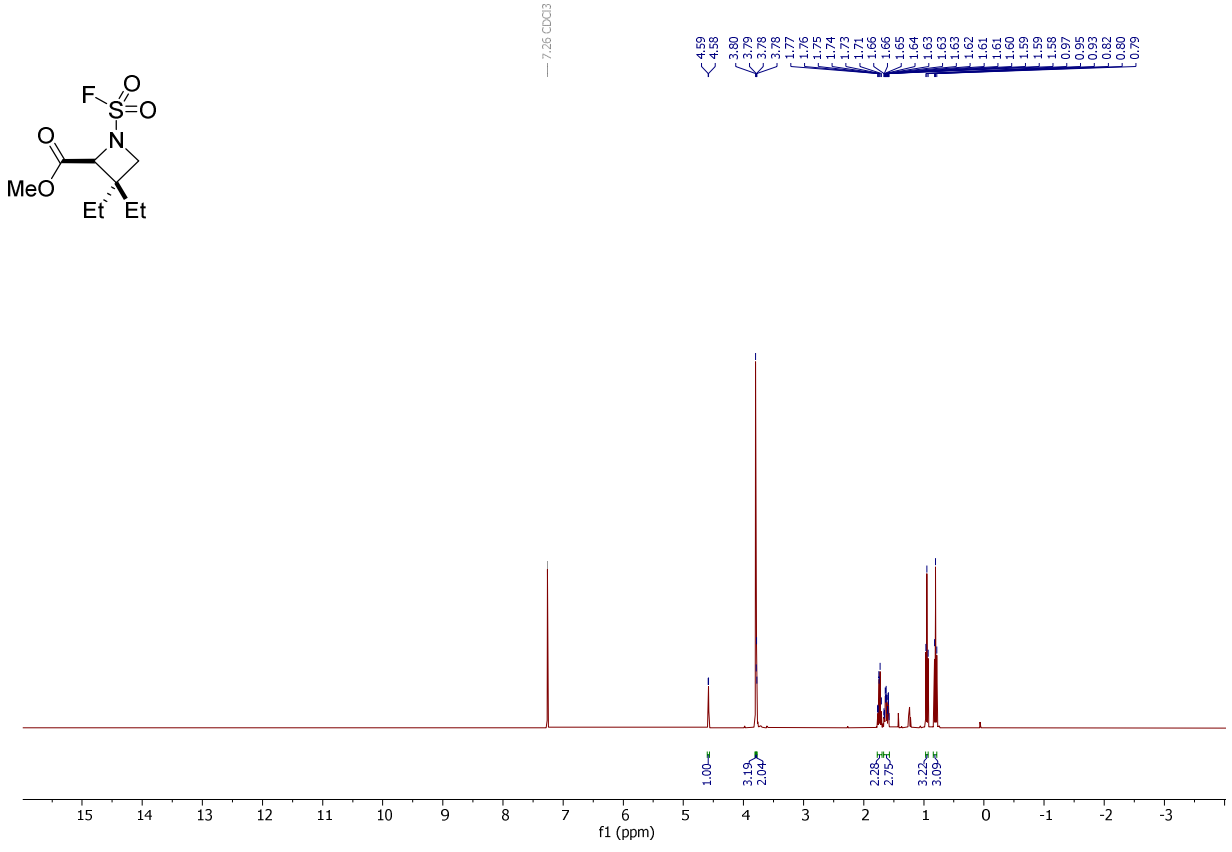


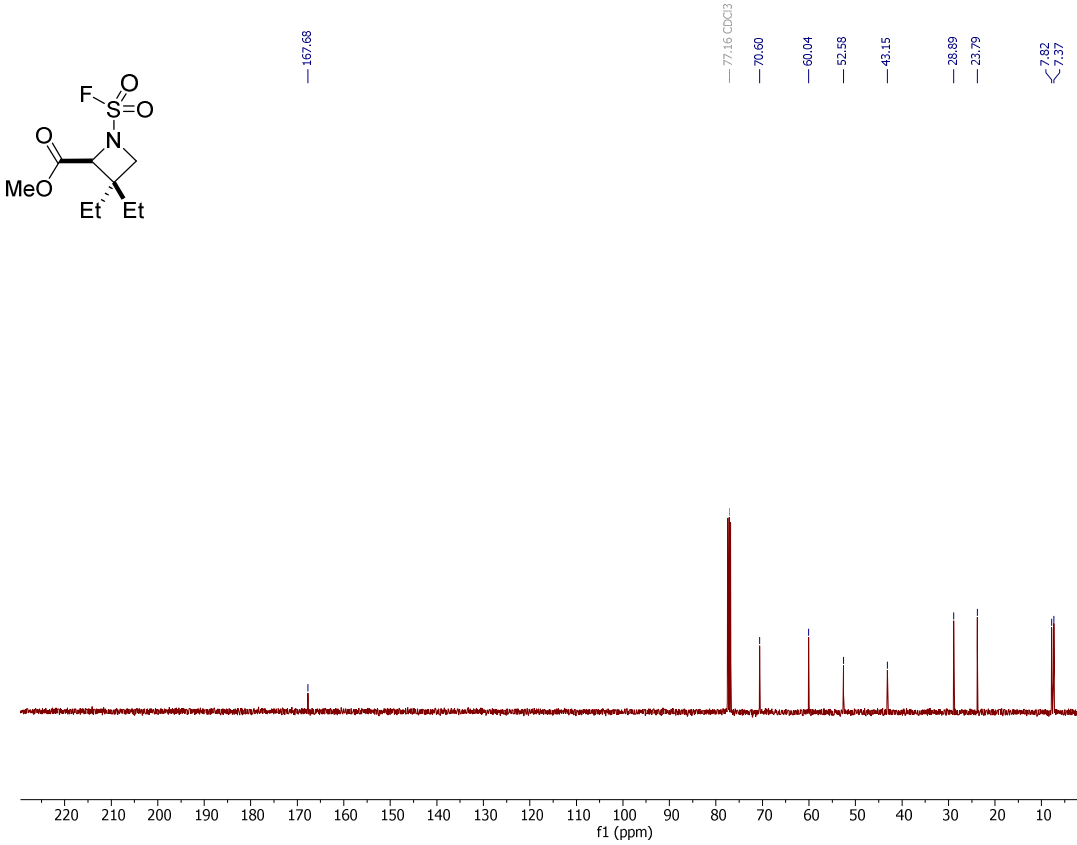
Benzyl ((S*)-1-((R*)-3,3-diethyl-2-(4-methoxyphenyl)azetidin-1-yl)-1-oxo-3-phenylpropan-2-yl)carbamate (8) and Benzyl ((S*)-1-((S*)-3,3-diethyl-2-(4-methoxyphenyl)azetidin-1-yl)-1-oxo-3-phenylpropan-2-yl)carbamate (8')

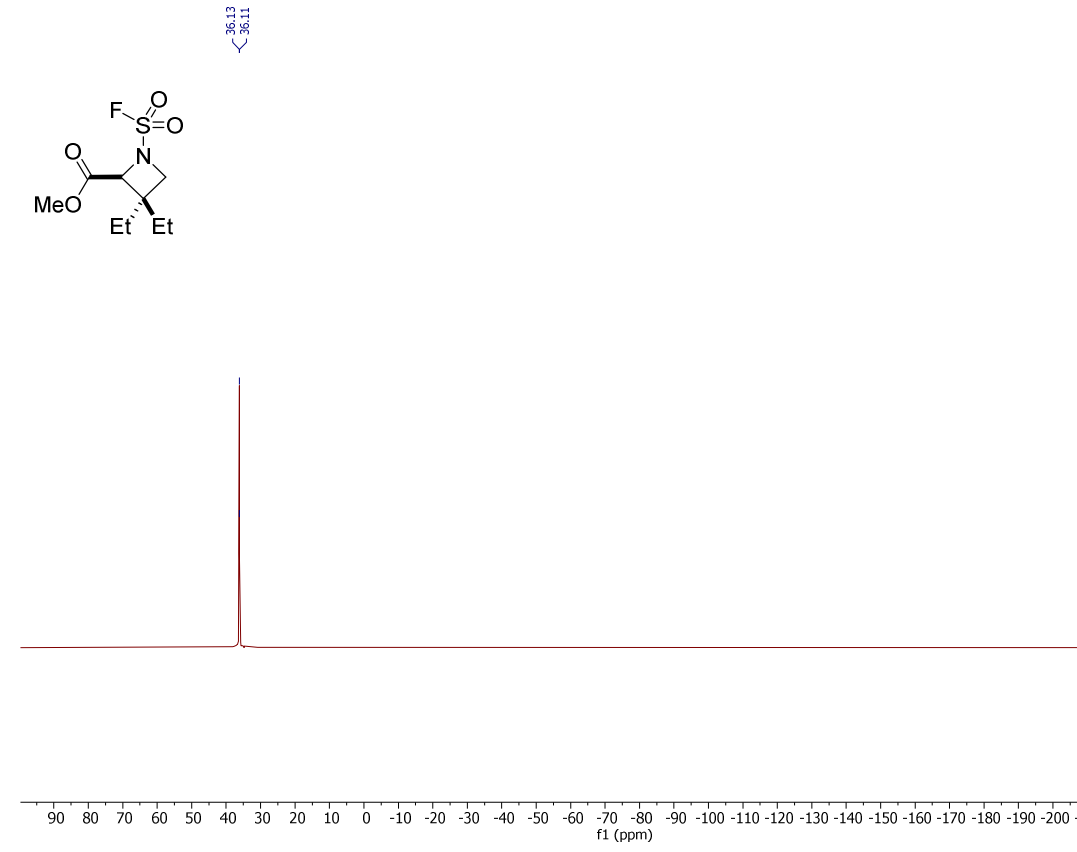




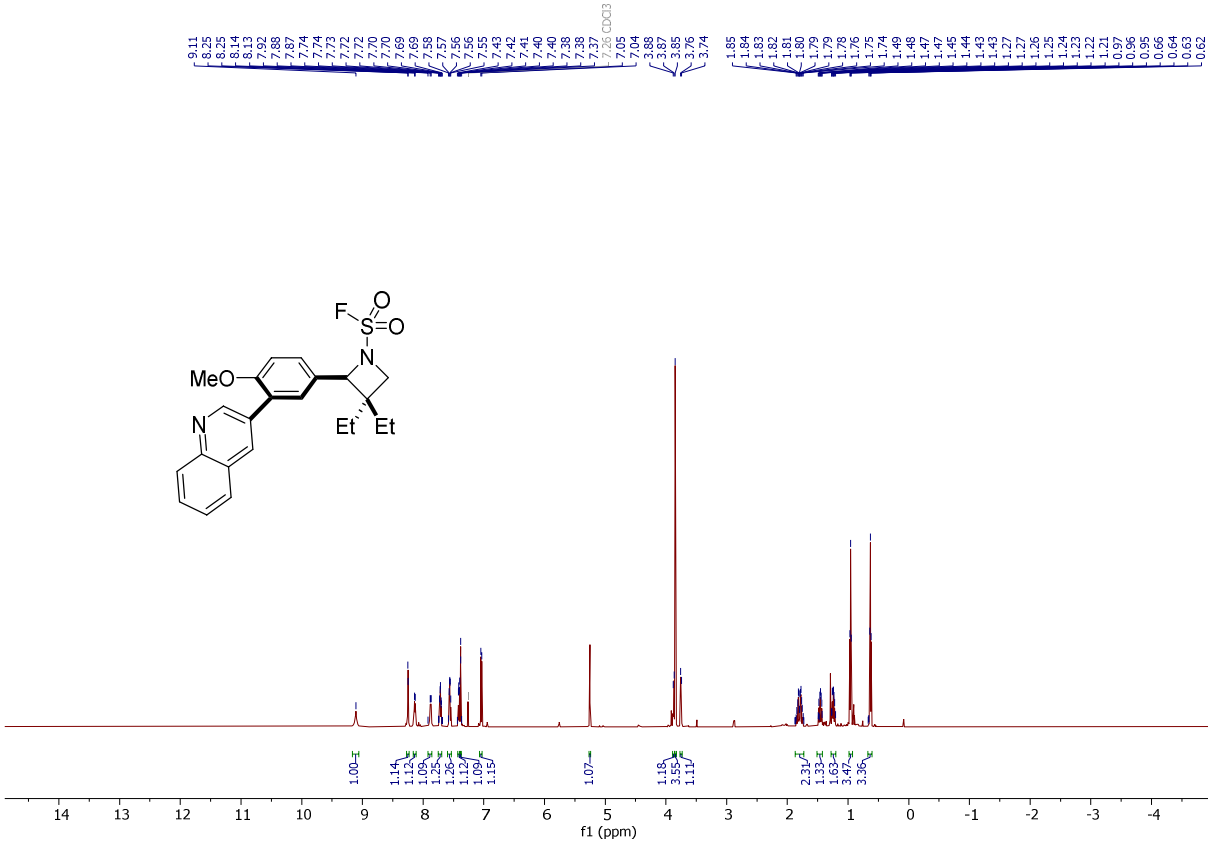
Methyl (*S**)-3,3-diethyl-1-(fluorosulfonyl)azetidine-2-carboxylate (9)

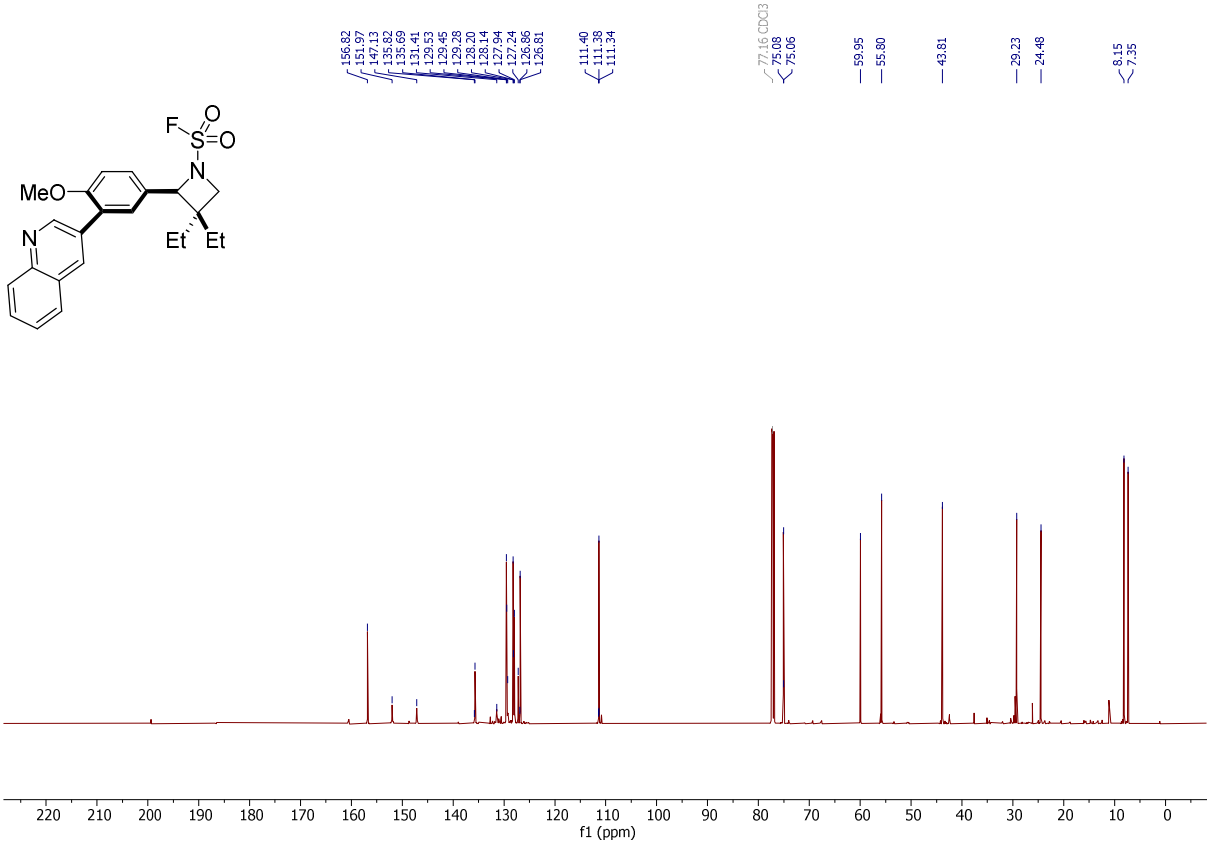


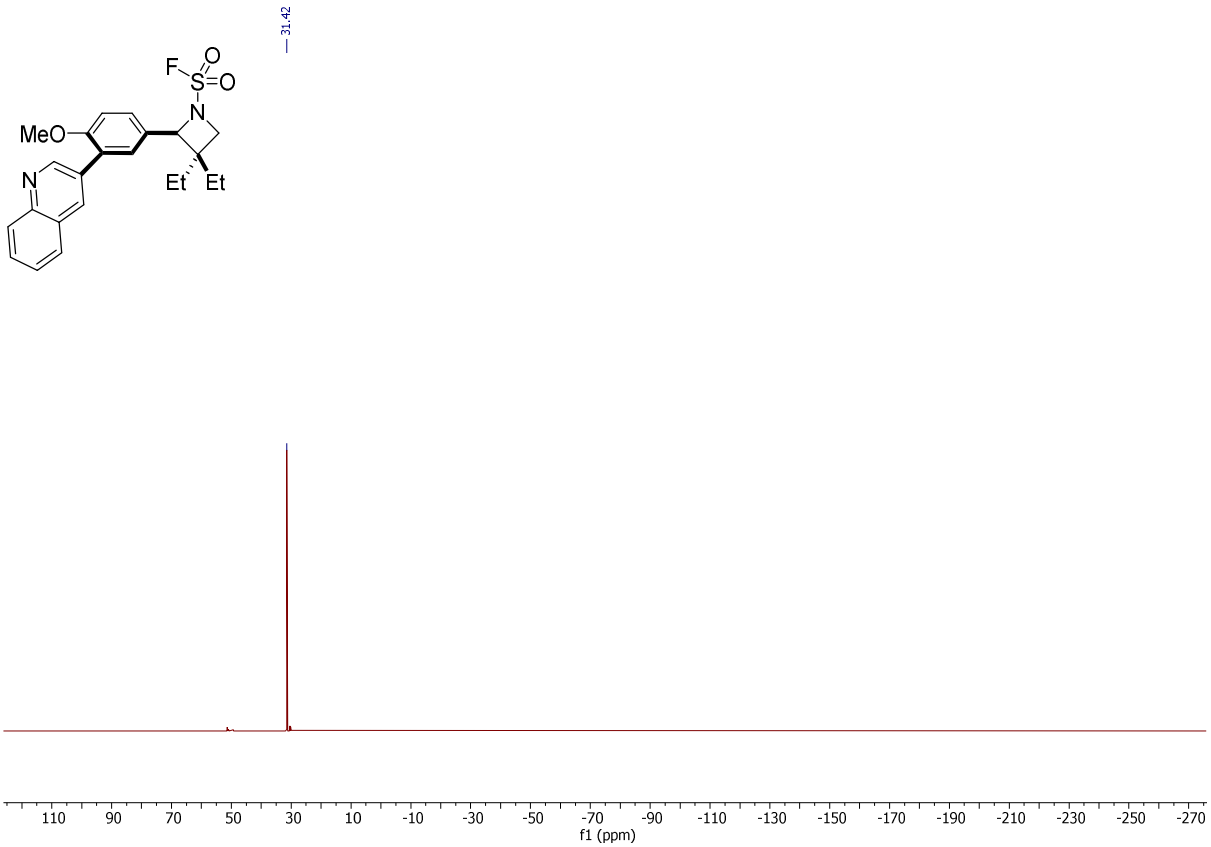

167.68
77.16 CDCl3
70.60
60.04
52.58
43.15
28.89
23.79
7.82
7.37
F
O
S
O
O
N
MeO
Et
Et
220 210 200 190 180 170 160 150 140 130 120 110 100 90 80 70 60 50 40 30 20 10 0 -10 -20
f1 (ppm)


36.13
36.11
F
O
S
O
O
N
MeO
Et
Et
90 80 70 60 50 40 30 20 10 0 -10 -20 -30 -40 -50 -60 -70 -80 -90 -100 -110 -120 -130 -140 -150 -160 -170 -180 -190 -200 -210 -220 -230 -240
f1 (ppm)

(*R**)-3,3-Diethyl-2-(4-methoxy-3-(quinolin-3-yl)phenyl)azetidine-1-sulfonyl fluoride (10)

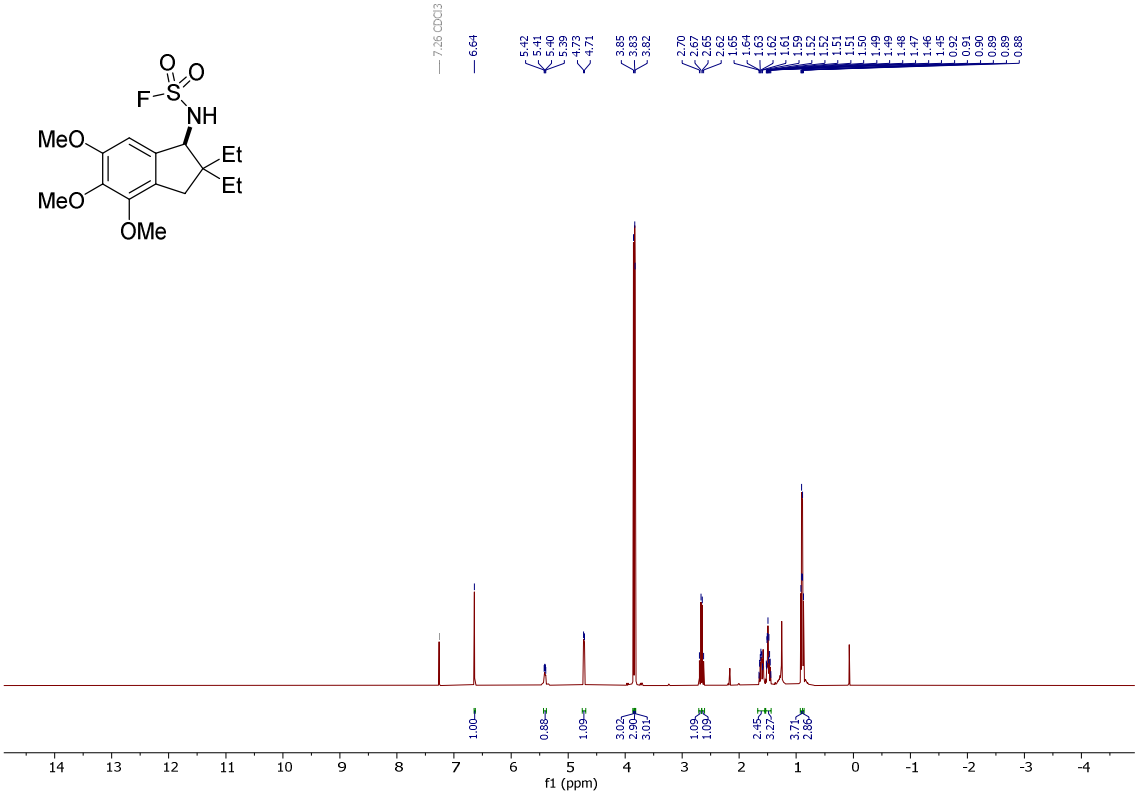


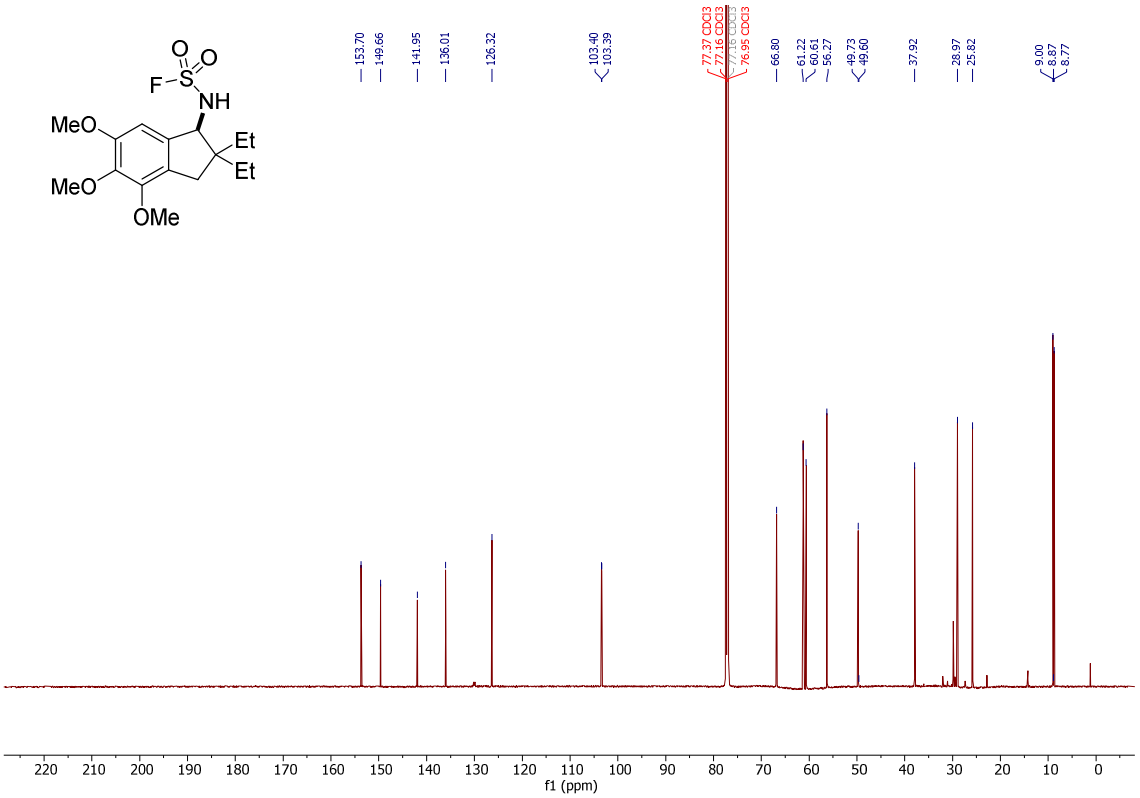

156.82
151.97
147.13
135.82
135.69
131.41
129.53
129.45
129.28
128.20
128.14
127.94
127.24
126.86
126.81
111.40
111.38
111.34
77.16 CDCl3
75.08
75.06
59.95
55.80
43.81
29.23
24.48
8.15
7.35
F
O
S
O
N
MeO
N
Et
Et
220 210 200 190 180 170 160 150 140 130 120 110 100 90 80 70 60 50 40 30 20 10 0
f1 (ppm)

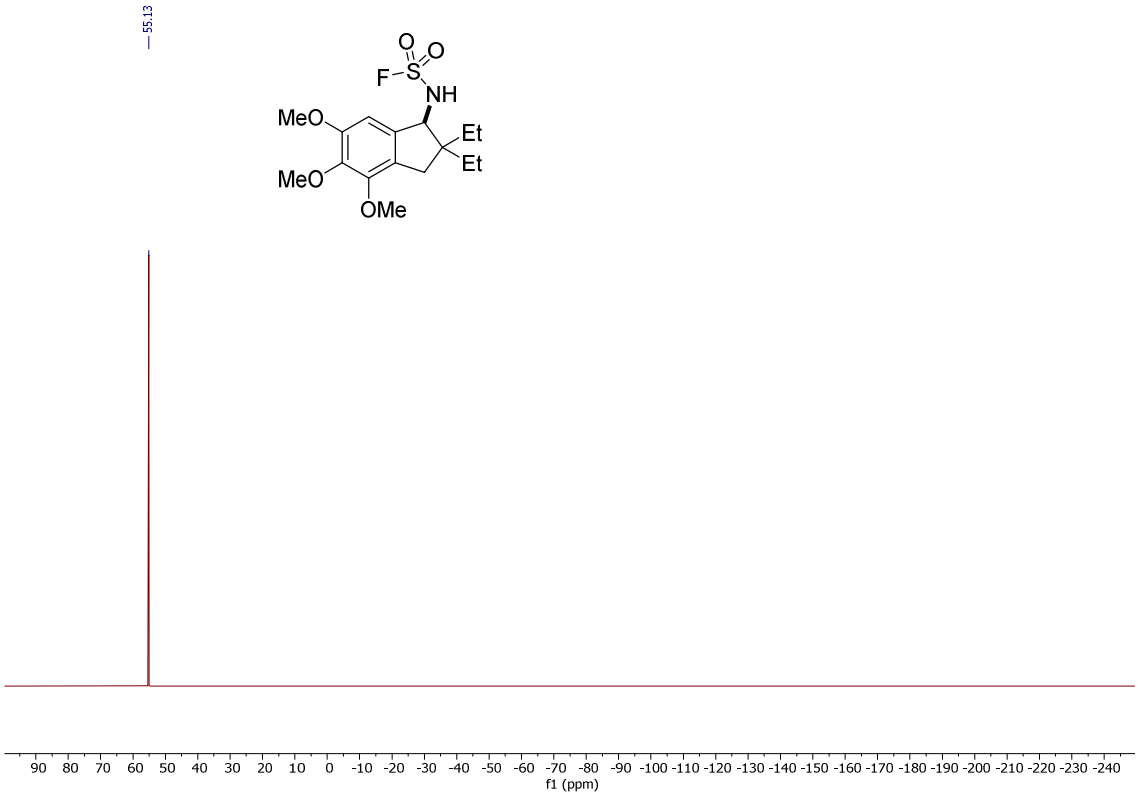

31.42
F
O
S
O
N
MeO
N
Et
Et
110 90 70 50 30 10 -10 -30 -50 -70 -90 -110 -130 -150 -170 -190 -210 -230 -250 -270
f1 (ppm)

Indane

(*S**)-(2,2-diethyl-4,5,6-trimethoxy-2,3-dihydro-1H-inden-1-yl)sulfamoyl fluoride (12)

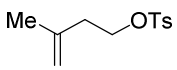


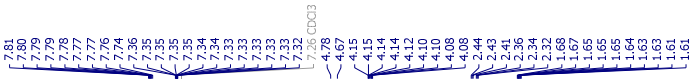


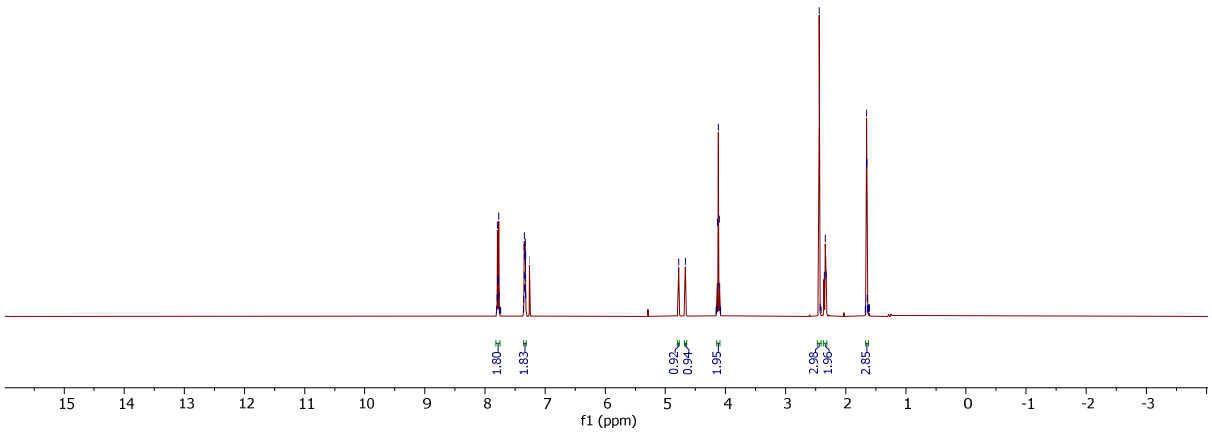

55.13
O
O
F
S
NH
MeO
MeO
OMe
Et
Et
90 80 70 60 50 40 30 20 10 0 -10 -20 -30 -40 -50 -60 -70 -80 -90 -100 -110 -120 -130 -140 -150 -160 -170 -180 -190 -200 -210 -220 -230 -240
f1 (ppm)

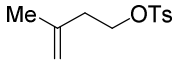
Alkenes

3-Methylbut-3-en-1-yl 4-methylbenzenesulfonate (13)

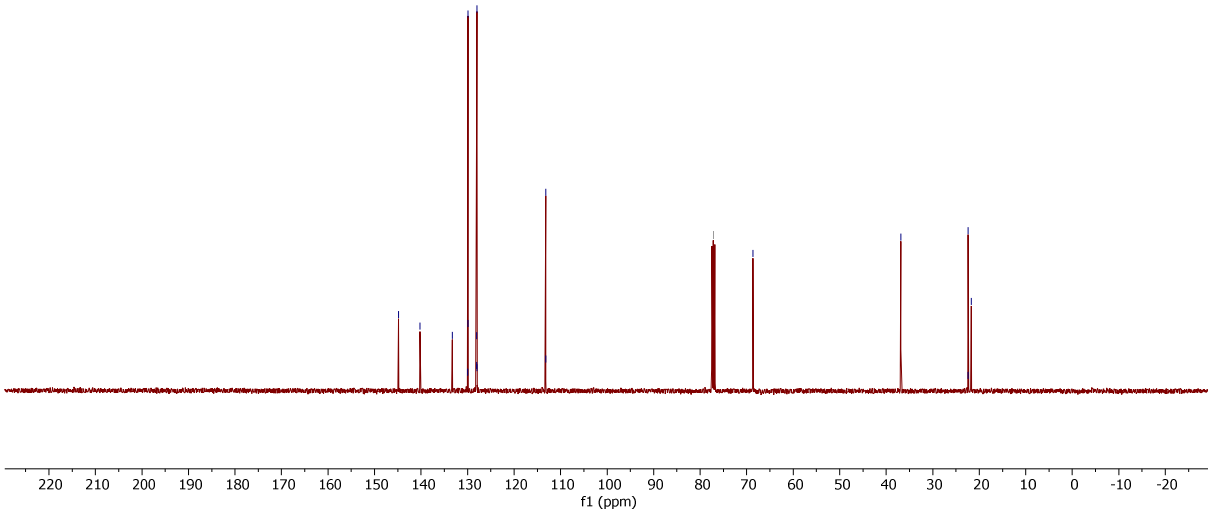




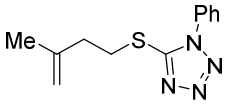


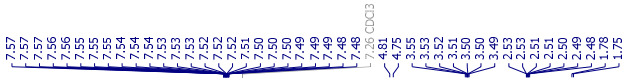


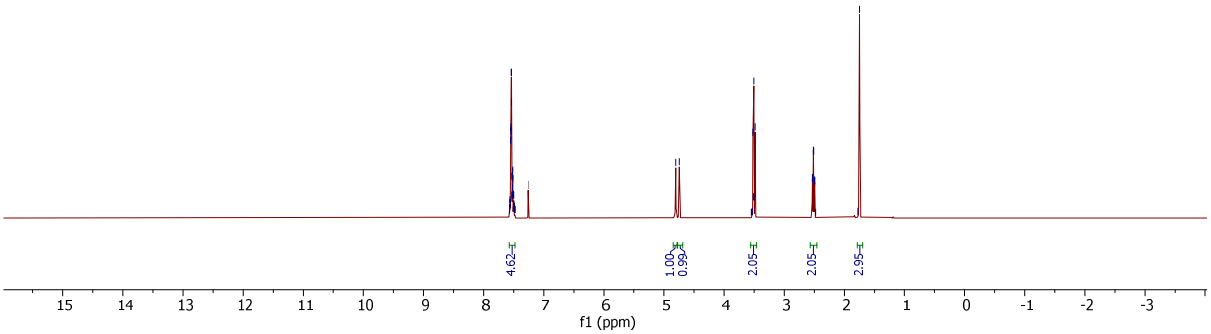


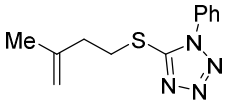


5-((3-Methylbut-3-en-1-yl)thio)-1-phenyl-1H-tetrazole (14)

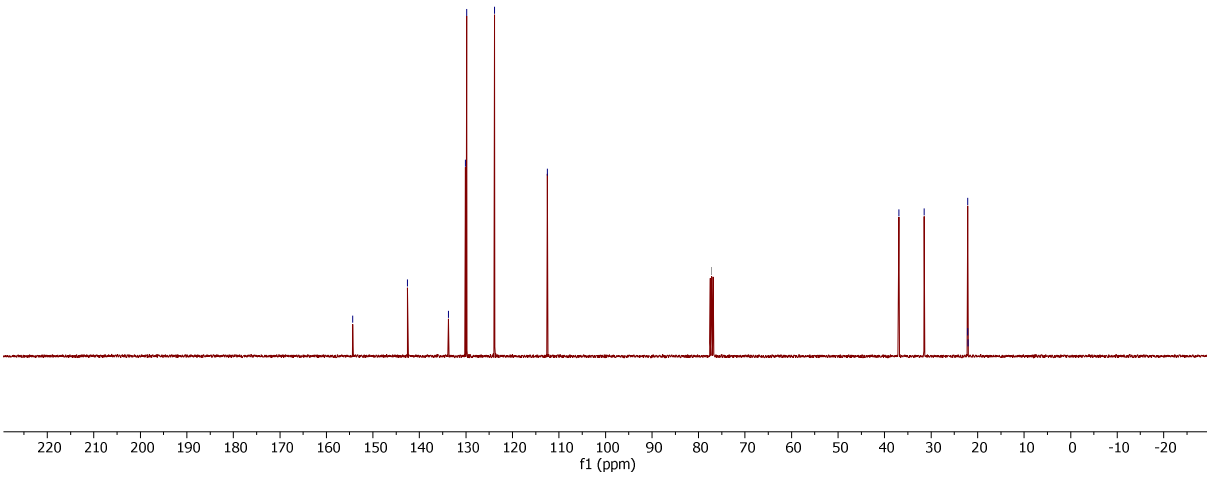






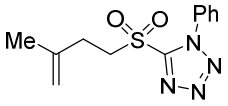


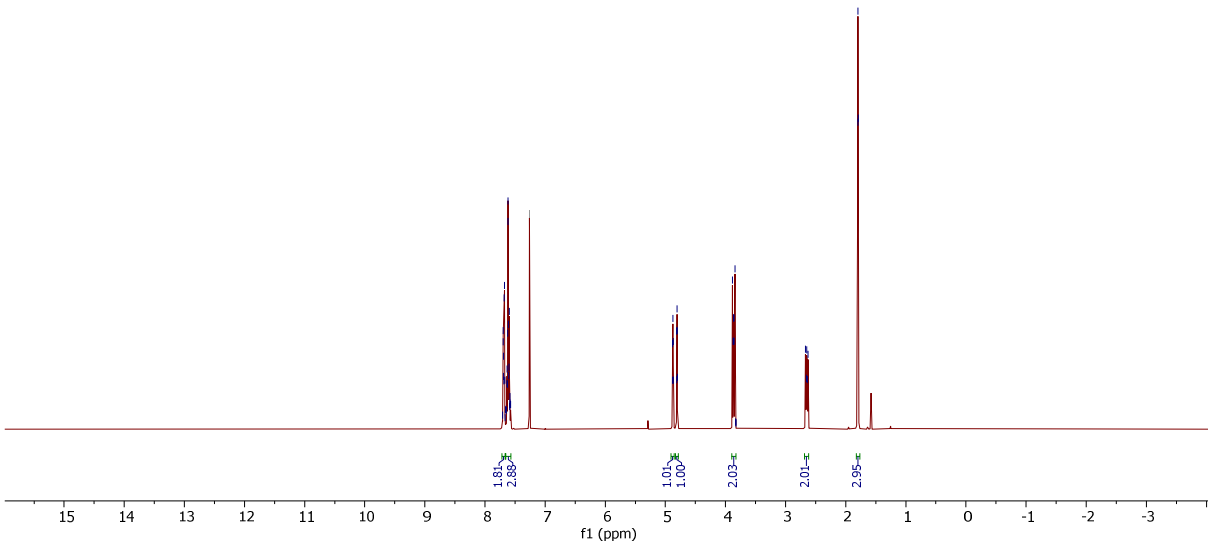




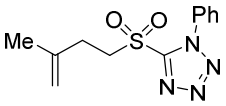
5-((3-Methylbut-3-en-1-yl)sulfonyl)-1-phenyl-1H-tetrazole (15)

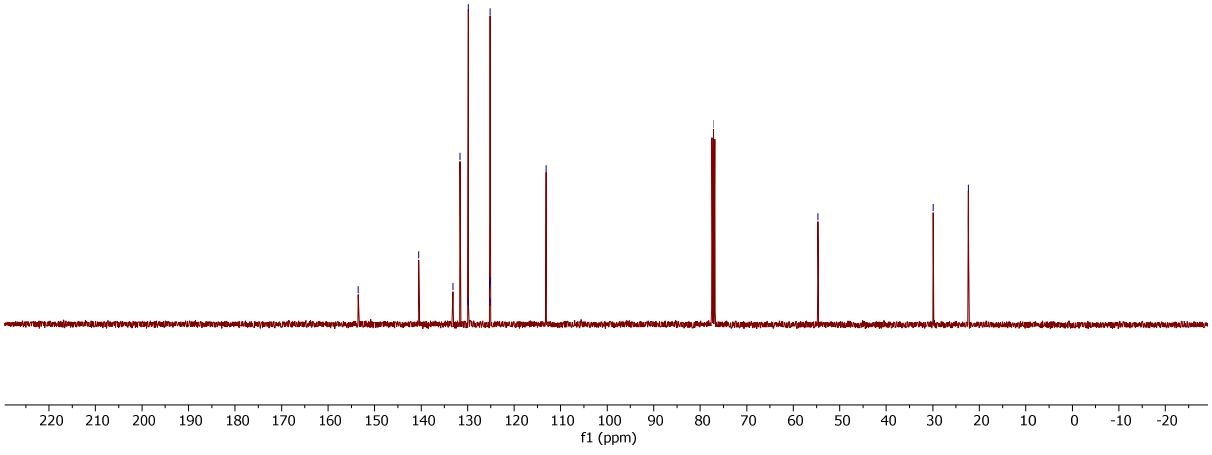






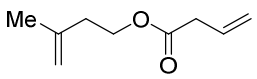


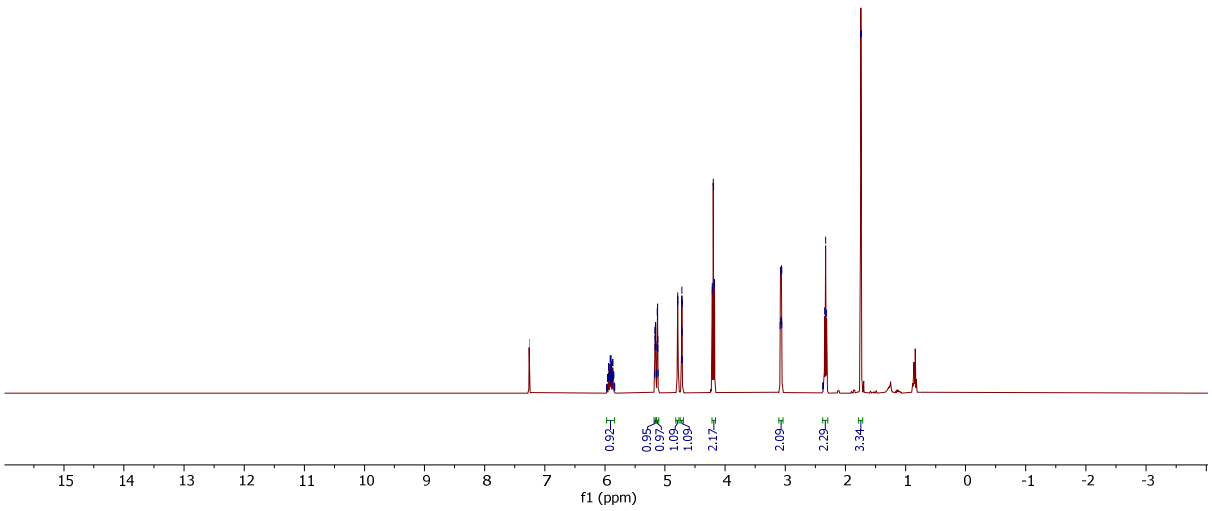


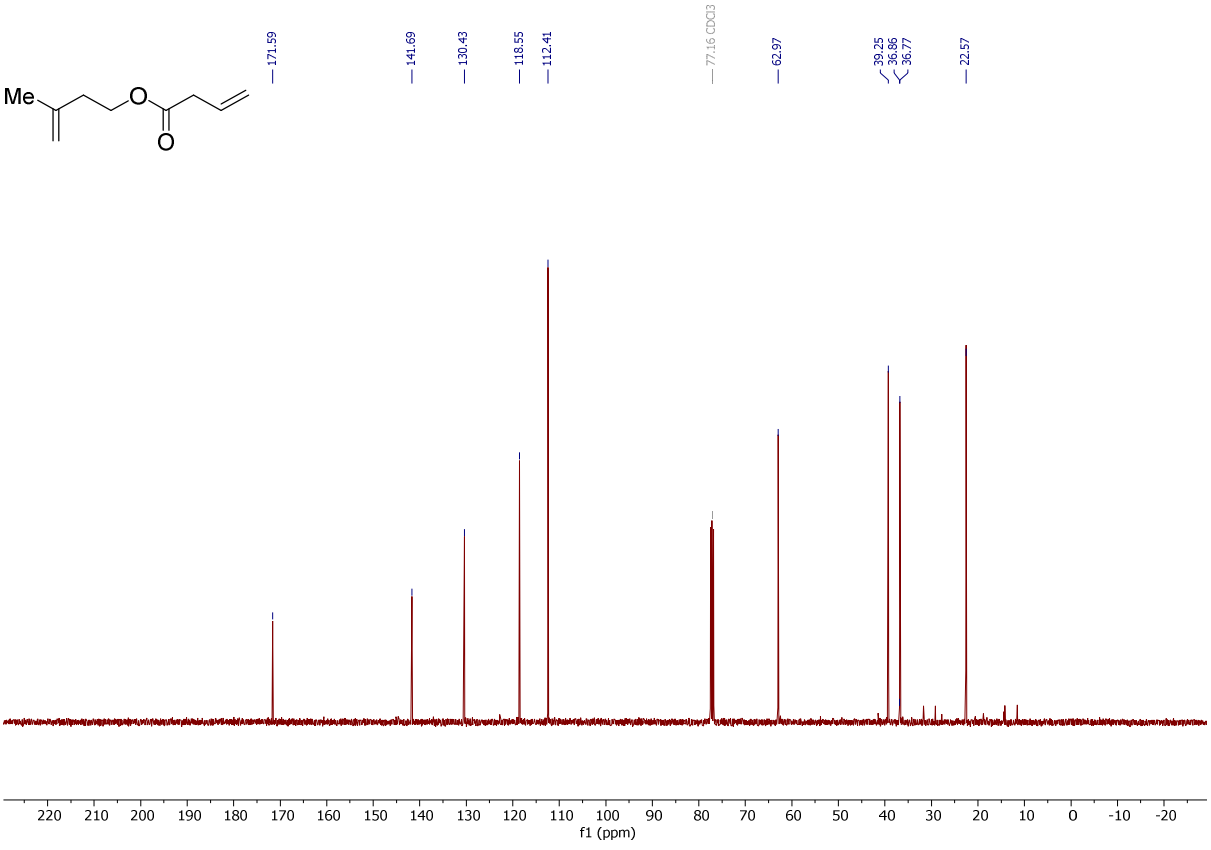


3-Methylbut-3-en-1-yl but-3-enoate (16)

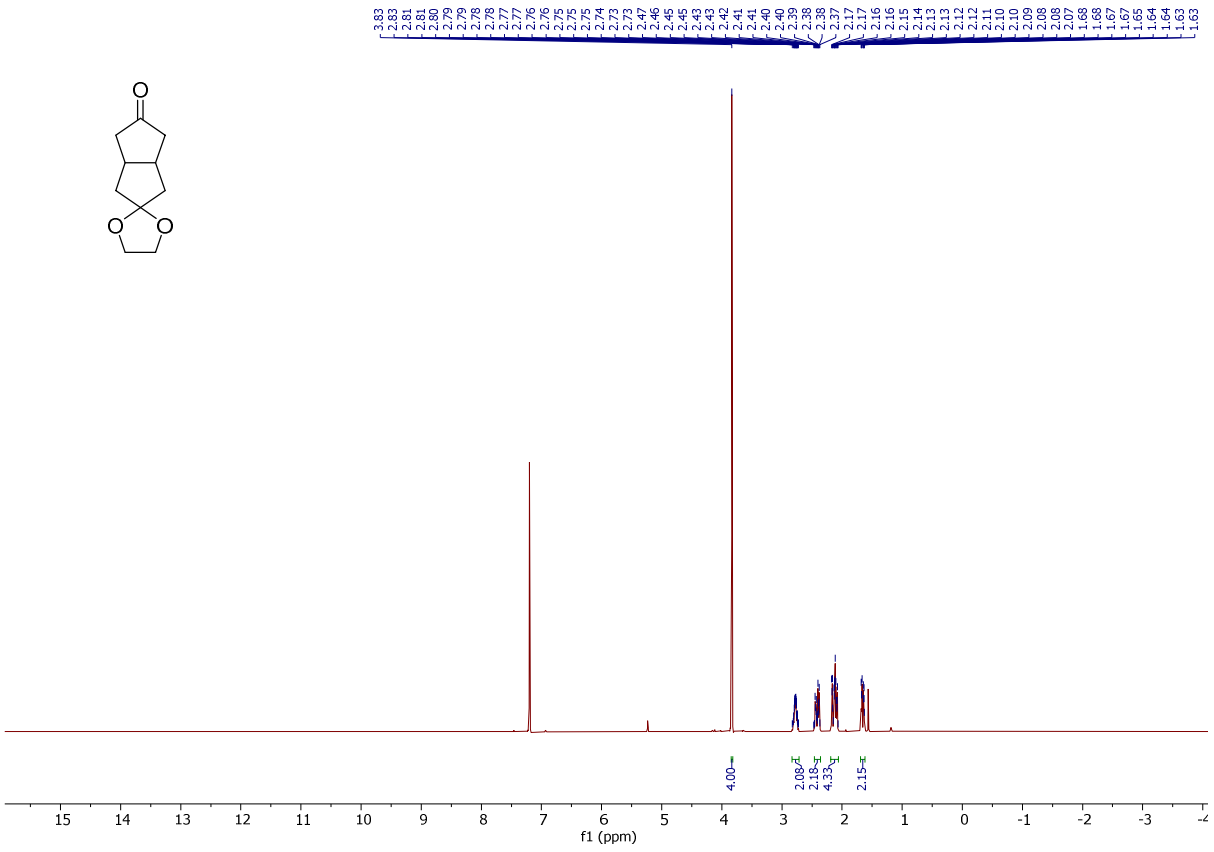


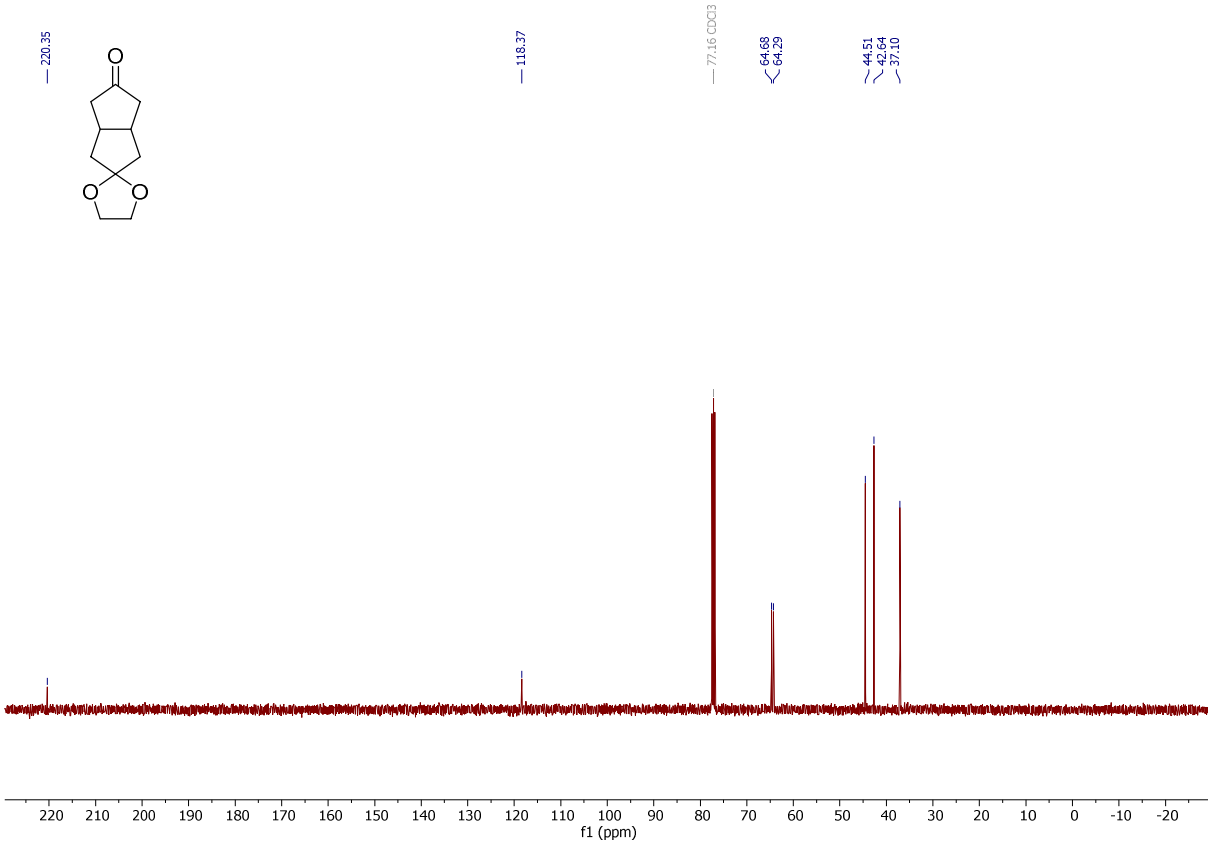




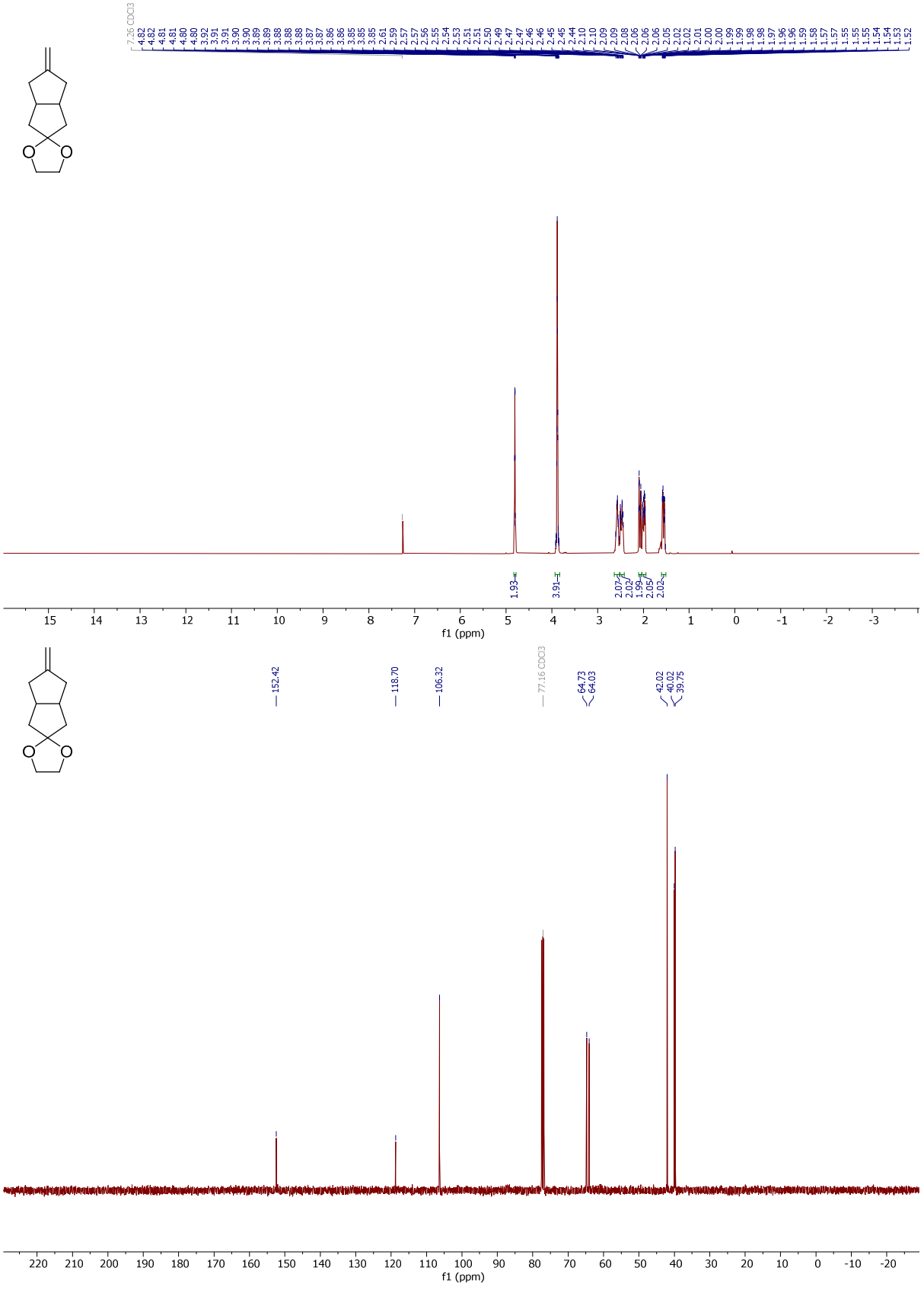


Tetrahydro-1H-spiro[pentalene-2,2'-[1,3]dioxolan]-5(3H)-one (17)

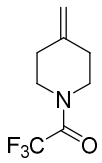


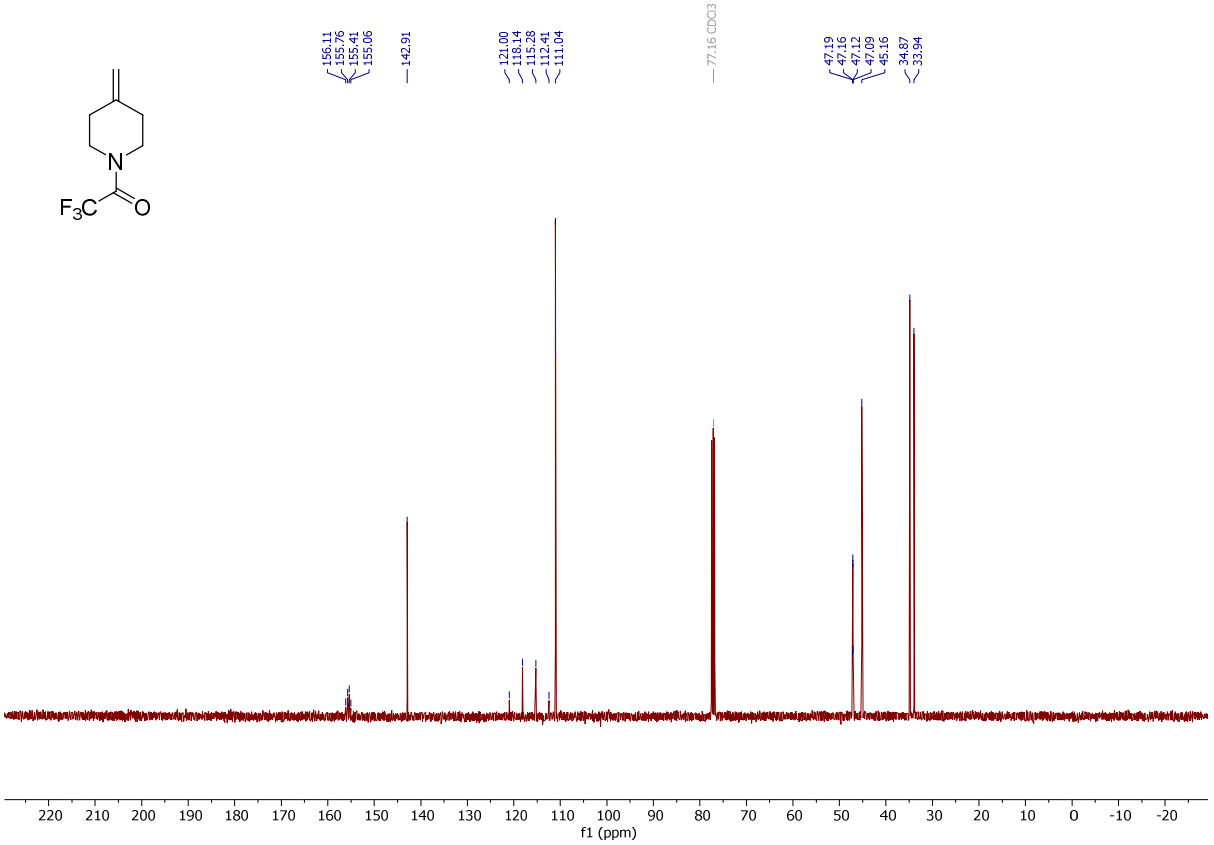


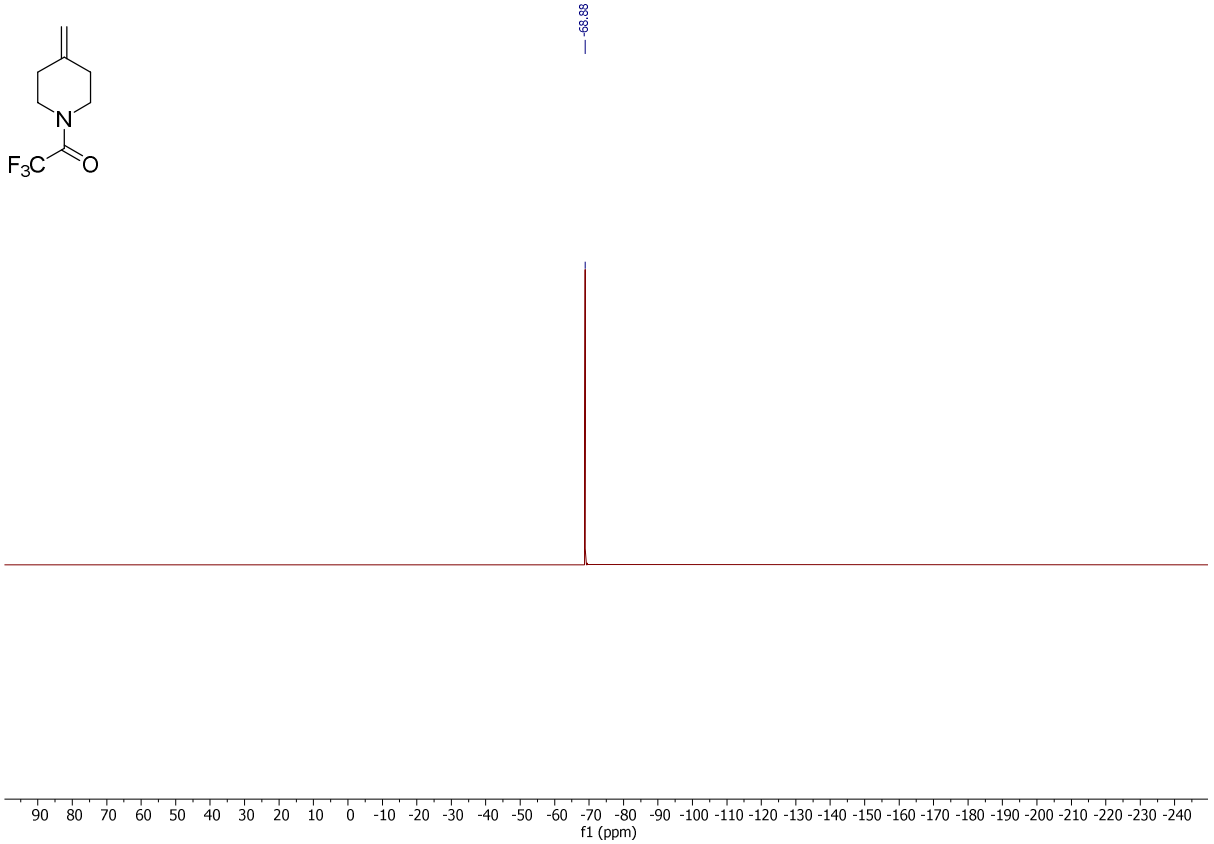
5-Methylenehexahydro-1H-spiro[pentalene-2,2'-[1,3]dioxolane] (18)



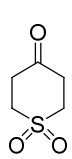
2,2,2-Trifluoro-1-(4-methylenepiperidin-1-yl)ethan-1-one (19)



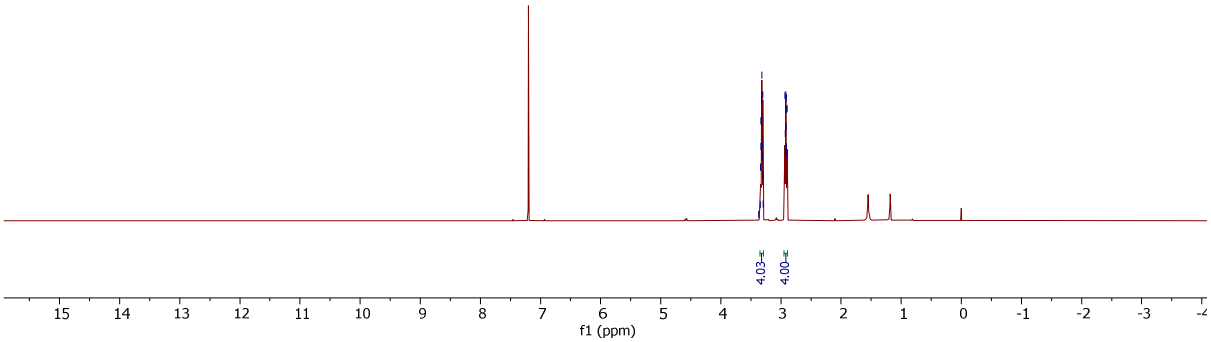

156.11
155.76
155.41
155.06
142.91
121.00
118.14
115.28
112.41
111.04
77.16 CDCl3
47.19
47.16
47.12
47.09
45.16
34.87
33.94
N
F3C
O
f1 (ppm)

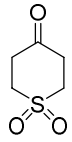

-68.88
N
F3C
O
f1 (ppm)

Tetrahydro-4H-thiopyran-4-one 1,1-dioxide (20)

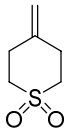


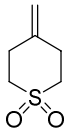




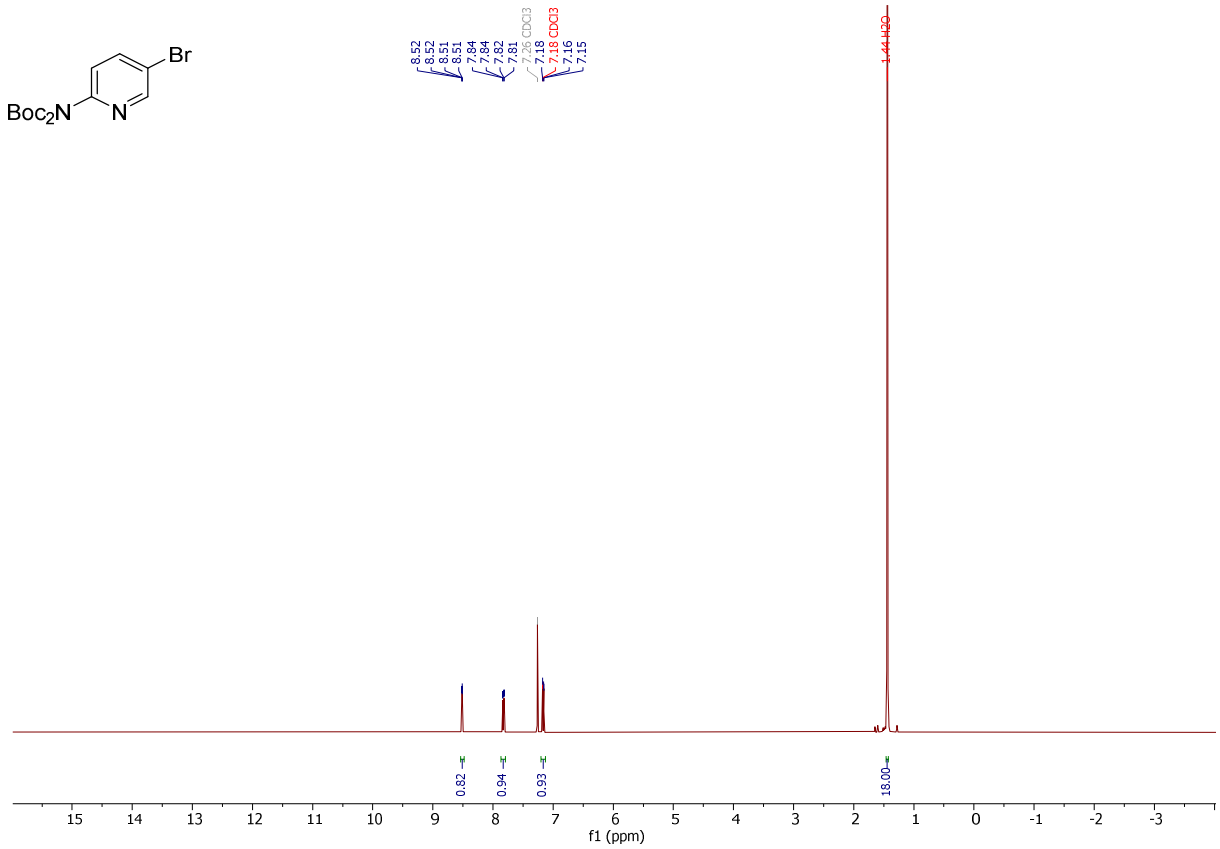


4-Methylenetetrahydro-2H-thiopyran 1,1-dioxide (21)

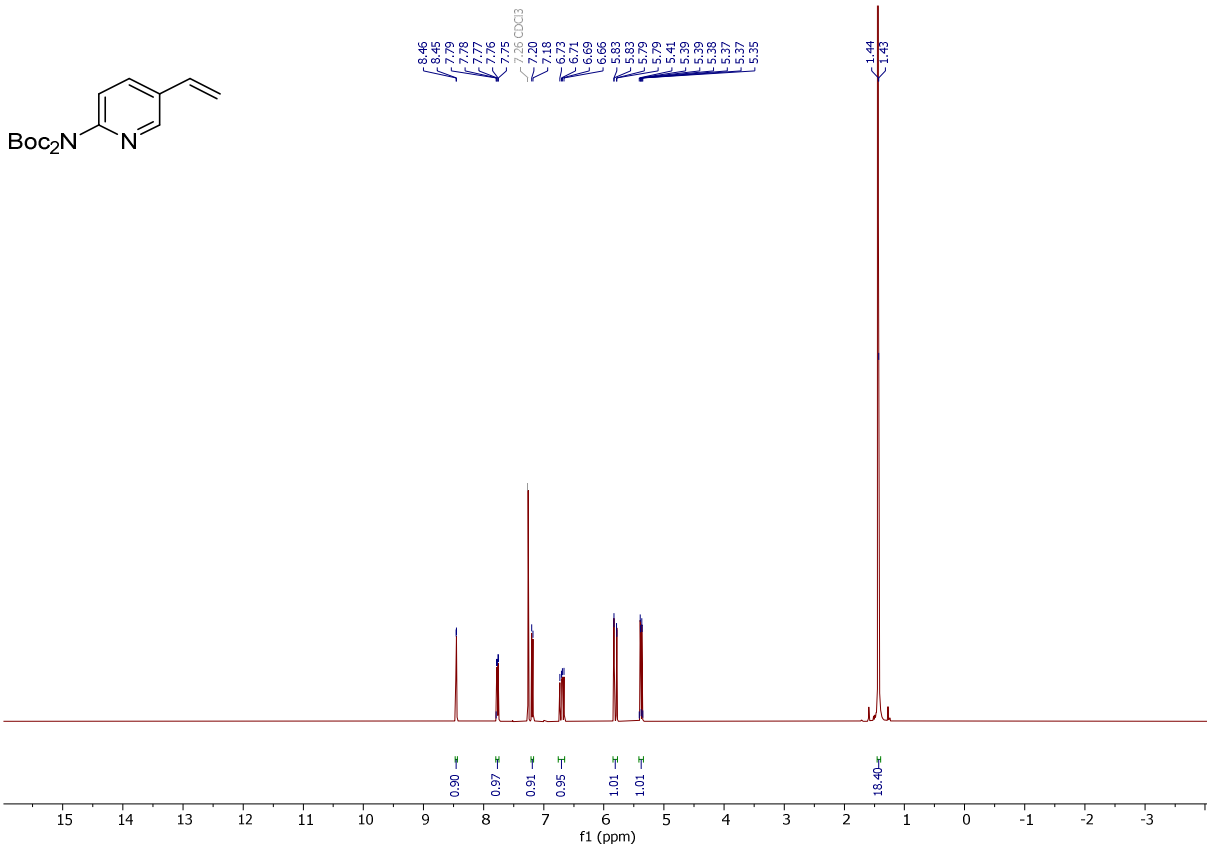


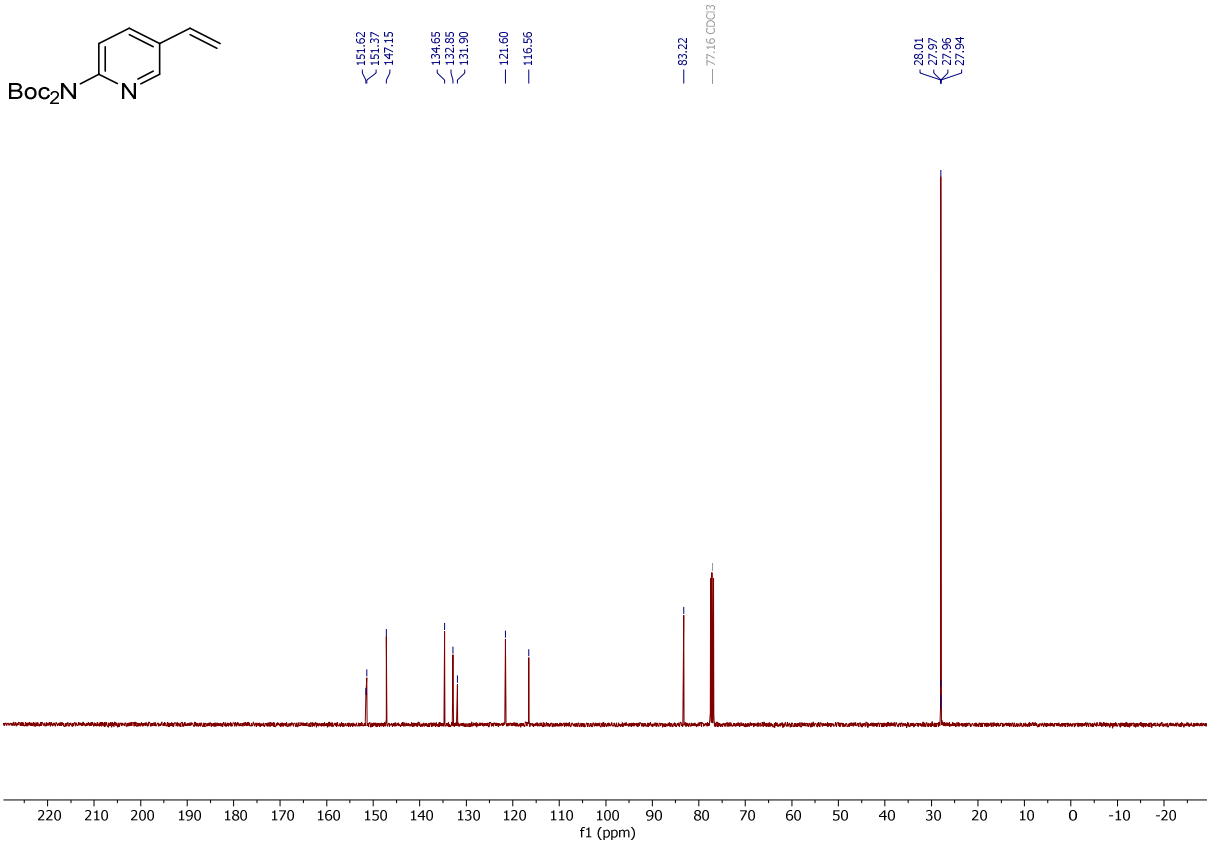


Tert-butyl (5-bromopyridin-2-yl)(*tert*-butoxycarbonyl)carbamate (22)

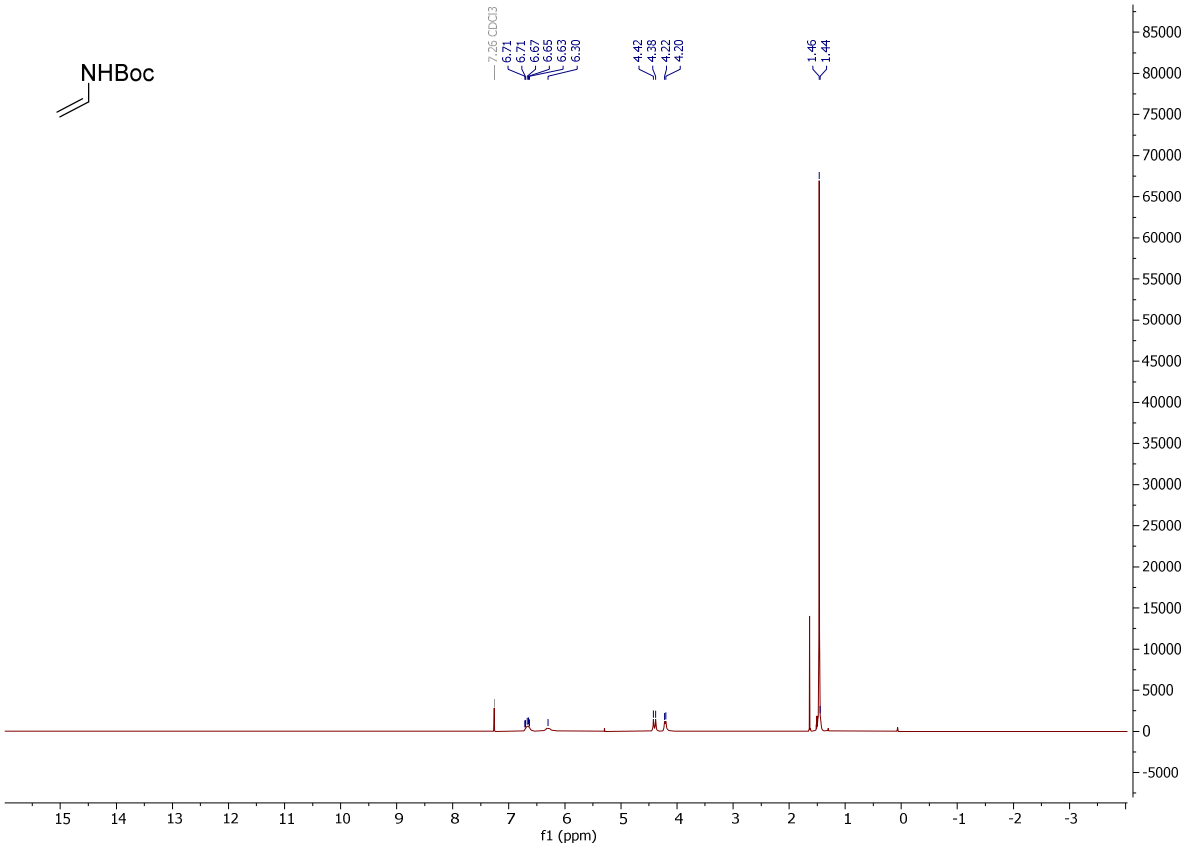


Tert-butyl (*tert*-butoxycarbonyl)(5-vinylpyridin-2-yl)carbamate (23)

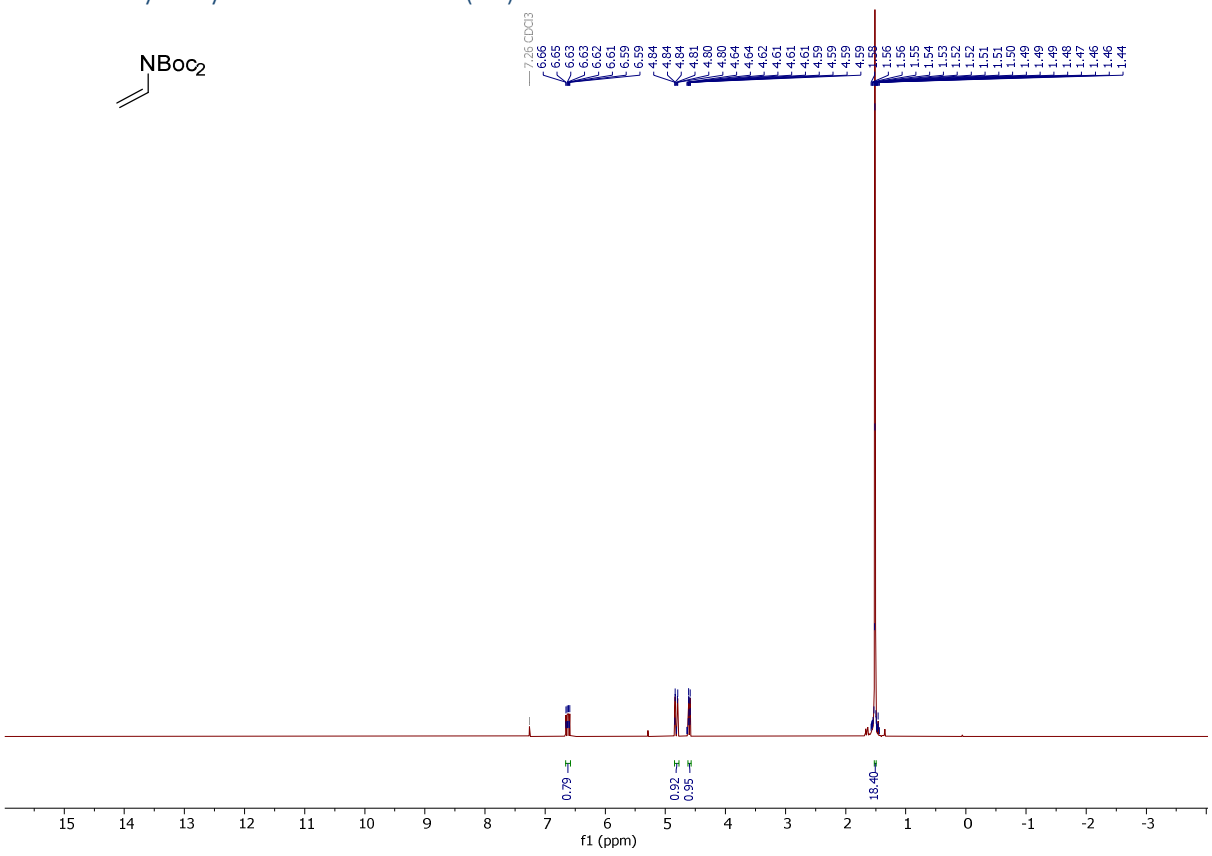


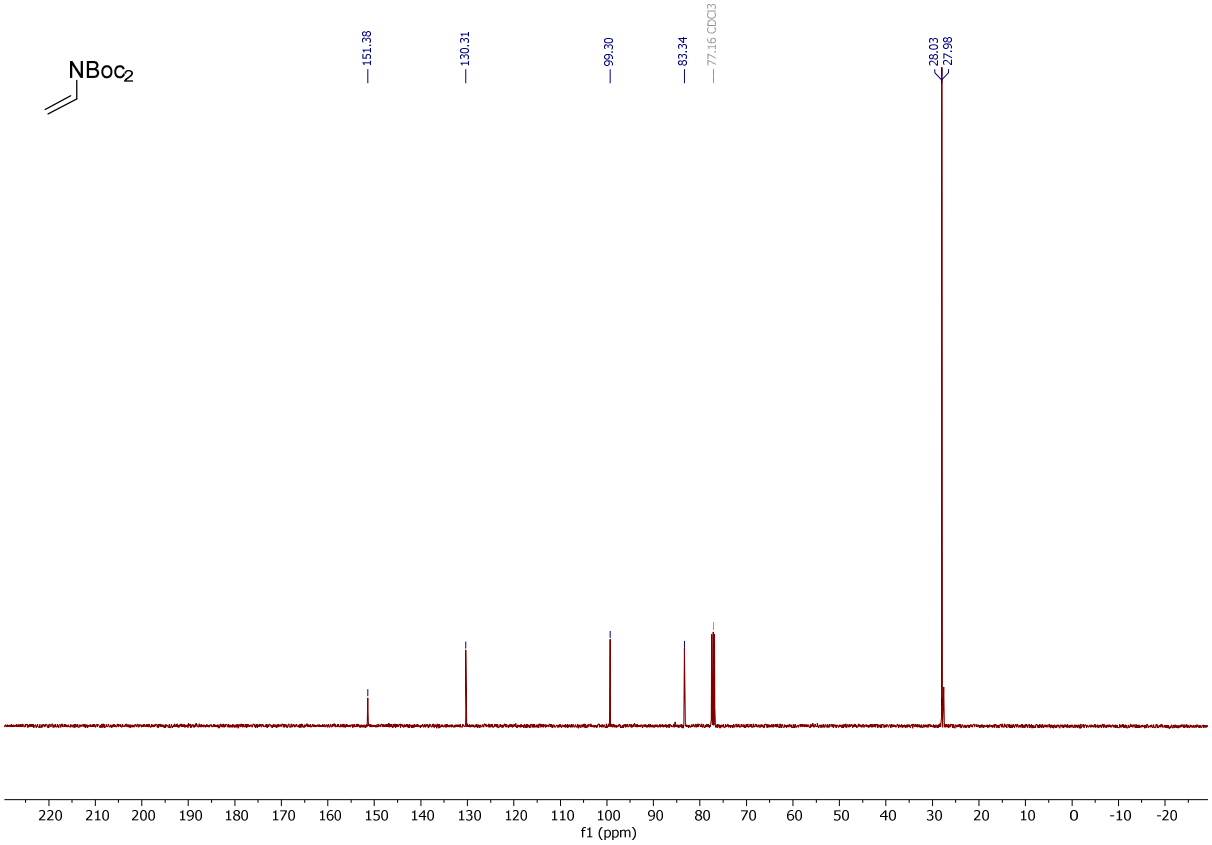


tert-butyl vinylcarbamate (24)

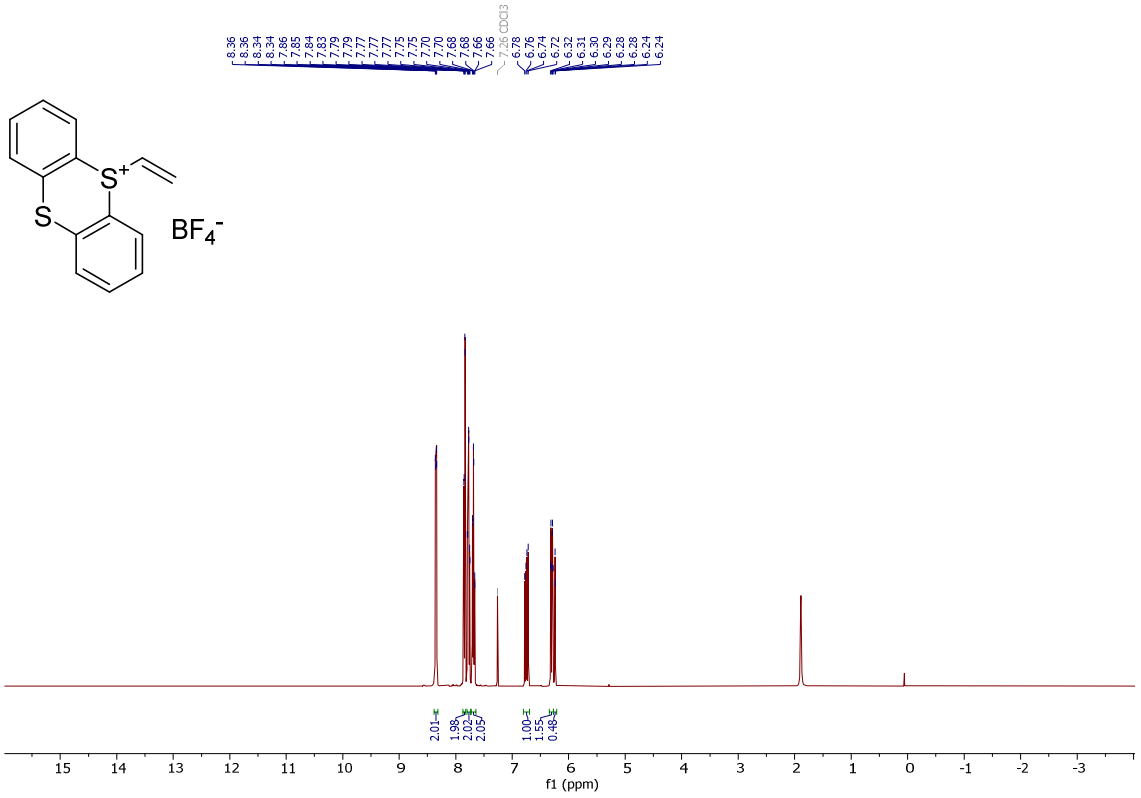


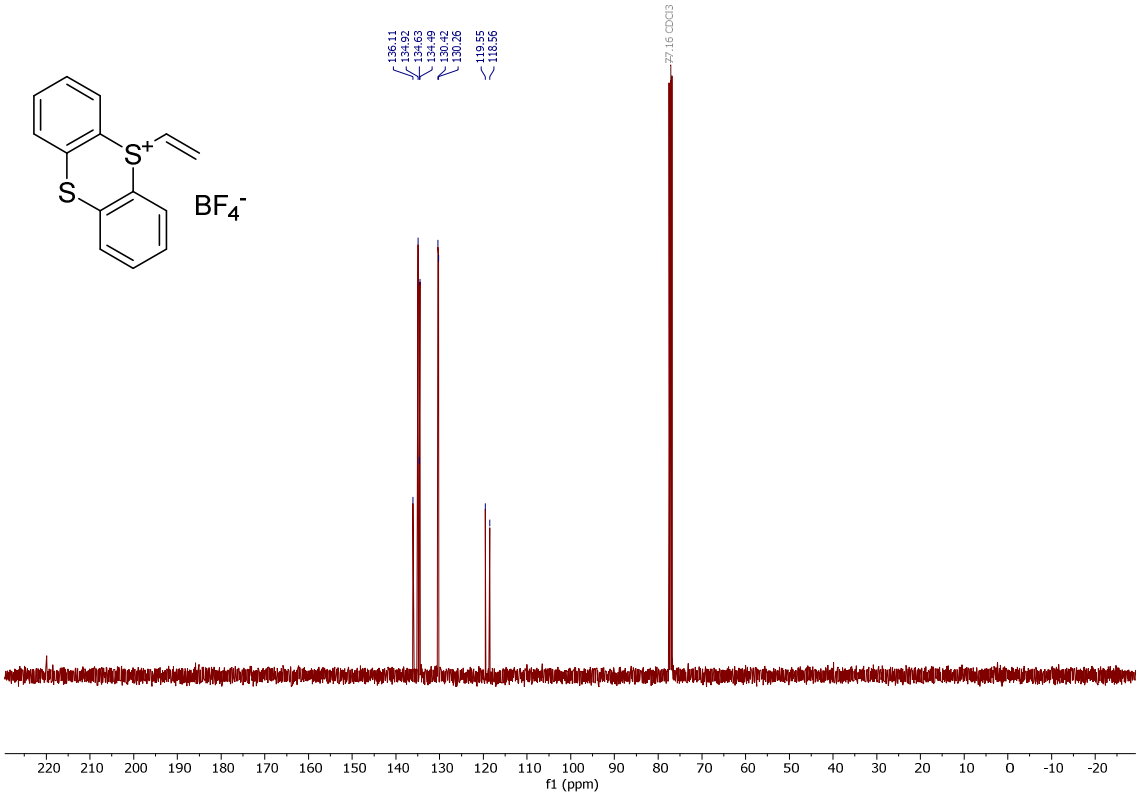
Di-*tert*-butyl vinyliminodicarbonate (25)

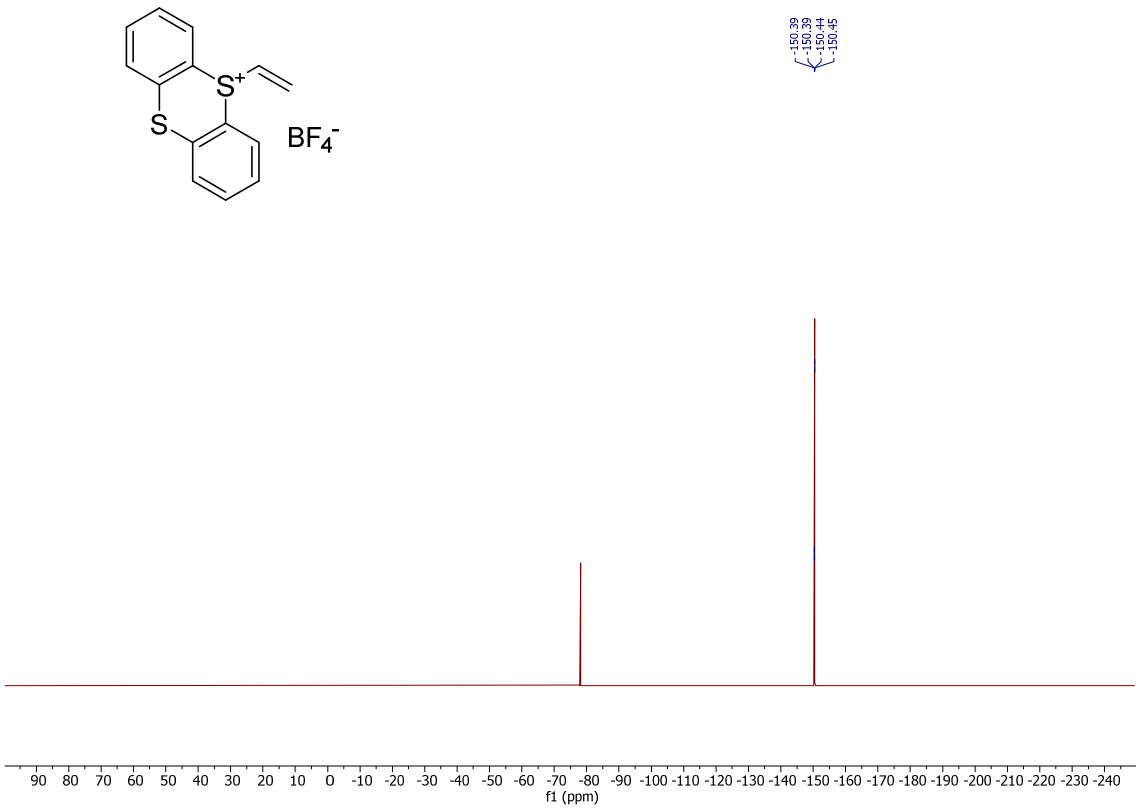




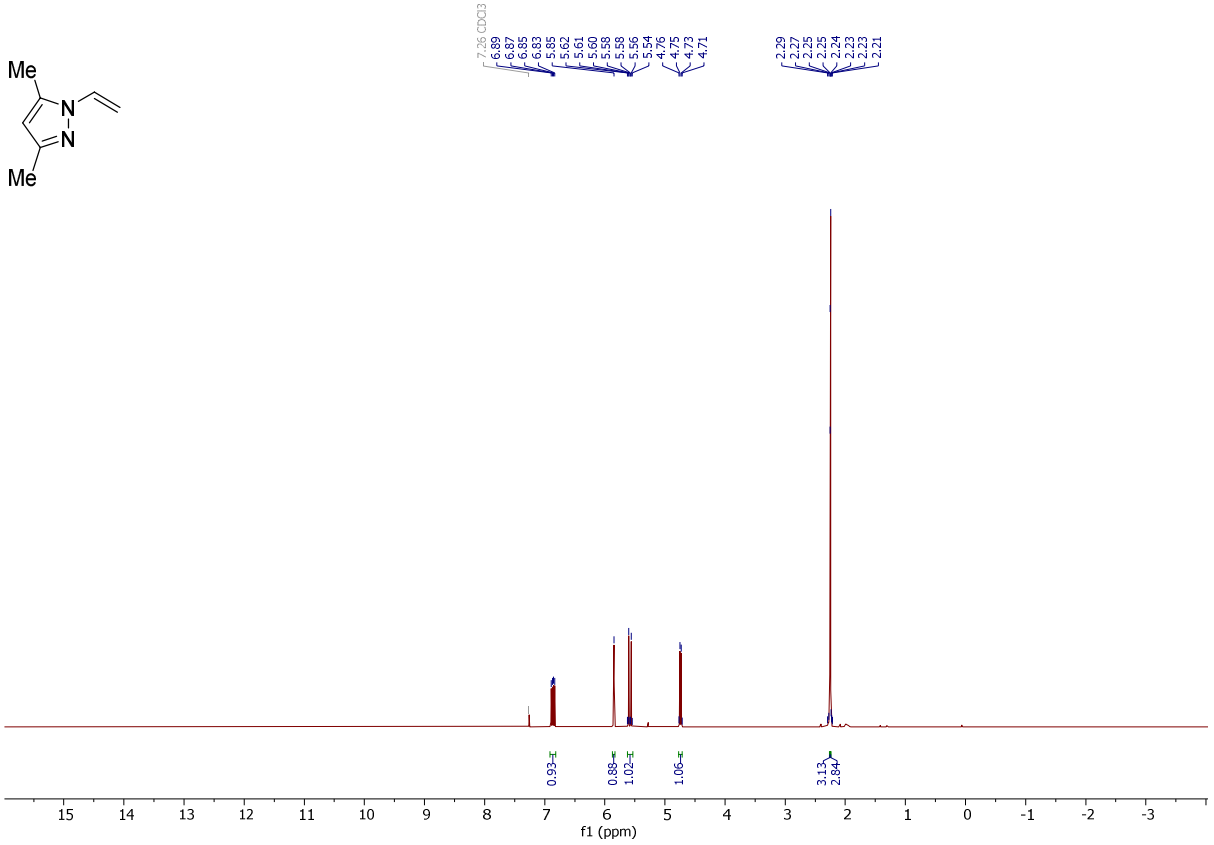
Vinyl thianthrenium tetrafluoroborate (26)

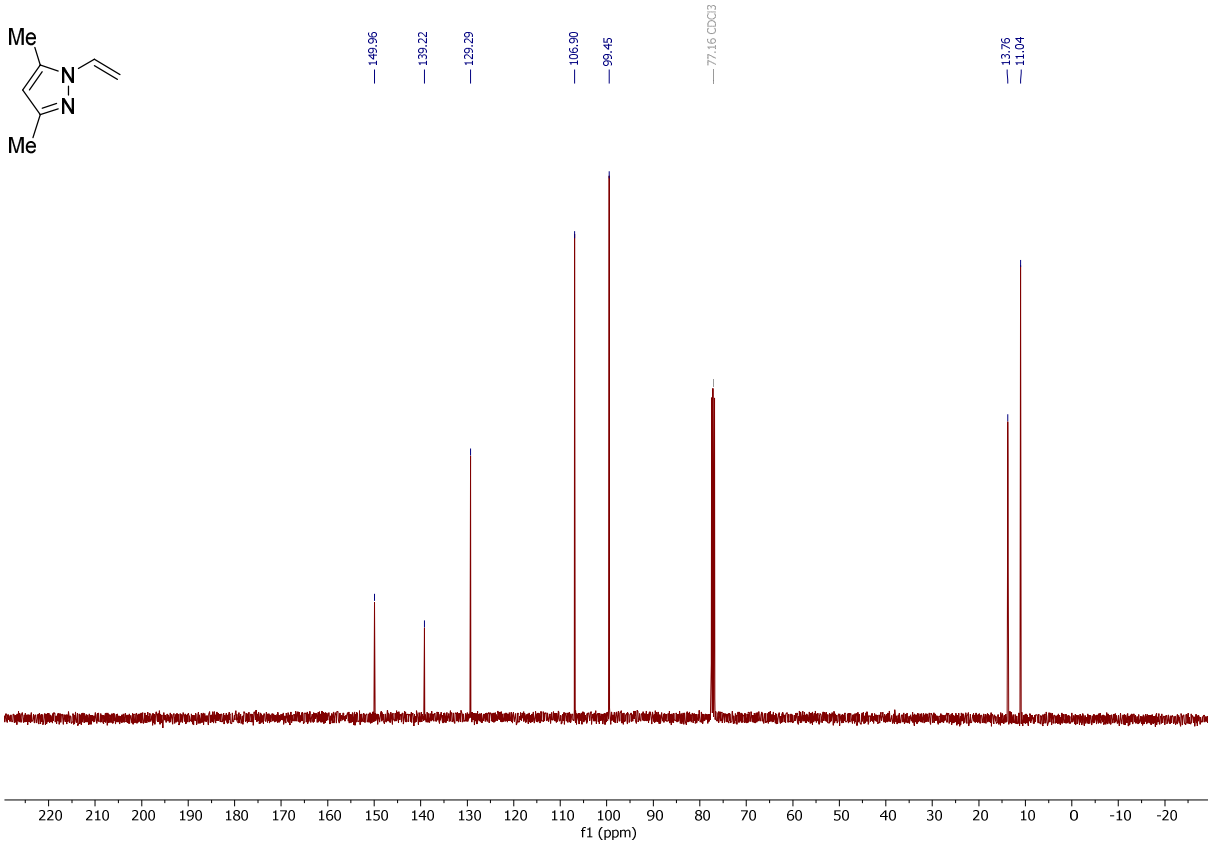



136.11
134.92
134.63
134.49
130.42
130.26
119.55
118.56
77.16 CDCl3
S+
S
BF4-
220 210 200 190 180 170 160 150 140 130 120 110 100 90 80 70 60 50 40 30 20 10 0 -10 -20
f1 (ppm)


150.39
150.39
150.44
150.45
S+
S
BF4-
90 80 70 60 50 40 30 20 10 0 -10 -20 -30 -40 -50 -60 -70 -80 -90 -100 -110 -120 -130 -140 -150 -160 -170 -180 -190 -200 -210 -220 -230 -240
f1 (ppm)

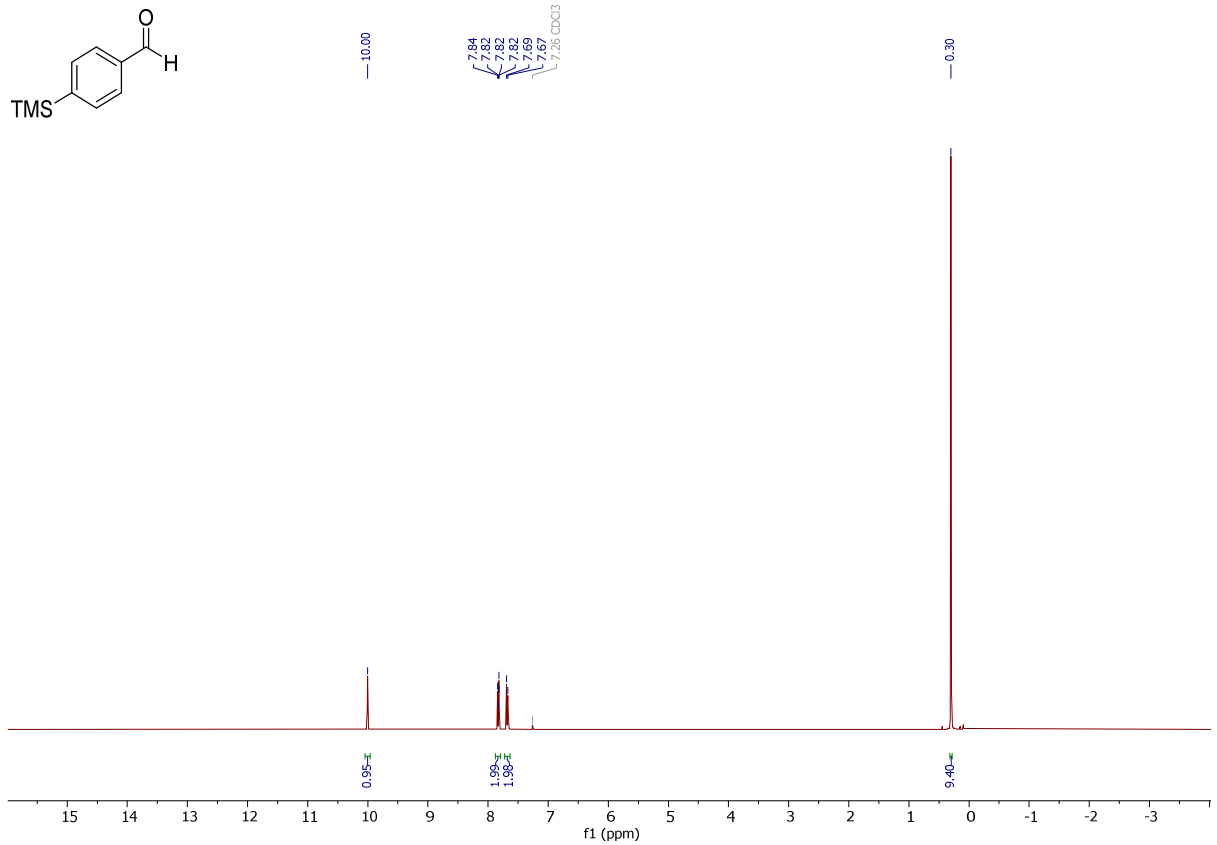
3,5-Dimethyl-1-vinyl-1H-pyrazole (27)

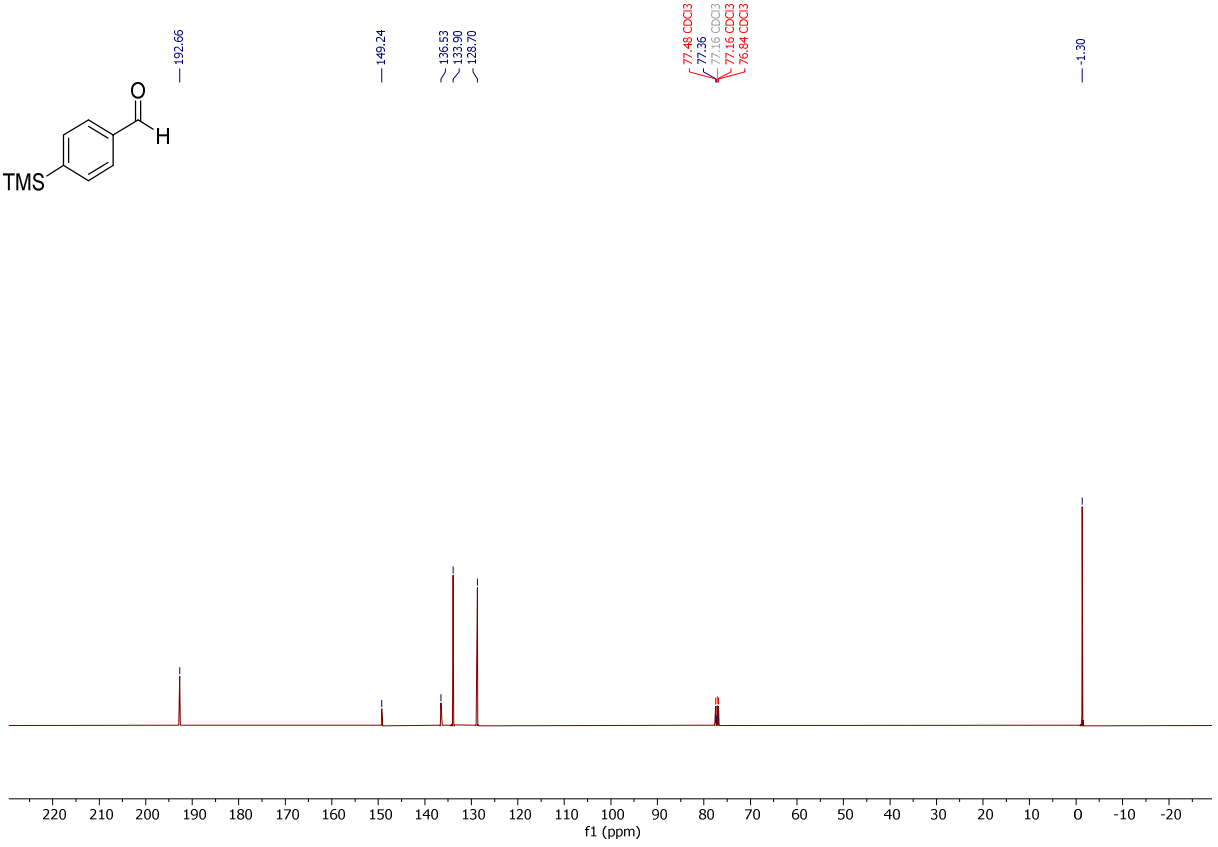




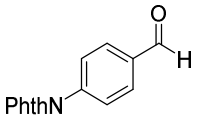
Aldehydes

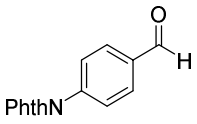
4-(Trimethylsilyl)benzaldehyde (28)



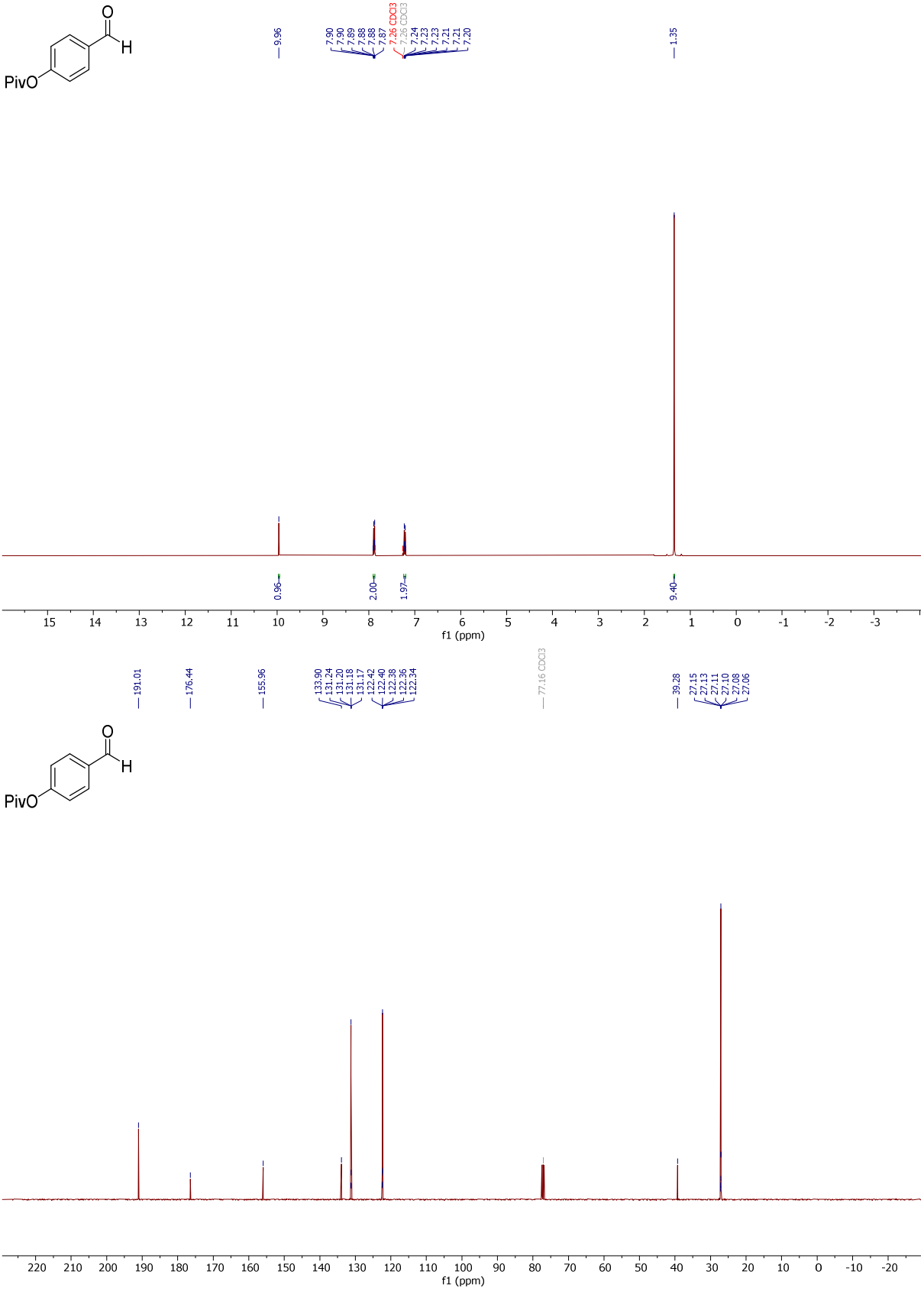


4-(1,3-Dioxoisoindolin-2-yl)benzaldehyde (29)

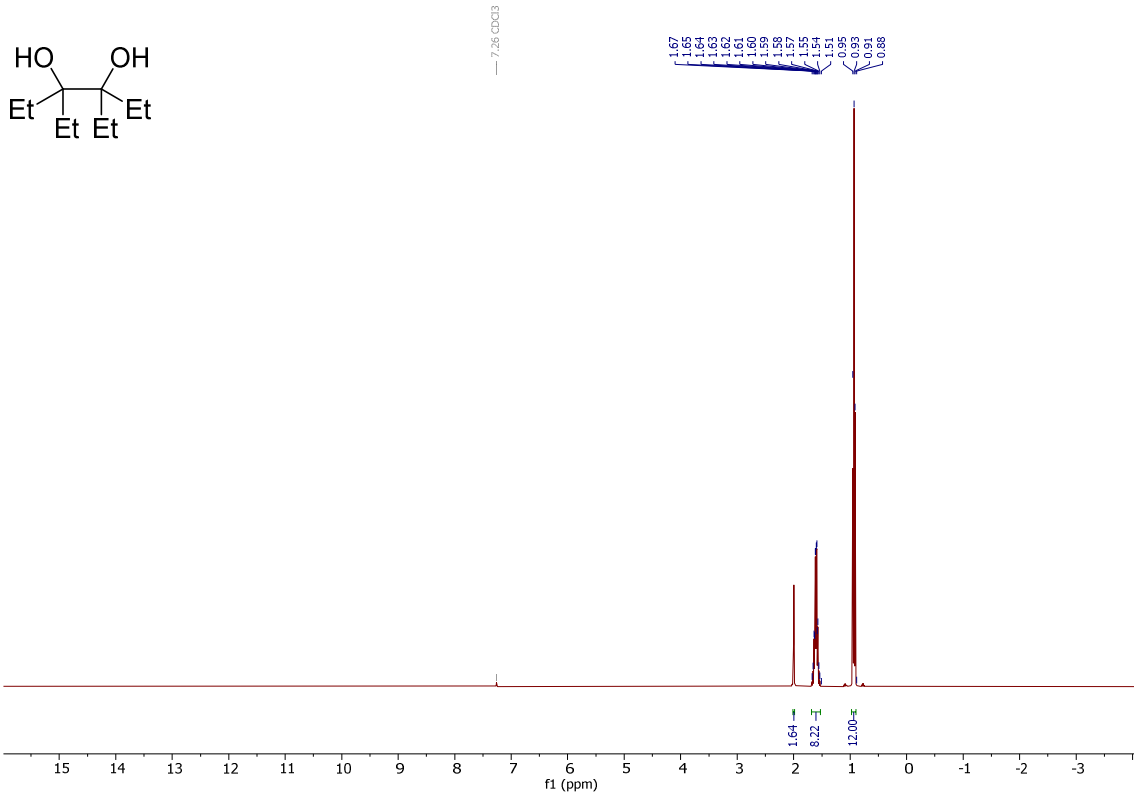


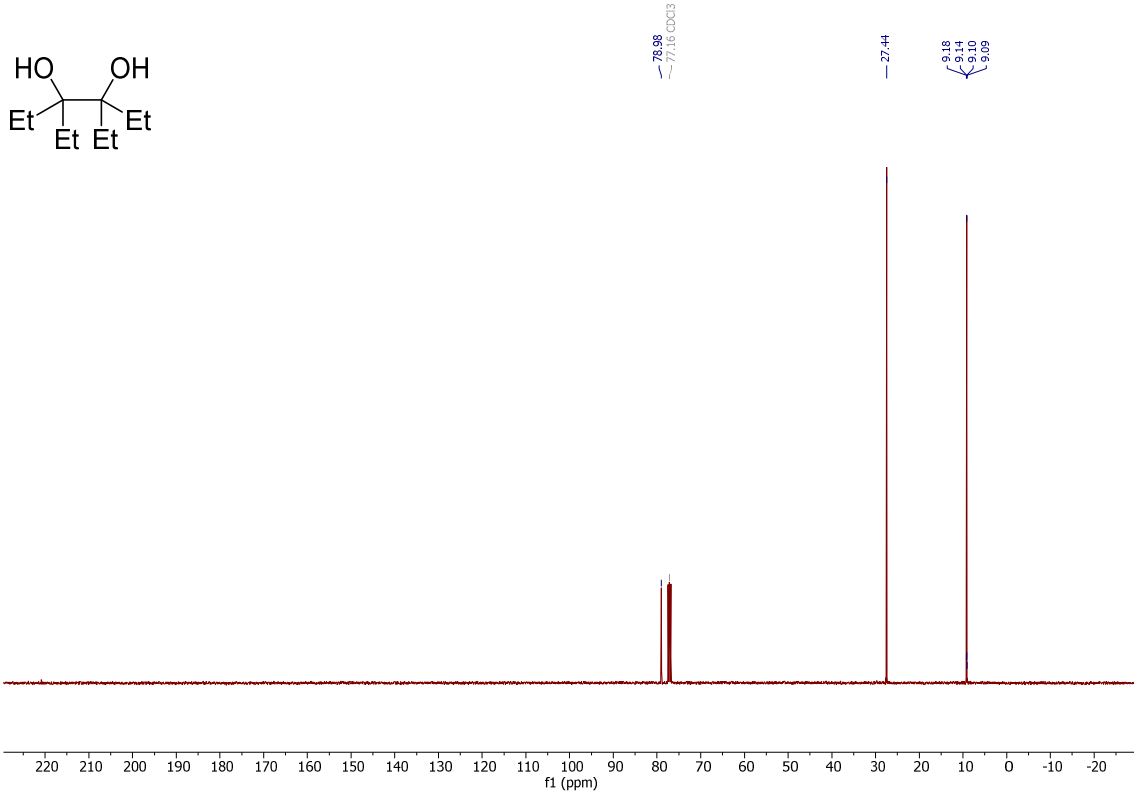


4-Formylphenyl pivalate (30)

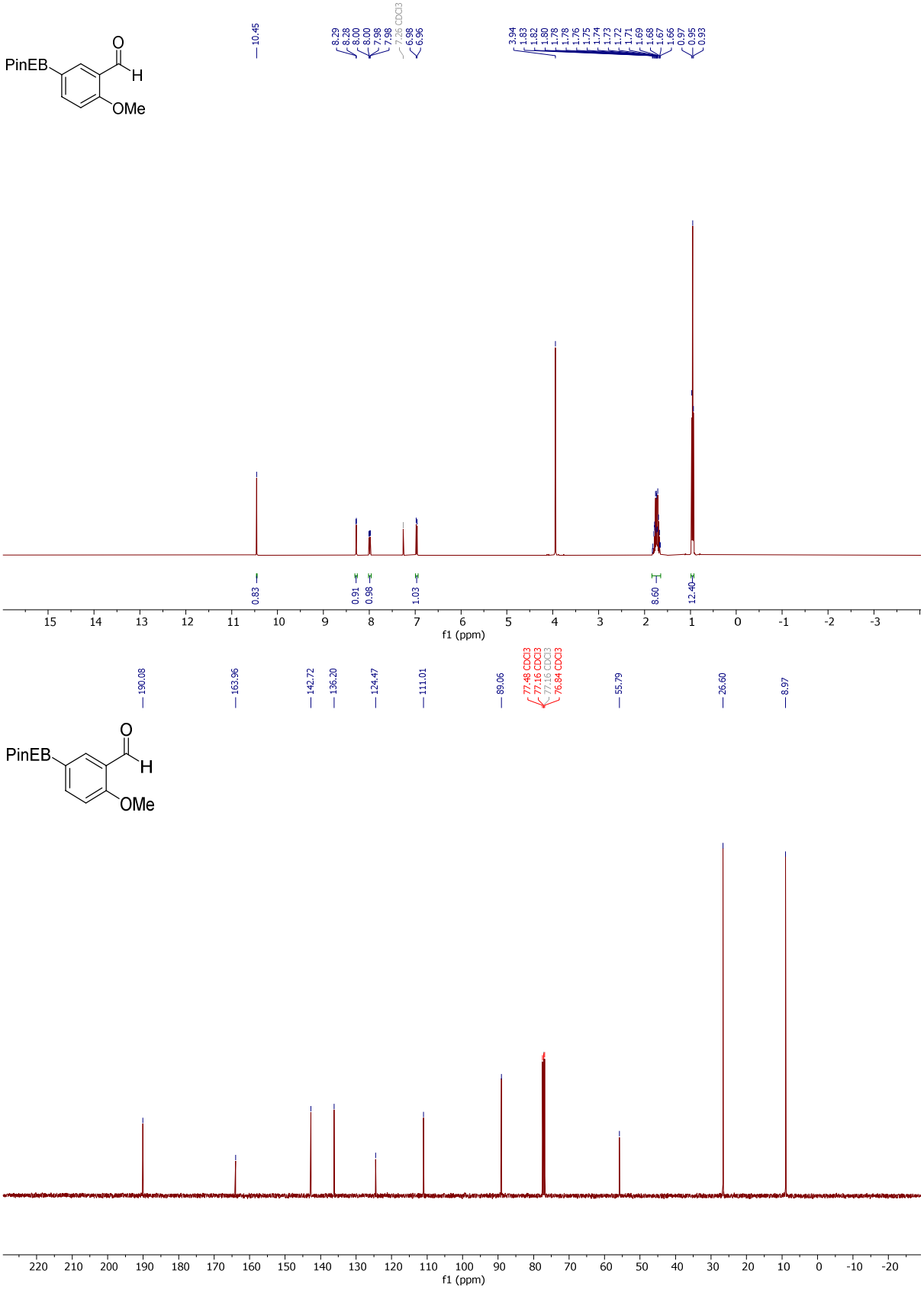


3,4-diethylhexane-3,4-diol (31)

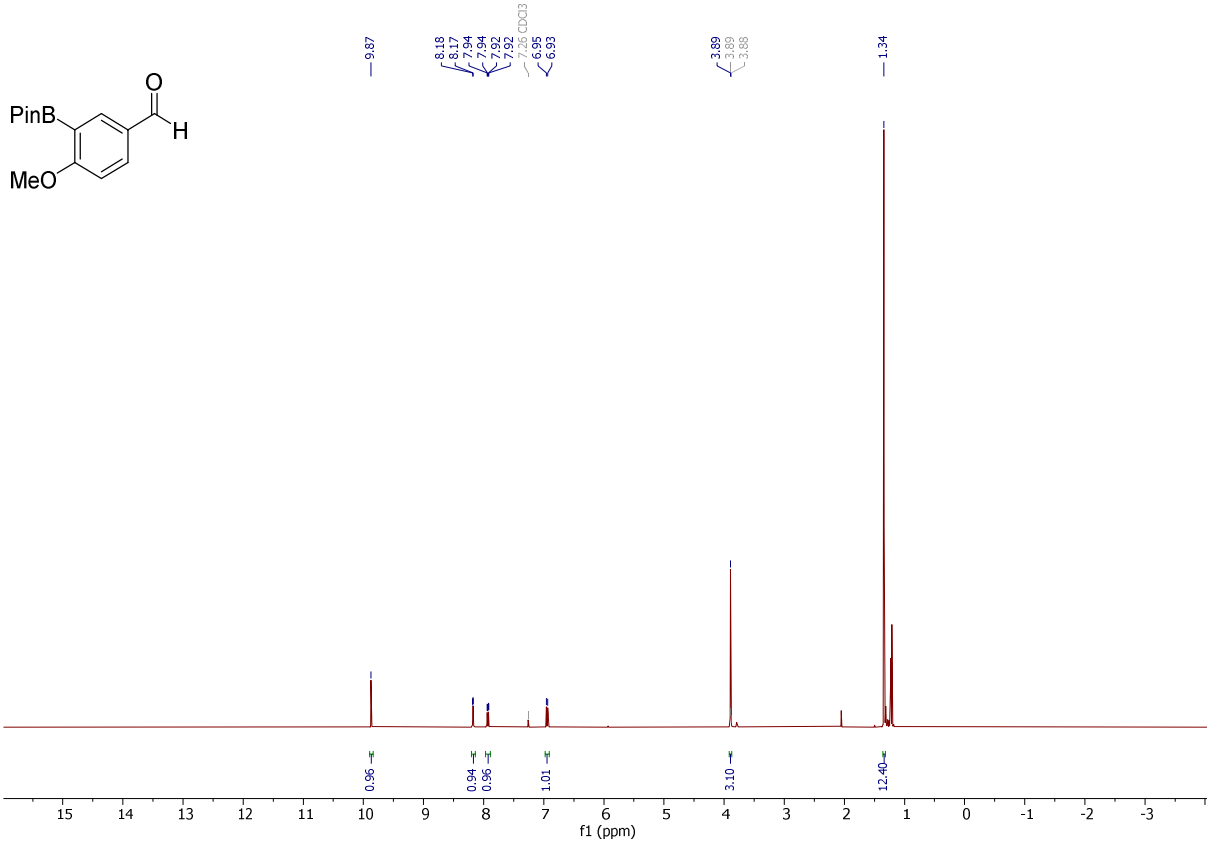


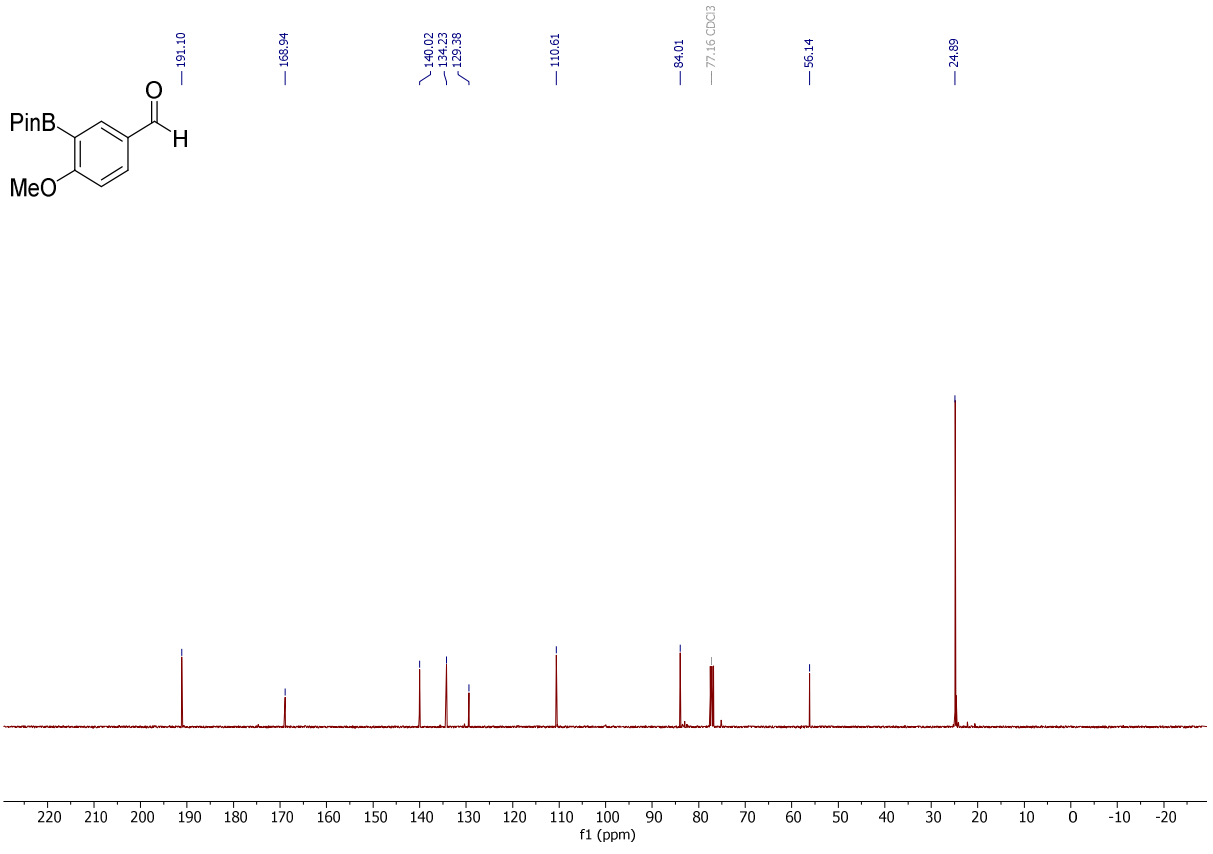


2-Methoxy-5-(4,4,5,5-tetraethyl-1,3,2-dioxaborolan-2-yl)benzaldehyde (32)

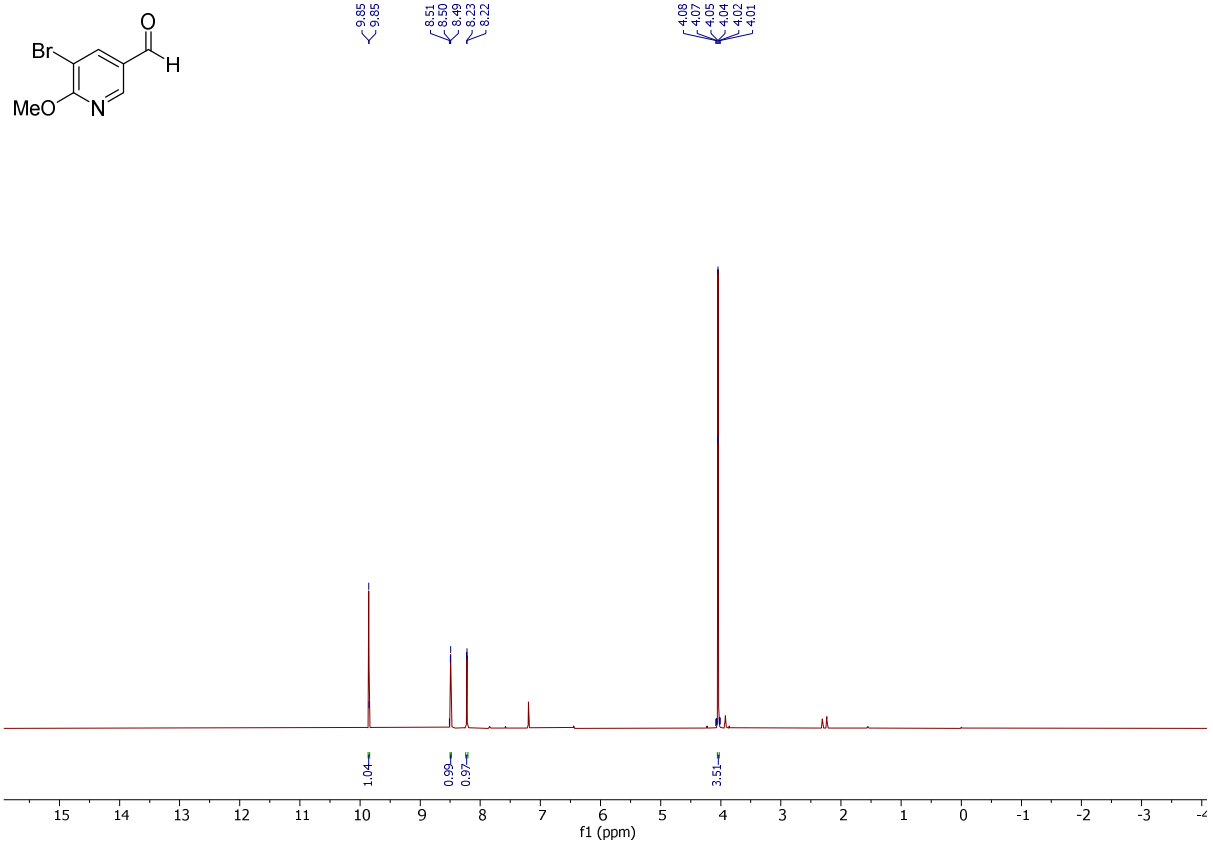


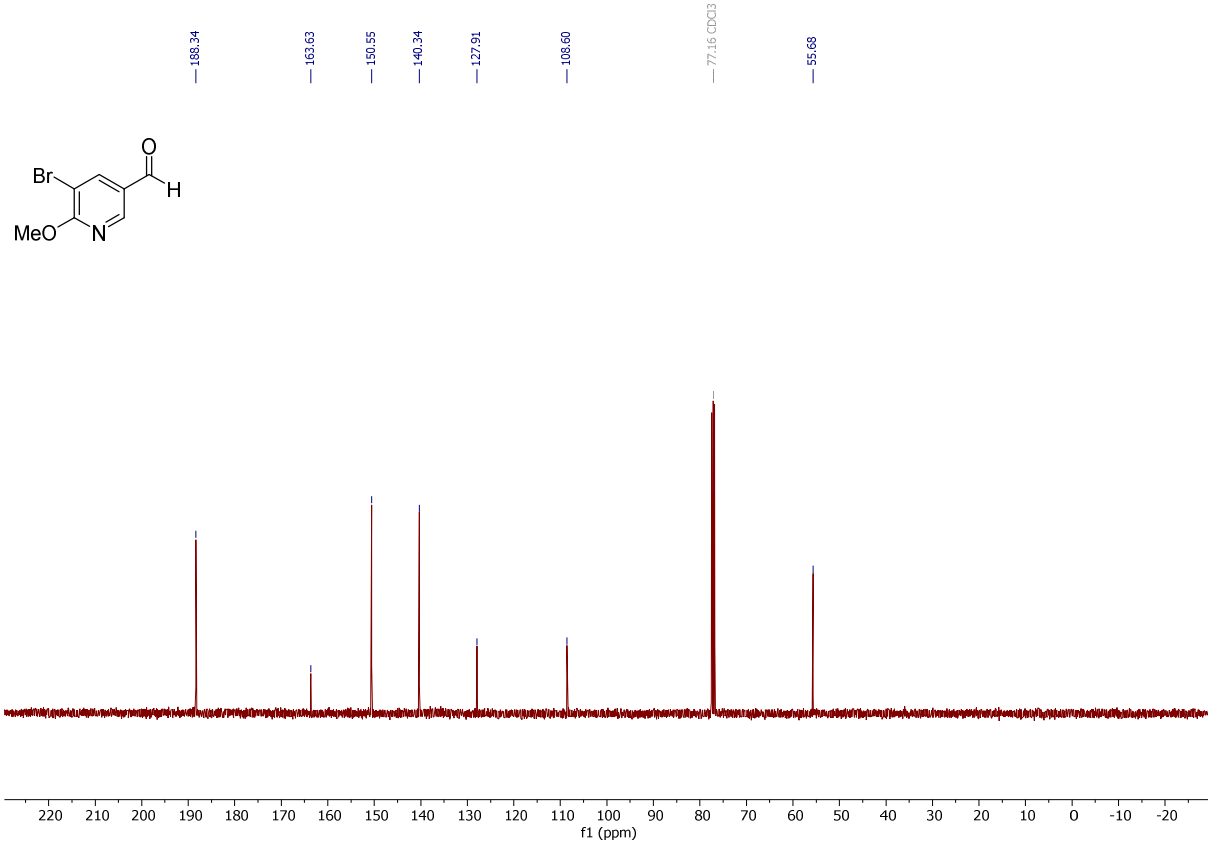
4-Methoxy-3-(4,4,5,5-tetramethyl-1,3,2-dioxaborolan-2-yl)benzaldehyde (33)



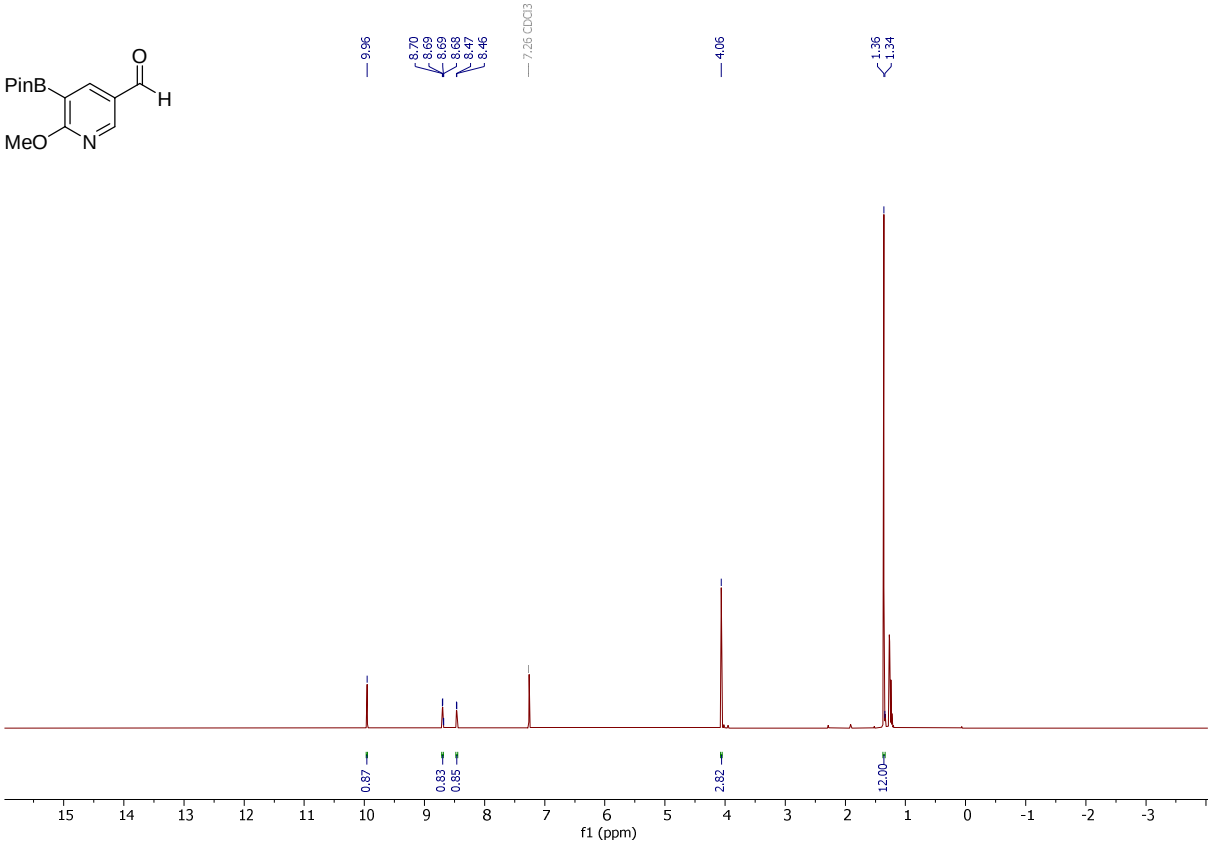


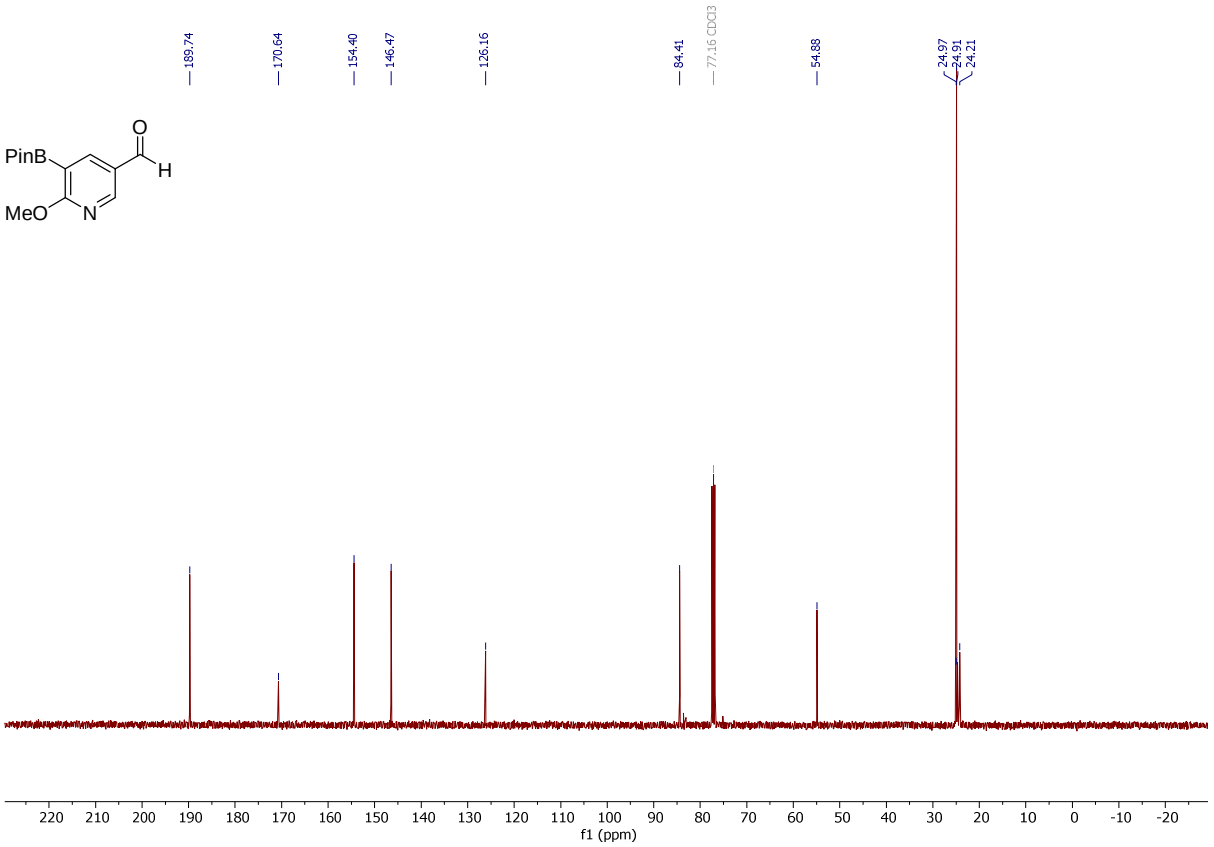
5-Bromo-6-methoxynicotinaldehyde (34)



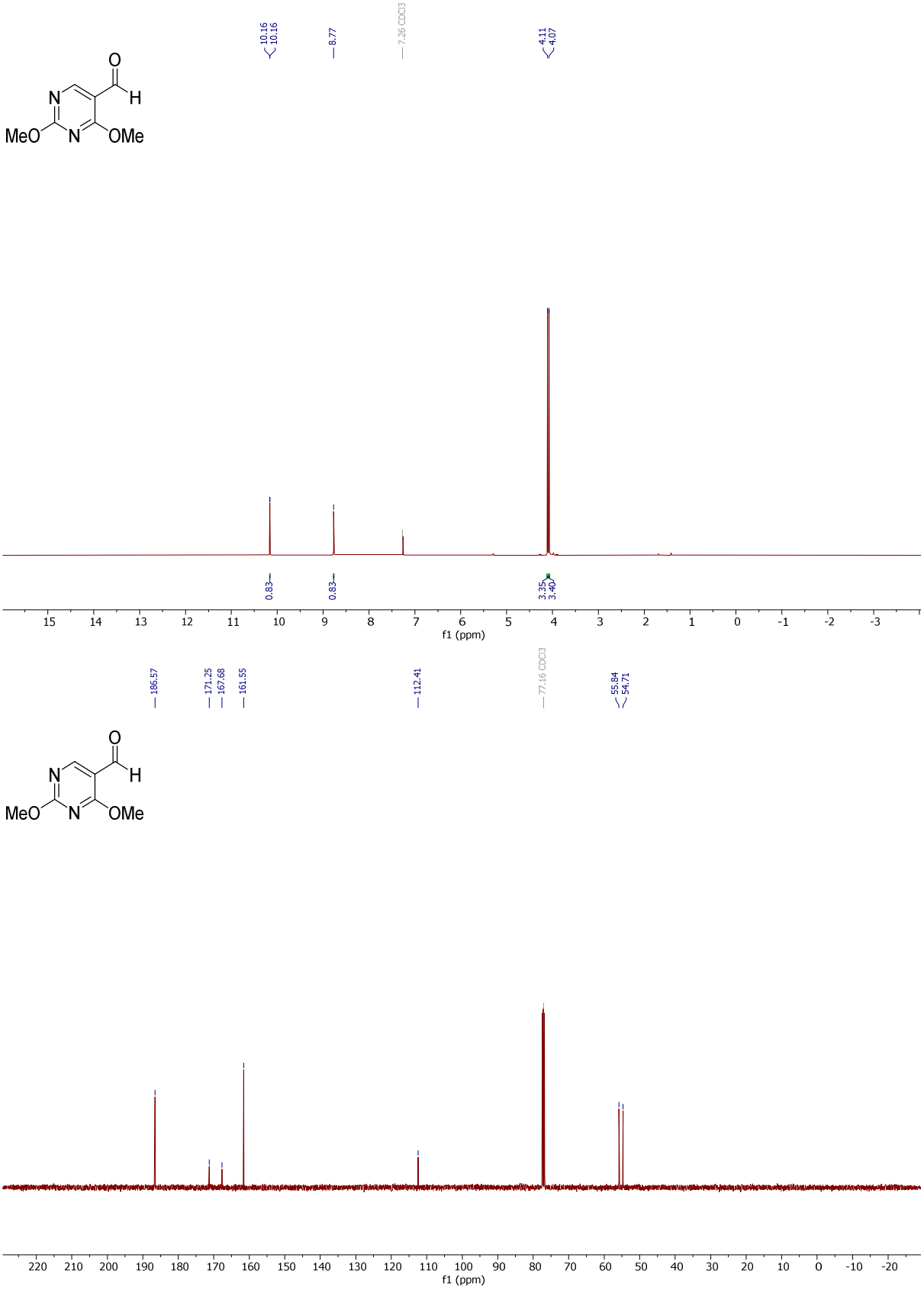


6-Methoxy-5-(4,4,5,5-tetramethyl-1,3,2-dioxaborolan-2-yl)nicotinaldehyde (35)



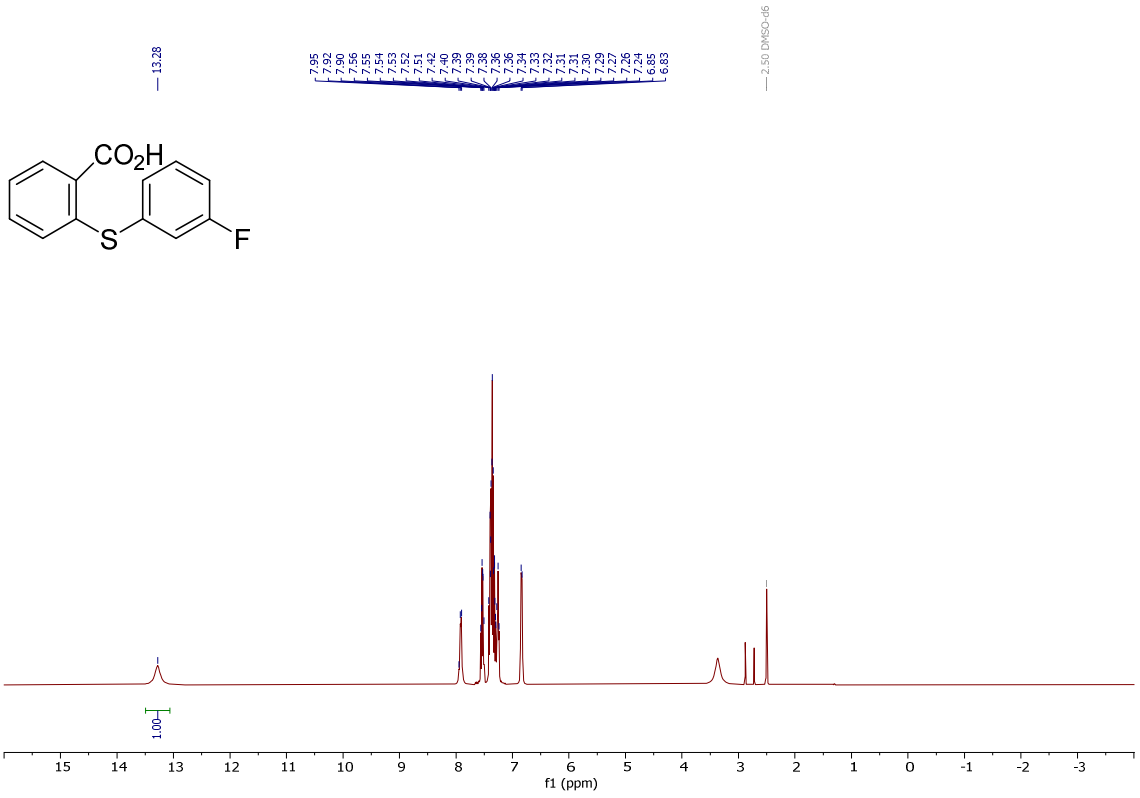

189.74
170.64
154.40
146.47
126.16
84.41
77.16 CDCl3
54.88
24.97
24.91
24.21
PinB
MeO
N
O
H
220 210 200 190 180 170 160 150 140 130 120 110 100 90 80 70 60 50 40 30 20 10 0 -10 -20
f1 (ppm)

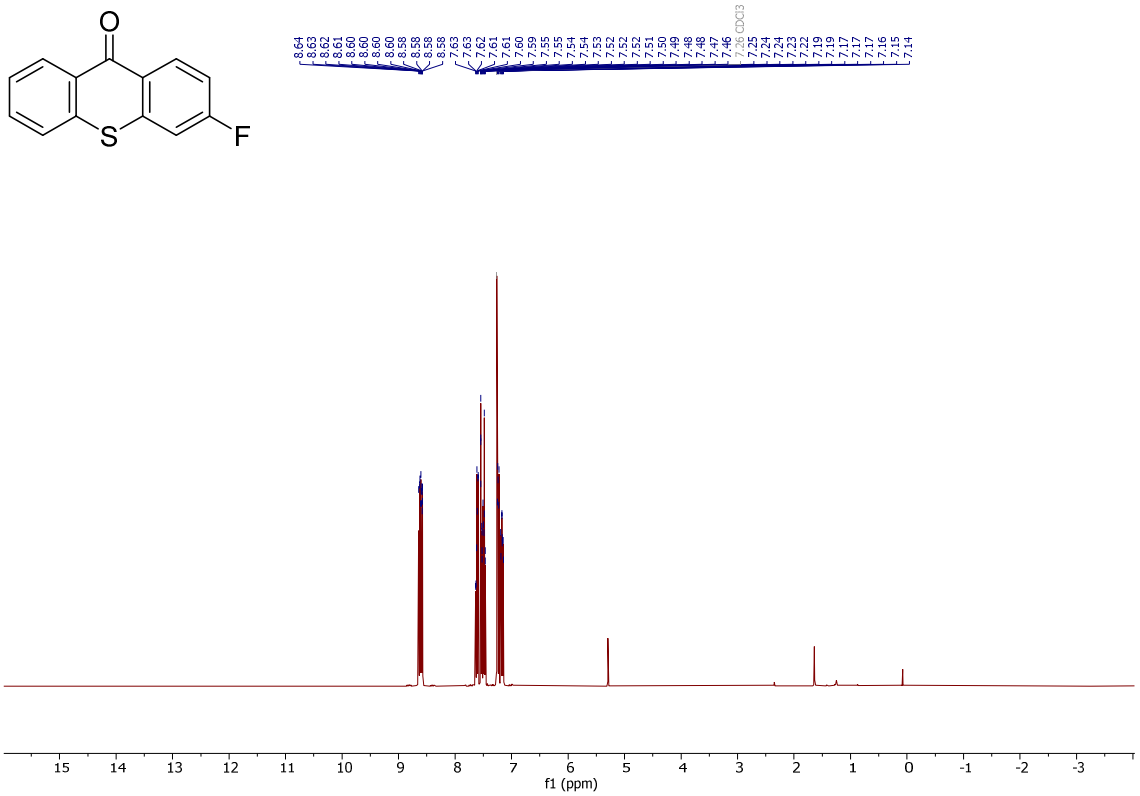
2,4-Dimethoxypyrimidine-5-carbaldehyde (36)

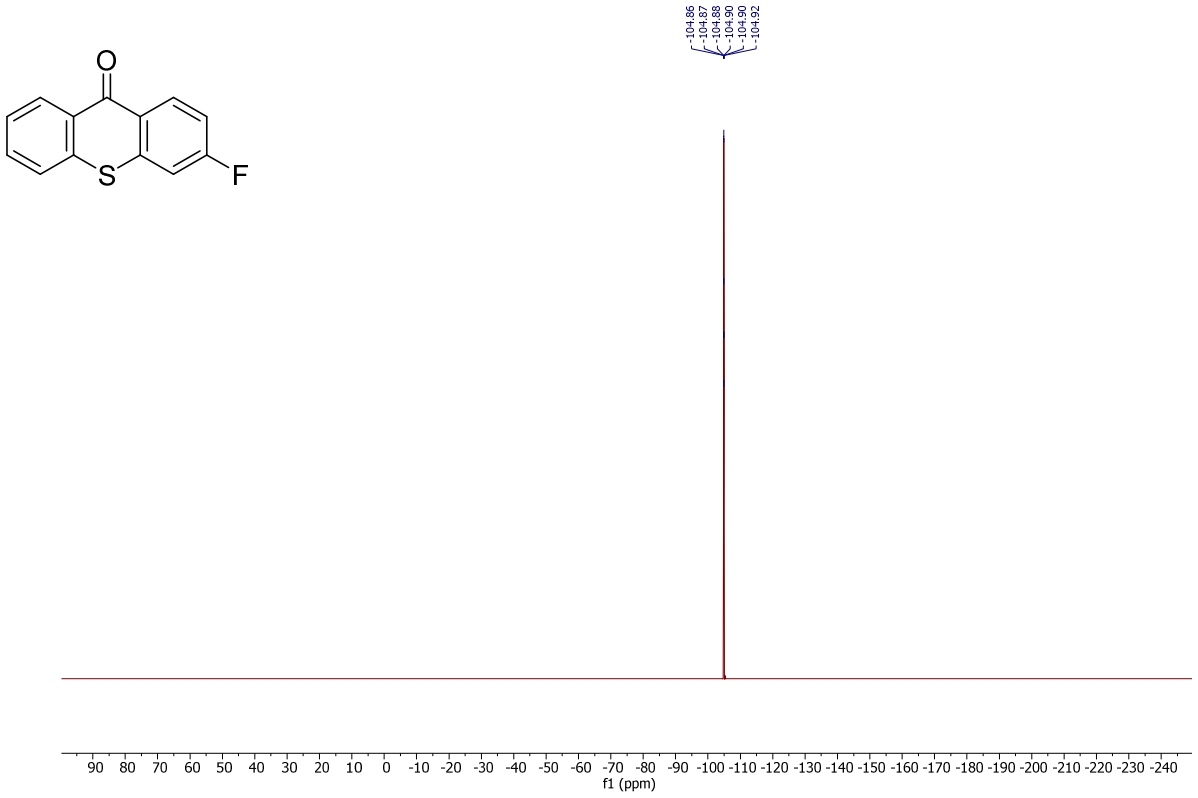


Photocatalysts

2-((3-fluorophenyl)thio)benzoic acid (37)






O
S
F
-104.86
-104.87
-104.88
-104.90
-104.90
-104.92
90 80 70 60 50 40 30 20 10 0 -10 -20 -30 -40 -50 -60 -70 -80 -90 -100 -110 -120 -130 -140 -150 -160 -170 -180 -190 -200 -210 -220 -230 -240
f1 (ppm)